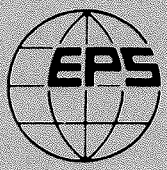

EUROPEAN
PHYSICAL
SOCIETY

INTERNATIONAL CONFERENCE ON HIGH-ENERGY PHYSICS

GENEVA, 27 JUNE – 4 JULY 1979

PROCEEDINGS

Volume 2

Sessions IV to VIII

CERN, European Organization for Nuclear Research, Geneva 1979

EUROPEAN
PHYSICAL
SOCIETY

INTERNATIONAL CONFERENCE ON HIGH-ENERGY PHYSICS

GENEVA, 27 JUNE – 4 JULY 1979

PROCEEDINGS

Volume 2

Sessions IV to VIII

CERN, European Organization for Nuclear Research, Geneva 1979

Copies of these Proceedings can be obtained from:

Scientific Information Service, CERN
CH-1211 Genève 23, Switzerland

Price (2 volumes) Sw.Fr. 30.-

CERN - Publications Group - RD/421 - 2000 - janvier 1980

CONTENTS

Volume 1

SESSION IV

HADRON PHYSICS

Chairmen: G. Bellini
G. Ekspong
G. Oades
Yu.D. Prokoshkin

Sci. Secretaries: W. Geist
P. Helgaker
E. Johansson
L. Lanceri
J.P. Martin
S. Maury
H. Plothow
C. Poyer

Rapporteurs talks:

M. Jacob	High p_T and jets
A.J.G. Hey	Particle systematics
V.A. Nikitin	Soft hadron reactions

Invited papers:

D. Treille	Photo- and hadroproduction of new flavours
G. Vegni	High energy interactions on nuclei
G. Höhler	High energy πN phase shift analysis
B. Povh	Very narrow states
Chan Hong-Mo	Theoretical implications of narrow hadron states
A.C. Irving	Hypercharge exchange reactions and hyperon resonance production

Contributed papers:

G. Thompson	The A_1 meson produced at 63 and 94 GeV/c in the reaction $\pi^- p \to \pi^-\pi^-\pi^+ p$
P. Weilhammer	Elastic and total $\pi^+\pi^-$ cross sections from a high statistics measurement of the reaction $\pi^- p \to \pi^+\pi^- n$ at 63 GeV/c
W.M. Geist	An analysis of charm searches in NN collisions
K. Barnham	Review of $K^{\pm} p$ physics
K.M. Terwilliger	Spin dependence in high p_T^2 elastic pp and np scattering
A. Bodek	Observation of prompt single muons and of missing energy associated with $\mu^+\mu^-$ pairs produced in hadronic interactions
D. Wegener	Quantum number effects in events with a charged particle of large transverse momentum
V. Picciarelli	$K^{*0}(890)$ polarization measurements in the hypercharge exchange reaction $\pi^- p \to K^{*0}(890)\Lambda^0/\Sigma^0$ at 10 GeV/c
Ning Hu	Scaling and the violation of scaling

HIGH P_T AND JETS

M. Jacob
CERN, Geneva, Switzerland

ABSTRACT

Recent developments in the field of high-p_t hadronic interactions are reviewed. They mainly refer to the jet structure of reactions with high-p_t secondaries and to the properties of hadronic jets. The relevance of quantum chromodynamics is assessed and a data-sampling illustrates successes and present problems. The question of prompt photons at high p_t is discussed. Recent results on wide angle πp elastic scattering are presented.

1. INTRODUCTION

Particle production at high transverse momentum (high p_t) has attracted much interest since the discovery of anomalously important yields at the CERN ISR in 1972. It is now well known that large-p_t secondaries are associated with a jet structure. The typical configuration is shown in Fig. 1.a). Two jets of hadrons are produced at wide angle, while forward and backward jets are also present, as is usually the case for hadronic reactions. The association of the two wide angle jets with the hard scattering and fragmentation of hadron constituents, as long discussed in the framework of the parton model (Fig. 1.b)), has now gained general currency. All expected features have been met with impressive success[1]. At present, quantum chromodynamics, as it can be used in its perturbative approximation, provides an attractive theoretical framework for a deeper understanding of the success of the parton model[2,3,4]. It allows for the computation of rates and predicts deviation from the too simple picture usually associated with the parton approach. While some semi-quantitative success can already be claimed, and while general agreement prevails that QCD subprocesses take a dominant rôle at very large p_t ($p_t > 10$ GeV/c), the situation is still unsettled. We are lacking data at collider energies ($\sqrt{s} \simeq 500$ GeV) which alone could provide full confidence in the QCD approach. Data should become available by 1981. Where plenty of data is already available (at $p_t \sim 5$ GeV/c say), QCD predictions have to involve too much parametrization of yet poorly understood effects to be amenable to any actual test. One also encounters evidence for some correlations which QCD is unable to meet in its simple "leading log" implementation and which may imply the relevance of more complicated effects, referred to as higher twist effects in the present vernacular.

We are at an interesting transition stage and the time which has elapsed since the Copenhagen meeting on "Jets in High Energy Collisions"[5] and the Tokyo Conference[6], which were the two landmarks in this field in 1978, has been a time of consolidation rather than a period during which new views or new challenges have emerged. At present there are far more precise and extensive data than was available at the time of the Tokyo Conference[7]. They are however basically supporting the jet picture which could already be claimed

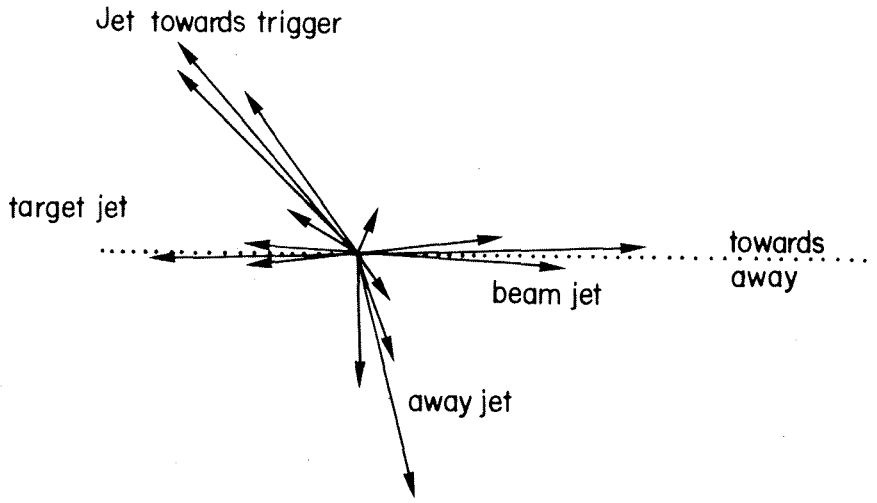

Fig. 1.a) : An idealized picture showing the two wide angle jets associated with the fragmentation of the scattered constituents. Also shown are the forward and backward jets typical of hadronic interactions.

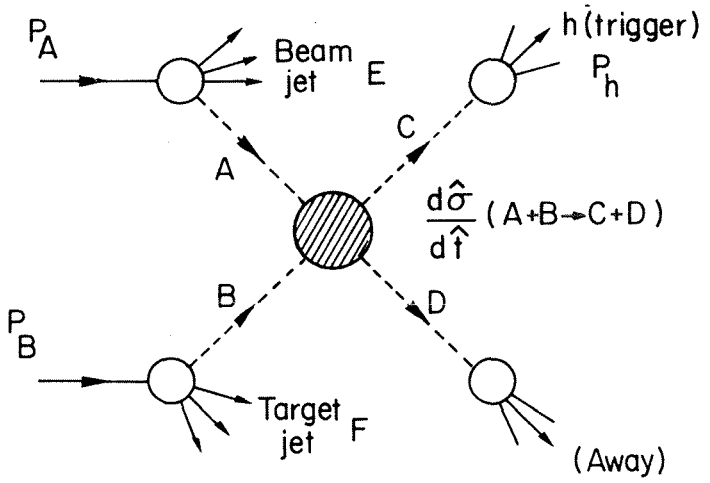

Figure 1.b) : The hard scattering approach to high-p_t production. Constituents A and B scatter into constituents C and D. The trigger particle is a fragment of constituent C.

as established by then. Insofar as these data provide stronger and wider support for the hard-scattering approach, they are a strong encouragement for further studies through which the nature, the relative rôle and the fragmentation modes of the relevant constituents should be established with some precision. Insofar as they certainly agree, at least at a qualitative level, with expectations based on QCD, there are as many challenging pieces of evidence for a more refined theoretical approach and as many sources of great expectation when considering experimentation at much higher energies.

The amount of new material is such that this review simply cannot do justice to all recent and interesting results. It is organized as follows. A data-sampling, aimed at illustrating the still better evidence for the jet structure which is now available, is first presented. This can be done without any specific reference to the nature of the relevant hadron constituents. We then turn to the study of recent experimental information which is more related to the actual nature of the basic mechanisms at work. Hints at QCD subprocesses becoming dominant at very high p_t are first reviewed. Evidence for this relies primarily upon the highest p_t data available, which correspond to inclusive π^o production. We then turn to a data-sampling again, choosing among recent results illustrating the complexity of the subprocesses or of correction terms rather than the overall simplicity which prevails at first sight. This has to do with specific effects expected in the framework of perturbative QCD. This has also to do with effects which could be associated with more complicated terms only, but which can be presently parametrized in terms of specific subprocesses. One of them is the well-known constituent interchange model (CIM)[1,8]. We conclude this review of high p_t and jets with the question of prompt photons at high p_t. It is a common feature of all models based on hard scattering among hadron constituents that the γ/π ratio should be much larger than α, and increase with p_t or more accurately with $x_t = 2p_t/\sqrt{s}$. Collecting evidence for a prompt photon component among an overwhelming background of π^o and η decays has however long been a challenging experimental question. Evidence for a prompt photon yield with a γ/π ratio increasing with p_t, and at the 20% level at p_t = 6 GeV/c, has now been reported.

Our present understanding of high-p_t processes is closely related to that of the energy behaviour of elastic scattering at fixed wide angle[1]. It is therefore deemed appropriate to close this report with some recent results on π-nucleon scattering in the 45 - 90° angular range. Even though the maximum beam energy is only 30 GeV, the relevant p_t is rather large by present standards.

2. THE JET STRUCTURE

Seldom are jets as clearly seen as in the actual event shown in Fig. 1.c). The peculiar (and now well understood) effect that most of the jet momentum on the trigger side is actually carried by the high-p_t particle used as a trigger notwithstanding, one is very close to the idealized picture of

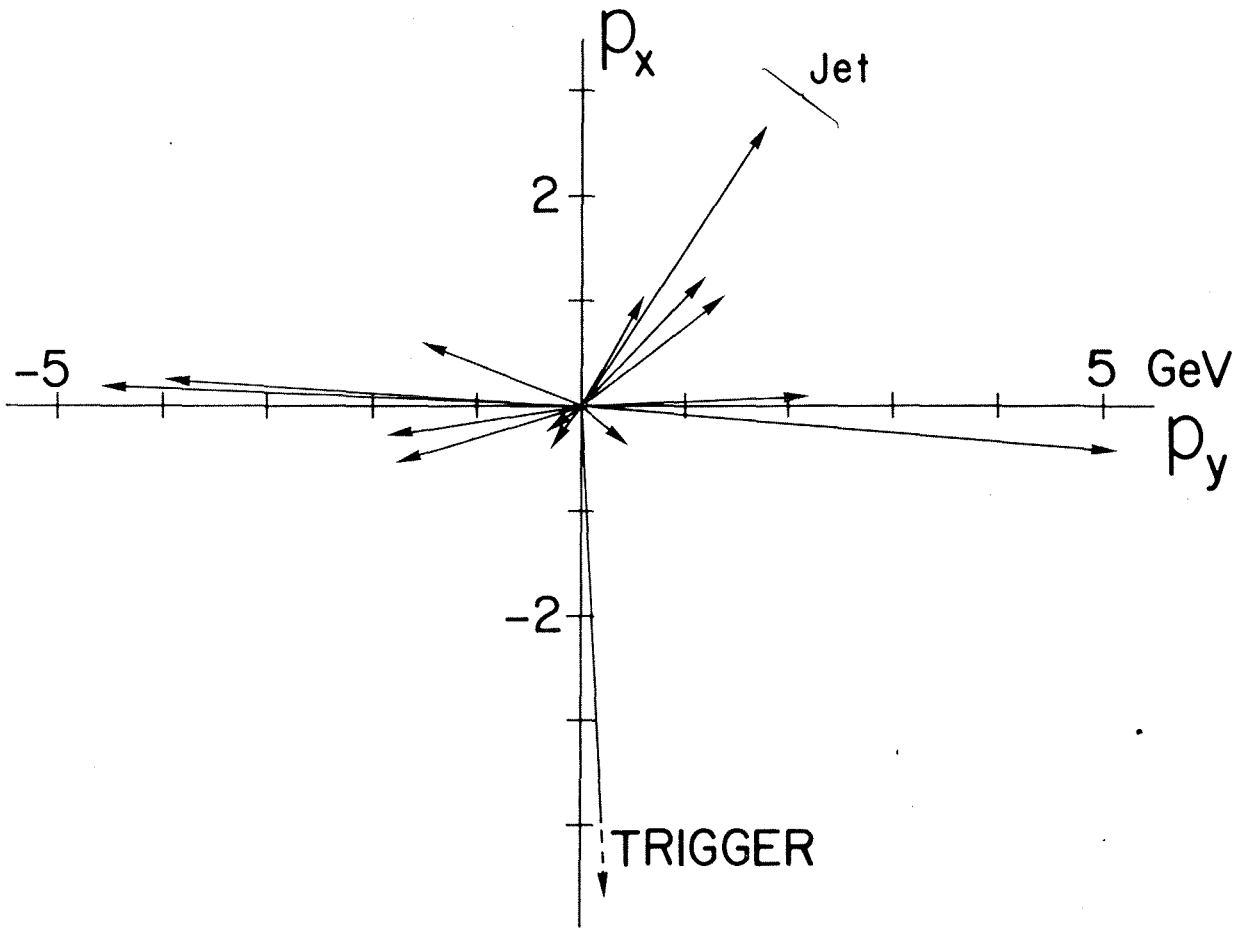

Fig. 1.c) : An event observed by the British-French-Scandinavian Collaboration at the ISR (R 413). A charged pion (with $p_t \simeq 9$ GeV/c) acts as a trigger. A jet of hadrons at wide angle is clearly seen on the other side even though only charged particles are recorded.

Fig. 1.a). Evidence of a jet structure more generally results from a now very wide array of correlation data[1,5,6]. Focussing on relatively high-p_t particles, which are more directly associated with the expected jets, one may first test for the angular (or rapidity) correlations which they must have among themselves as members of jets. We shall however not come back on evidence for jet-like rapidity correlations on the towards and on the away sides, which in standard vernacular are defined with respect to the detector used at triggering. No doubts remained already at the time of the Tokyo Conference[9]. We choose rather to present new data which better test the coplanarity structure of high-p_t reactions. All large-p_t particles should be in the plane defined by the hard-scattering subprocess. This simple (standard) jet picture is however not meant to exclude more complicated configurations, with for instance a third jet, the presence of which would spoil the coplanarity structure. In the framework of perturbative QCD this should also occur and we shall come back to it. The data displayed in Fig. 2 indicate that, up to a good level of approximation, there is no evidence against the coplanarity structure associated with the standard jet picture which one should at least contemplate for a while[10]. Figure 2.a) presents recent data from the Athens-Brookhaven-CERN-Syracuse Collaboration on azimuthal correlations among two high-p_t π^o's[11]. In an attempt to minimize what is expected by kinematical consideration alone, data are presented for increasing values of E_t, the global energy radiated transversally. In practice it is that of the two observed π^o's together with whatever is needed to balance the resulting transverse momentum. This is to be contrasted to a presentation of the data in terms of the observed transverse momenta which would force a coplanarity structure as favoured anyway in view of sharply falling rates with increasing p_t. Back-to-back peaks appear in the azimuthal correlations as the only prominent feature. Figure 2.b) shows recent data from the CERN-Saclay Collaboration at the ISR[12]. Displayed are the ratios of rates for the observation of fixed numbers N of charged particles for events selected by the observation of a high-p_t π^o (p_t > 5 GeV/c) and for "minimum bias" events. This is done toward and away from the trigger direction and also out of the plane. One clearly sees the increase expected from the presence of jets in the reaction plane, while nothing changes out of the plane.

Evidence for a jet structure has to go beyond angular correlations. In the standard jet picture one expects that particles associated with either jet should have but a limited transverse momentum with respect to the reconstructed jet axis. There was already some supporting evidence at the time of the Tokyo Conference[5,6]. More recent data confirm it and provide even more precise tests. Figure 3 illustrates progress made with some recent results from the CERN-Columbia-Oxford-Rockefeller Collaboration. They refer to the structure of the away side jet[13]. Figure 3.a) shows the axial symmetry of the jet. The distributions of jet fragments around the reconstructed jet axis (the away side jet) are shown for different cuts applied to the transverse momentum of the associated secondaries, the cutoff value increasing as one moves towards the centre. The axial symmetry remains. The angu-

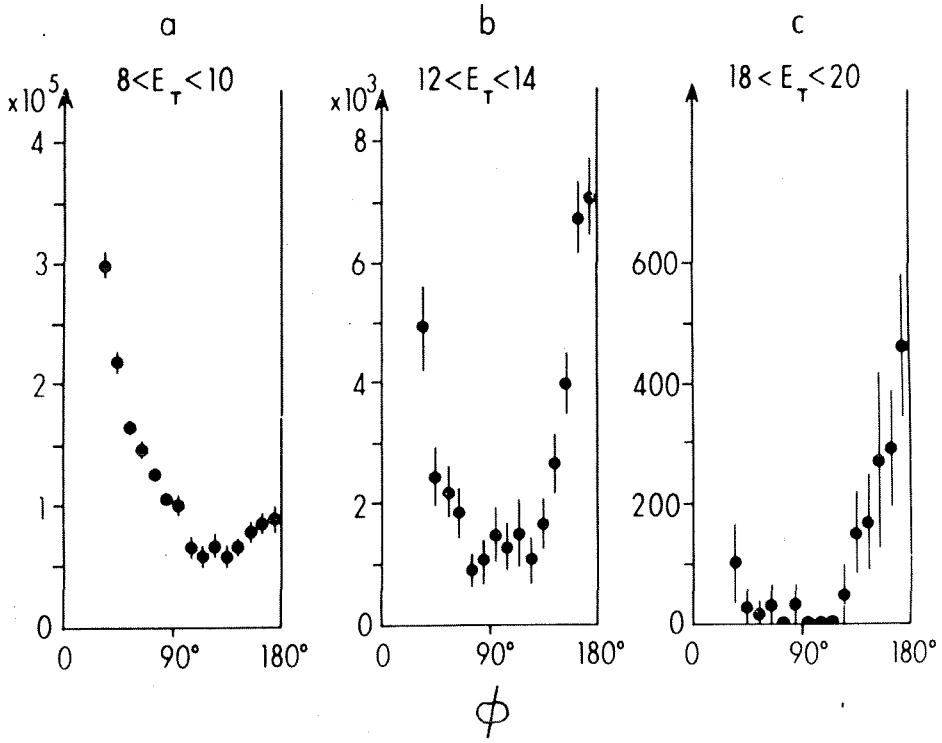

Figure 2.a) : Azimuthal correlation between two high-p_t π^o's for fixed values of E_t, the energy radiated transversally. It includes that of the two observed π^o's together with whatever momentum is needed to balance their transverse momenta. Data from the Athens-Brookhaven-CERN-Syracuse Collaboration, Ref. 11.

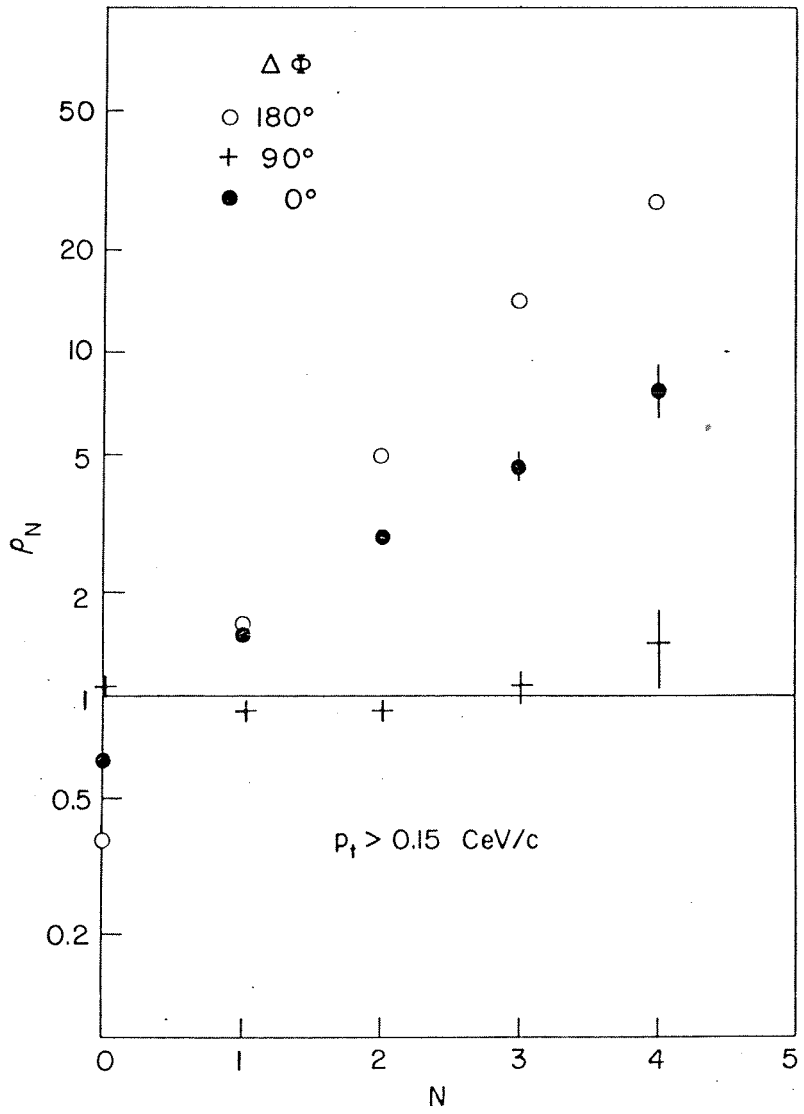

Figure 2.b) : Frequency ratio for the observation of a fixed number of charged particles, between reactions with a high-p_t π^o (p_t > 5 GeV/c) and typical hadronic reactions. The number of associated secondaries increases in the trigger plane (toward and away). Nothing changes out of the plane. Data from the CERN-Saclay Collaboration, Ref. 12.

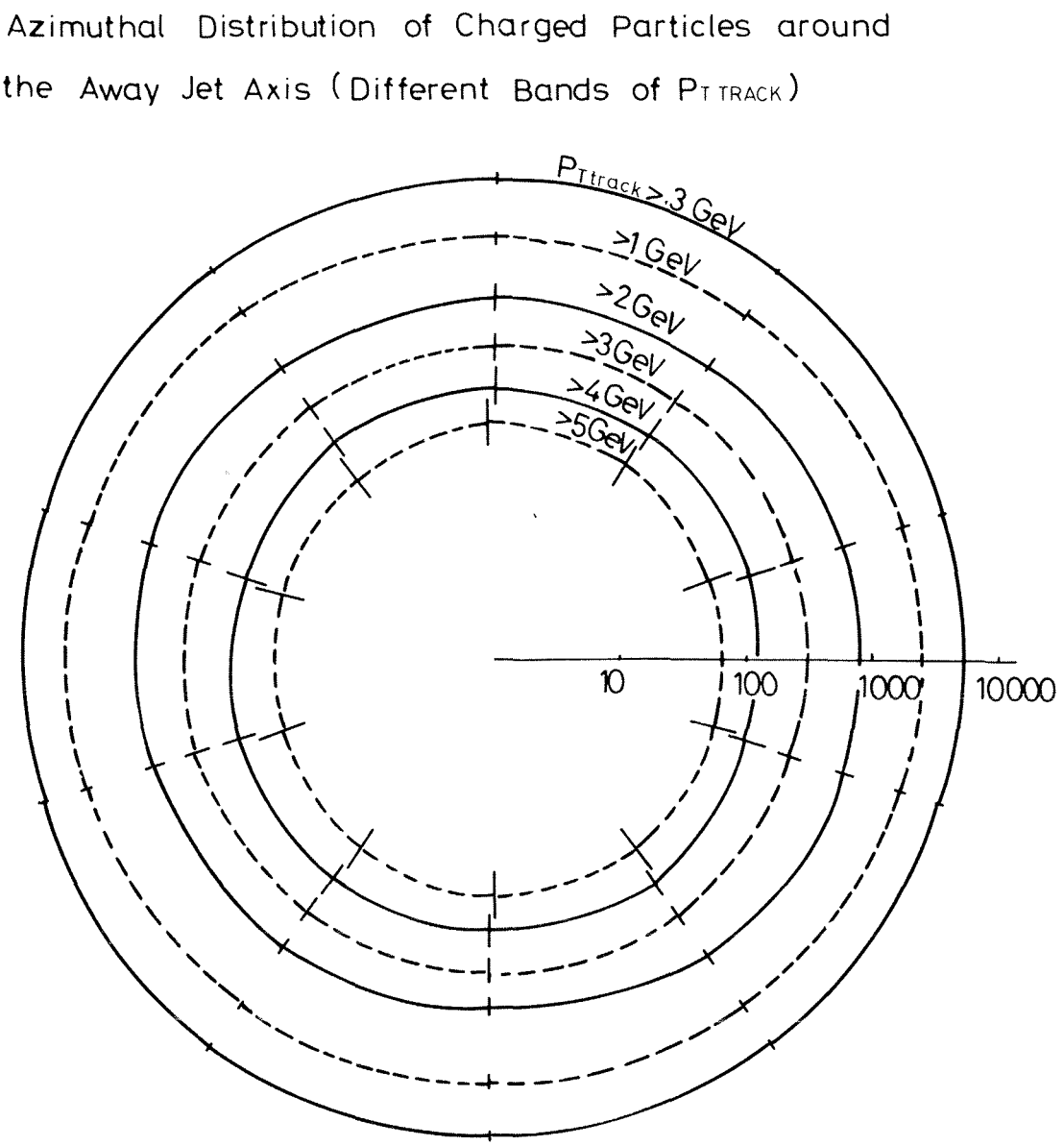

Figure 3.a) : Angular distribution of jet fragments around the reconstructed jet axis for different transverse momentum cutoff and relative yields. Data from the CERN-Columbia-Oxford-Rockefeller Collaboration, Ref. 13.

lar correlation also becomes sharper as the transverse momentum increases. This actually corresponds to a limited mean transverse momentum $\langle k_t \rangle$ with respect to the jet axis, as shown in Fig. 3.b). The mean value is practically constant as the trigger momentum is varied over a wide range.

New results on $\langle k_t \rangle$ have also been obtained by the CERN-Saclay Collaboration[12] though directly accessible to them is the component of the transverse momentum with respect to the jet axis which is in the reaction plane only. Using axial symmetry, as demonstrated by the CERN-Columbia-Oxford-Rockefeller Collaboration (Fig. 3.a)), they quote $\langle k_t \rangle = 0.55 \pm 0.05$ GeV/c in very good agreement with the data displayed in Fig. 3.b). Such a value of $\langle k_t \rangle$ can be considered to be in reasonable agreement with values reported in e^+e^- annihilation, provided that the comparison is made at large enough a value of x_L in order to eliminate the seagull effect which forces the global mean value down. At $x_L \sim 0.2$ say, preliminary data from PETRA seem to indicate a slow rise with energy, with $\langle k_t \rangle \simeq 0.45$ at 13 GeV and $\langle k_t \rangle \simeq 0.55$ at 27 GeV[14]. While jets in hadron interactions may appear to be slightly wider than those observed in e^+e^- annihilation at the same momentum, one should at present rather stress the overall agreement between the measured values of $\langle k_t \rangle$ in very different processes. Indeed, there is good agreement between the ISR values of $\langle k_t \rangle$ and values reported for deep inelastic neutrino scattering[15].

At present jets observed in hadron collisions meet properties associated with standard jets[10]. While there is no supporting evidence for the widening expected in the framework of QCD where the $\langle k_t \rangle$ distribution should eventually develop an unbounded component increasing as p_t at order $\alpha_s(p_t^2)$, it is however easy to convince oneself that the p_t values under study are still too low for such an effect to clearly appear over the distribution which merely parametrizes the hadronization of the jet, with a Gaussian shape often used[16,17].

Having ascertained angular correlations implied by a jet structure and a prominent jet property with a limited mean transverse momentum for jet fragments (Fig. 3.b)), we now turn to other expected jet properties. The fragments of a jet, among which π mesons dominate, should show a scaling distribution, each taking on the average a fixed fraction of the jet momentum. Figure 4.a) shows how scaling works for the fragments of the towards jet thus accompanying the trigger particle. The data, from the CERN-Saclay Collaboration, show the distribution in longitudinal momentum for charged secondaries associated with a high-p_t neutral trigger (one or several particles), scaled according to the trigger momentum. The distribution does not change as the trigger momentum varies from 5 to 8 GeV/c. Each associated particle carries on the average a fixed fraction z of the trigger momentum[12].

In order to better illustrate what is implied by scaling it is useful to write the expected distributions as they appear in a simplified model where an inverse power behaviour (p_t^{-n}) is used to approximate the inclusive

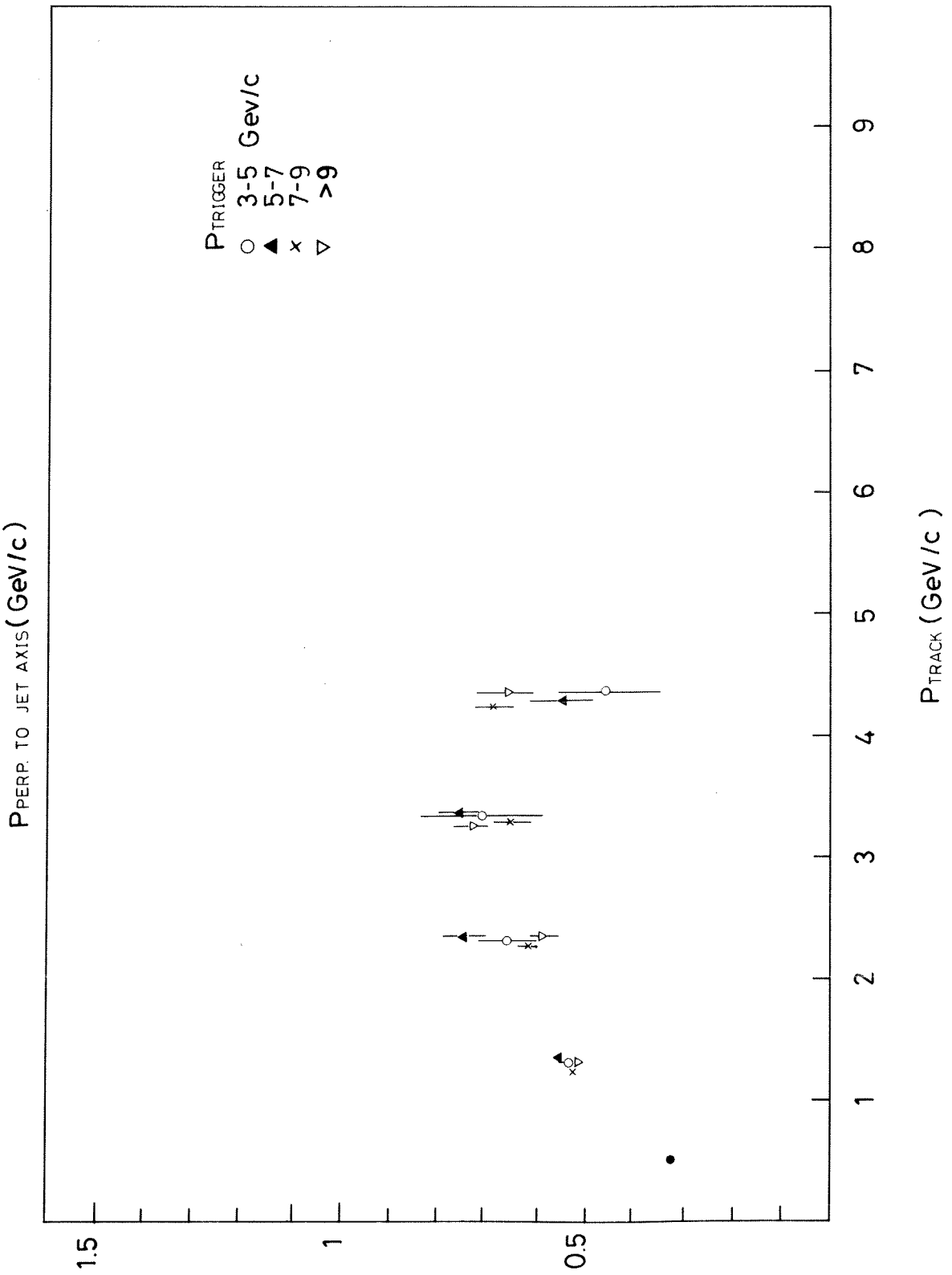

Figure 3.b) : Mean transverse momentum of jet fragments with respect to the jet axis for different trigger momenta. Data from the CERN-Columbia-Oxford-Rockefeller Collaboration, Ref. 13.

distribution at high p_t and where scaling distributions $F^i(x)$, $F^{ij}(x_1, x_2)$ ... are introduced for each fragmentation mode[18]. The distribution presented in Fig. 4.a) then simply reads:

$$\frac{1}{N}\frac{dN}{dz} = \frac{\int_0^1 x^n F(x, zx)\, dx}{\int_0^1 x^{n-1} F(x)\, dx} \qquad (1)$$

i.e. a function of z only (Fig. 4) with a numerical value depending much on the high x behaviour of the fragmentation functions.

Before claiming that scaling is well established one should however mention that the CERN-Columbia-Oxford-Rockefeller Collaboration does not concur to such a conclusion[13]. Observing charged particles associated to a neutral trigger they rather find that $\langle z \rangle$ falls with p_t (the distribution does not scale). The variation corresponds to about a factor 2 between 5 and 10 GeV/c[19] (Fig. 4.b)).

Though some evidence for scaling can be reported combining observations from different experiments, more work is certainly needed.

On the away side, general agreement prevails and all available results (many in number) show a scaling distribution provided that the trigger momentum is large enough (p_t > 3 GeV/c). One usually defines a variable x_e which is the fraction of the trigger momentum compensated by each observed secondary. Taking again the simplified model previously mentioned, and now assuming that the two jets balance exactly their transverse momenta[18] the distribution presented in Fig. 5) reads:

$$\frac{1}{N}\frac{dN}{dx_e} = \frac{\int_0^1 x^n F(x) F(xx_e)\, dx}{\int_0^1 x^{n-1} F(x)\, dx} \qquad (2)$$

i.e. a function of x_e only and, in practice, much different from $F(x_e)$.

Figure 5.a) shows recent data from the Athens-Brookhaven-CERN-Syracuse-Collaboration, which are those extending over the largest p_t range. They clearly demonstrate that, for each x_e value, the observed rate on the away side is independent of the trigger momentum. There was already good evidence for scaling at the time of the Tokyo Conference[4,5]. It is now overwhelming, as extensive data at very high p_t are available[11,12,13].

Figure 5.b) puts together ISR results already presented at the Tokyo Conference (CERN-Collège de France-Heidelberg-Karlsruhe Collaboration at lower p_t and British-French-Scandinavian at larger p_t, together with the new 8 GeV/c points from the CERN-Columbia-Oxford-Rockefeller Collaboration. Sca-

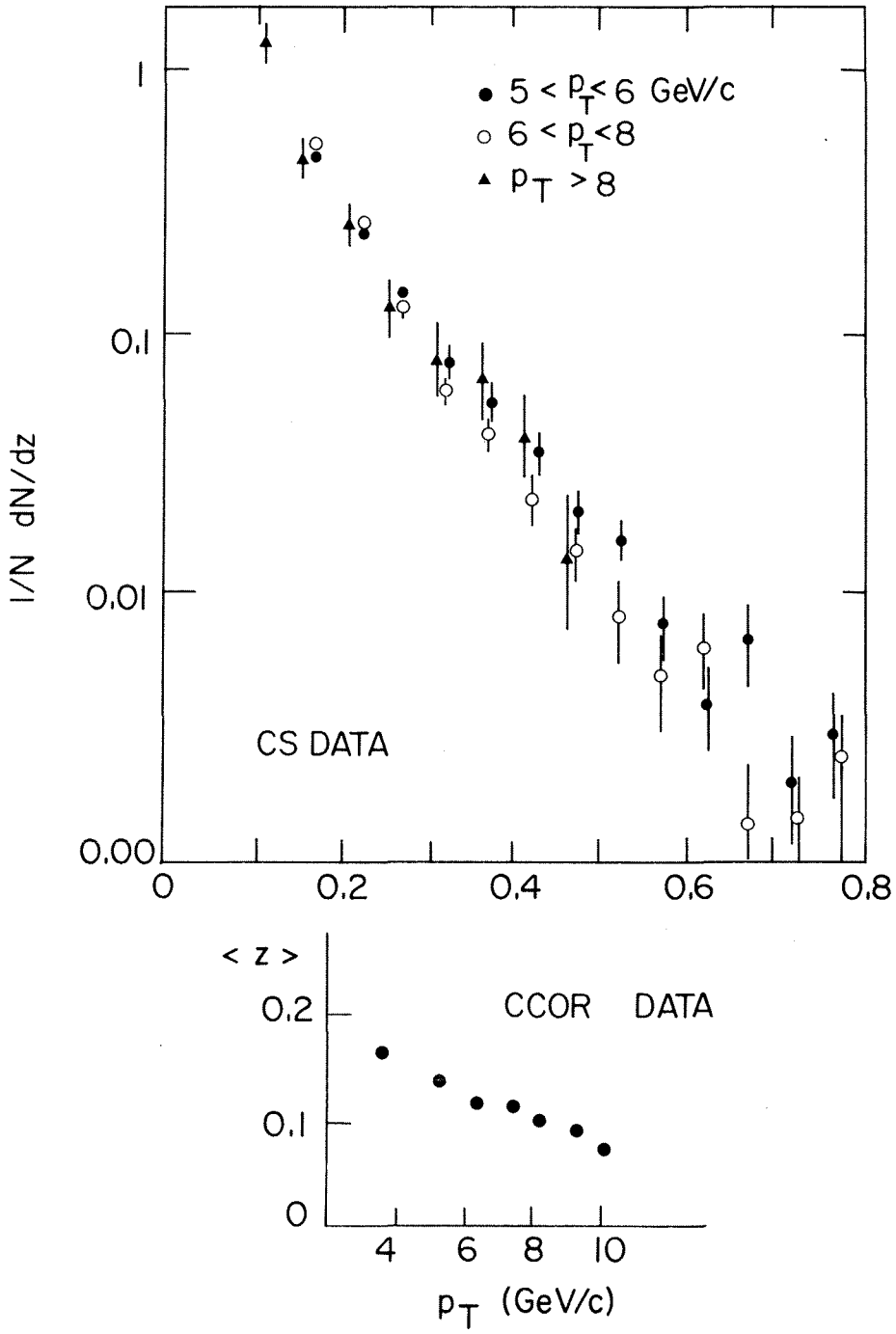

Figure 4.a) : Longitudinal distribution of charged particles associated with a high-p_t neutral trigger. The longitudinal momenta are scaled according to the trigger momenta. Scaling applies to the fragmentation of the trigger jet. Data from the CERN-Saclay Collaboration.

4.b) : Mean value of <z> as a function of the trigger momentum, as measured by the CERN-Columbia-Oxford-Rockefeller Collaboration. It should be constant for a scaling distribution!

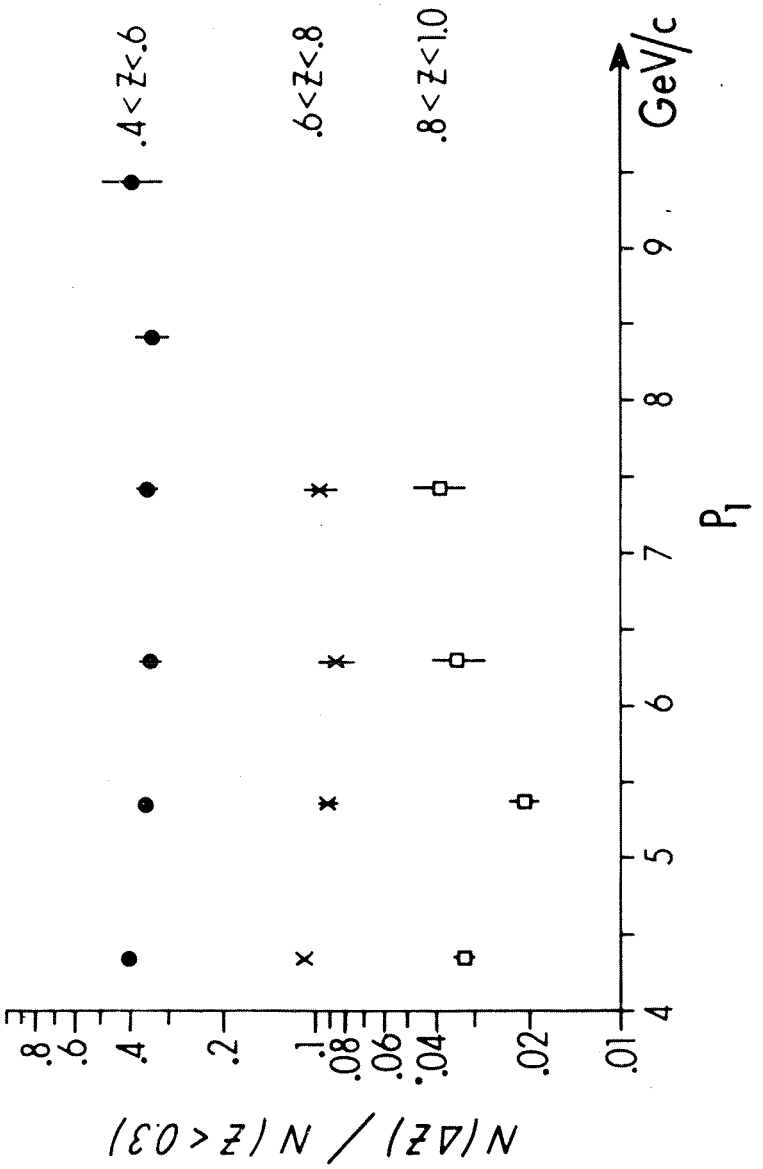

Figure 5.a) : Scaling on the away side. Data from the Athens-Brookhaven-CERN-Syracuse Collaboration. The yield for fixed values of x_e does not vary as p_t varies. The data are normalized to the yield at $x_e < 0.3$.

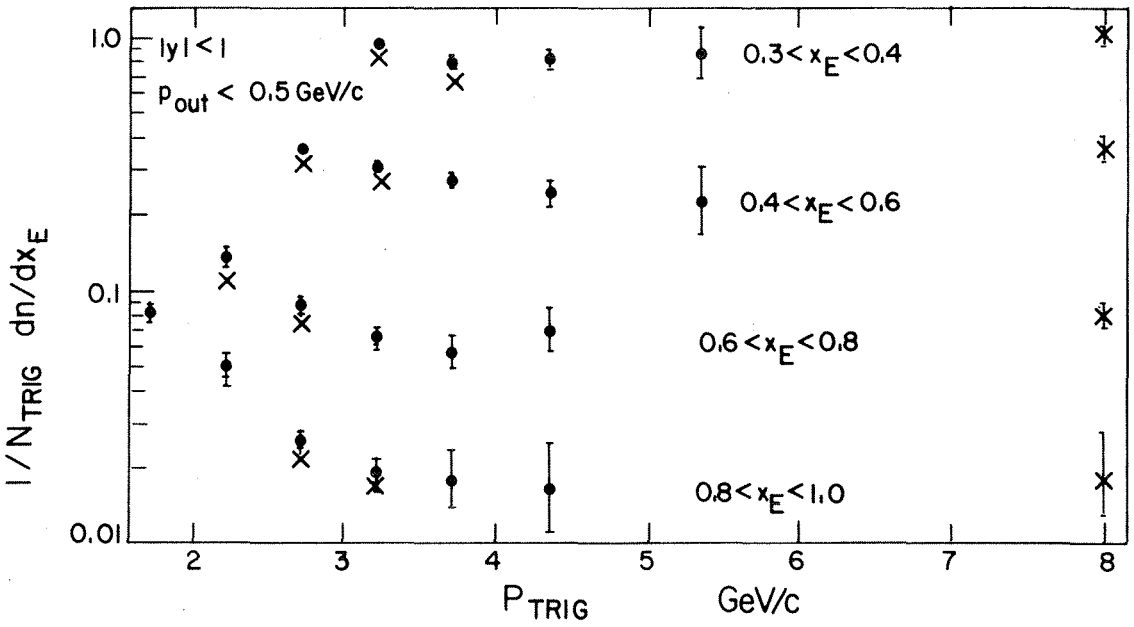

Figure 5.b) : Scaling on the away side. Data at lower p_t, Ref. 4, together with recent results from the CERN-Columbia-Oxford-Rockefeller Collaboration.

ling imposes itself as the trigger momentum becomes large enough and as the ratio between the trigger and away jet transverse momenta tends towards one.

An important consequence of scaling, and general ideas about jet fragmentation, is that the jet yield, collecting all particles associated with a jet, should be much larger than the single particle yield at the same p_t, usually considered when studying high-p_t processes. Considering again our simplified model in order to illustrate the point, the single-particle cross-section is readily related to the jet cross-section at the same p_t as follows:

$$\frac{d\sigma}{dp_t} = \frac{d\sigma^j}{dp_t} \int_0^1 x^{n-1} F(x)\, dx \qquad (3)$$

Since n is large (n ~ 10) and F(x) falls as x increases, the weighting factor provided by the integral is small, hence the large ratio between jet and single-particle yields. The detailed comparison between jet cross-sections and single-particle cross-sections is far more involved experimentally[20] and theoretically[21]. The response of the jet (calorimeter) detector has to be analyzed in terms of a Monte Carlo simulation, which cannot avoid some preconceived ideas about jets. Figure 6 shows the recent outcome[22] of E 260 at Fermilab (Caltech-UCLA-Fermilab-Illinois Collaboration). It gives the inclusive jet cross-section at 90°, together with the charged pion production cross-section measured at the same energy[23]: 200 GeV. The jet cross-section is typically two orders of magnitude above the single-particle cross-section, the ratio increasing with x_t ($x_t = \frac{2p_t}{\sqrt{s}}$) as expected[21].

Also shown in Fig. 6 are the results of a QCD calculation, the upper and lower curves corresponding to the production of a jet of given energy and momentum, respectively[22]. Which one should be preferred is unclear. This is ambiguous in perturbative QCD. For the values of p_t here considered jet pionization dissipates about 1 GeV in transverse momenta and masses. This corresponds to a difference in yield by an order of magnitude. The British-French-Scandinavian Collaboration has recently measured the inclusive jet cross-section at 2.6 GeV jet energy from an unbiased data sample[9]. It is found to be 150 times the single particle yield. The cross-section for a jet of 2.6 GeV momentum is lower by an order of magnitude. The jet to single particle ratio is also found to increase with x_t.

A large enhancement of the cross-section when considering a multi-particle system as opposed to a single-particle system at large p_t has also recently been reported from the analysis of K^-p interaction in BEBC at 110 GeV/c[24].

Figure 7.a) comes back on an effect which has been known for some time and which is of great relevance to the hard-scattering approach. It shows that pions are more efficient than protons at producing high-p_t jets (and high-p_t particles) and this the more so the larger x_t is. This is directly related to the fact that pion constituents carry a larger fraction of the particle momentum than proton constituents do.

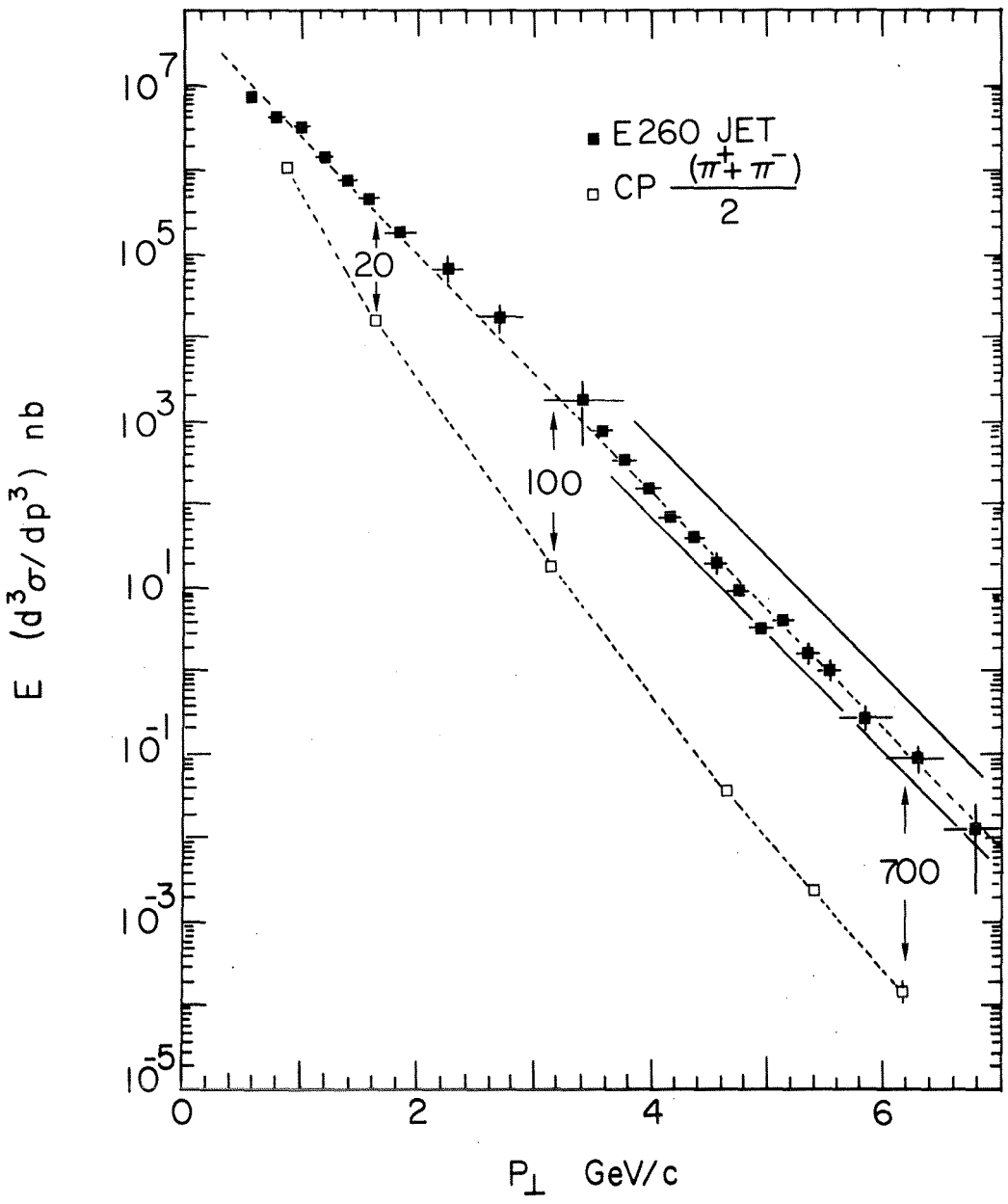

Figure 6 : Inclusive distribution for jets and for single particles. The jet data are from the Caltech-UCLA-Fermilab-Illinois Collaboration. The QCD calculation for jet production at fixed jet energy and fixed jet momentum brackets the data : G. Fox, private communication.

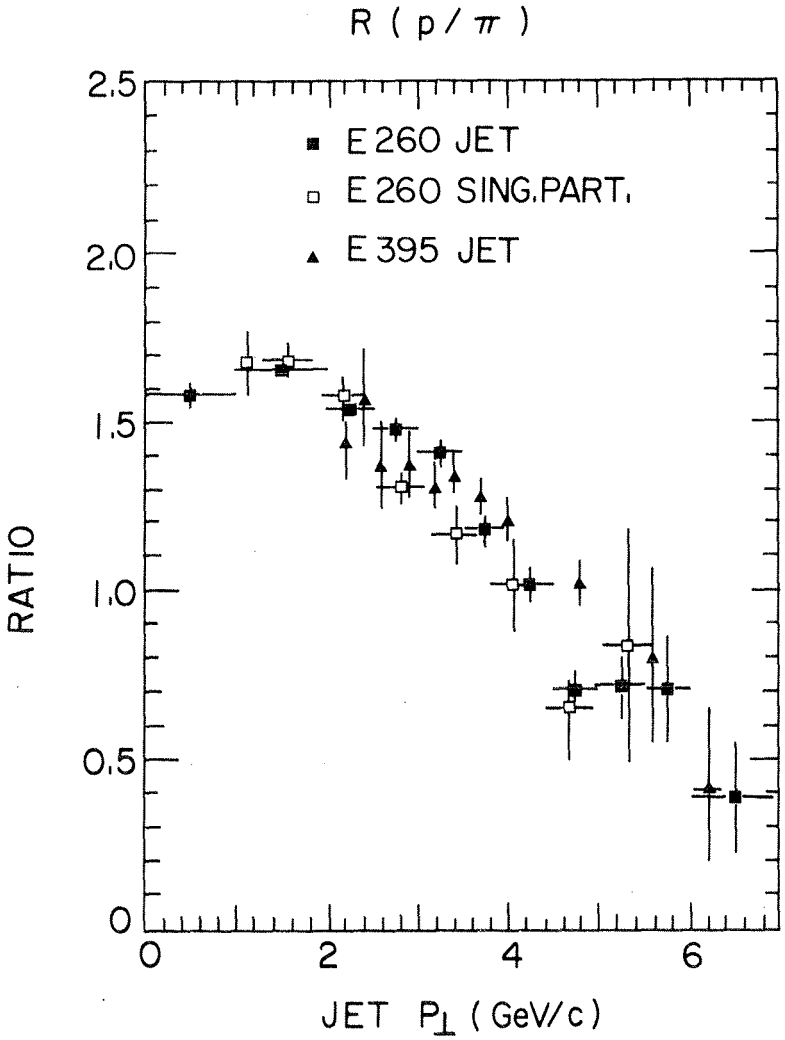

Figure 7.a) : The relative efficiency of proton and pion induced reactions. Ratio between the inclusive jet yield at 90° in proton- and pion-induced reactions. As p_t increases pions become more efficient. Data from E 260, Ref. 22.

A new feature, reported by Experiment 395 at Fermilab (Fermilab-Lehigh-Pennsylvania-Wisconsin Collaboration), is that the greater efficiency of pions actually refers to the production of jets emitted relatively forward, as again expected from pion constituents which take a larger fraction of the hadron they belong to[25]. Also shown (on Fig. 7.b)) are data obtained with a double arm calorimeter, setting one arm at 90° (as is the case for the inclusive jet yields, the ratio of which appears in Fig. 7.a)) and also at other angles and varying the direction of the other arm. As the production angle decreases, the relative efficiency of the pion beam increases.

A new result from the E 260 experiment is that the ratio between kaon and pion-induced reactions is compatible with one[22]. This holds from 1 to 5 GeV/c, and is shown in Fig. 8. More accurate data, extending over a wider p_t range would however be needed before one can conclude at similar distribution for strange constituent quarks. Antiprotons are also found to be slightly more efficient than protons at producing high-p_t jets (by 10% up to $p_t \approx 4$ GeV/c)[22].

The same reasoning which leads to a large ratio between the jet-production cross-section and the single-particle cross-section also implies that when triggering on a large-p_t particle one strongly favours infrequent fragmentation modes (or reaction processes), whereby most of the jet momentum is taken by a single particle[18,26]. One therefore expects that the accompanying momentum on the trigger side should increase with p_t in mean value while remaining relatively small (at the 10% level at most). This is shown to be the case by the British-French-Scandinavian results presented in Fig. 9[27]. The mean associated momentum for charged secondaries is shown as a function of the trigger momentum for different trigger particles. New is the relative rôle of the prominent resonances (ρ, K^*, Δ, ...) in contributing to the associated momentum. It is rather large, amounting to 25 to 50% of the observed value[28].

The complementary results displayed in Figs. 6 and 9 illustrate an important and general property of jet fragmentation. Whenever triggering on a high-p_t particle one is likely to select a particular and unlikely configuration whereby most (or practically all) the jet momentum is with one single particle (Fig. 1.c)). The production cross-section is thus greatly reduced. Conversely, triggering on a whole jet, a much larger production cross-section is observed. Such an effect is usually referred to as trigger bias.

Now that jet fragmentation properties can be considered as well established, at least within a first and good approximation, it is possible to turn to results for which the analysis of the data implies even more preconceived ideas about jet properties and relies on comparisons involving the pertinent Monte Carlo simulations. A very important question now tackled is that of the transverse momentum balance which is achieved among the two wide-angle jets only and, first, that of the actual occurrence of an away-side jet in all events triggered upon by the observation of a high-p_t particle. The

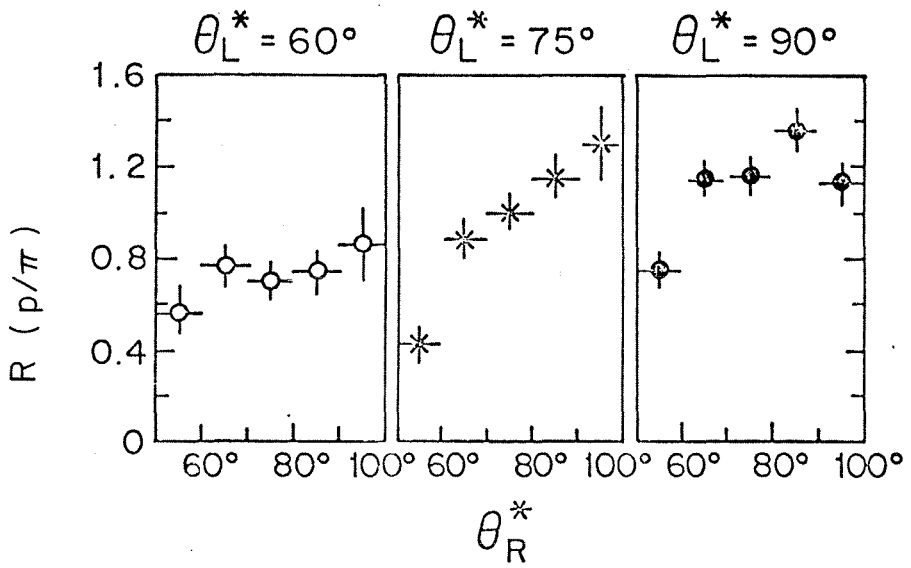

Figure 7.b) : Ratio between the double jet yield in proton- and pion-induced reactions. One calorimeter is set at 60°, 75° and 90°, the other at a different production angle. The increased efficiency of the pion is associated with a prevailing forward production. Data from E 395, Ref. 25.

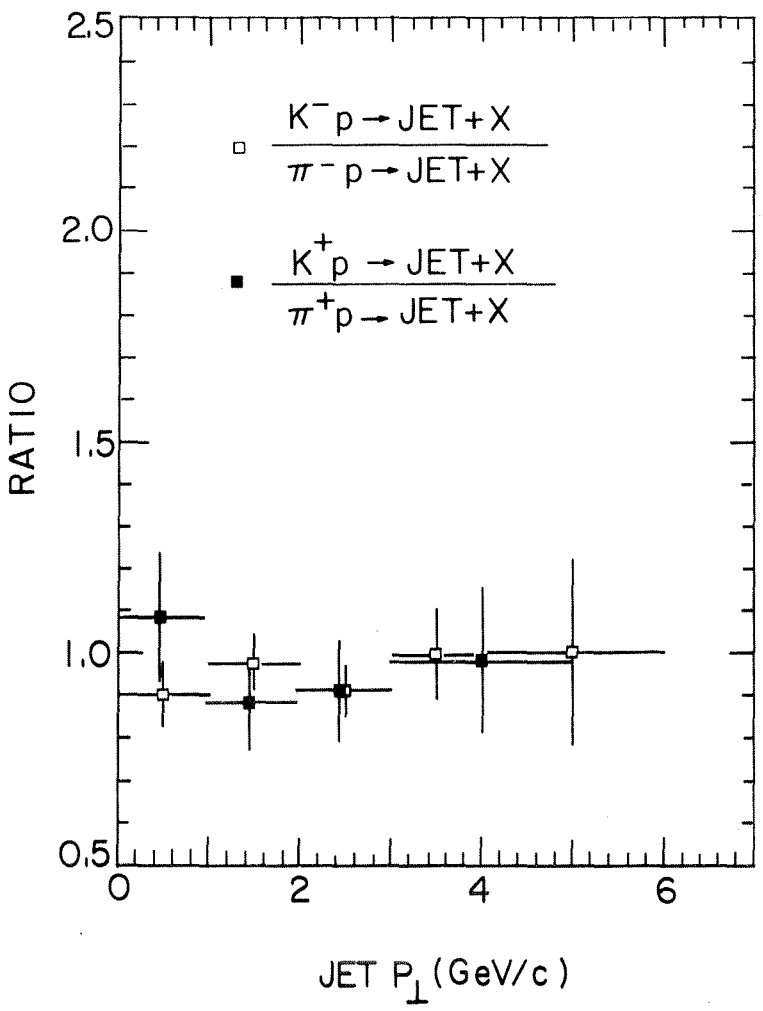

Figure 8 : The relative efficiency of kaon- and pion-induced reactions. Inclusive jet yields at 90°. Data from E 260, Ref. 22.

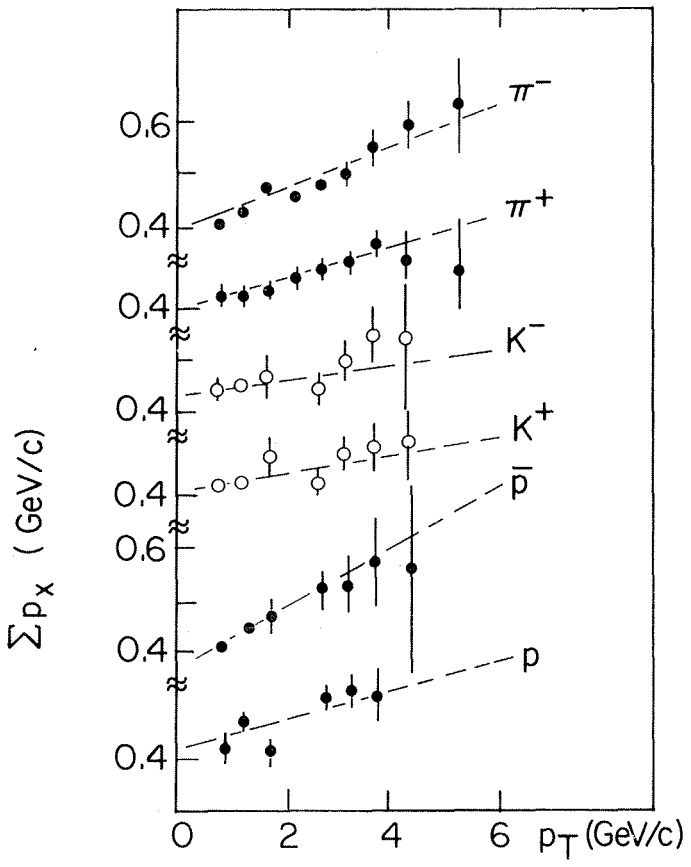

Figure 9 : The accompanying momentum to a high-p_t trigger particle. Shown is the mean momentum carried by charged particles produced in the direction of the trigger. Data from the British-French-Scandinavian Collaboration, Ref. 26.

limited solid angle and biased acceptance of detectors have long hampered such investigations. Figure 10 shows the result of a recent analysis made by the British-French-Scandinavian Collaboration, using data obtained with the SFM detector at the ISR[9].

The probability of observing an away-side jet remains low, increasing only from 0.1 at 2 GeV/c to 0.4 at 5 GeV/c. Yet it is compatible with that expected if there was an away-side jet in each event, provided that it is assumed that the transverse momentum of the away-side jet does not quite balance that of the trigger jet. A discrepancy of the order of 0.8 GeV/c would do (Fig. 10). This discrepancy is compatible with previous results from the same group showing how fast forward and backward particles partly balance the transverse momentum of the trigger particle[29].

Such a good but yet partial balancing of transverse momentum between two jets also appears in the double arm calorimeter results of E 395[24]. Figure 11.a) shows the momentum distribution observed in the away-side calorimeter (within two solid angles defined according to different fiducial limits) when triggering on a jet with a transfer momentum of 4 GeV/c. The distribution shows a peak which should be associated with a good collection of the away-side jet within the calorimeter. It is shifted to a lower p_t value. The p_t discrepancy observed in both cases should be in great part due to an obvious bias in favour of configurations with constituents moving in the direction of the triggering detector. This bias can however be overcome, triggering on both arms, requiring a particular value for the sum of the two transverse momenta. Figure 11.b) shows the p_t imbalance distribution observed when the sum of the two momenta should be between 4.5 and 5 GeV/c. The distribution peaks at zero with a full width at half maximum of 2.4 GeV/c. This imbalance distribution is in very good agreement with the value obtained by the CERN-Saclay Collaboration[12]. Their method is less direct since the jet momenta have to be reconstructed from a two π^o trigger (in two opposite arms) and the associated charged particles. Yet it covers a much higher p_t range, the sum of the two jet momenta being between 8 and 12 GeV/c.

We may conclude at this stage that there is now evidence for a typical configuration with two jets with approximately opposite transverse momenta.

While other configurations cannot be excluded at this stage, available data are compatible with two wide angle jets balancing their transverse momenta to a rather good approximation.

With confidence in present jet parametrization thus building up, it is now possible to attempt to reconstruct the actual jet shape from the detected particles, unfolding biases imposed by the detectors, and to estimate with some precision (~ 1 GeV say) the centre-of-mass energy of the two-jet system[30]. One is then in a position to compare jet fragmentation distributions and multiplicities (integrating over the inclusive fragmentation distribution) to those observed in e^+e^- annihilations and deep inelastic lepton scattering.

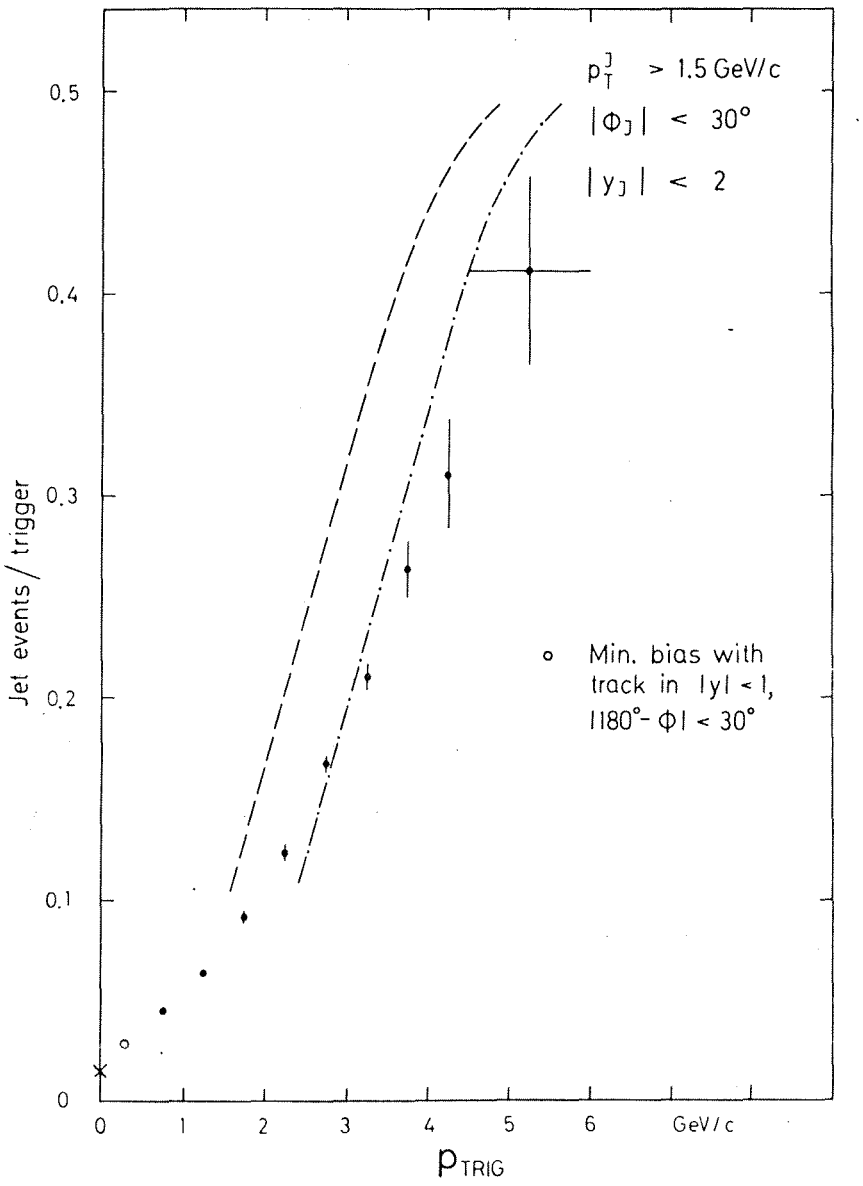

Figure 10 : Frequency of observing a jet on the away side. The low value corresponds to the limited solid angle of the detector. It is compatible with the occurrence of an away-side jet in each event with a high-p_t particle provided that the jet is assumed to have a transverse momentum lower (by 0.8 GeV/c) than the trigger momentum. British-French-Scandinavian Collaboration, Ref. 9. Full balancing (dashed curve) and balancing up to 0.8 GeV/c (dashed-dotted curve).

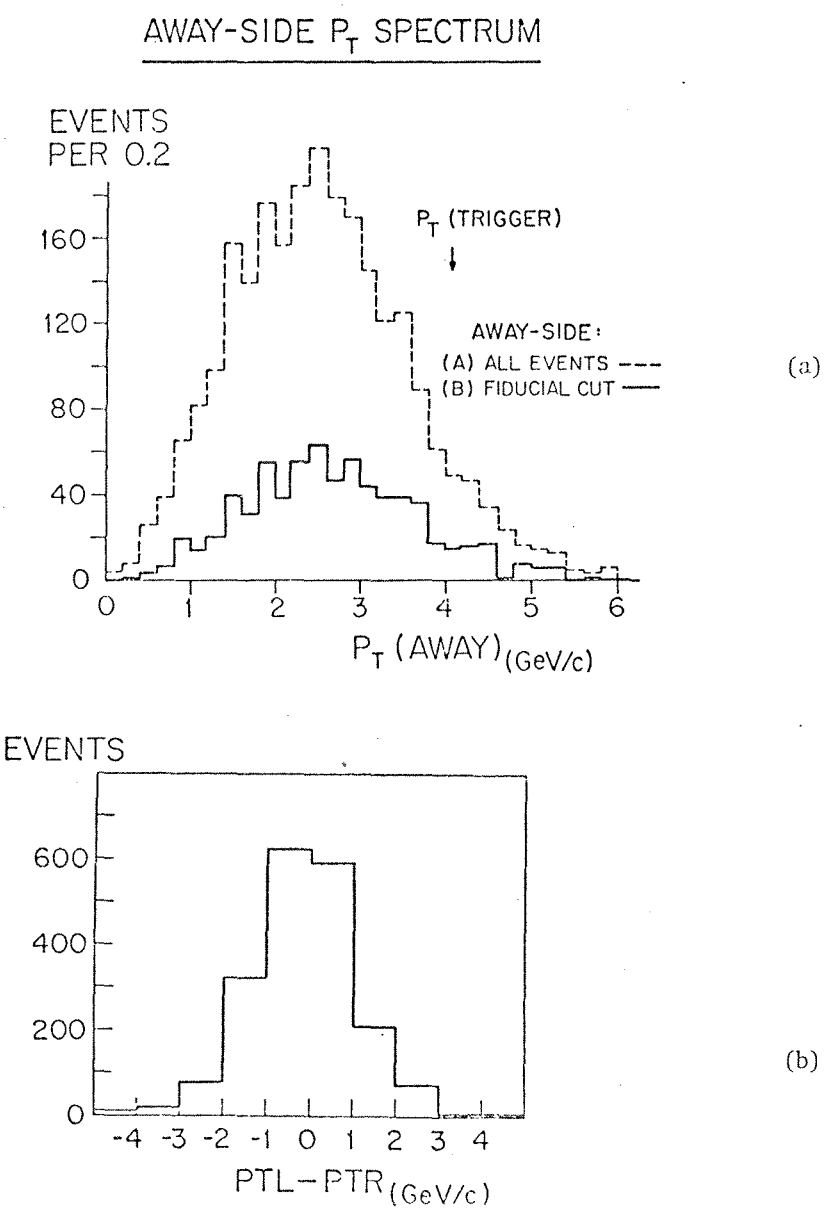

Figure 11.a) : Momentum collected in the away-side calorimeter when triggering on a jet with $3.95 < p_t < 4.2$ GeV/c. A good fraction of the trigger momentum is found to be balanced within the limited solid angle covered by the calorimeter. Data from E 395, Ref. 24.

11.b) : Discrepancy between the two-jet momenta when triggering on two calorimeters. Ref. 24.

Such a comparison is illustrated by Fig. 12.a). The jet fragmentation distribution F(x), reconstructed from the observed jet fragments, turns out to be amenable to an exponential parametrization in the range $0.2 < x < 0.8$. As does that observed in e^+e^- annihilation in the same energy range[31]. The values of the slope parameter are in good agreement for both sets of jets. The ISR data are from the British-French-Scandinavian Collaboration[9].

Figure 12.b) gives results on the mean charged jet multiplicity, reconstructed for a two-jet system. The lower energy points are obtained by the British-French-Scandinavian Collaboration[9], the higher energy ones by the CERN-Saclay Collaboration[12]. Also shown are results from e^+e^- annihilations[31] and from the analysis of deep inelastic neutrino scattering[15] at lower energies, and the PETRA data at higher energies which were reported at this Conference[32].

Again general agreement prevails. The British-French-Scandinavian Collaboration likes to emphasize the somewhat higher value of the multiplicity which they find as compared with the SPEAR values at the same energies[9]. At present one may perhaps however rather stress the apparent similarity which appears, at least at this level of investigation, between jets observed in quite different processes. Even though it may not stand up to a more refined analysis, this similarity should remain as a first approximation. In the future one should be more ambitious and try to differentiate between quark and gluon jets. More extensive data, collected with more sophisticated detectors, are however needed.

3. THE HARD SCATTERING PROCESSES

Having discussed the jet structure and jet properties we now turn to the dynamics of high-p_t production. In the hard-scattering approach, the inclusive distribution at angle θ takes the well-known form[1]:

$$E \frac{d\sigma}{d^3p} \sim \frac{1}{p_t^n} f(x_t, \theta) \qquad (4)$$

where the value of n and the form of the scaling function f depend on the nature of the relevant constituents, the type of basic interaction at work and the nature of the observed particles.

For pion inclusive distributions at $p_t < 6$ GeV/c, for which data have become precise and numerous, a very simple form holds with precision, namely (at 90^o)

$$E \frac{d\sigma}{d^3p} \sim \frac{1}{p_t^n} (1-x_t)^m \qquad (5)$$

with $n = 8.6$, $m = 10.6$ following a fit by the CERN-Columbia-Rockefeller-Saclay Collaboration[19]. This is not the behaviour a priori expected from QCD perturbative interactions among quarks and gluons for which (for mere scaling reasons) one should find $n = 4$. At the same time estimates for the pion yield turn out to be too small when calculated in a straightforward way[1].

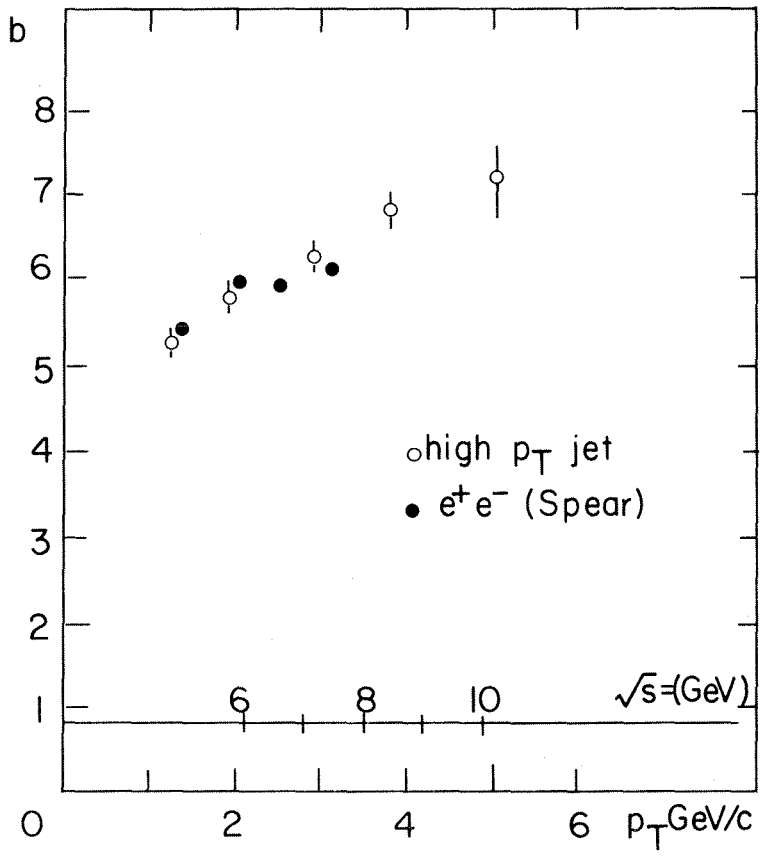

Figure 12.a) : Exponential fit to the jet fragmentation distribution for $0.2 < z < 0.8$. The slope is compared to that determined in e^+e^- annihilation and deep inelastic neutrino scattering. Data from the British-French-Scandinavian Collaboration, Ref. 9.

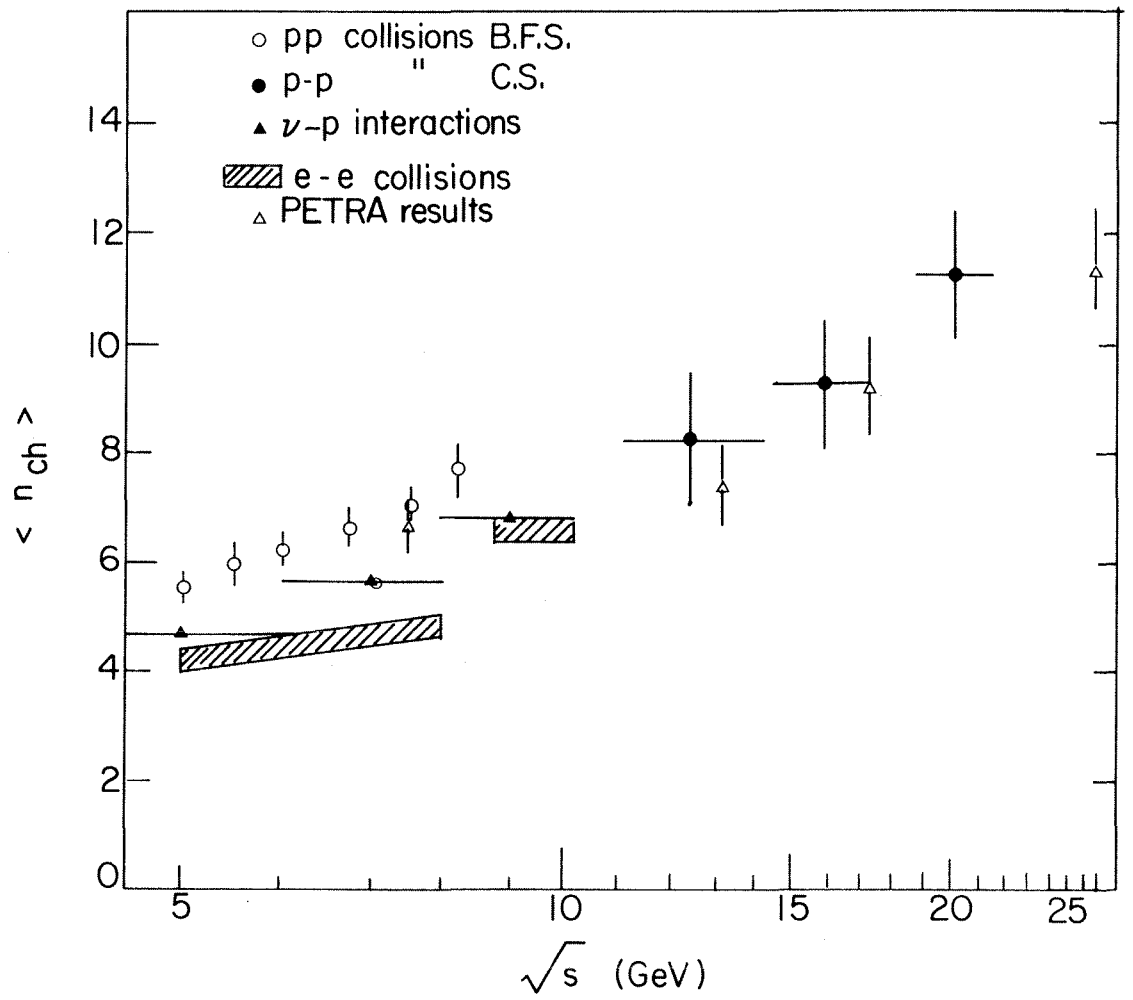

Figure 12.b) : Mean multiplicities as measured for high-p_t jets, e^+e^- annihilation and deep inelastic neutrino scattering. Data from the British-French-Scandinavian Collaboration, Ref. 9 and CERN-Saclay Collaboration, Ref. 12.

The observed behaviour has thus supported for a while models where scattering involving non-elementary constituents would be dominant. A much-quoted example is the constituent interchange model (CIM) which indeed predicts the observed behaviour (5) with values for n and m (8 and 9 respectively) in quite good agreement with the fitted values. With confidence growing in the ultimate relevance of QCD, and the many difficulties encountered by CIM, or any other related model when considered as the dominant process, a certain flexibility has to be implemented in all approaches[1].

Before discussing that, we concentrate on recent results in very high p_t production ($p_t > 10$ GeV/c) which provide a very strong hint at QCD subprocesses becoming the relevant ones. Figure 13.a) shows how the inclusive distribution of π^0 departs from above from the extrapolation of the behaviour (5), so successful at $p_t < 6$ GeV/c. The data cannot be reproduced with a single term of the form (5). They rather indicate the emergence of a new regime. Such a particular behaviour at very high p_t is obtained by three different collaborations with data on π^0 production. While in Fig. 13.a) we present the CERN-Columbia-Oxford-Rockefeller results at 3 energies, Fig. 13.b) puts the $\sqrt{s}$ = 62 GeV results of the CERN-Columbia-Oxford-Rockefeller, Athens-Brookhaven-CERN-Syracuse, and CERN-Saclay-Zurich Collaborations on the same plot. I think that discrepancies are not relevant and will eventually disappear with a better understanding of the responses of the different detectors. The convergence of conclusions should be rather stressed. Using data at 52 and 62 GeV to separate the p_t and x_t dependence, the fitting parameter n which results (5) shows a clear change with x_t. According to CCOR, $n \simeq 8$ for $x_t < 0.25$ and $n \sim 5$ for $x_t > 0.30$. According to ABCS, $n \simeq 8$ for $x_t < 0.25$ and $n \sim 4$ to 5 for $x_t > 0.25$. Finally, CSZ, fitting (first) in the $0.2 < x_t < 0.45$ range, obtain $n = 6.6 \pm 0.8$. There is a clear deviation between the highest p_t data and the well advertized n = 8 behaviour of the lower p_t ones. A new regime sets in. It is compatible with expectation based on QCD. Indeed, it was almost common knowledge that, if the QCD subprocess had any relevance, the p_t^{-8} regime could not continue beyond 10 GeV/c.

At present there is a general consensus among theorists that QCD subprocesses do eventually become dominant, and that very high p_t production should be discussed in terms of quark and gluon scattering yielding quark and gluon jets. While such conclusions are still only tentative, they lead to anticipation of spectacular effects at collider energies ($p\bar{p}$ interactions at $\sqrt{s}$ = 540 GeV). This point is worth being illustrated and Fig. 14 gives rates as now predicted[33]. The expected effects are spectacular. Calculated rates depend however on the handling of scaling violations and on the choice made for quark and gluon distributions and fragmentation functions. Experimenting at collider energies one should be dealing with large effects which are very sensitive to still poorly controlled parametrizations which are of great importance in QCD calculations[34].

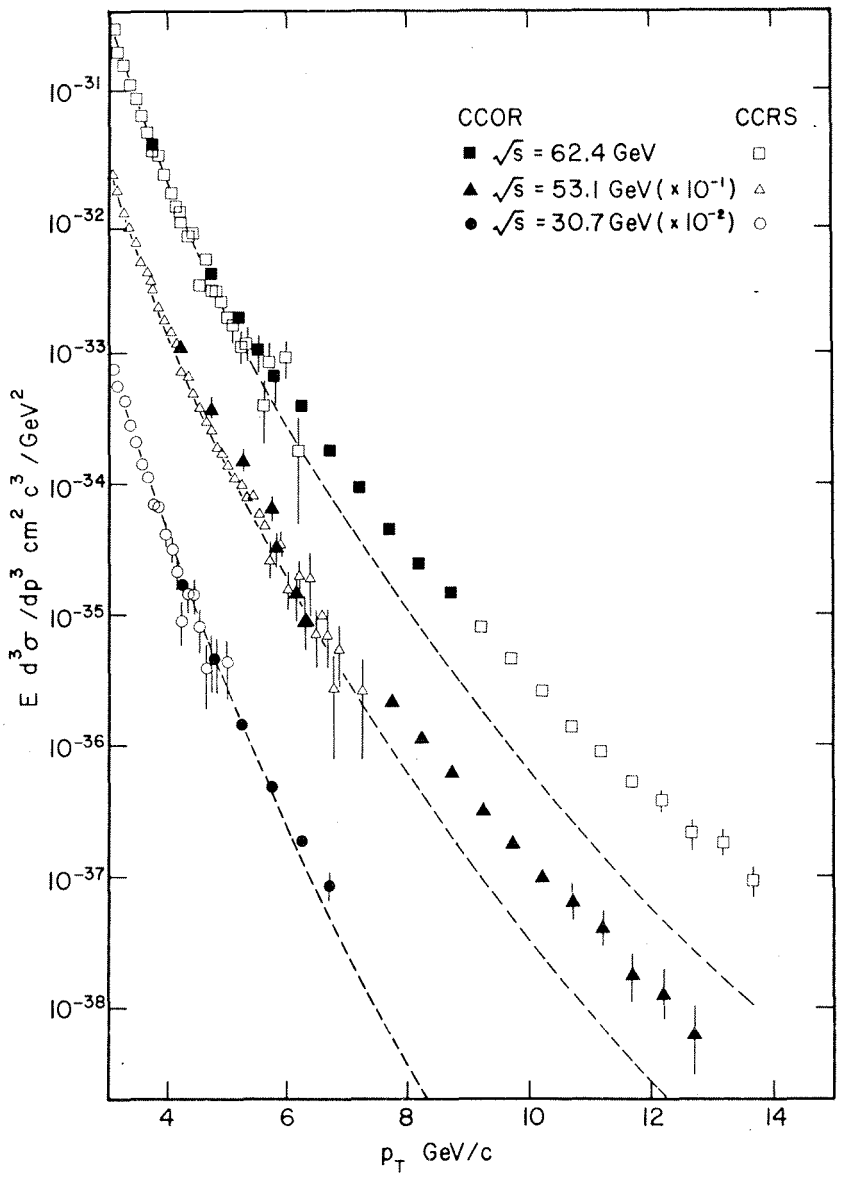

Figure 13.a) : Inclusive π^0 yields at very large p_t. Inclusive yields at 3 different energies. The dashed curves correspond to a fit (relation 5) to the lower p_t results (CCRS).

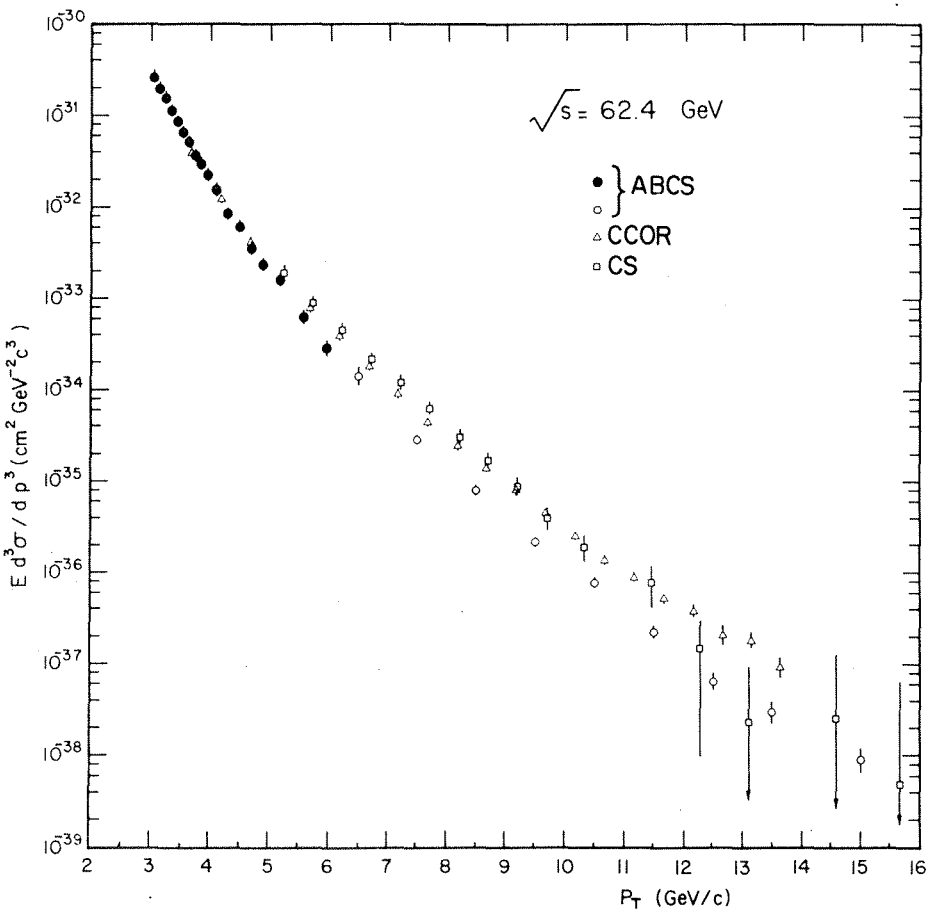

Figure 13.b) : Inclusive π^0 yields at very large p_t. Inclusive yields at $\sqrt{s}$ = 62 GeV as reported by the CCOR, CS and ABCS Collaborations at the ISR.

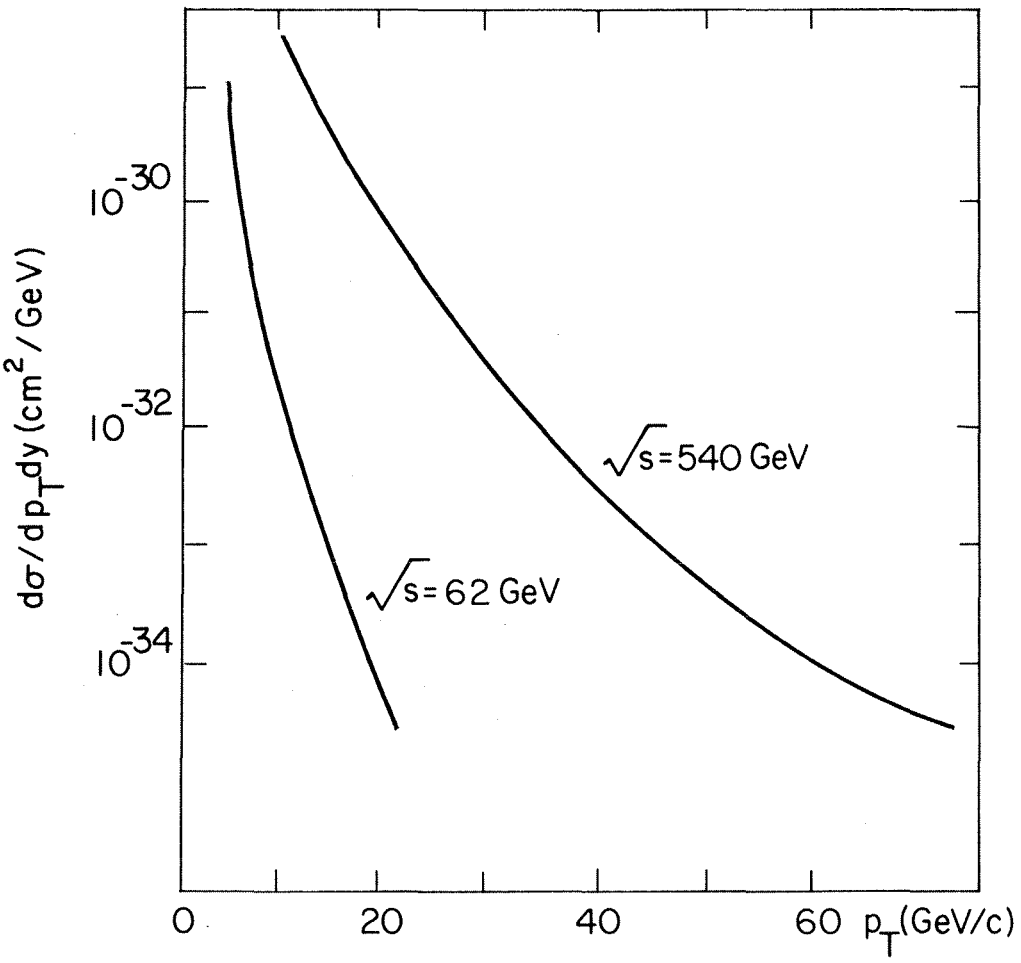

Figure 14 : Anticipated jet yields in $p\bar{p}$ collisions at ISR, $\sqrt{s}$ = 62 GeV, and collider, $\sqrt{s}$ = 540 GeV, energies. Standard QCD calculation (leading log approximation) for p_t > 10 GeV/c jet yields.

This review should however focus on the present situation, which is primarily concerned with data at $p_t < 10$ GeV/c in the 200 - 2000 GeV range. As previously stressed the jet structure is now well established, but the nature of the relevant subprocesses is still under investigation.

Granting the fact that perturbative QCD determines rates at very high p_t, it should also be of some relevance at lower p_t. Nevertheless, an actual calculation has immediately to face important correction terms. Some of them have to do with scaling violation effects expected to be important at medium p_t. Constituent motion should further contribute to making the observed p_t dependence steeper as the result of an obvious bias which was already discussed and the relevance of which becomes relatively weaker as p_t increases. The analysis is also complicated by the relative rôle of quarks and gluons which change with p_t in a trigger-dependent way. While one has to acknowledge the fact that the overall picture becomes rather complicated and that parametrized corrections may dwarf perturbative contributions, a fair amount of success prevails. As discussed in detail by R. Field at the Tokyo Conference[6], calculations do lead to an acceptable agreement with data, the effective p_t dependence eventually obtained being much steeper than the input behaviour associated with basic QCD subprocesses[35]. This does not exclude however that specific subprocesses of a more involved nature (higher twist effects in QCD) could be also relevant and contribute to producing effects which cannot be reached by QCD in its "leading log" implementation[8].

If one wishes to isolate best that contribution which belongs to perturbative QCD at moderate p_t, symmetric pair triggers offer an interesting handle, and this for two reasons. On the one hand, constituent motion effects are no longer emphasized by the triggering process as they are with single particle-triggers. On the other hand, an a priori competitive contender at medium p_t such as CIM is suppressed by the symmetry imposed on the trigger. Figure 15.a) shows symmetric pair data of the Chicago-Fermilab-Stony Brook Collaboration for $\pi^+\pi^-$ production at 400 GeV[36], together with a QCD calculation performed by the Bielefeld Group[37]. The main corrections correspond to scaling violations. Agreement prevails. However, in view of all the parametrization which has to be made with constituent distributions and fragmentation functions, it is important to check such a success over as wide an energy range as possible. It is therefore gratifying to see that the predictions made for symmetric π^0 pairs at ISR energies are indeed in very good agreement with recent results from the CERN-Columbia-Oxford-Rockefeller Collaboration[13] reported at this Conference. This is shown in Fig. 15.b), and builds confidence in using QCD at medium p_t values, even if important scaling violations have to be acknowledged.

Also shown in Fig. 15.a) are the respective contributions of the different subprocesses[35]. This illustrates in particular the overwhelming rôle of gluons for $x_t < 0.2$ and the relatively small rôle of pair formation, which is a particularly interesting process for the production of new flavours.

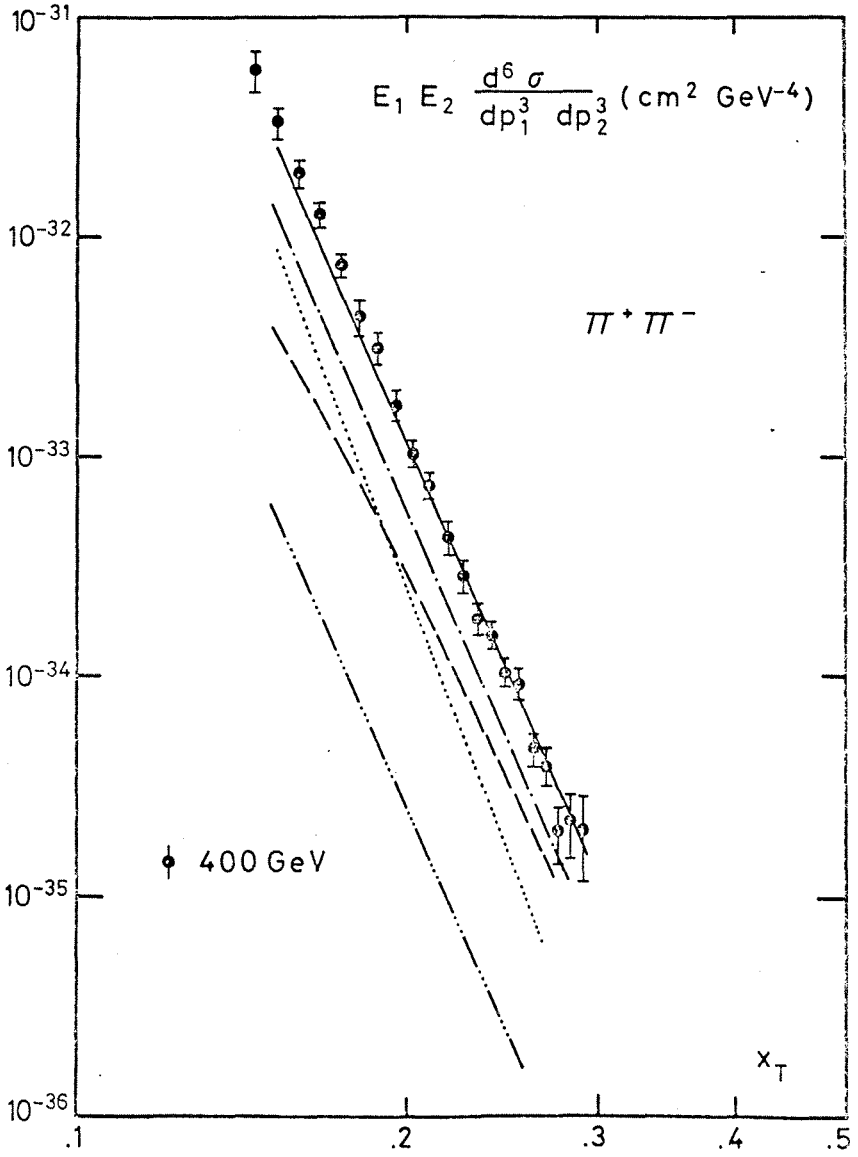

Figure 15.a) : Contributions of the various QCD subprocesses to the symmetric pair cross-section at 400 GeV versus x_t: $qg \to qg$ (-·-), $gg \to gg$ (....), $qq \to qq$ (---) and $gg \to q\bar{q}$ (-···-). The sum corresponds to the solid line. Data from Ref. 35.

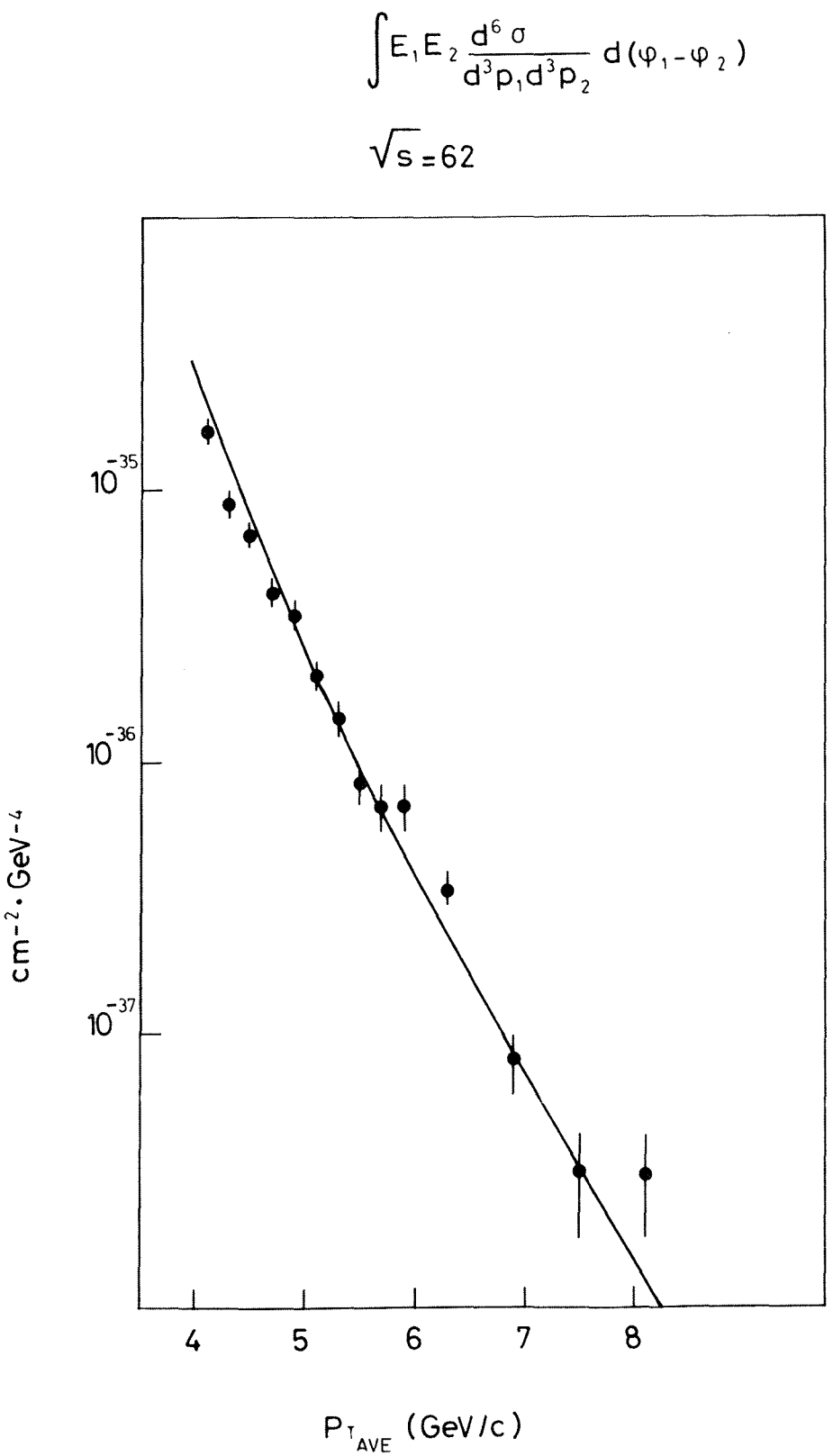

Figure 15.b) : Symmetric pair yield for $\pi^0\pi^0$ at $\sqrt{s}$ = 62 GeV. Recent results from the CERN-Columbia-Oxford-Rockefeller Collaboration (Δp_t < 1 GeV/c), preliminary data with a possible normalization error of 40% and predictions from Ref. 36.

It has often been emphasized that the comparison between pion- and proton-induced reactions should help to sort out the dominant mechanisms. While symmetric pair triggers suppress the CIM contribution, using an incident pion beam should enhance it. In connection with this, recent results from the Chicago-Princeton collaboration reported at the Conference[38] (Fig. 16) show that the ratio R between the π^- and π^+ yield is practically independent of p_t, whereas dominance of CIM, with the incident pion being globally scattered, would obviously impose a rising value of R with p_t. The observed behaviour is actually in good agreement with predictions based on the dominant rôle of QCD subprocesses, the difference between two calculations illustrating different parametrization of the pion structure function. These calculations give however too small a rate even though the ratio comes out right.

With such success, one could feel prompted to conclude that QCD, as used in its perturbative implementation, folding in all hadronization effects, meets experimental data in a satisfactory way[21,39,40]. It should however now be stressed that there are many results which point at more involved processes. As emphasized by J. Owens[40], the observed inclusive proton yield is an order of magnitude above estimates based on QCD calculations, while its p_t^{-12} dependence is in good agreement with CIM dominance. Baryon production at medium p_t may thus reveal a particular type of subprocess. Quantum correlation data which, while modest, are definitely present also indicate the presence of contributions which do not enter perturbative QCD, The results of the British-Scandinavian Collaboration of a year ago, which indicated a dependence of the positive over negative excess observed on the away side, on the nature of the triggering particle[5,6] are now complemented by more recent results from E 260 at Fermilab[41]. Shown in Fig. 17 is the reconstructed away-jet charge for different trigger particles as recently determined by the British-French-Scandinavian Collaboration[9]. The away-jet charge varies in a way as to partially compensate the charge of the trigger particle.

Such charge correlation effects among high-p_t particles are valuable clues for the presence of processes for which QCD cannot provide a full account in its "leading log" form.

It should be stressed that the main charge correlations observed are found among members of the same jet and tend to a partial charge compensation within the jet. An extensive study of charge correlations has been made by the CERN-Collège de France-Heidelberg-Karlsruhe Collaboration[42], using medium p_t triggers. Recent results involving higher p_t triggers have been reported by the CERN-Saclay Collaboration[12]. The amount of charge correlation among the two largest p_t charged particles is assessed though the value of a quantity r, which is defined as the ratio between the number of pairs with opposite charges to twice the square root of the number of pairs of positives times the number of negatives. Deviations from 1 thus measures the amount of correlations. Values of $r = 1.52 \pm 0.05$, 1.60 ± 0.03 and 1.00 ± 0.03 are reported for particles within the trigger-side jet, the away-side jet and for leading charged fragments in the two opposite jets, respectively.

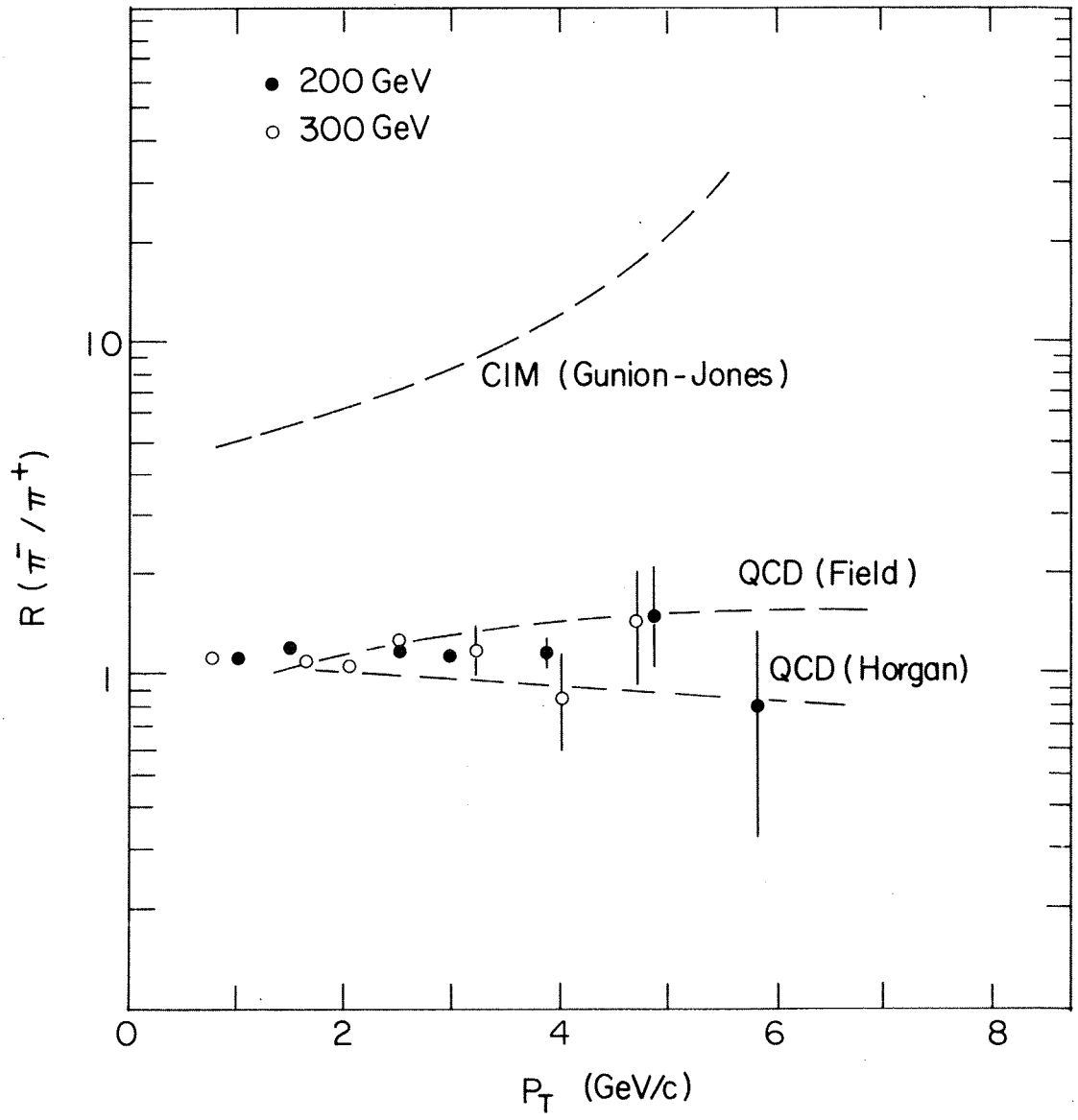

Figure 16 : Ratio of the π^- to π^+ yield in π-p induced reactions. Data from the Chicato-Princeton Collaboration, Ref. 37.

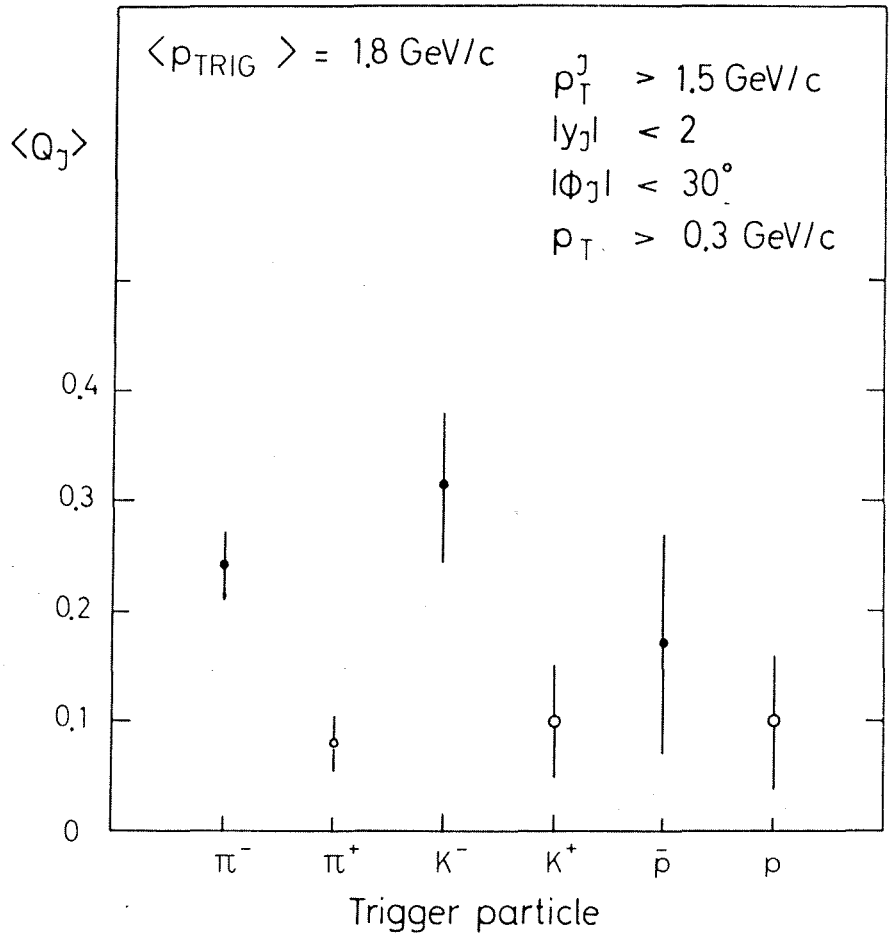

Figure 17 : Reconstructed jet charge on the away side. The mean charge varies with the kind of trigger particle used. Data from the British-Scandinavian Collaboration, Ref. 9.

Continuing data-sampling for special effects, it is considered appropriate to report a recent result by the Athens-Brookhaven-CERN-Syracuse Collaboration. This is shown in Fig. 18.a). The x_e distributions for π^o observed opposite to a high-p_t π^o show a systematic wiggle departure from an exponential fit (with a slope of the order of 7) which is well-determined by the data in the $0.3 < x_e < 0.6$ range which both correspond to large p_t and high statistics[43]. The wiggle could bear witness to a specific process whereby the two jets would consist of one high-p_t π^o only (the so-called quark-fusion process). A probability for such a jet configuration at the 0.2% level would be enough to account for the observed effect, a value not incompatible with one of the π^o's being a misidentified γ ray. The effect is also observed in the $\eta\pi$ configuration and cannot be blamed on a photon-π^o misidentification on both sides. The existence of the effect is however challenged by results from the CERN-Columbia-Oxford-Rockefeller Collaboration, also presented at this Conference, and shown in Fig. 18.b)[13]. In this case, an exponential fit is tailored over a larger x_e region and any attempt at a wiggle out of the exponential fit does not appear. One should then stress that the slope is definitely smaller ($B \simeq 5.3$) than the value used in Fig. 18.a) ($B \simeq 7$). Such a controversy should be resolved later. At present one may stress the common and a priori solid result of both experiments, namely the existence of some structure in the x_e distribution. If exponential fits are attempted, they have to be limited to a certain x_e range. A faster drop at lower x_e could be followed by a more gentle one at larger x_e but, as hinted at in Fig. 18.a), more structure could be present.

While we have thus singled out effects which point at something special (baryon production, charge correlation, structure in the x_e distribution) which are worth exploring in much greater detail, it remains that according to present knowledge, the QCD contribution, as calculated in a by now standard way with large scaling violations[21,39], appears as a successful contender for typical configurations at medium p_t values, where most of our available data are. It is then worth looking beyond the standard jet picture for effects which one should also expect in this framework. We concluded that it is still premature to look for jet widening with reconstructed jets. A noticeable effect is however likely to appear rather easily in the acoplanarity of the two jets. The incident particle and the direction of the trigger particle define a scattering plane (Fig. 1.b)) which should contain the opposite-side jet. This it does to a good approximation (Fig. 2). While the standard parton approach would allow for but a limited transverse momentum with respect to that plane, p_{out} in the usual vernacular, QCD imposes an unbounded value, increasing with p_t though at the order α_s only.

To the extent that the direction of the trigger-side jet is not precisely defined by the trigger particle and that one has to allow for some "primordial" transverse motion of the constituents, there should be some acoplanarity, usually parametrized by an exponential distribution in p_{out} and $\langle p_{out} \rangle$

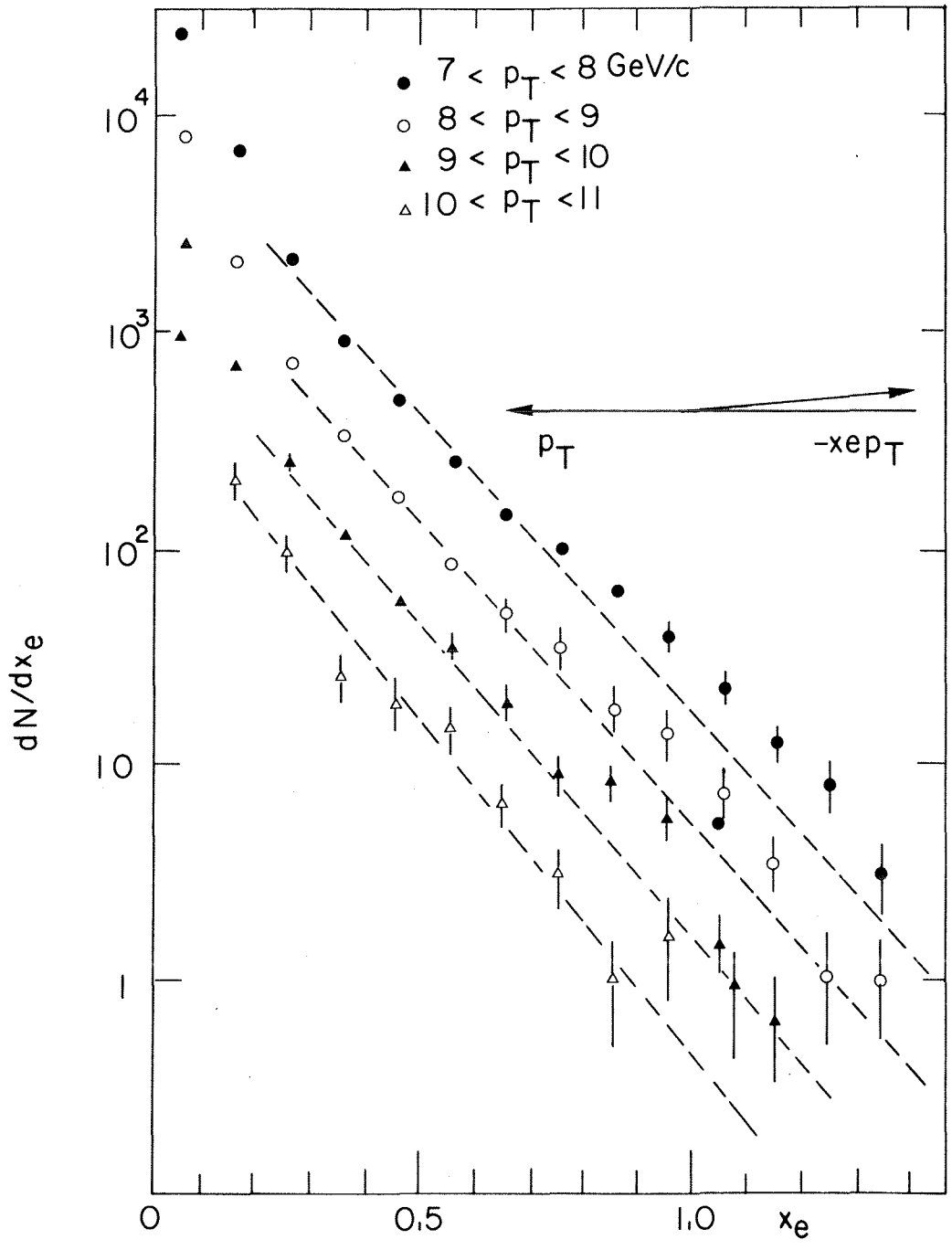

Figure 18.a) : x_e distribution for π^o with π^o trigger particle. Data from the Athens-CERN-Brookhaven-Syracuse Collaboration, Ref. 41.

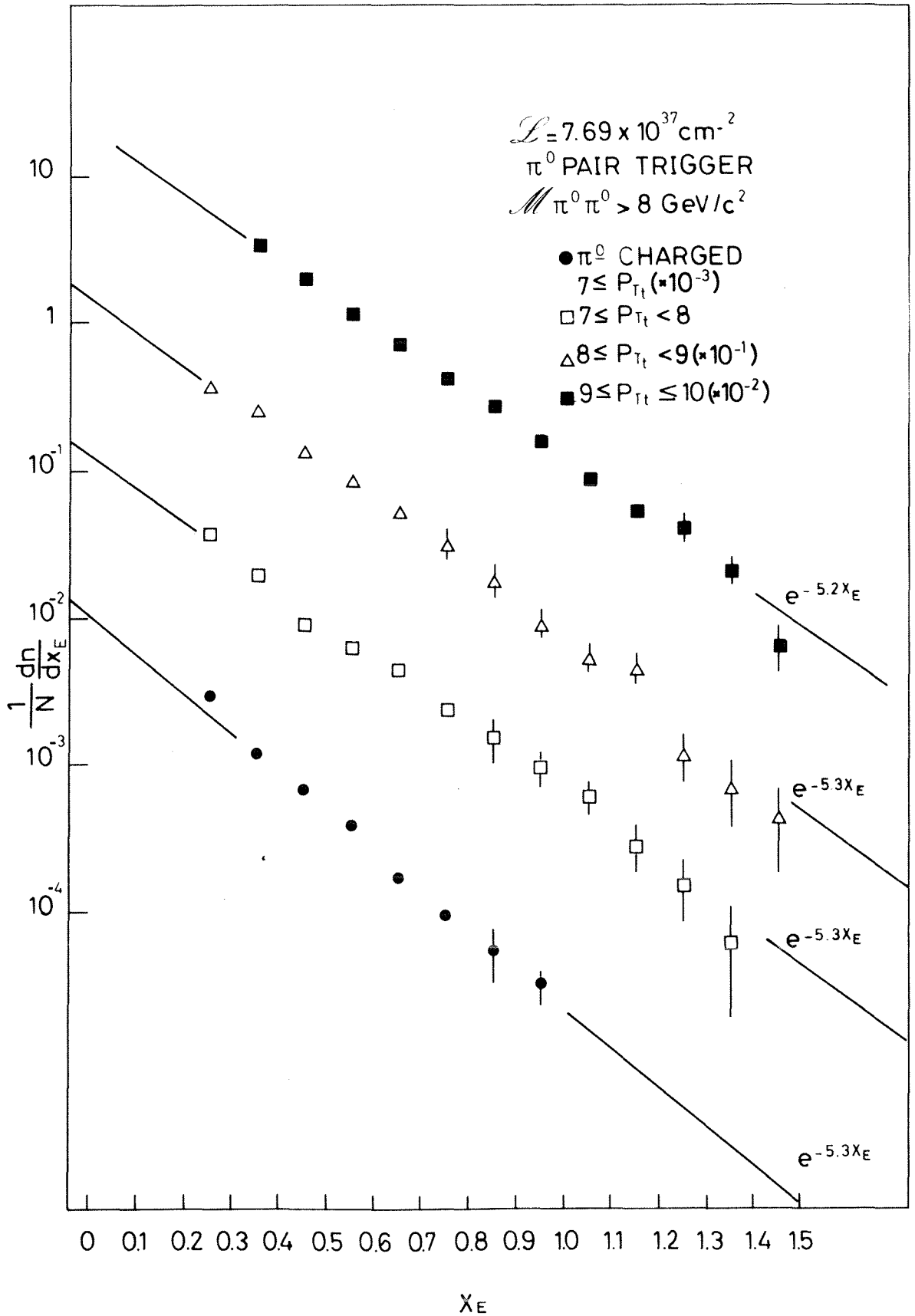

Figure 18.b) : x_e distribution for π^0 with π^0 trigger particle. Data from the CERN-Columbia-Oxford-Rockefeller Collaboration, Ref. 13.

should increase with x_e. Following perturbative QCD one should however expect $\langle p_{out} \rangle$ to also increase with p_t at fixed x_e, as radiated gluons break the coplanarity structure. Figure 19.a) shows the values of $\langle p_{out} \rangle$ recently reported by the CERN-Columbia-Oxford-Rockefeller Collaboration[13], for different trigger momentum values. They refer to the component out of the scattering plane for high-p_t particles of the away-side jet. The increase with p_t is clear. It should be stressed that $\langle p_{out} \rangle$ is not sufficient information insofar as one needs to search for a p_{out}^{-2} "tail", departing from an overall exponential distribution of $d\sigma/dp_{out}^2$, which is taken as parametrizing hadronization and primordial motion lumped together. Figure 19.b) gives the actual p_{out} distribution, as measured by the Athens-Brookhaven-CERN-Syracuse Collaboration for different x_e and p_t ranges. One clearly sees the widening of the distribution as x_e (and p_t at fixed x_e!) increases. Nevertheless, one cannot go beyond an overall exponential parametrization though with a decreasing slope as p_t increases. It is still impossible to point separately at calculable perturbative effects and parametrized non-perturbative ones. Yet a QCD calculation, facing all the intricacies of the $2 \to 3$ processes, which has recently been carried out by a DESY Group[44], reaches a remarkable agreement with the data. One may at least say that looking at a particularly sensitive parameter, p_{out}, the observed behaviour, which definitely departs from the standard parton model predictions, is compatible with that expected in perturbative QCD.

4. THE PROMPT PHOTON QUESTION

It is a common feature of all hard-scattering approaches that prompt photons should be seen at high p_t with a relative yield much larger than α. Photons are natural hard constituents and, while their production may be damped down by α as compared with that of hadrons, this comparison should refer to the production of a jet and not to that of a single meson. If one takes into account the relatively low yield of single particles as compared to a jet at high p_t, one readily concludes that there is a sizeable γ/π ratio.

In perturbative QCD, where quark-gluon scattering plays an important rôle, the subprocess $g\mathbf{q} \to \gamma q$ is the natural source of prompt photons[45]. The γ/π ratio is controlled by the fragmentation of a jet into a leading π; it increases with x_t. In the CIM approach prompt photons are eventually favoured over pions by a weaker p_t dependence[46]. The γ/π ratio should increase with p_t as p_t^2 to also become much larger than α even though the trigger jet consists of only one meson by construction.

While the γ/π^0 ratio has been an important theoretical issue for some time[1], the experimental situation was long uneasy[19]. This stems from the fact that prompt photons have to be singled out among a huge π^0 background, something which the often quantized nature of the detector (lead glass blocks) makes a formidable problem to tackle. At this Conference, results from the Athens-Brookhaven-CERN Collaboration have been presented as evidence for a

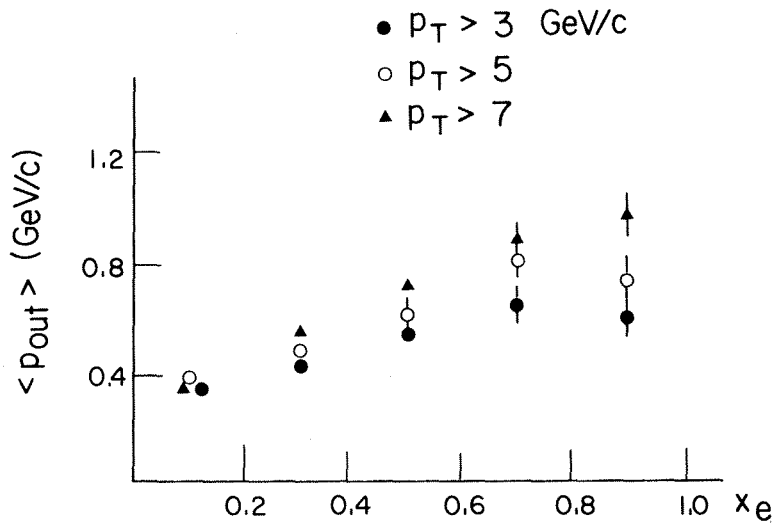

(a)

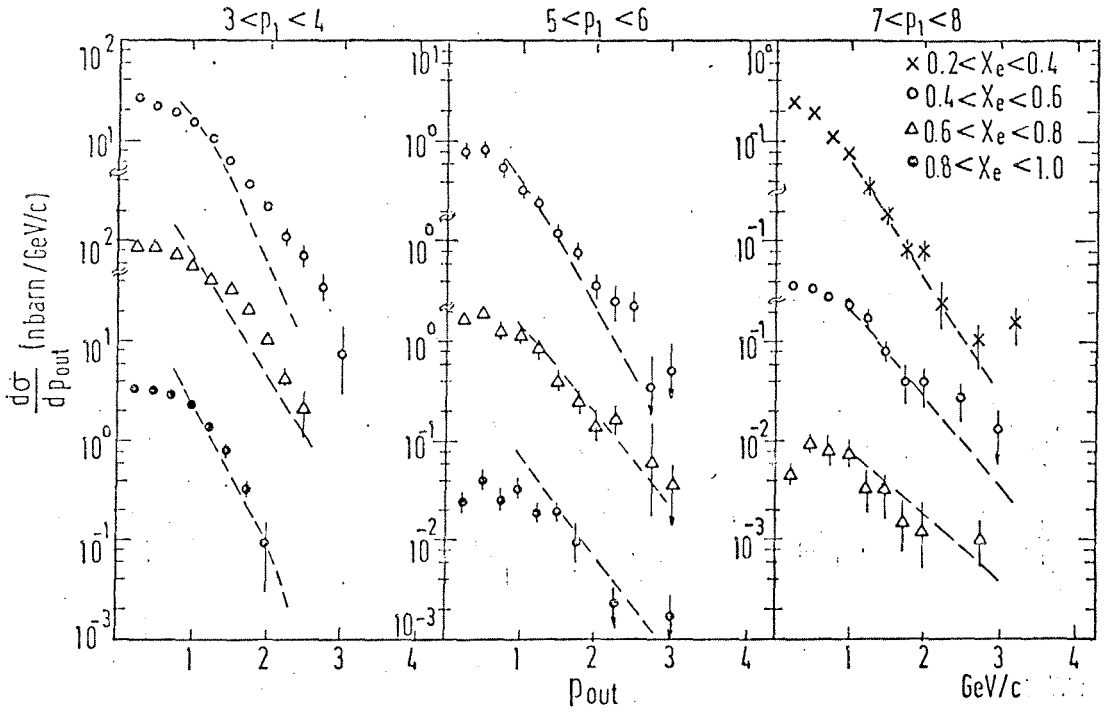

(b)

Figure 19.a) : The variation of $\langle p_{out} \rangle$ with x_e for different trigger momenta. Data from the CERN-Columbia-Oxford-Rockefeller Collaboration, Ref. 13.

b) : The $\langle p_{out} \rangle$ distribution for different x_e ranges and different trigger momenta. Data from the Athens-Brookhaven-CERN-Syracuse Collaboration, Ref. 11. Also shown (dashed curves) are the results of a QCD calculation, following well the widening of the $\langle p_{out} \rangle$ distribution with increasing p_t, Ref. 42.

γ/π^0 ratio at the 20% level at $p_t \simeq 6$ GeV/c[47]. The use of a liquid argon lead calorimeter is of great help in differentiating π^0's and prompt photons. This is discussed in detail in the report by C. Fabjan[48]. The data are presented in Fig. 20.a). Also presented, in Fig. 20.b), are data obtained earlier by the Rome-Brookhaven-CERN-Adelphi Collaboration using a lead glass detector[49]. They are compatible with the newer and more precise data from the ABC Collaboration, which extend beyond 6 GeV/c. The observed ratios (Fig. 20.a)) can be considered to be in semi-quantitative agreement with calculations[45,46]. It is still premature to claim an x_t as opposed to a p_t dependence. This beautiful experimental result will certainly prompt further effort to extend the p_t range to higher values and, on the theorists side, for more involved calculations.

5. ELASTIC SCATTERING AT WIDE ANGLES

From a theorist's point of view, the behaviour of elastic scattering at wide angle cannot be dissociated from the analysis of inelastic high-p_t phenomena[1]. One expects a new regime to take over the overwhelming Regge contribution at small angle. The differential cross-section at fixed angle should eventually decrease with increasing energy as an inverse power only, namely:

$$\frac{d\sigma}{dt} \sim s^{-n} f(\theta) \qquad (6)$$

The situation is a priori more complicated than when studying inclusive processes or jet production. Nevertheless, the same subprocesses should be at work. The smallness of the rates make such studies very difficult. At this Conference recent results on meson-proton scattering up to 90^o, at 20 and 30 GeV/c incident momentum, have been reported by the CERN-Annecy-Genova-Copenhagen-Oslo-UC London Collaboration[50]. The agreement with dimentional counting rules is reasonable[51]. Figure 21.a) shows the π-p elastic scattering cross-section and the solid curves correspond to a CIM fit to the π+p data at 20 GeV/c. The fall of the cross-section at 90^o which is followed over 4 orders of magnitude meets expectations. However, as shown in Fig. 21.b), agreement is only approximate. While these data contribute evidence for a new regime, which meets expectations based on hard scattering ideas, the question of elastic scattering at wide angle is only barely explored.

6. CONCLUSION

Many new and important pieces of data have become available since the Tokyo Conference. We are now more knowledgeable about high-p_t processes and, while perhaps not much wiser than a year ago, certainly far more confident in our understanding of the pertinent dynamics, insofar as previous assumptions have become fact. Expectations based on the parton model have met with great success. Quantum chromodynamics not only provides a promising framework but can now claim at least a semi-quantitative success[52]. High-

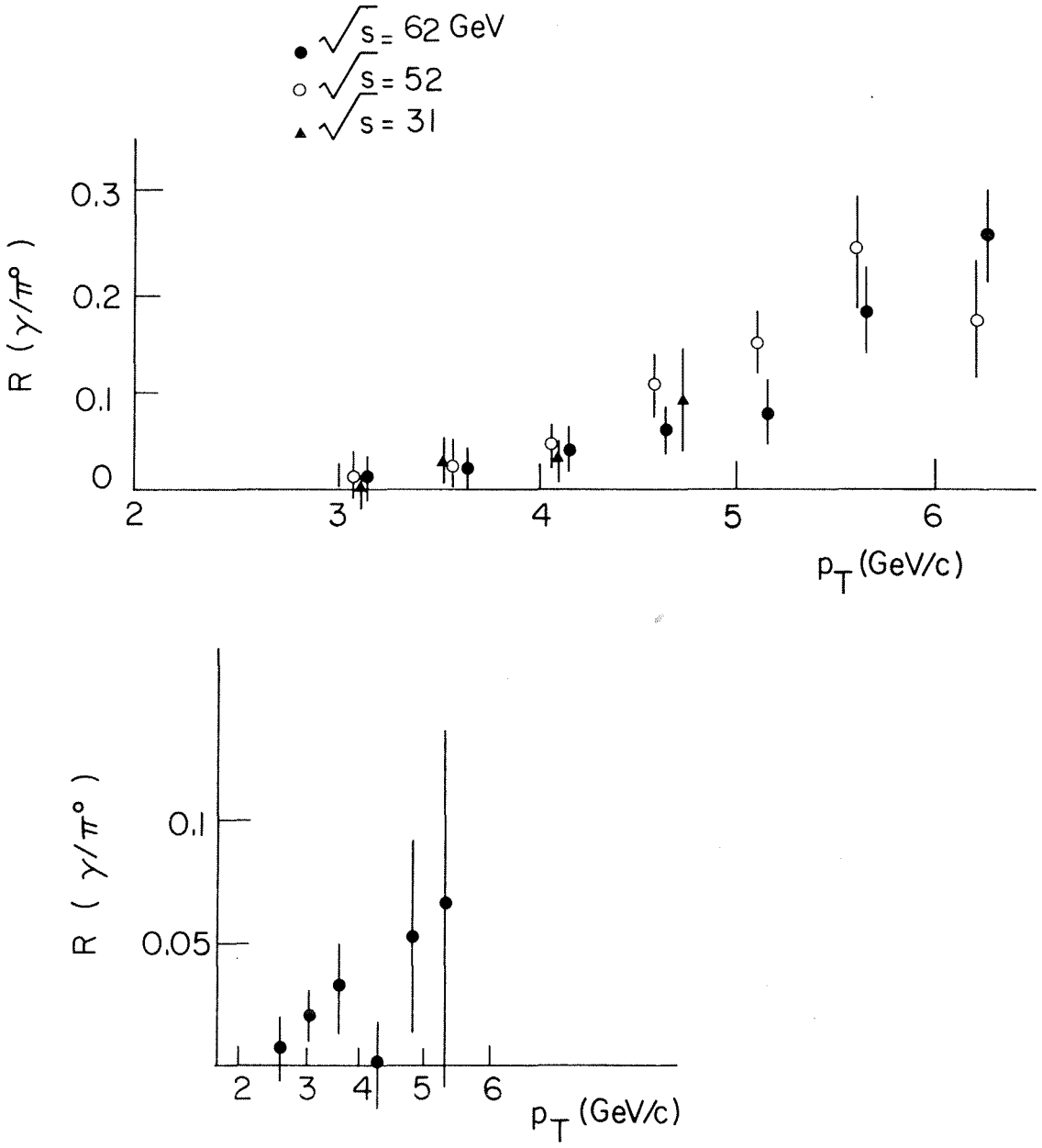

Figure 20.a) : The prompt photon yield. The γ/π^0 ratio as a function of p_t at $\sqrt{s}$ = 31, 52 and 62 GeV. Data from the Athens-Brookhaven-CERN Collaboration, Refs. 45 and 46.

b) : The γ/π^0 ratio as a function of p_t at $\sqrt{s}$ = 52 GeV. Data from the Rome-Brookhaven-CERN-Adelphi Collaboration, Ref. 47.

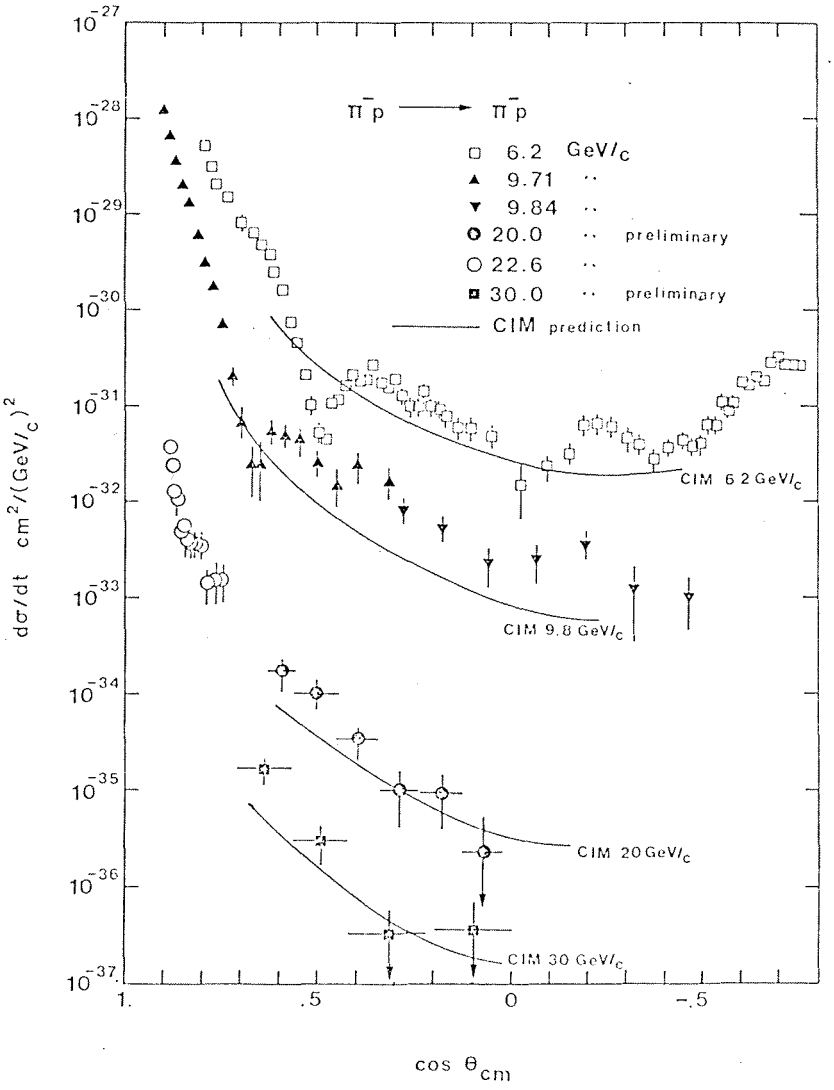

Figure 21.a) : Differential cross-section for π-p elastic scattering. The new results are at 20 and 30 GeV/c. CERN-Annecy-Genova-Copenhagen-Oslo-UC LOndon Collaboration, Ref. 49. The solid lines correspond to a CIM fit to the π^+p data at 20 GeV/c.

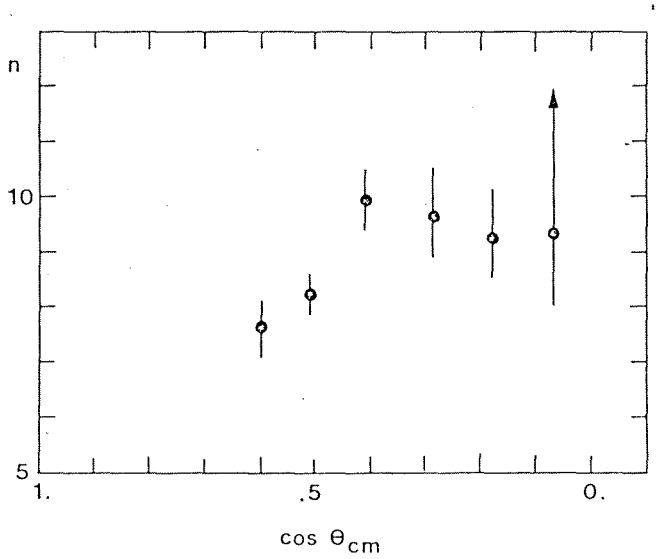

Figure 21.b) : The fitted n parameter at different scattering angles. It should be 8 in the CIM approach. Data at different energies (9.7 to 30 GeV) have been used.

p_t phenomena stand out as a clear and beautiful example of hadron interactions at the constituent level.

At present one can see further investigations as developing along two main lines. On the one hand, and as already emphasized, great expectations are put on interactions at collider energies[53]. This is where spectacular effects are expected, with large counting rates for high-p_t jets (Fig. 14) and where predictions based on QCD can be put to a thorough test. While many anticipated effects should show up in a clear way, or disprove through their absence some of our present ideas, it should be stressed that the values of x_t which will actually be accessible because of falling rates will remain small (at least at the $p\bar{p}$ collider). Wide angle jets, which are more easily identifiable will thus be mainly associated with gluons according to present views. Clear valence-quark jets will have to be looked for as high-energy jets at small angles and sorting out jet fragments will be very difficult.

On the other hand, further studies at present energies (in the 200 - 2000 GeV range) thus offer the opportunity to analyse in some detail the relevance and fragmentation properties of different types of constituents. Extensive quantum number correlation studies and jet triggering should be possible with new detectors[54]. This should greatly enlarge the type of data available. While there is now some evidence that scaling violations and expected corrections are large enough to modify the basic QCD perturbative input in such a way as to reach reasonable agreement with the data, the actual amount of higher twist effects which may still be necessary is a challenging and topical question. Such processes could well contribute a significant amount to the single-particle trigger yield. Oddly enough, correlation studies with jet triggering could eventually be the best way to demonstrate their relevance. While QCD is a complete theory, what it predicts is not fully known yet and we may use experimentation for clues. The question of high-p_t baryons and that of prompt photons certainly deserves further experimental investigation. In the latter case, the results reported at this Conference should be a great encouragement for further investigation.

ACKNOWLEDGEMENTS

I would like to express my gratitude to several experimental groups at the CERN-ISR for detailed discussions of their latest data, a fruitful collaboration with many colleagues which it is sad to translate here acrostically only: ABCS; BFS; CCHK; CCOR; CS. I am indebted to G. Fox for a very helpful exchange of correspondence and benefitted much from the reviews on high-p_t physics presented by M. Tannenbaum, J. Owens and W. Selove at the 1979 Moriond meeting. I am indebted to R. Horgan for informative discussions and I would like to thank again here particularly P. Darriulat and P. Landshoff for a now long collaboration on high-p_t physics. Ch. Redman has kindly brought this report to its present form.

REFERENCES

1) High-p_t phenomena have been discussed in a series of review articles which were written in turn as the analysis of high-p_t hadronic processes gradually developed. An extensive survey is obtained from D. Sivers, S. Brodsky and R. Blankenbecler, Phys. Reports 23 C, 1 (1976); S. Ellis and R. Stroynowski, Rev. Mod. Physics 49, 753 (1977); M. Jacob and P.V. Landshoff, Phys. Reports 48, 285 (1978).

2) C.T. Sachrajda, Phys. Letters 40, 213 (1978); D. Amati, R. Petronzio and G. Veneziano, Nucl. Physics B 140, 54 (1978); 146, 29 (1978).

3) H.D. Politzer, Proc. XIX Internat. Conf. on High Energy Physics, Tokyo, 229 (1978 and M.K. Gaillard "QCD Phenomenology", Rapporteur talk at this Conference.

4) For a detailed survey of the applications of quantum chromodynamics to hard-scattering processes, see Yu. L. Dokshitzer, D.I. Dyakonov and S.I. Troyan, Phys. Reports, to be published (1979) and R. Field, La Jolla Lecture Notes (1978), Calt 68-696.

5) Proc. Copenhagen Meeting on "Jets in High Energy Collisions", Physica Scripta 19, 69 (1979).

6) Proc. XIX Internat. Conf. on High Energy Physics, Tokyo (1978). In particular: R. Sosnowski, 693 and R. Field, 743.

7) The new experimental results practically all come from the exploitation of large detectors which were already completed at the time of the Tokyo Conference. This review therefore does not have to present any of these detectors - a welcome excuse for a theorist rapporteur. The major new detectors of experiment R 807 at the CERN ISR is presently at the completion stage. References 1 and 5 can be consulted for a presentation of the major detectors at CERN and at Fermilab.

8) S. Brodsky, Physica Scripta 19, 154 (1979).

9) An extensive survey of precise rapidity correlations, as more recently obtained, is to be found in M.G. Albrow et al., Studies of Proton-Proton Collisions at the CERN-ISR with an identified charged hadron of high transverse momentum at 90°, Nucl. Phys. B, to be published (1979). CERN/EP/79-56.

10) R. Field and R.P. Feynman, Nucl. Phys. B 136, 1 (1978).

11) C. Kourkoumelis et al., Correlations of High Transverse Momentum π^0 Pairs Produced at the CERN-ISR, CERN-EP 79-36, Nucl. Phys. to be published.

12) A. Clark et al., Large Transverse Momentum Jets in High Energy Proton-Proton Collisions, submitted to this Conference.

13) A. Angelis et al., Physica Scripta 19, 99 (1979), and contribution to this Conference.

14) G. Zech "Jets in e^+e^- Annihilation" Moriond meeting, Les Arcs (1979) - Preliminary Pluto data; P. Söding "Jet Analysis", Report to this Conference - Preliminary Tasso Data.

15) W.G. Scott "Neutrino '78", Int. Conf. on Neutrino Physics, Purdue University 1978 (ed. E.C.Fowler). J.C. Vander Welde, Physica Scripta 19, 173 (1979).

16) G. Sterman and S. Weinberg, Phys. Rev. Letters 39, 1436 (1977); E. Farhi, Phys. Rev. Letters 39, 1587 (1977).

17) This is the occasion to stress that quoting a mean value should not be enough since this assumes a particular shape which may change as p_t increases. To the extent that topical features are a Gaussian shape usually associated with the parametrization of the yet non-calculable fragmentation of each jet component, and a tailing distribution associated with the perturbative branching of the jet, having the full distribution is of great importance.

Even though there is at present no direct evidence in favour of QCD, it is impressive that no expectation based on QCD is found in sheer disagreement with any data. In view of the present interest raised by QCD it is therefore deemed appropriate to refer to its predictions at each stage at the risk of overdoing it.

18) S. Ellis et al., Nucl. Phys. B 108, 93 (1976); M. Jacob and P.V. Landshoff, Nucl. Phys. B 113, 395 (1976). The p_t^{-n} parametrization lumps together the p_t and x_t dependence, hence a rather high effective value for n. It is successful over a wide p_t range.

19) For a detailed discussion, see the general review of M. Tannenbaum, Proc. Moriond Meeting, Les Arcs (1979).

20) C. Bromberg et al., Phys. Rev. Letters 38, 1447 (1977); C. Bromberg et al., Nucl. Phys. B 134, 189 (1978); C. Bromberg et al., Phys. Rev. Letters 42, 1202 (1979).

21) R.P. Feynman, R. Field and G. Fox, Nucl. Phys. B 128, 1 (1977); Phys. Rev. D 18, 3320 (1978).

22) C. Bromberg et al., Jet Production in 200 GeV/c Hadron-Proton Collisions, Caltech preprint 1979. I am indebted to G. Fox for an exchange of correspondence. J. Rohlf, Caltech Thesis, in preparation.

23) D. Antreaseyan et al., Phys. Rev. Letters 38, 112, 115 (1978).

24) M. Deutschmann et al., Aachen III B/WA28-1 (1979).

25) W. Selove, High p_t Jet Studies at Fermilab, UPR-70 E (1979). Proceedings of the Moriond Meeting, Les Arcs (1979).

26. J.D. Björken, Acta Phys. Polon B 5, 145 (1974).

27) M.G. Albrow et al., Nucl. Phys. B 145, 305 (1978). K. Hansen, Proceedings of the Tokyo Conference.

28) H. Bøggild, Proc. Moriond Meeting, Les Arcs (1979); NBI/HE 79-6.

29) M.G. Albrow et al., Nucl. Phys. B 135, 461 (1978).

30) The Rapporteur has to trust the experimental collaborations in their reconstruction of the centre-of-mass energy for the two-jet system and their unfolding of all trigger bias effects. This requires involved Monte Carlo simulations.

31) G. Hanson, Moriond Meeting, Les Arcs (1978); SLAC PUB 2118 (1978); G. Hanson et al., Phys. Rev. Letters 35, 1609 (1975).

32) G. Wolf, "High Energy Trends", Rapporteur Talk at this Conference.

33) R. Horgan, CERN, private communication.

34) J. Gunion "The Realm of Gluons", UC Davis (1978); W. Furmanski and S. Pokorski, CERN th 2665 (1979). R. Field in Refs. 4, 5 and 6.

35) B. Combridge et al., Phys. Lett. 70 B, 234 (1978).

36) H. Jöstlein et al., Phys. Rev. Letters 42, 146 (1979).

37) R. Baier, J. Engels and B. Petersson, Symmetric Pairs at Large Transverse Momenta as a Test of Hard-Scattering Models, BI.TP 79/10.

38) B. Pope, Contribution to this Conference.

39) A. Contogouris et al., Phys. Rev. D 17, 2314 (1978).

40) J. Owens, Quantum Chromodynamics and Large Momentum Transfer Processes. Invited talk at the Coral Gables Conference "Orbis Scientiae" (1979).

41) C. Bromberg et al., "Production and Correlations of Charged Particles with High p_t in 200 GeV $\pi^{\pm}p$, $k^{-}p$ and pp Collisions", UCLA 1123 (1979).

42) D. Drijard et al., "Quantum Number Effects in Events with a Charged Particle at Large Transverse Momentum - 1", CERN/EP-78; "Quantum Number Effects in Events with a Charged Particle of Large Transverse Momentum - 2". Paper submitted to this Conference; D. Wegener, invited talk at this Conference.

43) C. Kourkoumelis et al., "Measurement of π^{o} Fragments from Jets Produced in pp Collisions at the CERN ISR", CERN-EP/79-57.

44) Z. Kunszt et al., DESY 79/28, 79/34 (1979). I am indebted to Z. Kunszt for an informative discussion on this point.

45) R. Field, Tokyo Conference, 743 (1978); A. Contogouris et al., Scale Violation Effects in Large p_t Direct Photon Production, McGill (1979).

46) R. Rückl et al., SLAC PUB 2115 (1978).

47) C. Kourkoumelis et al., Direct Production of High p_t Single Photons in pp Collisions at the CERN-ISR; paper contributed to this Conference.

48) C. Fabjan, Invited talk at this Conference.

49) E. Amaldi et al., Phys. Lett. 77 B, 240 (1978).

50) R. Almas et al., Meson-Proton Large-Angle Elastic Scattering at 20 and 30 GeV/c. Submitted paper to this Conference.

51) J. Gunion, Phys. Rev. D 8, 287 (1973).

52) R. Feynman, R. Field and G. Fox, Phys. Rev. D 18, 3320 (1978). G. Fox, "Application of Quantum Chromodynamics to High-p_t Hadron Production". Invited talk at the Coral Gables Conference "Orbis Scientiae" (1978).

53) This applies to the SPS used as a $p\bar{p}$ collider and later to the Fermilab doubler used the same way. This also applies to Isabelle; see BNL 50648.

54) Experiment R 807 for instance at the ISR. For a detailed review see ISR Workshop documents 2-7 and 2-14 (1977).

PARTICLE SYSTEMATICS

Anthony J.G.Hey
Physics Department, Southampton University, England.

ABSTRACT

Several aspects of hadron spectroscopy are reviewed. For the baryons, the status of the even parity 70 multiplets is examined in some detail. For the mesons, a rapid survey of the state of the $q\bar{q}$ multiplets leads on to a discussion of the identification of the 0^{++} mesons as $(q^2\bar{q}^2)$ configurations. A brief account of Jaffe and Low's approach to this problem via the P-matrix is included. Throughout the review the interesting interplay between ideas from non-charmed and charmed hadron spectroscopy is underlined.

0. INTRODUCTION

In this talk I shall concentrate on the spectroscopy of the 'light' hadrons - those composed of u, d and s quarks - but I will try to convince you that insights gained here may be of use for charmed hadron spectroscopy. Instead of attempting a comprehensive review, the discussion will be restricted to a few of the recent developments that I believe to be important and I will therefore make an attempt to set these in context. The selection of topics clearly reflects my personal opinions and omission does not necessarily constitute a value judgement.

A few words of warning. It is now fashionable to attach to everything the label, "predicted by QCD". In fact, despite favourable auguries, the confinement problem has not yet been solved and there are no rigorous results from QCD for hadron spectroscopy. Nevertheless, QCD has given some interesting clues and suggestions: I will attempt to separate these possible "QCD successes" from successes not specifically related to QCD. As always, good phenomenology must tread a delicate path between "random assumption models" on the one hand, and "rigorous theory" on the other.

1. THE BARYONS

1.1 The Harmonic Oscillator Shell Model

To set the scene for our discussion of the low-lying baryon resonances it is helpful to review the expectations of the simplest quark model - the non-relativistic harmonic oscillator model. In this theory the dynamics of the three quarks in a baryon are described by a non-relativistic Hamiltonian with harmonic forces between each pair of quarks

$$H = \frac{\underline{p}_1^2}{2m_1} + \frac{\underline{p}_2^2}{2m_2} + \frac{\underline{p}_3^2}{2m_3} + \tfrac{1}{2}K|\underline{r}_{12}|^2 + \tfrac{1}{2}K|\underline{r}_{23}|^2 + \tfrac{1}{2}K|\underline{r}_{31}|^2 \qquad (1.1)$$

In the SU(3) (and SU(6)) limit all quark masses are equal

$$m_1 = m_2 = m_3 = m \qquad (1.2)$$

and the centre of mass motion may be separated off in the usual fashion. The relative

quark motion is then described by two independent harmonic oscillators whose coordinates are conventionally chosen to be

$$\underline{\rho} = \frac{1}{\sqrt{2}} (\underline{r}_1 - \underline{r}_2) \tag{1.3}$$

and

$$\underline{\lambda} = \frac{1}{\sqrt{6}} (\underline{r}_1 + \underline{r}_2 - 2\underline{r}_3) \tag{1.4}$$

Notice that the ρ-oscillator is antisymmetric, and the λ-oscillator symmetric, under exchange of quark labels 1 and 2. The spatial wavefunctions obtained by exciting these oscillators then have the corresponding permutation symmetry. Under the assumptions that quarks have spin $\frac{1}{2}$ and are colour triplets, and that the low-lying hadrons are colour singlets and are composed of three active flavours of quarks (u, d, s), the allowed wavefunctions for baryons may be enumerated:-

$$|\, 3q \,\rangle = \underbrace{|\, \text{flavour} \,\rangle\, |\, \text{spin} \,\rangle\, |\, \text{space} \,\rangle}_{\text{Antisymmetric}} \underbrace{|\, \text{colour} \,\rangle}_{\underline{1}_C}$$

$$\underbrace{\qquad\qquad\qquad\qquad}_{\text{SU(6)} \times \text{O(3)}}$$

Symmetric Antisymmetric

The spectrum of the lowest SU(6) x O(3) multiplets in the harmonic oscillator shell model is shown in Figure 1. Clearly the equal spacing of the levels and the degeneracy structure are specific to the choice of harmonic interactions: introduction of a non-harmonic perturbation alters these splittings and lifts the degeneracies.

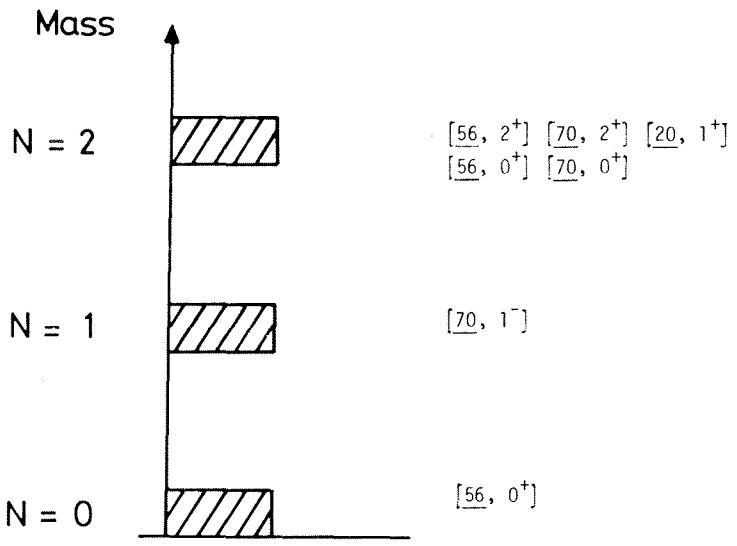

Figure 1 Spectrum of allowed SU(6) x O(3) multiplets in the harmonic oscillator quark shell model. The mass is labelled by the principal quantum number N of the harmonic oscillator and multiplets are labelled by their SU(6) representation, and their orbital angular momentum and parity, L^P.

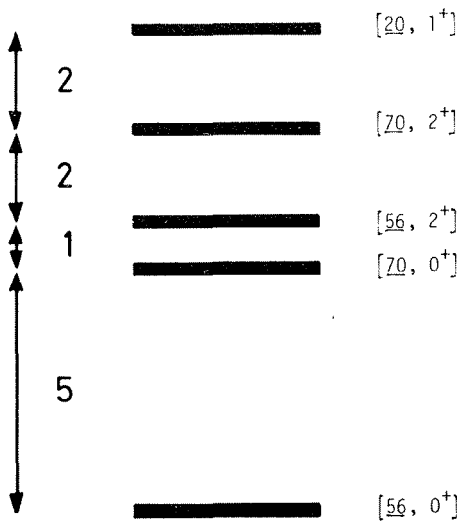

Figure 2 Pattern of splitting of N=2 Band Multiplets caused by a non-harmonic perturbation.

In fact, there is an amusing general result[1]: in first order perturbation theory, the pattern of splitting of the N=2 multiplets is independent of the form of the perturbing potential $U(\underline{r}_{ij})$. This pattern is shown in Figure 2; it has the attractive feature of lowering the radial excitation of the ground state - the $[\underline{56}, 0^+]$ multiplet - and raising the enigmatic $[\underline{20}, 1^+]$ multiplet, relative to the remaining $\underline{56}$ and $\underline{70}$'s.

1.2 Algebraic SU(6) Models

Over the past decade or so there have been two main types of attempt to bring order to the enormous amount of experimental data available on baryon resonances. Both are algebraic rather than dynamical in character - in that they parametrize the data in terms of a small number of unknown SU(6) reduced matrix elements instead of using a specific quark model, embodying many assumptions about quark dynamics, to predict matrix elements. It is appropriate to briefly review the ingredients and achievements of both these approaches in order to set more recent developments in context:-

(1) SU(6) Mass Operator Analyses[1-7]

The mass operator for baryon resonances is parametrized in terms of 2-body SU(6) tensor operators. To reduce the large number of possible operators, specific assumptions are made as to which operators have an important effect on the spectrum and which may be discarded. Detailed fits to the masses of all resonances within the low-lying negative and positive parity SU(6) multiplets have been performed, using harmonic oscillator wavefunctions for the quarks. The unknown reduced matrix elements are determined by a careful choice of "well-known" input states and the model then predicts the masses and SU(6) composition of all the remaining states. In particular, specific predictions are made for the masses of (as yet) unobserved resonances.

(2) $SU(6)_W$ Decay Operator Analyses[8-13]

These models concentrate on decay systematics and assume that resonance decay takes place via meson emission from a single active quark. The single quark transition operator is parametrized by the most general allowed $SU(6)_W$ structure. No detailed forms for the spatial wavefunctions are used but an SU(6) x O(3) classification of the resonant states is assumed. Again, the small number of reduced matrix elements are determined by a fit to data thus allowing the decay properties of hitherto unobserved states to be predicted.

It is clear that these two approaches are complementary to each other: to predict where best to look for a missing state one needs both the mass and the decay properties of the state. Most of the early mass fits took no account of the decay systematics of resonances while the decay fits made no attempt to explain the observed SU(6) mass splittings. It would clearly seem desirable to obtain a consistent picture of both aspects of an SU(6) multiplet - although it must be emphasized that the use of SU(6) symmetry for masses and of $SU(6)_W$ symmetry for decays involves different theoretical assumptions. What then is the status of such attempts?

1.3 Status - Pre-1978

Negative Parity States: $[\underline{70}, 1^-]$

(i) SU(6) mass fits[7, 14] were able to obtain a good description of the observed negative parity resonances below about 2 GeV.

(ii) $SU(6)_W$ decay analyses[11-13] enjoyed great success in correlating elastic and inelastic resonant amplitudes. In particular, the agreement with the inelastic amplitude signs for the reactions

$$\pi N \to N^* \to \pi\Delta$$

and

$$\bar{K}N \to Y^* \to \pi\Sigma^*(1385)$$

determined by isobar model analyses was spectacular. A recent isobar analysis of the $\pi^+ p$ channel[15] confirms this good agreement and also confirms the ρN amplitude signs predicted by such an SU(6) model[12].

(iii) Simultaneous SU(6) mass and decay fits were found to fail.[4, 7, 14] The basic reason for the incompatibility of these mass and decay analyses may be illustrated by the following example. Physical states are found to be mixtures of pure SU(6) states. In particular, the $\frac{1}{2}^-$ N^* resonances are mixtures of quark spin $\frac{1}{2}$ and $\frac{3}{2}$ SU(6) $\underline{70}$ states. e.g.

$$|\, S11(1530) > \; = -\sin\theta_s |^4 8> + \cos\theta_s \; |\, ^2 8 > \qquad (1.5)$$

In order to accomodate the observed ΛK decay of the higher mass S11(1670), decay analyses immediately require substantial mixing

$$\theta_s \sim -30^0$$

(in the conventions of reference 11). On the other hand, the specific assumptions of the mass operator fits[14] tied the amount of mixing to the mass difference of the S11(1530) and the D13(1520). Thus the S11 states were predicted to be essentially unmixed - in contradiction with the decay analysis result. The situation for the more complicated 3-way mixing of the Y^*'s is similar, but less clear cut.

Positive Parity States

The mass fits predicted[7] that the S=0 and S=-1 states of the four N=2 band multiplets - $[56, 0^+]_2$, $[\underline{56}, 2^+]$, $[\underline{70}, 0^+]$ and $[\underline{70}, 2^+]$ - should all lie below about 2.1 GeV in mass. The $[\underline{20}, 1^+]$ states are higher than this. Physical states are now mixtures of <u>different</u> SU(6) multiplets.

In contrast to this SU(6) picture of the positive parity states, decay analyses[11-13] obtained good agreement with data by only invoking $[\underline{56}, 0^+]$ and $[\underline{56}, 2^+]$ multiplets. In fact, the mass analyses themselves found the particular states used in the decay analyses were predominantly <u>56</u> in character with only a small <u>70</u> contamination. Nevertheless, the existence of even parity <u>70</u> multiplets at low mass, or indeed at all, was brought into question.

To bring out the issues more clearly, Table 1 lists all two, three and four star, positive-parity resonances below 2.1 GeV, according to the 1978 edition of the Particle Data Group compilation[16].

Table 1

Positive-parity states below 2.1 GeV according to the Particle Data Group 1978 compilation. (One star resonances have been omitted.) States with controversial SU(6) assignments have been ringed.

	N	Δ	Σ	Λ
	$\frac{1}{2}^+$ (1470)	$\frac{3}{2}^+$ (1690)	$\frac{1}{2}^+$ (1660)	$\frac{1}{2}^+$ (1600)
	$\frac{5}{2}^+$ (1688)	$\frac{5}{2}^+$ (1890)	$\frac{1}{2}^+$ (1880)	$\frac{1}{2}^+$ (1800)
	$\frac{1}{2}^+$ (1780)	$\frac{1}{2}^+$ (1910)	$\frac{5}{2}^+$ (1915)	$\frac{5}{2}^+$ (1815)
	$\frac{3}{2}^+$ (1810)	$\frac{7}{2}^+$ (1950)	$\frac{7}{2}^+$ (2030)	$\frac{3}{2}^+$ (1860)
	$\frac{7}{2}^+$ (1990)		$\frac{3}{2}^+$ (2080)	$\frac{5}{2}^+$ (2110)
	$\frac{5}{2}^+$ (2000)			
Total Number of States	6	4	5	5

Four of these states - NP11(1780), NF17(1990), ΛP01(1800) and ΛF05(2110) - were assigned by Jones, Dalitz and Horgan[7] to the [70, 0^+] and [70, 2^+] multiplets. Litchfield, Cashmore and Hey[11, 12] on the other hand suggested that these four states may be more economically assigned to higher-lying 56 multiplets. The motivation for this suggestion was based on a count of missing states. Tables 2 and 3 list the S=0 and S=-1 states required for the 56 and 70 multiplets: the existence of even parity 70's requires twice as many Y^*'s than for 56 multiplets. The number of states required by the mass fits and the number of observed states is as follows:-

	N^* and Δ^*	Σ^* and Λ^*
Predicted (Tables 2 and 3)	19	33
Observed (Table 1)	10	10

In view of the large discrepancy it seemed fair to question the evidence for positive parity 70's. Why have the missing states not been observed in partial wave analyses? - or at the very least, the missing states with high spin?

Table 2

Predicted S=0 and S=-1 states of the [56, 0^+] and [56, 2^+] multiplets.

	N	Δ	Σ	Λ
[56, 0^+]				
$^2_8$	$\frac{1}{2}^+$		$\frac{1}{2}^+$	$\frac{1}{2}^+$
$^4_{10}$		$\frac{3}{2}^+$	$\frac{3}{2}^+$	
[56, 2^+]				
$^2_8$	$\frac{5}{2}^+$		$\frac{5}{2}^+$	$\frac{5}{2}^+$
	$\frac{3}{2}^+$		$\frac{3}{2}^+$	$\frac{3}{2}^+$
		$\frac{7}{2}^+$	$\frac{7}{2}^+$	
$^4_{10}$		$\frac{5}{2}^+$	$\frac{5}{2}^+$	
		$\frac{3}{2}^+$	$\frac{3}{2}^+$	
		$\frac{1}{2}^+$	$\frac{1}{2}^+$	
Total no. of states	3	5	8	3

Table 3

Predicted S=0 and S=-1 states of the $[\underline{70}, 0^+]$ and $[\underline{70}, 2^+]$ multiplets.

	N	Δ	Σ	Λ
$[\underline{70}, 0^+]$				
$^2_8$	$\frac{1}{2}^+$		$\frac{1}{2}^+$	$\frac{1}{2}^+$
$^4_8$	$\frac{3}{2}^+$		$\frac{3}{2}^+$	$\frac{3}{2}^+$
$^2_{10}$		$\frac{1}{2}^+$	$\frac{1}{2}^+$	
$^2_1$				$\frac{1}{2}^+$
$[\underline{70}, 2^+]$				
$^2_8$	$\frac{5}{2}^+$		$\frac{5}{2}^+$	$\frac{5}{2}^+$
	$\frac{3}{2}^+$		$\frac{3}{2}^+$	$\frac{3}{2}^+$
	$\frac{7}{2}^+$		$\frac{7}{2}^+$	$\frac{7}{2}^+$
$^4_8$	$\frac{5}{2}^+$		$\frac{5}{2}^+$	$\frac{5}{2}^+$
	$\frac{3}{2}^+$		$\frac{3}{2}^+$	$\frac{3}{2}^+$
	$\frac{1}{2}^+$		$\frac{1}{2}^+$	$\frac{1}{2}^+$
$^2_{10}$		$\frac{5}{2}^+$	$\frac{5}{2}^+$	
		$\frac{3}{2}^+$	$\frac{3}{2}^+$	
$^2_1$				$\frac{5}{2}^+$
				$\frac{3}{2}^+$
Total no. of states	8	3	11	11

Summary of Pre-1978 Status

It is clear that the overall situation was far from satisfactory. Mass operator analyses - at least with their present choice of operators - failed to fit masses and decays simultaneously. They were thus unable to answer the question of why the missing $\underline{70}$ states had not been observed. Decay analyses were very successful but were more limited in ambition. In particular, no attempt was made to obtain an understanding of either the observed mass spectrum or the mixing matrices. Moreover, both approaches lack much intuitive appeal. We now turn to more recent developments which go some way toward clarifying these questions and answering these objections.

1.4 Post-1978 Developments

Although, as stressed in the introduction, there are few, if any, areas of hadron spectroscopy which can be said to provide evidence for specific QCD effects, it is certainly true that the paper of de Rujula, Georgi and Glashow[17] sparked off a revival of interest in non-relativistic potential models for the baryon spectrum. The new feature of this paper was the inclusion of a short-range potential arising from coloured gluon exchange between quarks, in addition to a long-range confining potential. Isgur and Karl[18-21] and other authors[22-30] have examined in detail the consequences of this gluon exchange potential for the excited baryon multiplets.

I will discuss in some detail the specific non-relativistic oscillator model of Isgur and Karl since, in addition to a treatment of the one-gluon corrections, it has another very interesting feature - although one which has nothing specific to QCD. This is the phenomenon of 'kinematic mixing' - SU(6) configuration mixing arising simply from the non-equality of non-strange and strange quark masses.

(a) Coloured Gluon Exchange

The non-relativistic reduction of the one-gluon exchange contribution to the Hamiltonian leads to the so-called Breit interaction. This contains a magnetic dipole-dipole interaction of the form (for two quarks i and j)

$$H^{ij}_{\text{Hyperfine}} = A\{\frac{8\pi}{3}\,\underline{S}_i.\underline{S}_j\delta^3(\underline{\rho}) + \frac{1}{\rho^3}(3\underline{S}_i.\hat{\underline{\rho}}\,\underline{S}_j.\hat{\underline{\rho}} - \underline{S}_i.\underline{S}_j)\} \qquad (1.6)$$

where $\underline{\rho} = \frac{1}{\sqrt{2}}(\underline{r}_i - \underline{r}_j)$. The first term is the Fermi contact term, which only operates when the pair (ij) have zero orbital angular momentum, and the second term is a spin tensor force which is operative only when the pair have non-zero orbital angular momentum.

For the ground state, only the contact term contributes and this term is responsible for the Δ-N and ρ-π splitting. The non-Abelian nature of coloured gluon exchange is reflected in the fact that the Δ-N and ρ-π splitting have the same sign, in agreement with experiment. This term is also responsible for the Σ-Λ splitting of the ground state baryons.[17]

For the $[\underline{70}, 1^-]$ both terms should be present and Isgur and Karl have made a quantitative study using harmonic oscillator quark wavefunctions. For the non-strange baryons, the contact term splits the $^2 8$ states from the $^4 8$ and $^2 10$ states in good qualitative agreement with the observed states. The presence of the tensor force does not alter this qualitative success but does induce mixing between the pure $^2 8$ and $^4 8$ states since

$$< S = \tfrac{3}{2} \mid H_{\text{tensor}} \mid S = \tfrac{1}{2} > \neq 0 \qquad (1.7)$$

The detailed calculations of Isgur and Karl[18, 20] predict little mixing for the D13 states but find substantial mixing for the S11 resonances; namely

$$\theta_s \sim -30^0$$

in good agreement with decay analyses[11, 13]. Before euphoria sets in some comments are in order:

(1) The reason for the discrepancy between mass and decay analyses now seems to be identified: Tensor forces were explicitly rejected in the early mass operator analyses.

(2) The mass operator analyses explicitly retained spin-orbit forces: the model of Isgur and Karl ignores them entirely, despite the fact that the Breit interaction has a specific spin-orbit contribution. It certainly seems clear that the data does not require

strong spin-orbit forces and several authors[20, 29, 31-33] have investigated the possibility that there is a substantial cancellation between the L.S force from vector gluon exchange and from a(presumed) scalar confining potential.

(3) From a theoretical point of view, the relevance of the non-relativistic treatment of single gluon exchange is not obvious. Indeed similar success for the ground state hadrons was obtained, at about the same time as de Rujula et al., in the framework of the MIT Bag[34], in which the quarks are highly relativistic. Even in the context of a 'non-relativistic' potential model, a recent re-analysis[30] of the Hamiltonian of de Rujula et al. shows that the quarks are in fact moving relativistically and 'relativistic corrections' must be treated with caution.

(b) Kinematic Mixing

The basic mechanism for this type of configuration mixing was first noticed in the context of the MIT Bag.[35] Isgur and Karl, however, chose instead the much more tractable non-relativistic harmonic oscillator Hamiltonian. The basis of the effect is merely the observation that SU(3) breaking via quark masses

$$m_s > m_u$$

requires that the frequency of the λ-oscillator is lower than that of the ρ-oscillator

$$\omega_\lambda < \omega_\rho$$

The ρ- and λ-modes have been defined by equations 1.3 and 1.4: the two types of oscillations may be visualized by the one-dimensional analogy shown in Figure 3.

A simple illustration of this mechanism of work is given by the Σ-Λ splitting of the $\frac{5^-}{2}$ states of the $[\underline{70}, 1^-]$.[19] For the ground state Σ and Λ we have

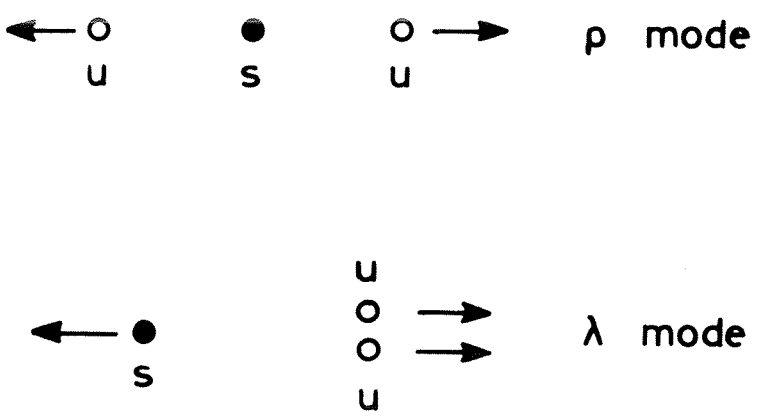

Figure 3 One-dimensional representation of ρ and λ oscillator modes

$$\Sigma\ \tfrac{1}{2}^{+}(1190) > \Lambda\ \tfrac{1}{2}^{+}(1115)$$

whereas we find

$$\Sigma\ \tfrac{5}{2}^{-}(1760) < \Lambda\ \tfrac{5}{2}^{-}(1830)$$

in the $[\underline{70}, 1^{-}]$. This reversal may be understood by considering the symmetries of the non-strange quarks in these states. Both Σ and Λ have the non-strange quarks coupled to spin 1 and a colour $\bar{3}$: the product of the isospin and spatial wavefunctions must therefore be symmetric. Thus

$$\Sigma : (I = 1) \to (12)_S \ \lambda\text{-mode}$$

and

$$\Lambda : (I = 0) \to (12)_A \ \rho\text{-mode}$$

so that the Σ is predicted to be the lighter state. Inclusion of the gluon exchange contribution reduces the splitting somewhat, but does not alter the conclusion.[19)]

The most important consequence of this kinematic effect concerns the mixing of the Y^*'s. The pure SU(6) states are not diagonal in the ρ, λ - basis: on diagonalisation the highest mass Y^*'s correspond to pure ρ-states. Under the standard assumption that resonance decays are described by single-quark operators a fascinating selection rule emerges. Kaon emission from a Y^* must necessarily involve the strange quark: since for the ρ-mode it is the non-strange quarks that are orbitally excited we obtain the result:

$$(Y^*)_\rho \not\to \bar{K}N \qquad (1.8)$$

This is illustrated schematically in Figure 4. It is interesting that this phenomenon - that the higher mass Y*'s of the $[\underline{70}, 1^{-}]$ tend to couple only weakly to $\bar{K}N$ - had been noticed empirically by Rosner and Petersen[36)], and by Faiman[37)], (who termed this "Ideal mixing for Baryons").

For the $[\underline{70}, 1^{-}]$, the mixing generated by the simple SU(3) mass splitting provides qualitative agreement with the observed mixing of SU(6) Decay analyses.[13)] What of the positive-parity baryons? The oscillator states of the N=2 level may be characterized as $\rho\rho$, $\rho\lambda$ and $\lambda\lambda$: Of these, only the $\lambda\lambda$ modes can couple to $\bar{K}N$ via a single quark operator. Thus there is the immediate prediction that many Y^*'s will essentially decouple from the $\bar{K}N$ formation channel. Isgur and Karl have investigated this in detail including a non-harmonic perturbing potential and gluon corrections.[21)] The qualitative expectation is borne out by their results: their most spectacular example concerns the $\frac{3}{2}^{+}\Lambda^*$ states. At the N=2 level, including the $\underline{70}$'s $\underline{\text{and}}$ the $\underline{20}$, seven $\frac{3}{2}^{+}\Lambda^*$ resonances are expected: the kinematic mixing $\underline{\text{decouples all but one}}$ of these states from $\bar{K}N$. According to the Particle Data Group, only one such resonance has been observed!

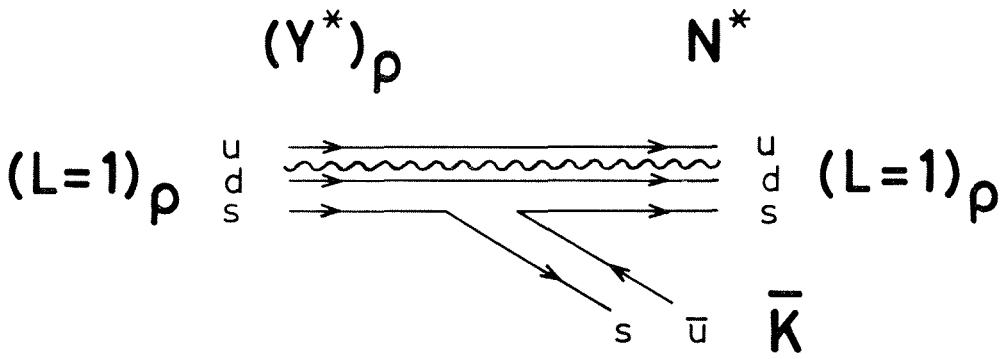

Figure 4 Quark line diagram illustrating the selection rule $(Y^*)_\rho \not\to \bar{K}N$.

Again, some additional comments are in order:

(1) The most spectacular decouplings occur for the Λ^* resonances: Σ^*'s do not in general decouple from $\bar{K}N$. There are still some missing Σ^* states which should couple to $\bar{K}N$ but in the specific model of Isgur and Karl these are either above 2 GeV, or involve low-spin states. With the present state of Y^* phase-shift analyses, it is plausible that there may be no conflict with the existence of even parity 70's.

(2) It would therefore seem that the most severe constraints on this model arise from the well-explored non-strange sector, where no decoupling of N^*'s and Δ^*'s is predicted. Even here after two new phase-shift analyses[38, 39] this year, the question is not resolved. An example will illustate this point. Isgur and Karl predict two $\Delta_{\frac{1}{2}}^{3+}$ states around 1950-2000 MeV. The analysis of Cutkosky et al. finds one state, the $\Delta_{\frac{1}{2}}^{3+}(1910)$ but include the comment that "alternate fits containing additional resonances are possible".

1.5 Conclusions

(1) A plausible case can be made for the existence of even-parity 70's. The integrity of phase shift analyses in not finding hitherto "theoretically desirable states" is impressive.

(2) Given the extent of configuration mixing in the S=-1 sector of the N=2 Band multiplets, it is no longer clear to me than an SU(6) classification is useful. Perhaps it is preferable to work directly with a quark basis that distinguishes strange and non-strange quarks.

1.6 Implications for Charmed Baryons

After the beautiful semiquantitative success of the Isgur-Karl model for non-charmed baryons, it is of interest to investigate the predictions of an extension of this model to the charmed quark sector. For the $[70, 1^-]$ the lowest-lying Λ^* is the $\Lambda_{\frac{1}{2}}^{-}(1405)$,

corresponding to a λ-mode excitation. Using the $\Lambda_c \frac{1}{2}^+(2.25)$ state to determine the charmed quark mass, Copley et al.[40] predict that the corresponding $\Lambda_c \frac{1}{2}^-$ state is probably stable against strong decay! They suggest a search for the electromagnetic decay

$$\Lambda_c(\tfrac{1}{2}^-) \rightarrow \Lambda_c(\tfrac{1}{2}^+) + \gamma$$

which is certainly of experimental interest.

2. THE MESONS

2.1 $(q\bar{q})$ Spectroscopy

Figure 5 shows the spectrum of $q\bar{q}$ nonets predicted by a harmonic oscillator quark model. Again, deviations from this pattern are caused by the inclusion of non-harmonic forces, spin-spin and spin-orbit forces and so on. A recent investigation,[41] for example, claims evidence for spin-tensor forces in the spectrum of observed mesons.

There is no time to review in detail all the experimental contributions on meson resonances that were presented in the parallel sessions of this conference. Instead, I shall give a very cursory survey of the current status of the N=1 and N=2 $(q\bar{q})$ multiplets.

(1) 2^{++}, 3^{--}

These leading trajectory nonets remain in good shape and little essential has changed since the Tokyo conference.[42]

(2) 1^{++}, 1^{+-}

For these multiplets there has been some clarification. I was particularly impressed by the enormous statistics of the data on 3π and Kππ channels presented at this conference

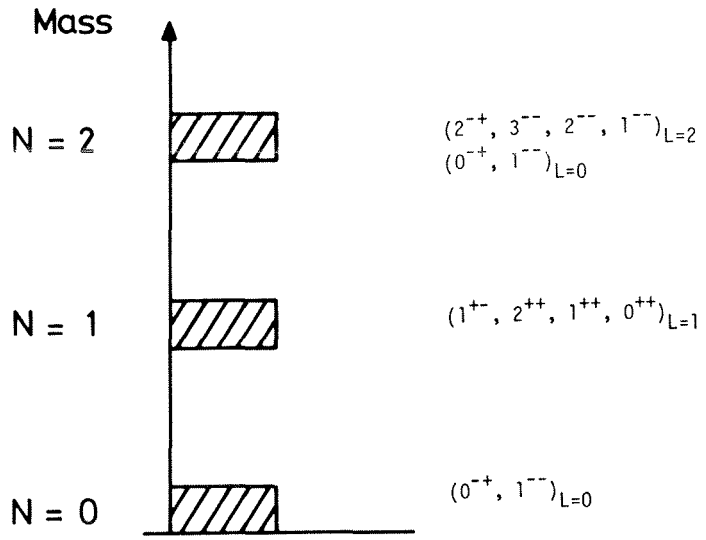

Figure 5 $(q\bar{q})$ multiplets of the Harmonic Oscillator Model. Nonets are labelled according to the principal quantum number N and the orbital angular momentum L, as well as their spin, parity and charge conjugation J^{PC}.

by members of the ACCMOR collaboration.[43, 44] Their analysis confirms the existence of two resonant states in the Q region of $K\pi\pi$, and a convincing resonant amplitude is seen in the 1^{++} (I=1) $\pi\rho$ channel: They quote an A_1 mass of around 1300 MeV. It is now a little embarassing that after so many years living without an A_1, there are now claims for an A_1 resonance at 1100[45, 46], 1300 in this experiment, and even[47] at 1500 MeV! It must be said, however, that the statistics of the present (diffractive production) experiment are an order of magnitude better than previous ones. We must wait until the dust settles.

(3) 2^{-+}, 2^{--}

Only the A_3 I=1 2^{-+} state has been confirmed[48], but there should soon be a detailed isobar analysis of the L region of $K\pi\pi$, which should show two $I=\frac{1}{2}$ states as in the Q region. I probably ought not to mention the hint of some 'extra' activity in the 2^{-+} I=1 channel that may not be explicable by a single resonance .....

(4) 0^{-+}, 1^{--} : Radial excitations

The isobar analyses[43, 44] of $K\pi\pi$ and 3π show new indications of possible K'(~1400) and π'(~1300) states. In view of these masses, and in the absence of any confirmation of the ρ'(1250) from present e^+e^- experiments[49] the ρ'(1600) looks a safer bet for theorists to model as the radial excitation of the ρ. Definite statements about possible ω' and ϕ' states are still awaited.

(5) N=4, L=3 Band?

An I=1 5^{--} state has been deduced from a moments analysis of a K^+K^-n(by missing mass) experiment.[50] The favoured mass and width are 2.30 GeV and 270 MeV, respectively. Figure 6 shows this state on an almost forgotten Chew-Frautschi plot.

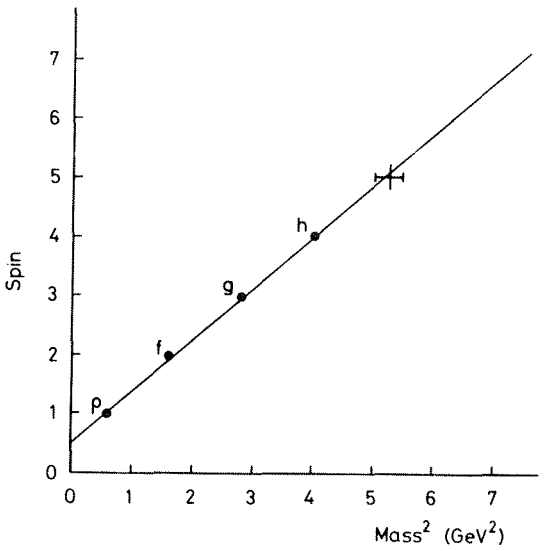

Figure 6 Chew-Frautschi plot including the new 5^{--} state.

2.2 $(q^2\bar{q}^2)$ Spectroscopy and the 0^{++} Mesons

In 1976 Jaffe challenged the orthodox view of the low mass 0^{++} mesons as $(q\bar{q})_{L=1}$ states and proposed their assignment as "crypto-exotic" $q^2\bar{q}^2$ states.[51] In general, multi-quark $q^2\bar{q}^2$ states are expected to be rather broad because of the possibility of super-allowed fall-apart decays (Figure 7). However, for the 0^{++} states coloured gluon exchange is effective in lowering the zeroth order $q^2\bar{q}^2$ mass significantly. In Jaffe's original calculations in the MIT Bag the following identification was possible

$$\frac{1}{\sqrt{2}}(u\bar{u} + d\bar{d})s\bar{s} \sim S^*(993)$$

$$u\bar{d}s\bar{s}, \text{ etc} \sim \delta(976)$$

$$u\bar{u}d\bar{d} \sim \varepsilon(700)$$

The ε-state was predicted to be very broad owing to its fall-apart decay to $\pi\pi$, but the S^* and δ states must couple to $K\bar{K}$ and are narrow because of the closeness of the $K\bar{K}$ threshold. Despite the encouraging qualitative success of these assignments there was a problem with the prediction of the accompanying κ state at around 900 MeV: the $K\pi$ phase shift is certainly not resonant below 1 GeV. Moreover, an exotic I=2 S-wave $\pi\pi$ state is predicted around 1100 MeV: the relevant phase shift is repulsive up to at least 1500 MeV. What are we to make of all these predictions?

2.3 The P-Matrix

In a recent paper, Jaffe and Low[52] have made some interesting observations concerning "mass" predictions for $q^2\bar{q}^2$ states. They argue that "masses" calculated for $q^2\bar{q}^2$ in the MIT Bag do not in general correspond to physical resonances. The motivation for their

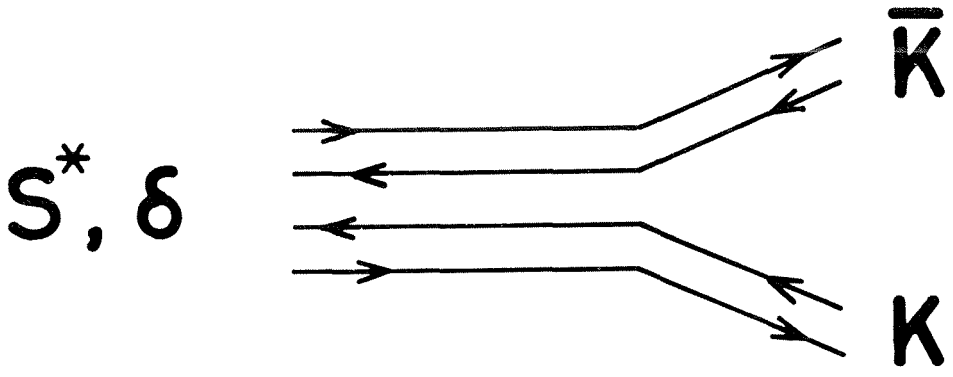

Figure 7 Quark line diagram for superallowed "fall-apart" decay of a $q^2\bar{q}^2$ state.

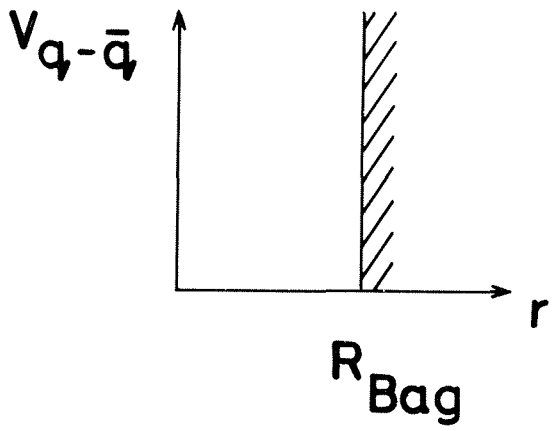

Figure 8 Bag approximation to the $q-\bar{q}$ confinement potential

analysis is sketched below.

For a $(q\bar{q})$ system coupled to an overall colour singlet, the Bag may be considered as approximating the colour confining potential by an infinite square well (Figure 8). A colour singlet $(q^2\bar{q}^2)$ system, on the other hand, has projections on to $(q\bar{q})(q\bar{q})$ systems both with colour octets coupled to an overall singlet,and with colour singlets.

$$[q^2\bar{q}^2]_{1_c} \rightarrow [(q\bar{q})_{8_c} - (q\bar{q})_{8_c}]_{1_c}$$
$$[q^2\bar{q}^2]_{1_c} \rightarrow [(q\bar{q})_{1_c} - (q\bar{q})_{1_c}]_{1_c}$$

For the colour octet component a colour confining potential such as Figure 8 is appropriate: for the colour singlet projection, however, some weak non-confining potential is expected (e.g. Figure 9). In Bag calculations this component has been artificially confined.

A tacit premise of all quark model calculations of resonance masses is a narrow resonance approximation: this is clearly invalid for $q^2\bar{q}^2$ states with their large fall-apart decay modes. In the absence of realistic calculations of fissioning Bags and so on, Jaffe and Low have proposed the "P-matrix" in an attempt to obtain a relation between observed phase-shifts and Bag model $q^2\bar{q}^2$ "primitives". The term "primitive" is introduced to underline the fact that these are not necessarily physical states.

An idea of their approach may be gained by considering an analogy[52] of S-wave scattering from a weak square well potential of radius b (Figure 10). For such a

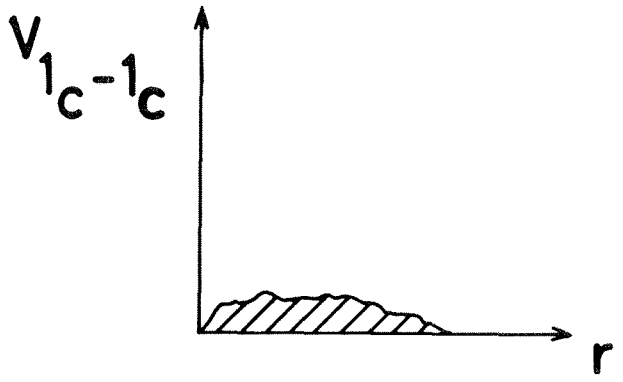

Figure 9 An artist's impression of a weak non-confining $(q\bar{q})_{1_c} - (q\bar{q})_{1_c}$ potential.

potential there are no bound states or resonances and the phase shift is found by solving the Schroedinger equation for $r < b$ and for $r > b$ and equating $\psi'(r)/\psi(r)$ at $r=b$. One obtains the condition

$$q \cot q\, b = k \cot(kb + \delta(k)) \tag{2.1}$$

where the three momenta are related by

$$q^2 = k^2 - 2mV$$

Now consider the following question. What is the connection, if any, between the phase shift $\delta(k)$ of this problem, and the eigenvalues of an infinite square well of radius b? (Figure 11). The eigenvalues of the infinite square well problem are obtained by imposing the boundary condition

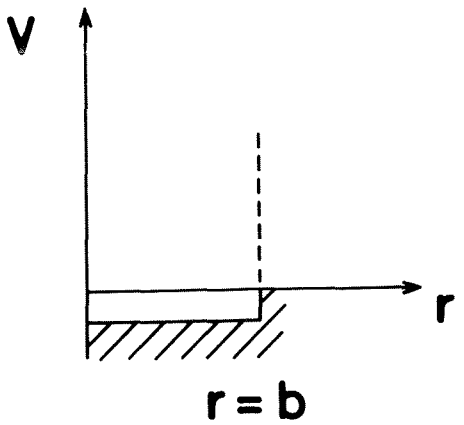

Figure 10 Weak square-well potential.

$$\psi(b) = 0 \tag{2.2}$$

corresponding to a pole in the logarithmic derivative

$$\left.\frac{\psi'(r)}{\psi(r)}\right|_{r=b} = q \cot qb \tag{2.3}$$

These occur for values of q such that

$$q_n b = n\pi$$

These are the infinite set of "primitives" for this problem. Is there a connection between these primitives q_n and the phase-shift $\delta(k)$ of our original problem? The answer is yes: primitives correspond to values of q such that q cot qb has a pole. By the definition of the phase-shift (equation 2.1) this occurs at values of k where the quantity

$$P(k) = k \cot(kb + \delta(k))$$

has a pole. Thus the primitives of the infinite square well correspond to values of k satisfying

$$\delta(k) = n\pi - kb$$

where $\delta(k)$ is the phase-shift of our weak potential problem.

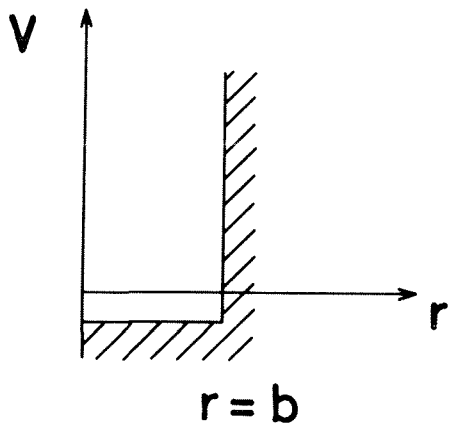

Figure 11 'Artificial' Infinite Square Well Potential.

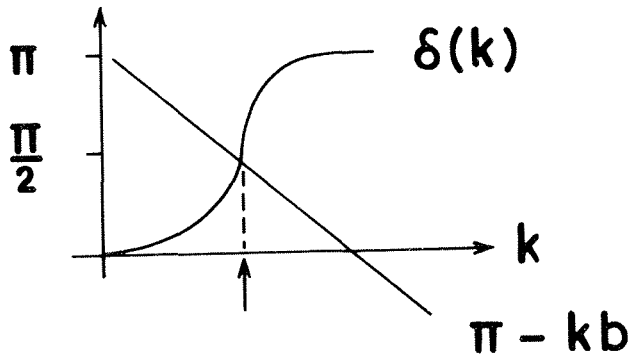

Figure 12 Position of P-matrix pole for narrow resonance.

Consider two examples:-

(1) Strong Forces, Narrow Resonance

This is analogous to the situation we expect for genuinely confined channels. The position of the P-matrix pole is most easily exhibited by a plot of $\delta(k)$ and π-kb versus k (Figure 12). The phase-shift rises rapidly through $\pi/2$ and the P-matrix pole is rather insensitive to the value of b and close to where $\delta(k)$ passes through $\pi/2$.

(2) Weak Forces, No Resonances

This is analogous to the situation we expect for unconfined channels. Despite the absence of resonant states there will be P-matrix poles. Figure 13 shows three cases:

(a) No potential: $\delta(k) \equiv 0$

The P-matrix pole is at $k=\pi/b$: Jaffe and Low call this the "compensation mass" M_{comp}. It is clearly very sensitive to the choice of b.

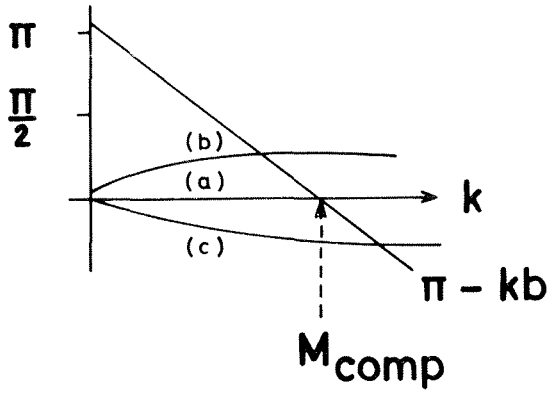

Figure 13 Position of P-matrix poles for (a) No interaction, (b) Weak attraction and (c) Weak repulsion. Case (a) defines the "compensation mass" M_{comp}.

(b) Weak attractive potential: $\delta(k) > 0$
The pole in the P-matrix is lower than the compensation mass.

(c) Weak repulsive potential: $\delta(k) < 0$
In this case the P-matrix pole is at a mass larger than M_{comp}.

This I hope illustrates the idea of Jaffe and Low. They have applied their formalism to S-wave πK and $\pi\pi$ phase-shifts and find P-matrix poles corresponding to all the Bag model primitives. For example, they find poles in the $K\pi$ channel at 960 MeV and in the I=2 $\pi\pi$ channel at 1.04 GeV, in good agreement with the original Bag estimates.[51] Jaffe and Low make a further strong claim: the relative splittings of the S-wave I=2 and I=0 $\pi\pi$ P-matrix poles with respect to the compensation mass correspond to "direct experimental evidence for the repulsive color magnetic interactions predicted in exotic channels by QCD".

It is clear that these results need careful examination. For example, one question is the sensitivity of the results to the choice of b. On physical grounds one expects

$$b \sim R_{Bag}$$

and Jaffe and Low have detailed arguments and consistency checks for their precise choice.

2.4 Conclusions

(1) Predictions of resonant masses for multiquark states certainly need care: for such states the narrow resonance approximation is clearly invalid.

(2) If we accept the $(q^2\bar{q}^2)$ identification for the 0^{++} states below 1 GeV, there are presumably some additional $(q\bar{q})_{L=1}$ 0^{++} states at higher masses. There are some hopeful signs of 'extra' activity in S-wave $\pi\pi \to K\bar{K}$ around 1300 MeV. At the moment the theoretical situation is confused: Martin and Ozmutlu[53] are unable to find any satisfactory multi-resonance description of the I=0 S-wave.

2.5 Implications

An obvious extrapolation of the idea of multiquark states is the inclusion of charmed quarks. Several authors[54-56] have looked at such states and naive estimates put several $c\bar{c}q\bar{q}$ states below the ψ'. One must re-examine these predictions in the light of Jaffe and Low's analysis of $q^2\bar{q}^2$ mesons. If any narrow states survive they could lead to curious decays of the ψ' and the possibility of charged "χ-like" states!

There have also been attempts to[57 - 59] explain the structure in the e^+e^- total cross section around 4 GeV in terms of a high orbital angular momentum approximation for $c\bar{c}q\bar{q}$ states.

3. CONCLUDING REMARKS

Before concluding I want to try to demonstrate that there are still interesting questions to ask of hadron spectroscopy.

The first question concerns multiquark hadrons. If we have granted acceptance to a $q^2\bar{q}^2$ interpretation of the scalar mesons, then we must assume other multiquark hadrons exist - in particular $q^4\bar{q}$ states.[60-64] Estimates in the MIT Bag of the lowest-lying negative parity $q^4\bar{q}$ states include many states in well-explored regions of phase-shift analyses. An extreme, and, in my opinion, a not very successful suggestion,[64] challenges the usual assignment of resonances to the $qqq[\underline{70}, 1^-]$. However, given our experience in the meson sector, Bag predictions must be regarded as 'primitives' and some sort of P-matrix analysis performed. A recent paper[65] claims some success along these lines.

The second question concerns the I=0 1^{+-} and 1^{++} states of the usual $(q\bar{q})_{L=1}$ multiplets. No I=0 partners of the B are known and the D and E mesons sit rather uneasily in the 1^{++} nonet. Given the success of non-relativistic potential models for charmonium, it seems worthwhile to try to extrapolate such models down to strangeonium. One such attempt is by Barbieri et al.[66] These authors determine the strange quark mass scale by fitting to the $\phi(s\bar{s})1^{--}$ state and then predict the P-wave and radially excited S-wave $(s\bar{s})$ states. They obtain reasonable agreement for the $f'(s\bar{s})2^{++}$ around 1.6 GeV,and predict a $\phi'(s\bar{s})1^{--}$ state at about 1.7 GeV. The situation with regard to the 1^{++}, 1^{+-}, and $0^{++}(s\bar{s})$ states is not so clear and probably warrants further attention.

Thirdly, I wish to bring to your attention some other curious states. Given Bjorken's beautiful argument[67] for the existence of glueballs and constituent gluons, what about $q\bar{q}g$[68] and qqqg states. Although it is difficult to make firm estimates for the properties of these states they deserve serious attention. One signal perhaps for mesons might be a J^{PC} exotic state: so far there is little encouragement from experiment.

To conclude:

(1) Clear evidence for the existence of non $q\bar{q}$ or qqq states is needed from experiment

(2) There are still interesting questions for light quark spectroscopy

(3) There is an interesting interplay between the charmed and non-charmed sectors.

ACKNOWLEDGEMENTS

Many people were helpful in my preparation of this talk: amongst the many I must thank are Hugh Burkhardt, Roger Cashmore, Jon Ellis, Bob Jaffe, Peter Litchfield and Alan Martin.

* * *

REFERENCES

1) R.Horgan and R.H.Dalitz, Nucl.Phys.B66, 135 (1973).

2) D.W.Greenberg and M.Resnikoff, Phys.Rev.163, 1844 (1967).

3) D.R.Divgi, Ph.D. Thesis, Univ. of Maryland (1970).

4) M.Jones, R.Levi Setti and T.Lasinksi, Nuovo Cimento 19A, 365 (1974).

5) R.Horgan and R.H.Dalitz, Nucl.Phys.B71, 546 (1974).

6) R.Horgan, Nucl.Phys.B71, 514 (1974).

7) M.Jones, R.H.Dalitz, and R.Horgan, Nucl.Phys.B129, 45 (1977).

8) D.Faiman and D.E.Plane, Nucl.Phys.B50, 379 (1972).

9) F.J.Gilman, M.Kugler and S.Meshkov, Phys.Rev.D9, 715 (1974).

10) A.J.G.Hey, J.L.Rosner and J.Weyers, Nucl.Phys.B61, 205 (1973).

11) A.J.G.Hey, P.J.Litchfield and R.J.Cashmore, Nucl.Phys.B95, 516 (1975).

12) R.J.Cashmore, A.J.G.Hey and P.J.Litchfield, Nucl.Phys.B98, 237 (1975).

13) P.J.Litchfield, R.J.Cashmore and A.J.G.Hey, contribution to the 1976 Oxford Conference on Baryon Resonances, edited by R.T.Ross and D.H.Saxon.

14) R.Horgan, invited contribution to the 1976 Oxford Conference on Baryon Resonances, edited by R.T.Ross and D.H.Saxon.

15) K.W.J.Barnham et al., "An Isobar Model Partial Wave Analysis of Three-Body Final States in π^+p Interactions from Threshold to 1700 MeV centre-of-Mass Energy", Imperial College preprint 1979, IC/HENP/78/3.

16) Particle Data Group, Phys.Lett.75B, 1(1978).

17) A.de Rujula, H.Georgi and S.Glashow, Phys.Rev.D12 147 (1975).

18) N.Isgur and G.Karl, Phys.Lett.72B, 109 (1977).

19) N.Isgur and G.Karl, Phys.Lett.74B, 353 (1978).

20) N.Isgur and G.Karl, Phys.Rev.D18, 4187 (1978).

21) N.Isgur and G.Karl, Phys.Rev.D, to be published.

22) D.Gromes and I.O.Stamatescu, Nucl.Phys.B112, 213 (1976).

23) H.J.Schnitzer, Phys.Rev.D13, 74 (1976).

24) D.Gromes, Nucl.Phys.B130, 18 (1977); ibid B131, 80 (1977).

25) W.Celmaster, Phys.Rev.D15, 1391 (1977).

26) L.J.Reinders, Journal of Physics G, to be published.

27) U.Elwanger, Heidelberg University preprint HD-THEP-78-1 (1978).

28) I.M.Barbour and D.K.Ponting, Glasgow University preprint 1979.

29) D.Gromes and I.O.Stamatescu, Heidelberg University preprint HD-THEP-79-3.

30) M.Böhm, Würzburg University preprint 1979.

31) A.B.Henriques, B.H.Kellett and R.G.Moorhouse, Phys.Lett.64B, 85 (1976).

32) H.J.Schnitzer, Phys.Lett.65B, 239 (1976); ibid 69B, 477 (1977).

33) Lai-Him Chan, Phys.Lett.71B, 422 (1977).

34) T.A.DeGrand, R.L.Jaffe, K.Johnson and J.Kiskis, Phys.Rev.D12, 2060 (1975).

35) T.A.DeGrand and R.L.Jaffe, Ann.Phys.(N.Y.)100, 425 (1976).

36) W.P.Petersen and J.L.Rosner, Phys.Rev.D6, 820 (1972).

37) D.Faiman, Phys.Rev.D15, 854 (1977).

38) G.Höhler, F.Kaiser, R.Koch and E.Pietarinen, Karlsruhr University preprint TKP-78-11 (1978).

39) R.E.Cutkosky, C.P.Forsyth, R.E.Hendrick and R.L.Kelly, Carnegie-Mellon University preprint COO-3066-117/LBL-8553 (1979).

40) L.A.Copley, N.Isgur and G.Karl, Carleton University preprint (1979).

41) B.R.Martin and L.J.Reinders, Phys.Lett.78B, 144 (1978).

42) R.J.Cashmore, review talk of the International Conference on High Energy Physics, Tokyo 1978.

43) G.Thompson, contributed paper to this conference.

44) M.Cerada, contribution to the Hadron spectroscopy parallel session at this conference.

45) Ph.Gavillet et al., Phys.Lett.69B, 119 (1977).

46) A.Ferrer et al., Phys.Lett.74B, 287 (1978).

47) R.Aaron, R.S.Longacre and J.E.Sacco, Ann.Phys. (N.Y.) 117, 56 (1979).

48) G.Thompson, contribution to the Hadron Spectroscopy parallel session at this conference.

49) J.Augustin, invited speaker at this conference.

50) E.Lorenz, contribution to the Hadron Spectroscopy parallel session at this conference.

51) R.L.Jaffe, Phys.Rev.D15, 267 (1977).

52) R.L.Jaffe and F.E.Low, Phys.Rev.D19, 2105 (1979).

53) A.D.Martin and E.N.Ozmutlu, Durham University preprint (1979); and A.D.Martin, contribution to the Hadron Spectroscopy parallel session at this conference.

54) L.B.Okun and M.B.Voloshin, Moscow preprint ITEP-152 (1976).

55) H.J.Lipkin, FERMILAB-Pub-77/57-THY.

56) A.de Rujula and R.L.Jaffe, contribution to 1977 Meson Spectroscopy Conference, Northeastern University, published by the American Institute of Physics.

57) G.L.Shaw, P.Thomas and S.Meshkov, Phys.Rev.Lett.36, 695 (1976).

58) C.Rosenzweig, Phys.Rev.Lett.36, 697, (1976).

59) Kuang-Ta Chao, Oxford University preprint 27/79 (1979).

60) M.Fukugita, K.Konishi and T.H.Hansson, Phys.Lett.74B, 261 (1978).

61) H.Högaasen and P.Sorba, Nucl.Phys.B145, 119 (1978).

62) M.De Combrugghe, H.Högaasen and P.Sorba, CERN preprint TH-2537 (1978).

63) P.J.G.Mulders, A.Th.M.Aerts and J.J.de Swart, Nijmegen University preprint THEF-NYM-78-3 (1978).

64) D.Strottman, Los Alamos preprint (LA-UR-78-3088) 1978).

65) C.Roiesnel, MIT preprint CTP-787 (1979).

66) R.Barbieri, R.Kögerler, Z.Kurst and R.Gatto, Nucl.Phys.B105, 125 (1976).

67) J.D.Bjorken, rapporteur's report to this conference.

68) D.Horn and J.E.Mandula, Phys.Rev.D17, 898 (1978).

* * *

DISCUSSION

Chairman: Yu.D. Prokoshkin

Sci. Secretaries: W.M. Geist and J.P. Martin

Chan Hong-Mo: You divided baryon spectroscopy into a pre-QCD and a post-QCD era, the latter being characterized by the work of Isgur and Karl. I wish to point out that the relation to QCD of these new fits is almost purely temporal in that they were done after QCD became popular, but in rather little else. At the level we are considering, namely one-gluon-exchange, QCD enters at two places: i) colour dependence in terms of the colour charges λ_i of the quarks; ii) the vector nature of the gluon. To test (i), one must have systems with different colours. In the baryon, however, all subsystems, namely quarks q and diquarks qq, have colour 3 so that no colour dependence can be tested. The vector nature (ii) of the gluon implies certain relative strengths between the spin-spin, spin-orbit and tensor terms. Isgur and Karl kept the spin-spin and tensor terms but dropped the spin-orbit term, which, as you pointed out, is mainly an assumption. One has not therefore tested the vector nature of the gluon. It is not excluded that one can get equally good fits with other combinations of spin-dependent forces. For example, there is a new preprint by Goldstein and Maharana in which they claim to obtain an equally good fit with quadrupole forces based on a quark-diquark model.

A.J.G. Hey: It is clear that you are not testing much QCD. There are many assumptions in the Isgur and Karl analysis which you have to worry about before you can claim that it was derived from QCD. I agree that the relation of QCD to the spectrum, at the moment, is very tenuous, except if you believe the analysis of Jaffe and Low. They claim to see the direct effect of the colour magnetism term. That is a possibility. The analysis of Goldstein which gives evidence for quark-diquark structure of baryons was based upon the assumption that 70-plets do not exist at low mass. I am not so clear that this evidence is valid. Therefore I am very sceptical about analyses which make as a keystone of their starting point the fact that 70-plets are not observed.

Chan Hong-Mo: Yes, my remark applies only to the baryons. For multiquark states, one has subsystems of different colours so that the colour dependence can be tested. This is one good reason why they are interesting. Also, I did not mean to blame you for unwisely ascribing to QCD any success of the recent fits to the baryon spectrum -- I was just unhappy that the truth is not more clearly stated in the literature.

A.J.G. Hey: I agree on the baryons.

P. Minkowski: For the absence of L·S-force there is a clear case when you state what the non-strange $^5/_2^-$, $^3/_2^-$, $^1/_2^-$ baryon states -- what you call ^{4}8, where the total spin is $^3/_2$ -- there is no visible mass splitting.

A.J.G. Hey: I agree. But one has to understand for whatever reason L·S-forces are suppressed in the baryon spectrum.

P. Minkowski: Maybe we learn more by a discussion of the equations written down by Leutwyler, Stern et al., who have such a model for mesons: your oscillator model, relativistic and no L·S-forces whatsoever.

A.J.G. Hey: I looked into the paper about the model you are talking about. I am afraid the greatest of its successes was correctly predicting the position of the $\eta_c(2.8)$.

H.J. Schnitzer: I should emphasize that the baryon model of Isgur and Karl is the only one which agrees with similar models of meson spectroscopy.

A.J.G. Hey: In my opinion the models for meson spectroscopy are premature. There are not enough data on the q-$\bar{q}$ excitations of the mesons. I discussed fits similar to those of Isgur and Karl in the meson sector. They predict all these states at masses which we have looked for and they have no reason why we do not see them. And before we do not have some more experimental evidence I take all the spectroscopists' calculations with a pinch of salt.

J. Rosner: Are you able to place any theoretical bounds on the mass of the A_1?

A.J.G. Hey: No comment.

C.S. Kalman: We have calculated the four-quark ground state using the formalism of Isgur and Karl in a paper to be considered in the Parallel Session on Hadron Spectroscopy. The hyperfine treatment is identical with Jaffe and the parameters are obtained *solely* from baryon data. The lowest mass is roughly 300 MeV higher than Jaffe's E(700) and is in fact bang on the ρ mass.

A.J.G. Hey: OK. There are no reliable models for predicting masses.

SOFT HADRON REACTIONS

V.A. Nikitin,
JINR, Dubna, USSR

The domain of research which is the subject of the present report is often referred to as "old physics" at this conference. It is not clear to me what this term means: respect or disdain. On the one hand, hadronic reactions with small momentum transfer give only an indirect reflection of particle structure which makes them not attractive enough.

On the other hand, just in this very domain we were convinced of the validity of the fundamental principles of quantum field theory and worked out some rather general semiphenomenological theories (such as Regge poles) which give a satisfactory description of a large variety of soft hadronic reactions. Finally the concepts of quark-parton model advanced by "new physics" are being checked and developed in the field of hadron interaction with small momentum transfer. The important task now is to establish links and to develop a common language for "old" and "new" domains.

Some 50 reports have been submitted to the section "Hadron interactions" at this conference. I start my review with two-body reactions.

I. BINARY REACTIONS

1. Elastic scattering

The Arizona-Dubna-Fermilab collaboration /1/ reports on the results of a study of proton-helium elastic scattering in an energy range of $40 \leqslant E \leqslant 400$ GeV and a momentum transfer of $0.003 \leqslant |t| \leqslant 0,5$ $(GeV/c)^2$.

The internal helium gas jet target has been used. The stacks of silicon detectors have registered recoil nuclei. An example of the measured differential cross-section is shown in fig. 1.

The slope parameter of the diffraction pHe cone $(b(s,t) = \frac{d}{dt}(\ln \frac{d\sigma}{dt}))$ has been obtained (fig. 2). The striking feature of the functions $b_{pp}(s)$, $b_{pd}(s)$, and $b_{pHe}(s)$ is that they do not tend to one universal slope with increasing s. In the approximation of one effective pole (pomeron) all elastic hadronic processes should show the unique rate of shrinkage b_1 $(b_o + b_1 \ln s)$. Fig. 2 shows that it is not the case in reality.

As has been pointed out by Yu.I.Asimov et al. /3/, the effect may arise from the energy dependence of the Glauber corrections. The rate of shrinkage for pd scattering is

$$b_1 \approx \frac{S(t)}{\left(S(t) - \frac{\Delta\sigma}{2\sigma_t}\right)} \left(2\alpha' + c\frac{\partial}{\partial \ln s}\left(\frac{\Delta\sigma}{2\sigma_t}\right)\right) \qquad (1)$$

instead of $b_1 = 2\alpha'$ as it is the one pole approximation. Here S(t) is the deuteron formfactor, $\Delta\sigma = 2\sigma_{tpN} - \sigma_{pd}$ the defect of the total cross section and α' the slope of the effective trajectory. The second term violates the universal behaviour of b (s). Another feature of (1) is specific t-dependence of b_1. Since the denominator decreases with increasing

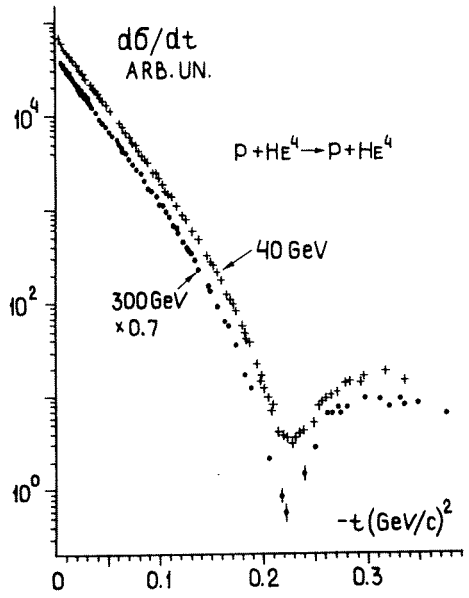

Fig. 1. pHe-elastic scattering differential cross section

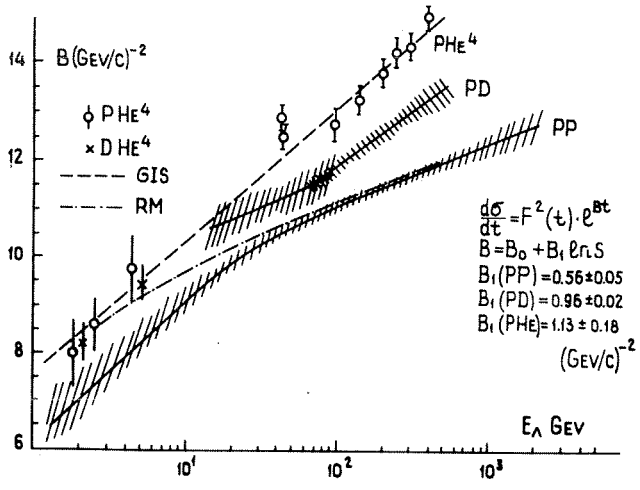

Fig. 2. Comparison of the slope parameters of the proton-light nuclei elastic scattering. For the references to original papers see/2/.

$|t|$, the rate of shrinkage is expected to be larger for larger $|t|$.

For pHe scattering the prediction /3/ has been made: $b_1(t \approx 0) = 1.35$, $b_1(t = 0.07) = 2.8$ $(GeV/c)^2$. The data of /1/ are accurate enough to get b and b_1 in different t-intervals. The result is presented in fig. 3. The value of b_1 $(t \approx 0)$ is close to the prediction /3/ but the rate of shrinkage seems to be t-independent. This disagreement with the model is not very surprising since helium nucleus is much more compact than deuteron, and, perhaps, screening corrections require more delicate treatment. The importance of essential improvement of the Glauber model is shown in fig. 4, where the comparison is made of the differential cross-section of the reaction pHe --> pHe with the calculation from the Glauber formula. The single-Gaussian approximation is used as an input for the pN amplitude and helium formfactor in version I of the Glauber formula. In the second version the double-Gaussian parametrization is used in order to fit better the data on pp and eHe elastic scattering. Both versions fail to reproduce the data.

In the same experiment /1/ a $(He + H_2)$ gas mixture has been used as a target. This made it possible to perform absolute normalization of the pHe data and, using the optical theorem, to determine the total cross-section of pHe interactions. This is shown in fig. 5 together with the total

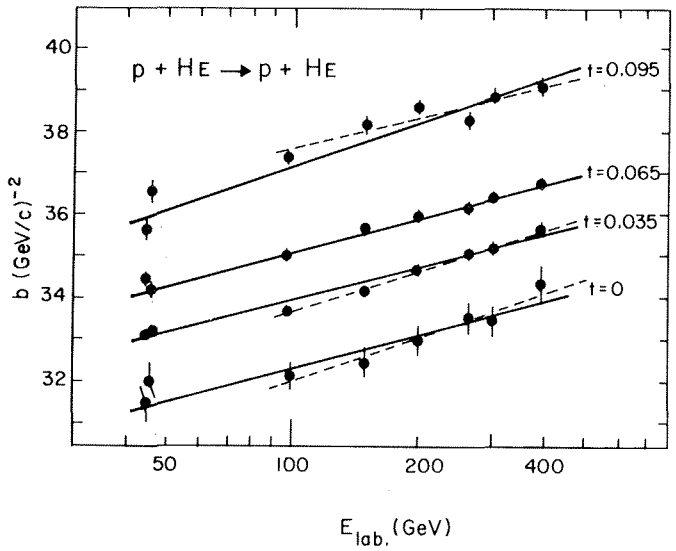

Fig. 3. The b-parameter of elastic pHe scattering as a function of s and t. The rate of shrinkage b_1 does not depend on t.

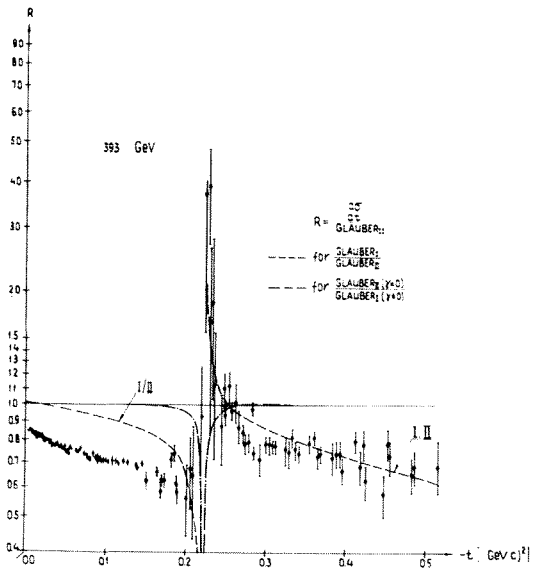

Fig. 4. Comparison of the differential cross-section of elastic pHe scattering with the Glauber model prediction.

cross sections of pp and pd interactions. The geometrical scaling (GS) relation

$$\sigma_t \sim b \sim r^2(s) \sim \ln s \quad (2)$$

is in good agreement with the data on σ_t and b (shown in fig. 5) at an energy of $E_L \gtrsim 150$ GeV. The concept of GS is usually treated as an empirical rule and now is often used as a criterion for the construction of models of binary hadron reactions [4,5]. It is worth noticing that GS has a ground in Regge theory with pomeron:

$\alpha(0) = 1 + \Delta$, $\Delta = 0.06$ [6].

It should hold with an accuracy of a few per cent in an energy range up to several TeV. This version Regge theory gives a good description of rising σ_{tot}, $\rho = \mathrm{Re}A/\mathrm{Im}A$ and some other data [6,7].

C.Lewin et al. [8] have presented the data on elastic $K^{\pm}p$ interactions at 32.1 GeV/c. The analysis made in this paper includes also some other $K^{\pm}$ data available at higher energies. In particular, the GS rule

$$\frac{d\sigma}{dt}(s,t) = \quad (3)$$
$$= r^{-4}(s) \cdot f(r^2(s) \cdot t); \quad \sigma_t \sim r^2$$

tested. As is shown in fig. 6, the GS in the form (3) holds for $K^{\pm}$ elastic scattering with an absolute accuracy of ~ 0.5 mb/GeV^2 at energies above 70 GeV.

Since the experiments [8] have been done with K^+ and

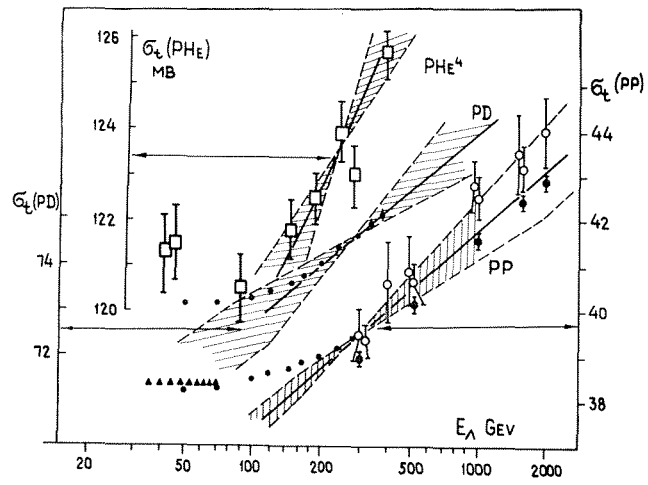

Fig. 5. Comparison of the behaviour of the total cross section with the GS relation (2). The new data on σ_{tot}(pHe) and b(pHe) are taken from /1/.

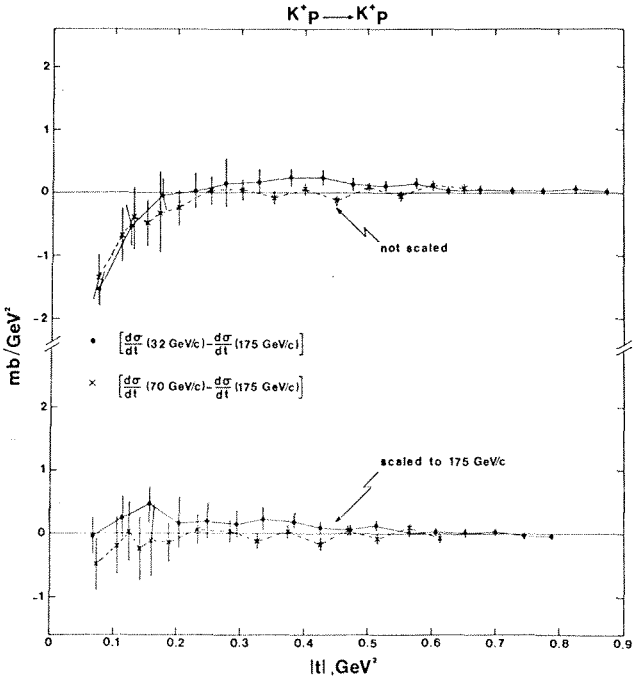

Fig. 6. Comparison of the differential cross section of elastic K+p scattering at different energies. The GS (3) holds at an energy higher 70 GeV.

K^- under the same conditions, the data are relevant to study the difference of the $K^\pm p$ cross section. In terms of Regge model the scattering amplitude reads

$$A(K^\pm p) = IP + R^+ \mp R^- ,$$

where $R^\pm$ are the reggeon contributions with $\pm$ - signatures.

$$Im\,R^-(t) = \frac{\left(\frac{d\sigma}{dt}\right)_{K^-} - \left(\frac{d\sigma}{dt}\right)_{K^+}}{\sqrt{\left(\frac{d\sigma}{dt}\right)_{K^-} + \left(\frac{d\sigma}{dt}\right)_{K^+}}} \qquad (4)$$

The data show that the function (4) is peripheral and may be parametrized as

$$Im\,R^-(s,t) = \alpha\, e^{\beta t} J_0(r\sqrt{-t})$$

$$\alpha = c\, s^{-0.58 \pm 0.04}$$

This function is shown in fig.7 in impact parameter space.

R.Henzi and P.Valin have submitted to this conference paper /9/ devoted to discussion of the recent FNAL and ISR data on elastic pp scattering at large momentum transfer. They have developed the type of optical model, where the cross section of elastic scattering is expressed via the inelastic overlap function G_{in} (s,b) in b-space

$$\frac{d\sigma}{dt}(s,t) = \qquad (5)$$

$$\pi\left(\int_0^\infty (1-\sqrt{1-G_{in}})\, J_0(b\sqrt{-t})\, b\, db\right)$$

In this relation unitarity is taken into account. The expansion

$$1-\sqrt{1-G_{in}} \approx 1/2\, G_{in} - 1/4\, G_{in}^2 \cdots$$

suggests the interpretation of G_{in} as the "Born term". This gives hopes that G_{in} (s,b) may have a simple structure. The real part of the amplitude and spin terms are neglected. The G_{in} (s,b) is chosen as Gaussian with a small "edgy" correction necessary in order to reproduce the diffraction zero of $d\sigma/dt\,(t)$

at - t ≈ 1,4. The number of parameters is 8. They are functions of lns. At fixed energy the model retains 5 parameters. As is seen in fig.8, the model is able to describe all the published pp differential cross sections, and an extrapolation prediction is made to higher energy.

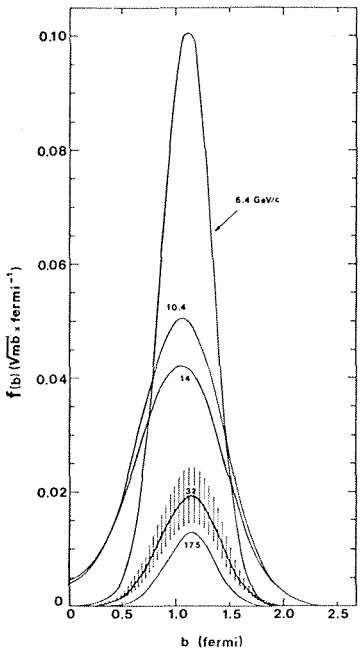

Fig. 7. The profile function of (4).

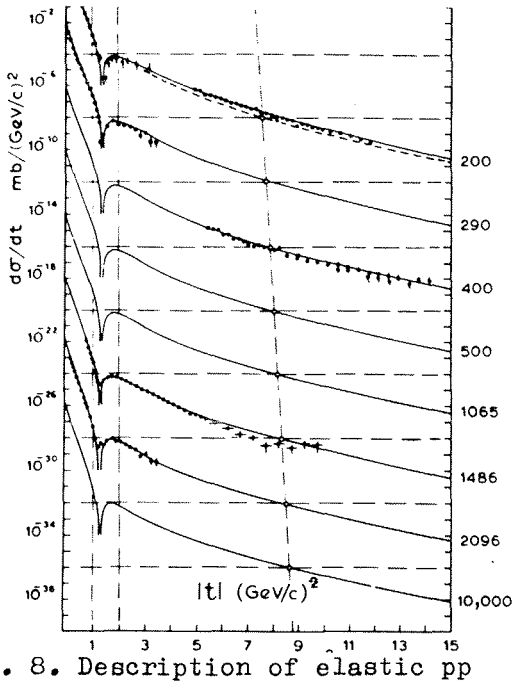

Fig. 8. Description of elastic pp scattering by formula (5).

Unfortunately we do not know how to relate different reactions (say, pp and $\bar{p}p$) in this purely phenomenological models. The parameters are practicaly constrained by no general principles. If a new experiment requires to change them, we can hardly learn a lesson from it.

The spin degrees of freedom introduce a good deal of complexity into the hadron behaviour. For example, pp scattering is controlled by five amplitudes. An experimental guidance is particularly important here. A new measurement of polarization in pp elastic scattering at 150 GeV/c is reported by G.Fidecaro et al. /10/ The result is based on a sample of $\sim 10^6$ events of elastic scattering off the polarized target where the left - right asymmetry is observed. The result is presented in fig. 9.

The polarization P always comes when the interference of spin flip and spin nonflip waves take place.

$$P \cdot \frac{d\sigma}{dt} \sim Im\,(A_{nf} A_f^*)$$

Paper /4/ treats binary reactions in terms of Regge poles with absorptions. The latter is regarded as a unitary correction to the pole contribution and is expressed again via Regge-like amplitudes. The matrix element of each pole R in b-space reads as $m_R(b) = R(b) - iR(b) \cdot m_{ef}(b)$ where m_{ef} is the effective pomeron amplitude. Both IP and R have a spin flip part. The first

zero in polarization at $-t \approx 0,5$ occurs because of zero of ReR, and the second zero at $-t \approx 1,4$ is due to changing the sign of JmIP.

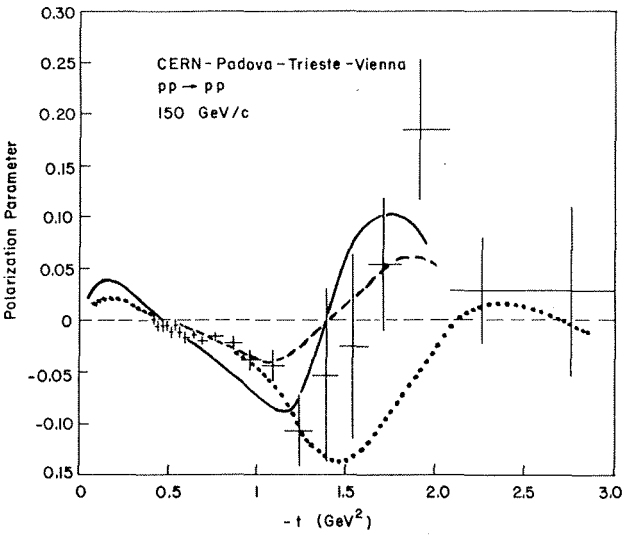

Fig. 9. Polarization in pp elastic scattering. The theoretical curves are:
G.L.Kane, 100 GeV /4/
W.Majerotto, 150 GeV /5/
C.Bourrely, 150 GeV /11/.

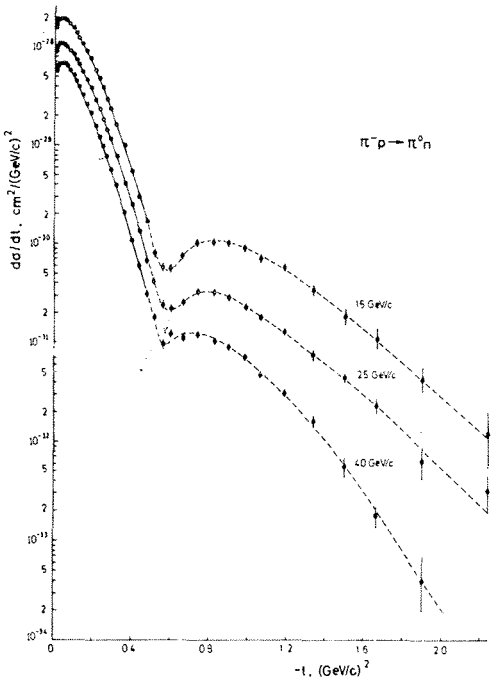

Fig. 10. Differential cross section of the reaction $\pi^- p \to \pi^0 n$

The eikonal model for binary reactions has been developed in /5/. The eikonal is constructed from Regge-like amplitudes in a pure pole approximation. The effective pomeron is chosen phenomenologically similar to /9/ (see (5)) and it does not contain a spin flip component.

The very different approach is tried in /11/. The proton is considered as a rotating extended object. The incident particle has different velocities relative to the left and right edges of the spinning target.

This obviously leads to the left - right asymmetry in scattering. The model operates with the arbitrary function $\omega(b)$, where ω is the frequency of rotation and b is the impact parameter. Notice that a similar idea has been used /12/ for the analysis of spin effects in inelastic hadron interactions.

The theoretical predictions mentioned here are checked against the experimental result /10/ in fig. 9. The calculation of /4,5/ is in qualitative agreement with the data. The effect predicted in /4/ is larger probably due to the spin flip component in the pomeron term.

New data on polarization of higher accuracy and at higher energy are welcome.

2. Charge exchange reactions

Four papers by W.D.Apel et al./13/ are devoted to a study reactions

$$\pi^- p \to \pi^0 n,\ \eta n,\ \eta' n,\ \omega n$$

in an energy interval of 15-40 GeV. The cross sect. with high statistics and over a wide range of t reported on. Their general feature is a dip at t = 0 which shows evidence for spin structure of the reactions. It has been found (for first 3 reactions) that the spin flip and spin nonflip amplitudes can be parametrized, for small $|t|$, as exponential with the same slopes. So

$$\frac{d\sigma}{dt} = \frac{d\sigma}{dt}(0)(1 - gct)e^{ct}$$

where g and c are logarithmic functions of s.

An example of the differential cross section is shown in fig. 10. The effective ρ and A_2 trajectories are determined (figs. 11, 12). The ρ trajectory is linear. The A_2 trajectory is also linear at $0 \lesssim |t| \lesssim 0.4$ and passes through the ρ, A_2, g and h mesons. But at $|t| > 0.7$ it has a complex behaviour. This problem requires more investigation at higher energies. Based on the ratio of the cross sections for the reactions $\pi^- p \to \eta n$, $\pi^- p \to \eta' n$ at t = 0 $R(\eta'/\eta) = 0.55 \pm 0.06$, the singlet-octet mixing angle for pseudoscalar mesons is found to be $\theta = -(18.2 \pm 1,4)°$

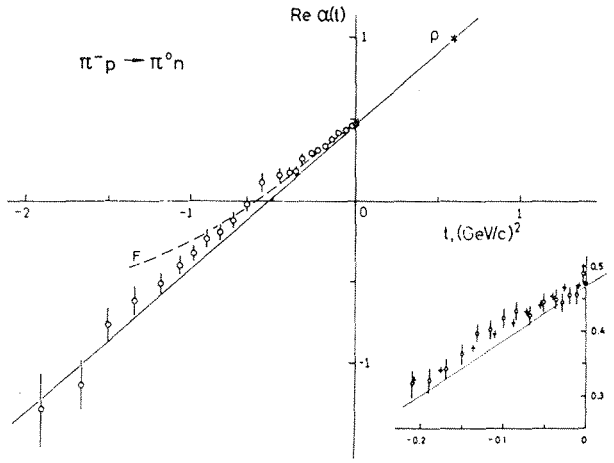

Fig. 11. Effective ρ-trajectory (from the reaction $\pi^- p \to \pi^0 n$).

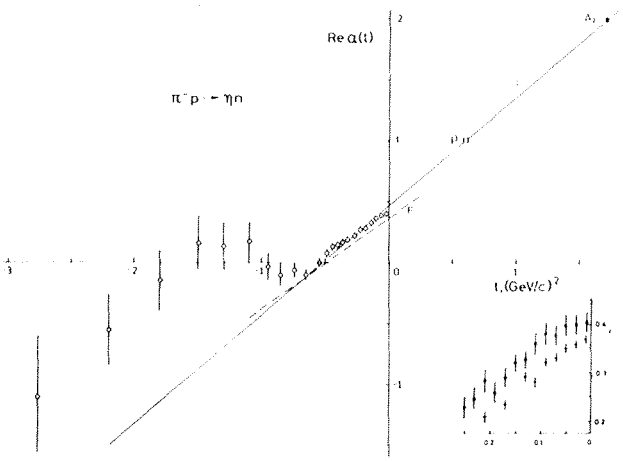

Fig. 12. Effective A_2-trajectory (from the reaction $\pi^- p \to \eta^0 n$).

The data are reported on the density matrix for ω meson. In particular, the relation $\rho_{00} = 1 - 2\rho_{1-1}$ holds, hence these data require no unnatural parity exchange for producing ω's of helicity 1.

II. DIFFRACTIVE DISSOCIATION

1. Definition and general properties

The reactions of diffractive dissociation are among favourite ones already for a long time. They can be distinguished by the following set of criteria.

a) The cross sections σ (s) are nearly s-independent.

b) The t-distribution has a forward peak.

c) The involved particles may

change only spin, parity and mass (zero quantum number exchange).

d) The factorization rule holds.

e) ρ =ReA/ImA $\approx$ 0.

f) The Morrison - Gribov rule is approximately valid

$$P_a = P_c\ (-1)^{J_a - J_c}$$

(P is parity, J is spin).

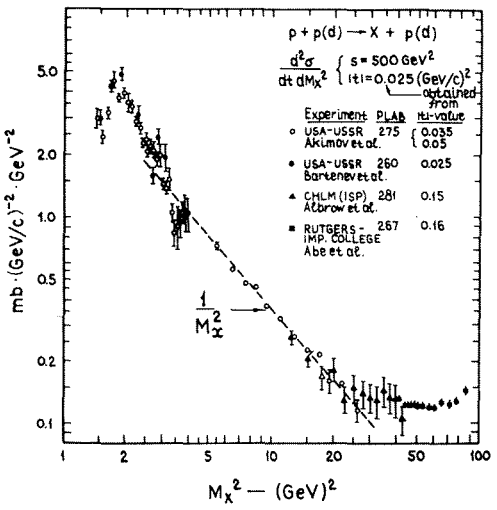

Fig. 13. Example of the double differential cross section of the proton diffraction dissosiation.

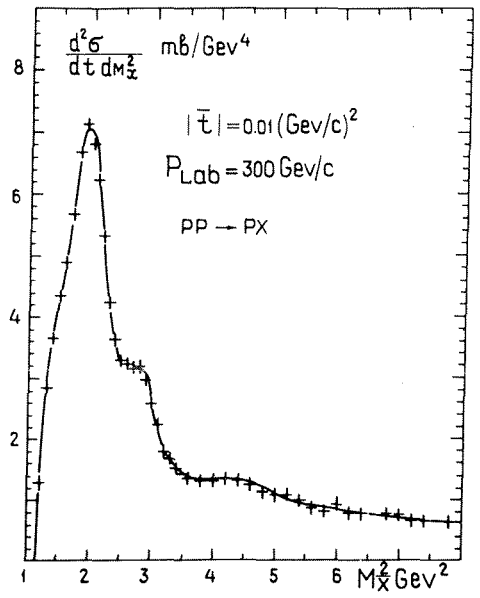

Fig. 14. Low mass proton DD in the reaction pp -- Xp.

A typical behaviour of the cross section $d^2\sigma/dtdm_x^2$ of the proton diffractive dissociation (DD) pp -> Xp is shown in fig. 13. There is an enhancement at a low mass of system x. Then the drop follows by $\sim m_x^{-2}$ and subsequently the leveling takes place. The low mass part of proton DD has been studied with high precision in paper /14/.

The result is shown in fig. 14. The nature of the peak at $m_x^2 \approx 1{,}9$ GeV^2 is not quite clear. Partially it may be explained by Deck effect (creation of system x through the scattering of virtual pion of incident particle off the target with small momentum transfer). But an appreciable contribution of isobar N (1400) is not excluded.

In accordance with an intuitive image of the DD, the forward peak at small t always has a perfect exponential shape. An example is shown in fig. 15. It is borrowed from paper /15/, where the DD of π^- on some nuclei is studied. The observed slope parameter b is in good correspondence with the radius, r, of nuclei: $b = r^2/4, r = cA^{1/3}$.

2. Parton picture of diffractive dissociation

I.Pomeranchuk and E.Feinberg (1956) /16/, M.Good and W.Walker (1960) /17/

suggested to consider the hadron as a superposition of some elementary states $|\psi_K\rangle$

$$|h\rangle = c_K |\psi_K\rangle, \quad \langle\psi_{K'}|\psi_K\rangle = \delta_{K'K}$$

which are eigenstates of the interaction operator

$$T|\psi_K\rangle = t_K |\psi_K\rangle$$

so t_k^2 is the probability of the state $|\psi_K\rangle$ to interact. The amplitude of elastic scattering is written as

$$\mathrm{Im}\, A_{el} = \langle h|T|h\rangle = \sum_K |c_K|^2 t_K = \langle t\rangle$$

and the DD cross section is

$$\sigma_{DD} = \sum_K |\langle\psi_K|T|h\rangle|^2 - \sigma_{el} = \langle t^2\rangle - \langle t\rangle^2$$

what is the dispersion of t over k. So t_k must be essentially different in order to give rise to inelastic diffraction.

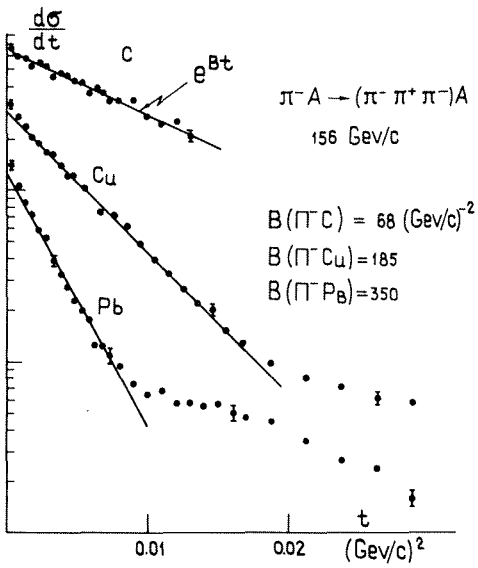

Fig. 15. Differential cross-section of pion DD on nuclei.

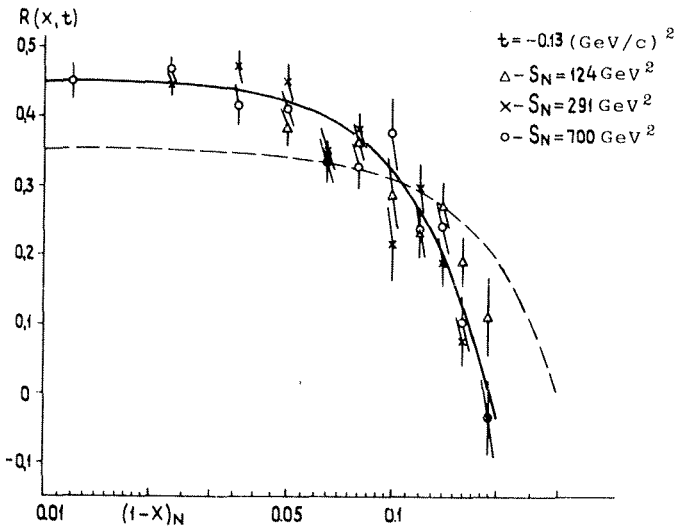

Fig. 16. Comparison of the differential cross sections of the reactions pp -> Xp and pd --> Xd, which shows the vanishing of the screening correction for $(1 - x) \approx 0.1$. The smooth curve - fit to the data of parton model /19/.

Mietinnen et al. /18/ have proposed to interpret the states as hadron states with k wee partons. The wee partons may have different impact parameters and rapidities which leads to the dispersion of t_k.

B.Kopeliovich et al./19/, starting with the same idea, have developed the two-component model, where $t_0 = 0$ (hadron without wee parton does not interact; it is passive component) and $t_k = t$ (active component). In this approximation the sign of the imaginary part of the DD amplitude is found to be negative.This leads, in particular, to a new interesting phenomenon of antishadowing in DD on nuclei.

The illustration of antishadowing effect in DD proton on deutron pd -> Xd, is done graphicaly below. The involved vertexes have the signs as follows : (p -> p, +), (p -> x,-), (x -> x,+), (x' -> X,-)

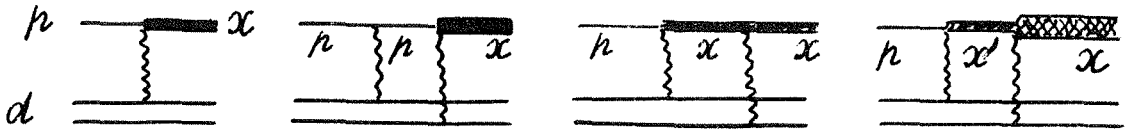

	a	b	c	d
I	+	-	-	-
II	-	+	+	-

I. The sign of amplitude in conventional Glauber model.
II.The sign of amplitude in the parton model /19/.

In the version II graph d) gives antiscreening effect.

The data on the reaction pd -> Xd confirm the predicted effect,which is displayed in the change of the sign of scattering correction when m_x increases (fig. 16).

3.Coherent inelastic diffraction of neutron on deutron

The results are reported on the experiment on pd and dd collisions at ISR /20/. The reaction nd --- (p π^-)d is studied at a c.m. energy of 37 and 53 GeV. A new interesting interference phenomenon is observed in the low mass differential cross section $d^2\sigma/dtdm^2$ (t), where the shoulder appears around $-t \approx 0.3$ (see fig. 17). The interpretation of the data is made on the basis of Glauber multiple scattering theory extended to the inelastic case, where the input is given by the elementary diffractive amplitude on free nucleons and by the total cross section of diffractive states. Three types of input amplitudes are used.

$$T_{\Delta\lambda}(t) = i c_{\Delta\lambda} e^{at} J_{\Delta\lambda}(R\sqrt{-t})\, e^{i\Delta\lambda\varphi}$$

$$(d\sigma/dt)_{NN\to(N\pi)N} = \sum_{\Delta\lambda} |T_{\Delta\lambda}|^2 \qquad (6)$$

where $\Delta\lambda$ is the amount of the helicity flip; the parameters $c_{\Delta\lambda}$ depend on the mass of the $(N\pi)$ - system. The sum includes 5 terms ($\Delta\lambda = 0 - 4$).

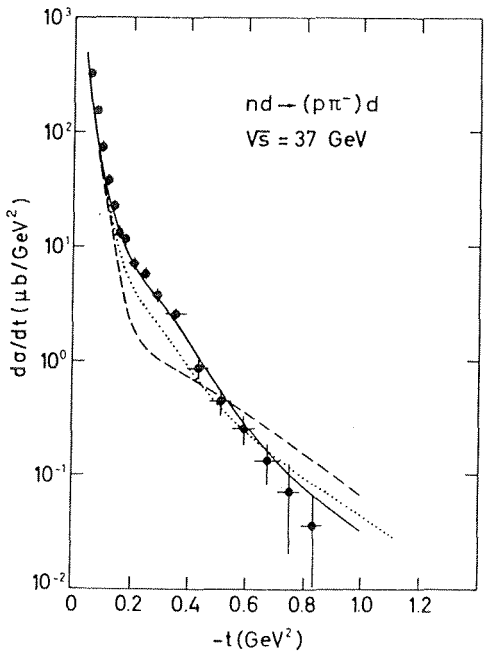

Fig. 17. Differential cross section of the reaction $nd \to (p\pi^-)d$ for a mass interval of $1,3 \leq m(\pi^- p) \leq 1,44$ GeV. The curves are calculated according to the generalized Glauber model. The input amplitude is taken in the form (6,7,8): —(6), --- (7), ... (8).

The second type of amplitude is characterized by having a nonzero real part, only a helicity conserving term and a central profile in b-space. The square of this amplitude is directly determined from nucleon-nucleon experiments as well.

$$T(t) = i\,(a_1 e^{b_1 t} + a_2 e^{b_2 t} e^{i\varphi}) \qquad (7)$$

The third type of amplitude is chosen with properties which are intermediate between the first and second cases

$$T(t) = iaJ_0(R\sqrt{-t})e^{at} + be^{\beta t}$$

The comparison of these three models with experiment (fig.17) shows that only the first one yields a positive result.

To summarize, the interference effect observed in coherent nucleon DD on deuteron is very sensitive to the structure of the elementary DD amplitude. In the light of this, the deuteron can be considered as an interferometer for hadronic states. Although the approach discussed here /20/ successfully describes the data, one has to bear in mind that the Glauber model is far from perfection. The simplest critical remark concerns the rescattering of the diffractive state $(p\pi)$. We do not know the value and structure of the rescattering vertex. This point is especially important in view of the result of paper /19/, where the constructive interference is treated as an antishadowing nature of double scattering correction.

4. Triple Regge analysis of diffractive hadron scattering

Triple Regge formalism is widely used to analyse DD reactions in the

region $s \gg m_0^2$, $m^2 \gg m_0^2$, $s/m^2 \gg 1$ (m_0 is the hadron mass, and m is the excited state mass). The inclusive cross section in triple Regge formalism is graphically expressed as

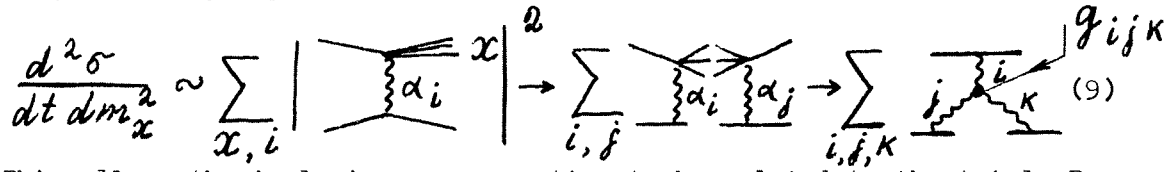

(9)

This allows the inclusive cross section to be related to the triple Regge coupling functions $g_{ijk}(t)$

$$\frac{d^2\sigma}{dt\,dm_x^2} = \sum_{i,j,k} G_{ijk}(t)\, s^{\alpha_i(t)+\alpha_j(t)-2} \times m_x^{\alpha_k(0)-\alpha_i(t)-\alpha_j(t)} \qquad (10)$$

Here G_{ijk} absorbs signatures and reggeon-particle vertex functions. This formula gives a phenomenological foundation for experimental data systematics.

Three papers on this subject have been submitted to this conference. The authors of /7/ analyse the data on $\sigma_{totpp}(s)$ and on the reaction pp --> Xp at small momentum transfer and $120 \leq s \leq 700$ GeV^2. They pass on to the level of reggeon-quark interactions, so, instead of (9), the graphs are considered:

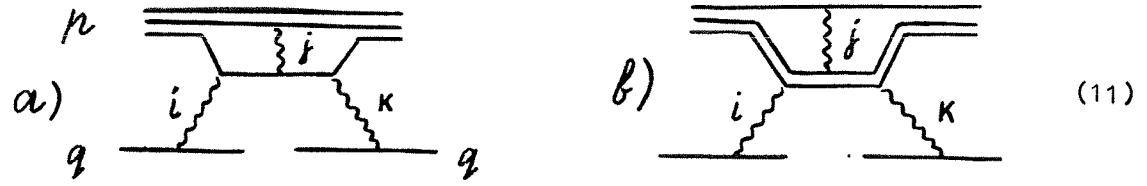

(11)

In fact, the triple reggeon vertex function is not involved, but it is calculated from the reggeon-quark (11a) or reggeon diquark vertex (11b). The graph (11b) yields a better data description, The contribution of different terms to (10) is shown in fig. 18. Pomeron with an intercept of $\alpha(0) = 1.06$ has been chosen in this analysis.

Paper /21/ is devoted to a triple Regge analysis of inclusive proton production in K^-p interactions at 32 GeV/c. Since the data refer to rather low energy and to high mass ($0.15 \leq m_x^2/s \leq 0.35$) of the diffractively produced system, the analysis includes only two terms: RR$\mathbb{P}$ and $\pi\pi$R. The differential cross section of the reaction K^-p --> Xp and its description by (10) is shown in fig. 19. The pion-proton inclusive cross section of the reaction $\pi^-p \to \pi^-X$ in the beam fragmentation region at an energy of 147 GeV has been described by means of triple Regge formula (10) in paper /22/. It is proved that the set of parameters found in the analysis of the reaction pp --> Xp provides a good agreement with the $\pi^-p \to \pi^-X$ data.

The summary of solutions of different triple Regge analyses is given in Table I.

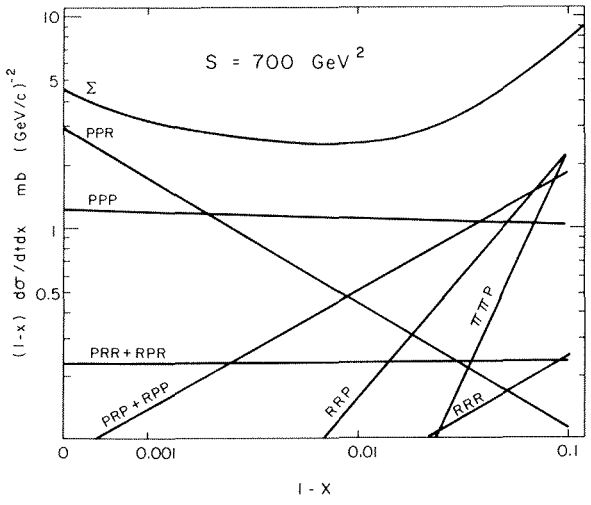

Fig. 18. Contributions of different triple Regge terms to the inclusive cross section of the reaction pp→Xp at -t = 0.05. The calculation is done by the reggeon-diquark model /7/.

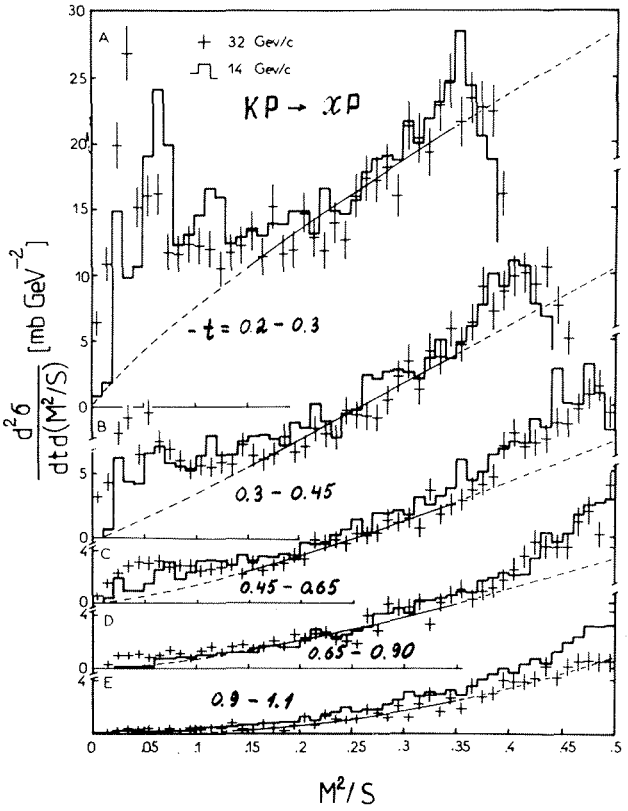

Fig. 19. Triple Regge analysis of the $K^- p \to Xp$.

TABLE I. Parameters G_{ijk} (t = 0) mb/GeV^4 of three-Regge expansion

Vertex	$\alpha_{IP}(0) = 1.06$ CD	MT	$\alpha_{IP}(0) = 1$ CD	FF	KK	AB
PPP	1.56	0.81	2.93	2.55	3.24±0.3	--
	--	--	--	--	6.9 ±1	--
PPR	0.94	0.96	2.42	4.42	3.2 ±0.6	--
RRP	13.0	27.2	18.5	31.6	7.2 ±2	20.±3
PRR	--	--	--	--	-9.3 ±2	--
RRR	83.7	32.2	18.1	18.1	51.8 ±8	--
R	--	--	--	--	--	49.±12

CD - S.Chu, B.Desai /24/. pp
MT - S.Mukhin, V.Tsarev /7/. pp
KK - Y.Kazarinov, B.Kopeliovich /25/. pp
AB - Y.Arestov, V.Babintsev /21/. $K^- p$

To conclude, the triple Regge analysis provides a significant step towards a combined description on the total cross section, elastic scattering and inclusive distributions for pp, Kp and πp systems, which are all related through factorization and unitarity.

III. INCLUSIVE REACTIONS

1. Scaling violation in the central region

New extensive data on inclusive cross sections in the fragmentation and central regions are reported at this conference by bubble chambers collaborations /22, 26, 27, 28, 29/. Inelastic collisions $\pi^{\pm}$ p, pp, $K^{\pm}$p have been studied in an energy range of 8 - 147 GeV. One of the typical x-distributions is shown in fig. 20 /26/.

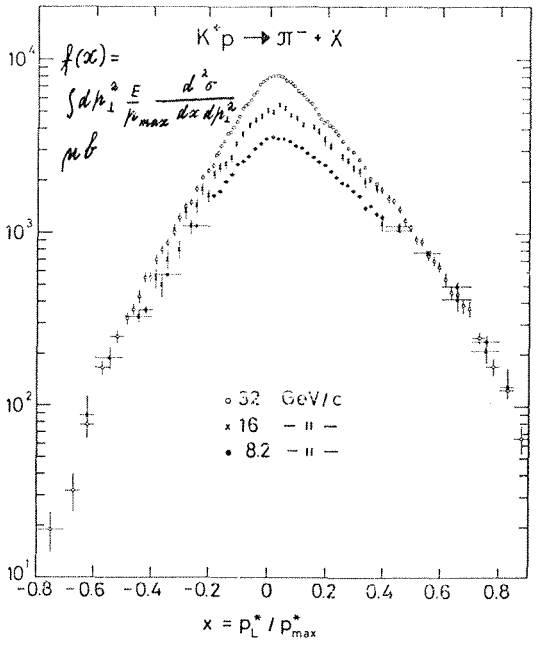

Fig. 20. Structure functions of π^- produced in the reaction $K^+p \to \pi^- X$.

This is inclusive π^--production in the reaction

$K^+p \to \pi^- + X$ at energies of 8 - 32 GeV. Comparison of structure functions at different energies clearly shows that early scaling holds in the fragmentation region at $|x| > 0{,}5$ and scaling is violated in the central region. The behaviour of the structure function

$$f(x,s)\Big|_{x\approx 0}^{p_L^* \approx 0} = \frac{1}{\sigma_t} \int E^* d^2\sigma/(dp_L^* dp_T^2)\, dp_T^2$$

is reproduced by the relation

$$f(x,s) = b + c_0 s^{-1/4} + ds^{-1/2} \qquad (12)$$

This type s-dependence may be understood in terms of double-Regge expansion

$$PP = b \quad , \quad PR = ds^{-1/2}$$
$$RR = c_0 s^{-1/4} \qquad (13)$$

In this diagram c denotes inclusively observed particle. It is easy to prove that in this scheme the charged particle multiplicity should behave as

$$n_{ch} = a + b\ln s + cs^{-1/2} + ds^{-1/2} \ln s \qquad (14)$$

The compilation of data on f (x 0,s) is presented in fig. 21. We see that data do behave as (12) in an energy interval of up to 2 TeV. Experiments support the relation (14) as well. The relation (12) literally taken says that at high energy we shall approach the scaling invariance. But at present it is hard to say where exactly the scaling limit is if it exists at all.

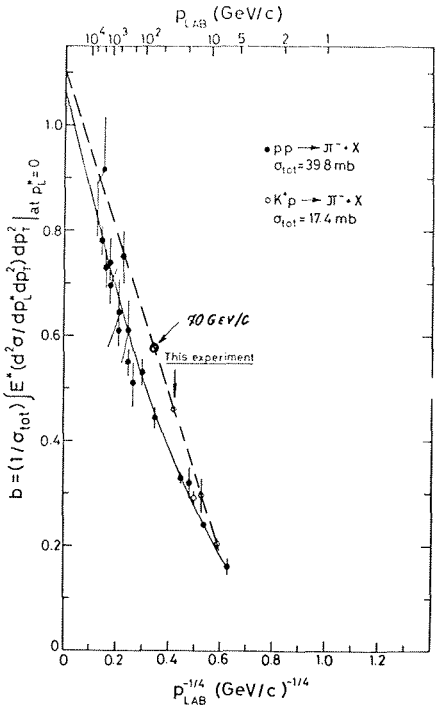

Fig. 21. Complication of data on the behaviour of inclusive cross section in the central region.

An interesting alternative approach to the scaling problem has been suggested by A.Capella et al. /30/.

In the dual topological model the pomeron has a cylindrical topology and its s-channel contents, obtained by cutting, are two uncorrelated chains corresponding to a multiperipheral picture of particle production (fig. 22). The rapidity density of produced particles is given by the superposition of two independent rapidity distributions. Each of them is scaling-invariant. When energy rises, the interval of their overlapping becomes wider. This leads to increasing the density in the central region.

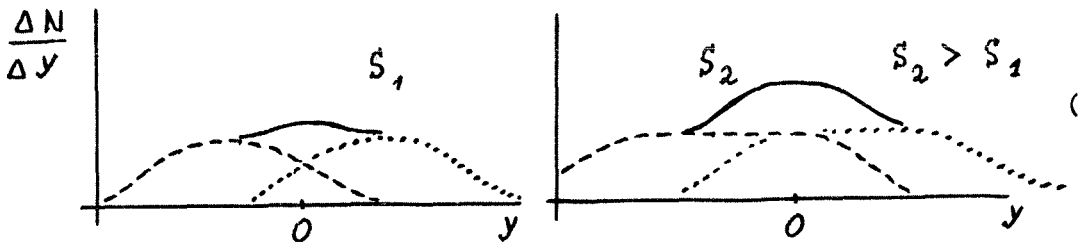

(15)

The energy dependence of the central plateau height for pp inelastic interactions is shown in fig. 23. The model /30/ is in agreement with data. In order to distinguish between the possibilities (12) and (15), one has to get data at energy higher than attainable now.

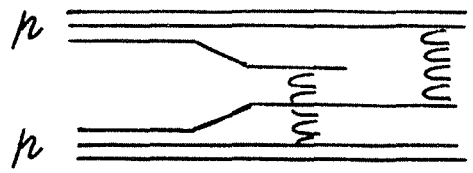

Fig. 22. Two-chain model for pp scattering obtained by cutting the cylindrical pomeron.

2. Evaluation of the total cross section of K interactions

The reaction $K^+p \to \Delta^{++}x^\circ$ has been studied in paper /31/. At small momentum transfer it is dominated by π - exchange. An evidence for π dominance is obtained from the t-distribution, where the narrow peak with slope $b \approx r_\pi$ is clearly observed at small t' and in the target fragmentation region. This makes it possible to apply the Chew-Low extrapolation procedure in order to calculate the total cross section of K π interactions for different effective mass (or c.m. energy)

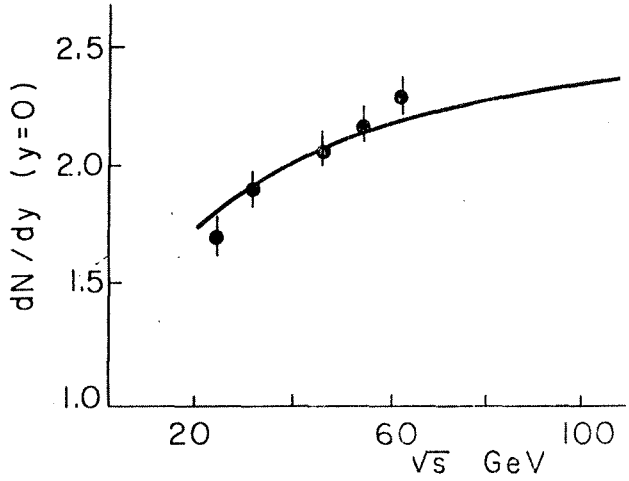

Fig. 23. Energy dependence of the central plateau height for pp --> p X. The solid curve is the model /30/ of cylindrical pomeron.

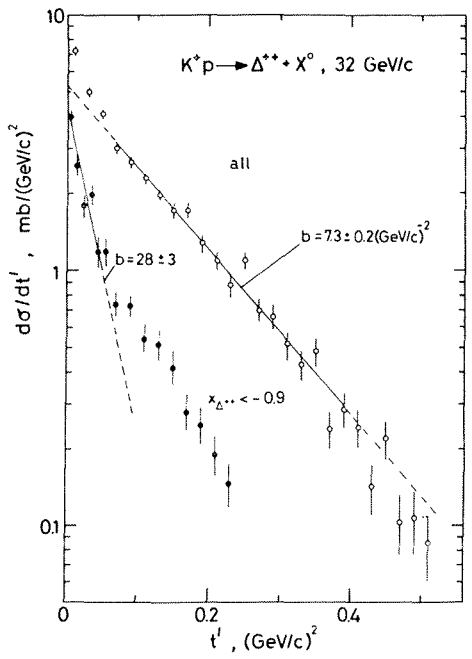

Fig. 24. Differential cross section of the reaction $K^+p \to \Delta^{++}X^o$.

of the K π system. The result is presented in fig. 25. The two known resonances are seen. The surprise is that at high mass ($m_{K\pi} \approx 5$ GeV) $\sigma_{tot}(K\pi) \approx$ 22 mb which is twice as large as the value estimated by the factorization relation $\sigma_{tot}(K\pi) = (\sigma_{tot}(\pi p)\,\sigma_{tot}(Kp)/\sigma_{tot}(pp) \approx 11$ mb. The high value of $\sigma_{tot}(K\pi)$ may indicate the existence of some unknown resonances. But, being more careful, one could suspect the validity of π-pole approximation used in the Chew-Low extrapolation.

3. Property of low p_T-distributions

It is known that a low p_T part of the secondary hadron spectrum may be described by the expression known in the statistical model

$$\frac{d\sigma}{dp_T} = C\sqrt{E_T}\,p_T \exp(-E_T/T), \quad (16)$$

where $E_T = p_T^2 + m^2$ and parameter T has the meaning of hadron temperature. It has been found that $T \approx m_\pi$ is universal for a great number of reactions and secondary hadrons.

Some new data on this subject have appeared at the conference.

The reactions

$\pi^- p \to m\pi + x$; m = 2,3,4

have been studied at a 40 GeV energy of incident π^- in paper /32/. The pionic systems ($m\pi$) are chosen in order to investigate their transverse momentum distribution. Figure 26 shows the mean transverse momentum of the pionic system as a function of its mass. It is found that p_T has nearly a linear dependence on mass and is not sensitive to the charge and number of particles in the system. The temperature determined by (16) is also remarkably constant: $T \approx 130$MeV.

In paper /33/ a similar consideration has been applied

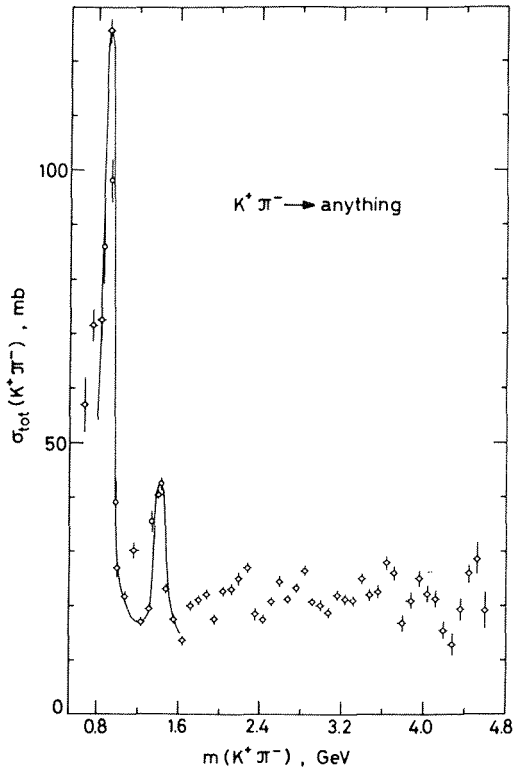

Fig. 25. Total cross section of K π interactions obtained from the reaction $K^+p \rightarrow \Delta^{++}x^0$.

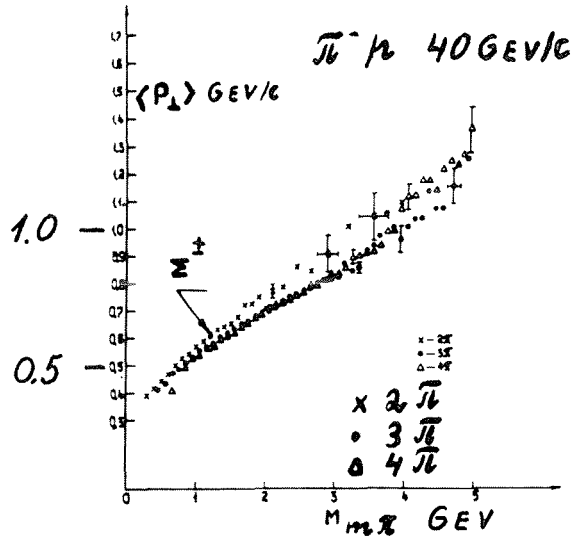

Fig. 26. Average transverse momentum as a function of the pionic mass.

for $\Sigma^\pm$ produced in the reaction $K^-p \rightarrow \Sigma^\pm x$. The average transverse momentum for $\Sigma^\pm$ is marked in fig. 26. It fell on the curve of the pionic systems. This once more demonstrates a statistical nature of the transverse momentum spectra, where all the particles and systems of particles get into equilibrium, and nature makes no distinctions between them.

In the K^-p experiment /34/ single and double vertex diffractive events are separated.

$$K^-p \text{ --- } (n \quad K^-) + p$$
$$\text{--- } K^- + (n \quad p)$$
$$\text{--- } (n \quad K^-) + (n \quad p);$$

$n = 2,4$. ($p_{K^-} = 32$ GeV/c)

These processes are selected by the maximum rapidity gap method. The rapidity and angular distributions of K*, K, Δ, p are analysed in the rest frame of the diffractively produced system. These distributions are mainly symmetric. Some leading effect of protons for decaying the system (p2 π) is explained by the Deck model. The p_T distributions of the decay products of the diffractive system are reasonably well described by the statistical model (16) with a temperature close to m π (see fig. 27).

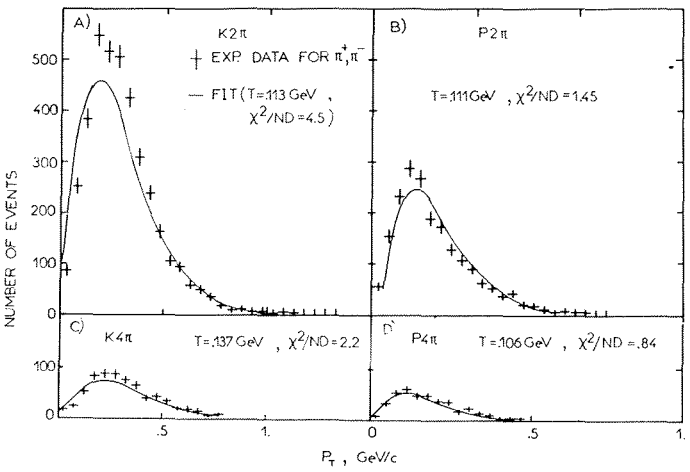

Fig. 27. p_T distributions of π -mesons from decay of the diffractively produced ($n\pi$,K), ($n\pi$,p) systems. Solid lines--statistical model (16).

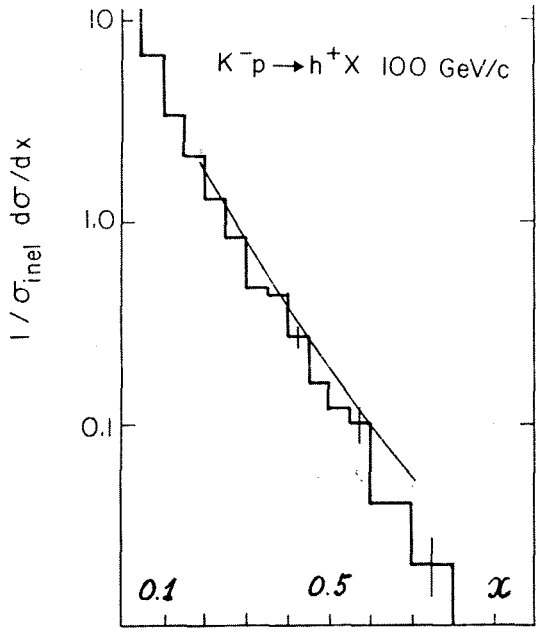

Fig.28. Check of the quark fragmentation model (17) (solid curve) against experimental data on the reaction $K^-p \to \pi^+ x$.

4. Single-particle inclusive reactions and the quark--parton model

A number of articles have been published in the last few years devoted to the explanation of low p_T hadron reactions in terms of the quark-parton model /38/. There are several approaches to the subject.

In the quark fragmentation model the interaction is due to wee parton (quark), and almost all of the initial momentum is carried away by the remaining (one or two) valence quarks. Then these constituents fragmentize into the final state. The x-distributions of inclusively observed particles are then given by the incoherent sum of contributions from "decaying" quarks.

In the paper /35/ the model of quark fragmentation is implemented to describe the inclusive cross section of K^-p interactions at 110 GeV. Assuming that the fragmentizing quark carries a fraction x_o of initial momentum ($x_o \approx 1$), one has the following expression for K fragmentation into hadron h:

$$\frac{1}{\sigma_{in}} \frac{d\sigma}{dx} = \frac{1}{2} \left(D_c^h\left(\frac{x}{x_o}\right) + D_{\bar{u}}^h\left(\frac{x}{x_o}\right) \right) \qquad (17)$$

The fragmentation function D(x) is known experimentally from lepton-hadron interactions.

There is a good agreement between the prediction of model (17) and experimental data. One example of their correspondence is shown in fig. 28. Similar results have been obtained for the region of proton fragmentation.

The second approach is usually referred to as the quark recombination model. According to this model, fragments are produced via the recombination of valence quark with sea antiquark (or vice versa).

For the reactions of K^- fragmentation $K^-p \to \pi^\pm x$ this may be illustrated graphically as follows:

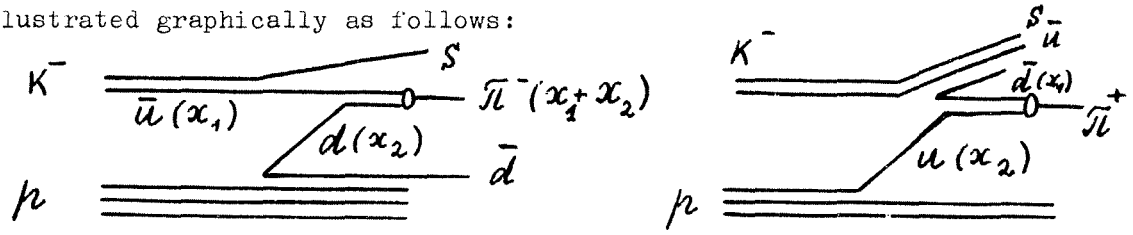

The x-distribution of the fragment reads

$$\frac{2E}{\sqrt{s}\,\sigma_{in}}\,\frac{d\sigma}{dx} = \int F(x_1x_2)\,R(x_1,x_2,x)\,\frac{dx_1}{x_1}\,\frac{dx_2}{x_2}\,, \qquad (18)$$

where F is the joint probability of $q\bar{q}$ momentum distribution.

$$F(x_1,\ x_2)=F_q(x_1)\cdot F_{\bar{q}}(x_2)\cdot \beta\cdot(1-x_1-x_2) \qquad (19)$$

Here $F_{q,\bar{q}}$ are the quark distribution functions, $\beta\,(1-x_1-x_2)$ the phase-space factor and R is the recombination function.

$$R = \frac{x_1}{x}\,\frac{x_2}{x}\,\delta\left(1-\frac{x_1}{x}-\frac{x_2}{x}\right) \qquad (20)$$

We see how the inclusive cross section in this model is related to the quark momentum distributions. This approach provides an interesting check of a quark-parton picture of the hadron behaviour. It can be also used to determine the valence quark distribution in mesons for which there is no information from lepton- hadron collisions.

The model (18-20) has been successfully used for the description of K^- fragmentation at 110 GeV [35]. In particular, the shape of the valence quark momentum distribution in the kaon is found to be $\sim (1-x)^{1.0\pm0.3}$. This result is compatible with the valence quark distribution in the pion derived from low p_T hadron data by the same method.

The inelastic $\bar{p}p$ interaction at 32 GeV/c has been studied in paper [36]. It is shown that the x-distribution of $\pi^\pm$ - mesons in the fragmentation region of p and $\bar{p}$ is compatible with the prediction of a quark-parton model of the type (18).

The ratio $R = \pi^+/\pi^-$ in the proton fragmentation region shows interesting features: it depends on the type of incident particle and its energy [37]. For example, at E = 16 GeV and $x \approx 0.7$ $R_{\pi^+p} \approx 10$, $R_{pp} \approx 5$ and $R_{\pi^-p} \approx 1.5$. When energy rises, R seems to approach the scaling limit $R \approx R_{pp} \approx 5$. The models outlined above cannot account for these effects. An additional mechanism is suggested [37] which can be described by means of triple Regge and valence quark annihilation.

We see that parton concepts appear to be useful for understanding gross

features of data and promise to give a key for common description of lepton-hadron and hadron-hadron interactions. But at the present stage the parton model contains some weak points: it is not well-founded on theoretical principles and contains somewhat arbitrary assumptions (phase-space factor in (19) and recombination function (20)). It is known experimentally that the contribution of resonances to multiparticle production is large ($\sim$ 80%). This effect may mask true quark distributions. Scaling violation and gluonic effects need a further analysis.

IV. CONCLUSION

Let us summarize the main results which have been reviewed in this report.

1. The consequences of quantum field theory which have been tested in experiments on binary reactions are found to be valid in an energy range of up to 2 TeV.

2. The rate of shrinkage of the cones of elastic pp, pd and pHe scattering is different. The model of inelastic screening gives a qualitative explanation of data.

3. The total cross section of pHe interactions rises in an energy interval of 100-400 GeV.

4. π^-p charge exchange reactions show that $\alpha_\rho(t) \approx \alpha_{A_2}(t)$ at $0 \leq |t| \leq 0.7$. The meson octet-singlet mixing angle is $\theta \simeq -18°$.

5. Deuteron serves as an analyzer of the pp $\to$ Xp scattering amplitude. Different helicity states in this amplitude are important.

6. Triple Regge expansion gives a satisfactory common description of pp, Kp and π p diffractive processes.

7. The nature of scaling violation at $x \approx 0$ is not clear. There are two alternative explanations: double Regge expansion and dual topological pomeron model.

8. The quark-parton model provides a means for common understanding of lepton-hadron and hadron-hadron collisions.

Here is an obvious suggestion of new experiments which would resolve some of the above problems.

1. It is worthwhile to continue studies of elastic and diffractive dissociation reactions of protons with light nuclei. Since pd and dd experiments at ISR were successful, it seems reasonable to extend this program on a wider sample of nuclei.

2. The lack of $\bar{p}p$ and $\bar{p}A$ data may be made up by a gas jet target experiment using an antiproton storage ring.

3. The study of inelastic pp interactions at a polarized target is welcome. This experiment will apply new serious restrictions on the quark-parton model.

4. The like-particle interference phenomenon should be investigated using statistics of one or two orders of magnitude higher than that accessible now by means of a bubble chamber /39/.

I want to express my deep gratitude to all the authors of contributions to this conference who had fruitful discussions with me and were patient enough explaining me some specific topics of their study. These stimulating contacts helped me a lot in the preparation of this report.

R e f e r e n c e s

1. E.Jenkins et al. to be published in Phys. Rev.
2. V.A.Nikitin, Elem. part and nuclei, v. 10, 581 (1979), ibid S.V.Mukhin, V.A.Tsarev, v. 8, 990 (1977) (russian).
3. Y.J.Azimov et al. JETP Lett., 23, 131 (1976) (in russian).
4. G.L.Kane and A.Seidl, Rev. Mod. Phys., 48, 309 (1976).
5. W.Majerotto, Forts. der Physik, 24, 237 (1976).
6. B.S. Kopeliovich and L.J.Lapidus, JETP, 71, 61 (1976) (russian).
7. S.V.Mukhin, V.A.Tsarev, JINR preprint E2-12293 (1979).
8. C.Lewin et al., paper 202; P.V.Shliapnikov et al., paper 226.
9. R.Henzi and P.Valin, papers 107, 108 and Nucl. Phys. B148, 513 (1979).
10. G.Fidecaro et al., Polarization measurements in pp elastic scattering at 150 GeV/c.
11. C.Bourrely and J.Soffer to be published Phys,Rev. D 19.
12. J.J.Levintov, ITEP-144 (1978).
13. W.D.Apel et al., papers 263, 264, 265, 266.
14. E.Jenkins et al., to be publieshed.
15. D.Berg et al., paper 34.
16. E.L.Feinberg and I.Ya.Pomeranchuk, Suppl. Nuovo Cim,111, 652 (1956).
17. M.A.Good and K.D.Walker, Phys. Rev., 120, 1857 (1960).
18. H.J.Mietinnen et al., Phys. Rev. D18, 1969 (1978).
19. B.Z.Kopeliovich et al., paper 182 and JINR preprint E2-12288 (1979).
20. G.Goggi et al., paper 207.
21. Yu.Arestov et al., paper 240.
22. R.Migneron, J.L.Robinson, Triple pomeron coupling and pion inclusive scattering, paper 296.
23. R.Field and G.Fox, Nucl. Phys. B80, 367 (1974).
24. S.Y.Chu at al., Phys. Rev., D13, 2967 (1976).
25. Yu.Kazarinov et al., JETP, 70, 1152 (1976) (russian).
26. J.V.Ajinenko et al., papers 66, 200, 225.
27. De Wolf et al., paper 67.
28. R.T.Van de Valle et al., paper 106.
29. Yu.Arestov et al., paper 127.
30. A.Capella et al., Phys. Lett., 81B, 68 (1979).
31. P.V.Sliapnikov et al., Study of reaction $K^+p \to \Delta^{++}x^\circ$ at 32 GeV.
32. N.S.Angelov et al., JINR, P1-12110, Dubna (1979).
33. H.Böttcher et al., paper 92.
34. Y.Arestov et al., paper 171.
35. F.Mandel et al., paper 28.

36. Yu.Arestov et al., paper 127.
37. B.Buchbeck et al., paper 155.
38. K.P.Das and R.C.Hwa. Phys. Rev. Lett. 69 B, 459 (1977).
D.W.Duke and F.E.Taylor, Phys. Rev. D1788 (1978).
R.Diebold, Proc. of the 19th Int.Conf. on High Energy Phys., p.666, Tokio (1978).
39. V.V.Babintsev et al., paper 122.

* * *

DISCUSSION

Chairman: Yu.D. Prokoshkin

Sci. Secretaries: W.M. Geist and J.P. Martin

R. Henzi (comment): As you have mentioned, at fixed energy there are five parameters in our analysis which correspond roughly to the total cross-section, the forward slope, the positions of the diffraction zero and of the 2nd diffraction maximum and to the height of the latter. Outside of these points the differential cross-section shows upward curvatures which might require further parameters, however these curvatures are correctly predicted by the model. A rescattering analysis of these results can be done which shows that these curvatures are rescattering effects and that the diffraction zero at 1.4 $(GeV/c)^2$ is "accidental" in nature and I would like to go on record saying that other such "accidental" diffraction zeros are possible but not before $|t| \approx 30$ $(GeV/c)^2$.

G. Goggi: In our ISR experiment on pd and dd elastic scattering we observed that the large inelastic shadow corrections that contribute at these energies are very sensitive to the form of triple-Regge parametrization of pp → pX data that is used as input. In the light of this, could you comment on the analysis of p^{4}He elastic scattering?

V.A. Nikitin: We made an attempt to apply the Glauber formula. The input NN inelastic amplitude was similar to what Alberi and Goggi used. We achieved a reasonably good description of the proton-helium diffractive cross-section. But it is not clear how to treat the x-x vertex (i.e. jet-jet transition): at least two parameters have to be introduced. We feel it is a weak point of the inelastic scattering model. In its present form, it has no clear correspondence with the parton model.

PHOTO- AND HADROPRODUCTION OF NEW FLAVOURS

D. Treille
CERN, Geneva, Switzerland

ABSTRACT

The hadroproduction and photoproduction of charm are reviewed. A rich but still confused set of data is now available. Possible evidence for beauty is reported.

I will concentrate mostly on the hadroproduction of charm, with a brief mention of beauty and various references to strangeness. Such studies give us information about the production and dressing of heavy quarks; eventually they can also provide interesting results on the spectroscopy of new particles. Many new data are available: but the field is yet in its infancy and much confusion has to be sorted out.

To identify charm production, we can:

- either look directly at the decay of charm, with emulsions or an equivalent technique;
- or use as an indicator the few known channels into which it decays. This leads to:

i) indirect measurements of charm production, by detecting the prompt leptons from its semi-leptonic channels (e, μ, ν, eμ, etc.);

ii) bump hunting (Kπ, K$\pi\pi$, K$\rho\pi$, etc.): there we can benefit from the zero width of charmed objects and eventually the exoticity of decay channels, while the difficulties generally arise from combinatorial problems.

1. EMULSIONS

We look for charged or neutral decays close (50 μ to a few mm) to the primary vertex. Early hyperon decays or the interactions of secondaries can simulate charm decay, and if we evaluate the probability of such a background, we find that single "accidents" will never be a convincing proof. We must either look for double accidents, where the two decays are seen, or back the emulsion with a spectrometer providing the identification and the effective mass of the decay products. An example of the first kind[1] is shown in Fig. 1: if it is interpreted as D^0 and $\bar{D}^0$ decay, the lifetime and cross-section are in good agreement with the world values. As far as we know, only two such events do exist[2]. An example of the second kind, from WA58 at CERN[3], is described by Fig. 2, which shows a very likely candidate for $\bar{D}^0$ decay. The mass and quantum number are correct. The measured lifetime (2.3×10^{-14} s) is short, but it could be shown that the scanning method of this experiment favours early decays. The missing companion can have gone into neutrals.

A past emulsion experiment[4] gave a quite embarrassing upper limit for charm hadroproduction of ~ 1.5 μb at 300 GeV: however, Fig. 3 shows that with the presently admitted charm lifetime ($\sim 5 \times 10^{-13}$ s) this limit can be one order of magnitude higher. The disagreement with the other measurements would then disappear.

Finally, since scanning emulsions is time-consuming and difficult, other techniques providing a similar spatial resolution should be invented. Figure 4 shows an interesting event obtained in LEBC, the newly built small LH_2 bubble chamber at CERN[5]. The V^0 and secondary vertex contained in this event are not visible on the figure owing to the loss of

resolution during the reproduction. But we can look at the scale and at the size of a bubble of BEBC shown for comparison, and appreciate the quality and resolving power of this chamber.

2. INDIRECT MEASUREMENTS

2.1 Prompt ν

I report here on the results of the CERN neutrino beam dump (second version). Its principle is well known[6]. The detectors were BEBC, the CDHS[7], and CHARM[8] spectrometers. Gargamelle was no longer there. The target density was varied, and an extrapolation to infinite density allowed to get the prompt ν signal. Table 1 [9] gives the available numbers for all prompt signals observed. Summarizing it:

i) all three experiments agree on the value of the prompt signal and find what CDHS found in the first run;

ii) they do not contradict the equality of $(\nu_\mu + \bar{\nu}_\mu)$ and $(\nu_e + \bar{\nu}_e)$ signals, but do not prove it either;

iii) the separation of the polarities in the prompt signals is as yet preliminary and will always be affected by large uncertainties.

iv) the interpretation in terms of charm decay is probably right. Extracting a cross-section requires some knowledge of the longitudinal distribution of the charm parents. In principle, information on this does exist in the data (for instance, through the observed E_ν distribution): the constraint will not be very strong but a good lower limit should be obtained[10]. Generally quoted values for the charm production cross-section are ∿ 40 μb (for $A^{2/3}$) and 10 μb (for A).

2.2 Prompt μ

An experiment performed at FNAL (Fig. 5) has found a prompt μ signal[11] at moderate p_T and small x ($10 < E^{\mu^+} < 60$ GeV for 400 GeV protons). In that region the prompt signal is about equal to the pair signal. They also see a signal in $\mu^+\mu^-$ + missing energy. Interpreting both as a manifestation of charm, they get cross-sections in the 20 μb region. Prompt $e^\pm$ signals have been discussed in the past.

2.3 eμ, ee

Experiment No. R702 at the CERN Intersecting Storage Rings (ISR)[12] gave results on charm production in the central region. From their three-arm spectrometer (Fig. 6) they get eμ, e^+e^- same-side, e^+e^- opposite-side pairs. Discarding the mass regions with too much background (ψ, ρ, Dalitz $e^\pm$) they fit all data with a production model inspired by Bourquin and Gaillard[13] (and therefore relevant only for central production). They get a charm cross-section of 10.1 ± 2.3 μb per unit of rapidity in the central region.

3. DIRECT SIGNALS

Three experiments[14] at the ISR have obtained signals of Λ_c^+ [and D^+ in one case[15]] production (Figs. 7 to 10). All three observe the signal at quite large x. This forward production is strongly favoured by their trigger and selection procedure. The cross-sections they measure are in rough agreement (Table 2) and lead, with reasonable assumptions[16] on branching ratios, to charmed baryon production in the 50-100 μb region. This is not a surprise for some theorists[17] who expect this from a purely diffractive mechanism.

They clearly demonstrate that besides central production another mechanism for charm production is at work. A quite flat x distribution for Λ_c is likely, if one refers to Λ production from protons. However, it is a surprise for D^+, which seems quite different from K's. It is necessary to invoke some type of recombination mechanism[18] which does not seem to apply for strangeness.

4. SUMMARY OF RESULTS

A full understanding of how charm is hadroproduced is obviously missing. However, we can at least put some order in the data and re-evaluate them with a common set of assumptions. For instance, a reasonable guess is probably to assume an $A^{0.9}$ dependence, since this value is observed for Drell-Yan pairs at the same mass. It has been shown[19] that such a treatment reduces the most outstanding discrepancies and exhibits a crude excitation curve (Fig. 11). Comparing these results with the theoretical predictions (or postdictions)[20], we observe that first-order QCD calculations are somewhat low, which is not a surprise since they describe only central production. The best fits come from models which in one way or the other go beyond this first-order approximation.

5. BEAUTY

Here we mean bound states (such as $b\bar{u}$) of the b quark ($\sim$ 5 GeV, charge = $-1/3$) with ordinary ones. They cannot lie far from 5.3 GeV. It has been shown[21] that if they are produced more abundantly than the T, they are not long-lived ($< 10^{-8}$ sec). In the most likely models, for instance the KM model[22] they are predicted[23]

i) to have a lifetime of $O(10^{-14}$ s);

ii) to decay mostly by a $b \to c \to s$ cascade.

Both properties suggest which experimental methods should be used to search for them. For hadroproduction of such objects, predictions differ widely[24]. However, we can guess that relative to the T they are at least as abundant as charm relative to the ψ.

Finally, it is certain that their detection will be difficult unless extremely constrained decay channels do exist. A clever suggestion[25] is that the B could have a few percent probability to decay into ψ + strangeness. This could look futuristic. However, WA11 [26] at CERN was able to check it. They select final states having a $\psi \to \mu^+\mu^-$; they measure all other particles and identify some of them. A compact arrangement of multiwire proportional chambers (MWPC) allows for a good reconstruction of V^0's. Owing to the extreme selectivity of their trigger and their high luminosity, their sensitivity is quite impressive for such an open spectrometer. One entry in Fig. 13 corresponds to a production cross-section of 10 pb. This figure shows the effective mass for $\psi K^0\pi^\pm + \psi K^-\pi^+$ combinations obtained without any sophisticated cut; $\psi K^+\pi^-$ has not been used because the K^+ signature is more ambiguous. The least one can say is that the 4σ effect in Fig. 13 should encourage more work along these lines. If it is due to naked beauty, it would correspond to a production cross-section of $\sim$ 100 nb, which is by no means unrealistic[24].

6. PHOTOPRODUCTION

The CIF Collaboration at FNAL reported the first observation of the D in photoproduction for a mean γ energy of $\sim$ 100 GeV [27]. It is seen in $K^\pm\pi^\pm$ (Fig. 14). The exploration of other

channels supports this without adding much significance. A production model assuming diffractive $D\bar{D}$ production leads to a cross-section of 600 ± 240 nb for $D^0\bar{D}^0$. There is nothing new on $\bar{\Lambda}_c$ production since last year[28]. The WA4 experiment at CERN provides upper limits already quoted at Tokyo[28]: more results will be available at the FNAL eγ meeting. The present data, shown in Fig. 15 together with some predictions, do not allow any definite conclusions. However, it is likely that the "excess" observed in σ_{tot} at FNAL[28] is not entirely due to charm production.

REFERENCES

1) H. Fuchi et al., DPNU-8-79, March 1979.

2) For the first one, see N. Ushida et al., Lett. Nuovo Cimento 23, 577 (1978).

3) Presented by A. Conti at this conference (parallel session 1).

4) See G. Coremans Bertrand et al., Phys. Letters 65B, 480 (1976).
D.J. Crennell et al., Rutherford preprint RL 78-051A (1978).

5) J. Lemonne et al., NA13 proposal, CERN/SPSC 77-44 and CERN/SPSC 78-91.

6) See, for instance, K. Kleinknecht, Proc. Int. Conf. on High-Energy Physics, Tokyo, 1978 (Physical Society of Japan, Tokyo, 1979), p. 378, or
H. Wachsmuth, Proc. Topical Conf. on Neutrino Physics, Oxford, 1978 (Science Research Council, Rutherford Lab., Didcot, 1978), p. 233.

7) T. Hansl et al., Phys. Letters 74B, 139 (1978).

8) Presented by W. Kozanecki at "Neutrino-79", Int. Conf. on Neutrinos, Weak Interactions and Cosmology, Bergen, 1979.

9) Presented by P. Schmid, by S. Loucatos, and by P. Monacelli at this conference (parallel session 1).

10) K.W.J. Barnham and N.S. Craigie, IC/HENP/78/24 (1978).

11) Abstract No. 1 submitted to this conference, and paper contributed by B.C. Barish et al. to this conference, communication by A. Bodek.
See also B. Barish, Proc. Int. Conf. on High-Energy Physics, Tokyo, 1978 (Physical Society of Japan, Tokyo, 1979), p. 383.

12) Presented by A. Clark at this conference (parallel session 1), and CERN EP/79-13 (February 1979).

13) M. Bourquin and J.M. Gaillard, Nucl. Phys. B114, 334 (1976).

14) ACCDHW Collaboration (Split field), D. Drijard et al., communication by H. Frehse.
ACHMNC (Lampshade), K.L. Giboni et al., communication by F. Muller.
Los Angeles-Saclay (R603), W. Lockman et al., UCLA 1125 (1979), communication by P. Schlein.

15) D. Drijard et al., Phys. Lett. 81B, 250 (1979).

16) J.G. Korner et al., DESY 78/13 and 78/53 (1978).

17) G. Gustafson and C. Peterson, Phys. Lett. 67B, 81 (1977).

18) J. Ranft, KMU-HEP 7903 (1979).

19) W. Geist, Paper contributed to this conference.

20) H.M. Georgi et al., HUTP-78/A008 (1978)*.
C.E. Carlson et al., SLAC PUB 2212 (1978).
J. Babcock et al., Phys. Rev. D 18, 162 (1978).
Y. Ezawa et al., preprint from Ehime University, Matsuyama 790.
H. Fritzsch and K.H. Streng, CERN-TH 2520 (1978).
B.L. Combridge, CERN-TH 2574 (1978).

21) R. Diebold, Proc. Int. Conf. on High-Energy Physics, Tokyo, 1978 (Physical Society of Japan, Tokyo, 1979), p. 666.
G. Giacomelli, Proc. Int. Conf. on High-Energy Physics, Tokyo, 1978 (Physical Society of Japan, Tokyo, 1979), p. 53.

22) M. Kobayashi and K. Maskawa, Progr. Theor. Phys. 49, 652 (1973).

23) V. Barger et al., Phys. Rev. Lett. 42, 1585 (1979).
R.E. Shrock et al., Phys. Rev. Lett. 42, 1589 (1979).

24) Most of the authors of Ref. 20 give predictions for $B\bar{B}$ states.

25) H. Fritzsch, CERN-TH 2648 (1979).

26) R. Barate et al., Paper presented at the 13th Rencontre de Moriond, Les Arcs, 12-24 March 1978.

27) Presented by S. Holmes at this conference (parallel session 1).

28) E. Gabathuler, Proc. Int. Conf. on High-Energy Physics, Tokyo, 1978 (Physical Society of Japan, Tokyo, 1979), p. 841.

Table 1

	CDHS	CHARM	BEBC
Mass (tons)	∿ 500	99	12.5
Distance from target (m)	890	910	820
ν flux dilution	0.85	0.81	1
Solid angle (μsr)	10.2	6.9	10.0
Events/(ton$\cdot 10^{17}$ p)			
E_{sh} > 10 GeV			
ρ = 1/3: 0 μ	0.65 ± 0.10	0.65 ± 0.06	0.90 ± 0.17
1 μ	1.19 ± 0.10	1.06 ± 1.07	1.33 ± 0.21
0 μ/1 μ	0.54 ± 0.08	0.61 ± 0.07	0.68 ± 0.16
ρ = 1: 0 μ	0.33 ± 0.04	0.38 ± 0.03	0.31 ± 0.05
1 μ	0.52 ± 0.03	0.48 ± 0.03	0.43 ± 0.05
0 μ/1 μ	0.64 ± 0.08	0.79 ± 0.07	0.72 ± 0.14
ρ = ∞: Excess $\overset{(-)}{\nu}_e$ (NC + CC)	0.11 ± 0.08[a]	0.19 ± 0.05	
Excess $\overset{(-)}{\nu}_\mu$ (CC)	0.19 ± 0.07	0.19 ± 0.06	
Excess 0 μ	0.17 ± 0.08	0.25 ± 0.05	
$e^- + e^+$ (E_ν > 10 GeV)			0.13 ± 0.03[b]
$\mu^- + \mu^+$ (E_ν > 10 GeV)			0.30 ± 0.13[b]

a) Deduced from the results
b) Preliminary, obtained by combining old and new results.

Table 2

ACCDHW Collaboration (Split field)

x range $\begin{cases} \Lambda_c^+ \to \bar{K}^{*0} p & 0.5 < x < 0.9 \\ \Lambda_c^+ \to K^- \Delta^{++} & 0.35 < x < 0.95 \end{cases}$

Angular distribution: $\propto e^{-2p_T}$

	$\bar{K}^{*0}p$	$K^-\Delta^{++}$
$\frac{d\sigma}{dy}$ = const	Bσ = 6.2 μb	Bσ = 6.7 μb
$\frac{d\sigma}{dx}$ = const	Bσ = 3.0 μb	Bσ = 3.3 μb

ACCMNR Collaboration (Lampshade)

Kinematic region $\begin{cases} 10 < M_X < 28 \text{ GeV/c}^2 \\ 0.3 < x < 0.8 \\ 0 < p_T < 1 \text{ GeV/c} \end{cases}$

$\Lambda_c^+ \to K^- p \pi^+$ Bσ = 0.7-1.8 μb

$\Lambda_c^+ \to \Lambda^0 \pi^+ \pi^+ \pi^-$ Bσ = 0.3-0.7 μb

Los Angeles - Saclay

0.75 < x < 0.90

$\Lambda_c^+ \to K\bar{p}n^+$ Bσ = 2.8 ± 1 μb

$\Lambda_c^+ \to \Lambda^0 \pi^+ \pi^+ \pi^-$ Bσ = 2.3 ± 0.3 μb

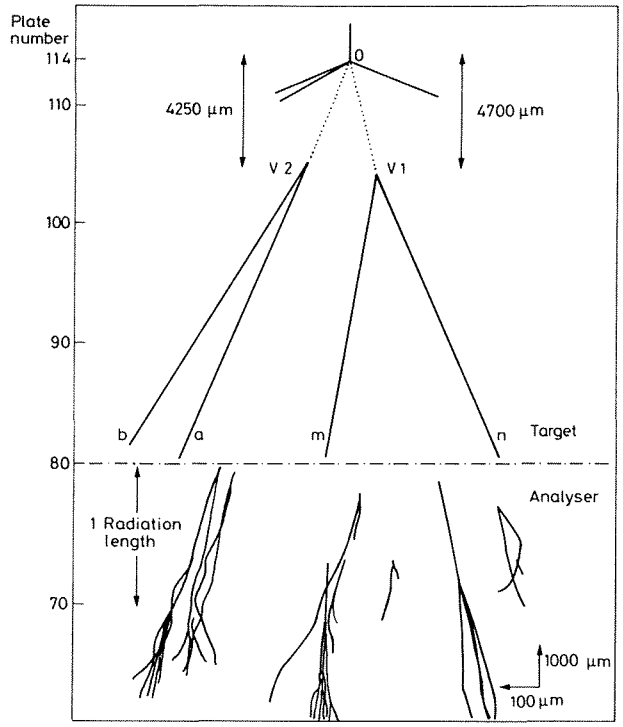

Fig. 1 Schematic view of an event in an emulsion chamber showing a double decay. There is a strong momentum imbalance for each V^0. Both decaying particles could be D^0's with missing K^0's.

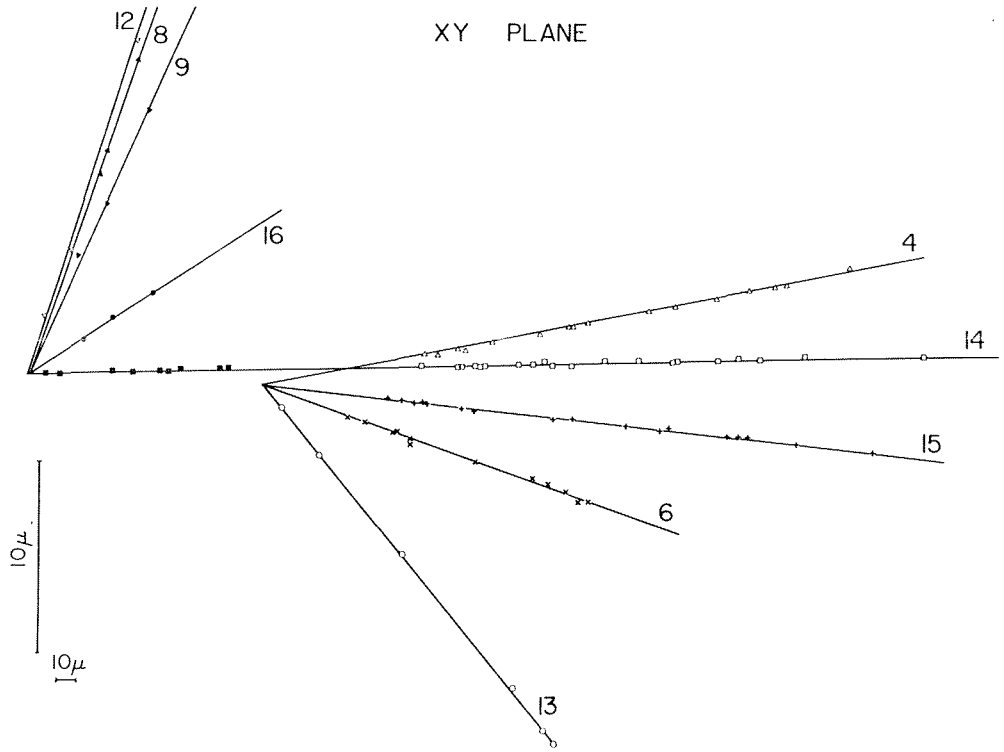

Fig. 2 An emulsion event from photoproduction (WA 58 at CERN). A neutral star with four prongs has all its prongs measured in the Ω spectrometer; one is identified as a K^+. The other three are compatible with π. The effective mass of the $(K\pi\pi\pi)^0$ system is (1867 ± 10) MeV.

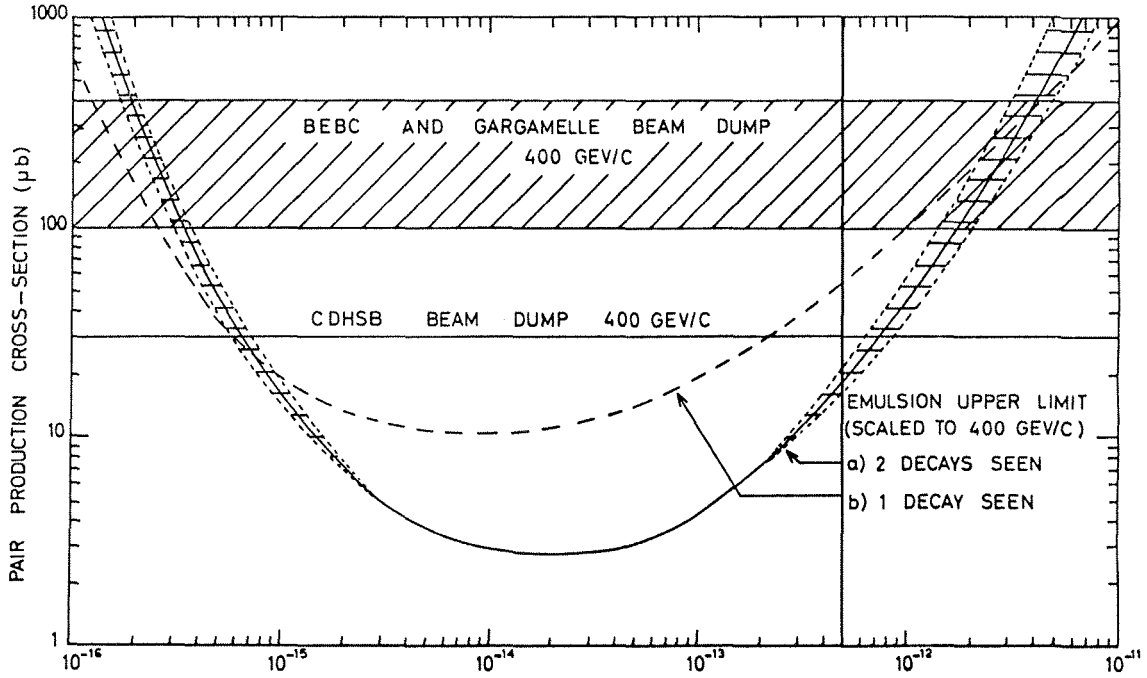

Fig. 3 Upper limit versus lifetime for charm hadroproduction (from G. Coremans Bertrand et al., Ref. 4). The measurement from Gargamelle should be ignored.

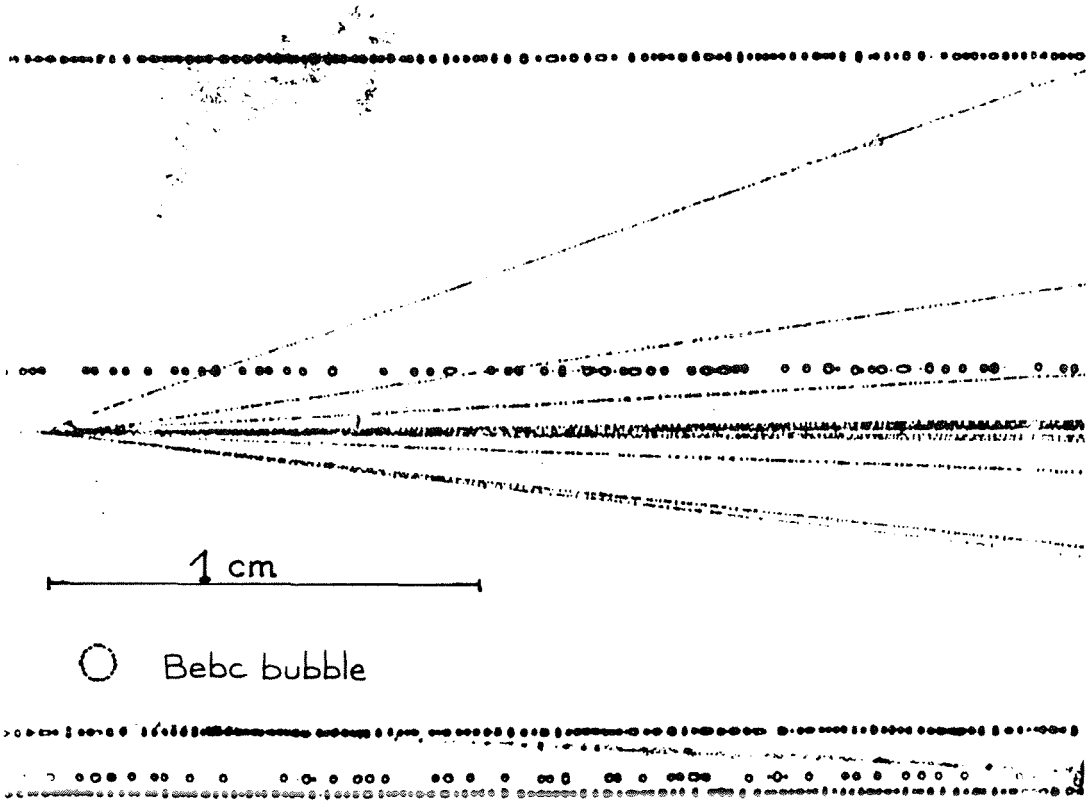

Fig. 4 A cliché from the LEBC bubble chamber

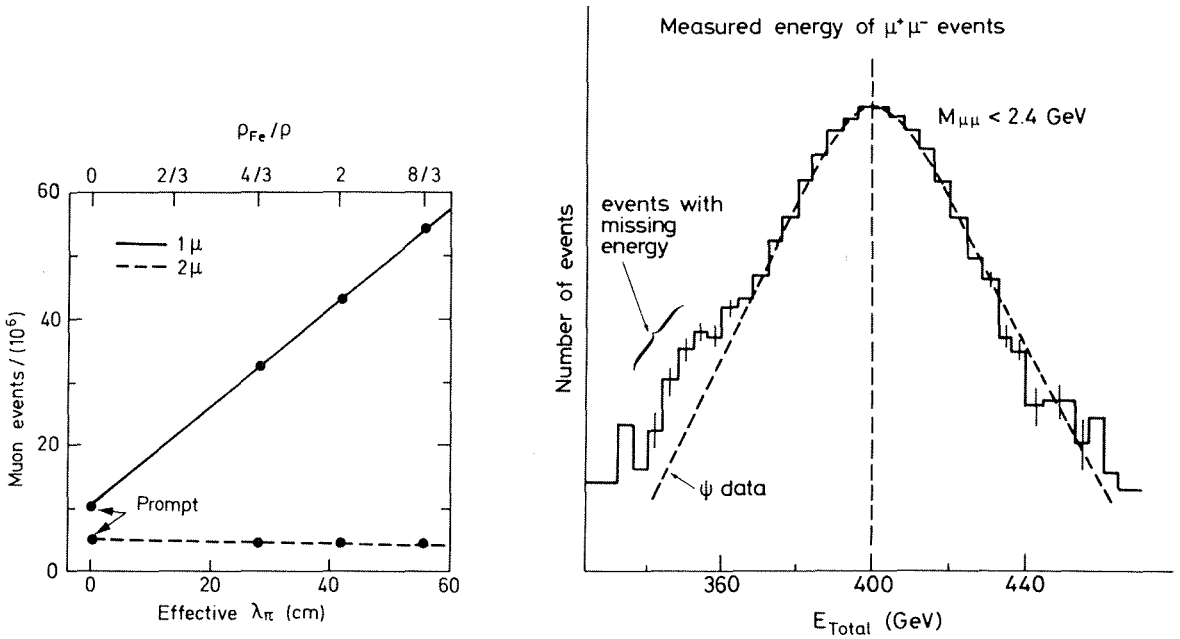

Fig. 5 The evidence for a prompt μ signal (a) and missing energy in $\mu^+\mu^-$ events (b)

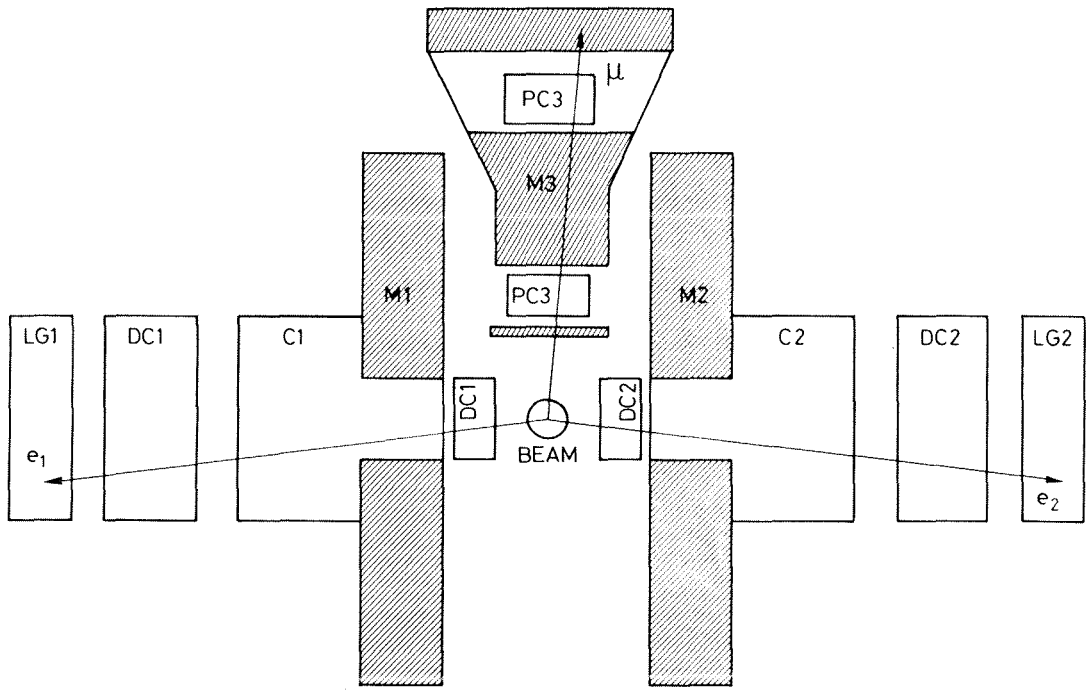

Fig. 6 The three-arm spectrometer of CERN-Saclay-ETH (R 702) experiment

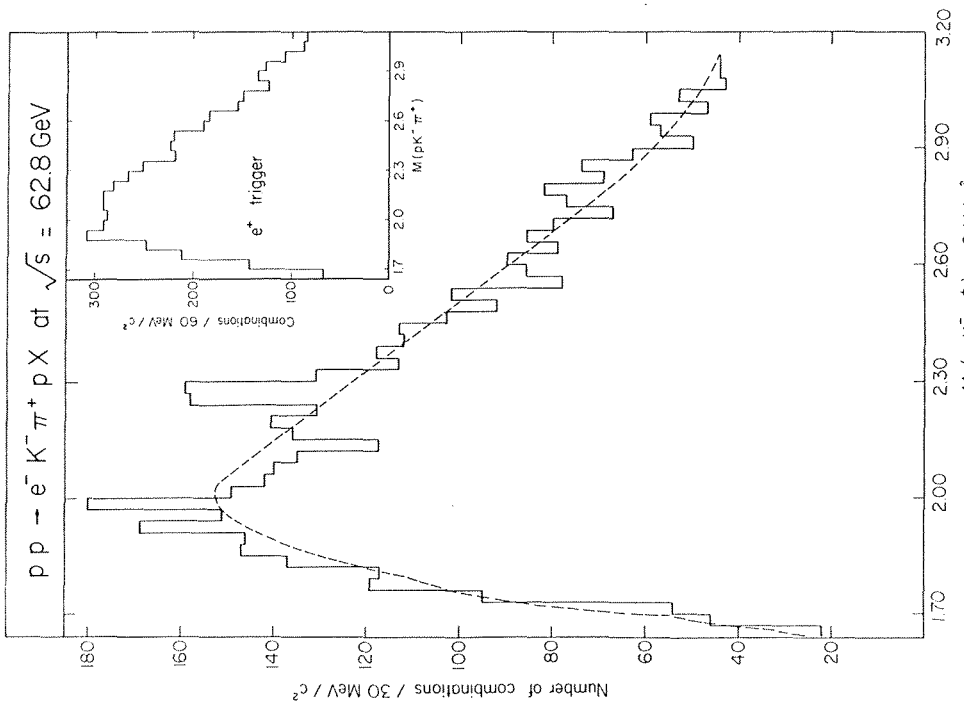

Fig. 8 The Λ_c^+ from ACCDHW (e trigger, low x)

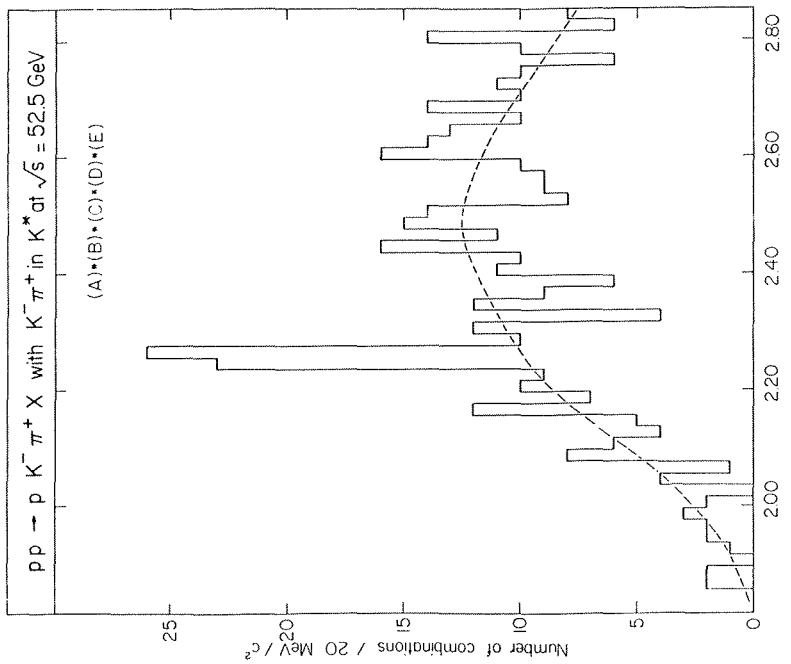

Fig. 7 The Λ_c^+ from ACCDHW (K trigger, large x)

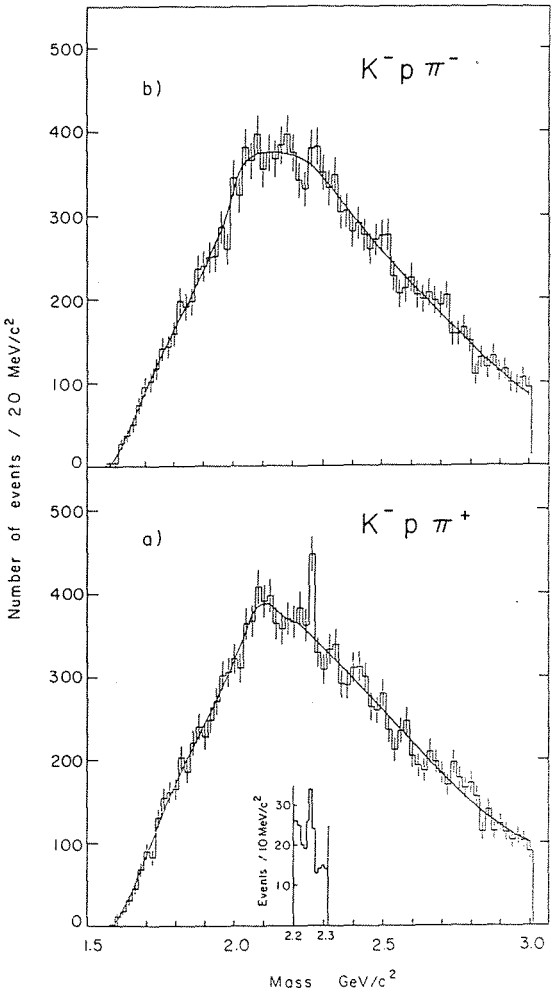

Fig. 9 The Λ_c^+ from ACHMNC (diffractive trigger)

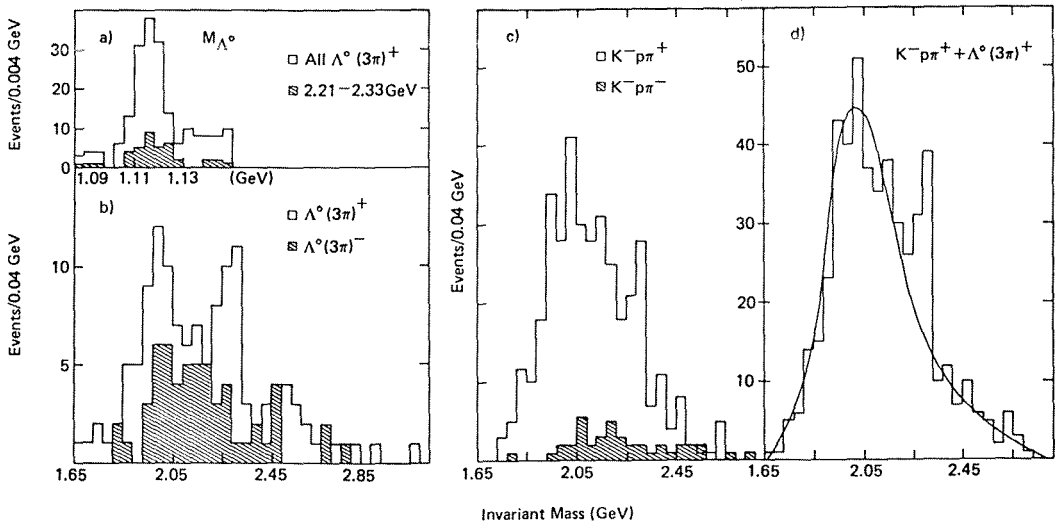

Fig. 10 The Λ_c^+ from Los Angeles-Saclay

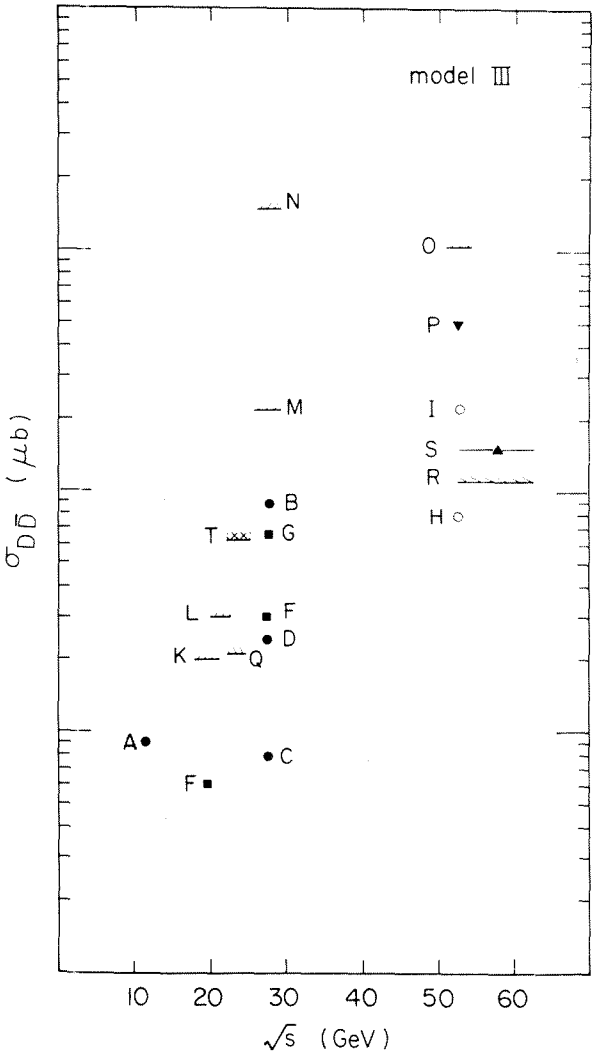

Fig. 11 Charm production excitation curve according to one of the models (III) considered in Ref. 19

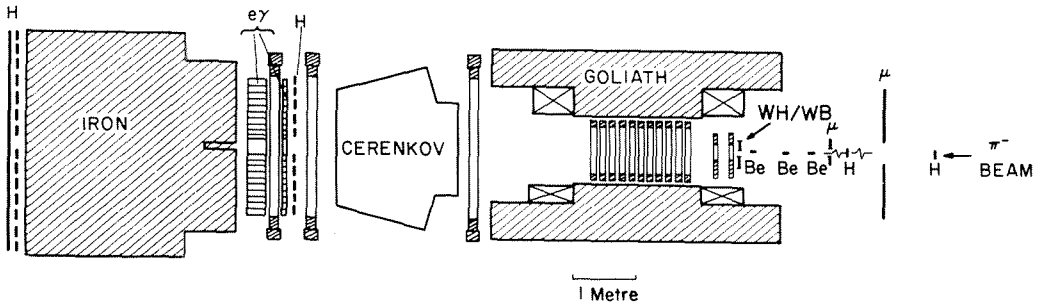

Fig. 12 The WA 11 spectrometer

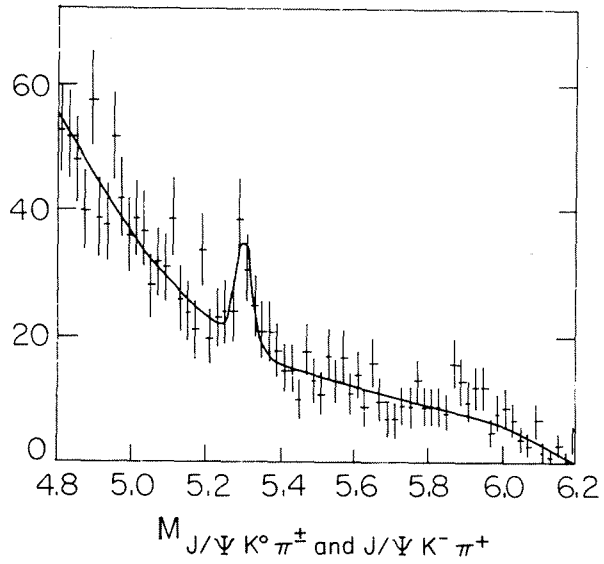

Fig. 13 The ψKπ spectrum from WA 11

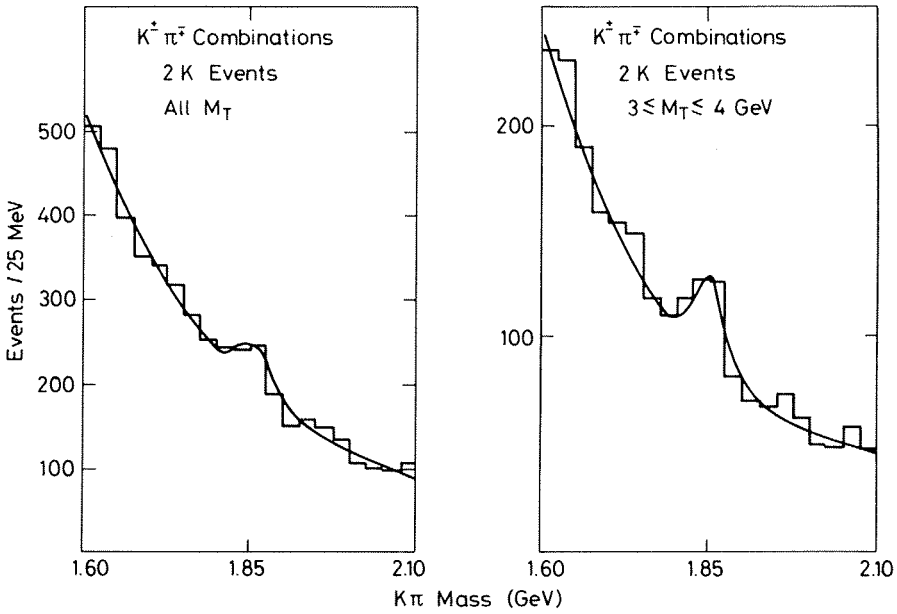

Fig. 14 The D → Kπ from the FNAL-CIF Collaboration

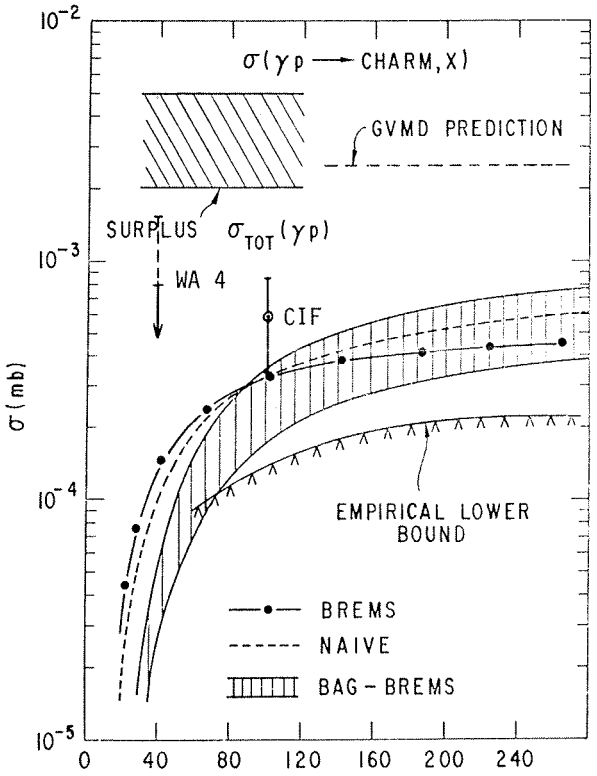

Fig. 15 Predictions and results in charm photoproduction. The results given by CIF are for $D^0\bar{D}^0$ only. The upper limits from the WA 4 experiment at CERN depend on the channel explored.

HIGH ENERGY INTERACTIONS ON NUCLEI

G. Vegni
Istituto di Fisica dell'Università and INFN, Milano, ITALY

ABSTRACT

Multihadrons production and coherent or semicoherent reactions on nuclei allow information about such intriguing topics as space--time development of particle production and interactions of resonances with nucleons. Some of the latest results are here summarized, with particular emphasis on the coherent and semicoherent channels, in connection with the criticisms and suggestions recently developed regarding the so called σ_2 cross-section (for the interactions of resonances with nucleons), as it is obtained from the A dependence of diffractive production on nuclei.

The two main lines, in which at present the nucleus is used as a tool to better understand elementary hadronic properties are:

a) the study of multiparticle production disregarding the final state of the nucleus, but looking at the number of emitted particles as a function of the rapidity y (or pseudorapidity η), p^2, Feynman's X_L, etc. for different nuclear sizes A (or $\bar{\nu} = \sigma_{hp} \cdot A/\sigma_{hA}$, the number of mean free paths in the nucleus from a "standard" point of view).

A comparison between the above quantities for different incident hadrons, at different energies (i.e. different "time of transit" in the nucleus) and with the equivalent distributions obtained on free proton, is an otherwise unavailable source of information about the space-time development of the elementary hadron-hadron processes and in regard to the way, and the extent to which nuclear matter reacts as a conglomerated target.

As it is known, different theoretical approaches on these subjects were developed: Multiperipheral models [1], Energy Flux model [2], Quark-Parton models [3], all of these mainly concerning the space-time development; and cumulative effects [4] or coherent tube models [5] in which the other point of view is mainly taken into account.

b) the analysis of coherent and semicoherent interactions, i.e. the study of the production of well-defined hadronic systems when the nucleus is left in a well-known state (either fundamental or excited).

Besides the original interest in using the nucleus as a filter to select and study particular spin-parity systems, mainly in the diffractive channels, growing attention has been paid in recent years to the results of the measurement of the so called "σ_2" parameter.

In the Glauber-Kölbig and Margolis (GKM) [6] formalism this parameter stands for the unstable produced system nucleon cross-section (a further quantity not otherwise available). Many different criticisms and suggestions were recently expressed about the above interpretation [7]; as we are going to see later on, the peculiar trend of the results obtained so far has strengthened both criticisms and suggestions.

According to some of these views, the amount of space-time required by the elementary hadronic systems to develop themselves does not allow to obtain σ_2 with the meaning of interaction cross-section of a "fully developed" system.

Such criticism is supported by the observation that multiparticles production on nuclei display little or no cascading. Instead it is suggested that it should be possible to obtain

more elementary information from σ_2 such as the distribution of cross sections for the eigenstates of diffraction, on the assumption that the eigenstates are parton states and the latter interact independently with the nuclear target (H.L. Miettinen and J. Pumplin [7d]).

Other views, though,suggest that σ_2 can be obtained from refining the GKM formalism: G. Fäldt and P. Osland [8] introduce, as corrections, spin flip terms in the production amplitudes to avoid or reduce the diminishing values of σ_2 with increasing produced masses.

In a paper presented at this Conference B.C. Kopeliovich et al. [9] argue that, when treating the inelastic diffraction on nuclei with a quark-parton eigenstate method, the inelastic diffractive amplitude turns out to have the opposite sign to the elastic amplitude. The authors' conclusion is that the neglecting of this correction is a reason for the diminishing values of σ_2.

Because of the space available I will try to discuss the recent findings concerning point b (coherent and semicoherent reactions) a little more extensively whereas, as far as point a (multiparticle production) is concerned, I shall confine myself to pointing out a few interesting features in three recent experiments. Extensive reviews on multiparticle production were recently made by W. Busza [10], A.M. Baldin [4], T. Ferbel[11].

I am also going to briefly discuss a recent result in the analysis and interpretation of the inelastic total hadronic cross-section on nuclei.

MULTIPARTICLE PRODUCTION

Two experiments were recently carried out at energies ranging between 20 and 50 GeV. For many aspects this is a not much explored region of transition, at higher energies many parameters being weakly or not at all depending on the energy. A remarkable example of this is given by the ratio $R = \langle n \rangle_A / \langle n \rangle_H$ where $\langle n \rangle_A$ is the mean multiplicity of shower particles in nuclei and $\langle n \rangle_H$ is the equivalent in free proton interactions [10].

In Fig. 1 this ratio R, for incident pions at 40 GeV/c, is given as a function of the nuclear size (using the already defined parameter $\bar{\nu}$), for different intervals of pseudorapidity $\eta = \ln[\mathrm{tg}(\theta_{lab}/2)]$.

The data were obtained, using optical spark chambers, from the Bologna, Dubna, Helsinki, Milan, Moscow, Warsaw and Wien Collaboration at the Serpukhov accelerator [12]. No magnetic field was used with the exception of a small percentage of pictures which were used to evaluate the subtraction of the slow protons (in Fig.1 the protons with $\beta \lesssim .7$ are subtracted).

It is evident that there are limited cascading effects at large angle, while there is no cascading effect at all, but absorption, at large η (in forward direction). Another interesting result from the same experiment comes from the analysis of the pseudorapidity distributions for different charged multiplicity and different nuclear targets. Normalized curves, obtained on carbon from propane bubble-chamber data, completely describe the distributions for all the different nuclei (see Fig.6 in ref.12):it is possible to deduce that the shape of the pseudorapidity distributions is independent from the target nucleus but is dependent only on the charged multiplicity of the events.

Furthermore this experiment confirms what has already been observed at other energies, namely the linear dependence of the multiplicity dispersion $D = \sqrt{\langle N^2 \rangle - \langle N \rangle^2}$ on the mean multiplicity distribution $\langle N \rangle$.

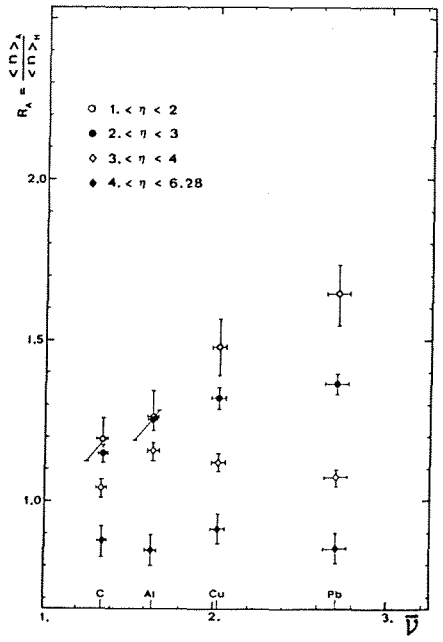

Fig. 1 - R vs $\bar{\nu}$ for different η region (from ref.12)

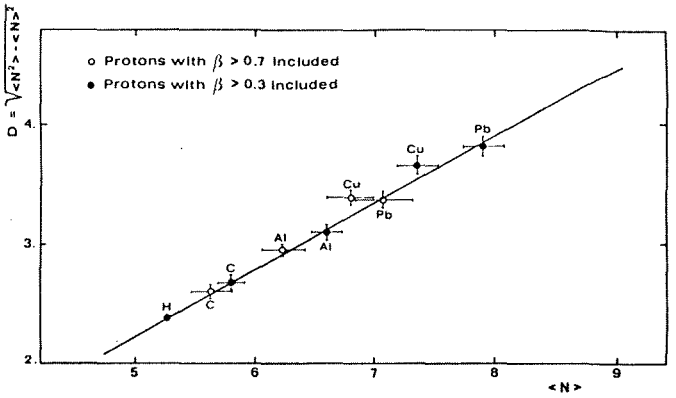

Fig.2 - D vs <N> (from ref.12).

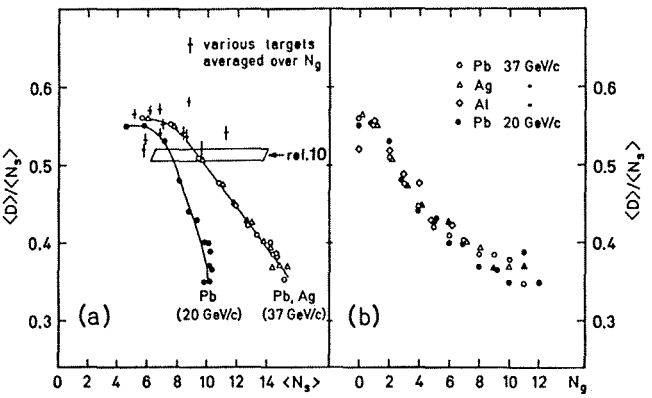

Fig.3 - Normalized dispersion <D>/<N>. a) as a function of <N> and b) as a function of Ng (N and N_S are here equivalent) (from ref.14).

As it is shown in Fig.2 the corresponding points for each nucleus lie on the straight line obtained as best fit to the π^-p world statistics by A. Wroblewski [13].

This result seems to support the hypothesis that in hadron nucleus interactions the multiplicity distribution scales in the same way as in the hadron nucleon ones. In particular this provides further indirect evidence for the validity of KNO scaling, also for hadron nucleus collisions (see e.g. W. Busza [10]), as predicted by the coherent tube model.

A systematic deviation from KNO scaling was observed instead in another experiment within the same range of energies· the one performed at CERN by M.A. Faessler et al. with π^-,K^- and $\bar{p}$ at 20 and 37 GeV/c [14].

The set-up was characterized by a non-magnetic detector (CsI(Tℓ) scintillation and Lucite Cerenkov detectors),which made it possible to distinguish between fast and slow particles ($\beta_{cut} \simeq 0.7$), as in the emulsion data, but with the advantage of having a well-defined target nucleus. Interesting features are provided by the correlations between slow (N_g) and fast (N_S) particles angular and multiplicity distributions.

In particular the authors show that the ratio D/<N> is no longer constant,but is decreasing when <N> is increased as a function of N_g (and not as a function of the atomic weight A, as in the previous analysis), see Fig.3a,b.

Other interesting considerations allowed by the systematic measure of the gray (g) tracks in this experiment, result from the pseudorapidity distribution as a function of N_g and of incoming energy.

The authors found an upper region in η showing a depletion and a lower region showing an increase in the number of fast particles (see Fig.12 in ref.14); the border η_c depends both on the incoming energy and on the number of collisions. As the authors point out, this trend is quite different from the prediction of many of the present models.

The interest of a separate analysis of the energy dependent and the energy independent components of shower particles multiplicities has been shown by A. Andersson et al. in a paper presented at this Conference and by I. Otterlund in a previous paper [15].

Analysing the results of many $\pi^{\pm}A$ experiments they infer that the ratio between energy dependent components in hA and hp reactions is independent of energy and close to the $\bar{\nu}$ number of collisions between the incident hadron and the target nucleons.

The two above mentioned experiments were both performed in absence of magnetic fields, so pseudorapidity η, and not rapidity $y=\frac{1}{2}\ln(E+p_{\prime\prime})/(E-p_{\prime\prime})$ was used as main variable in the analysis of the results.

D. Chaney et al. (Rochester, Fermilab, Northwestern Coll. [16]) performed a study of neutron-nuclei multihadron production up to 400 GeV/c (max at $\sim$300 GeV/c) at the Fermilab, using a 80" x 24" x 72" magnet with scintillation counters and magnetostrictive-readout wire spark chambers. A major result of this detailed experiment to which I would like to draw attention is the observation that trends in the data differ markedly when examined in terms of rapidity y rather than pseudorapidity η.

Fig. 4 and Fig.5 show fits of the form A^{α} (A atomic weight) to the cross-sections presented as functions respectively of y and η. (One should keep in mind that $\alpha \simeq 2/3$ would imply that the multiplicity is independent of nuclear size and that there are neither cascading nor absorption effects of the hadronic system produced in the initial collision).

The comparison with the model predictions lead to contradictory results depending on whether y or η distributions are used: in the first case the data show a definite dependence on A, in that α falls well below a value of 2/3 at large rapidity (against the simple multiperipheral and energy-flux cascade model predictions, but in favour of multi-Regge pole exchange models [1]); in the second case the data are consistent with a lack of dependence on A for $5 < \eta < 7$, followed by a large increase in α for $\eta > 7$. The authors suggest that this increase might be due, partially at least, to electromagnetic contamination, so the data might

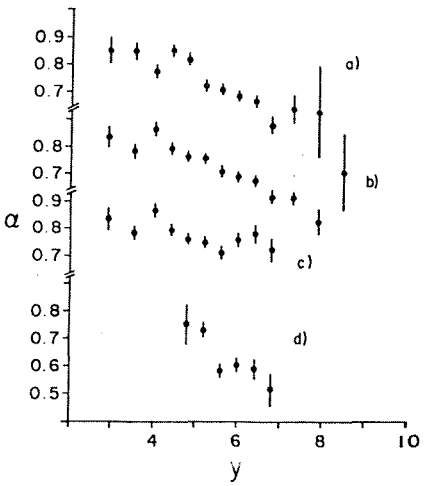

Fig. 4

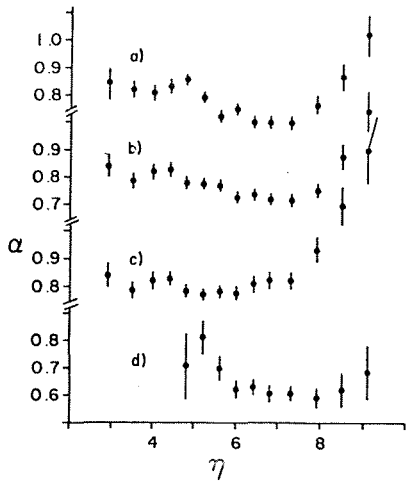

Fig. 5

Fig.4 - Atomic-weight dependence of the cross section as a function of rapidity. a) all negative particles b) all positive's (pion mass assumed) c) positive "pions" d) protons (from ref.16).

Fig.5 - The same as in Fig.4 but as a function of pseudorapidity (from ref.16).

agree with the Parton-Cascade model , which predicts a moderate increase at large η.

In conclusion from the general findings of the above three experiments there ensues a confirmation of the particular transparency of the nuclear matter to the forward produced particles.

There is qualitative agreement with the predictions of many of the current models, but, at least at the present level of the analyses, none of these models seems to provide an understanding of all the production phenomena.

Some discrepancies in the experimental results (e.g. in the KNO scaling validity and in the η and y distributions which we have already been discussing) claim for further and perhaps more systematic and detailed investigations, including use of magnetic fields.

The decreasing of the inelastic total hadronic cross sections on nuclei, at increasing energies (observed in recent years with incident neutrons[17] and K_L^0[18]) was a further case of "a priori unexpected" transparency of nuclear matter to hadronic particle crossing. Recent measurements of γ nucleus hadronic total cross sections up to 140 GeV have shown similar behaviour (D.O. Calwell et al.[19]).

In Fig. 6 $A_{eff}/A = \sigma_{\gamma A}/(Z\sigma_{\gamma p} + (A-Z)\sigma_{\gamma n})$ is shown at increasing γ energies. The full line comes from L.Bertocchi's and D. Treleani's calculations[20]; they introduce large mass intermediate states into a Vector Dominance Model. This introduction, as in the case of the neutron and K_L^0 cross sections, produces screening effects; this fact can be interpreted as if the incident hadronic component of the γ dissociates into a possible higher mass state at one point and recombines at another within the nucleus. (Dotted lines correspond to simple VDM plus point-like photon).

COHERENT AND SEMICOHERENT INTERACTIONS

In the paper submitted to this Conference by T. Ferbel[11b,c] we find summarized the preliminary results of an experiment (Rochester-Minnesota-Fermilab Coll.) on coherent production with π^-, K^-, $\bar{p}$ at 156 and 260 GeV/c on C, Al, Cu and Pb targets, performed at the Fermilab with digit wire/PWC spectrometer. Fig. 7 shows the 3π invariant mass distribution at 156 GeV/c; beyond the usual $A_1(\rho_0\pi^-)$ low mass enhancement around 1100 MeV there is a possible structure in the A_2(1310 MeV) region.

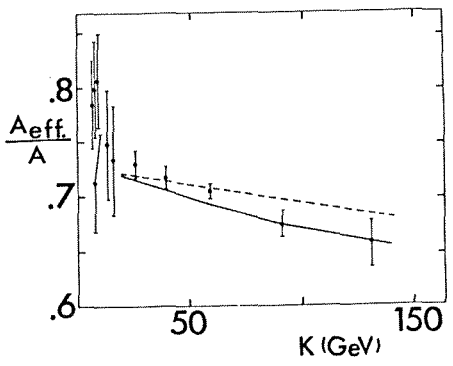

Fig.6 - E_{eff}/A vs γ energies (for Cu target). The data are from ref.19, the curves from ref.20.

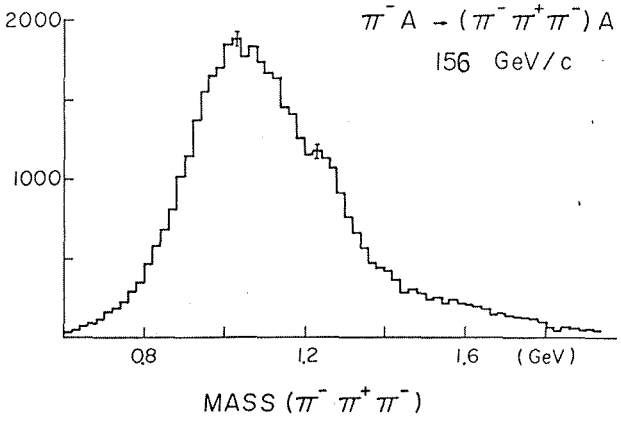

Fig.7 - Coherently produced 3π invariant mass (from ref.11b).

TABLE I

Meson	Radiat. Width
$\rho^- \to \pi^-\gamma$	50 ± 10 keV
$K^{*-} \to K^-\gamma$	∿ 50 keV
$A_2^- \to \pi^-\gamma$	∿ 450 keV
$A_1^- \to \pi^-\gamma$	∿ 600 keV

At these energies the Coulomb excitation becomes important and the authors can measure the radiative decay widths Γ_γ of unstable elementary particle $b \to a + \gamma$ by means of a generalization of the Primakoff formula for the production of a particle b in the Coulomb field of a nucleus. The results are summarized in Table I.

At the Serpukhov accelerator the Bologna, Dubna, Helsinki, Milan, Warsaw, Wien Coll. performed an experiment of coherent production $\pi^- A \to \pi^-\pi^-\pi^+ A$ with incident pions at 40 GeV/c on 9 nuclear targets from Be to Pb.[21] The set-up consisted in the M.I.S. optical spectrometer (1.3 x 1.5 x 5 m^3 - $B_{max} \simeq$ 17 Kgauss), scintillation counters to define the forward acceptance cone and to anticoincide charged recoils at very large angle, and a large MWPC to select the charged multiplicity. About 700.000 pictures were collected; the present analysis is based on half the statistics.

The coherent sample of events is selected in the region of $d\sigma/dt$ (up to the first minimum) in which the ratio of coherent signal to incoherent background is more favourable.

Fig. 8a, b display the invariant mass distributions (obtained with light nuclei) for $\pi^+\pi^-$ systems, when the corresponding 3π masses are respectively in the A_1 and A_3 region.

As it is possible to see, ρ_0 and respectively, ρ_0 and f_0 productions are dominating. The corresponding 3π invariant mass distributions - always for the "coherent sample" - are shown in Fig.9a. In addition to the large accumulation in the A_1 region an accumulation in the A_3 (1640 MeV) region is evident.

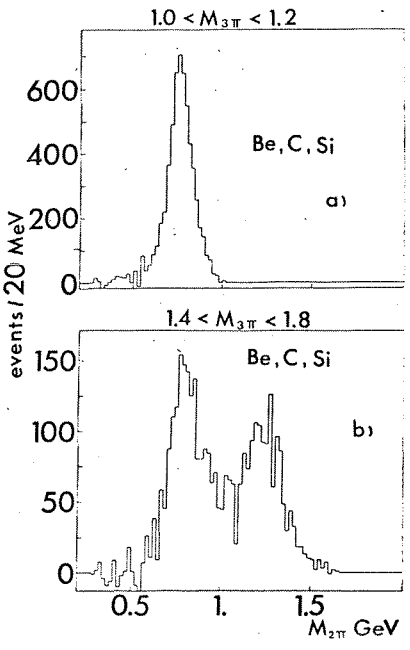

Fig.8- a) $M^*\pi^+\pi^-$ (for the "coherent sample" in light nuclei) when $1.0 \leq M^*_{3\pi} \leq 1.2$ GeV.
b) idem when $1.4 \leq M^*_{3\pi} \leq 1.8$ GeV (from ref.21).

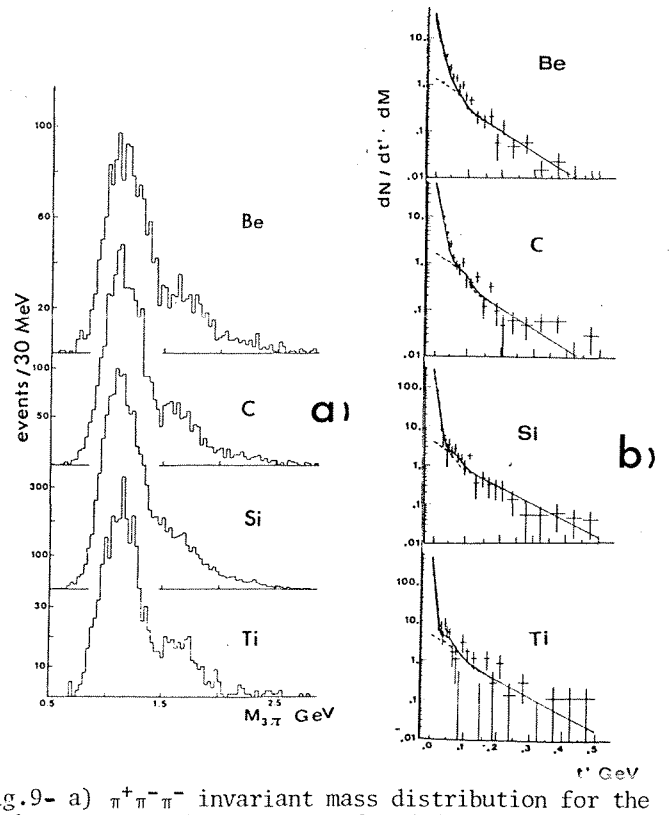

Fig.9- a) $\pi^+\pi^-\pi^-$ invariant mass distribution for the "coherent sample" separately for different light nuclei.
b) t' differential distribution for the same samples of events. Fitted curves are from the GKM model - see the text (from ref.11).

The equivalent distributions for heavier nuclei display the same trend with a light reduction at the highest masses due to the nuclear form factors. Fig.9b shows differential t' distributions ($t'=t-t_{min}$; $t_{min}=(M^*_{3\pi}-m_\pi)^2/4p^2_{inc}$) for the events with $1.<M^*_{3\pi}<1.2$ GeV.

The fit to the t' distribution is obtained from the relation:

$$\frac{d^2\sigma}{dt'dm^*} = \frac{d^2\sigma_{coh}}{dt'dm^*} + \frac{d^2\sigma_{incoh}}{dt'dm^*} \qquad (1)$$

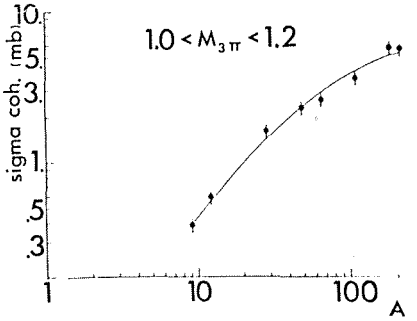

Fig.10- σ_{coh} vs A for $1.0\lesssim M^*_{3\pi}\lesssim 1.2$ GeV. Fitted curve from form.(3) (from ref.21)

The incoherent term $d^2\sigma_{incoh}/dt'dm^*$ is proportional to the differential production on free proton and includes a factor of correction owing to the bias in the detection of low protons, introduced by the set-up.

In this first approach the coherent term is obtained from the old Glauber-Kölbig and Margolis formalism [6]:

$$\frac{d^2\sigma_{coh}}{dt'dm^*} = C_0 e^{-bt}A^2|F(t',m^*,p_{inc},\sigma_1,\sigma_2,\alpha_1,\alpha_2)|^2 . \qquad (2)$$

where $C_0 = \left(\frac{d^2\sigma_{nucleon}}{dt'dm^*}\right)_{t'=0}$ and σ_2 (the unstable system-nucleon cross-section) are taken as free parameters, σ_1 is the incident pion-nucleon total cross-section, and α_1 and α_2 are the corresponding real to immaginary part ratios of the forward elastic scattering amplitude (σ_1 and α_1 are taken from the literature). After subtraction of the incoherent background it is possible to obtain:

$$\sigma_{coh}(\Delta m^*, \Delta t') = \int_{m_1^*}^{m_2^*}\int_0^{t'} \frac{d^2\sigma_{coh}}{dt'dm^*}\, dt'dm^* \qquad (3)$$

An overall fits of formula (1) or (3) to the data of the different nuclear targets yields the parameter σ_2 for different $M^*_{3\pi}$ intervals. Fig.10 shows σ_{coh} vs A with the fitted curve from formula (3).

Preliminary results obtained by the collaboration are:

$1.0\lesssim M^*\lesssim 1.2$ GeV, $\sigma_2=16.2$ mb ($\Delta\sigma_{2stat} = \pm 1.9$ mb, $\Delta\sigma_{2syst} = {}^{+\ 2.3}_{-\ 1.2}$ mb)

$1.6\lesssim M^*\lesssim 1.8$ GeV, $\sigma_2=15.7$ mb ($\Delta\sigma_{2stat} = \pm 1.9$ mb, $\Delta\sigma_{2syst} = \pm 4$ mb)(+)

Fig. 11a,b is a compilation of the world present data on σ_2 measures, respectively for incident pions and incident neutrons or protons. The data are displayed in function of the masses of the produced system. As it is possible to see the general trend in both cases is a decreasing of σ_2 with the increasing of M^*, with some evidence of a small rise at

(+) The big systematic errors will be reduced in the near future with a more refined extimation of the overall efficiencies. Allowing the parameter α_2 to slightly variate around zero ($-.5\lesssim\alpha_2\lesssim.5$) or using the differential form.(1) instead of the integrated form.(3) in the fit, have no remarkable effects within the errors.

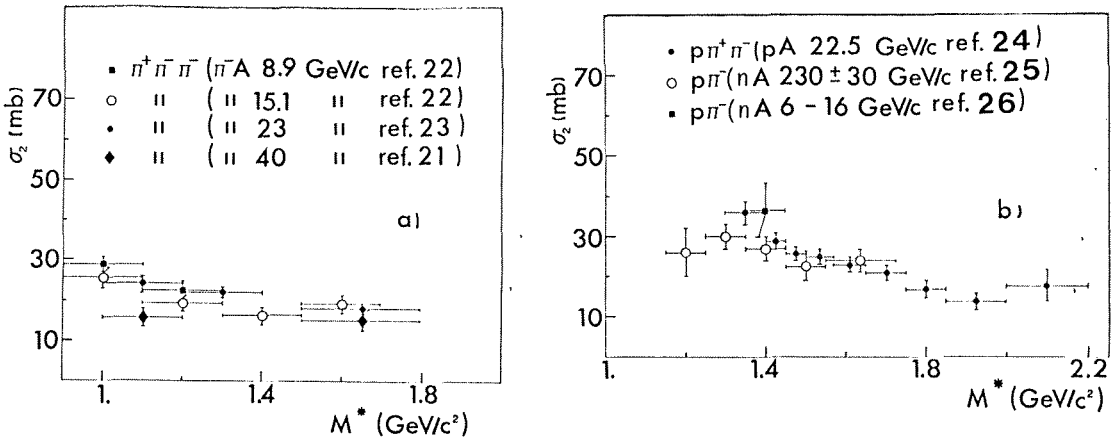

Fig. 11a,b - Compilation of σ_2 measures obtained, in the frame of the GKM formalism, from the A dependence of diffractive production on nuclei a) for incident pion beams b) for incident protons or neutrons.

the upper limit "allowed" for coherent production at each energies(+). Another feature is that, as far as the present data are concerned, there is a constant decrease of σ_2 at fixed M^*, with the increasing of the incident energy.

This last feature seems to be in evident and intuitive correlation with possible effects of the space-time evolution of the produced system. Furthermore it is of remarkable interest that, both for incident pions and nucleons, there are situations in which σ_2 is less than the incident hadron-nucleon cross-section(++).

As it was pointed out earlier, many theoretical ideas were developed in order to account for these features. When the different collaborations reanalyze their data - as they are planning to do[21,23] - by introducing at least such corrections as suggested by Fäldt and Osland [8], it will be very interesting to see whether and to what extent these corrections (which in principle seem to maintain the original meaning of σ_2) will change the σ_2 values.

At the Serpukhov accelerator semicoherent elastic scattering on carbon

$$\pi^- + {}^{12}C \rightarrow \pi^- + {}^{12}C^* \quad (J^P = 2^+)$$
$$\qquad\qquad\qquad\qquad\quad \downarrow \rightarrow {}^{12}C + \gamma \ (4.44 \text{ MeV})$$

was investigated by the Dubna-Milan Collaboration[21,27]: the total elastic cross section was measured with 25 and 40 GeV/c incident pions; furthermore, the differential elastic cross section was also obtained at 40 GeV/c.

The experimental set-up was the same as the one used for the experiment on coherent interactions on nuclei [21], except for the vertex detector.

(+) M^*_{max} is related through t_{min}, as before, defined to the incident momentum; for large t_{min}, because of the nuclear form factor, the coherent production becomes negligible.

(++) I remember that other peculiarites in the σ_2 behaviour cames from the measures for different spin parity states (e.g. in the A_1 region σ_2, always in the GKM frame, is ranging between 15 and 25 mb for $J^P=1^+$ and between 50 and 60 mb for $J^P=0^-$)[22,23]. Not yet partial wave analysis is performed in the two recent experiments above discussed.

The experimental data were selected with a counter technique, looking at the coincidence between the scattered pion and the 4.44 MeV photon from the $J^P=2^+$ carbon excited state detected by a NaI counter. A polystyrene Live Target was used in order to reduce incoherent background.

The value obtained for the integrated cross section at 40 GeV/c in the $0.0032 \lesssim |t| \lesssim 0.27$ $(GeV/c)^2$ four-momentum transfer range is

$$\sigma = (1.16 \pm 0.11) \text{ mb}$$

According to the theoretical models, this t-range at 40 GeV/c covers more than 99% of the angular distribution, so the above value nearly corresponds to the total semicoherent elastic cross-section.

At 25 GeV/c the t-range was $0.0013 \lesssim |t| \lesssim 0.10 (GeV/c)^2$; the corresponding integrated cross-section is

$$\sigma = (0.80 \pm 0.25) \text{ mb.}$$

In this case the correction to be applied to obtain the total cross-section is model--dependent.

For a detailed analysis of the elastic semicoherent reaction the angular distribution of the scattered pions was measured at 40 GeV/c of incident momentum in 15.000 pictures taken with the M.I.S. optical spectrometer.

Fig. 12 gives the distribution of $d\sigma/dt$ for 760 selected "semicoherent" events.

The experimental data were compared with the recent theoretical calculations of L. Bertocchi and C. Troncon.[28] These parameter-free calculations were developed, in the frame of the Glauber theory, by using the hadron amplitudes obtained from hadron scattering on proton targets, and nuclear form factors from nuclear elastic and inelastic (for the 0^+-2^+ transition) electron scattering.

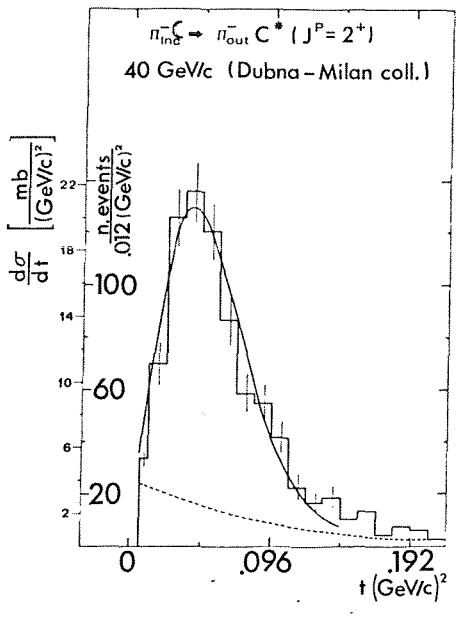

The elastic semicoherent cross-section is calculated to be 1.20 mb at 40 GeV/c and 1.18 mb at 25 GeV/c (for the same t intervals as the experimental ones). In Fig.1 the theoretical curve, added to an exponential background(+), is superimposed to the experimental distribution in absolute value (without fit); the comparison yields χ^2/degrees of freedom = 8.2/8, corresponding to a confidence level of 40%.

The conclusion is that there exists a good agreement between the experimental data and this parameter-free theoretical calculation, not only

Fig.12 - $d\sigma/dt$ distribution for the "semicoherent" selected sample (from ref.21). Dotted line corresponds to an exponential background; full line corresponds to the Bertocchi-Troncon's[28] theoretical calculations.

(+) The remaining incoherent background in the selected sample was estimated from the NaI pulse height distributions, and it was found to have an exponential "slope" consistent with elastic scattering on nucleon. In this experiment no use of time of flight measurement was made because of the particular set-up geometry. Such measurement would further reduce the already low background.

as far as the total elastic cross section is concerned but also the shape of the differential distributions, up to 40 GeV energy.

The previously found discrepancies[29,30] between experimental data and theoretical previsions no longer subsist. Consequently it is now possible to consider again the semicoherent channels, as originally proposed by L. Stodolski[31] and O.Piccioni[29], as channels in addition to or as an alternative to the coherent ones, useful to a better understanding of particular aspects of the elementary hadronic processes at high energy(+).

More generally it is clear that all the questions recently raised on the hadronic interactions on nuclei (absorption cross-sections, space-time development of the produced system etc.) should also be present in the studies of the semicoherent channels and that the particular clearness of these channels (due to the 4.44 γ's signature) would add useful information to the general experimental frame. For instance G. Fäldt and P. Osland suggested that their modifications to the GKM calculation to obtain the σ_2 parameter could be more easily tested in the semicoherent channels[8].

Another interesting experiment in which the nucleus (in this case the deuteron) is used as a useful tool ("a hadronic interference", as the authors put it ...) has been recently performed by G. Goggi et al.[34] at the CERN Intersecting Storage Rings; they used proton and deuteron colliding beams with the Split-Field Magnetic detector.

The experiment studies the coherent diffraction dissociation

$$pd \to (p\pi^+\pi^-)d \quad \text{at } \sqrt{s}=53 \text{ GeV}$$

and

$$nd \to (p\pi^-)d \quad \text{at } \sqrt{s}=37 \text{ GeV}.$$

(For comparison, an analysis is also made of the corresponding diffractive channels on protons).

The authors analyze the data in the frame of the "Glauber formalism" but with two different kinds of description of the elementary nucleon-nucleon production amplitude: a) in a standard hypothesis (central model) b) in a peripheral description.

Besides they include the elicity flip amplitude, following the suggestions of Hümble, Fäldt and Osland.

Fig.13 is an example of $d\sigma/dt$ experimental distribution for p-d reactions ($1.6<M_{p\pi^+\pi^-}<1.8$ GeV) - the continuous line corresponding to the peripheral model, the dashed curve to the "central" model. The agreement of experimental data with the first model is clear.

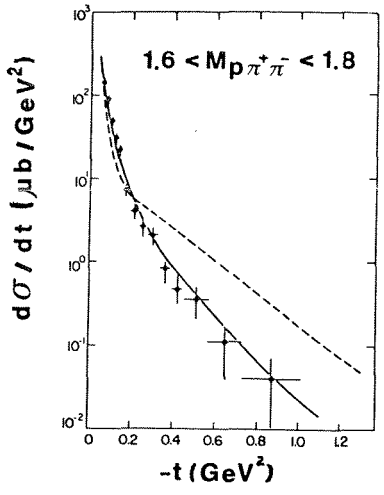

Fig. 13 - Comparison between peripheral and central model (see the text) (from ref.34).

(+) The 3π production on semicoherent channel had already been investigated with a low resolution magnetic spectrometer at 6 GeV/c by Ascoli et al. [32]; for a discussion of this channel see also V.V. Balashov et al.[33]

Fig.14, on the other hand, depicts the contribution of no spin-flip ($\Delta\lambda=0$) amplitude (dashed line) and of the $\Delta\lambda=1$ amplitude (full line) to the peripheral model (interval $1.44<M_{p\pi^+\pi^-}<1.6$ GeV is shown as an example). The effect of "dip filling" of this last curve is evident.

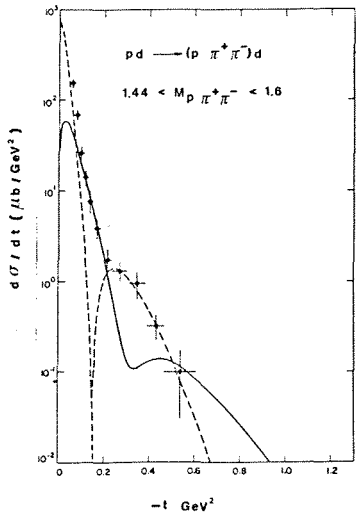

The authors also try to interpret the experimental results with the "central model" and to leave the σ_2 parameter free. They demonstrate that this leads to an underestimation of σ_2 with the increasing mass of the diffracted system. (This is evident also at a simple inspection to Figure 13).

This observation seems to fit in very well with the general frame of the previously discussed analysis.

Fig.14 - Comparison of contributions of no spin flip and spin flip amplitude in the peripheral model (from ref.34).

CONCLUSIONS

Both multiparticle production and coherent interactions seem to be deeply related to the space-time development of hadronic systems, even if no clear quantitative description of the phenomena is obtainable so far from this point of view.

In the coherent experiments, more careful analyses of the present data are in progress and it will be interesting to see the effects of the introduction of the suggested refinements to the previous theoretical frame.

Particular channels, such as the semicoherent ones, seem to provide the possibility of clear discrimination between different hypotheses.

A few discrepancies between phenomenological analyses in multiparticle production claim for further detailed and systematic measurements.

REFERENCES

1) See, for example, a) J. Koplik and A.H. Mueller, Phys. Rev. D12 (1975) 3638. b) A. Capella and A. Krzywicki, in Proc. of "Recent Developments in High Energy Physics" Campione d'Italia October 1977 p.369. c) G. Białkowski, ibid. p.393.

2) K. Gottfried, Phys. Rev. Lett. 32 (1974) 957.

3) See, for example, a) O.V. Kancheli, IEPT Lett. 18 (1974) 274. b) S.J. Brodosky et al., Phys. Rev. Lett. 39 (1977) 1120. c) A. Białas, et al., Acta Phys. Pol. B8 (1977) 585.

4) A.M. Baldin, Proc. 19th Int. Conf. High Energy Physics - Tokyo 1978 p.455.

5) See, for example, a) A. Dar, invited talk at Topical Meeting on Multiparticle Production at Very High Energy - Trieste (1976) . b) C. Bergström and S. Fredriksson, Preprint TH 2505-CERN (1978).

6) K. Kölbig and B. Margolis, Nucl. Phys. B6 (1968) 85 and references there.

7) a) L. Van Hove, in "Particle Interactions at Very High Energies" edited by D. Speiser et al. (Plenum, New York, 1973). b) A. Białas and W. Czyz, Acta Phys. Pol. B5 (1974) 523. c) L. Caneschi and A. Schwimmer, Nucl. Phys. B133 (1978) 408. d) H.L. Miettinen and J. Pumplin, Phys. Rev. Lett. 42 (1979) 204.

8) G. Fäldt and P. Osland, Nucl. Phys. 87B (1975) 445.

9) B.Z. Kopeliovich et al., Preprint J.I.N.R. E2-12288 (1979) contr. paper 189 to this Conf.

10) W. Busza, Acta Phys. Pol. B8 (1977) 333.

11) a) T. Ferbel, Proc. 19th Int. Conf. High Energy Phys.- Tokyo 1978 p.465. b) T. Ferbel, Review Talk presented to the First Workshop on Ultra Relat. Nucl. Collis. LBL (1979) and private communication. c) D. Berg et al., contr. paper 34 to this Conference.

12) P.L. Frabetti et al., Preprint CERN-EP/79-42 (April 1979) to be published on Nucl. Phys. B.

13) A. Wroblewski, Proc. 8th Int. Symp. on Multip. Dynamics, Kayserberg 1977 p.37.

14) M.A. Faessler et al., Preprint CERN-EP/79-15 (Febr.1979) to be published on Nucl. Phys. B.

15) I. Otterlund, Technion-PH-79 (1979) and B.A. Andersson et al., Contr. Paper 61 to this Conf.

16) D. Chaney et al., Preprint COO-3065-221 (June 1979).

17) P.V.R. Murty et al., Nucl. Phys. B92, 269 (1975).

18) A. Gsponer et al., Phys. Rev. Lett. 42 (1979) 9.

19) D.O. Caldwell et al., Phys. Rev. Lett. 42 (1979) 553.

20) L. Bertocchi and D. Treleani, Preprint "Effect of the Large Intermediate Masses on the Hadronic Properties of the Photon" ICTP 1979 and private communication.

21) a) Bologna, Dubna, Helsinki, Milan, Warsaw Coll., Contributed paper 282 to this Conference. b) A.T. Abrosimov et al., Invited paper presented by G. Bellini to the II Intern. Symp. on Hadron Structure and Multip. Prod. - Kazimierz, 20-26 May 1979. c) P.L. Frabetti et al., IFUM 231/AE (1979).

22) P. Mühlemann et al., Nucl. Phys. B59 (1973) 106.

23) T.J. Roberts et al., Phys. Rev. D18 (1978) 59.

24) R.M. Edelstain et al., Phys. Rev. Lett. 38 (1977) 185.

25) W. Mollet et al., Phys. Rev. Lett. 39 (1977) 1646.

26) W.C. Carithers et al., Proc. of "Top. Conf. on High Energy Collisions Involving Nuclei" Trieste 1974 (Ed. Compositori) p,307.

27) a) T. Bettinazzi et al., Proc. Triangle Seminar on Recent Developments in High Energy Physics, Campione d'Italia, 1977 (Ed. Compositori, Bologna 1978), p.429. b) P.L. Frabetti et al., Preprint CERN EP/79-49 to be published on Nucl. Phys. B.

28) L. Bertocchi and C. Troncon, Nuovo Cimento 45A (1978) 238.

29) W. Melhop et al., Prof. Topical Seminar on High Energy Collisions Involving Nuclei, Trieste 1974 (Ed. Compositori, Bologna 1975) p.85.

30) J.L. Groves et al., Phys. Rev. D15 (1977) 47.

31) L. Stodolsky, Phys. Rev. 144 (1966) 1145.

32) V.V. Balashov et al., Phys. Lett. 49B (1974) 120.

33) G. Ascoli et al., Phys. Rev. Lett. 31 (1973) 795.

34) G. Goggi et al., Preprint CERN EP/79-43, Contributed paper 207 to this Conference.

HIGH ENERGY πN PHASE SHIFT ANALYSIS

G. Höhler
Institut für Theoretische Kernphysik, Universität Karlsruhe, Germany

ABSTRACT

We give a summary of recent work on πN phase shift analysis above 2 GeV/c lab. momentum. In particular we discuss improvements of the "1978 Karlsruhe-Helsinki solution" and problems with discrepancies between experimental data.

1. INTRODUCTION

In the mass range up to about 2 GeV the most important nucleon resonances have been discovered in the phase shift analyses of the CERN[1] and Saclay[2] groups (1967-73). However their method led to increasing difficulties at higher momenta, in particular because of the sharp cut-off of the partial wave expansion and the "shortest path method" for the continuation in energy.

In more recent phase shift analyses[3-5] the sharp cut-off has been replaced by a soft one, using convergence test function methods. Furthermore the continuation in energy is performed by imposing analyticity constraints.

Cutkosky et al.[5] chose analyticity along certain hyperbolas in the Mandelstam plane. At present this group has just completed the analysis in the mass range 1.35 - 2.16 GeV and it can be expected that they will proceed to higher momenta in the near future.

Pietarinen preferred fixed-t analyticity[3] which has also been used in investigations of our group[6]. The results of our subsequent collaboration are described in Ref.[4].

The choice of the fixed-t analyticity constraint has the advantage that crossing symmetry is taken into account and that data are available in the large momentum interval from threshold up to 200 GeV/c. The t-range is limited to $|t| < 0.5$ GeV^2 by the condition for the convergence of the Legendre expansion, but it turns out that the uncertainty does not increase too much if one extends the range to about 1 GeV^2. Together with isospin invariance this analyticity constraint for all invariant amplitudes is strong enough to lead to a unique solution.[+)]

Originally fixed-t analyticity has been expressed in terms of dispersion relations[9]. But for numerical work it is much more convenient to use an expansion method which has been developed by Pietarinen in Ref.[3]. At first I had doubts whether one can perform accurate calculations on a computer with a power series which has about 60 terms, but a comparison with the evaluation of dispersion integrals and the study of a case where the result can be expressed analytically convinced me that this method is reliable.

[+)] A special problem occurred with the new Rutherford data for charge-exchange differential cross sections and polarizations[7]. We found that these data cannot be well fitted together with the other data and the analyticity constraints and that the difficulty is not due to a violation of isospin bounds. A similar observation was made by Cutkosky et al.[5] who used a different method. See also the discussion of these data in Ref.[8].

However, there is one case in which dispersion relations are useful in addition to the expansion. If data above the resonance region are analysed, an acceptable solution should have amplitudes which approach a well-defined asymptotic behaviour. Since reliable theoretical predictions are not known, one has to assume different models with adjustable parameters. I think that dispersion relations are well suited for this part of the analysis. The result can then be used in order to incorporate the high energy behaviour in the ansatz for the expansion.

Several authors have claimed that the analytic properties which are embodied in dispersion relations can equally well be implemented by writing "derivative analyticity relations" which can be handled more easily[10]. However it has been shown that this method is reliable only at very high energies, where it is essentially equivalent to the well-known "analytic parametrizations" of other authors. It is hard to see how it can be useful in the resonance region, and even at 10 GeV/c it could happen that effects which are "non-local in energy" are appreciable[11].

In his first attempt to analyse the data up to 10 GeV/c Pietarinen[12] omitted the large angle and backward data ($|t| > 3$ GeV^2), showing that one can nevertheless derive fairly accurate results for the partial waves as long as the angular momentum is not too large. Our more recent calculations include data at all angles[4].

At present we are performing a new analysis in the high energy region which takes into account the large data set of Jenkins et al.[13]. It covers the angular region $|\cos \Theta_{cm}| \leq 0.35$ at 2 - 9.7 GeV/c ($\pi^- p$) and 2 - 6.3 GeV/c ($\pi^+ p$) respectively and represents a major improvement of the experimental information. Furthermore we have just received the new charge-exchange data of Miyake et al.[14] at 2 - 3 GeV/c which will also be very helpful.

Before discussing details and results of our work, I would like to mention the work of other authors in this field.

E. Ferrari[15] has investigated the high energy behaviour of the partial waves up to 10 GeV/c, starting from the invariant amplitudes of Hecht et al.[7] and from the "Karlsruhe-Helsinki 1978" solution (Ref.[4]).

Pierrard[16] performed an amplitude analysis at 40 GeV/c, using the results of his group for the polarizations and for the spin-rotation parameters. Furthermore he extended the work of Hecht et al.[7] to this energy. It turned out that he was not able to fit the spin-rotation parameters at $|t| > 0.2$ GeV^2 with this method. Since we noticed a similar difficulty, we shall pay special attention to this question in our new analysis.

A. Hendry's phase shift analysis[17] in the range 1.6 - 10 GeV/c makes use of a model based on the impact parameter representation in a first step. Then the fit is improved by varying the phase shifts in the neighborhood of this solution. In general his Argand diagrams look similar to ours. It will be of interest to check whether his invariant amplitudes are compatible with the analyticity constraints.

A similar remark applies to the phase shift analysis of D. Chew[18] for all π^+p data in the range 0.6 - 2.3 GeV/c. She used a method proposed by E. Barrelet[19]. It starts with a determination of the zero trajectories of the transversity amplitudes from the experimental data. The result is then used in an ansatz for the angular dependence of the phase of the transversity amplitude at fixed energy. In some cases her results for the nucleon resonances show large deviations from those of other authors[4,5]. For the discussion of this discrepancy it will be of interest to compare her zero trajectories with those derived from the phase shifts of Refs.[4,5] and to check, whether the invariant amplitudes reconstructed from her phase shifts are compatible with our analyticity constraints.

We have also studied zero trajectories in detail[20], because their simplicity (in the case of invariant amplitudes) is an interesting information for attempts to formulate a model for pion-nucleon scattering. Furthermore strong fluctuations in zero trajectories in a certain energy range indicate that the phase shift solution is not satisfactory.

2. STATUS OF NUCLEON RESONANCES ABOVE 2 GeV

As mentioned above a large number of new experimental data has become available only very recently. Up to now we have only included the π^+p data of Jenkins et al.[13] below 5 GeV/c. Our results are still preliminary and we have not yet made an attempt to redetermine the masses and widths.

Δ-resonances: Δ(2416) is a well-established resonance not only because of its Argand diagram but also because it gives the main contribution to a pronounced bump in the total cross section. There is in addition a much weaker effect Δ(2468) G39, of which the mass is not yet well determined. The best candidates at higher momenta are Δ(2990) K3,13 and Δ(2794) I3,13, which contribute to the small enhancement of the total cross section at 2850 MeV. Finally there are weaker resonance-like effects in L3,17, where the real part becomes zero near 3200 MeV, and in M3,19.

A comparison with Hendry's table[17] shows an approximate agreement with his $T_{\ell+}$ resonances. But at the position of his $T_{\ell-}$ resonances our solution shows at most some wiggles (for instance in K3,13) but no significant resonance structures.

D. Chew[18] found a D33 resonance Δ(2173). In this region we see no significant structure, whereas Cutcosky et al.[5] list a very weak effect at 2010 ± 100 MeV.

N-resonances: Since our "1978" solution has not yet been updated, I shall only mention that there is an approximate agreement with Hendry's table[17] up to a mass of 3 GeV, except for D15, where we find in addition a two star resonance N(2228).

Of course the main question is whether the above structures in the Argand diagrams are really belonging to resonances poles of the amplitudes. Otherwise it would not make sense to compare the "resonance parameters" with the predictions for the excited states of the nucleon from quark models, as it is being done for instance in Refs.[21].

First one can see that, starting with the ideal case of Δ(1233), the Argand diagrams[4,22] show a continuous variety of "resonance circles" which finally leads to the small

wiggles of K3,13 etc. This is expected, since the resonances become more and more inelastic at higher energies.

However one should also notice the following effect. The curves for Im $T_{\ell\pm}$ start to rise at a certain energy, which is higher for higher ℓ, and finally they approach an almost constant behaviour, sometimes after having a peak. Qualitatively this pattern follows from the fact that, above 1 - 2 GeV/c, the data show a diffraction peak which depends only slowly on energy, i.e. it is a geometrical effect. It can be calculated in a simple way, if one assumes an exponential shape for the imaginary part of the non-flip amplitude, which dominates the diffraction peak[23].

The projection of the non-flip amplitude gives for each ℓ only a combination of two partial waves and one has to insert information on the spin-flip amplitude, if one wants to obtain each partial wave separately. This makes some of the Im $T_{\ell\pm}$ steeper and others flatter and it pushes some of the Re $T_{\ell\pm}$ to the positive side, although the general background at high energies is negative (for isospin 3/2). Since the spin-flip amplitude can be determined completely only if one has not only polarization data but also spin-rotation data, the accuracy would be improved if a new spin-rotation experiment would be carried out in a suitable kinematical region.

Even if the increase of Im $T_{\ell\pm}$ comes from geometrical reasons, it could produce a resonance-like variation of the real part, if it is rapid enough. This follows from the partial wave dispersion relation (see also Ref.[24]).
Fig. 1 shows some results of our partial wave analysis.

3. DETERMINATION OF πN AMPLITUDES ABOVE THE RESONANCE REGION

In Ref.[4] we have presented the results of our earlier work in this field, which are based on fits of the data to invariant amplitudes constrained by fixed-t analyticity. At present we are working on an improved version, in which we spend a greater effort in studying discrepancies between different data sets[25].

We noticed that the new CERN Coulomb interference data of Burq et al.[26] do not join smoothly with the Fermilab data which start at slightly larger $|t|$ values (Fig. 2). A study of the t-dependence of the logarithmic slopes b(t) (Fig. 3) showed that both data sets can be connected by a smooth curve, i.e. a possible reason for the discrepancy is a renormalization error of the Fermilab data[27]. Unfortunately it turns out that one needs a renormalization of 11 % for the 50 GeV/c data of Ayres et al.[27], although the estimate of the authors for the systematic error is 3 %. The 50 GeV/c data of Akerlof et al.[27] require a renormalization of 15 %.

We have also reanalyzed the Coulomb interference data of Foley et al.[30], inserting the prediction for the real part from our evaluation of the dispersion relation and solving for the forward slope b(0) and a possible renormalization factor. We find renormalizations of the order of 5 % and appreciably smaller values of b(0) than the authors.

The shape of b(t) at small $|t|$ shows an unexpected increase which is enforced by the data of Burq et al.[26]. It is of great interest in connection with models for diffraction scattering, since one expects a contribution from the cut which starts at $t = + 0.08$ GeV^2.

Finally we have written the differential cross section in terms of the invariant amplitudes C and A, using the fact that the contribution of A is negligible at high energies in our t-range[6]. This allows us to determine the imaginary part of the amplitude $C \equiv A'$, taking the real part from an evaluation of the dispersion relation. It turns out that Im C(s,t)/Im C(s,0) has a small momentum dependence in the large interval from 3 to 175 GeV/c (Fig. 4). This is related to the fact that the logarithmic slope b(t) in the interval $0.2 < |t| < 0.5$ GeV^2 is constant within the errors in the range 6 - 140 GeV/c (no shrinkage) (Ref.[25]).

The analysis of the πN charge exchange data has usually led to the conclusion that reggeized ρ-exchange is strongly dominating. A small difficulty lies in the fact that the intercept $\alpha_\rho(0) = 0.481 \pm 0.004$ is somewhat different from the same quantity as determined from the difference of the total $\pi^\pm$p cross sections: $\alpha_\rho(0) = 0.54 \pm 0.03$.

Following a remark by Bourrely et al.[28], Borie and Jakob[29] have recently calculated the electromagnetic corrections to the invariant amplitude B for elastic scattering. It turns out that the corrections are appreciable at 40 GeV/c and that they are increasing relative to the hadronic amplitude with energy. If the elastic polarization data are included together with the charge-exchange data for an analysis of the isospin odd amplitude, as it is usually done, the previously neglected electromagnetic corrections lead to difficulties with the simple ρ-exchange model which need further attention.

REFERENCES

1) S. Almehed and C. Lovelace, Nucl. Phys. 40 B (1972) 157

2) R. Ayed, Thesis (Université de Paris-Sud, 1976) and CEA-N-1921. Only date available in 1973 have been taken into account

3) E. Pietarinen, Nucl. Phys. B 49 (1972) 315, Nuovo Cimento 12 A (1972) 522, Nucl. Phys. B 107 (1976) 21

4) G. Höhler, F. Kaiser, R. Koch and E. Pietarinen, Handbook of Pion-Nucleon Scattering. Physics Data 12-1, 1979

5) R.E. Cutcosky et al., COO-3066-116 and LBL-8552, COO-3066-117 and LBL 8553. Earlier version: Proceedings of the Topical Conference on Baryon Resonances, 1976

6) G. Höhler and R. Strauss, Zeitschr. f. Physik 232 (1970) 205
G. Höhler and H.P. Jakob, Zeitschr. f. Physik 268 (1974) 75
H. Hecht, H.P. Jakob and P. Kroll, Nucl. Phys. B 71 (1973) 1

7) R.M. Brown et al., Nucl. Phys. B 117 (1976) 12 and B 144 (1978) 287

8) G. Höhler, H.P. Jakob, F. Kaiser and G. Brandenburger, Analysis of πN Charge-Exchange Data at Intermediate Energies. KfK 2735 (Feb. 1979)

9) G.F. Chew, M.L. Goldberger, F. Low and Y. Nambu, Phys. Rev. 106 (1957) 1337

10) J.B. Bronzan et al., Phys. Lett. 49 B (1974) 272
D.P. Sidhu et al., Phys. Rev. D 11 (1975) 1351
U. Sukhatme et al., Phys. Rev. D 12 (1975) 3431

11) G. Eichmann and J. Dronkers, Phys. Lett. 52 B (1974) 428
G. Höhler in Hadron Interactions at Low Energies, Ed. D. Krupa and J. Pisut 1975, p. 11
G. Höhler, H.P. Jakob and F. Kaiser, Phys. Lett. 58 B (1975) 348
A. Bujak and O. Dumbrais, J. Phys. G, Nucl. Phys. 2 (1976) No. 9

12) E. Pietarinen, Phys. Lett. 61 B (1976) 461

13) K.A. Jenkins et al., Phys. Rev. Lett. 40 (1978) 425, 429

14) Private communication. Theses of Y. Suzuki and M. Minowa, Kyoto University 1979

15) E. Ferrari, Nuovo Cimento A, in print

16) J. Pierrard, Thesis, Université de Paris-Sud CEA-N-2028

17) A. Hendry, Phys. Rev. Lett. 41 (1978) 222

18) D. Chew, CERN preprint (15th June 1979)

19) E. Barrelet, Nuovo Cimento 8A (1972) 331 and thesis (Paris 1970)

20) G. Höhler and I. Sabba-Stefanescu, Singularities of Zero Trajectories of Scattering Amplitudes, Zeitschrift für Physik, in print
E. Borie, W. Gampp, G. Höhler, R. Koch, I. Sabba-Stefanescu, Zero Trajectories of Invariant πN Amplitudes, Karlsruhe preprint $TKP_8$78-18 and unpublished work on zeros of transversity amplitudes. See also Ref.

21) R.H. Dalitz and L.J. Reinders, High-lying baryon multiplets in the hadronic quark shell model
M. Böhm, The masses of the non-strange baryon resonances in a quark model. Preprint, University of Würzburg
D. Gromes and I.O. Stamatescu, Baryon spectrum and the forces between quarks.
We have listed only some of the most recent preprints. Earlier references are given in these papers
S.D. Protopopescu and N.P. Samios, Light hadronic spectroscopy, to appear in Annual Review of Nuclear and Particle Science, 1979

22) Review of Particle Properties, Particle Data Group. April 1978 edition

23) G. Höhler and H.P. Jakob, Zeitschrift für Physik 261 (1973) 371

24) J.S. Ball and W.R. Frazer, Phys. Rev. Lett. 7 (1961) 204

25) G. Höhler, F. Kaiser and H.P. Staudenmaier, The Shape of the $\pi^- p$ Diffraction Peak, Karlsruhe preprint TKP 79-4

26) J.P. Burq et al., Phys. Lett. 77 B(1978) 438 and CERN report

27) D.S. Ayres et al., Phys. Rev. D 15 (1977) 3105, C.W. Akerlof et al., Phys. Rev. D 14 (1976) 2864

28) C. Bourrely and J. Soffer, Lett. Nuovo Cimento 19 (1977) 569

29) E. Borie and H.P. Jakob, Phys. Lett. 78 B (1978) 323

30) K.J. Foley et al., Phys. Rev. 181 (1969) 1775.

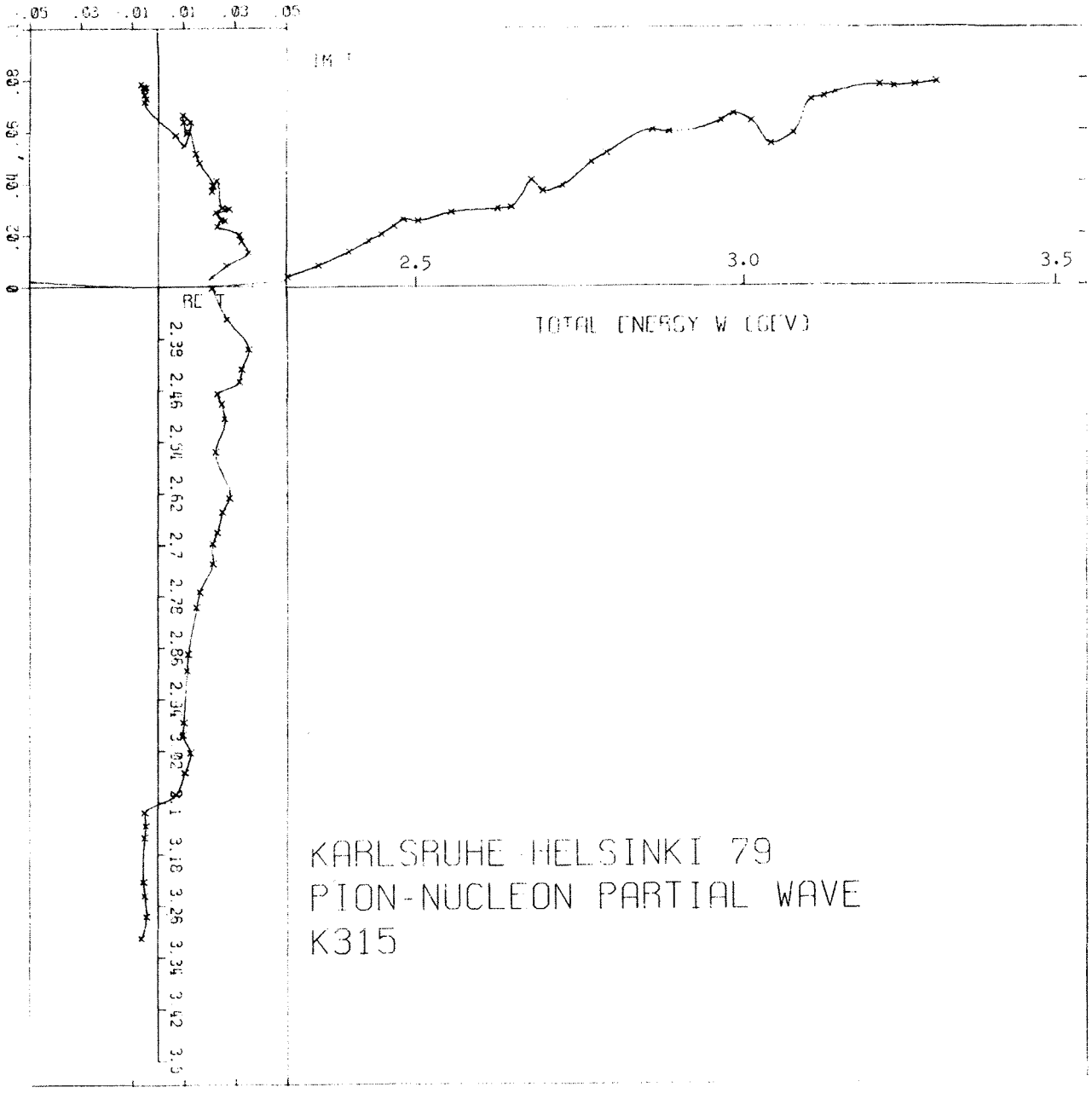

Fig. 1 Our preliminary result for the result for the partial wave K3,15. The s-dependence at fixed t of the π^+p data of Jenkins et al.[13] shows at some t-values pronounced structures in the region of this resonance.

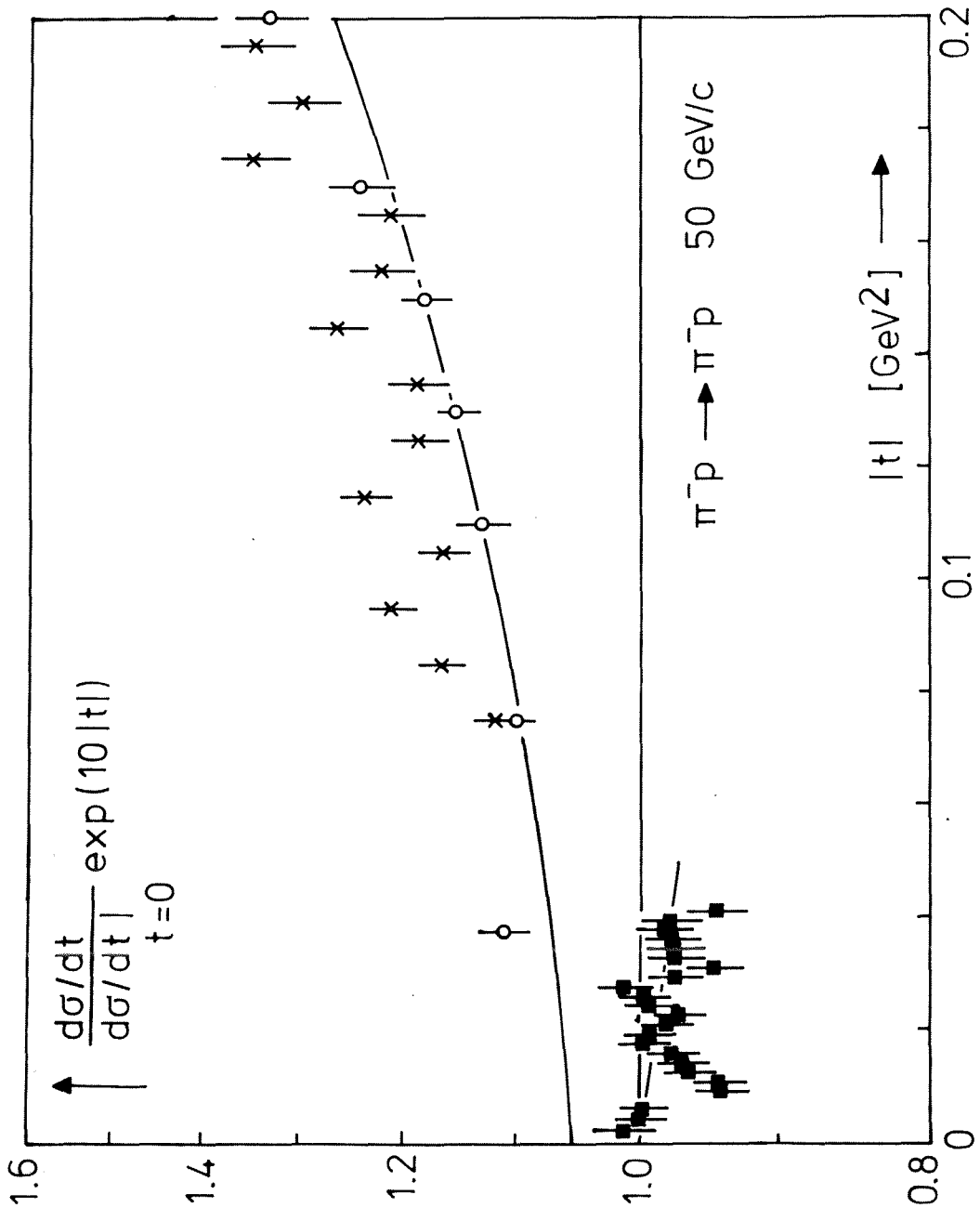

Fig. 2 A discrepancy between published data at 50 GeV/c. We have plotted the strong interaction part of the π^-p differential cross sections of Burq et al.[26]: ● Ayres et al.[27]: ○ and Akerlof et al.[27]: ×. The solid lines are the fits of Burq et al.[26] and of Ayres et al.[27].

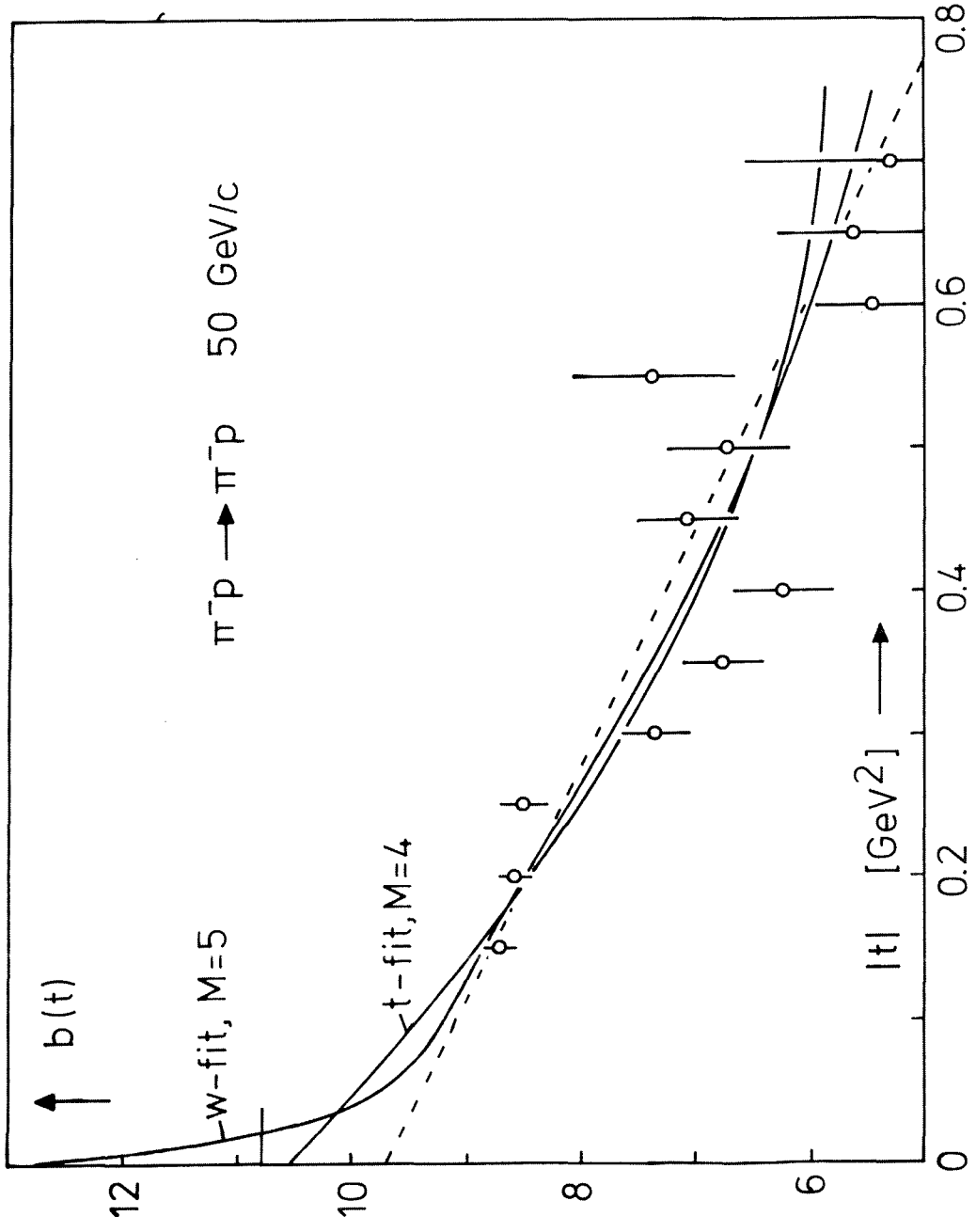

Fig. 3 The t-dependence of the logarithmic slope b(t) at 50 GeV/c (Ref. 25). We have performed simultaneous fits to the data of Burq et al.[26] and Ayres et al.[27], using a renormalization factor in the second case. The solid lines follow from different parametrizations. The dashed line is the fit of Ayres et al.[27]. The points are best straight line fits to the data of Ayres et al.[27] in intervals $\Delta t = 0.2$ GeV^2. Burq et al.[26] give $b(o) = 10.6 \pm 0.3$ GeV^{-2}.

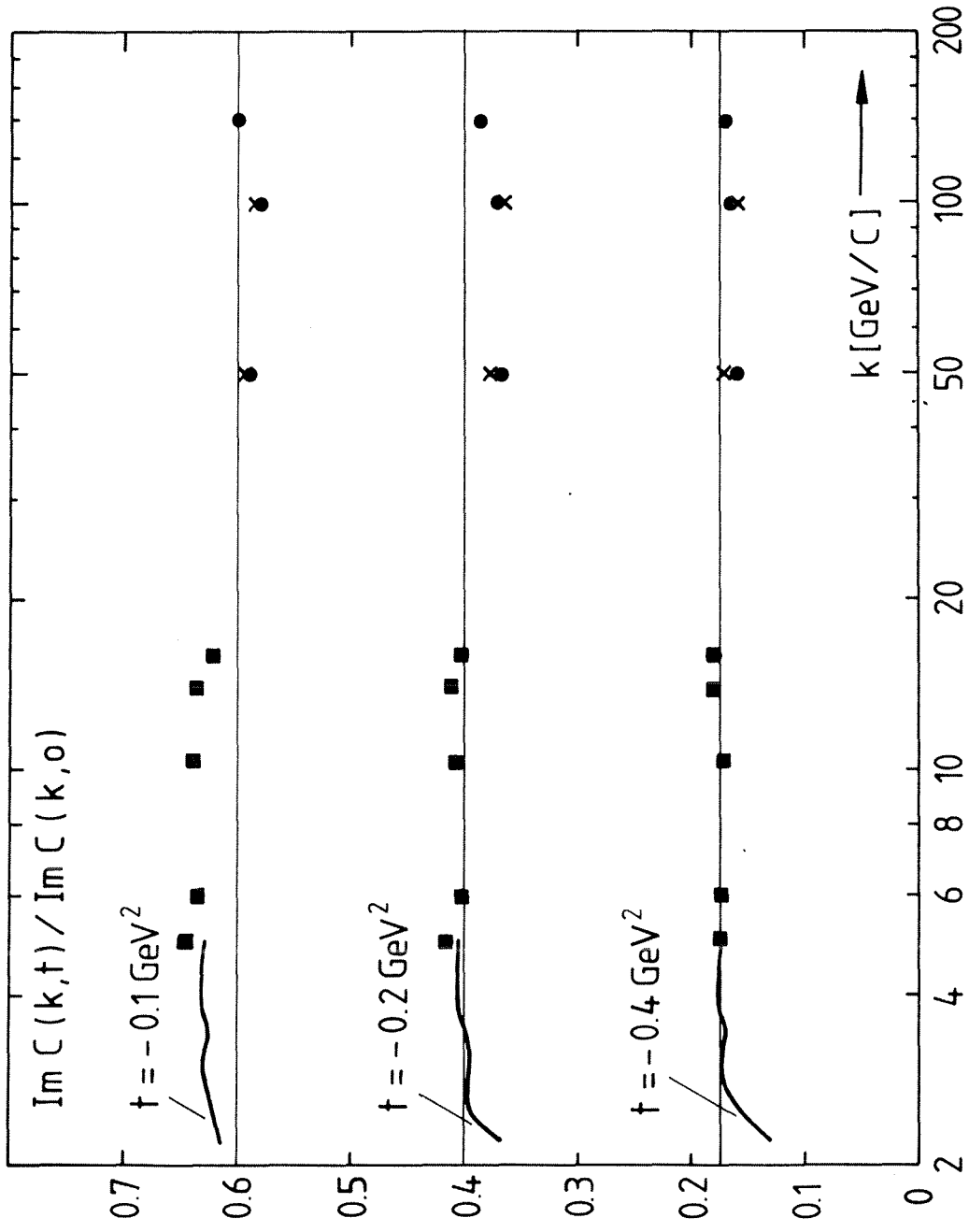

Fig. 4 Momentum dependence of the ratio Im C(s,t)/Im C(s,0) from the renormalized data. The procedure has been described in the text (see also Ref. 25).

VERY NARROW STATES

B. Povh
Max-Planck-Institut für Kernphysik, Heidelberg, Germany

ABSTRACT

In the $\bar{p}p$ system narrow resonances have been observed at 1.94, 2.02 and 2.2 GeV. The search for narrow baryonium states has begun. Recent experiments trying to verify their existence failed to do so. A set of new experiments searching for baryonium is in progress.

1. INTRODUCTION

Quite some time ago the concept of baryonium was introduced to antiproton physics based on formal considerations[1,2]. But it was not before the S resonance was established rather firmly[3,4,5] that one started to speculate about the existence of narrow baryonium states. Only with a sufficient number of narrow states in the $\bar{N}N$ system can one hope to learn about the baryon structure by studying baryonium states.

There is, however, no really good theoretical argument for the existence of narrow $\bar{N}N$ resonances. The central concern is to explain why the annihilation which dominates the low energy $\bar{p}p$ interaction does not smear out the narrow states. In the model of baryonium by Rossi and Veneziano[2] the Zweig-Iizuke-Okuba rule applied to the conservation of the junction of the three quarks in a baryon hinders annihilation. In the model of Chan[6] narrow baryonium states are states with intrinsic colour excitation and thus cannot decay directly into either $\bar{N}N$ or mesons. But finding narrow baryonium states of the first, second or of some other type would rather teach us about the baryon structure than being a consequence of some theoretical prediction.

The question of narrow baryonium states has to be settled experimentally. The possibility of having access to a systematic study of the baryon structure via baryonium spectroscopy makes experimentalists so persistent in their search for baryonium.

When accepting this invitation to talk about the present experimental status of the search for baryonium I was quite sure that I would be able to give a definite answer as to the existence or non-existence of narrow baryonium states. But some of the hurried experiments trying to confirm their existence and possibly to find new ones failed to show any indication of the baryonium. The second generation experiments just being started will do, I hope, a careful job in scanning the $\bar{N}N$ system for narrow states. But at present the situation in baryonium physics is still as confusing as it used to be. Nevertheless, I find it quite useful to give a status report and to reconsider the alternative approaches in the search for baryonium.

There are two main approaches in the baryonium search. The first one is based on the assumption that the baryonium is a rather extended object,

extended if compared to the normal mesons. This idea originated from the potential model of $\bar{p}p$ resonances but is also common to the diquark-diantiquark model of baryonium. Therefore preference is given to using low energy $\bar{p}$ on hydrogen or deuterium targets to populate the baryonium states. The second type of experiments aims at investigating $\bar{p}p$ pairs produced in "high"-energy hadron-hadron or photon-hadron collisions. In one exclusive measurement several kinematical conditions of produced particles can be efficiently used to select the best trigger for baryonium production.

2. FORMATION EXPERIMENTS

The S resonance has been observed in several experiments, for instance in 1974 in an experiment by a group at Brookhaven[3] in the total cross section for antiprotons on hydrogen and deuterium. The resonance was found to be quite narrow, with a width of only about 10 MeV. Considering the annihilation channel, which dissipates an energy of 2 GeV, this width is very small. But it is also small if scattering alone is taken into account, since the resonance is 60 MeV above the proton-antiproton threshold. Two groups at CERN have been searching for such narrow resonances in the $\bar{p}p$ formation cross section at $\bar{p}$ momenta below 700 MeV/c; in this momentum region a good energy resolution can be achieved with the present experimental techniques. Both groups observed[4,5] narrow resonances at a 1.94 GeV mass in both the elastic and the annihilation channels, with about equal cross sections. Since the phase space available for the annihilation is much larger than that for the elastic scattering, it is obvious that the 1.94 GeV resonance is predominantly due to the elastic channel.

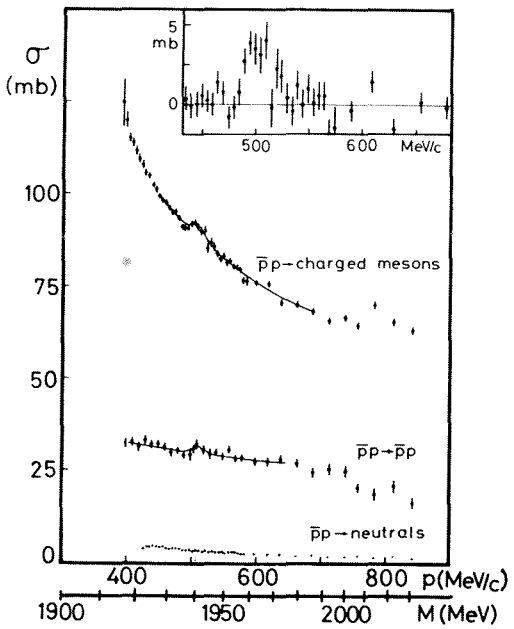

Figure 1: The excitation function for the pp annihilation into charged particles and for elastic scattering. The resonance seen at 505 ± 15 MeV/c corresponds to a c.m. energy of 1939 ± 3 MeV.

Figure 1 displaying the results of a Heidelberg group demonstrates the weakness of the signal-to-noise ratio when resonances are to be observed in formation experiments. Further evidence for the S resonance was reported at the Tokyo conference[7], but these results also suffer from poor statistics. Recently, Tripp et al.[8] repeated the Carrol[3] experiment and did not find any indication of the S resonance. In view of the weak signal of the S resonance in the total cross section I cannot believe that this resonance can be observed at all in a transmission experiment using a wide momentum bite without knowing its mean momentum. At KEK in Japan an experiment by Fujii et al.[4] which is comparable in effort to that of the Heidelberg group will soon be finished.

3. PRODUCTION EXPERIMENTS

3.1 "High" energy

Some two years ago two narrow resonances in the $\bar{p}p$ system were observed at 2.02 GeV and 2.2 GeV in an experiment with 9 and 12 GeV π^- on hydrogen performed with the Ω spectrometer at CERN[10]. An indication of the S resonance was also observed. In the reaction $\pi^- + p \to (p_f\pi^-)(\bar{p}p)$ the four-constraint fit was applied as to select the proper channel ($\bar{p}p$ against $K^+K^-, \pi^+\pi^-$) and to render possible the introduction of further kinematical cuts to improve the signal-to-noise ratio. It should be pointed out that the 2.02 GeV resonance shows up in the spectrum without any kinematical cuts. With more restrictive cuts, essentially reducing the $\bar{p}$ produced in the forward direction, the spectrum in Fig. 2 is obtained.

At the Washington meeting in 1979 Carroll et al. reported on a similar experiment at Brookhaven: $\pi^+ + p \to (p_f\pi^+)(\bar{p}p)$ in which no resonance was observed. As this study is unpublished it is difficult to judge its credibil-

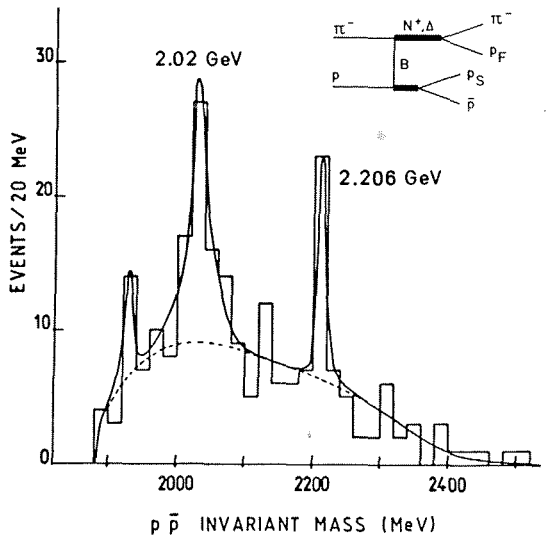

Figure 2: The distribution of the $\bar{p}p$ invariant mass with a $\cos\Theta < 0$ and a $1175 < M(p_F\pi^-) < 1300$ MeV selection for the sample of the two 9 + 12 GeV/c runs.

ity. It is believed, however, that in this experiment no four-constraint fit could be applied and the quality of the data may not have been sufficiently good as to observe narrow resonances.

Two experiments checking the Ω experiments will soon be performed with the same precision but higher statistics, namely at Brookhaven by S.V. Chung et al. on MPS investigating $\pi^- p \to (\pi^- p_f)(\bar{p}p)$ at 12 GeV/c and 16 GeV/c and at CERN (WA 56 Ω') investigating $\pi^+ p \to \Delta^{++}(\bar{p}p)$ and $\pi^+ p \to p_f(p\bar{n})$ at 20 GeV/c pion momentum.

At SLAC a $\gamma + p \to p(\bar{p}p)$ measurement has been analyzed but not yet been published. At CERN in the WA4 experiment the same reaction was studied and found to be worth repeating as to look for S-meson production.

Let me mention also another Brookhaven experiment looking for low mass in the $\bar{p}p$ system[11]. The reaction used was $np \to (\bar{p}p)X$ with the $(\bar{p}p)$ pairs produced in the forward direction. While φ and Λ (1520) clearly show up in the (K^-K^+) and (K^-p) invariant mass spectra, no narrow $(\bar{p}p)$ resonance has been observed.

3.2 "Low" energy

Baryonium states below the $\bar{p}p$ threshold were preferentially searched for by using stopped $\bar{p}$[12,13] and by looking for radiative capture in $\bar{p}p \to \gamma + X$. This reaction was suggested according to the belief that baryon states close to the $\bar{p}p$ threshold have deuteron-like properties[1] and the radiative capture to baryonium states may compete with the annihilation.

In an experiment at CERN[14] three gamma lines were discerned. If interpreted as gammas leading to baryonium states, these states would have masses 1.68, 1.65 and 1.4 GeV. The statistics in this experiment, however, is too poor, which is rather typical for baryonium search, to furnish conclusive evidence on narrow states below the $\bar{p}p$ threshold.

It was pointed out[15] that the $\bar{p}p \to \pi^- + X$ reaction should have all the required properties for populating baryonium states at the threshold, just like the $\bar{p}p \to \gamma + X$ reaction has, but in addition with a much higher cross section. In fact, this reaction is the analog to the $pp \to \pi d$ reaction which is well known for its high cross section (1.4 mb/sr) at 1.3 GeV/c incoming protons. Presently, an experiment is under way at CERN[14] aiming at verifying the existence of baryonium states below 2 GeV mass.

3.3 Knock-out reaction

Of some limited use for the search for baryonium states at the threshold is the reaction $\bar{p} + d \to p + (\bar{p}n)$. In this reaction one of the nucleons in the deuterium is replaced by the $\bar{p}$. This reaction clearly favours a large size object. Its limitation is due to the very small mass bite that can be reached. Replacing a nucleon has a large probability only if the momentum transfer to the baryonium state is of the order of the Fermi momenta of the nucleons in the deuteron. This limits the mass region that can be investi-

gated by this reaction to about 40 MeV below and above the $\bar{p}p$ threshold. Two experiments using this reaction have recently been finished, one at Brookhaven and the other at CERN, but neither has been analysed yet.

4. CONCLUSIONS

I would like to emphasize once again that the problem of baryonium is not just a problem of the existence of a single resonance in the $\bar{p}p$ system, but rather of the existence of sufficient states as to render baryonium spectroscopy possible. This explains the search for such states in a rather large "mass" bite.

During the last two years the existence of three narrow resonances in the $\bar{p}p$ system at 1.94, 2.02 and 2.2 GeV has been indicated. Some recent experiments trying to verify their existence failed to do so. To my opinion, none of these experiments has a higher credibility than the previous ones. And I am rather optimistic and hope that the current experiments searching for baryonium will soon yield positive results.

We should not forget, however, that there are some broad structures (100-200 MeV) in the $\bar{p}p$ cross section which are attributed to the T, V and U resonances and which should be carefully investigated. We should not forget the lesson we just learned from experiments at Argonne on the pp interaction. It took 20 years to find out that the pp cross section is not flat if one looks carefully enough, and there exists strong evidence for diproton resonances. This result would have been of great significance for understanding the nucleon-nucleon interaction had it been known earlier. It still may be of importance when comparing the nucleon-nucleon to the nucleon-antinucleon interaction.

* * *

REFERENCES

1) J.L. Rosner, Phys. Rep. 11C, 189 (1974); C. Rosenzweig, Phys. Rev. Lett. 36, 697 (1976); G.F. Chew, LBL Preprint 5391 (1976); G.F. Chew, contribution to the Third European Symposium on Antinucleon-Nucleon Interactions, Stockholm, 1976; L.N. Bogdanova, O.D. Dalkarov and I.S. Shapiro, Ann. Phys. 84, 261 (1974).

2) G.C. Rossi and G. Veneziano, CERN Preprint TH-2287, to be published in Nucl. Phys. B.

3) A.S. Carroll et al., Phys. Rev. Lett. 32, 247 (1974).

4) V. Chaloupka et al., Phys. Lett. 61B, 487 (1976).

5) W. Brückner et al., Phys. Lett. 67B, 222 (1977).

6) H.H. Chan, following contribution.

7) S. Sakamoto et al., contribution to the Tokyo Conf. 1978, preprint.

8) R.D. Tripp, pivate communication.

9) T. Fujii, private communication.

10) P. Benkheiri et al., Phys. Lett. 68B, 483 (1977).

11) A.S. Carroll et al., Phys. Rev. D19, 1950 (1979).

12) T. Kalogeropoulos et al., Phys. Rev. Lett. 35, 824 (1975).

13) P. Pavlopoulos et al., Phys. Lett. 72B, 415 (1978).

14) R. Bertini et al., proposal, CERN/PSC/78-15 (1978).

15) G. Dosch and B. Povh, MPI-H-1978-V6 (1978).

* * *

DISCUSSION

Chairman: G. Ekspong

Sci. Secretaries: S. Maury and H. Plothow

S.J. Lindenbaum: You stated that the Carrol et al. experiment at the BNL/MPS was similar to the CERN Ω experiment on baryonium and so far did not have a clear contradiction of it. You also stated that the Chung et al. experiment was also planned at the MPS at BNL to check the CERN baryonium experiment. Carroll et al. studied π^+p.

The Chung et al. experiment at MPS observed π^- + p at 12 GeV/c and at 16 GeV/c some time ago. This is similar even in trigger to the CERN Ω experiment. Our BNL/CCNY group collaborated in this experiment. The estimated data taken at 12 GeV/c is about twice the CERN data. At 16 GeV/c we have taken five times more data than that. Owing to various mundane reasons the data are still being analysed. This experiment is the only one similar to the CERN Ω experiment and should be expected to clearly confirm or contradict it.

B. Povh: I agree with your statement about the Carroll et al. and the Chung et al. experiments. I am not aware, however, that the Chung et al. experiment has already been performed and is awaiting analysis.

THEORETICAL IMPLICATIONS OF NARROW HADRON STATES

Chan Hong-Mo,
CERN, Geneva, Switzerland.

ABSTRACT

Various theoretical interpretations of narrow hadron states unconnected with new flavours are reviewed, with special emphasis on narrow baryoniums above the $N\bar{N}$ threshold which are believed to be indicative of a new phenomenon, due probably to colour, never before realized in hadron spectroscopy.

In the last two years there have been frequent experimental reports of narrow hadron states in the mass region 1.5-3.0 GeV. Most of them are associated with $B\bar{B}$ channels, either through their production or their decay, and are therefore called "baryoniums" by experimenters. A partial list of the most interesting examples is given in Table 1. Some narrow structures are reported also in meson-baryon channels. For example, in a contribution to this conference, evidence is presented for a state at 3.17 GeV with width $\lesssim$ 20 MeV and decaying mainly into three strange particles, e.g. $K\bar{K}Y$. Unfortunately, in nearly all cases the evidence is as yet inconclusive and is still being hotly debated among experimenters. This is, however, a purely experimental question to which I am not competent to add my own opinion. Here I am concerned only with their possible interpretation in case they do exist.

Table 1

Mass (GeV)	Width (MeV)	Seen in
1.68	$\sim$ 20	$p\bar{p} \to \gamma X$ $e^+e^- \to X$
1.936 (S)	4-8	$p\bar{p} \to X$ $p\bar{p} \to p\bar{p}$ $p\bar{p} \to \bar{p}p$
2.020	$\lesssim$ 20	$\pi^-p \to \Delta(p\bar{p})$
2.204	$\lesssim$ 20	$\pi^-p \to \Delta(p\bar{p})$
2.95	$\lesssim$ 20	$\pi^-p \to (p\bar{p}\pi^-)X$

Let us consider for the moment only "baryoniums"; but most of our arguments are immediately generalizable to other cases. The first question to ask, of course, is why they are so narrow, their masses and quantum numbers being such that there are plenty of open mesonic channels into which they can decay. The situation is reminiscent of the familiar case of J/ψ, which is also very narrow yet not forbidden to decay into ordinary particles by any known selection rule. Although still not fully understood, this so-called OZI suppression has some explanation in terms of either the quark-gluon model or the unitarized dual model,

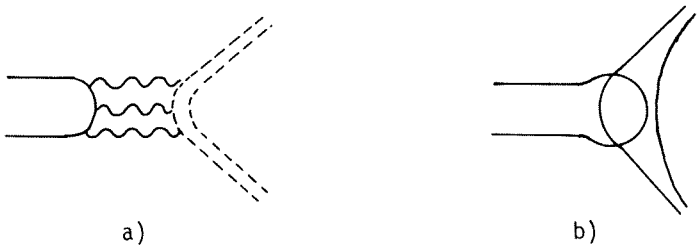

Fig. 1

as illustrated in Fig. 1. In either case, however, the argument relies on the supposition that J/ψ is associated with a new quark (charm), which makes it hard for the resonance to decay directly into ordinary particles.

Can the same argument be applied to baryonium? *A priori* No! True, baryoniums are associated with $B\bar{B}$ channels in much the same way as J/ψ is associated with charm. Indeed, once above the $N\bar{N}$ threshold they are seen to decay preferentially into final states with a $B\bar{B}$ pair. Yet, as far as we see, these $B\bar{B}$ channels are not distinguished from meson channels by any new quantum numbers. We are accustomed to think of a baryon as being made up of three ordinary quarks, which have no difficulty in recombining with the three antiquarks in an antibaryon to form mesons. Indeed, the large annihilation cross-section for $N\bar{N}$ collisions testifies to the soundness of this assertion. Of course, it is not entirely excluded that a baryon may be distinguished from a general three-quark system by some hidden internal structure. For example, it has been suggested that the three quarks in a baryon are linked together by a junction, as illustrated in Fig. 2a, which takes some effort to dissolve. In that case, the model of Fig. 2b for baryonium will be inhibited from decaying into mesons by much the same mechanism as the OZI suppression in Fig. 1b -- instead of the charm quark pair in Fig. 1, a junction pair has now to be annihilated, as depicted in Fig. 2c. When put in this way, models like this can hardly be regarded as an explanation for baryonium but just as a replacement of a new phenomenon by a new assumption. They are therefore to be justified by theoretical arguments outside the topic under discussion, such as connection to QCD, connection to duality, or internal consistency. In my opinion, however, none of the current versions of such models is as yet convincingly justified in this manner.

There is, however, an easier way of suppressing the decay into mesons of a system containing both quarks and antiquarks; namely, by separating the quarks from the antiquarks by an angular momentum barrier. This is more economical than the junction-type models just

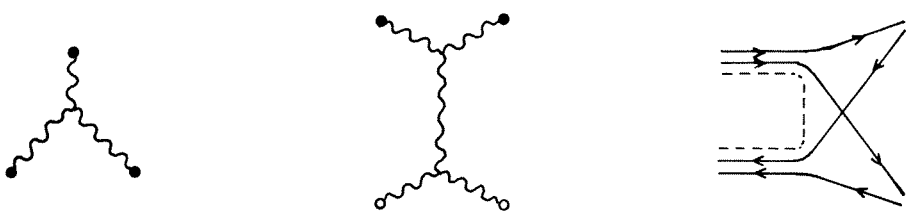

Fig. 2

discussed, since no new assumption is involved except that quarks carry angular momentum, which presumably most of us are ready to accept. The only question is a quantitative one, namely whether this kinematical suppression is sufficient to explain the phenomenon experimentally observed. For example, the barrier effect cannot apply to zero L states, nor can it be expected to yield mesonic widths of much less than a few MeV. Experimentally all existing baryonium candidates with identified quantum numbers have spin ≥ 3 and, except for S(1.936), no width has as yet been measured to be less than the usual experimental resolution of around 20 MeV. At present, therefore, there is no compelling empirical reason for assuming that there is any suppression mechanism other than the angular momentum barrier.

Even accepting the barrier argument, there are still two possibilities for baryonium:

i) nucleon-antinucleon states held together by ordinary nuclear forces;
ii) diquark-antidiquark states held together by confinement forces.

Nuclear forces, being short-ranged, are incapable of forming metastable states with very high angular momentum or very high mass -- also, tightly bound states are very unstable because of annihilation. Hence, for alternative (i), one expects metastable baryoniums only around the $N\bar{N}$ threshold. On the other hand, the confinement potential is not only long-ranged but is supposed even to increase with distance. It is capable, therefore, of forming baryonium states essentially with any angular momentum and any high mass. Around the threshold region, however, the two versions are not readily distinguishable except by detailed calculations of the resonance spectrum and decay widths. Unfortunately, models of either category are not yet sufficiently developed for doing very accurate calculations. It may be said in general that (i) predicts many more baryonium states below the $N\bar{N}$ threshold than does (ii), but the present experimental information can be comfortably accomodated in either without lending any strong support.

Once mesonic decays are suppressed by any mechanism, narrow states below and just above the $N\bar{N}$ threshold can be expected. One has therefore no difficulty in explaining the existence of such states as (1.68) and S(1.936) in Table 1 in any of the models discussed above, although some may be more specific in their predictions than others. Difficulty arises, however, for those narrow states which are reported some way above the $N\bar{N}$ threshold, such as the (2.020), (2.204), and (2.95) of Table 1. Indeed, it is here that the main interest of the whole subject lies. None of the arguments presented above can suppress the decay of a resonance into final states containing an $N\bar{N}$ pair, so that above the $N\bar{N}$ threshold such states will in general be broad. We have already asserted that nuclear resonant states of $N\bar{N}$ [alternative (i)] are very unstable above the $N\bar{N}$ threshold. There have been some suggestions that possibly one can still obtain narrow states by forming bound states of excited nucleons, thus, $N^*\bar{N}^*$. However, since excited nucleons themselves decay readily, e.g. $N^* \to N\pi$, with large widths, narrow states obtained in this way cannot be of a general occurrence. On the other hand, diquark-antidiquark resonances, in decaying into $B\bar{B}$, require the creation of a $Q\bar{Q}$ pair; thus $(QQ)\div(\bar{Q}\bar{Q}) \to (QQQ) + (\bar{Q}\bar{Q}\bar{Q})$. Such decays are very similar to the decays of ordinary excited meson and baryon resonances, e.g. $f \to \pi\pi$, which also require a quark pair creation; thus $(Q)\div(\bar{Q}) \to (Q\bar{Q}) + (Q\bar{Q})$. The expected widths of such decays are thus of the order of 100 MeV as for ordinary hadrons, not the small widths of < 20 MeV experimentally observed. Hence if these states really exist, they are indicative of a new phenomenon never before realized in hadron spectroscopy.

What, then, is a possible explanation? In my opinion there is at present only one viable suggestion, namely colour. In the current picture of quark confinement, quarks carry a colour charge corresponding to the representation 3 of colour SU(3). A diquark can then have colour $3 \times 3 = \bar{3}$ or 6. Similarly, an antidiquark has colour 3 or $\bar{6}$. There are therefore two ways of forming a colour singlet diquark-antidiquark resonance, namely $(QQ)^{\bar{3}}\text{--}(\bar{Q}\bar{Q})^{3}$ or $(QQ)^{6}\text{--}(\bar{Q}\bar{Q})^{\bar{6}}$, where superscripts denote colour. The former can decay readily into $B\bar{B}$ pairs as indicated above, thus $(QQ)^{\bar{3}}\text{-}\cdot\text{-}(\bar{Q}\bar{Q})^{3} \to [(QQ)^{\bar{3}}Q^{3}]^{1} + [(\bar{Q}\bar{Q})^{3}\bar{Q}^{\bar{3}}]^{1}$; but not the latter, since a colour-6 diquark cannot combine with a colour-3 quark to form a colour-singlet baryon: $6 \times 3 = 8 + 10 \not\ni 1$. In order to decay into $B\bar{B}$, the resonance $(QQ)^{6}\text{--}(\bar{Q}\bar{Q})^{\bar{6}}$ must first mix with $(QQ)^{\bar{3}}\text{--}(\bar{Q}\bar{Q})^{3}$, but there are indications, both theoretical and phenomenological, that such an effect will decrease with increasing separation between the diquark and the antidiquark. The implication is then that for large L the resonances $(QQ)^{6}\text{--}(\bar{Q}\bar{Q})^{\bar{6}}$ will have their decays into $B\bar{B}$ channels suppressed and can therefore retain a narrow width even high above the $N\bar{N}$ threshold. Thus if the existence of such narrow states is confirmed by future experiment, it may be considered a triumph for the current theory of colour confinement.

How can we test that these tentative narrow states are indeed colour molecules of the type $(QQ)^{6}\text{--}(\bar{Q}\bar{Q})^{\bar{6}}$ and not the consequence of some previously unknown effect? First, if our interpretation is correct, then they are not isolated cases -- there must be a whole family of them corresponding to the various orbital separations L and the various spin configurations of the diquarks from which they are formed. Secondly, since other modes are suppressed, they prefer to decay by cascade into one another, emitting mesons; thus:

$$(QQ)^{6}\text{-}\overset{L}{-}\text{-}(\bar{Q}\bar{Q})^{\bar{6}} \to (QQ)^{6}\text{-}\overset{L'}{-}\text{-}(\bar{Q})^{3}\text{-}\cdot\text{-}(\bar{Q})^{3} \to (QQ)^{6}\text{-}\overset{L'}{-}\text{-}(\bar{Q}\bar{Q})^{\bar{6}} + (Q\bar{Q})^{1} \ .$$

Thirdly, they are predicted to have reasonable production cross-sections but are hard to form in the direct channel of $N\bar{N}$ collisions, this prediction having to do with the strong dependence of colour mixing on the mass t of the $QQ\bar{Q}\bar{Q}$ system, somewhat analogous to violations of the OZI rule. These are all quite unusual properties which are useful for distinguishing the colour interpretation from other alternatives.

Finally, making more explicit use of the existing models for colour confinement, such as the one-gluon exchange model for hyperfine splittings and the MIT bag model for the Regge slope (both already tested in ordinary meson and baryon spectroscopy), one can calculate approximately the spectrum of such narrow baryoniums in terms of just a couple of parameters. Figure 3 is an example of such a calculation. Knowing the spectrum, one can then proceed to predict other properties such as the detailed cascade pattern of each resonance. It would seem that if these states really do exist, then their interpretation as colour molecules could be tested quite unambiguously. Unfortuantely, as mentioned in the beginning, the experimental situation is chaotic, but the scanty information available, taken uncritically, is not inconsistent with the predictions, as seen also in Fig. 3.

It is clear that very similar arguments can be extended to other multiquark systems. For example, we can have resonances such as $(QQ)^{6}\text{---}(QQ\bar{Q})^{\bar{6}}$ with baryon number 1, which would again have difficulty in decaying into ordinary hadrons, thus acquiring a narrow width even at high mass, and would prefer to decay by cascade into each other, emitting mesons. Hence if these conjectures are confirmed it would appear that we have just opened up a whole new and intriguing area of hadron spectroscopy which is almost equal in complexity to inorganic chemistry.

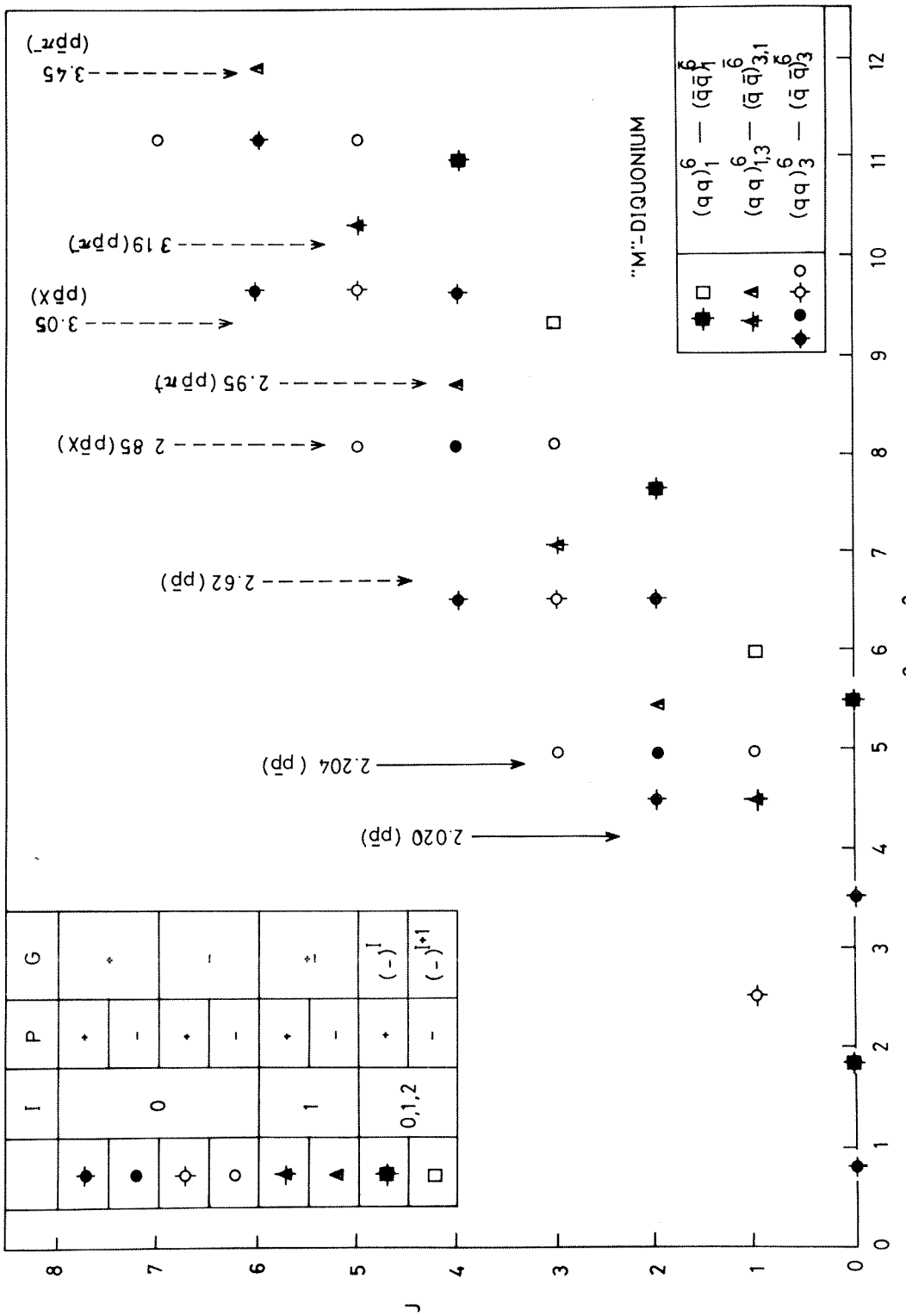
J
M² (GeV²)
I
P
G
0
1
0,1,2
+
−
±
2.020 (pp̄)
2.204 (pp̄)
2.62 (pp̄)
2 85(pp̄X)
2.95 (pp̄π)
3.05 (pp̄X)
3 19(pp̄π)
3.45 (pp̄π)
"M²-DIQUONIUM
(qq)₁⁶ — (q̄q̄)₁⁶
(qq)₁,₃⁶ — (q̄q̄)₃,₁⁶
(qq)₃⁶ — (q̄q̄)₃⁶

Fig. 3

It is regrettable that no detailed bibliography is possible with the limited space allotted. We quote only a random selection of references.

For reviews of experiments see:

B. Povh, invited talk, this conference.

L. Montanet, 5th Int. Conf. on Experimental Meson Spectroscopy, Boston, 1977; CERN preprint EP/PHYS 77-22; and Proc. 13th Rencontre de Moriond, Les Arcs, 1978 (ed. J. Tran Thanh Van) (Editions Frontières, Dreux, France, 1978) "Phenomenology of Quantum Chromodynamics", p. 285.

For models of baryonium suppressing mesonic decays by other mechanisms than just angular momentum, see for example:

M. Imachi et al., Progr. Theor. Phys. 57 (1977) 517.

G.C. Rossi and G. Veneziano, Nucl. Phys. B123 (1977) 507.

G.F. Chew, CERN preprint TH 2671 (1979).

For models of baryonium as nuclear $N\bar{N}$ states, see for example:

R. Vinh Mau, Proc. 13th Rencontre de Moriond, Les Arcs, 1978 (ed. J. Tran Thanh Van) (Editions Frontières, Dreux, France, 1978) "Phenomenology of Quantum Chromodynamics", p. 273.

For colour models of narrow states, see for example:

Chan Hong-Mo and H. Høgaasen, Phys. Lett. 72B (1977) 121 and Nucl. Phys. B136 (1978) 401.

R.L. Jaffe, Phys. Rev. D 17 (1978) 1444.

Chan Hong-Mo et al., Phys. Lett. 76B (1978) 634.

* * *

DISCUSSION

Chairman: G. Ekspong

Sci. Secretaries: S. Maury and H. Plothow

O. Pène: Do you not believe that a big angular momentum between diquark and antidiquark might imply a centrifugal barrier effect which would also prevent a large width into $p\bar{p}$ even if diquark-antidiquark is in a $3\text{-}\bar{3}$ state, since phase space is smaller than for ordinary hadron decays with analogous angular momentum; and, on the contrary, that $6\text{-}\bar{6}$ diquark-antidiquark states would decay into mesons because colour forces push apart the two quarks in a diquark?

Chan Hong-Mo: No, I do not believe either statement. First, high angular momenta do not prevent ordinary mesons and baryons from decaying readily into mesons and meson-baryon, respectively. I do not see why they should suppress $B\bar{B}$ decays of diquark-antidiquark systems. I am sure one can construct models in which this is so (I understand that some of Dr. Pène's collaborators are authors of one such model), but I see no reason why one should accept these model assumptions rather than some others. Secondly, I do not believe that $6\text{-}\bar{6}$ diquoniums will decay readily into mesons, basing my statement on the MIT bag model which to me is a more realistic model for confinement than the potential model which Dr. Pène uses. In the bag model, high-L $6\text{-}\bar{6}$ diquoniums are kinematically forbidden to split into two high-L mesons. I refer you to a paper of Høgaasen and myself on the subject in Phys. Letters (1978).

HYPERCHARGE EXCHANGE REACTIONS AND HYPERON RESONANCE PRODUCTION

A.C. Irving

Department of Applied Mathematics and Theoretical Physics, Liverpool University, Liverpool L69 3BX, U.K.

ABSTRACT

A review is presented of recent high statistics results on hypercharge exchange processes. Intermediate energy data on helicity non-flip dominated processes (Σ production) and on helicity-flip processes (Σ^* production) reveal complicated and strongly energy-dependent systematics for exchange degeneracy breaking. Preliminary data at 70 GeV/c show evidence of the expected effects of high-lying J-plane singularities at $|t| \gtrsim 0.5$. No existing model, or simple modification thereof, can describe the major features of the new data.

1. INTRODUCTION

In this short report I shall discuss what lessons may be learned from the recent experimental results on hypercharge exchange (HYCEX) processes. The latter represent one of the final attempts to achieve a simple understanding of two-body hadronic exchange mechanisms. Since the instigation of these experiments to measure

$$K^- p \to \pi^- \Sigma^+ \qquad (1a)$$

$$\pi^+ p \to K^+ \Sigma^+ \qquad (1b)$$

and

$$K^- p \to \pi^- Y^*(1385)^+ \qquad (2a)$$

$$\pi^+ p \to K^+ Y^*(1385)^+ \qquad (2b)$$

there has been an increasing suspicion that we may, as it were, be attempting to discover QED by measuring uranium-lead scattering. Nonetheless, these HYCEX processes, together with their charge-exchange (CEX) analogues have already provided valuable information about such global, phenomenological features as Regge pole dominance, exchange-degeneracy and absorption effects. These laboriously accumulated systematics must be held in store for the day when "complete solutions" for the hadronic interaction are being tested.

Particular attractions of processes (1) and (2) are that they readily yield polarisation information, they test line-reversal symmetry (LRS) and hence EXD, they exhibit both helicity-flip and non-flip dominated cross-sections (processes (1) and (2) respectively) and they are simply related by SU(3) to CEX processes.

2. HYCEX FOLKLORE

"One may wax eloquent for many a moon on the standard folklore applied to the hypercharge exchange reactions. Here rather than a full core dump,

we present a restrained soliloquy".

G.C. Fox (Nucl. Phys. B56, 386 (1973))

The exchange amplitude structure of reactions 1a,b can be expressed as

$$K^- p \to \pi^- \Sigma^+ = V+T \equiv A_R \tag{3a}$$

$$\pi^+ p \to K^+ \Sigma^+ = -V+T \equiv A_C \tag{3b}$$

In a 2-Regge pole model ($V \equiv K^*(890)$, $T \equiv K^{**}(1420)$) these amplitudes would be

$$V = \beta_V \, ie^{-i\pi\alpha_V/2} s^{\alpha_V} \tag{4a}$$

$$T = \beta_T \, e^{-i\pi\alpha_T/2} s^{\alpha_T} \, . \tag{4b}$$

Let us denote the differential cross-sections for processes 1a,b by σ_R, σ_C respectively (R ≡ Real, C ≡ Complex in a dual solution). The quantity $\tilde{\cos}\varphi_{VT}$ [1], defined by

$$\tilde{\cos}\varphi_{VT} \equiv (\sigma_R-\sigma_C)/(\sigma_R+\sigma_C) = 2|V/T|\cos\varphi_{VT}/[1+|V/T|^2] \tag{5}$$

gives some measure* of the spin-averaged relative phase difference φ_{VT} between vector and tensor exchanges. In a 2-pole model (4)

$$\tilde{\cos}\varphi_{VT} = 2\lambda \sin\tfrac{\pi}{2}(\alpha_V-\alpha_\pi)/[1+\lambda^2], \tag{6}$$

where $\lambda(s,t) = (\beta_V/\beta_T)s^{\alpha_V-\alpha_T}$. Thus $\tilde{\cos}\varphi_{VT}(t) \equiv 0$ if weak EXD ($\alpha_V(t) = \alpha_T(t)$) holds. It should also vanish when $\alpha_V(t) = 0$ if vector exchange has a nonsense wrong-signature zero: $\beta_V \sim \alpha_V(t)$ (cf. ρ in $\pi^- p \to \pi^0 n$). In the latter case, σ_R and σ_C would exhibit a cross-over at this t-value (-0.4?). Even if EXD does not hold, $\tilde{\cos}\varphi_{VT}$ should vary <u>slowly</u> with s assuming $|\alpha_V-\alpha_T|$ is not too large (the K^* spectrum suggests less than 0.1-0.2) and that leading Regge poles do indeed dominate. Any zero structure would be independent of s.

Denoting helicity flip and non-flip amplitudes by F and N respectively, the polarisation P is given by

$$P\sigma = -2\mathrm{Im}[NF^*] \tag{7}$$

so that

$$P_R\sigma_R + P_C\sigma_C = -2\mathrm{Im}[N_V F_V^* + N_T F_T^*]. \tag{8}$$

---

* $2x/(1+x^2)$ differs from 1 by less than 20% for $0.5 < x < 2$.

In any 2-pole model this must vanish so that

$$P_R = -P_C(\sigma_R/\sigma_C). \tag{9}$$

The vector and tensor polarisation contributions to eqn. (8) are respectively analogous to those in $\pi^- p \to \pi^0 n$ and $\pi^- p \to \eta n$. If weak EXD holds, $\sigma_R = \sigma_C$ so that

$$P_R = -P_C. \tag{10}$$

If strong EXD holds ($\beta_V/\beta_T = \tan\pi\alpha/2$, $\alpha = \alpha_V = \alpha_T$), then $F_R, N_R \sim$ real and $F_C, N_C \sim e^{-i\pi\alpha}$ so that

$$P_R = P_C = 0. \tag{11}$$

Simple coupling arguments [1] tell us that the Σ cross-sections (1) and Y^* cross-sections (2) will be helicity non-flip and flip dominated respectively. One should study both.

3. RECENT HYCEX DATA

Fig. 1 shows σ and P for reactions (1) at 7 and 10 GeV/c as measured in the experiment by Berglund et al [2] at CERN. In this counter experiment and in the hybrid experiment of the SLAC/Imperial College collaboration [3),4)] particular attention was paid to reducing relative normalisation errors between the $K^- p$ and $\pi^+ p$ channels.

In this figure one notices: i) A cross-over in the cross-sections ($\sigma_R > \sigma_C$ at small t) which moves to smaller t as s increases. ii) A marked change in slope near t = -.5 (pole/cut interference?). iii) The EXD violation drops rapidly with energy. iv) The polarization is large and approximately mirror symmetric (eqn. 10). It does not decrease with s in this range. Fig. 2 shows $\widetilde{\cos}\varphi_{VT}$ for this data set and those of refs. 3,4.

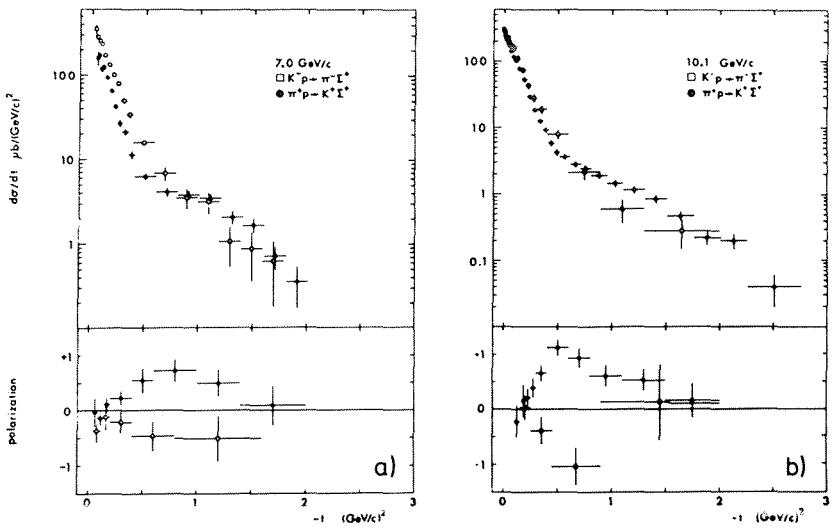

Fig. 1 HYCEX data from ref. 2.

The plots of $\widetilde{\cos\varphi}_{VT}$ vs.t shown in fig. 2 show many of the above features more clearly. At 7 GeV/c there may be some systematic differences at small t between the data of ref. 2 and those of ref. 4. We see:

(i) The rapid s-dependence of $\widetilde{\cos\varphi}_{VT}$ excludes any 2-pole model.

(ii) The Navelet and Stevens [5] (NS) pole + low-lying effective cut model (solid curve in fig. 2a) reproduces the t dependence of $\widetilde{\cos\varphi}_{VT}$ well. The absorption model of Hartley and Kane [6] (HK) with high-lying cuts does not, having too pronounced an EXD violation (dotted curve of fig. 2a). Girardi [7] has recently applied a model with dual Regge-Pomeron, Regge-Regge and Regge-Pomeron-Regge cuts [8] to HYCEX data. The secondary cuts do indeed give $\widetilde{\cos\varphi}_{VT}$ a rapid s-dependence. Since the Regge-Pomeron cuts are the traditional ones [1] which produce $\sigma_C > \sigma_R$, one expects that, asymptotically, $\widetilde{\cos\varphi}_{VT} < 0$ for all t. However, already by 10 GeV/c the model predicts $\widetilde{\cos\varphi}_{VT}$ to be negative (-.3 at t = -.5) whereas the data are still positive.

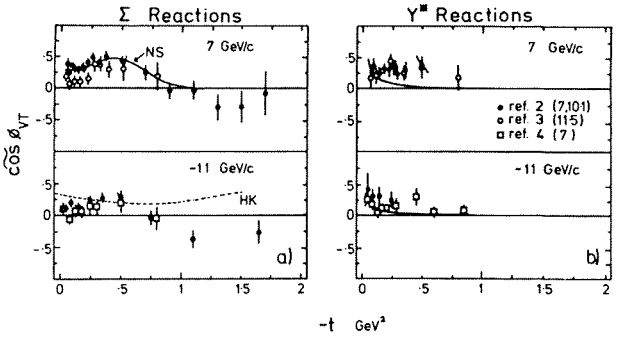

Fig. 2 $\widetilde{\cos\varphi}_{VT}$ for the Σ and Y^* data of refs. 2,3 and 4. The Σ data of ref. 2 are actually at fixed t' rather than t. This makes little difference.

(iii) The $\widetilde{\cos\varphi}_{VT}$ values for the Y^* processes (2) are very large. This can be partially explained [3] by the kinematic behaviour $\sigma \sim (t_{min}-t)$ expected in a helicity flip dominated reaction $[t_{min}(KY^*) < 0,\ t_{min}(\pi Y^*) > 0]$. The solid curves in fig. 2b give the predictions of weak EXD modified by this kinematic effect. Its major effect is at low $|t|$ and s. In the related processes $KN \to K\Delta$, $\bar{K}N \to \bar{K}\Delta$ where t_{min} is much smaller, this effect is quite insufficient to explain the large values of $\widetilde{\cos\varphi}_{VT}$ at 4-6 GeV/c.

Some idea of the discrepancies between the different data sets, both old and new, can be obtained from fig. 3.

We note that:

(i) At large $|t|$, preliminary FNAL $\pi^+p \to K^+\Sigma^+$ data from ref. 9 lie above the simplest Regge pole extrapolations from lower energies as exemplified by the NS model curves superimposed. Classical absorption models [6] predict this (see below).

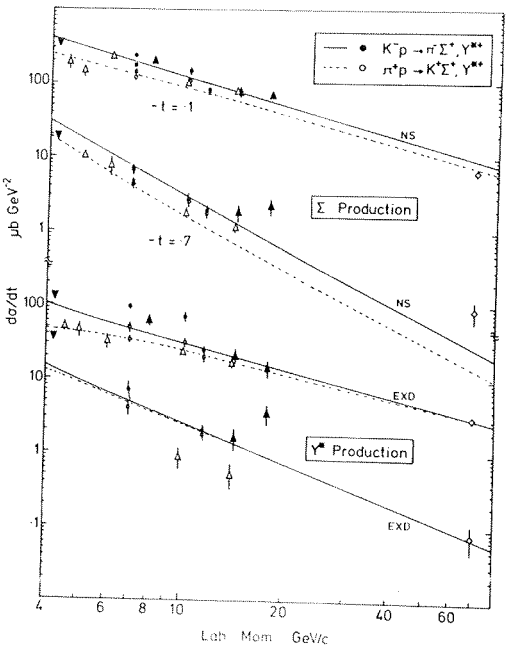

Fig. 3 $d\sigma/dt$ at fixed $|t|$ (.1 and .7) for processes (1) and (2). The recent data of refs. 2, 4 and 9 are distinguished by the symbols ○, □ and ◇ respectively.

(ii) The curves through the Y^* data correspond exactly to those of fig. 2b, i.e. weak EXD + kinematics). The basic pole dependence ($\bar{\alpha}(t = -.1) = .43$, $\bar{\alpha}(t = -.7) = .08$) has been chosen arbitrarily just to guide the eye. The kinematic effect is small compared to discrepancies between data sets.

The result of fits, $\sigma \propto s^{2\alpha_{eff}(t)-2}$, to the π^+p data is summarised in the α_{eff} plots of fig. 4.

(i) Below 10 GeV/c and for $|t| \lesssim 1$, α_{eff} for $\pi^+p \to K^+\Sigma^+$ is much above the expected trajectory $\alpha_{K^*} \simeq .35 + .9t$, presumably due to the destructive effects of low-lying cuts.[5] That of $K^-p \to \pi^-\Sigma^+$ (not shown) is closer to expectation.[2]

(ii) Over the higher momentum range (10-70 GeV/c) α_{eff} at small t is nearer the leading pole trajectory but deviates at larger t. It is reminiscent of the classical absorption model expectation, exemplified in the figure by the prediction of Hartley and Kane[6] for this range (dotted curve). The structure in α_{eff} at $t = -.5$ corresponds to the fact that $d\sigma/dt$ still has a shoulder at $|t| \gtrsim .5$ at 70 GeV/c. Pure Regge pole models tend to have a smooth (exponential) $d\sigma/dt$ in these particular processes (1,2). The structure seen at FNAL[9] is good evidence for cut effects. The K^-p data at FNAL energies is not yet available.

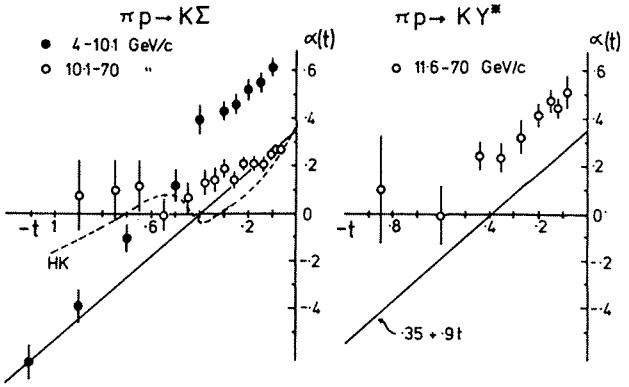

Fig. 4 $\alpha_{eff}(t)$ evaluated over the momentum ranges shown. The 4-10.1 GeV/c data are from ref. 2. The Y^* data used were those of ref. 3,9. Using the data of ref. 2 instead of ref. 3, α_{eff} is changed by $\Delta \propto \simeq -.07$.

(iii) Normalisation discrepancies prevent any firm conclusions about the Y^* data.

Overall we see that the evidence is very much against weak EXD even for the helicity flip dominated processes. Approximate agreement between σ_R and σ_C at one momentum ($\sim$11 GeV/c)[3] is not sufficient evidence for EXD. A model with approximately EXD K^*, K^{**} poles supplemented by low-lying cuts[5] fits the intermediate energy data very well. However, traditional high-lying absorptive cuts must also be present since the polarisation in $\pi^+p \to K^+\Sigma^+$ remains quite large ($\sim$50%) at 70 GeV/c[9] and since the α_{eff} at large t rises over the higher energy range. Existing models (e.g. ref. 5,6, 7,10) are insufficiently complicated to reproduce these features.

4. Y^* PRODUCTION AMPLITUDES

The weak hyperon decay allows one to reconstruct the spin amplitudes of each Y^* process (2) up to 2 undetermined pieces of information, one of which is the overall phase. If transversity spin quantisation is used, one can

express the results as 4 amplitude moduli (fig. 5) and 2 relative phases. The 11.5 GeV/c data for $K^-p \to \pi Y^*$ [11] are very similar to those at 4.2 GeV/c.[12] All data agree with the naive quark model expectation (dotted line on fig. 5) that

$$|T_{m_{Y^*} m_p}| = \begin{cases} 0 \\ \frac{1}{\sqrt{2}} \end{cases} \text{ acc. as } |m_{Y^*} - m_p| = \begin{cases} 2 \\ 0 \end{cases} \qquad (12)$$

except at small $|t'|$. These deviations are not so surprising since the cross-section already shows a finite helicity non-flip component (zero if equation 12 holds) at $t' \simeq 0$. Transversity double-flip can only arise in the quark model via double scattering and so the deviations from (12) should drop with energy. Apart from $|T_{-3/2\ 1/2}|$, the data are consistent with this. The preliminary data at 7 GeV/c, however, show the opposite trend, if any. One must await the final data.

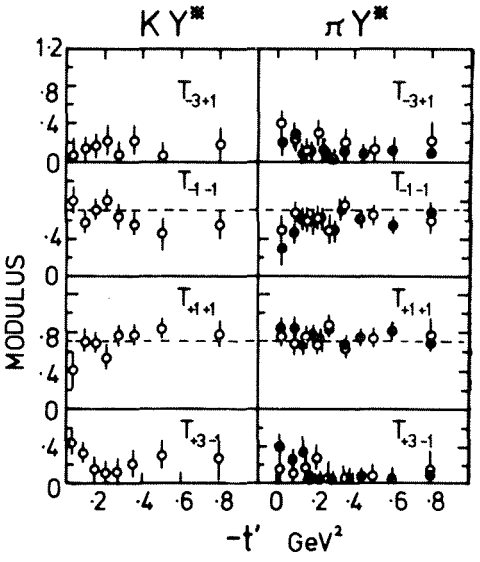

Fig. 5 Transversity amplitude moduli of reactions (2) at 11.5 GeV/c (0)[11] and at 4.2 GeV/c for $K^-p \to \pi Y^*$ ( )[12]. The amplitudes are normalised to unity.

Looking at the differences between KY^* and πY^* amplitudes, one notices that the deviations from the quark model follow different patterns. However, one notices, quite empirically, that the 7 and 11.5 GeV/c data satisfy

$$|T_{m',m}(KY^*)| \simeq |T_{-m',-m}(\pi Y^*)| \qquad (13)$$

in this normalisation, although I know of no theoretical justification for this.

5. OUTLOOK

Basic Regge ideas still represent our only global understanding of the huge mass of long-range hadronic interactions. Hypercharge exchange reactions (1) and (2) provide a particularly severe test of these ideas. The latest data, while confirming these at a qualitative level, also underline the depth of our ignorance when it comes to the details. Believers in QCD will not see this as a significant problem - one simply has to demonstrate confinement, check a few simple perturbative predictions of short distance phenomena and leave the rest to the chemists.

In conclusion, the data from this latest (and probably the last) generation of two-body hadronic experiments is of very high quality indeed and provides many answers. It is unfortunate that few can remember what

the questions were.

Acknowledgements

I thank T.S. Virdee for communicating experimental results prior to publication and H. Navelet for providing model calculations. I am also grateful to CERN Theory Division for support during preparation of this report.

* * *

References

1) A.C. Irving and R.P. Worden, Phys. Reports 34C, 117 (1977), and references therein.

2) A. Berglund et al., Phys. Letters 57B, 100 (1975); ibid. 73B, 369 (1978). Nucl. Phys. B (to be published).
A. Berglund, Univ. of Stockholm Thesis (1978).

3) J. Ballam et al., Phys. Rev. Letters 41, 676 (1978), and private communication from V. Cautis (1979).

4) P.A. Baker et al., preliminary data in Imperial College preprint IC/HEMP/78/21 submitted to the XIX int. conf. on high energy physics, Tokyo, Japan (1978); finalised data to be submitted to Nucl. Phys. B (private communication from T.S. Virdee).

5) H. Navelet and P.R. Stevens, Nucl. Phys. B104, 171 (1976).

6) B.J. Hartley and G.L. Kane, Nucl. Phys. B57, 175 (1973).

7) G. Girardi, J. Phys. G3, 1031 (1977).

8) G. Girardi et al., Nucl. Phys. B69, 107 (1974).

9) M.W. Arenton et al., Argonne report ANL-HEP-RP-78-24.

10) G.L. Kane and A. Seidl, Rev. Mod. Phys. 48(2), 309 (1976).

11) C.V. Cautis et al., SLAC-PUB-2233 (1978), submitted to Nucl. Phys. B. J. Ballam et al., IC/HEMP/78/22 submitted to the XIX int. conf. on high energy physics, Tokyo, Japan (1978).

12) S.O. Holmgren et al., Nucl. Phys. B119, 261 (1977).

THE A_1 MESON PRODUCED AT 63 AND 94 GeV/c IN THE REACTION $\pi^- p \to \pi^-\pi^-\pi^+ p$

ACCMOR COLLABORATION

(Amsterdam-CERN-Cracow-Munich-Oxford-Rutherford)

G. Thompson (Contact Person)

Department of Nuclear Physics, Oxford University, UK.

1. ABSTRACT

The results are presented of partial wave analyses of almost 600,000 events from the reaction $\pi^- p \to \pi^-\pi^-\pi^+ p$ at 63 and 94 GeV/c and with a higher momentum transfer trigger. The shape of the 1^+S $(\rho\pi)$ mass spectrum changes substantially as a function of t, and is not compatible with predictions of the Deck model. In addition, the phase of this partial wave rises by $\sim 90°$ over a mass range of 400 GeV/c^2 relative to 0^-P, 2^-P and the 2^+D production phases. These features provide compelling evidence for a resonant A_1 of mass $\sim$1280 MeV/c^2 and width $\sim$300 MeV/c^2 and indeed a rescattering model with such a state fits the data well.

2. INTRODUCTION

In the naive quark model, a p-wave $q\bar{q}$ should give rise to two, I = 1, spin-parity $J^P = 1^+$ mesons. The positive G-parity candidate, the B(1235) has been long established in the $\omega\pi$ decay mode. The negative G-parity A_1, presumed to decay $\rho\pi$, has defied certain identification principally because of the confusion of pion diffractive dissociation (Deck Model) into the same final state at low $(\rho\pi)$ masses. Attempts to use charge exchange reactions[1] to eliminate this background have met the problem of low statistics and increased complication from the I = 0 channel. Small cross-sections also affect similar attempts to use baryon exchange reactions[2] though here there are specific claims for a comparatively narrow resonance of mass $\sim$1.04 GeV/c^2. This experiment uses very high statistics (some order of magnitude greater than the previous highest forward production experiment[3]) and a more detailed model for coherent background to detect the need for such a resonant state.

The data of this publication come from 598,128 events of the reaction

$$\pi^- p \to \pi^-\pi^-\pi^+ p$$

with incident momenta of 63 and 94 GeV/c on the ACCMOR WA3 forward spectrometer[4]. The momenta are high enough to ensure that in the mass region investigated, the three pion vertex is well separated from the baryon and there is no possibility of N* contamination within the reaction. There is uniform geometric acceptance in momentum transfer (t') and for the purposes of analysis the events are selected in bins $0.0 < |t'| < 0.05$ (GeV/c)^2 (low t') and $0.05 < |t'| < 0.7$ (GeV/c)^2 (high t'). Additionally a 94 GeV/c sample was taken with a selective high t' trigger and here the data is subdivided in bins of $0.16 < |t'| < 0.3$ (GeV/c)^2, and $0.3 < |t'| < 0.7$ (GeV/c)^2 (collectively, very high t').

Within these $|t'|$ bins the data has been subject to two energy independent partial wave analyses based on the isobar model of sequential decay*. In this paper intensities of a given partial wave refer to the acceptance corrected number of events in a given bin

---

* For a detailed comparison of the SLAC amplitude analysis and the University of Illinois density matrix formalism, as used here, see Ref. 4.

multiplied by an appropriate diagonal density matrix element and relative phases are those of an off-diagonal element, though, in this area, the rank of the density matrix is close enough to unity to identify this with the phases between true proton spin amplitudes.

Throughout, the data has been fitted in the Gottfried-Jackson (t channel), frame in mass bins of 20 MeV/c^2 compatible with the (3π) mass resolution of σ = 10-12 MeV/c^2. Within each bin a rough $|t'|$ dependence has been imposed on each wave found from separate fits with 100 MeV/c^2 mass cuts and small t' divisions.

The spectroscopic nomenclature will assume the result of negligible contribution from unnatural parity exchange and, unless stated otherwise, that production is in the predominant M = 0 mode.

3. RESULTS OF THE PARTIAL WAVE ANALYSIS

The intensity of the s-wave $\rho\pi$ $J^P = 1^+$ state (1^+S) is shown for 93 GeV/c data in Fig. 1,2 (a), (b), the 63 GeV/c data appearing similar to Fig. 1. There is little s dependence

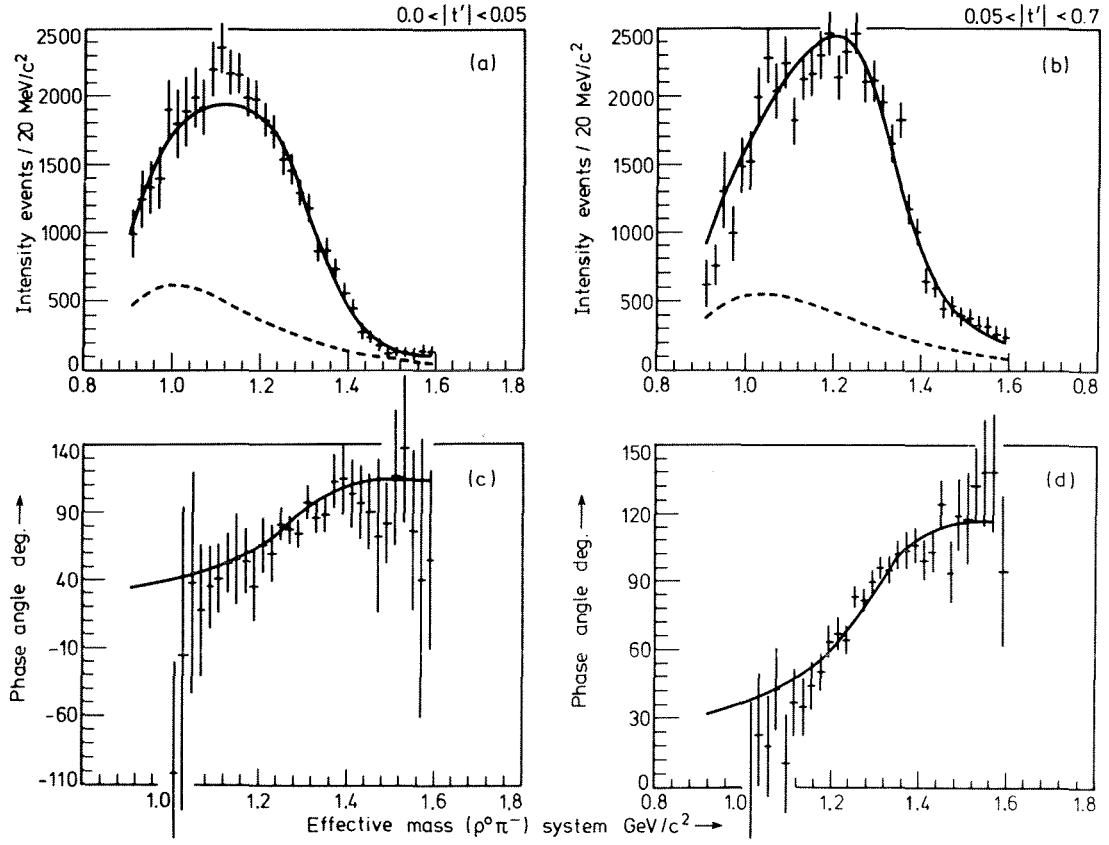

Fig. 1: 94 GeV/c data, 1^+S intensity (a,b) and phases (c,d) relative to $2^+ D_{M=1}$

of the spectrum shape for a given $|t'|$ cuts, but comparison between 1(a) and 1(b) and with 2(a) and 2(b) shows that at a given s there are some large changes in shape as a function of t'. From low to high t' the qualitative change is from a broad peak in the 1.1 GeV/c^2 region, to a flat top from 1.1 to 1.3 with rapid fall off, to, finally, a narrower peak in the 1.3 GeV/c^2 region. It is certainly clear that a resonance alone could never describe these phenomena, and it will become equally clear that no simple diffractive model can

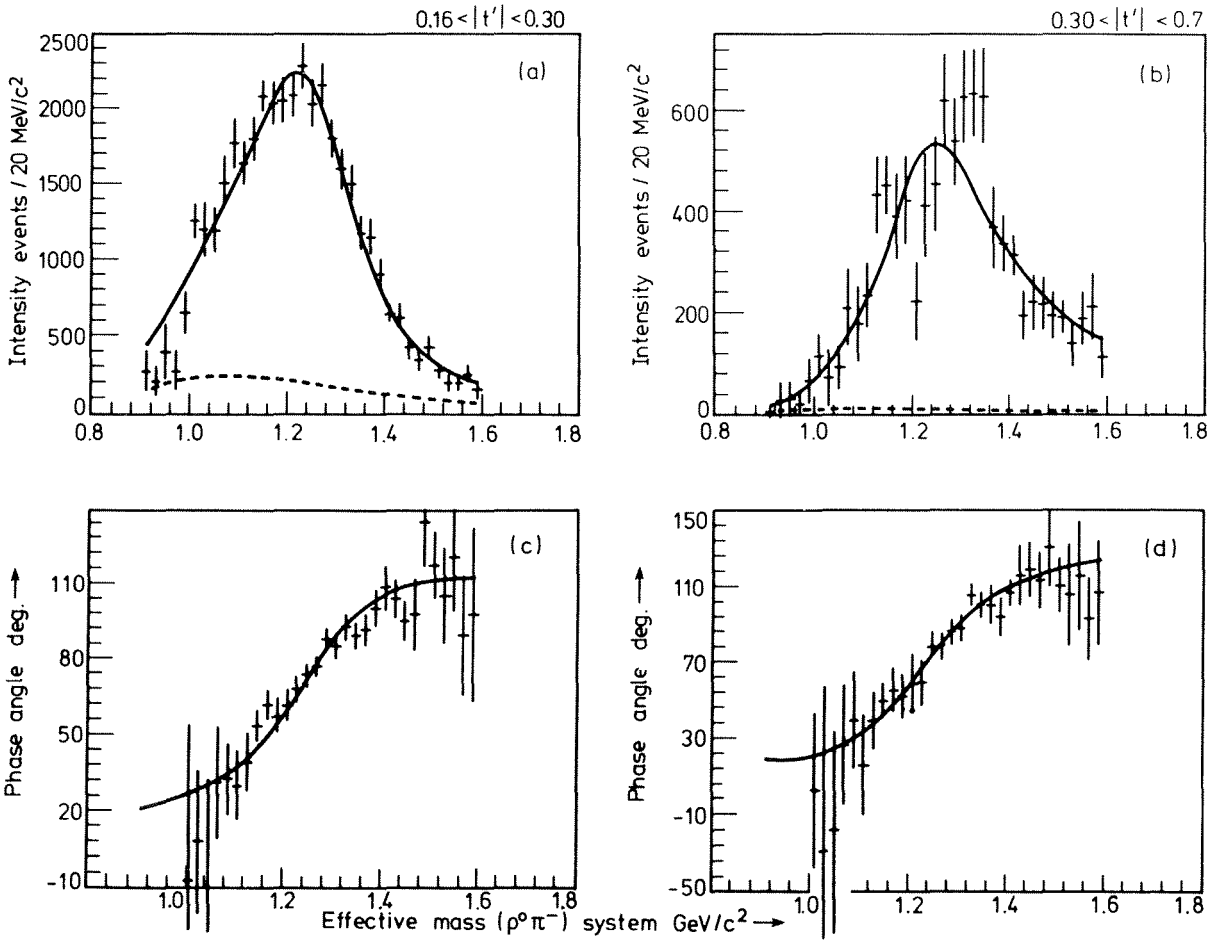

Fig. 2: 94 GeV/c data high t', 1^+S intensity (a,b) and phases (c,d) relative to $2^+D_{M=1}$

duplicate this behaviour either.

This data would not support narrow resonances at masses around 1.1 GeV/c^2, unless highly unlikely conspiracies damp resulting phase variation.

If there is any resonant content in the mass spectrum it should be evident from a sizeable change in the production phase of the 1^+S partial wave. The relative phases with respect to the other major waves in the low mass region are displayed for 93 GeV/c data, high t', in Fig. 3. Those with respect to 1^+P ($\varepsilon\pi$) and 0^-S ($\varepsilon\pi$) show, at most, excursions of only 20-30° and are compatible with previous experiments. Those with respect to $0^-P(\rho\pi)$ and $2^-P(\rho\pi)$ show positive evidence for large phase changes in the vicinity of 1.3 GeV/c^2. Below 1.1 GeV/c^2 there are problems with ambiguous solutions but it is clear that at higher masses there is a discrepancy which may only be resolved by supposing the forward motion of some reference phases (1^+P, 0^-S) or the reverse motions of others (0^-P, 2^-P).

A solution to this difficulty may be found by reference to the 1^+S - $2^+D_{M=1}$ phase difference (Fig. 4). It may be noted that in both |t'| regions there is a large backward movement corresponding to the A_2 meson[5] but this is by no means the full ∿180° as expected from a pure Breit-Wigner and indeed the edges of the distributions may indicate

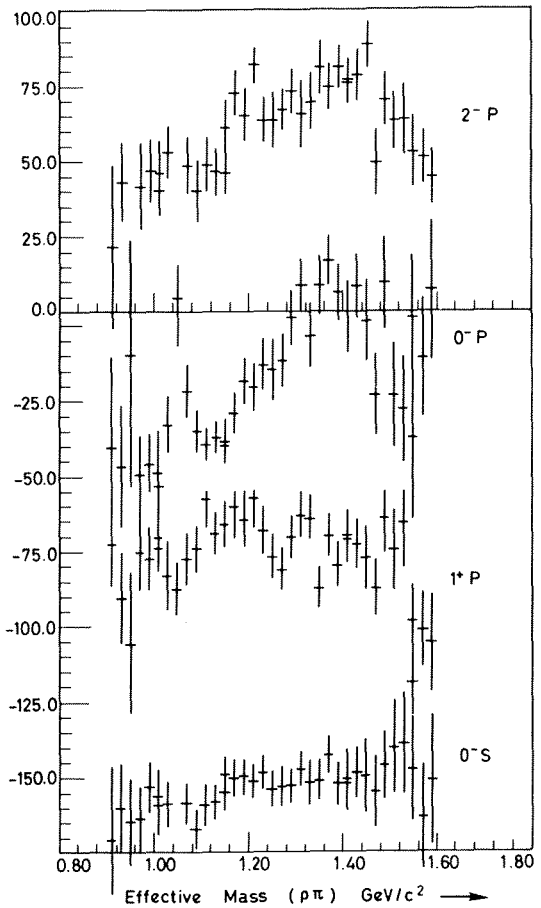

Fig. 3: 94 GeV/c data, phase relative to 0^-S, 0^-P, 1^+P, 2^-P at high t'

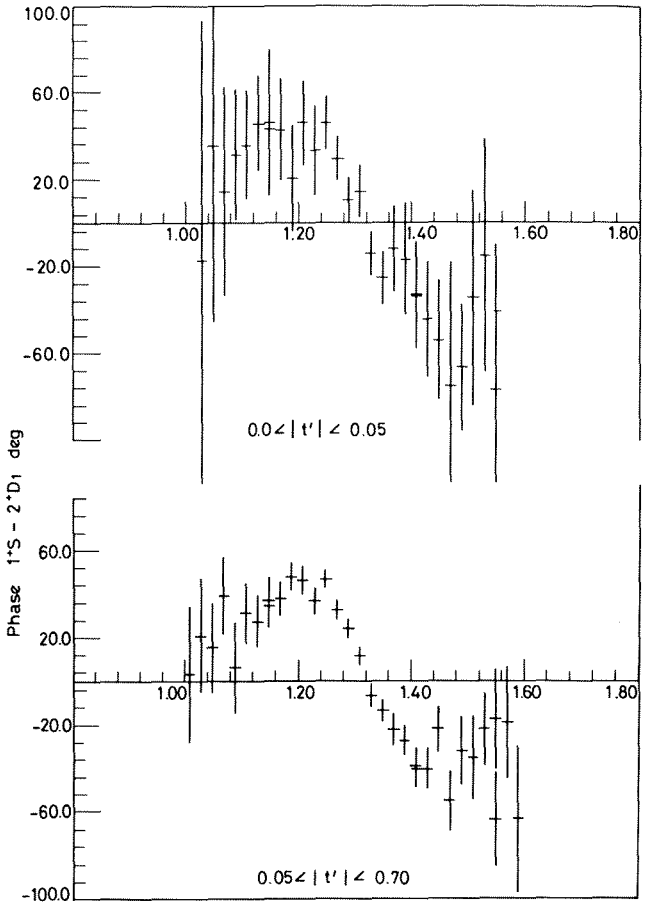

Fig. 4: 94 GeV/c data, phase relative to $2^+D_{M=1}$ at low t' and high t'

residual forward motion of the 1^+S contribution. When the fitted A_2 parameters are used to predict the absolute phase motion of that wave and this is subtracted from the data of Fig. 4, the result, seen in Figs. 1 and 2, is that the forward motion of the 1^+S phase by $\sim 90°$ is indeed confirmed in the 1.2-1.4 GeV/c^2 region.

There is thus a strong indication from both intensity and phase that a resonant object with mass $\sim$1.3 GeV/c^2 is being produced with a rather flatter $|t'|$ differential cross-section than a background with which it is produced coherently. To further elucidate the spectrum, it is, therefore, necessary to adopt a model in which the standard Deck-type diagram is modified by a resonant state, which will be produced both directly and in interference with this mechanism.[6]

3. MODEL DEPENDENT FITS

The solid lines of Figs. 1 and 2 display the results of a rescattering model at 94 GeV/c. With the standard trigger at 63 and 94 GeV/c there is an acceptable χ^2 in intensity and phase for a seven parameter fit simultaneous in low and high t' data. In Fig. 2, for the very high t' data at 94 GeV/c, separate normalisation has been allowed for (a) and (b) because of doubts about the ability with which the intensity of Deck mechanisms may be calculated at high average t' . Throughout, the diffractive component is a projection of a OPE Deck type model. Separate tests have shown that the inclusion of ρ exchange diagrams

and possible reggeisation make qualitatively minor changes. With the exception of the very low level found above $|t'| = 0.3$ GeV/c^2 each fit agrees to within ∿20% with the absolute predictions of such models to the intensity that would be present if there were no resonant component (dashed lines). The kinematic component alone can only contribute a maximum of ∿30° phase change (zero without reggeisation) and even if normalised upwards invariably peaks too soon and too shallowly to be at all compatible with these high statistics data.

In each of the different $m(3\pi)$ and t' regions fitted, the values of the fit parameters are consistent and indicate the need for an A_1 resonance of mass 1280 ± 40 MeV/c^2, width 300 ± 30 MeV/c^2. Production appears to be with a momentum transfer slope ∿7 (GeV/c)$^{-2}$ to be compared to the overall intensity in this region of 10.1 ± 0.9 (GeV/c)$^{-2}$. The production phase prefers to be about -50° with respect to pure Deck, though tests have shown that this parameter is not crucial to the good agreement of intensity and phase shapes. Indeed fits to another rescattering model[7] in which this phase is held constant at zero cannot be ruled out and also call for resonance parameters at roughly the same values.

4. CONCLUSIONS

The absolute magnitude of the 1^+S $(\rho\pi)$ partial wave and its substantial change of shape as a function of momentum transfer has proved to be incompatible with diffractive Deck mechanisms. A broad peak at around 1.3 GeV/c , seen better at higher $|t'|$, and an accompanying large phase change in the data provides compelling evidence for a resonant A_1. Fits to a model in which such a state provides rescattering corrections to a simple Deck model produce satisfactory χ^2 and indicate a mass 1280 ± 40 MeV/c^2 and width 300 ± 30 MeV/c^2.

5. REFERENCES

1. Baltay et al, Phys. Rev. Lett. 39, 591, (1977).
2. Gavillet et al, Phys. Lett. 69B, 119, (1977).
3. Antipov et al, Nuc. Phys. B63, 141 and 153 (1973).
4. Spalding, Thesis, Oxford University, 1979.
5. The A_2 meson produced at 63 and 94 GeV/c in the reaction $\pi^-p \to \pi^-\pi^-\pi^+p$. This Conference.
6. Aitchison and Bowler, Journal of Phys. G. 3, 1503 (1977).
7. Basdevant and Berger, Phys. Rev. D16, 657 (1977).

ELASTIC AND TOTAL $\pi^+\pi^-$ CROSS SECTIONS FROM A HIGH STATISTICS MEASUREMENT OF THE REACTION $\pi^-p \to \pi^+\pi^-n$ AT 63 GeV/c

C. Daum, L. Hertzberger, W. Hoogland, S. Peters, P. Van Deurzen,
NIKHEF-H, Amsterdam, The Netherlands.

A. Berglund, V. Chabaud, B. Hyams, H. Tiecke, P. Weilhammer,
CERN, Geneva, Switzerland.

A. Dwurazny, H. Palka, G. Polok, K. Rybicki, M. Turala, J. Turnau, A. Zalewska,
Institute of Nuclear Physics, Cracow, Poland.

H. Becker, G. Blanar, M. Cerrada, H. Dietl, J. Gallivan, M. Glaubman, R. Klanner, E. Lorenz, G. Lütjens, G. Lutz, W. Männer, U. Stierlin,
Max Planck Institute, Munich, Germany.

I. Blakey, M. Bowler, R. Cashmore, J. Loken, J. Spalding, G. Thompson,
Nuclear Physics Laboratory, University of Oxford, Oxford, U.K.

B. Alper, C. Damerell, A. Gillman, J. Hardwick, F. Wickens,
Rutherford Laboratory, Chilton, Didcot, Oxfordshire, U.K.

(Presented by P. Weilhammer)

ABSTRACT

A sample of about 230 000 events of the reaction $\pi^-p \to \pi^+\pi^-n$, measured with a magnetic forward spectrometer set up in an unseparated π^- beam with a momentum of 63 GeV/c at the SPS has been analysed in terms of one pion exchange. The elastic $\pi^+\pi^-$ cross section has been determined using an extrapolation to the pion pole in the mass range up to $m_{\pi^+\pi^-} = 4$ GeV. The total $\pi^+\pi^-$ cross section is obtained via the optical theorem.

1. INTRODUCTION

A large acceptance forward wire chamber spectrometer using two large magnets was set up in a hadron beam at the SPS. Besides a number of other exclusive and inclusive channels, the reaction

$$\pi^-p \to \pi^+\pi^-n \qquad (1)$$

was studied at 63.2 GeV beam energy. The purpose of this measurement was twofold: (i) to study the production mechanism of resonances in the $\pi^+\pi^-$ system up to high momenta and large momentum transfers, and (ii) to investigate $\pi^+\pi^-$ scattering at the highest attainable $\pi^+\pi^-$ centre-of-mass energies.

In this paper we report first results from a determination of elastic and total $\pi^+\pi^-$ cross sections obtained from a sample of more than 60 000 events with a mass $m_{\pi^+\pi^-} \geq 2.0$ GeV. A comparison with the features of $\bar{p}p$ scattering is given.

2. APPARATUS AND TRIGGER

A schematic layout of the spectrometer is shown in Fig. 1. The essential feature of the spectrometer is the use of two large aperture forward magnets in series. The first one, with a gap of $260 \times 60 \times 90$ cm^3 and a bending power of 9 kGm, analyses the momentum of low

energy particles in the range from 300 MeV to about 3 GeV with good acceptance and the second one with a gap of $150 \times 50 \times 110$ cm^3 and a bending power of 20 kGm, provides an accurate momentum measurement for particles up to 100 GeV. Before and after the first magnet 24 and 20 planes of wire spark chambers (I and II) (0.25 mm resolution/plane) gave an accurate determination of particle trajectories. There were a further 18 planes of large wire chambers (IIIa,IIIb,IIIc) arranged in three groups and interspaced by two large Čerenkov (Č1,Č2) hodoscopes behind the second magnet. The 50 cm long liquid H_2 target was surrounded by a barrel of Pb scintillator sandwich anticoincidence counters (F) with only a small hole upstream for the beam to enter and a rectangular exit window matching the magnet apertures to let the forward moving secondary particles pass. Three further arrays of Pb scintillator sandwich counters (G,H) were installed downstream from the target to redefine windows. The gap of the first magnet was also lined with Pb scintillator sandwich counters.

Two 32 element counter arrays (P2/3) behind the first magnet and a set of two proportional wire chamber planes (P1), one with vertical wires and the other with 15^o inclined wires (1 mm pitch), set up directly behind the target, could be used for selecting a desired multiplicity of secondary charged particles. The direction of the incoming beam was determined by a set of 10 proportional wire chamber planes. Two standard CEDAR Čerenkov counters and one threshold Čerenkov counter served for efficient discrimination of incoming π's, K's, and protons in the beam. A telescope of five scintillation counters was used to define the incoming beam. A small scintillation counter D_2 after the second magnet could be used to signal non-interacting beam particles.

The trigger condition for the selection of reaction (1) was an incoming negatively-charged particle, selected by the beam counters and two charged particles in the forward direction defined by two hits in either one of the two proportional wire planes P1 and two hits in the counter array P2/3 with back-to-back counters in P2 and P3 in coincidence. This trigger condition is however not yet sufficient to select reaction (1) efficiently since there is a very high electromagnetic background of forward two-prongs caused by a beam and a knock-on electron with an energy above 300 MeV, most frequently produced in the H_2 target. An anticoincidence signal from the D_2 counter cannot be used in the trigger since this would veto forward going π^-'s from reaction (1), which comprise a large fraction of the high mass $\pi^+\pi^-$ events. We therefore applied a special anticoincidence logic to eliminate these knock-on electrons, making use of the fact that those δ-electrons are emitted with a very small opening angle with the beam and therefore all arrive at one side of the counter array P2/3 behind the first magnet. Two-prong events, having a coincidence hit in the central P2/3 element (on which the beam was focused) and in the D_2 counter, in addition to a hit on any one element on the "negative" side of the P2/3 array were rejected.

Additionally, all anticoincidence signals from the counters F, G and H vetoed the trigger in order to reject events with additional charged or neutral particles outside the solid angle defined by the magnet apertures. In this way the trigger rate was cut down to an acceptable level ($\sim$20 triggers per 10^5 incoming beam particles).

3. DATA PROCESSING AND EVENT SELECTION

A total of about $5.8 \cdot 10^6$ triggers, including calibration runs for determining losses of

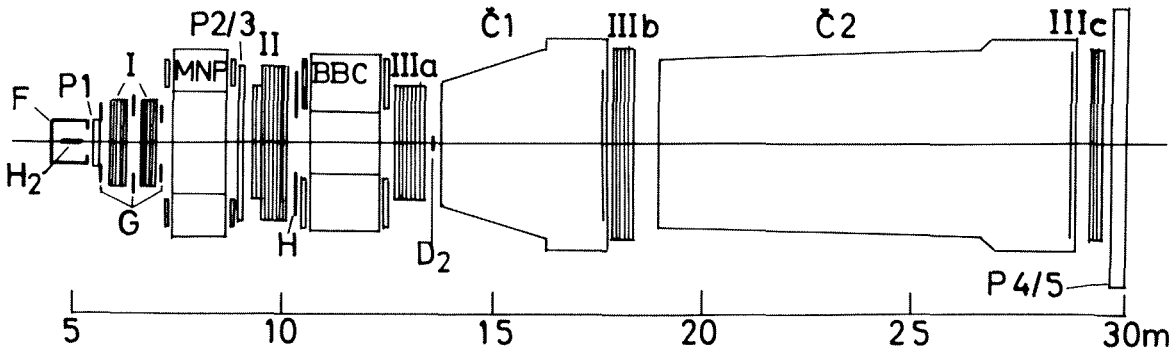

Fig. 1 Schematic layout of the WA3-Spectrometer.
H_2 : Hydrogen Target; MNP,BBC : Spectrometer Magnets;
I,II,IIIa,b,c : 80 planes of Wire Spark chambers;
P1 : MWPC's:, P2/3 : 32 element counter arrays;
F,G,H,D,P4/5 : Pb-Scintillator-Sandwich Veto Counters;
Č1,Č2 : Hodoscopic Threshold Čerenkov Counters.

good events caused by the trigger conditions, were recorded. All events were processed through a geometry and kinematics program which had about 98% efficiency to fully reconstruct events with two charged forward going particles. After appropriate cuts applied in order to select a clean sample of events of reaction (1) we obtained about 230 000 good $\pi^+\pi^-$ events. In Fig. 2a the mass spectrum is shown for the observed events and after acceptance corrections (see chapter 4). In the following we will concentrate on the data in the high mass region.

4. METHOD OF ANALYSIS

The raw data shown in Fig. 2a have to be corrected for geometrical acceptance losses. The $\pi^+\pi^-$ events are characterized by the following parameters:

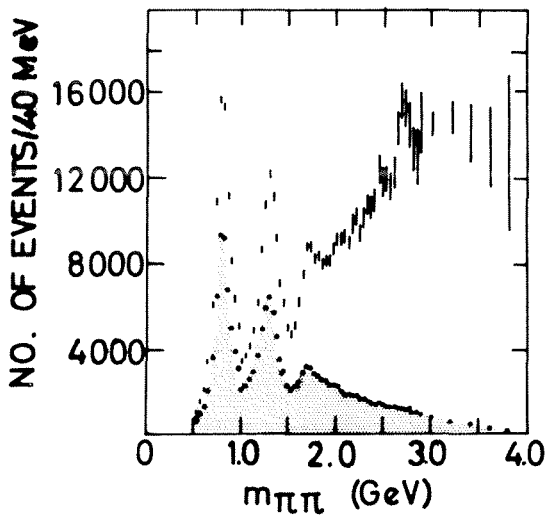

Fig. 2a $\pi^+\pi^-$ Mass Spectrum
dots : observed
lines : acceptance corrected

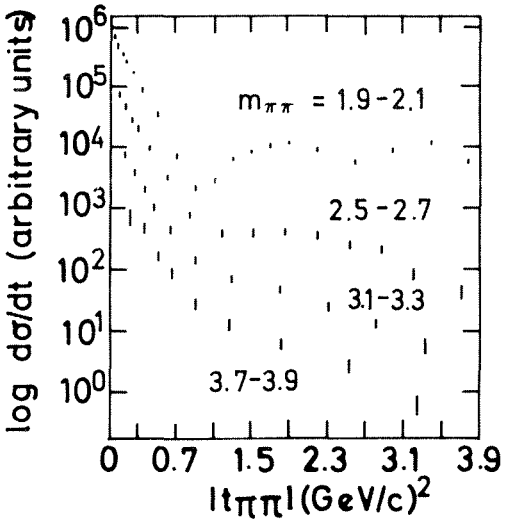

Fig. 2b Differential $\pi^+\pi^-$ Cross Sections $\frac{d\sigma^{\pi\pi}}{dt_{\pi\pi}}$ for 4 different $m_{\pi^+\pi^-}$ mass intervals

$m_{\pi^+\pi^-}$: rest mass of the $\pi^+\pi^-$ system

t_{pn} : four momentum transfer to the nucleon

$\cos\theta,\phi$: decay angles of the π^- in the $\pi^+\pi^-$ rest system in the t-channel helicity frame

$t_{\pi\pi} = -2q^2(1-\cos\theta)$ is the four momentum transfer between the incoming and outgoing π^-

$q = \frac{1}{2}\sqrt{m^2_{\pi\pi} - 4m^2_{\pi}}$ -- momentum of each pion in the centre-of-mass of the $\pi^+\pi^-$ system.

The geometrical acceptance of the $\pi^+\pi^-$ events is calculated by a Monte Carlo method. Events are generated at fixed $m_{\pi^+\pi^-}$, t_{pn} values isotropically in ϕ. Since the observed events exhibit a strongly forward peaked $\cos\theta$ distribution, in particular at high $\pi\pi$ masses, the Monte Carlo events have been generated with a $\cos\theta$ distribution derived from the observed events. In this way we ensure that the statistical error of the Monte Carlo calculation is small compared to the error on the observed events over the whole $\cos\theta$ range using the minimal computer time necessary.

At higher dipion masses ($m_{\pi\pi} \lesssim 2$ GeV) we observe $t_{\pi\pi}$-distributions which show more and more a forward-peaked diffractive pattern. A description of this distribution in terms of moments of spherical harmonics needs too many high order terms to be practical. Therefore the $\cos\theta$ distribution was fitted independently in 20 $\cos\theta$-bins of varying bin size.

Our data show that spherical harmonics moments $\langle Y_{\ell m}\rangle$ with $m \geq 2$ are negligible for $|t_{pn}| \lesssim 0.2$ GeV^2. It is therefore possible to describe the ϕ-dependence of the double differential cross section by

$$\frac{d^2\sigma}{d\cos\theta d\phi} = I_0(\cos\theta) + I_1(\cos\theta) \cdot \cos\phi \qquad (2)$$

In a first step this expression is fitted in given $m_{\pi\pi}, t_{pn}$ intervals in each of 20 $\cos\theta$ bins using a least squares method ($\Delta m_{\pi\pi} = 0.2$ GeV, $0 < |t_{pn}| < 0.2$ GeV^2).

The resulting I_0, I_1 are used as input to a maximum likelihood program in which the I_0, I_1 of (2) are also parametrized as functions of t_{pn}.

These parametrizations can be derived from a generalization of the poor man's absorption model[1] by Ochs and Wagner[2]

$$I_0 = \frac{-t_{pn}}{(m_\pi^2 - t_{pn})^2} F_0^2(t_{pn}) |T|^2 + \frac{|C_A|^2}{m^2_{\pi\pi}} F_1^2(t_{pn}) \left|\frac{dT}{d\theta}\right|^2 \qquad (3)$$

$$I_1 = \frac{\sqrt{-t_{pn}}}{(m_\pi^2 - t_{pn})} F_0(t_{pn})\, F_1(t_{pn})\, \mathrm{Re}\, \frac{C_A}{m^2_{\pi\pi}} \frac{d}{d\theta} |T|^2 \qquad (4)$$

$T(m_{\pi\pi},\cos\theta)$ is the $\pi\pi$ scattering amplitude

C_A is the absorption strength parameter

$F_i(t)$ form factors

These formulae contain the required small $t_{\pi\pi}$-behaviour

$$I_1 \propto \sin\theta \propto \sqrt{-t_{\pi\pi}} \qquad (5)$$

and for the second term in I_0

$$I_0^{(2)} \propto \sin^2\theta \propto |t_{\pi\pi}| \quad .$$

We assume C_A to be real. Preliminary fits using a Regge-type parametrization showed that the second term in formula (3) $I_0^{(2)}$ is smaller than 10% over the whole $t_{\pi\pi}$-region. In the small $t_{\pi\pi}$-region which is used to extract the total $\pi\pi$ cross section it vanishes $\propto|t_{\pi\pi}|$. From this contribution we therefore expect a contamination of the elastic $\pi\pi$-cross section of less than 10%. Its contribution to the total cross section can be neglected.

We incorporate in our fits the minimal contribution only which is obtained by neglecting a relative phase change between T and $\frac{dT}{d\theta}$.

We take $F_0^2(t_{pn}) = F_1^2(t_{pn}) = e^{b(t_{pn}-m_\pi^2)}$ and obtain

$$\begin{aligned} I_0 &= \frac{-t_{pn}}{(m_\pi^2 - t_{pn})^2}\, e^{b(t_{pn}-m_\pi^2)} \cdot T_0^2 + e^{b(t_{pn}-m_\pi^2)} \cdot \frac{1}{4} T_1^2 \\ I_1 &= \frac{\sqrt{-t_{pn}}}{m_\pi^2 - t_{pn}}\, e^{b(t_{pn}-m_\pi^2)} \cdot T_0 \cdot T_1 \end{aligned} \qquad (6)$$

where $T_0 = |T|$

$$T_1 = \frac{2C_A}{m_{\pi\pi}} \left|\frac{dT}{d\theta}\right|$$

T_0, T_1 are again fitted independently in 20 $\cos\theta$ bins, the slope b is taken to be the same for all $\cos\theta$ in a given $m_{\pi\pi}$ bin. We do not demand $T_1 \propto \frac{dT}{d\theta}$ in our fits.

Using the Chew-Low formula

$$\lim_{(t_{pn} \to m_\pi^2)} \frac{d^3\sigma}{dm_{\pi\pi}\, dt_{pn}\, d\cos\theta} = \frac{m_{\pi\pi}^2\, q_\pi}{4\pi\, m_p^2\, p_{Lab}^2} \frac{g^2}{4\pi} \frac{-t_{pn}}{(m_\pi^2 - t_{pn})^2}\, e^{b(t_{pn}-m_\pi^2)} \frac{d\sigma_{\pi\pi}^{el}}{d\cos\theta}$$

one obtains directly the pole-extrapolated elastic $\pi\pi$-cross section

$$\frac{d\sigma_{\pi\pi}^{el}}{d\cos\theta} = T_0^2 \Big/ \left(\frac{m_{\pi\pi}^2\, q_\pi}{4\pi\, m_p^2\, p_{Lab}^2} \cdot \frac{g^2}{4\pi} \right)$$

where p_{Lab} = beam momentum
$g^2/4\pi$ = 2×14.6 = pion nucleon coupling constant
m_p = mass of proton .

In Fig. 2b the fitted values T_0^2 are shown for four $m_{\pi\pi}$ mass bins ($1.9\ \text{GeV} < m_{\pi\pi} < 2.1\ \text{GeV}$, $2.5\ \text{GeV} < m_{\pi\pi} < 2.7\ \text{GeV}$, $3.1\ \text{GeV} < m_{\pi\pi} < 3.3\ \text{GeV}$ and $3.7\ \text{GeV} < m_{\pi\pi} < 3.9\ \text{GeV}$) as a function of $t_{\pi\pi}$. This pole extrapolated differential $\pi^+\pi^-$ cross section follows an exponential in the $|t_{\pi\pi}|$ interval $0 < |t_{\pi\pi}| < 0.7\ \text{GeV}^2/c^2$ for all $m_{\pi\pi}$ mass bins.

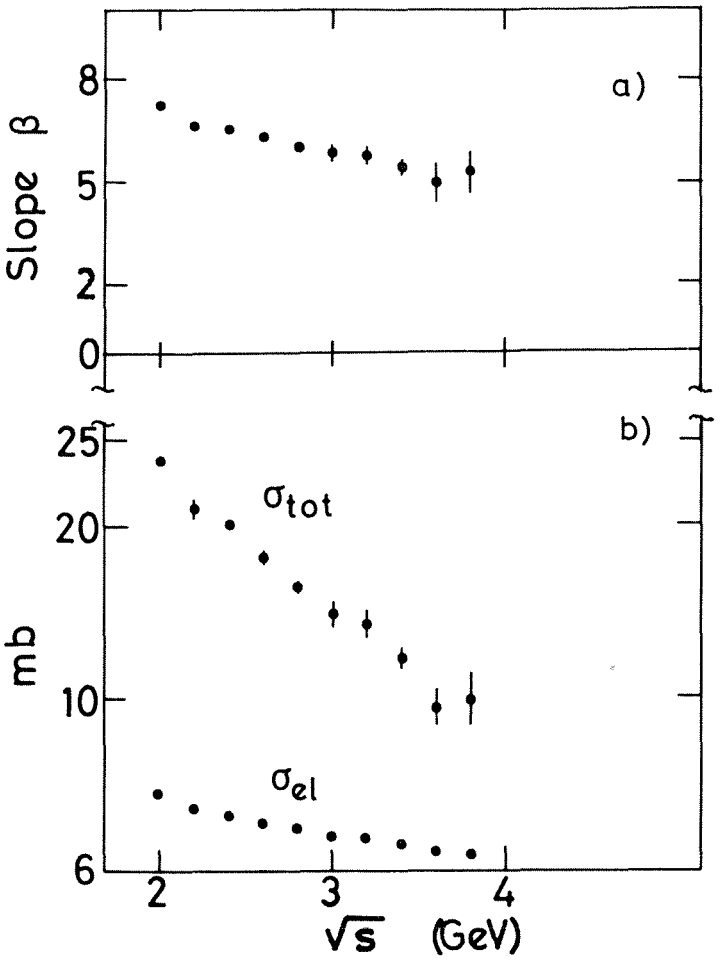

Fig. 3a Slope of $\frac{d\sigma^{\pi\pi}}{dt_{\pi\pi}}$ fitted in the interval $0 < t_{\pi\pi} < 0.7$ $(GeV/c)^2$

Fig. 3b Total and Elastic $\pi^+\pi^-$ cross sections. Errors are statistical only.

The value of the forward $\pi^+\pi^-$ elastic cross section was then determined by fitting an exponential $A\, e^{\beta t_{\pi\pi}}$ to these distributions in each $m_{\pi\pi}$ bin. The values for the slope parameters as a function of $m_{\pi\pi}$ are shown in Fig. 3a.

The total $\pi^+\pi^-$ cross section can now be determined through the optical theorem assuming that the $\pi\pi$ scattering amplitude is purely imaginary in the forward direction. The values thus obtained together with the elastic $\pi^+\pi^-$ cross section, which is calculated by integrating the distribution T_0^2 over $\cos\theta$, are shown in Fig. 3b as a function of $\sqrt{s} = m_{\pi\pi}$. The errors shown in Fig. 3b are statistical only. We estimate in this preliminary analysis the systematic error on the elastic cross section to be 40%, giving an error of 20% for the total cross section. This systematic error is due to uncertainties in the procedure of the extrapolation to the pion pole, of the extrapolation to $t_{\pi\pi} = 0$ and also to the preliminary status of the absolute cross section normalization. We believe that we might be somewhat too low in our cross section due to these systematic effects, since the total cross section at the ρ-meson peak, evaluated in the same way, comes out about 10% below the unitarity bound.

5. DISCUSSION OF RESULTS

The following major features of high energy $\pi^+\pi^-$ collisions in the energy range from $\sqrt{s}$ = 2 GeV to 4 GeV can be observed in our data:

(i) the total cross section still decreases very strongly in the observed energy interval (from about 25 mb to 10 mb). This indicates that $\pi^+\pi^-$ scattering at these energies is not yet purely diffractive.

(ii) The elastic $\pi^+\pi^-$ cross section is decreasing even more strongly than $\sigma_{\pi\pi}^{tot}$ as a function of $\sqrt{s}$. Its value varies from 20% to 10% of the total cross section.

(iii) The elastic differential $\pi^+\pi^-$ cross section follows an exponential shape at low $|t_{\pi\pi}|$. The slope exhibits antishrinkage ($\beta \simeq 7$ (GeV/c)$^{-2}$ at $\sqrt{s}$ = 2 GeV and $\beta \simeq 5$ (GeV/c)$^{-2}$ at $\sqrt{s}$ = 4 GeV).

(iv) The differential cross section has a marked dip around $t = 1$ (GeV/c)^2 at low $\sqrt{s}$, which disappears at higher $\sqrt{s}$.

Around $\sqrt{s}$ = 2 GeV our measured $\sigma_{\pi\pi}^{tot}$ and $\sigma_{\pi\pi}^{el}$ agree with results from a previous bubble chamber experiment[3] at 25 GeV/c. At higher $\sqrt{s}$ our cross section values continue to decrease, whereas Ref. 3 claims a flattening off to a constant value around $\sqrt{s}$ = 3 GeV. One should, however, note that the data sample of Ref. 3 consisted of only about 500 events above $m_{\pi^+\pi^-}$ = 2 GeV.

A comparison with the only other measured hadron-antihadron scattering process, $\bar{p}p \to \bar{p}p$, in the equivalent energy range of $E_{\bar{p}}^{Lab}$ = 3 GeV to 8.5 GeV, shows a very similar pattern: $\sigma_{\bar{p}p}^{tot}$ falls from about 80 mb to 55 mb, the slope of $d\sigma^{\bar{p}p}/dt$ is about twice as large as the slope of $d\sigma^{\pi\pi}/dt$ and also exhibits antishrinkage ($\beta^{\bar{p}p} \simeq 14$ (GeV/c)$^{-2}$ to 12.5 (GeV/c)$^{-2}$) and the ratio $\sigma^{el}/\sigma^{tot} \simeq 20\%$. One also finds the same dip structure in $d\sigma^{\bar{p}p}/dt$ at low $E_{\bar{p}}^{Lab}$ around $t = 0.4$ (GeV/c)^2.

Interpreting the $\pi^+\pi^-$ cross section in terms of an optical model with $\sigma^{tot} \sim R^2$, R representing the extension of the target, indicates that the radius of the pion is about $\frac{1}{2}$ times the radius of the nucleon ($R_\pi \simeq \frac{1}{2}$ fm). From Regge theories[4,5,6] one expects, if factorization is valid, that at very high energies $\sigma_{\pi^+\pi^-} = \frac{\sigma_{\pi^-p}}{\sigma_{pp}}$. Taking our highest energy points one gets $\sigma_{\pi^+\pi^-} = \frac{(27\text{ mb})}{(40\text{ mb})} \simeq 18$ mb, which does not agree with our measured value of 9.7 mb. Predictions based on a model of scattering between the constituent quarks in the different particles[7] give $\sigma_{\pi^+\pi^-} = \frac{2(\sigma_{\pi^-p})^2}{\sigma_{pp}+\sigma_{\bar{p}p}} \simeq 14$ mb, $\beta_{\pi\pi} = 5.8$ (GeV/c)$^{-2}$ and $R_\pi = 0.65$ fm, somewhat higher than our measured values for these quantities.

6. CONCLUSIONS

We have analysed reaction (1) in terms of $\pi^+\pi^-$ scattering for masses $m_{\pi^+\pi^-} \geq 2$ GeV. We find that the $\pi^+\pi^-$ differential, the integrated elastic and the total cross sections have similar energy dependences as observed in $\bar{p}p$ scattering at equivalent energies. The geometrical extension of the pion, as defined in optical models, comes out about 0.5 fm. The values of the total $\pi\pi$ cross section and the exponential slope of the differential cross section are lower than predictions of both the Regge model and the quark model of high energy $\pi\pi$ scattering.

REFERENCES

1) P.K. Williams, PR D1 (1970) 1 12.

2) W. Ochs and F. Wagner, PL 44 B (1973) 271; F. Wagner, NP B58 (1973) 494.

3) W.L. Robertson et al., PR D7 (1973) 9.

4) V.N. Gribov and I. Pomerantchuk, PRL 8 (1962) 343.

5) M. Gell-Mann, PRL 8 (1962) 263.

6) W. Abbe, PR 160 (1967) 1519.

7) E. Strauner, PRL 20 (1968) 1258.

AN ANALYSIS OF CHARM SEARCHES IN NN COLLISIONS

W.M. Geist
CERN - Geneva, Switzerland

ABSTRACT

D^+-meson production was recently observed in pp collisions at the ISR. Here, a systematical comparison of all relevant experimental data is performed. By confronting various simple models with all available data conclusions concerning characteristics of charm production can be drawn.

1. INTRODUCTION

Recently the production of charmed particles was observed for the first time in pp interactions at the CERN ISR [1(a, b)]. Many other experiments were dedicated to charm production in hadronic interactions but only indirect evidence [2-12] or upper limits for the cross section [13-27] were obtained. No consistent picture of inclusive charmed meson production, which is supposed to contribute most to the charm cross section, has emerged so far [28].

This is probably due both to the fact that the non-emulsion experiments covered only distinct and limited regions of phase space and to the various ways of extracting cross sections from the measurements.

In the present analysis, four possible forms of the differential cross section for D-meson production are assumed to perform the calculation of the total charm cross section is an identical way for all published non-emulsion NN experiments.

They differ only by the longitudinal dependence of the production amplitude.

2. DETAILS OF ANALYSIS

Emulsion experiments [25-27, 29, 30] are omitted here. The remaining NN experiments are classified according to the types of (double)-inclusive reactions and charmed particle decays to which they are sensitive.

Throughout the paper, N,C,D,ℓ,h denote a nucleon, a charmed particle (baryon or meson), a D meson, a lepton and the decay products from a hadronic decay of a charmed particle; additional hadrons are symbolized by $X^{(')}$:

- Single prompt lepton production [2-11]:

$$\begin{array}{l} NN \to C + X \\ \quad\ \big\lfloor\!\to \ell + X' \end{array} \quad . \qquad (1)$$

- Inclusive multihadron production [1(a-b), 13-17]:

$$\begin{array}{l} NN \to C + X \\ \quad\ \big\lfloor\!\to h \end{array} \quad . \qquad (2)$$

- Inclusive production of lepton-antilepton pairs [12,18,19]:

$$\begin{array}{l} NN \to C_1 + C_2 + X \\ \qquad\quad \hookrightarrow \bar{\ell} + X'' \\ \quad \hookrightarrow \ell + X' \end{array} \qquad \bar{\ell} = e^{\pm}e^{\mp},\ e^{\pm}\mu^{\mp} \tag{3}$$

- Inclusive production of multihadron systems in association with a single lepton [1(b),20]:

$$\begin{array}{l} NN \to C_1 + C_2 + X \\ \qquad\quad \hookrightarrow h \\ \quad \hookrightarrow \ell + X' \end{array} \quad . \tag{4}$$

The analysis of the above experimental data starts from the basic assumption that the dominant contribution to the charm cross section in all regions of phase space to which the experiments were sensitive is due to D mesons production (i.e. C = D in reactions (1) to (4)). With a Monte-Carlo method D-meson were generated according to four models:

- Model 1:

$$E\,\frac{d\sigma}{d\bar{p}}\bigg|_D = g(y)e^{-\alpha p_T} \tag{5}$$

is chosen such that

$$\int E\,\frac{d\sigma}{d\bar{p}}\bigg|_D dp_T^2 \sim (1-x)^3, \text{ (central production)}; \tag{6}$$

$(E, \bar{p})$ denotes the four-momentum of the $(\bar{D})$ meson, p_T, x and y are its transverse momentum, Feynman variable and rapidity in the c.m. system, α is a slope parameter.

- Model 2:

$$\frac{d^2\sigma}{dy\,dp_T^2} \simeq \text{const. } e^{-\alpha p_T} \ . \tag{7}$$

This ansatz has been tried since the requirement for approximate consistency of the D^+ cross section measured at moderate x [1(a)] and the e/π ratio obtained at small x [11] at the same c.m. energy calls for a rather y independent differential cross section (sect. 3).

- Model 3: one may assume that charmed mesons are produced as follows:

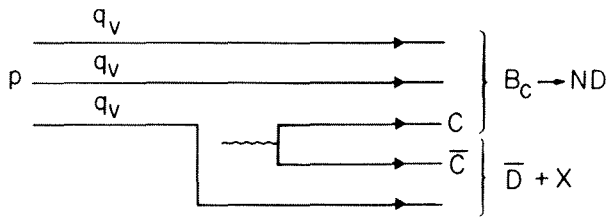

in which a c quark recombines with two valence quark q_V [31] to give an excited charmed baryonic state B_c which may decay into a nucleon and a D meson.

For simplicity, the invariant differential cross section of model 1 was used for $\bar{D}$ production and $d\sigma/dxdp_T^2 \sim \text{const. } e^{-2p_T}$ for B_c production. The distribution of the effective ND mass M was parametrized as

$$\frac{d\sigma}{dM} \sim (M-M_{th})e^{-(M-M_{th})\beta} \tag{8}$$

with a threshold mass $M_{th} = m_N + m_D$ and a free parameter β (see below),

- Model 4: since there is a large cross section for single diffraction [32], also the following reaction was considered:

$$NN \rightarrow NN^* \quad , \quad N^* \rightarrow ND\bar{D} \tag{9}$$

The following differential cross section for N^* production was used [33]:

$$\frac{d}{dt\ dM^*} \sim e^{-6t}\ \frac{d\sigma}{dM^*} \ . \tag{10}$$

The effective $ND\bar{D}$ mass M^* distribution was parametrized analogous to model 3.

A further assumption common to all models is that the average transverse momentum of $(\bar{D})$ mesons is 1 GeV/c, which determines the parameter β in eq. (8) and corresponds to $\alpha = 2\ \text{GeV/c})^{-2}$ for models 1 and 2.

For the calculation of lepton/pion ratios a good description of the experimental inclusive pion spectra has to be found. With a Monte-Carlo program, pions were generated such that the transverse momentum spectra for pions at $\sqrt{s} = 53$ are reproduced in the range $0.2 \lesssim p_T \lesssim 1.6$ [34,35] as well as the pion rapidity distributions measured at fixed values of p_T at a c.m. system energy $\sqrt{s} = 53$ GeV [36,37].

For the semileptonic decays in reactions (1), (3) and (4), it was assumed that there is a 60% (40%) contribution from decays $D \rightarrow eK^*(890)\nu$ ($D \rightarrow eK\nu$) to the total semi-leptonic D decay. Analytic expressions for the lepton momentum distributions were used [38]. The resulting summed lepton distribution fits the data [39] very well.

The cross sections σ_i, i = 1...4, from models 1 to 4 were determined according to the relation $\sigma_i = R_i\sigma_0$ from the published cross sections σ_0; R_i is the inverse of the acceptance obtained from model i relative to that from the model used by the authors.

3. RESULTS

All published cross sections are shown in fig. 1(a) and listed in table 1, labelled by capital letter, which are also used to indicate the experiments in fig. 1. All cross sections have been (re)calculated for a semi-leptonic branching ratio $B_{SL} = 10\%$ [40], a hadronic branching ratio $B(D^0 \rightarrow K\pi) = 2.2\%$ [40] and the power dependence $A^{0.9}$ of the inclusive D cross section on the atomic number A of the target material which hold for the inclusive μ-pair production in the D mass region [41]. The original cross sections have been updated, whenever possible, for a 60% (40%) contribution from the decay $D \rightarrow eK^*\nu$ ($D \rightarrow eK\nu$) to the semi-leptonic D decays. Finally, cross sections

were multiplied by a factor 2 in the case of reactions (2) and (4) to take into account the undetected charge state of $(\bar{D})$ mesons.

It should be mentioned that at ISR energies there is a factor of ~ 200 between the lowest (S) and the largest (P) published cross section value.

Now, results of the present analysis are given in table 1 and shown in figs 1(b) and 1(c) for models 2 and 3.

The beam dump experiments would give the cross sections listed in lines A,B,C,D of table 1 and shown in fig. 1(b,c) (same symbols). From models 1 and 3, one calculates an average ν energy $\langle E_\nu \rangle_W$ after weighting with the $(\bar{\nu})$-N cross section of $\langle E_\nu \rangle_W \approx 90 \div 100$ GeV which is consistent with the data [5,42]; whereas models 2 and 4 predict $\langle E_\nu \rangle_W \gtrsim 120$ GeV. Correspondingly, the calculated ν flux is in better agreement with the data [42] in case of models 1 and 3 (not shown). The measurements of [6] (E) cannot be reanalyzed with the present method.

Measured μ/π ratios are shown in fig. 2; μ from μ-pairs had been subtracted. The μ/π ratios calculated for p targets from models 1 to 4 are shown for a charm cross section $\sigma_{D\bar{D}} = \sigma_\pi \cdot 10^{-3}$ ($\sigma_\pi := \frac{1}{2}(\sigma(\pi^+) + \sigma(\pi^-))$, [7]) including a branching ratio B_{SL} of 10%. Models 2 to 4 describe the 400 GeV/c data best. A central production mechanism yields rather low values at large x which was already found in [38,43]. From adjusting the curves to the data the cross sections in line F of table 1 were determined. The influence of the lepton spectrum of the semi-muonic decay on the model predictions is demonstrated by the dashed line in fig. 2(b).

At the CERN-ISR e/π ratios have been measured at c.m. polar angles $\theta_{c.m.} = 30^0$ and 90^0 [10,11] as functions of transverse momentum. The data in the relevant kinematic range are shown in fig. 3(d). Only data above a transverse momentum of 500 MeV/c will be considered. At smaller values, the subtraction of the background is rather unsafe partly because of lack of knowledge about η/π^0 ratios [44]. There is some uncertainty concerning the influence of the e-pair veto on the actual e/π ratio, even more so for that data of [10] (H) which were normalized to pion spectra measured without veto. The contribution from ρ, ω, ϕ decays to the e/π ratios was calculated from the ρ and ϕ cross sections of [45] and [46] with the assumption $\sigma_\omega = \sigma_\rho$; the resulting curve for $\theta_{c.m.} = 30^0$ is shown in fig. 3(a). The charm cross sections can now be deduced from the corrected data by adjusting the predictions from models 1 to 4 in fig. 3(a,b,c) to the data at transverse momenta above 500 MeV/c; the curves have been drawn for $\sigma_{D\bar{D}} = \sigma_\pi \cdot 10^{-3}$, $\sigma_\pi = 150$ mb [47], and $B_{SL} = 10\%$. The influence of the assumed p_T distribution of D mesons on the model prediction and of the shape of the lepton spectrum from semi-leptonic decays has some consequences for the model predictions, as can be seen in fig. 3 (a,b) (dotted line). Within the errors, the predictions from all models 1 to 4 are roughly consistent with the data [11]yielding the cross sections in line J of table 1.

The data of [12] give rise to the cross sections in line S of table 1, when interpreted in terms of the four models.

From the D^+ production measured at the ISR [1(a)] the cross sections in line P of table 1 were obtained. The cross section from model 1 of $\gtrsim$ 5 mb is clearly inconsistent with the measured e/π ratio mentioned above [11].

Finally, the data of all experiments giving upper limits for the cross sections have been reanalyzed in the framework of the four models. The results are given in table 1 and partly also in fig. 1(b,c).

5. CONCLUSIONS

A comparison of fig. 1(a) and figs 1(b,c) reveals that a production amplitude which is a weak function of x (models 2 and 3) reduces the discrepancy between the various ISR experiments from a factor ∿ 200 to a factor of ∿ 3.5 between the data from D^+ production and from lepton pairs. Model 1 and 3 have the virtue of discribing the mean measured neutrino energy from the beam dump experiments best. The μ/π ratios as functions of Feynman x are rather well reproduced by model 2, 3 and 4. It seems that model 1 (central production) and model 4 (diffractive production) exhibit the largest inconsistencies with the data. On the other hand, appropriate contributions from both model 1 and model 4 would also give rather y independent cross sections at high energies.

To summarize, some features of the data slightly favour D-meson production mechanisms with unexpectedly large contributions from forward production. Clearly, the experimental findings have to be corroborated before drawing safe conclusions. In the framework of such a mechanism, a typical charmed meson cross section for ISR energies would be ∿ 300 μb(*) in pp collisions compared to a cross section of less than 50 μb/N at beam energies of 400 GeV/c.

Acknowledgements

I am very grateful to all my colleagues from the CERN-Collège de France-Heidelberg-Karlsruhe Collaboration for discussions, especially to Drs D. Drijard, R. Sosnowski and H. Wahl. In particular, I would like to thank Dr. H.G. Fischer for helpful contributions.

(*) A cross section of ∿ 45 μb is found in [1(b)] for Λ_c production assuming $d\sigma/dx(\Lambda_c)$ = const.

REFERENCES

[1] (a) CCHK Collaboration, D. Drijard et al., Phys. Lett. 81B (1979) 250;

(b) CCHK Collaboration, D. Drijard et al., paper submitted to this Conference.

[2] A.E. Asratyan et al., Phys. Lett. 79B (1978) 497.

[3] Gargamelle Collaboration, P. Alibran et al., Phys. Lett. 79B (1978) 134.

[4] CDHS Collaboration, T. Hansl et al., Phys. Lett. 74B (1978) 139.

[5] ABCLOS Collaboration, P.C. Bosetti et al., Phys. Lett. 74B (1978) 143.

[6] J.P. Dishaw et al., SLAC-PUB-2291, submitted to Phys. Lett.

[7] J.G. Branson et al., Preprint.

[8] J.G. Branson et al., Phys. Rev. Lett. 38 (1977) 457.

[9] H.W. Brown et al., Preprint;
B.C. Barish et al., Preprint.

[10] F.W. Büsser et al., Nucl. Phys. B113 (1976) 189 and Phys. Lett. 53B (1974) 212.

[11] L. Baum et al., Phys. Lett. 60B (1976) 485.
M. Barone et al., Nucl. Phys. B132 (1978) 29.

[12] A. Chilingarov et al., Phys. Lett. 83B (1979) 136.

[13] E.J. Bleser et al., Phys. Rev. Lett. 35 (1975) 76.

[14] M.A. Abolins et al., Phys. Lett. 73B (1978) 355.

[15] W.R. Ditzler et al., Phys. Lett. 71B (1977) 451.

[16] D. Bintinger et al., Phys. Rev. Lett. 37 (1976) 732.

[17] J.C. Alder et al., Phys. Lett. 66B (1977) 401.

[18] R. Lipton et al., Phys. Rev. Lett. 40 (1978) 608.

[19] L. Baum et al., Phys. Lett. 68B (1977) 279.

[20] D. Spelbring et al., Phys. Rev. Lett. 40 (1978) 605.

[21] M. Binkley et al., Phys. Rev. Lett. 37 (1976) 578.

[22] G. Blanar et al., Phys. Lett. 38 (1977) 192.

[23] J.G. Branson et al., Phys. Rev. Lett. 38 (1977) 580.

[24] A.M. Jonckheere et al., Phys. Rev. D16 (1977) 2073.

[25] G. Coremans-Bertrand et al., Phys. Lett. 65B (1976) 480.

[26] W. Bozzoli et al., Lett. al Nuovo Cimento 19 (1977) 32.

[27] J.P. Mundra et al., Lett. al Nuovo Cimento 18 (1977) 554.

[28] See, e.g. R. Diebold, Rapporteur's Talk at the 19th Int. Conf. on High Energy Physics, Tokyo, 1978.

REFERENCES (Contd')

[29] P.L. Jain and B. Girard, Phys. Rev. Lett. 34 (1975) 1238.

[30] N. Ushida et al., Lett. al Nuovo Cimento 23 (1978) 577.

[31] L. Van Hove, TH 2628-CERN, 12 February 1979.
J. Ranft, SLAC-PUB-2052 and Preprint KMU-HEP 79-03.

[32] See e.g. CHLM Collaboration, G. Albrow et al., Nucl. Phys. B108 (1976) 1.

[33] P.M. Kooijman, Thesis, Utrecht Rijksuniv. April 1979.

[34] British-Scandinavian Collaboration, K. Guettler et al., Phys. Lett. 64B (1976) 111.

[35] British-Scandinavian Collaboration, B. Alper et al., Nucl. Phys. B87 (1971) 19.
CCRS Collaboration, F.W. Büsser et al., Nucl. Phys. B106 (1976) 1.

[36] British-Scandinavian Collaboration, B. Alper et al., Nucl. Phys. B100 (1975) 237.

[37] CERN-Bologna Collaboration, P. Capiluppi et al., Nucl. Phys. B79 (1974) 189.

[38] I. Hinchchiff and C.H. LlewellynSmith, Nucl. Phys. B114 (1976) 45.

[39] See, e.g. J. Kirkby, SLAC-PUB-2231 (1978).

[40] B.H. Wiik and G. Wolf, DESY 78/23, May 1978.

[41] J.G. Branson et al., Phys. Rev. Lett. 38 (1977) 1334.

[42] H. Wachsmuth, Invited Talk given at the Topical Conference on Neutrino Physics, Oxford, 2-7 July 1978.

[43] M. Bourquin and J.M. Gaillard, Nucl. Phys. B114 (1976) 334.

[44] E. Amaldi et al., ROM 78-114, November 1978.

[45] British-French-Scandinavian Collaboration, M.G. Albrow et al., CERN Preprint, December 1978, submitted to Nucl. Phys. B.

[46] CCHK Collaboration, D. Drijard et al., paper submitted to this Conference.

[47] U. Amaldi et al., Nucl. Phys. B145 (1978) 367.
E. Nagy et al., Nucl. Phys. B150 (1979) 221.
L. Baksay et al., Nucl. Phys. B141 (1978) 1.

[48] E.J. Siskind et al., CALT 68-665.

TABLE 1

Symbol	First author, ref.	Reaction, beam (c.m.s.) energy, model	Further assumptions	$\sigma_{D\bar{D}}$(μb) per nucleon, full phase space	$\sigma_{D\bar{D}}$(μb) per nucleon, full phase space (updated)	$\sigma_{D\bar{D}}$(μb) model 1	$\sigma_{D\bar{D}}$(μb) model 2	$\sigma_{D\bar{D}}$(μb) model 3	$\sigma_{D\bar{D}}$(μb) model 4
A	Asratyan PL 79B (78) 497	pFe → νX 70 GeV/c model of [43]	A^1 B_{SL} = 10%	5 ± 4	$A^{0.9}$: 7.5 ± 6	7.5	3.8	9	3
B	Alibran PL 79B (78) 134	pCu → νX 400 GeV/c model of [43]	$A^{2/3}$ σ_{inel} = 40 mb	320^{+150}_{-100}	$A^{0.9}$, σ_{inel} = 33 mb: 170^{+78}_{53}	100	50	90	25
C	Hansl PL 79B (78) 139	pCu → νX 400 GeV/c $E\frac{d\sigma}{d\vec{p}} \sim (1-x)^3 e^{-2.8p_T}$	$A^{2/3}$ σ_{inel} = 37 mb	30	$A^{0.9}$, σ_{inel} = 33 mb: 12	11	4	8	3
D	Bosetti PL 79B (78) 143	pCu(Be) → νX 400 GeV/c $E\frac{d\sigma}{d\vec{p}} \sim (1-x)^3 e^{-2p_T}$	$A^{2/3}$ σ_{inel} = 33 mb	100	$A^{0.9}$: 38	33	12	24	7
E	Dishaw SLAC-PUB-2291	pFe → νX 400 GeV/c $E\frac{d\sigma}{d\vec{p}} \sim (1-x)^3 e^{-2.8p_T}$	-		$A^{0.9}$: 820	-	-	-	-
F	Branson preprint	pCu → νX 400 GeV/c pFe → νX 200 GeV/c $E\frac{d\sigma}{d\vec{p}} \sim (1-x)^4 e^{-2.5p_T}$	A^1 $E\frac{d\sigma}{d\vec{p}}(\pi) \sim (1-x)^5$ σ = 100(90) mb	400 GeV/c: < 59 200 GeV/c: < 26	$A^{0.9}$: < 90 < 90 < 39	< 90 < 39	7.5 3	30 6	18 4.5
G	Brown preprint	pFe → νX 400 GeV/c $E\frac{d\sigma}{d\vec{p}} \sim (1-x)^5 e^{-2.5p_T}$	A^1 60% D → eKν 40% D → $eK^*\nu$	35	$A^{0.9}$: 52	46	69	68	138

TABLE 1 (Cont'd)

Symbol	First author, ref.	Reaction, beam (c.m.s.) energy, model	Further assumptions	$\sigma_{D\bar{D}}$(μb) per nucleon, full phase space	$\sigma_{D\bar{D}}$(μb) per nucleon, full phase space (updated)	$\sigma_{D\bar{D}}$(μb) model 1	$\sigma_{D\bar{D}}$(μb) model 2	$\sigma_{D\bar{D}}$(μb) model 3	$\sigma_{D\bar{D}}$(μb) model 4
H	Busser NP B113 (76) 189	$pp \to eX$ at 90^0 $\sqrt{s}$ = 53 GeV	–	–	–	50	90	70	–
I	Barone NP B132(78)29 Baum PL 60B(76)485 Block NP B140(78)525	$pp \to eX$ at 30^0 $\sqrt{s}$ = 53 GeV	$\frac{\eta}{\pi^0} = 0.11e^{0.8p_T}$ σ_π = 200 mb	680^{+270}_{-160}	σ_π = 150 mb: 510^{+203}_{-120}	135	220	240	320
		model see NP B140(78)525							
K	Bleser PRL 35 (75) 76	nBe → KπX ∿ 200 GeV/c $\frac{d\sigma}{dx}$ = const.	A^1 (?)	< 8	$A^{0.9}$: < 20	< 23	< 23	< 20	< 10
L	Abolins PL 73B (78) 355	nBe → KπX ∿ 250 GeV/c $\frac{d\sigma}{dx\, dp_T^2} \sim e^{-5x} e^{-2p_T}$	A^1 (?)	< 28	$A^{0.9}$: < 70	< 50	< 30	< 40	< 18
M	Ditzler PL 71B (77) 451	pBe → KπX 400 GeV/c	A^1	–	–	D^0 < 113 $\bar{D}^0$ < 88	< 200 < 163	< 238 < 88	< 3275 < 2638
N	Bintinger PRL 37 (76) 732	$pCH_2 \to K\pi X$ 400 GeV $E\frac{d\sigma}{d\vec{p}}\Big\|_\psi = E\frac{d\sigma}{d\vec{p}}\Big\|_D$	$B_{\mu\mu}\sigma_\psi$ = 10 nb	D^0 < 135 $\bar{D}^0$ < 180	$A^{0.9}$, $B_{\mu\mu}\sigma_\psi \approx 20$ mb [48]: D^0 < 632 $\bar{D}^0$ < 842	< 842 < 1123	< 1520 < 2036	< 1778 < 1123	< 24 944 < 33 251
O	Alder PL 66B (77) 401	$pp \to K\pi X$ $\sqrt{s}$ = 53 GeV model of [43]		D^0 < 410 $\bar{D}^0$ < 365	< 820 < 730	< 820 < 730	< 1180 < 1050	< 1490 < 730	< 15 260 < 13 620

TABLE 1 (Cont'd)

Symbol	First author, ref.	Reaction beam (c.m.s.) model	Further assumptions	$\sigma_{D\bar{D}}$(μb) per nucleon full phase space	$\sigma_{D\bar{D}}$(μb) per nucleon full phase space (updated)	$\sigma_{D\bar{D}}$(μb) model 1	$\sigma_{D\bar{D}}$(μb) model 2	$\sigma_{D\bar{D}}$(μb) model 3	$\sigma_{D\bar{D}}$(μb) model 4
P	Drijard PL 81B (78) 250	$pp \to K^{*}\pi X$ $\sqrt{s}$ = 53 GeV $\frac{d\sigma}{dx\, dp_T^2} \sim (1-x)^3 e^{-2p_T}$	$B(D^+ \to K^{*}\pi)$ = 0.66 $B(D^+ \to K\pi\pi)$	2500 ± 1500	5000	> 5000	560	480	380
Q	Lipton PRL 40 (78) 608	nBe → μ + e + X 300 GeV/c $E\frac{d\sigma}{\vec{dp}} \sim e^{-5x} e^{-1.5 p_T^2}$	B_{SL} = 15% $A^{0.84}$ 100% D → ℓ$K^{*}\nu$	< 15	B_{SL} = 10% $A^{0.9}$: < 21	< 18	< 26	< 22	< 40
R	Baum PL 77B (78) 397	pp → μ + e + X $\sqrt{s}$ = 53 GeV model of [43]	B_{SL} = 11% 50% D → e$K^{*}\nu$	< 76	B_{SL} = 10% 60% D → e$K^{*}\nu$ < 97 μb	< 90	< 180	< 110	-
S	Chilingarov PL 83B (79) 136	pp → μ + e + X e + e + X $\sqrt{s}$ = 53 GeV modified version of [43]	50% D → e$K^{*}\nu$	21.9 ± 5	21.9 ± 5	45	150-220	110-220	-
T	Spelbring PRL 40 (78) 605	nBe → μ + Kπ + X 300 GeV/c $E\frac{d\sigma}{\vec{dp}} \sim e^{-5x}\, e^{-1.5 p_T^2}$	$A^{0.84}$ B_{SL} = 15% $B_{K\pi}$ = 3% 100% D → ℓ$K^{*}\nu$	< 44	B_{SL} = 10%/$B_{K\pi}$ = 2.2% $A^{0.9}$: < 112	< 82	< 53	< 62	< 44

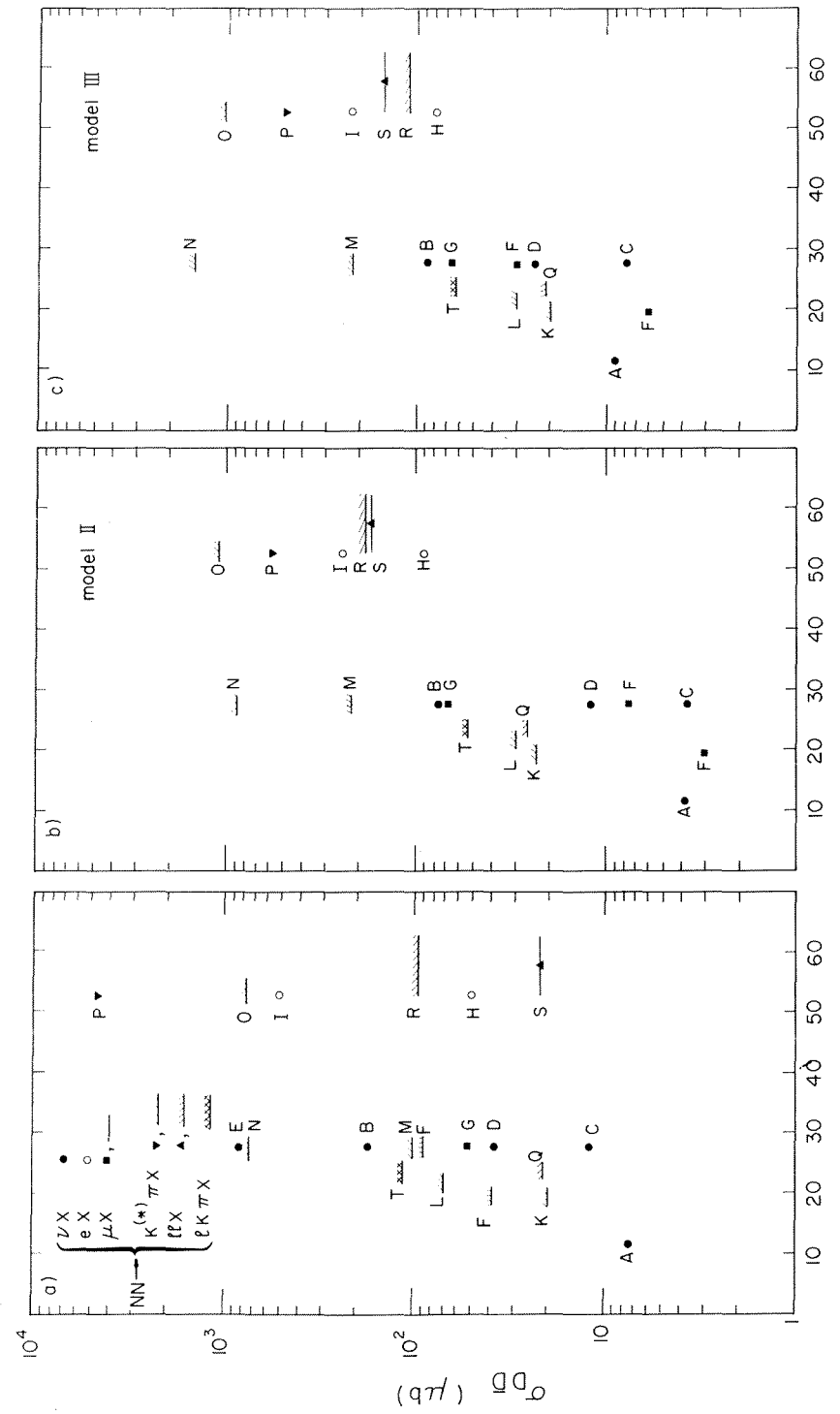

Fig. 1 (a) Inclusive D-pair cross sections $\sigma_{D\bar{D}}$ per nucleon and upper limits from [1(a),2-12,13-20]; they have been updated wherever possible (see text and columns 5 and 6 of table 1 for details). (b) Same as fig. 1(a), but recalculated with model II. (c) Same as fig. 1(a), but recalculated with model III.

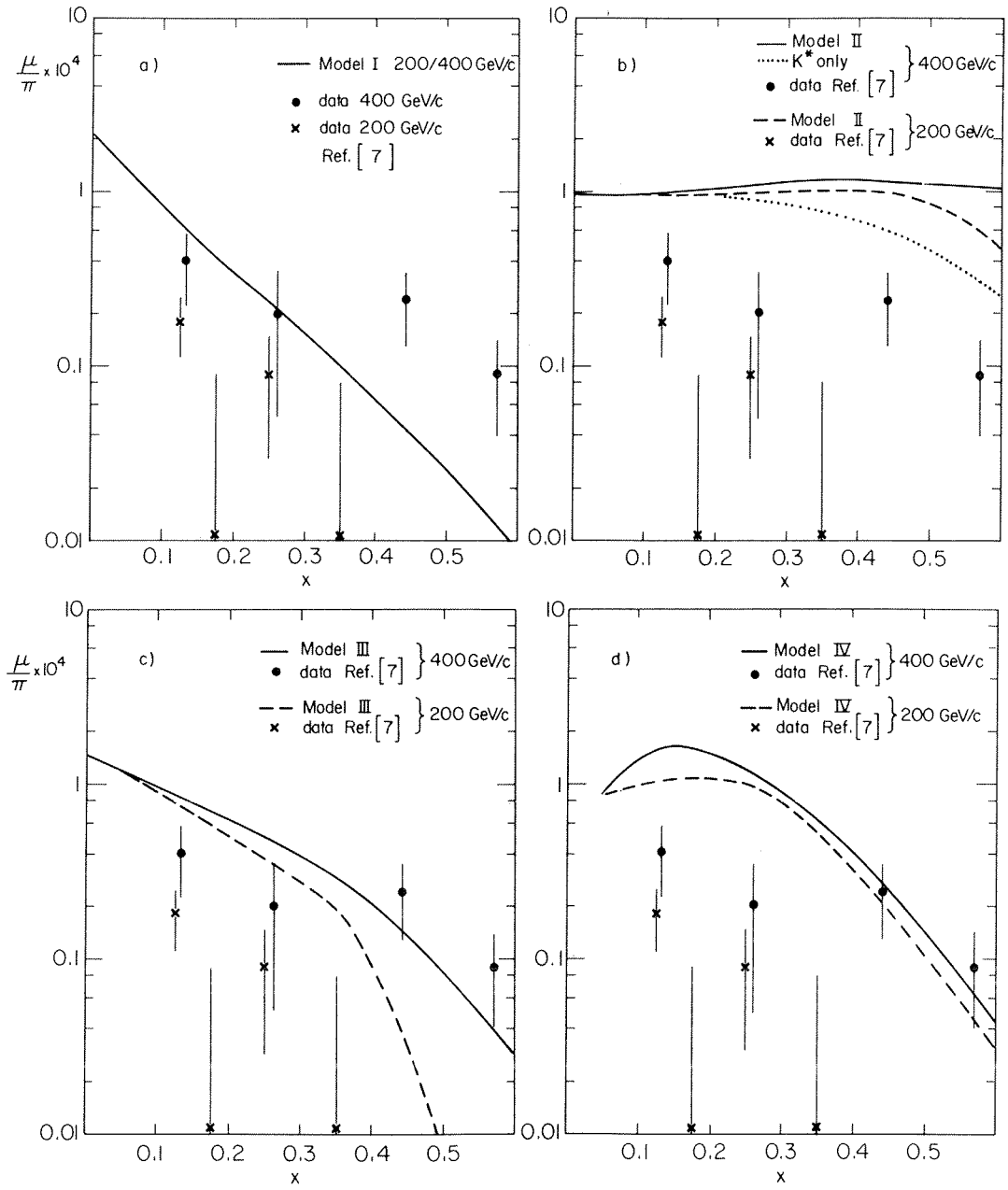

Fig. 2 (a) Ratio of single prompt μ normalized to the pion flux as function of Feynman x at beam momenta of 400 GeV/c and 200 GeV/c. The curves were calculated from model I for proton targets with an inclusive D-pair cross section $B_{SL}\sigma_{D\bar{D}} = \sigma_{\pi} \cdot 10^{-4}$ [7] (see text). (b) Same as fig. 2(a), but with results from model II. The dotted line was calculated assuming a semileptonic branching ratio $B_{SL}(D \to \mu K^{*}\nu) = 10\%$. (c) Same as fig. 2(a), but with results from model III. (d) Same as fig. 2(a), but with results from model IV.

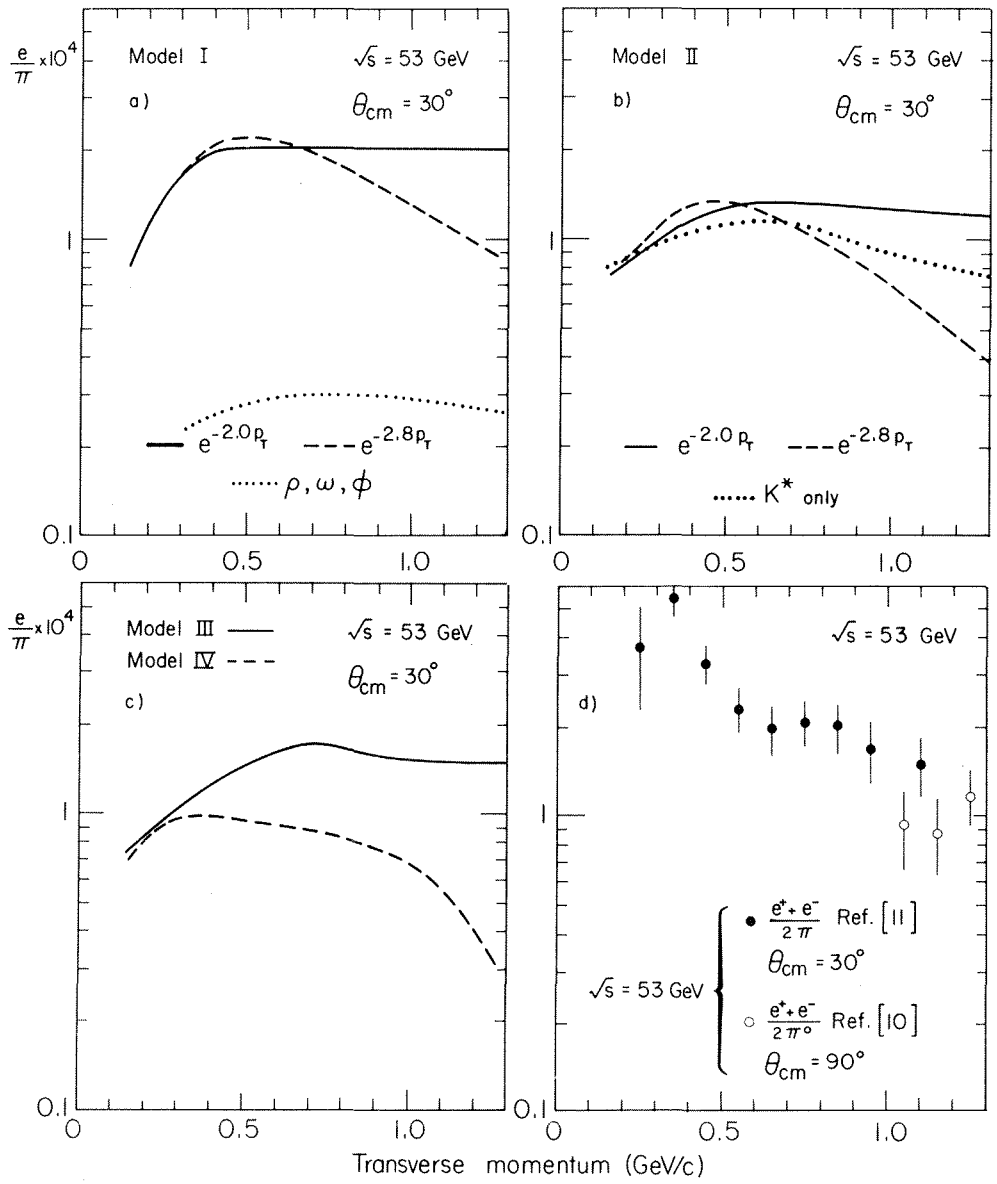

Fig. 3 (a) e/π ratios as functions of transverse momentum predicted by model I at a centre of mass energy of 53 GeV and a centre of mass polar angle θ_{cm} of 30^0 for $B_{SL}\sigma_{D\bar{D}} = \sigma_\pi \cdot 10^{-4}$ (solid line); a slope parameter of 2.8 $(GeV/c)^{-1}$ for the transverse momentum distribution of D-mesons gives the ratio indicated by the dashed line. The contribution from the decays of vectormesons is shown by the dotted line. (b) Same as fig. 3(a), but based upon model II; however, the dotted curve shows the model prediction resulting from B_{SL} $(D \to eK^*\nu) = 10\%$. (c) Same as fig. 3(a), but from model III (solid line) and model IV (dashed line). (d) e/π ratios as measured by [11] at a c.m.s. energy of 53 GeV at $\theta_{cm} = 30^0$ and by [10] obtained at $\theta_{cm} = 90^0$ as functions of transverse momentum.

REVIEW OF $K^{\pm}p$ PHYSICS

K.W.J. Barnham
Blackett Laboratory, Imperial College, London, England.

ABSTRACT

Some of the topics presented in the conference submissions corresponding to the 45 abstracts on $K^{\pm}p$ physics are discussed. The application of quark-parton model ideas to low-P_t hadronic interactions appears to be a fruitful approach. In particular two-particle correlations place stringent restrictions on the possible dynamical mechanisms. The presence of a strange quark in $K^{\pm}p$ interactions greatly extends the possible tests. Inclusive resonance production is also discussed. Mention is also made of the use of bubble chamber data as a standard of known physics with which to compare any new effects.

1. INTRODUCTION

Forty-five abstracts on the subject of $K^{\pm}p$ physics were received at the conference. In a short review I will clearly have to be subjective in my choice of topics. Since spectroscopy received good coverage in a series of well organised parallel sessions I will ignore the 11 abstracts on that subject. Probably the biggest change from previous conferences is the first appearance of a sizable number of papers, 9, from the high energy BEBC bubble chamber experiments, 70 GeV/c $K^{\pm}p$ and 110 GeV/c $K^{-}p$ (WA26-WA28). I have therefore decided to concentrate on the main subjects that these new experiments are studying and I will refer also to relevant work reported by the other experiments. I must apologise to any who are disappointed that their paper is not mentioned, and I hope they will appreciate the constraints of writing a short review of so many papers.

2. LOW-P_t QUARK-PARTON MODELS

Six papers[1a-f] were submitted with data relevant to the application of quark-parton model ideas, formulated in the deep-inelastic and high-P_t regimes, to soft hadronic processes. Refs. 2a-m contain many of the major theoretical contributions on this subject, but I do not claim that the list is exhaustive. Though the various models differ in detail the basic idea on which most of them rest is indicated schematically in fig. 1 for the proton fragmentation region. Both π^+ and π^- contain one of the valence quarks of the proton. Hence if we study the fastest π^+ and π^- in the fragmentation region i.e. $|x| \to 1$ (where x is x-Feynman $= 2P_L^{cms}/\sqrt{s}$) then we are probably observing a valence quark from the proton which has dressed itself up with a soft antiquark from the sea. Only if it is a valence quark will it reach such high $|x|$. Hence the high $|x|$ behaviour must be determined by the momentum distributions

of the valence quarks in the proton u(x) and d(x), assuming the sea quarks contribute little momentum.

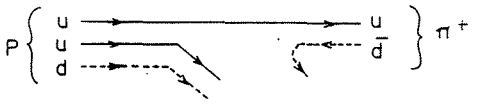

Fig. 1

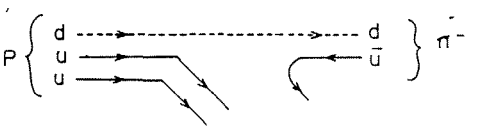

Quantitative applications of this idea clearly depend on the exact dynamics and kinematics of the quark interaction process and many of the authors in Refs. 2a-m have different prescriptions for these. However one quantitative prediction due to Ochs [2d] is independent of such detailed considerations. The ratio of the invariant x-Feynman distribution functions $f_p^{\pi^+}(x)$ and $f_p^{\pi^-}(x)$ should be given by

$$f_p^{\pi^+}(x)/f_p^{\pi^-}(x) \longrightarrow u(x)/d(x) \qquad (1)$$

where u(x) and d(x) are as measured in deep inelastic lepton scattering. In the absence of good lepton-neutron scattering data at high |x| one can compare with a prediction, due to Farrar and Jackson,[3] that this ratio should approach 5, assuming vector gluon exchange.

The prediction in equation (1) has been tested a number of times and seems to work well. In a submission to this conference[1b] the Serpukhov - Brussels - Mons - LPNHE - Saclay Collaboration have tested it for proton fragmentation in K^+p interactions at 32 GeV/c in the Mirabelle Chamber at Serpukhov. At first sight fig. 2a looks a perfect propaganda slide for these soft quark-model ideas since the ratio is tending to the Farrar-Jackson value of 5. However fig. 2b shows the same data (open circles) plotted as a function of x and one sees that statistics run out well short of x = -1. Furthermore in fig. 2b the full circles indicate the ratio after removal of 2-charged-prong events which, the authors point out, removes a large fraction of diffraction-dissociation events. Clearly the π^+/π^- ratio must come down after such a cut, as K^+p 2-prong events do not have negative tracks. However the authors wish to emphasis that the ratio is influenced strongly by the diffractive component which does not appear to have a place within these quark model ideas. In addition fig. 2b shows the effect on the ratio of demanding there be a slow proton in the event ($|t_{pp'}| < .6$ GeV^2). In a separate paper[7f] the same collaboration shows that such events are dominated by Δ^{++} production. This

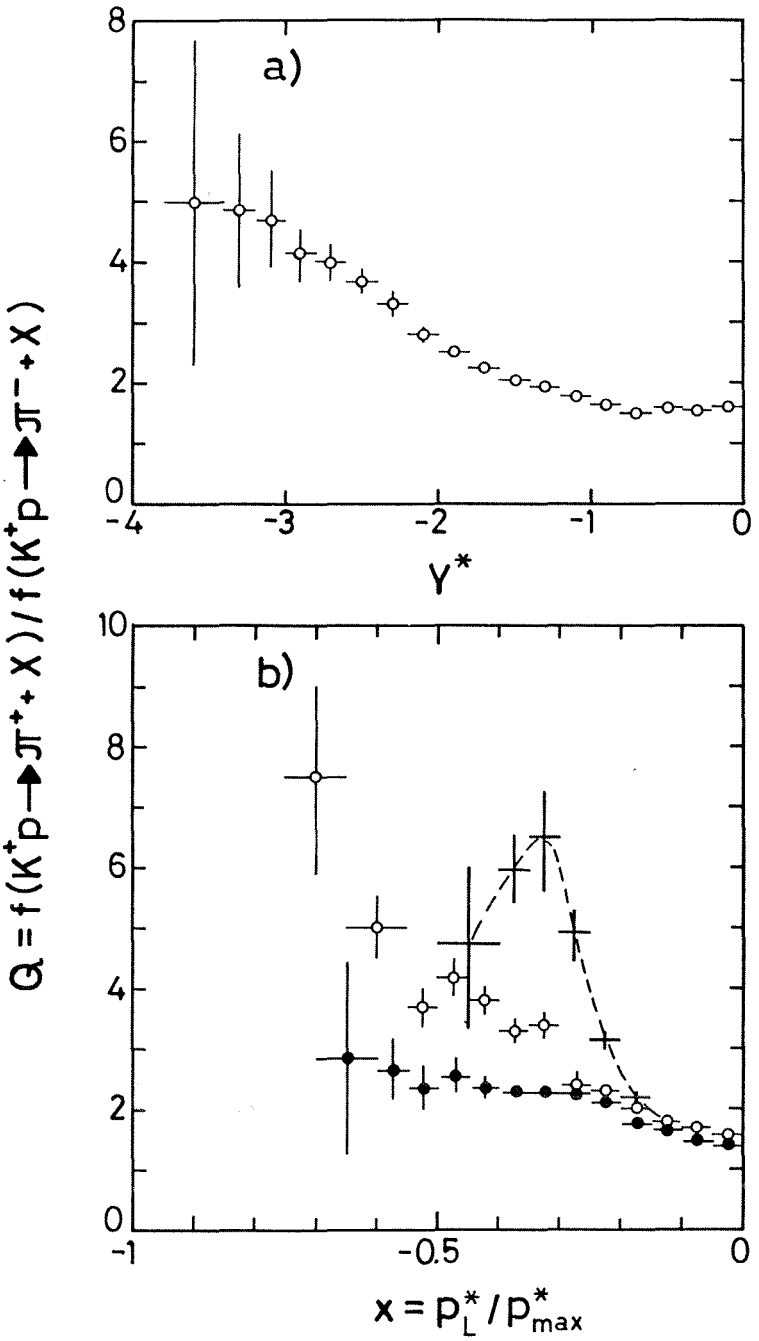

Fig. 2 The ratio of the structure functions for reactions $K^+p \to \pi^+ + x$ and $K^+p \to \pi^- + x$ at 32 GeV/c as a function of a) c.m. rapidity and b) x-Feynman . The crosses show the corresponding ratio for pions produced in association with protons with $|t_{pp}| < 0.6$ GeV^2. Full dots are for all events except inelastic 2-prongs.

is an example, therefore, of the influence resonance production can have on this ratio, a point which has been discussed previously [4].

A further word of caution about the interpretation of such ratios was made in the conference submission of Buschbeck et. al.[1f]. They point out that the π^+/π^- ratio in proton fragmentation depends on the incident particle for beam momenta below 100 GeV/c. It clearly should not do so if it is really measuring the proton structure.

One should bear these caveats in mind when interpreting the studies of soft quark ideas in Refs. 1a-f. One should also note that the presence of the strange quark in $K^{\pm}$ reactions greatly extends the scope of the tests which can be made of these ideas. In one conference submission [1e] the 110 GeV/c K^-p Collaboration has used this approach to make a preliminary determination of the momentum distribution s(x) of the strange quark in the kaon. From fig. 3a we see that the fast $\bar{K}^o$ distribution measures s(x) if these low-P_t quark-parton ideas are correct. The 110 GeV/c K^- collaboration, therefore, attempt to fit their K^o_s distribution with the recombination model using the same prescription as Hwa and Roberts used [2ℓ] to determine the pion quark momentum distribution. Assuming $s(x) = \bar{u}(x)$ they obtain an exponent (for $x > .3$):

$$s(x) \sim (1 - x)^{1.0 \pm 0.3}$$

to be compared with Hwa and Roberts result

$$u(x) \sim (1 - x)^{0.8 \pm .2}$$

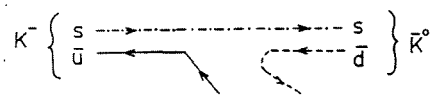

Fig. 3a

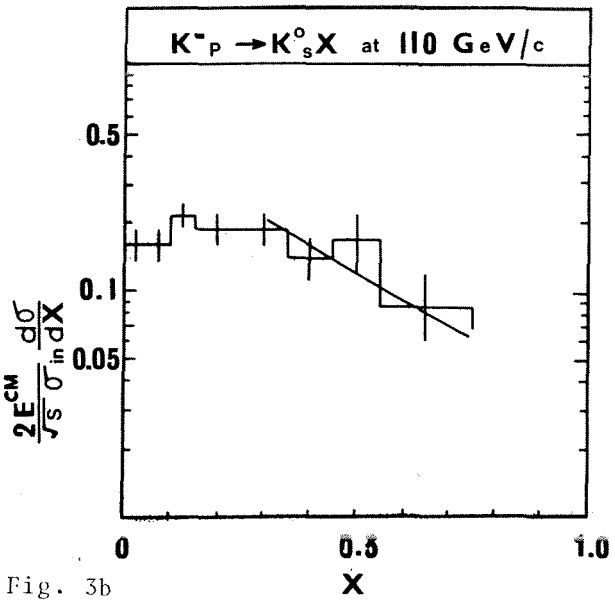

Fig. 3b

Fig. 3b Invariant inclusive x-distribution of neutral kaons in 110 GeV/c K^-p interactions. The solid curve represents the fit to the recombination model with s(x) in text.

Their analysis is preliminary and the statistics low, but the result suggests that the quark momentum distributions in the kaon are similar to those in the pion.

One of the most interesting extensions of these low-P_t quark-parton ideas is the study of two-particle correlations. Two such studies have appeared in the literature recently[5] and two conference contributions[1a, 1c] concentrate on this subject. The principle is illustrated by one of the tests made by the 32 GeV/c K^+p collaboration[1a]. First take a "trigger" particle at x-Feynman x_1. They consider $\pi^{\pm}$, K^0_S, Λ, $\bar{\Lambda}$ and K^{*+} (890) as triggers, which illustrates the wide range of tests made possible by kaon beams. Then they choose a second particle, a π^+ or π^-, at x-Feynman x_2. Important variable are:

$$x_{12} = x_1 + x_2 \qquad (2)$$

$$\text{and } \tilde{x}_2 = \frac{x_2}{x_2^{max}} = \frac{x_2}{1 - |x_1|} \qquad (3)$$

If we trigger on the fastest π^+ as in Fig. 4a then the second fastest π^+ probably also comes from a valence u quark. Triggering on a fast π^- as in Fig. 4b gives twice as many possibilities for an associated fast π^+ from one of the two valence u quarks. Hence these models predict the ratio:

Fig. 4a

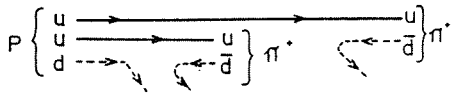

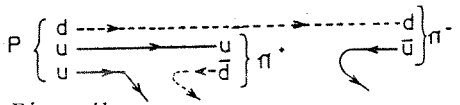

Fig. 4b

$$\left(\frac{\pi_1^- \pi_2^+}{\pi_1^+ \pi_2^+}\right) \to 2 \qquad \text{as } x_1, x_2 \to -1 \qquad (4)$$

In Fig. 5 we see that as $|x_1|$ increases the ratio of π^+ at $\tilde{x}_2$, for trigger π^- and trigger π^+, does approach 2 as $\tilde{x}_2$ increases.

Preliminary analysis of the WA3 Spectrometer experiment[1c] has taken these tests further and attempted to distinguish between two different possibilities for the dressing-up mechanism. These differ in their treatment

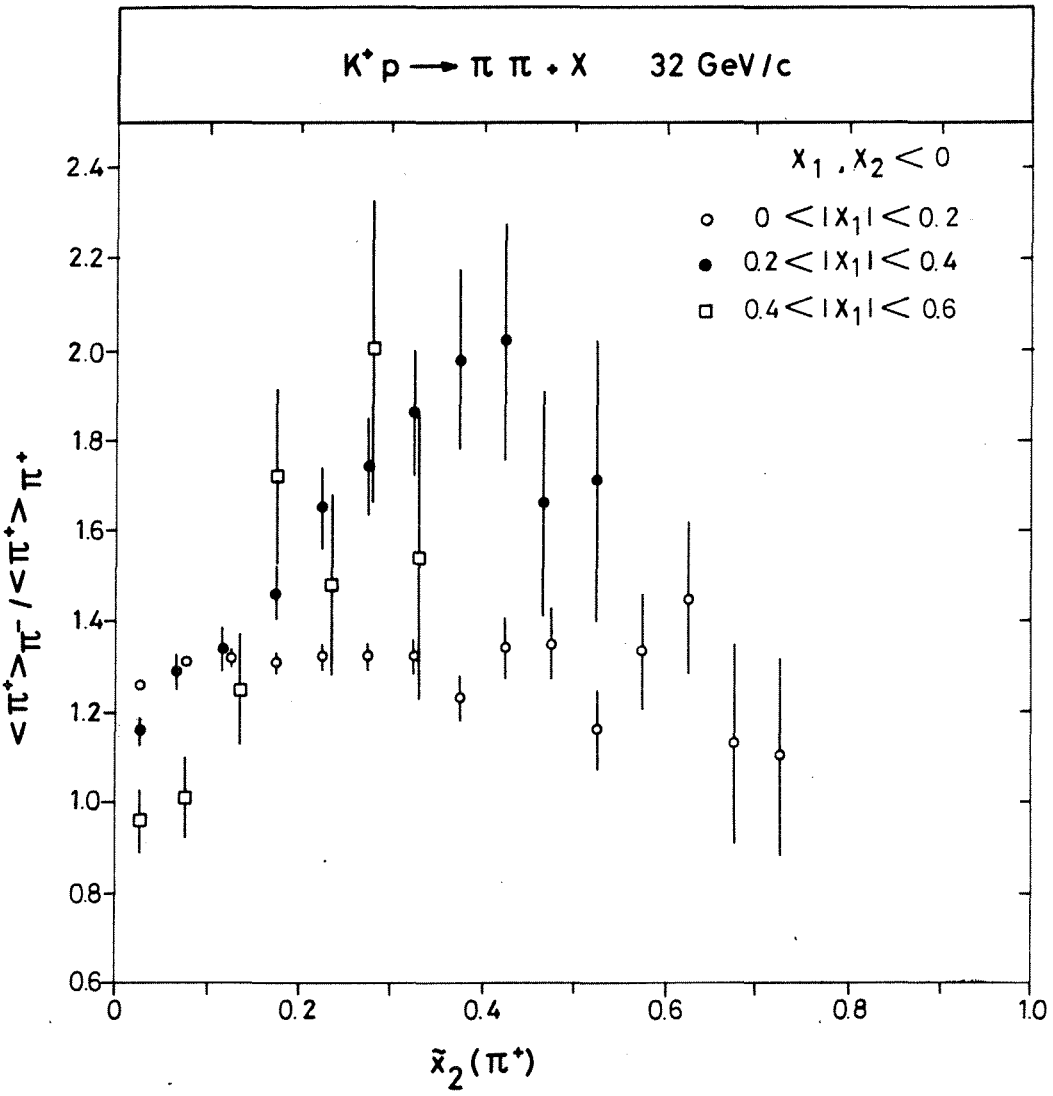

Fig. 5 Ratio of $\tilde{x}_2(\pi^+)$ distributions with π^- and π^+ trigger, respectively, for three intervals of trigger momentum x_1, in 32 GeV/c K^+p interactions.

of the second fastest particle. Strict devotees of the recombination doctrine (e.g. 2d, 2e) would say that the second fastest particle contained a valence quark. Hence if one triggers on a fast π^- as in Fig. 6a then a second fast π^- is possible by this mechanism when π^- is incident but not for K^- beams. This predicts that:-

$$\frac{(\pi_1^- \quad \pi_2^-)_{K^-}}{(\pi_1^- \quad \pi_2^-)_{\pi^-}} \rightarrow \quad 0 \qquad \text{as } x_1,\ x_2 \rightarrow +1$$

However, another school of thought (e.g. 2c, 2f, 2k) would have it that only one valence quark participated, leaving the other quark behind as in a nuclear stripping reaction. The leading quark then fragments, à la Field-Feynman[6]. According to this philosophy the second π^- would appear somewhere down the chain as in Fig. 6b. This would occur for both incident π^- and K^- except that both valence quarks can participate in the fastest π^- when the beam is π^-. Hence:-

$$\frac{(\pi_1^- \quad \pi_2^-)_{K^-}}{(\pi_1^- \quad \pi_2^-)_{\pi^-}} \rightarrow \quad \tfrac{1}{2} \qquad \text{as } x_1,\ x_2 \rightarrow +1$$

The WA3 data, Fig. 7a, clearly favour the strict recombination scheme.

However, the same experiment's data in Fig. 7b is a problem for both models. The π^+, a $(u\bar{d})$ combination, doesn't share a valance quark with the π^- $(\bar{u}d)$ or K^- $(s\bar{u})$. Hence on either model, if one triggers on a fast π^-, the fastest π^+ is formed from the sea, e.g. as the first link in the chain of Fig. 6b. Hence on both models:-

$$\frac{(\pi_1^- \quad \pi_2^+)_{K^-}}{(\pi_1^- \quad \pi_2^+)_{\pi^-}} \rightarrow \quad \tfrac{1}{2} \qquad \text{as } x_1,\ x_2 \rightarrow +1$$

It can be seen from Fig. 7b that this doesn't happen and clearly both classes of low-P_t models are going to have problems explaining this.

Fig. 6a

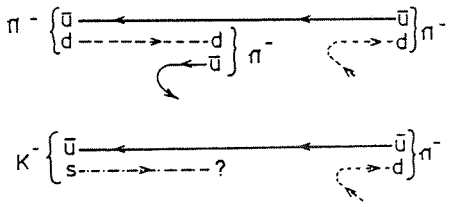

Fig. 6b

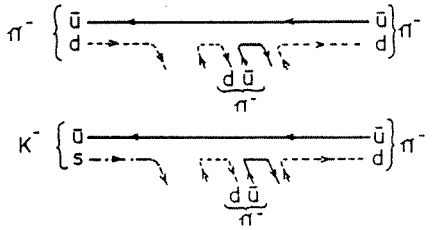

Experiment WA3, ACCMOR Collaboration
(preliminary data)

$$R_1 = \frac{K^- p \longrightarrow (\pi^-\pi^-) + X}{\pi^- p \longrightarrow (\pi^-\pi^-) + X} \text{ at 58 GeV/c}$$

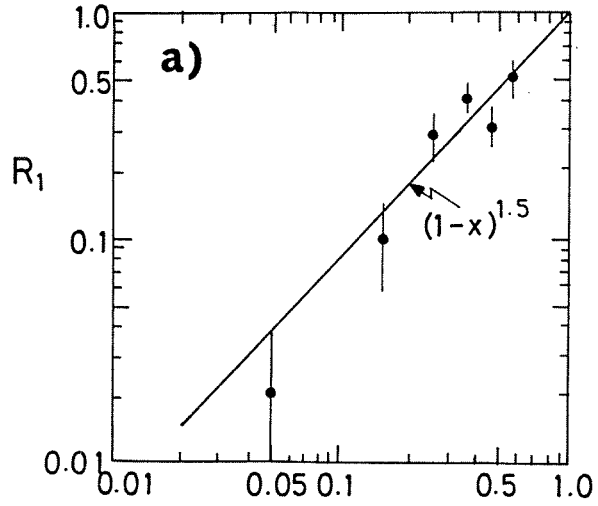

$$R_2 = \frac{K^- p \longrightarrow (\pi^+\pi^-) + X}{\pi^- p \longrightarrow (\pi^+\pi^-) + X} \text{ at 58 GeV/c}$$

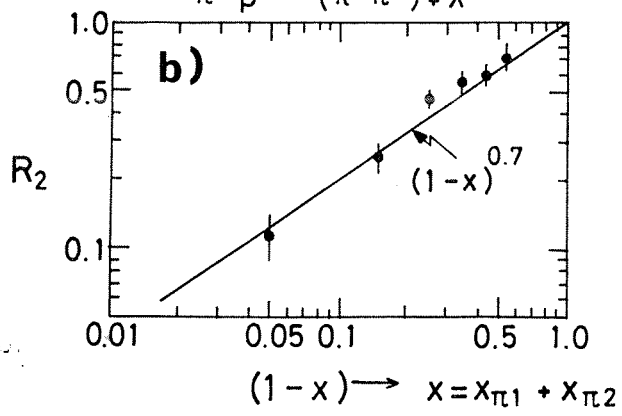

Fig. 7a Plot of the ratio R_1 as a function of $x = x_1 + x_2$ where $x = P_\pi / P_{BEAM}$ for K^-p and $\pi^- p$ reactions at 58 GeV/c.

Fig. 7b Plot of the ratio R_2 as a function of x.

Differences in s(x) and d(x) could be invoked, but this would run into conflict with the 110 GeV/c result that they appear similar as discussed earlier. Clearly more data on s(x) and d(x) and further tests of these low-P_t quark-parton models are required. The External Particle Identifier, a multicell ionization chamber which can separate π/K/p from $\sim$30 - 90 GeV/c was in use during the most recent BEBC run and should make a significant improvement to such studies.

3. INCLUSIVE RESONANCE PRODUCTION

It will not be possible to do justice to the many papers [7a-g] received on this subject. The inclusive Φ production [7a, b] is probably the most interesting as a study of the Okubo-Zweig-Iizuka rule. This data was reviewed by D.R.O. Morrison in a parallel session. The other vector mesons are the most popular subjects for study. The 32 GeV/c K^-p collaboration [7d] not only consider $K^{*-}(890)$ and $\bar{K}^{*0}(890)$ production but also, rather bravely, extract cross sections for the S=+1 states $K^{*+}(890)$ and $K^{*0}(890)$ and the tensor mesons $K^{*-}(1420)$ and $\bar{K}^{*0}(1420)$. In general their results agree with simple quark model predictions [8].

It is pertinent to consider whether such studies are possible in the new generation of high energy, and hence high multiplicity, bubble chamber experiments. Figs. 8a,b from the 70 GeV/c K^-p collaboration [7e] show that it is clearly possible for the $K^{*-}(890)$ but more problematic for the $K^{*0}(890)$. Commendably the authors allow in their fits for the effect of calling a real π^- a K^-. This is important because if the π^- came from a ρ^0 it would produce a peak at around .94 GeV mass rather than contribute smoothly to the background as is often optimistically assumed.

The 70 GeV/c K^-p cross sections are presented in Fig. 9, and they show no energy dependence. The new 32 GeV/c K^-p cross sections have also been added in Fig. 9.

Inclusive Δ^{++} production has been a fruitful source of study for many years. New results from the 32 GeV/c and 70 GeV/c K^+p collaborations [7f, g] submitted to this conference enable the P_{LAB} dependence to be plotted as in Fig 10. The 70 GeV/c result indicates that the fall in cross section below 32 GeV/c is levelling off. The 70 GeV/c K^+p collaboration also compare their cross section with the pp result [9]:-

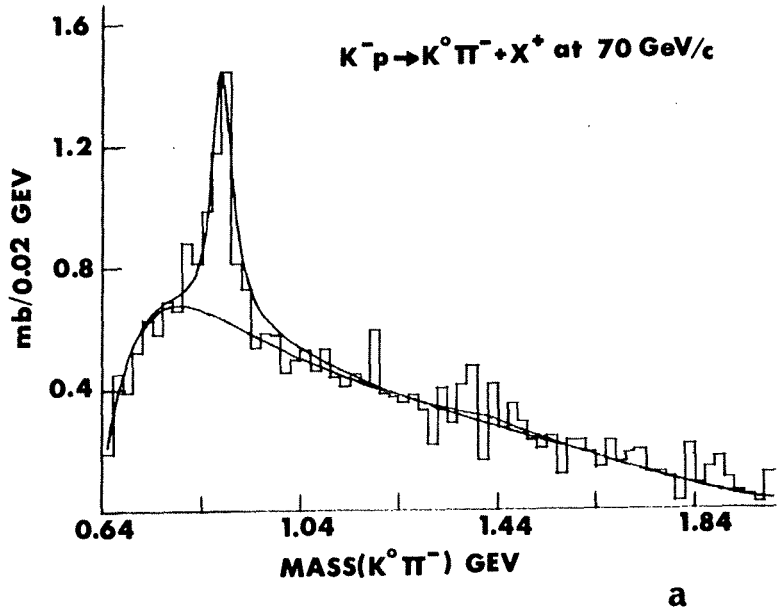

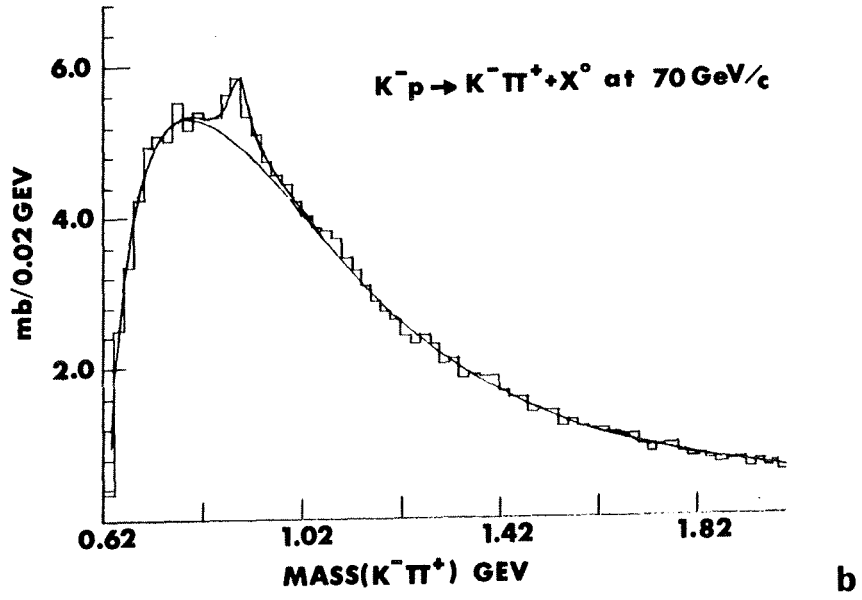

Fig. 8a $K^{o}\pi^{-}$ effective mass distribution in $K^{-}p$ interactions at 70 GeV/c. The lower curve shows the background and the upper curve the sum of background and resonance terms obtained by fitting.

Fig. 8b $K^{-}\pi^{+}$ effective mass distribution. Solid curves as in (a).

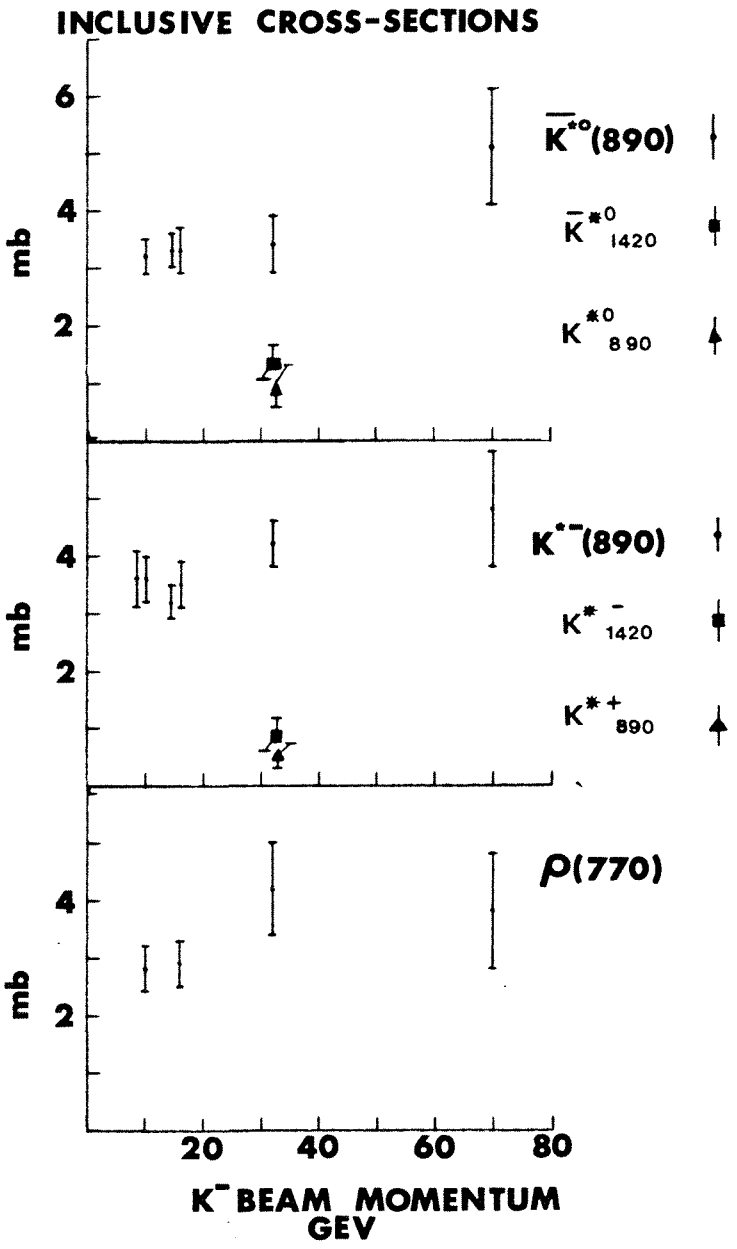

Fig. 9 The $\bar{K}^{*0}$, K^{*-} and ρ inclusive cross-sections in K^-p interactions as a function of K^- beam momentum.

$$\frac{\sigma(K^+p \to \Delta^{++}+x^o)}{\sigma(pp \to \Delta^{++}+x^o)} = 0.47 \pm .07$$

and point out that this is consistent with factorization since the ratio agrees with

$$\frac{\sigma_{TOT}(K^+p)}{\sigma_{TOT}(pp)} = 0.47$$

These results are, in fact, easily explained on a triple Regge picture. The relevant diagram is Fig. 11. The s-dependence is determined by the intercept of the top Reggeon $\bar{\alpha}(o)$. At high enough energies this should be the Pomeron which factorises. Hence the K^+R^- elastic scattering amplitude (or total cross-section by the optical theorem) should have the same ratio to the pR^- amplitude as the K^+p and pp total cross sections. Note also that when factorization occurs $\bar{a}(o)$ is the Pomeron intercept ($\gtrsim 1$) and the triple-Regge cross section becomes energy independent. The data in Fig.10 indicates this probably happens around 70 GeV/c.

In addition note that for incident K^- the R^-K^- scattering in Fig.11 is exotic and hence should be Pomeron dominated at much lower R^-K^- masses. The RK mass is the missing mass to the Δ^{++}, so kinematically this means at lower s values. Pomeron dominance was, in fact, observed in K^- interactions as low as 10 and 16 GeV/c [10a]. The cross section observed in 16 GeV/c K^-p reactions [10b] was 0.48mb or 0.62mb depending whether a Breit-Wigner fit or mass cut was used. The 70 GeV/c K^+p result is consistent with the higher figure. If this triple-Regge picture with Pomeron dominance is correct the 70 GeV/c and 110 GeV/c K^-p cross sections should be similer. These results are awaited with interest.

4. HADRON BUBBLE CHAMBER DATA AS A STANDARD FOR TESTING NEW PHYSICS

Three contributions to this conference [11a-c] presented results which I interpret as belonging in this category. The philosophy behind these comparisons is that hadronic bubble chamber data is standard, known physics, dominated by limited transverse momentum and logarithmically rising multiplicities. In addition the charged particles are measured with minimum experimental bias. Hence any new phenomena found in the apparently more

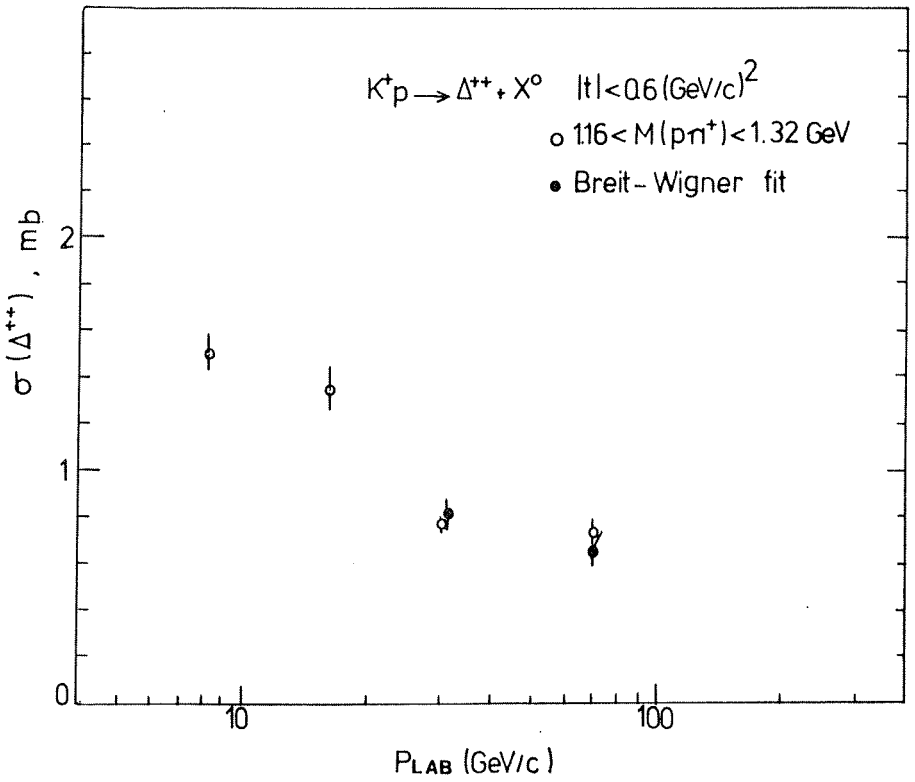

Fig. 10 Energy dependence of the Δ^{++} inclusive cross-section in K^+p interactions. The point at 32 GeV/c for $1.16 < M(p\pi^+) < 1.32$ GeV interval is calculated with the additional cut $\cos\theta_J < 0.8$.

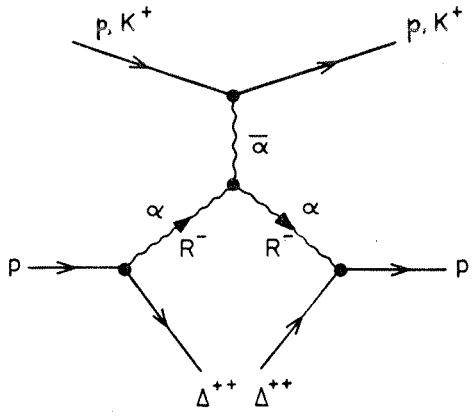

Fig. 11 Triple-Regge diagram for the reactions $K^+p \rightarrow \Delta^{++} + x^o$ and $pp \rightarrow \Delta^{++} + x^o$.

exciting fields of lepton physics should be compared with this "standard model" to see if the new physics was in fact already known or to see if it is due to experimental bias or analysis technique.

As an example consider the comparison made by the 110 GeV/c K^-p collaboration[11b] with the E-260 FNAL Calorimeter experiment[12]. The Calorimeter experiment observed, amongst other things, that the charged multiparticle rate at $P_t > 3$ GeV/c was a factor of 10 higher than the single particle rate. The popular interpretation of their results is that they were observing jet production. Taking exactly the same cuts as imposed by the Calorimeter set-up the bubble chamber collaboration show that their data has the same behaviour at much lower P_t and it extrapolates smoothly to the E-260 data as seen in Fig. 12a. Note also from Fig. 12b that the same general features are present at 16 GeV/c where hard scattering effects are certainly not expected to be important.

More quantitatively the 110 GeV/c K^- collaboration estimate that if they took a cut on their multiparticle systems with $P_t > 2$ GeV/c they would have a total of about 170 "jet" events in their sample. However, by performing a full, charged particle "sphericity" analysis (Fig. 13) they estimate that at most there are 30 events in the disc (i.e. 4-jet) corner. Hence the bulk of the high-P_t multiparticle systems are probably not jets.

Of course, such comparisons can work the other way and emphasise the significance of effects when differences are observed. In one conference submission[11c] the 70 GeV/c K^-p collaboration has studied the variation of $\langle P_t^2 \rangle$ of pions, relative to the K^- direction, as a function of s. They compare this with the rise in $\langle P_t^2 \rangle$, relative to the mean hadron direction, with W^2 (the square of the hadronic centre-of-mass energy) observed in νNe interactions by the ABCLOS collaboration[13]. Having shown that $\langle P_t^2 \rangle$ rises for both π^+ and π^- (Fib. 14a, b) they then show in Fig. 14c that the rise is less steep ($\sim$lns) than that observed in νNe ($\sim$s). Interestingly the increase proportional to s is a first-order QCD prediction. Here then the comparison is saying that perhaps something different is occuring in νNe reactions, or there is an experimental bias in the latter!

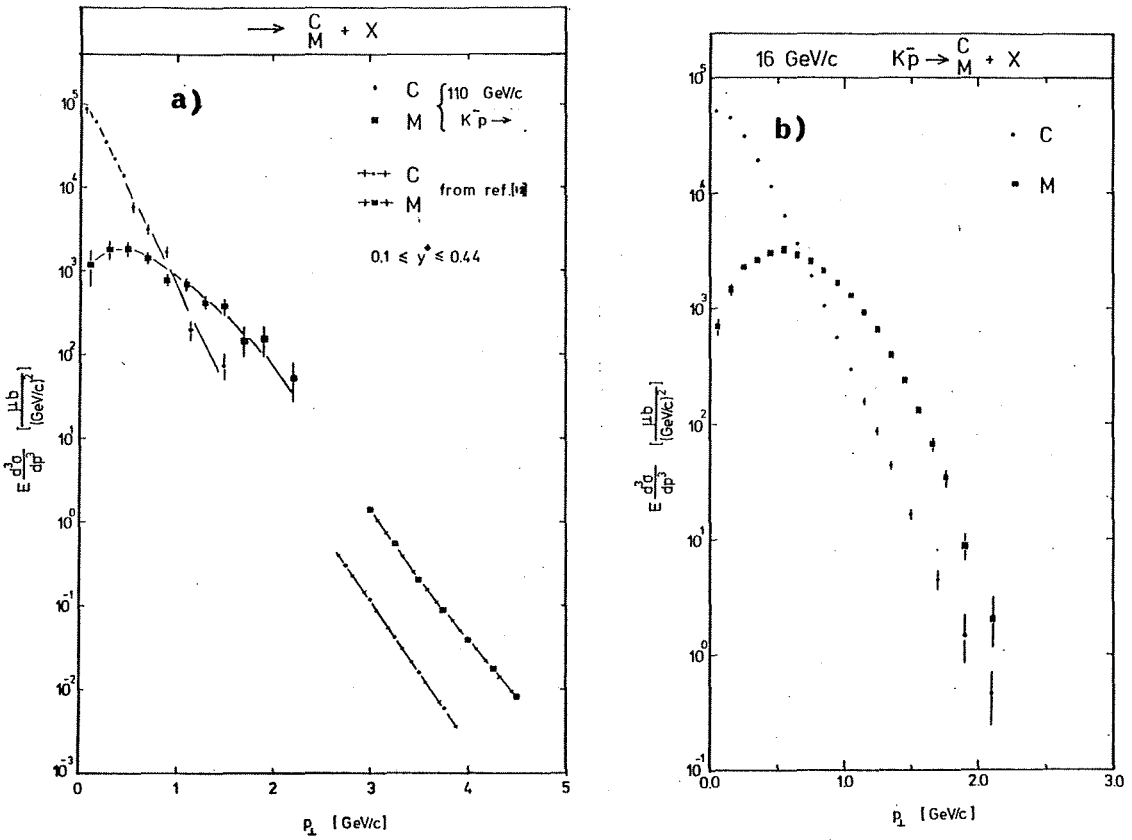

Fig. 12a P_t distribution of invariant cross-section of single charged particles C and multiparticle systems M in the rapidity range $0.1 \leq y^* \leq 0.44$. All constituents in the multiparticle systems in this figure have values $y^* > -0.5$. Also drawn are data taken from Fig. 23 of Ref. 12.

Fig. 12b As Fig. (a) but with data from K^-p interactions at 16 GeV/c.

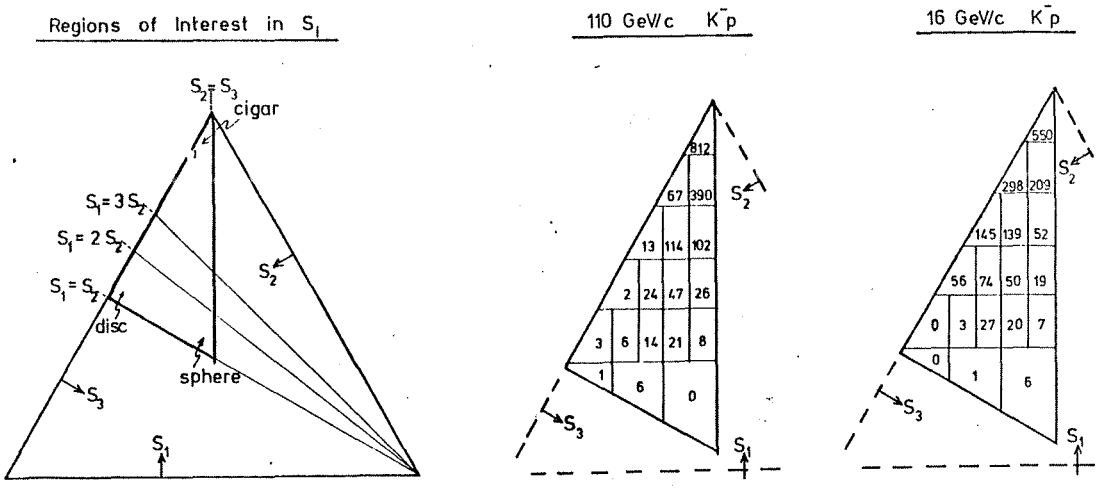

Fig. 13a Regions of interest in the sphericity variable.

Fig. 13b The population (number of events $\geq$ 4 prong) for 110 GeV/c K^-p data.

Fig. 13c The population for 16 GeV/c K^-p data. The number of events is normalized to the total number of events $\geq$ 4 prong at 110 GeV/c.

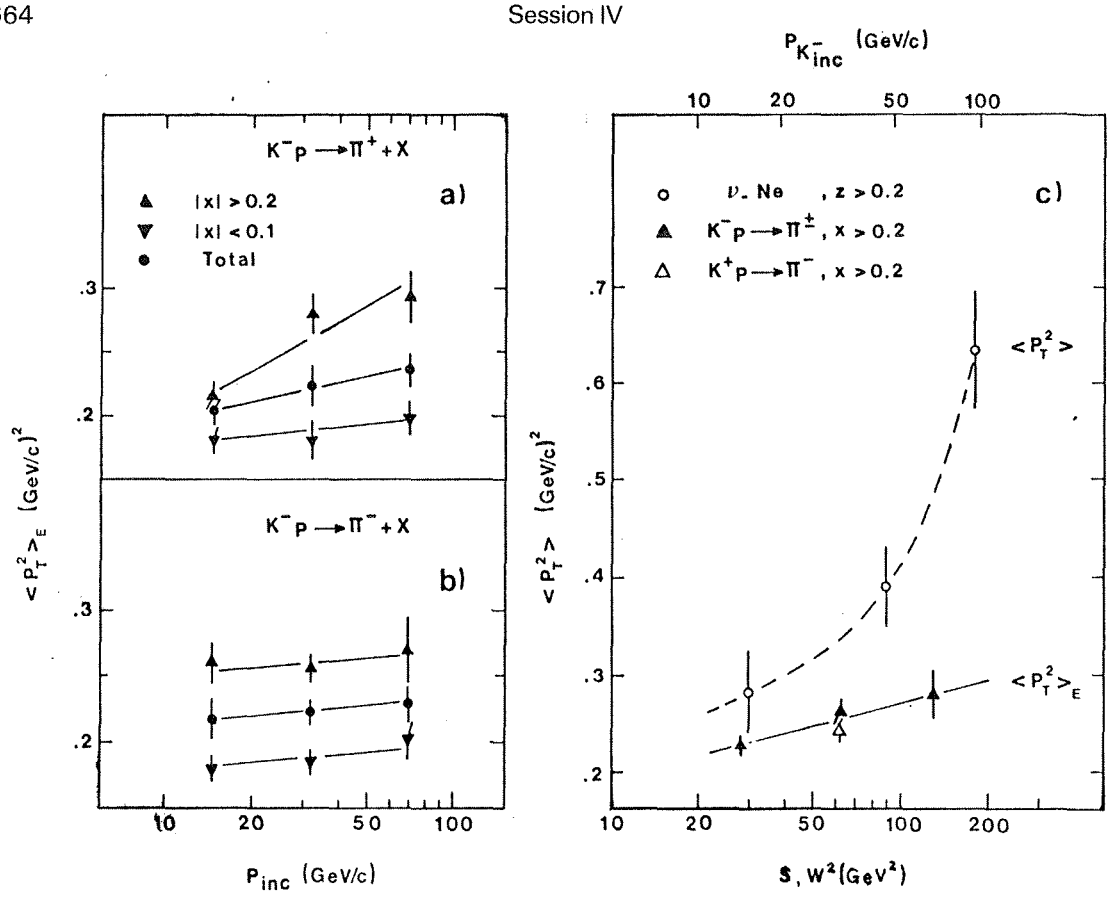

Fig. 14a Energy dependence of $<P_t^2>_E$ in various x-Feynman regions for π^+ in K^-p interactions. $<P_t^2>_E$ is P_t averaged over the invariant P_t distribution.

Fig. 14b As for (a) but for produced π^-.

Fig. 14c Energy dependence of $<P_t^2>_E$ in $K^\pm p \to \pi^\pm + x$ for x-Feynman >0.2 and of $<P_t^2>$ for the reaction $\nu Ne \to \mu^- +$ hadrons for z > 0.2.

One should conclude by admitting that these comparisons are not particular to incident K^+ or K^-. However, they do need good statistics, minimum bias, bubble chamber data.

5. APOLOGIES AND ACKNOWLEDGEMENTS

Of the subjects I have been unable to cover in this short review I must mention the studies of diffraction dissociation by the 32 GeV/c K^+p collaboration[14] and 70 GeV/c K^-p collaboration[15]. I apologise to these authors and refer interested readers to the original papers.

I have benefitted considerably from discussions on the topics described here with a number of colleagues but in particular E.A. De Wolf and W. Ochs.

REFERENCES

1a) Abstract 64. 32 GeV/c K^+p. E. A. De Wolf et al. Brussels, Serpukhov Collaboration.

b) Abstract 66. 32 GeV/c K^+p. I. V. Ajinenko et al. Serpukhov, Brussels, Mons, LPNHE, Saclay Collaboration.

c) Abstract 54. 58 GeV/c K^-/π^-p. Amsterdam, CERN, Cracow, Munich MPI, Oxford, Rutherford Collaboration and W. Ochs private communication.

d) Abstract 67. 70 GeV/c K^+p. Brussels, CERN, Genova, Mons, Nijmegen, Serpukhov, Tel Aviv Collaboration.

e) Abstract 28. 110 GeV/c K^-p. Aachen, Berlin, CERN, Cracow, London, Vienna, Warsaw Collaboration.

f) Abstract 155. B. Buschbeck, H. Dibon, H.R. Gerhold, W. Kittel.

2a) H. Goldberg, Nucl. Phys. B44 (1972) 149.

b) S. Pokorski and L. Van Hove, Acta Phys. Pol. B5 (1974) 229.

c) B. Andersson et al, Phys. Letts. 69B (1977) 221.

d) W. Ochs, Nucl.Phys. B118 (1977) 397.

e) K.P. Das and R.C. Hwa, Phys. Letts. 68B (1977) 459

f) S.J. Brodsky and J.F. Gunion, Phys. Rev. D17 (1978) 848.

g) D.W. Duke and F.E. Taylor, Phys. Rev. D17 (1978) 1788.

h) M.J. Teper, Rutherford Preprint RL-78-022/A (1978).

i) L. Van Hove, CERN TH-2628 (1979).

j) J. Ranft, Phys. Rev. D18 (1978) 1491.

k) A. Capella et al. Orsay Preprint LPTE 78/30 (1978)

ℓ) R.C. Hwa and R.G. Roberts, Z. Physik C1 (1979) 81.

m) P.V. Chliapnikov et al. Nucl. Phys. B148 (1979) 400.

For a review of the experimental situation see W.D. Shephard, Proc. IX Multiparticle Dynamics Symposium, Tabor, Czechoslavakia (1978).

3) G.R. Farrar and D.R. Jackson, P.R.L. 35 (1975) 1416.

4) R.G. Roberts, R.C. Hwa and S. Matsuda, Rutherford Preprint RL-78-040 (1978)

5) E. Lehman et al. Phys. Rev. D18 (1978) 3353
W. Lockman et al. P.R.L. 41 (1978) 680.

6) R.D. Field and R.P. Feynman. Phys. Rev D15 (1977) 2590.

Inclusive ϕ Production

7a) Abstract 59. 63, 93 GeV/c $K^{\pm}/\pi^{\pm}p$. Amsterdam, CERN, Cracow, Munich MPI, Oxford, Rutherford Collaboration.

b) Abstract 91. 10, 16 GeV/c $K^{-}/\pi^{+}p$ Aachen, Bonn, CERN, Cracow, London, Vienna, Warsaw Collaboration.

Other Inclusive Vector Mesons

c) Abstract 133. 147 GeV/c K^{+}, π^{+}, p/p. FNAL 30" Hybrid Consortium.

d) Abstract 170. 32 GeV/c $K^{-}p$. Y. Arestov et al. Serpukhov, Saclay, Aachen, Berlin, CERN, Vienna Collaboration.

e) Abstract 229. 70 GeV/c $K^{-}p$. C. Comber et al. Rutherford, Saclay, LPNHE Collaboration.

Inclusive Δ^{++}

f) Abstract 65. 32 GeV/c $K^{+}p$. P.V. Chliapnikov et al, Serpukhov, Brussels, Mons, Saclay, LPNHE Collaboration.

g) Abstract 106. 70 GeV/c $K^{+}p$. Brussels, CERN, Genova, Mons, Nijmegen, Serpukhov, Tel Aviv Collaboration.

8) V.V. Anisovich and V.M. Shekhter. Nucl. Phys. B55 (1973) 455.

9) H. Bialkowska et al. Nucl. Phys. B110 (1976) 300.

10a) P. Bosetti et al. Nucl. Phys. B81 (1974) 61.

b) J. Bartke et al. Nucl. Phys. B137 (1978) 189.

11a) Abstract 132. 147 GeV/c K^{+}, π^{+}, p/p. FNAL 30" Hybrid Consortium.

b) Abstract 161. 110 GeV/c $K^{-}p$. M. Deutschmann et al, Aachen, Berlin, CERN, Cracow, London, Vienna, Warsaw Collaboration.

c) Abstract 167. 70 GeV/c $K^{-}p$. J.M. Laffaille et al, Saclay, LPNHE, Rutherford Collaboration.

12) C. Bromberg et al. Nucl. Phys. B134 (1978) 189.

13) P.C. Bosetti et al, Nucl. Phys. B149 (1979) 13.

14) Abstract 201. 32 GeV/c $K^{+}p$. J. Saudraix et al, Saclay, LPNHE, Serpukhov, Mons, Brussels Collaboration.

15) Abstract 168. 70 GeV/c $K^{-}p$. J. Dumorchez et al, LPNHE, Saclay, Rutherford Collaboration. Université P. & M. Curie Preprint LPNHEP-79/06 (1979).

SPIN DEPENDENCE IN HIGH-$P_\perp^2$ ELASTIC pp AND np SCATTERING

D.G. Crabb, R.C. Fernow*), P.H. Hansen, J. Hauser, A.D. Krisch, B. Sandler†), T. Shima, and K.M. Terwilliger
University of Michigan, Ann Arbor, MI USA

E.A. Crosbie, L.G. Ratner, P.F. Schultz, and G.H. Thomas
Argonne National Laboratory, Argonne, IL USA

J.R. O'Fallon
Argonne Universities Association, Argonne, IL USA

A. Lin
Abadan Institute of Technology, Abadan, Iran

A.J. Salthouse
Bell Laboratories, Murray Hill, NJ USA

S.L. Linn and A. Perlmutter
Department of Physics and Center for Theoretical Studies, University of Miami, Coral Gables, FL and University of Michigan, Ann Arbor, MI USA

N.L. Karmaker
University of Kiel, Kiel, Germany

P. Kyberd
Oxford University, Oxford, England

ABSTRACT

Using the polarized proton capability of the Argonne ZGS we recently made $90°_{cm}$ measurements of elastic $p_\uparrow p_\uparrow$ scattering from 6 to 11.75 GeV/c, determining the parallel and anti-parallel pure initial spin state cross sections and the associated spin-spin parameter A_{nn} with the spins normal to the scattering plane. We find that the parallel to anti-parallel cross section ratio rises dramatically from $1.2\pm.06$ at $P_\perp^2=3.3$ $(GeV/c)^2$ to $3.2\pm.4$ at 4.8 $(GeV/c)^2$, similar to the $P_\perp^2$ dependence previously observed at the fixed laboratory momentum of 11.75 GeV/c. We have also extended our measurements at 6 GeV/c and find that A_{nn} has a small but sharp rise at $90°_{cm}$. In addition a month of 12 GeV/c polarized deuteron acceleration in the ZGS enabled us to measure A_{nn} at two points at 6 GeV/c for $n_\uparrow p_\uparrow$ elastic scattering: $A_{nn}=-.17\pm.04$ at $P_\perp^2=.8$, $A_{nn}=-.19\pm.05$ at $P_\perp^2=1.0$. These values are opposite in sign from the $p_\uparrow p_\uparrow$ results at the same momentum.

INTRODUCTION

The last few years our group has been studying the effects of spin states on elastic proton-proton scattering, attempting to measure these spin dependences out to the highest energies and momentum transfers available. The accelerator, the Argonne ZGS, is presently unique in its capability of accelerating polarized protons — intensities of nearly 10^{11} polarized protons per pulse have been accelerated to 11.75 GeV/c, with proton beam

*)Present address: Brookhaven National Laboratory, Upton, L.I., NY, USA
†)Present address: General Electric Co, Milwaukee, WI, USA

polarizations over 60%. The ZGS accelerator will be turned off this fall, the end of September, so future work on high energy spin-spin interactions will depend on the development of a polarized proton capability in one of the higher energy alternating gradient machines.

These spin-spin forces appear to have a dramatic $P_\perp^2$ dependence. As reported earlier[1] we observed that at a beam momentum of 11.75 GeV/c the ratio of the spin parallel to anti-parallel cross sections, the spin normal to the scattering plane, rises from approximately unity to four as $P_\perp^2$ goes from 3 to 5 $(GeV/c)^2$. Here we present the results of our recent $p_\uparrow p_\uparrow$ spin-spin measurements at $90°_{cm}$, now varying the laboratory beam momentum, covering the same $P_\perp^2$ range. We also have been able to make limited spin-spin measurements at 6 GeV/c in $n_\uparrow p_\uparrow$ elastic scattering and will compare them to our $p_\uparrow p_\uparrow$ 6 GeV/c results.

EXPERIMENT

The general layout of our experiments for $p_\uparrow p_\uparrow$ elastic scattering is shown in Fig. 1. The proton beam from the ZGS, incident from the left, is polarized up and down on alternate pulses. The beam polarization is determined by measurements of the spin dependent asymmetry in the scattering of the polarized beam off a liquid hydrogen target; the asymmetry parameter, A, is known from previous measurements. The beam then passes through a polarized proton target (PPT) of $C_2H_6O_2$, with a target proton polarization typically in the 70% range. Because of radiation damage with high beam intensities, the target material had to be annealed twice a day and changed every few days. Elastic scattering events from the PPT are identified with a two-arm magnetic spectrometer. Background from non-hydrogen events is estimated using hydrogen-free teflon beads to replace the target material.

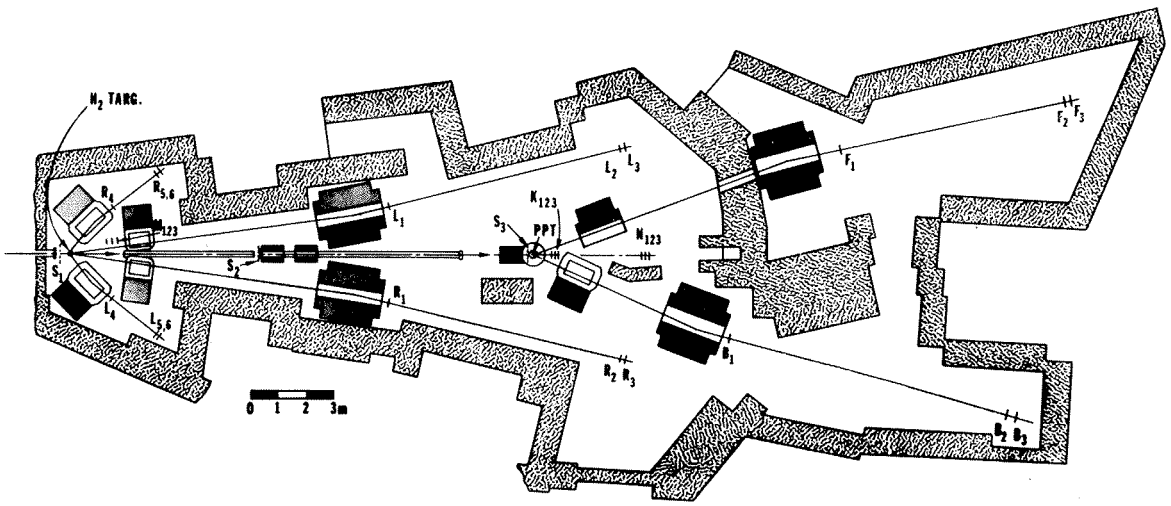

FIGURE 1: Layout of the experiment. The polarized beam passes through the liquid H_2 target and its polarization is measured. The beam then scatters in the polarized proton target (PPT) and the elastic events are counted by the F and B counters. The M,N, and K counters are intensity monitors, while S_1,S_2, and S_3 monitor the beam position.

For the neutron experiment the ZGS beam was 12 GeV/c polarized deuterons, therefore ∿ 6 GeV/c neutrons and protons, with polarization ∿ 50%. The hydrogen target polarimeter system discussed above was used to monitor the polarization of the protons in the deuteron - equivalent to the neutrons. Quasielastic n or p scatterings off the hydrogen in the PPT were again detected with the two arm spectrometer, with momentum analysis now only on the recoil proton (B) side. The forward neutron was detected with an anticoincidence counter followed by a brass-scintillator sandwich on the high energy forward (F) branch; the forward protons were detected with a single counter.

The accelerated deuteron intensity was 10^9/pulse, much lower than for protons, which limited our np data to two points.

In both experiments the observed polarization dependent cross sections, $d\sigma/dt\ (P_B, P_T)$, can be used to determine the associated Wolfenstein parameters: the asymmetry parameter, A, and initial state correlation parameter, A_{nn}, all spins normal to the scattering plane. The relation is:

$$\frac{d\sigma}{dt} = \langle\frac{d\sigma}{dt}\rangle [1 + (P_B + P_T)A + P_B P_T A_{nn}] \qquad (1)$$

The pure spin state cross sections are then:

$$\frac{d\sigma}{dt})_{\uparrow\uparrow} = \langle\frac{d\sigma}{dt}\rangle (1 + 2A + A_{nn})$$

$$\frac{d\sigma}{dt})_{\downarrow\downarrow} = \langle\frac{d\sigma}{dt}\rangle (1 - 2A + A_{nn})$$

$$\frac{d\sigma}{dt})_{\uparrow\downarrow} = \frac{d\sigma}{dt})_{\downarrow\uparrow} = \langle\frac{d\sigma}{dt}\rangle \quad (1 - A_{nn}). \qquad (2)$$

At $90°_{cm}$ in pp scattering A=0, and the parallel spin up and parallel spin down cross sections become equal.

RESULTS: 90° CENTER OF MASS EXPERIMENT

The present experiment went from a beam momentum of 6 GeV/c to 11.75 GeV/c, $P_\perp^2$ = 2.4 to 5.09 $(GeV/c)^2$. The constraint that A=0 at $90°_{cm}$ in pp elastic scattering was satisfied within the experimental errors.

Our present $90°_{cm}$ results, and those of earlier experiments[2)3)] are shown at the left in Fig. 2. Plotted is the ratio of the spin parallel cross section to the anti parallel cross section. From relations (2), since A=0, this ratio is

$$\frac{\frac{d\sigma}{dt})_{\text{parallel}}}{\frac{d\sigma}{dt})_{\text{antiparallel}}} = \frac{1 + A_{nn}}{1 - A_{nn}} \qquad (3)$$

This cross section ratio, rather flat and nearly unity in the intermediate $P_\perp^2$ region, increases quite dramatically, going from 1.2±0.06 at $P_\perp^2$ = 3.3 $(GeV/c)^2$ to 3.2±.4 at $P_\perp^2$ = 4.8 $(GeV/c)^2$, and appears to level off at ∿4 at the higher $P_\perp^2$. This rise with $P_\perp^2$ is remarkably similar to that observed in

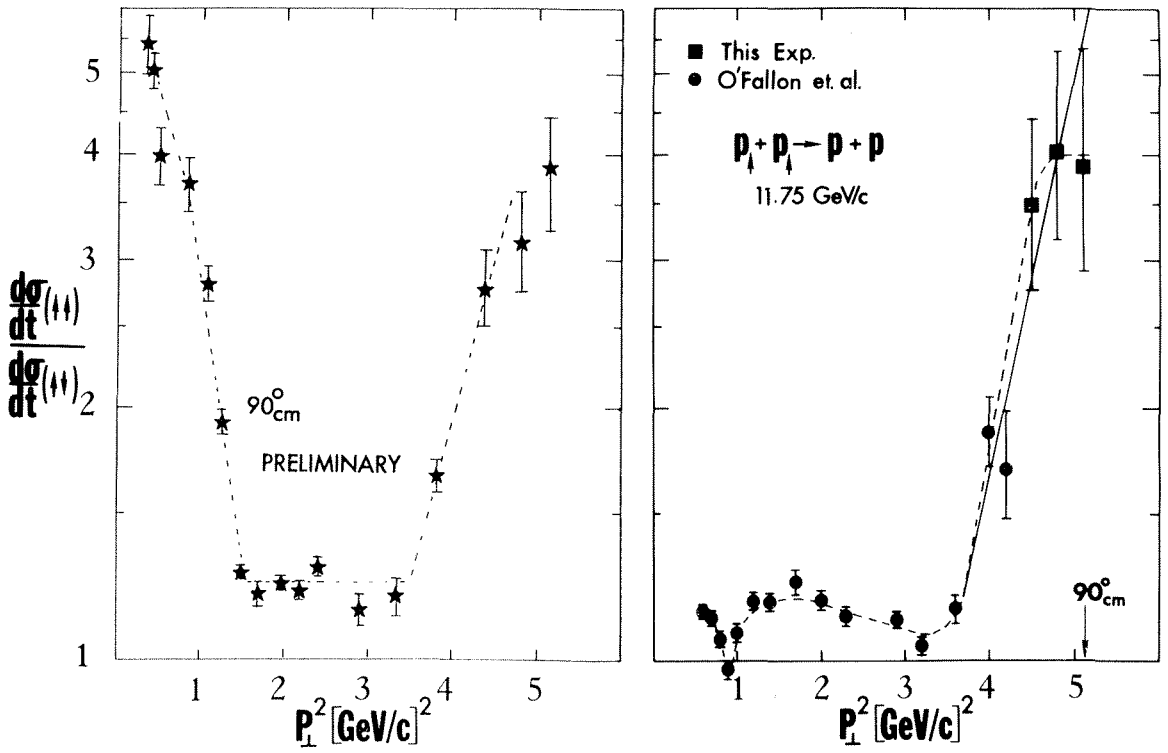

FIGURE 2: Plots of the $P_\perp^2$ dependence of the ratio of the differential elastic pp cross section in pure initial spins states. Left: $90°_{cm}$, varying beam momentum; the data for $P_\perp^2 \geq 2.4$ (GeV/c)^2 are from this experiment, the rest from Refs. 2), 3). Right: fixed beam momentum, 11.75 GeV/c, varying scattering angle; the plot is from Ref. 1). Both plots show similar high $P_\perp^2$ behavior: the spin parallel cross section increases dramatically relative to the spin antiparallel over the $P_\perp^2$ range of 3 to 5 (GeV/c)^2.

our previous experiment[1] at fixed beam momentum, 11.75 GeV/c, where the scattering angle was varied. These results are shown at the right in Fig. 2, also plotted using relation (3). Both ratios appear to rise over the same $P_\perp^2$ range.

np AND pp 6 GeV/c EXPERIMENTS

We obtained data from the 12 GeV/c polarized deuteron experiment at $P_\perp^2$ = .8 and 1 (GeV/c)^2. The values of A and A_{nn} for pp elastic scattering in our deuterium experiment agree with our more precise pp 6 GeV/c results,[4] giving us support for our np A_{nn} data. These are presented in Fig. 3. Also shown are our 6 GeV/c pp A_{nn} results - the sharp rise at $90°_{cm}$ is recent data. The large negative A_{nn} in np scattering is quite interesting. The antiparallel spin-spin interaction is larger than the parallel - opposite from the pp case.

We would like to thank E.F. Parker and the ZGS staff for their efforts in successfully accelerating the world's first high energy polarized deuteron beam, and in continuing the outstanding operation of the ZGS. We

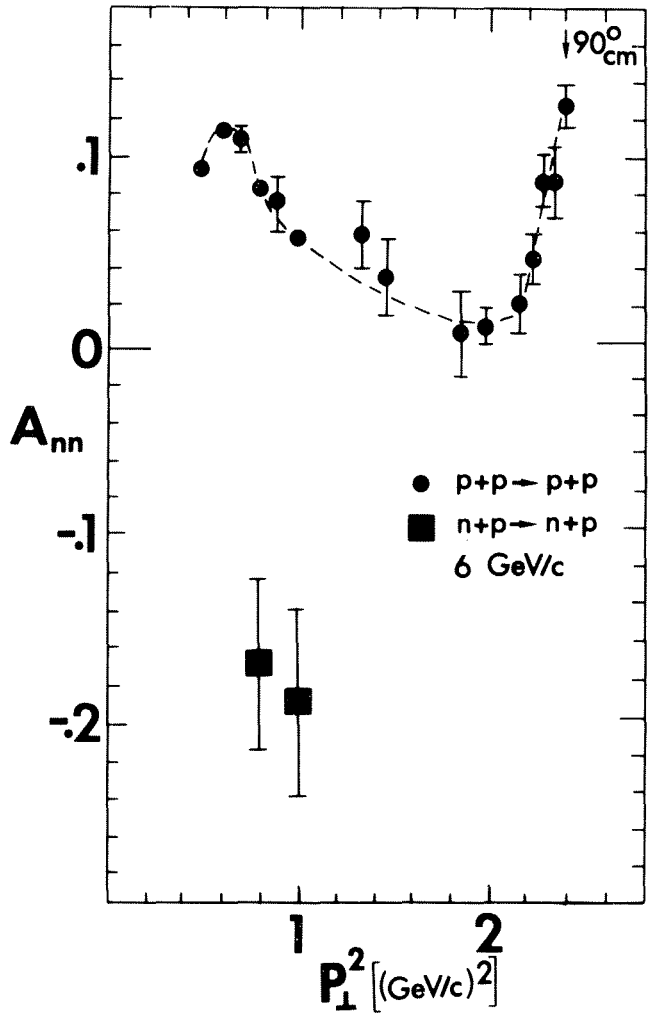

FIGURE 3: The spin-spin correlation parameter A_{nn} plotted against $P_\perp^2$ at 6 GeV/c beam momentum. Top: proton-proton elastic scattering. Bottom: neutron-proton elastic scattering. The np and pp results are quite different.

also thank R. Levine and M. Yatchman for helping in the design and construction of the neutron counter. This research was supported by a grant from the U.S. Department of Energy.

* * *

REFERENCES

1) D.G. Crabb et al., Phys. Rev. Lett. 41, 1257 (1978).

2) A. Lin et al., Phys. Lett. 74B, 273 (1978).

3) The two low momentum points are from a LAMPF experiment, H.B. Willard, et al., Proc. of Conf. on High Energy Physics with Polarized Beams and Polarized Targets, Argonne, 1978. G.H. Thomas, Ed. (A.I.P. New York 1979) 420.

4) R.C. Fernow, et al., Phys. Lett. 52B, 243 (1974). M. Borghini et al., Phys. Rev. D17, 24 (1978).

OBSERVATION OF PROMPT SINGLE MUONS AND OF MISSING ENERGY ASSOCIATED WITH $\mu^+\mu^-$ PAIRS PRODUCED IN HADRONIC INTERACTIONS*

B.C.Barish, J.F.Bartlett**, A.Bodek***, K.W.Brown, M.H.Shaevitz, E.J.Siskind
California Institute of Technology, Pasadena, CA. 91125, USA.
A.Diament-Berger†, J.P.Dishaw, M.Faessler††, J.K.Liu†††, F.S.Merritt, S.G.Wojcicki
Stanford University, Stanford, CA. 94305, USA.
Presented by A. Bodek (University of Rochester)

ABSTRACT

In a study of interactions of 400 GeV protons in a totally absorbing iron calorimeter we report two observations indicating the hadronic production of heavy short-lived weakly decaying particles. First we have observed a prompt muon signal in the region $.8 < p_t < 2.5$ GeV/c. The rate is comparable in magnitude to the prompt 2μ rate in the same kinematic region. In addition to detecting $\mu^+\mu^-$ events arising from electromagnetic sources (e.g., $\rho \to \mu^+\mu^-, \psi \to \mu^+\mu^-$ etc.) we have observed $\mu^+\mu^-$ pairs associated with a significant amount of missing energy indicative of final state neutrinos. Interpreting these data as production of $D\bar{D}$ pairs followed by single or double muonic decays leads to a model dependent estimate of total production cross-section of order 15 μb.

INTRODUCTION

The hadronic production of charmed particles had recently received considerable experimental and theoretical attention. QCD calculations predict cross-sections in the range 1-30 μb in 400 GeV p-N interactions[1], with gluon fusion probably giving the dominant contribution. Previous searches for charm production have produced widely varying results[2-6], ranging from upper limits of ∿1 μb/nucleon[2,3] at 400 GeV to a recently reported signal of ≈150 μb at the ISR[5]. The prompt neutrino signal reported by the CERN beam dump experiments[6], if interpreted as a charm signal, corresponds to a production cross-section of 25-50 μb/nucleon (assuming linear A dependence)[7].

One of the cleanest signatures of charm production would be the observation of a prompt single-muon signal, since the branching ratio of charm into $\mu\nu$ + hadrons is large (∿10%) and other sources of prompt single muons are negligible. Several experimental groups[2,8,9] have reported sizable prompt muon production, but previously only two[2,9] have attempted to separate 1-μ from 2-μ events (the latter are due primarily to electromagnetic rather than weak decays). The results of both of these groups were consistent with all the prompt muon signal originating from 2-μ events, but allowed a sizable single muon signal.

PROMPT SINGLE MUONS

We report here on the observation of a prompt 1-μ signal in the moderately high p_t ($0.8 < p_t^{\mu^+} < 2.5$ GeV) and low x_F ($10 < E^{\mu^+} < 60$ GeV) region produced by 400 GeV p-N interactions. We find approximately equal production cross-sections for 1-μ and 2-μ final states in this kinematic region. We also present evidence for the observation of missing energy (indicative of final state neutrinos) in association with hadronically produced $\mu^+\mu^-$ pairs, and relate it to the observed single muon signal.

* Work supported by the U.S.Dept. of Energy and the Nat. Sci. Foundation.
** Present address: Fermilab, Batavia, Illinois, 60510.
***Present address: University of Rochester, Rochester, N.Y., 14627.
† Permanent address: Department de Physique des Particules Elementaires, Saclay, France.
†† Present address: CERN, Geneva, Switzerland.
†††Presently with American Asian Bank, San Francisco, CA.

The experiment was performed in the Fermilab N5 beam with 400 GeV protons at typical intensities of 3-5 10^5/sec. The primary elements of the detector (Fig. 1) were a fine-grained target-calorimeter of variable density[10] (energy resolution of 3.5% at 400 GeV), a muon identifier (MI), and a toroidal muon spectrometer[11].

The data reported here were taken with a high-p_t trigger, which required a coincidence of both a beam and a muon trigger component. The muon component required the muon to remain in the same quadrant throughout the toroid system by requiring the appropriate coincidence of counters C, S2, ACR, T4 (which were divided into quadrants) and S1, T2, T3, MV (divided into half-planes). This requirement preferentially selected muons with high p_t ($p_t^{\mu^+} > .8$ GeV).

The beam component required an incident proton to pass through counters B0 and B1 (7.6×7.6 cm and 5.1×5.1 cm) and to interact within the first 10 plates of the calorimeter. To reject any background from upstream interactions, triggers were vetoed by the presence of any additional particles in the beam or halo counters within 95 nanoseconds of the trigger. Further beam information was provided by the pulse height of the trigger counters and by the incident proton's trajectory and momemtum, as measured by a spectrometer immediately upstream of the calorimeter. Interactions satisfying the beam trigger alone were scaled, and one out of each 2^{16} was recorded to provide a control sample of interactions without any muon requirement.

In the data analysis, software cuts were made to insure that the muon trigger counters were associated with a good trajectory, that the μ^+ enter the toroid system at least 17.5 cm from the axis (outside of the hole), and that the interaction point lie between plates 1 and 8 of the calorimeter. The muon trigger acceptance after all these cuts was greater than 50% over the range $1.0 < p_t^{\mu^+} < 2.5$ and $20 < E^{\mu^+} < 60$ GeV.

The majority of muons which triggered the apparatus were due to pion and kaon decays. This background was measured by uniformly expanding the first 25 plates (1 meter of steel) of the calorimeter, thereby proportionally increasing the mean path length and decay probability of hadrons in this region. Most of the hadrons decaying downstream of this region were produced by secondary or tertiary interactions, and consequently gave decay muons that were generally too low in energy to satisfy the trigger.

The experiment collected data at three different densities (keeping the mean interaction point fixed in space): fully compacted, expanded by a factor of 1.5, and expanded by a factor of 2. The mean calorimeter density in the compacted configuration was 3/4 that of steel due to the gaps (1.3 cm) between plates. After all software cuts, the rates in each density configuration were normalized to the beam trigger rates and plotted as shown in Fig. 2. As expected, the 2-μ rate is flat, and the 1-μ rate shows a linear increase with the effective pion interaction length. The 1-μ slope measures the rate from non-prompt decays, and the intercept of $(10.5\pm.5)10^{-6}$ at infinite density is the raw prompt 1-μ signal.

To obtain the true prompt single muon rate, the raw prompt 1-μ rate had to be corrected for several background sources:

a) $\mu^+\mu^-$ events with a low energy μ^- which ranged out in the calorimeter or muon identifier. A Monte-Carlo calculation using the measured $\mu^+\mu^-$ distributions gave a correction of $10 \pm 2\%$ (systematic errors included) of the raw prompt 1-μ signal. This component was subtracted from the 1-μ signal and added to the 2-μ signal.

b) Muons from decays of pions and kaons in the unexpanded part of the calorimeter (after

plate 25). A Monte-Carlo simulation of the hadron shower, which reproduced the mean shower profile measured in the experiment, gave a correction of 8±3% of the measured decay rate[12]. This corresponds to 16±6% of the prompt 1-μ signal.

c) A subtraction of 20±10% of the prompt 1-μ signal due to second order variation in the acceptance with density. These arise because, although the mean interaction point stays fixed, multiple scattering effects and production by secondaries move downstream when the calorimeter is expanded.Since the toroid hole subtends a larger angle for particles originating downstream, this yields a reduction of 4±2% in the acceptance of the expanded relative to the compacted configuration. This correction was obtained from the $\mu^+\mu^-$ events (which should be constant with density).

After all corrections, the measured prompt 1-μ rate was $(5.8\pm1.5)\times10^{-6}$ per incident proton and the 2-μ rate was $(5.9\pm.2)\times10^{-6}$; the errors are largely systematic. A natural explanation of this single muon signal would be production and subsequent decay via leptonic mode of new heavy hadrons, the most likely candidates being the charm particles. That same mechanism would also require a production (at a lower rate) of a pair of charged muons, both of which originate from the decay of charm particles. The muons from this process would have to be associated with a missing energy due to companion neutrinos emitted in the decay.

TWO PROMP MUONS WITH MISSING ENERGY

The total observed energy spectrum for $\mu^+\mu^-$ events ($E_{tot}=E_{\mu^+}+E_{\mu^-}+E_{calorimeter}$) is shown in Fig. 3. The dashed curve shown for comparison is the E_{tot} spectrum exhibited by beam interactions without final state muon. There is a pronounced enhancement of missing energy events for $m_{\mu^+\mu^-}<2.4$ GeV. We observe 227 $\mu^+\mu^-$ events with missing energy in excess of 45 GeV. An estimate of the double π,K decay background is provided by the 5 observed like sign dimuon events with large missing energy. Monte Carlo calculation of $K\bar{K}$ production and double decay also yields a background of 5 events. Also, since the toroid spectrometer is instrumented with acrylic calorimetry counters, we can rule out catastrophic muon energy loss in the steel as significant source of background. We conclude that all backgrounds are unlikely to contribute more than 10% of the observed $\mu^+\mu^-$ with missing energy signal.

INTERPRETATION

To estimate a charm production cross-section from these data, we have assumed that all the signal comes from the semileptonic decays D→Kμν (60%) and D→K*μν (40%) with a total semileptonic branching ratio of 8%. The inclusive D cross-section was assumed to increase linearly[13] with the atomic number A of the nucleus and was parameterized as

$$E\frac{d^3\sigma}{dp^3} = C\,(1 - x_F)^{\beta}\, e^{-\alpha p_t} \quad \text{(for inclusive D production)} \qquad (1)$$

The single muon data were consistent with values in the range $\alpha=2.0$-3.5 GeV^{-1} and $\beta>3$. Varying α and β over these allowed ranges yields charm cross-sections in the range 15-75 μb/nucleon. For $\beta=5$ and $\alpha=2.5$, the acceptance for the produced μ^+'s was 2.5% and the cross-section for D production was $\sigma_{D\bar{D}} = 36\pm9$ μb/nucleon. This model, in which the two charmed states are uncorrelated gives an acceptance of 0.14% for the $\mu^+\mu^-$ events with 45 GeV of missing energy and yields a charm cross-section of 22±8 μb. However, the $\mu^+\mu^-$ mass and momentum distributions do not fit this model.

In order to include the expected correlation between the D and $\bar{D}$ state we assume a

$D\bar{D}$ model production model

$$E\frac{d^3\sigma}{dp^3} = \frac{C}{M^3}(1-x_F)^{\beta} e^{-\alpha p_t} e^{-M/\sqrt{s}} \quad \text{(for } D\bar{D} \text{ production)} \qquad (2)$$

and calculated the fraction of $D\bar{D}$ double muonic decays which satisfy our trigger requirement, give 2 μ's that pass the muon cuts, and yield a measured missing energy in excess of 45 GeV. Here the kinematic variables in the above cross-section equation refer to the composite $D\bar{D}$ system (and $\sqrt{s}$=27.4). The acceptance was rather insensitive (to ±30%) to variations in α between 1.5 and 3.0 GeV^{-1} and γ between 0.0 and 17.5. For α=2.23, β=2.96 and γ=14.9 we obtain an acceptance of 0.39% yielding a charm cross-section of 8±3 μb. Using this same model we obtain a charm cross-section of 24±5 μb from the single muon data. Changing β from 2.96 to 6.0 changes the $\mu^+\mu^-$ acceptance from 0.39% to 0.24%. In general, the 2μ with missing energy data yield lower cross-sections than the prompt single muon data. We are presently investigating various distributions that will bring the two sets of data into better agreement, and still fit the measured distributions. (For example, making β larger appears to help.) Besides finding better parameters, we are investigating whether we are using an improper production mechanism, e.g. improper correlation between the D and $\bar{D}$ state, the possibility of different branching ratios for the charge and neutral states, a possible contribution from charmed baryon production etc. Until these model uncertainties are resolved by more fits to the experimental distributions, charm cross sections between 7 to 70 μb are consistent with the data. Also, the next run of Fermilab experiment[14] E595, which measures prompt single muons over a larger kinematic range, will help resolve the model uncertainties.

REFERENCES

1) C.Carlson and R.Suaya, SLAC-PUB-2212 (1978); and J.Babcock, D.Sivers, S.Wolfram, Phys. Rev. D18, 162 (1978); B.W.Lee, M.K.Gaillard, J.L.Rosner, Rev. Mod. Phys. 47, 277 (1975).

2) H.Kasha et al., Phys. Rev. Lett. 36, 1007 (1976); M.J.Lauterbach, Phys. Rev. D17, 2507 (1978).

3) C.Coremans-Bertrand et al., Phys. Lett. 65B, 480 (1976); also see D.Crennel et al., Phys. Lett. 78B, 171 (1978) and W.Bozzoli et al., Lett. al Nuovo Cimento 19,32 (1977).

4) W.Ditzler et al., Phys. Lett. 71B, 451 (1977); D.Spelbring et al., Phys. Rev. Lett. 40, 605 (1978).

5) D.Drijard et al., Phys. Lett. 81B, 250 (1979); other relevant ISR results include A.G.Clark et al., Phys. Lett. 77B, 339 (1978); and J.C.Alder et al., Phys. Lett. 66B, 401 (1977).

6) P.Alibran et al., Phys. Lett. 74B, 134 (1978); T. Hansl et al., Phys. Lett. 74B, 139 (1978); P.C.Bosetti et al., Phys. Lett. 74B, 143 (1978).

7) H.Wachsmuth, CERN/EP/PHYS 78-29 (presented at Topical Conference on Neutrino Physics, Oxford, England, July (1978)).

8) F.W.Busser et al., Phys. Lett. 53B, 212 (1974).

9) J.G.Branson et al., Phys. Rev. Lett. 37, 803 (1976).

10) J.P.Dishaw et al., (this experiment)--SLAC-PUB-2291 (March 1979), to be published in Physics Letters.

11) E.J.Siskind et al., (this experiment)--CALT-68-665 (March 1979), submitted to Physical Review D.

12) Recent measurements of downstream decays, using a similar trigger in a modified version (Fermilab E595) of this experiment, have confirmed this Monte-Carlo estimate.

13) We have used a total inelastic p-Fe cross section of 690 mb which is 12.4 mb/nucleon (A.S.Carrol et al., Phys. Lett. 80B, 319 (1979).

14) Caltech-Fermilab-Rochester-Stanford Collaboration.

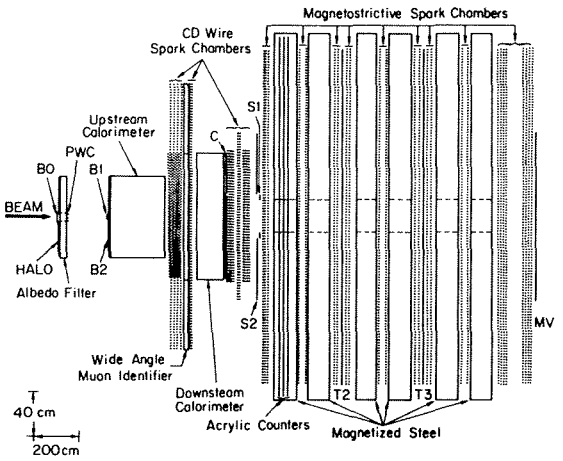

FIGURE 1

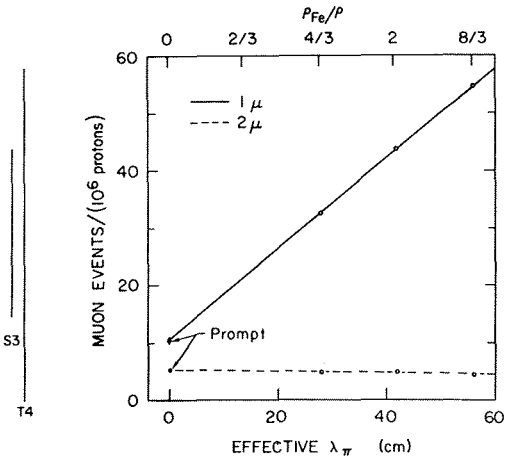

FIGURE 2

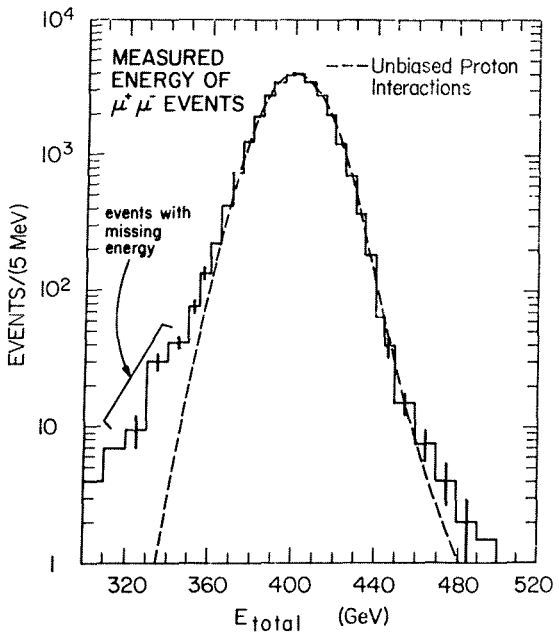

FIGURE 3

FIGURE CAPTIONS

1. The experimental setup.
2. The raw 1μ and 2μ experimental rates per 10^6 protons versus inverse density. After background subtractions the prompt 1μ and 2μ rates are equal.
3. The number of $\mu^+\mu^-$ events versus the total observed energy ($E_{total}=E_{\mu^+}+E_{\mu^-}+E_{calorimeter}$).

QUANTUM NUMBER EFFECTS IN EVENTS WITH A CHARGED PARTICLE AT LARGE TRANSVERSE MOMENTUM

(CHARGE CORRELATIONS IN JETS)

D. Wegener,
University of Dortmund*, Germany
(CCHK Collaboration)

ABSTRACT

Charge correlations of particles in an event with a large p_t trigger particle have been measured. The correlation length for the charge compensation of the hard scattered parton fragments is the same as observed in nondiffractive inelastic events. Part of the charge of the large p_t trigger particle is compensated by the soft particles of the "away jet". For the spectator fragments the same charge correlation distributions are observed as for nondiffractive inelastic events.

§ 1 INTRODUCTION

We present experimental results on charge correlations between particles produced in an event with a large p_t trigger [1,2]. By the application of proper cuts we try to study separately the charge compensation for particles of each of the four jets ("trigger jet", "away jet", "spectator jets") which occur in a large p_t event[3,4]. The measured distributions are compared with the corresponding ones observed in nondiffractive inelastic events [2,5].

The analysis is based on a sample of events with a positive or a negative large p_t trigger particle ($\langle p_T \rangle$ = 2.5 GeV/c) produced at a polar angle of $\langle \theta_\tau \rangle \approx 45^o$ [4,6]. The measurements have been performed at a center of mass energy of $\sqrt{s}$ = 52.5 GeV at the CERN-ISR with the Split-Field-Magnet (SFM) facility.

§ 2 DEFINITION OF EXPERIMENTAL QUANTITIES

To study the dynamics of the charge compensation process in large p_t reactions, we select a particle from one of the four jets and determine the "associated" (conditional) density of particle number and charge. These "associated" densities are obtained by selecting a particle h_2 from one of the four jets in a phase space interval around $\vec{p}_2$ and then evaluate the density of interest for the particles h_1 in the phase space interval around $\vec{p}_1$ for the rest of the event. The "associated particle density" is the density of particles of charge Q_1 at rapidity y_1, conditional to the observation of a particle at y_2 with the charge Q_2:

$$\rho^{Q_1Q_2}(y_1|y_2) = \frac{\rho^{Q_1Q_2}(y_1,y_2)}{\rho^{Q_2}(y_2)} \qquad (1)$$

ρ^{Q_1} and $\rho^{Q_1Q_2}$ are the single-particle and two particle densities respectively.

The "associated net charge density" is given by

$$q(y_1|Q_2,y_2) = \rho^{+Q_2}(y_1|y_2) - \rho^{-Q_2}(y_1|y_2) \qquad (2)$$

To study the charge compensation, we use the "associated charge density balance"

$$\Delta q(y_1|y_2) = q(y_1|-,y_2) - q(y_1|+,y_2) \qquad (3)$$

i.e. the change of the "associated charge density" at y_1, when the charge at y_2 is changed from negative to positive. This quantity allows to select the charge density distribution of these particles, which compensate the charge of the selected particle h_2.[1)]

§ 3 EXPERIMENTAL RESULTS

1. "CHARGE DENSITY BALANCE" ASSOCIATED WITH THE TRIGGER PARTICLE

The "associated charge density balance" Δq is shown in fig.1 as a function of y_1 for the case that the trigger particle of the large p_t event istaken as the selected particle h_2. The data are compared with Δq as measured in nondiffractive inelastic events.[2,5)] Both distributions show a sharp peak in the rapidity interval of the selected particle and coincide in the peak region, which is a clear indication of a strong local component contributing to the charge compensation. Moreover an indication for a weaker global charge compensation component exists for the large p_t event.

To separate the contributions of the four jets to the charge compensation of the large p_t trigger particle at (y_T, p_T, ϕ_T), fig.2 shows the dependence of Δq on the rapidity y and the azimuthal angle ϕ of the additional particles for two event configurations. They differ by the rapidity of the "away jet", fixed in phase space by its leading particle. As the leading particle of the "away jet" we choose that particle in the "away region" ($\phi = \langle\phi_T\rangle + 180^o \pm 30^o$) with the highest transverse momentum, which has to exceed 0.6 GeV/c, in order to reduce the chance of misidentification. In the upper part of fig. 2 Δq is plotted for these configurations, where the "trigger jet" and the "away jet" are in the same y-interval ("back to antiback" configuration), while in the lower part of fig.2 the rapidity difference between the "trigger jet" and the "away jet" is large ("back to back" configuration).

For both event configurations a peak of Δq is observed in the azimuthal angular interval of the trigger particle ($\phi \approx \langle\phi_T\rangle$), whose position in y is independent of the rapidity of the "away jet". This result demonstrates that part of the trigger charge is compensated by

low p_t particles of the "trigger jet" in agreement with observation of ref.4).

A peak of Δq in the azimuthal angular region opposite to the trigger particle ($\phi = \langle\phi_\tau\rangle + 180^o$) is also observed for both event configurations, but in contrast to the peak in the ϕ-interval of the trigger its position in rapidity follows that of the "away jet". This proves that part of the trigger charge is compensated by particles belonging to the "away jet". Since the charges of the leading particles in the "trigger jet" and in the "away jet" are uncorrelated [2,3], the observed charge flow between the "trigger jet" and the "away jet" is due to low p_t particles of the latter.

In addition to the two peaks of Δq already discussed, a flat contribution in ϕ shows up in fig.2, which is independent of y in a broad interval. This global component can be attributed to a charge flow between the "trigger jet" and the "spectator jets".

The observed three components contributing to the charge compensation of the trigger particle are in qualitative agreement with the expectations of the quark parton model [7]. From the investigation of the charge compensation of the leading particle in the "away jet" similar conclusions can be drawn as for the "trigger jet"[1].

2. "CHARGE DENSITY BALANCE" ASSOCIATED WITH A PARTICLE FROM THE "SPECTATOR JET"

To minimize the perturbation due to fragments from the "trigger jet" and the "away jet" in the study of the "spectator jet" fragmentation, only events have been analysed, where the "trigger jet" and the "away jet" are in a "back to antiback" configuration at $y < -0.7$. The selected particles of the "spectator jet" are localized at $y_2 > 0.5$.

For two intervals y_2 of the selected particle from the "spectator jet" Δq is plotted as function of y_1 in fig.3. The corresponding distributions for nondiffractive inelastic events, which have a selected particle in the same y_2 intervals, are included. The two distributions peak in the region of the selected particle and coincide in a wide rapidity region.

From this coincidence follows that for both event types the fragmentation of the corresponding parton is similar as far as charge compensation is concerned. In the case of the nondiffractive inelastic event it has been shown that a local compensation process dominates [2,5], which seems hold also for the "spectator jet" fragmentation. In addition the quark content of the two fragmenting systems is different [1,6], hence it follows from the present analysis that the adjustment of charges between the observed hadrons and the corresponding partons does not depend on the quark content of the fragmenting system.

§ 4 CONCLUSION

It is shown that local charge compensation dominates the fragmentation of the four jets of a large p_t event. The observed charge correlation length is the same as measured in nondiffractive inelastic events and in this sense is universal[8]. In addition a charge flow is observal between the different jets as expected in the framework of the quark parton model.

REFERENCES

* Work, supportet by the Bundesministerium für Forschung und Technologie, Bonn

1) CCHK Collaboration, D.Drijard et al., Paper 210

2) W.Hofmann, PhD thesis, Karlsruhe 1977 and report KfK 2489

3) R.P.Feynman et al.,Nucl.Phys.B.128 (1977) 1

4) CCHK Collaboration, D.Drijard et al., Nucl.Phys. B127 (1977) 1

5) CCHK Collaboration, D.Drijard et al., CERN/EP/PHYS 78-13 Nucl.Phys.B (in print)

6) CCHK Collaboration, D.Drijard et al., CERN/EP/PHYS 78-14 Rev. Nucl.Phys.B (in print)

7) P.Hoyer et al., Nordita 78/42

8) H.Satz, Nuovo Cim. 37A (1977) 141

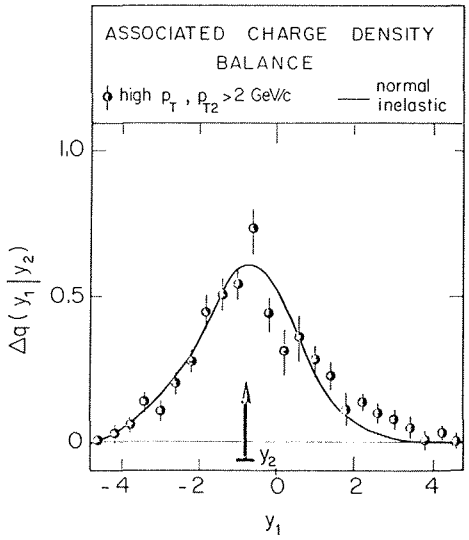

Fig. 1

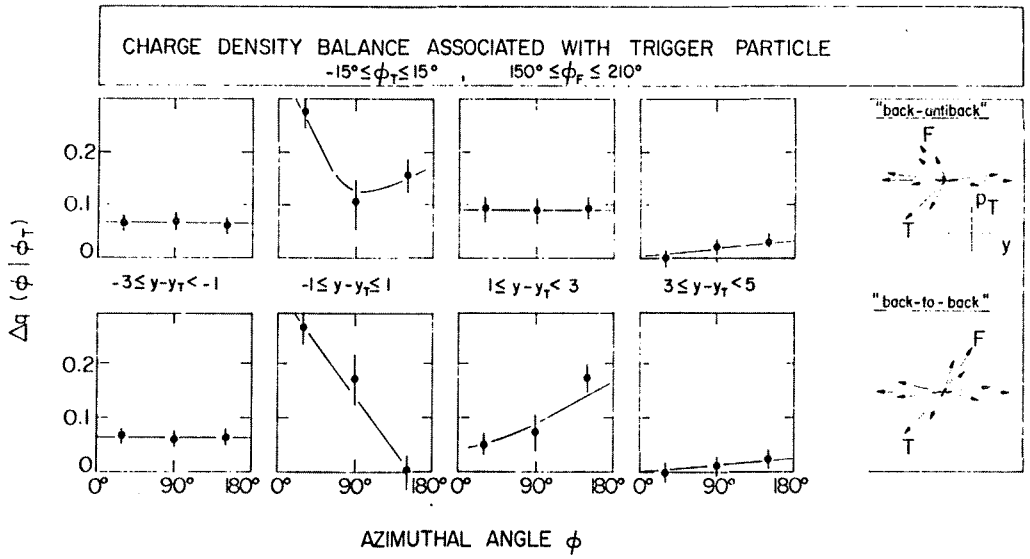

Fig. 2

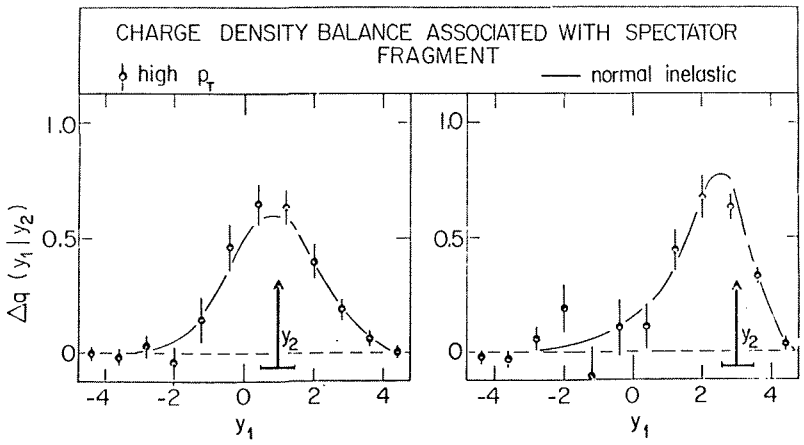

Fig. 3

$K^{*o}(890)$ POLARIZATION MEASUREMENTS IN THE HYPERCHARGE EXCHANGE REACTION $\pi^-p\to K^{*o}(890)\Lambda^\circ/\Sigma^\circ$ AT 10 GeV/c

Bari-Bonn-CERN-Daresbury-Glasgow-Liverpool-Milano-Vienna Collaboration.
Armstrong,Best,Bröring,Cluskey,Costa,Donald,D.N.Edwards,M.Edwards,Evangelista,French,Ghidini,Gordon,Houlden,Hughes,Lewis,Mandelli,Mättig,Miller,Mitaroff,Müller,Palano,Palazzi-Cerrina,Paul,Pensotti,Perini,Picciarelli,Pregernig,Rühmer,Strub,Thompson,Turnbull,Woodworth,Zito.

ABSTRACT

$K^{*o}(890)$ production in the hypercharge exchange reaction $\pi^-p\to K^{*o}(890)\Lambda^\circ/\Sigma^\circ$ at 10 GeV/c (28448 events) is discussed. An amplitude analysis in the t' range up to 1 GeV^2 shows that the production mechanism is dominated by Natural Parity Exchange (~84%). Comparisons are made with predictions from a Regge model and a quark model.

In this paper we present results on $K^{*o}(890)$ production in the reaction

$$\pi^-p\to K^{*o}(890)\ \Lambda^\circ/\Sigma^\circ \tag{1}$$

at 10 GeV/c. In particular, the K^{*o} polarization measurements have allowed a detailed amplitude analysis of reaction (1).

The data come from an experiment performed with the OMEGA Spectrometer[1] at the CERN PS. The apparatus was triggered by a forward going K^+ in the momentum range 4.9 to 9.8 GeV/c, selected by means of two Cerenkov counters (HPC,LPC) and scintillation counter hodoscopes (A,H1,H2). The trigger conditions are described in detail in Ref.(2).

A total of 1.1 million triggers of the type

$$\pi^-p\to K^+\ X^- \tag{2}$$

corresponding to a beam flux sensitivity of 10.5 events/nb was collected and then processed through modified versions of the pattern recognition and geometry program ROMEO[3] and the kinematics program KOMEGA[4].

The reaction

$$\pi^-p\to K^+\ \pi^-\ \Lambda^\circ/\Sigma^\circ \tag{3}$$

has been isolated by selecting the missing mass squared to the $(K^+\pi^-)$ system ($MM^2(K^+\pi^-)$) between 1.08 and 1.56 GeV^2 corresponding to the unresolved $\Lambda^\circ/\Sigma^\circ$ peak seen in Fig.1a. This procedure allows the $\Lambda^\circ/\Sigma^\circ$ to be considered irrespective of their charged or neutral decay. The $(K^+\pi^-)$ effective mass ($M(K^+\pi^-)$) distribution, shown in Fig.1b, is dominated by the $K^*(890)$ and $K^*(1420)$. Defining the $K^{*o}(890)$ in the $M(K^+\pi^-)$ range (0.84-0.96) GeV, we obtained a final sample of $K^{*o}\ \Lambda^\circ/\Sigma^\circ$ consisting of 28448 events. Fig.1c and 1d show respectively the missing mass squared to the K^{*o} and the $(K^+\pi^-)$ effective mass associated with the $\Lambda^\circ/\Sigma^\circ$.

Contamination from competing channels, the most important of which is

$$\pi^-p\to K^+K^-n \tag{4}$$

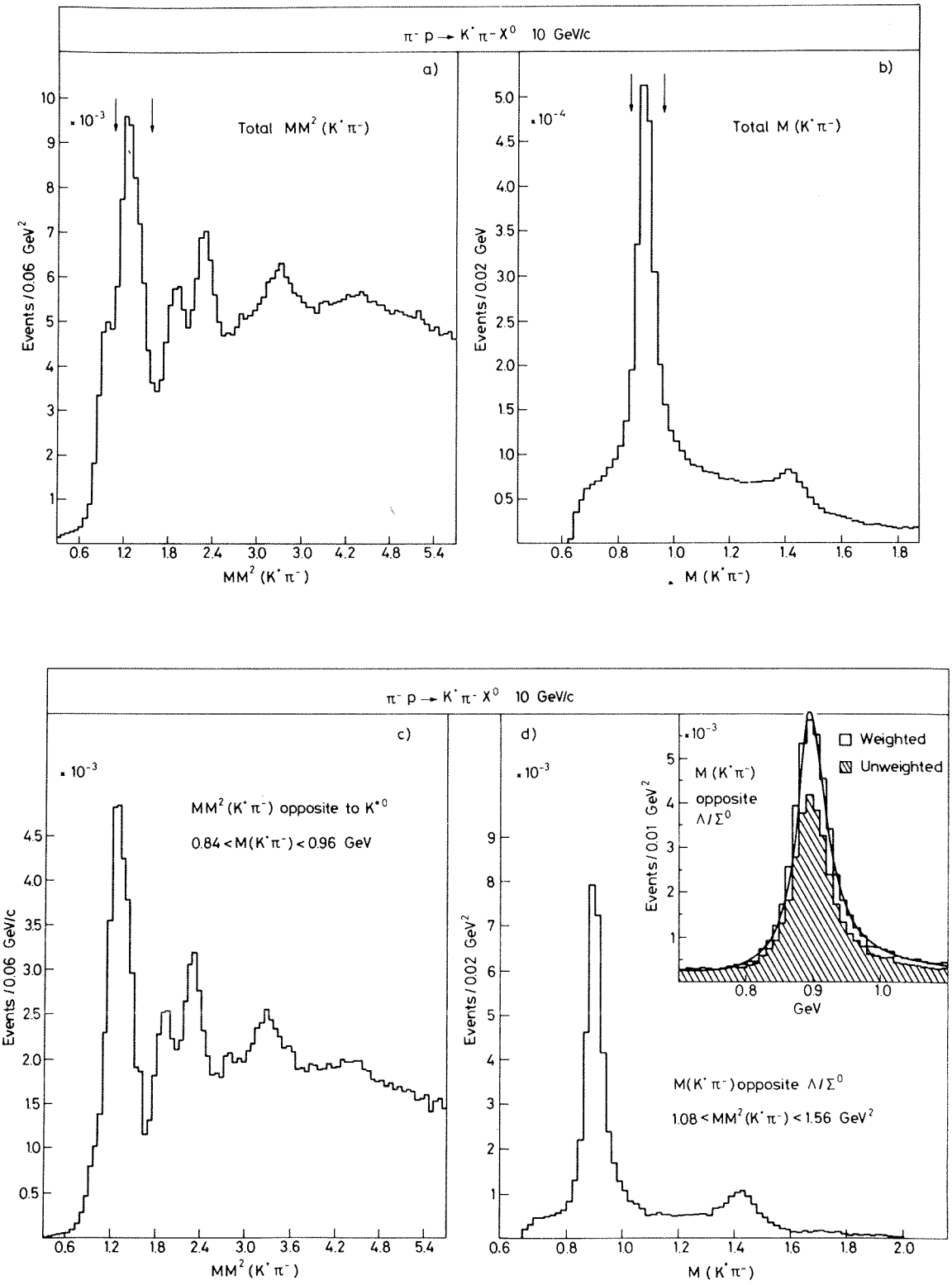

Fig. 1 Distributions of a) Missing mass squared to the $(K^+\pi^-)$ system (unweighted) b) Effective mass of the $(K^+\pi^-)$ system (unweighted) c) Missing mass squared to $(K^+\pi^-)$ for events with $0.84 < M(K^+\pi^-) < 0.96$ GeV (unweighted) d) Effective mass $M(K^+\pi^-)$ (unweighted) for events with a missing mass squared in the $\Lambda^\circ/\Sigma^\circ$ region (1.08-1.56 GeV^2). The region centred around the $K^{*0}(890)$ is shown in the inset. The curve superposed on the weighted distribution corresponds to the fit described in the text. The arrows indicate the cuts used to define the channel $K^{*0}\Lambda^\circ/\Sigma^\circ$.

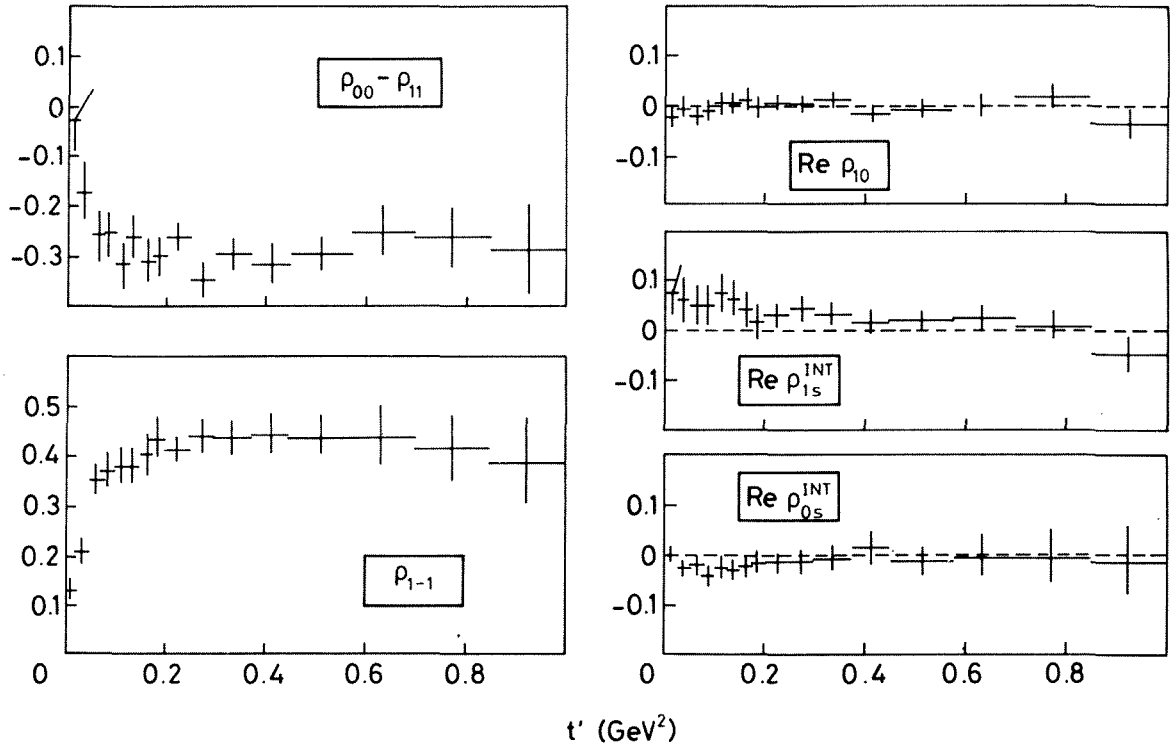

Fig. 2 Density matrix elements of the K^{*o} evaluated in the Gottfried-Jackson system as a function of t'.

cannot be avoided by this method. For the $K^{*o}(890)$ $\Lambda^\circ/\Sigma^\circ$ events the contamination varied from ~5% in the lowest t' interval to less than 1% for t'>0.1 GeV^2*. All events were also weighted to take into account the trigger geometrical acceptance and the losses due to the detecting system and reconstruction program. The fully weighted $(K^+\pi^-)$ mass spectrum for reaction (3) is shown in Fig.1d in the (0.7-1.1) GeV mass range (see inset).

The K^{*o} production and decay has been described in terms of the spin density matrix elements evaluated in the Gottfried-Jackson frame. Due to the existence of zero-acceptance regions ("holes") in the $(\cos\theta-\Phi)$ plane, we have used the linear algebra method[5] to fit the angular distributions. Since a fit to the $K^+\pi^-$ effective mass spectrum (see below) requires some background in addition to the P-wave Breit-Wigner in the $K^{*o}(890)$ region, we have attempted to describe the angular distributions by introducing a coherent S-wave. A good fit was obtained. The resulting density matrix elements (ρ_{ij}) are displayed in Fig.2 as a function of t' .

For an understanding of the production mechanism it is convenient to express the density matrix elements in terms of the actual wave amplitudes, namely S_o, P_o, P_+, P_-. Here S_o and P_o describe the contributions due to helicity-zero production in the K^{*o} mass region while, to leading order in energy, P_+ describes the helicity-one production by natural exchange (NPE) and P_- the production by unnatural parity exchange (UPE).

---

*) $t' = |t - t_{min}|$ where t is the four momentum transfer squared between the incident π^- and the $(K^+\pi^-)$ system.

Since no information is available on the $\Lambda^\circ/\Sigma^\circ$ polarization in this experiment, each amplitude is an incoherent sum over helicity-flip and non-flip at the nucleon vertex. The following formulae relate the measured parameters to the amplitudes[6].

$$\frac{d\sigma}{dt'} = |S_o|^2 + (|P_o|^2 + |P_+|^2 + |P_-|^2) \tag{5}$$

$$\frac{d\sigma}{dt'} (\rho_{oo}-\rho_{11}) = |P_o|^2 - \frac{1}{2}(|P_+|^2 + |P_-|^2) \tag{6}$$

$$\frac{d\sigma}{dt'} \rho_{1-1} = \frac{1}{2}(|P_+|^2 - |P_-|^2) \tag{7}$$

$$\frac{d\sigma}{dt'} \mathrm{Re}\rho_{10} = \frac{1}{\sqrt{2}} |P_o|\,|P_-|\,(\xi\cos\Psi)_{P_oP_-} \tag{8}$$

$$\frac{d\sigma}{dt'} \mathrm{Re}\rho_{os}^{INT} = |S_o|\,|P_o|\,(\xi\cos\Psi)_{S_oP_o} \tag{9}$$

$$\frac{d\sigma}{dt'} \mathrm{Re}\rho_{1s}^{INT} = \frac{1}{\sqrt{2}} |S_o|\,|P_-|\,(\xi\cos\Psi)_{S_oP_-} \tag{10}$$

where ξ is the degree of spin coherence at the nucleon vertex ($0 \leq \xi \leq 1$) and Ψ the relative phase between the amplitudes. From these formulae and the measured ρ_{ij}'s we find that:

i) NPE is the dominant mechanism since $(\rho_{oo}-\rho_{11})$ is large and negative and ρ_{1-1} is large and positive (see formulae (6) and (7)).

ii) For $t' < 0.05$ GeV^2 a significant UPE contribution is also present since $(\rho_{oo}-\rho_{11})$ and ρ_{1-1} are both small.

iii) For all t' values the interference terms are nearly zero, implying UPE amplitudes either out of phase ($\cos\Psi=0$) or vanishing, or complete incoherence ($\xi=0$).

Because of iii), our analysis is confined to the evaluation of the four amplitude moduli by means of the first three equations only. To solve the system unambiguously another independent measurement is needed. This can be provided by the mass distributions. On the basis of zero S-P interference in the K^{*o} region we assumed that the observed $K\pi$ mass spectrum could be described by a formula[7] of the type.

$$\frac{d\sigma}{dm_{K\pi}} = \varepsilon_S |M_S|^2 + (1-\varepsilon_S)\,|M_P|^2 \tag{11}$$

where M_S, M_P represent the mass dependent S- and P-wave amplitudes, assumed as an S-wave linear background and a P-wave relativistic Breit-Wigner function in the range (0.7-1.1) GeV, and ε_S measures the relative amount of S-wave. By fitting formula (11) to the total mass spectrum we obtained the curve drawn on Fig.1d with M_{K^*} = (0.897±0.001) GeV and Γ_{K^*} = (0.054±0.002) GeV. To obtain the amount of S-wave background as a function of t' the above formula was fitted to the $M(K^+\pi^-)$ distribution in each t' interval, keeping the mass and width fixed at the same values. These S-wave background events represent <10% of the total events in all t' intervals except for the two lowest where it rises to 30%.

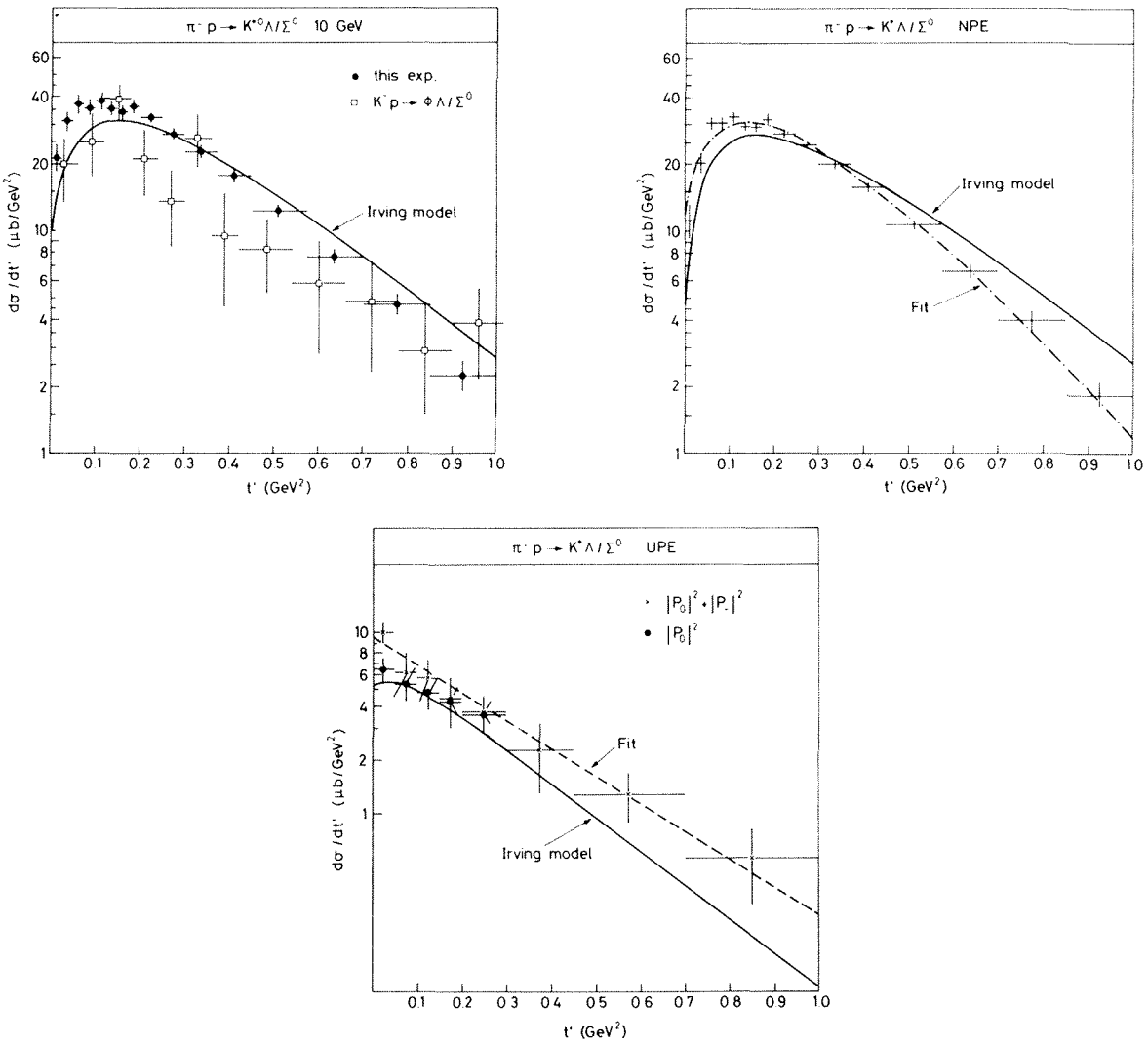

Fig. 3 a) $d\sigma/dt'$ distribution for K^{*o} production. Data from the reaction $K^-p \to \phi\,\Lambda^\circ/\Sigma^\circ$ at 10 GeV/c are also shown. The Irving model prediction is shown as a continuous line. b) $d\sigma^{NPE}/dt'$ distribution. The dashed curve is the fit discussed in the text. The Irving model prediction is shown as a continuous line. c) $d\sigma^{UPE}/dt'$ distribution. The dashed curve is a simple exponential fit (see text). The continuous line represents the Irving model prediction for the $|P_0|^2 + |P_-|^2$ contributions.

The P-wave amplitudes for different naturalities were then derived from eq.(5)-(7) and corrected to take into account the Breit-Wigner tails and $\Lambda^\circ/\Sigma^\circ$ mass cut. Fig.3a shows the P-wave differential cross section as a function of t'. The NPE part (Fig.3b) is dominant. Most of the UPE contribution (Fig.3c) is due to $|P_o|^2$. The helicity-one part $|P_-|^2$ (not shown) is small every-where and for $t' < 0.3$ GeV^2 compatible with zero.

Another possible approach to determine the moduli of the amplitudes is to fix the $|S_o|/|P_o|$ ratio to the value measured in a ($K\pi$) phase-shift analysis[8]. The results obtained in this way are similar to those displayed in Fig.3.

The NPE and UPE differential cross sections of Fig.4b and Fig.4c are different in shape and cannot be described by the same parametrization. The NPE part was fitted with the formula:

$$\frac{d\sigma^{NPE}}{dt'} = C(A+t')\ e^{-Bt'} \qquad (12)$$

and gave the following set of values: C = (431 ± 25) μb/GeV^4, A = (0.023 0.005) GeV^2 and B = (5.9±0.1) GeV^{-2} with a χ^2 per degree of freedom χ^2/ND=15.5/13. The fit is shown as a dashed line in Fig.3b. In (12) the purely exponential term corresponds approximately to the contribution of the zero net helicity flip. From the fit result we estimate that ~ 90% of the NPE term over the whole t' range (t'<1 GeV^2) is due to net helicity flip. To fit the UPE distribution a simple exponential was used, giving a slope B = (3.6±0.4) GeV^{-2} with χ^2/ND = 2.3/6.

The integrated cross sections for $K^{*o}(890)$ production corresponding to the various exchange terms, together with the results of similar studies at lower energies[9,10] are displayed in Fig.4. Comparing these sets of data we observe an increase of the NPE contribution from ~58% at low energy to ~85% at 10 GeV/c and corresponding decreases of the UPE helicity-zero (σ_o^{UPE}) from ~25% to ~14% and UPE helicity-one ($\sigma_{|1|}^{UPE}$) from ~17% to ~1%.

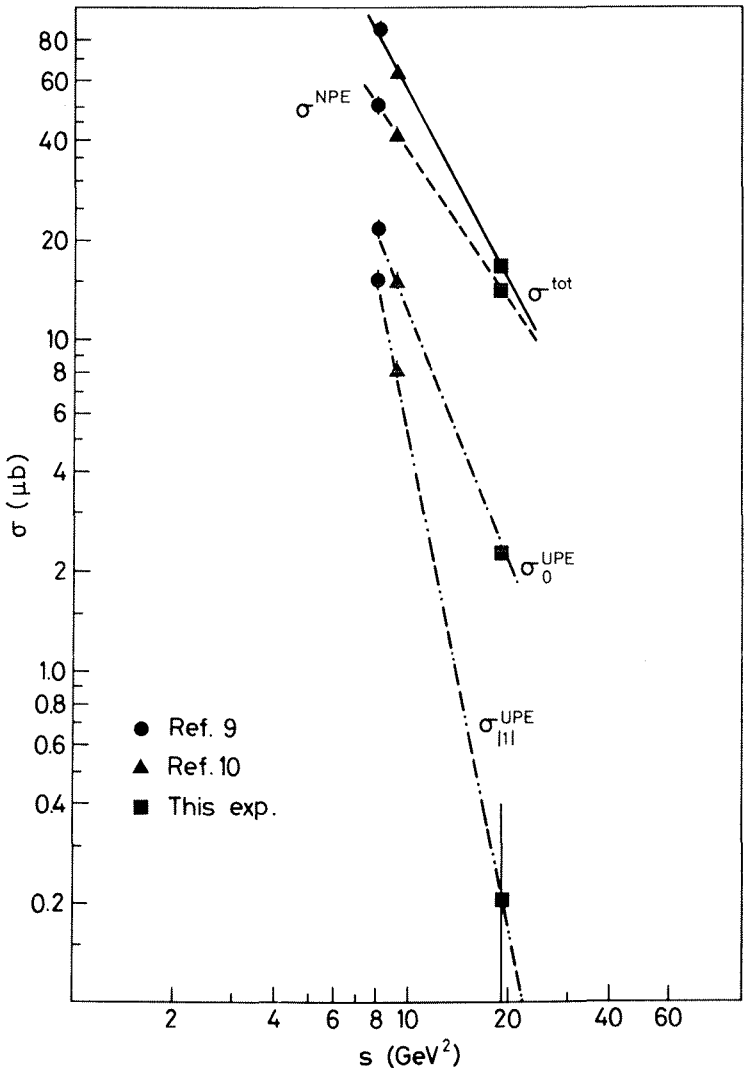

Fig. 4 Total and partial cross sections for the reaction $\pi^- p \to K^{*o} \Lambda^o/\Sigma^o$ for $t' < 1$ GeV^2 as a function of the center of mass energy squared. The lines correspond to the fits discussed in the text.

The various contributions were fitted with the formula $\sigma \propto s^n$, the values obtained for n being quoted in Fig.4 and the corresponding curves being drawn in Fig.4. Using the relation $n=2\alpha(o)-2$ we find $\alpha^{NPE}=(.25\pm.05)$ and $\alpha_o^{UPE} = (-0.3\pm.1)$ which may be compared with the values[11] of 0.35 for degenerate $K^*(890)/K^*(1420)$ trajectory exchange and -.223 for K trajectory exchange respectively.

The experimental results on reaction (1) can be compared with the prediction of a Regge model developed by Irving[11]. The full line curves drawn in Fig.3 represent the predictions of the model for the differential cross sections.

Independently of the exchange mechanism, both the quark model[12] and SU(3) plus factorization[13] require reaction (1) to have the same characteristics as the reaction

$$K^-p \to \phi \Lambda^\circ/\Sigma^\circ \qquad (13)$$

Good agreement has been found at low energy[9,13]. A previous paper[2] from this experiment presented results on reaction (13). The differential cross sections for the reactions (1) and (13) are compatible in shape (Fig.3a). The total cross sections for the two reactions differ by 2.5s.d. which accounts for the systematically lower values of $\frac{d\sigma}{dt'}$ for reaction (13). The limited statistics on reaction (13) prevents a more detailed comparison of the various exchange contributions.

To summarize, from the $K^{*o}(890)$ polarization measurement the following properties of reaction (1) have been deduced:

i) Natural Parity Exchange is the dominant production mechanism (~84% of the total). Most of it is accounted for by net helicity flip (~90%);

ii) the Unnatural Parity Exchange contribution is mainly associated with the $K^{*o}(890)$ helicity zero state;

iii) the density matrix elements representing interference between various UPE contributions are nearly zero for all values of t';

iv) K^{*o} production is reasonably described by the Regge model of Irving, and agreement with the prediction of the quark model and SU(3) is found in comparing reactions (1) and (13).

REFERENCES

1) O.Gildemeister, Int.Conf. on Instrumentation for High Energy Physics, Frascati (1973).

2) C.Evangelista et al., Nucl.Phys. B 127 (1977) 384.

3) F.Bourgeois et al., Pattern recognition methods for OMEGA and SFM spark chamber experiments, CERN report DD/DH/70-13. CERN ROMEO Users Manual.

4) CERN HYDRA Application Library.

5) G.Grayer et al., Nucl.Phys. B 75 (1974) 189.

6) P.Estabrooks et al., Nucl.Phys. B 106 (1976) 61.

7) M.Aguilar-Benitez et al., Phy.Rev. D6 (1972) 11.

8) P.Estabrooks et al., Nucl.Phys. B 113 (1978) 490.

9) D.Yaffe et al., Nucl.Phys. B 75 (1974) 365.

10) D.J.Crennel et al., Phys.Rev. D 6 (1972) 1220.

11) A.C.Irving and R.P.Worden, Physics Reports 34 (1977) 117.

12) A.Bialas and K.Zalewski, Nucl.Phys. B 6 (1968) 465.

11) M.Aguilar-Benitez et al., Phys.Rev.Lett. 28 (1972) 574.

SCALING AND THE VIOLATION OF SCALING

Ning Hu

Department of Physics, Peking University
Institute of Theoretical Physics, Academia Sinica

ABSTRACT

It is shown that the asymptotic freedom is not relevant in order to obtain scaling for the deep inelastic scattering process. By assuming that the quarks perform simple harmonic oscillations inside the hadron, reasonable pion and nucleon structure functions can be obtained.

We consider the deep inelastic scattering of the electron by the hadron. Choose the coordinate system in which the momenta P and q of the hadron and the virtual photon emitted by the electron satisfy the condition q = - P. In the following all momenta are understood as their components along the direction of P unless other wise indicated. The Feynman diagram of the process is shown in Fig. 1. The corresponding transition matrix element is

$$\langle k_1 k_2 \cdots k_n | M | Pq \rangle = \sum_m \sum_{p_i} \langle k_1 k_2 \cdots k_n | V_2 | p_1+q, p_2, \cdots p_m \rangle \frac{1}{P_0+q_0-E_1'-E_2-\cdots-E_m}$$

$$\langle p_1+q | J_\perp | p_1 \rangle \frac{1}{P_0-E_1-E_2-\cdots-E_m} \langle p_1 p_2 \cdots p_m | V_1 | P \rangle \qquad (1)$$

where $E_i = (p_i^2 + M_i^2)^{1/2}$ is the energy of the parton i, $E_1' = ((p_1+q)^2+M_1^2)^{1/2}$. V_1 and V_2 represent the effective vertex functions correspond to the shadowed parts in Fig. 1. They are closely related to the wave functions of the hadron states. No creation or annihilation of quark pairs by the virtual photon is considered, since they can be shown to be small. Write $p_i = x_i P$ with $0 \le x_i \le 1$ and $\sum_i x_i = 1$. When P is very large we have approximately $P_0 = P$, $E_i = x_i P + \mu_i^2/2x_i P$, $\mu_i^2 = p_i^2 + M_i^2$ and $E_1' = -(x_1 P + q) - \mu_1^2/(2x_1 P + q)$. The negative sign on the right side of the last expression arises from the fact that $x_1 P + q$ is negative. We have

$$(P_0 - E_1 - E_2 - \cdots - E_m)^{-1} \approx P / \sum_{i=1}^{m} x_i \mu_i^2 \qquad (2)$$

$$(P_0 + q_0 - E_1' - E_2 - \cdots - E_m)^{-1} \approx \left(2x_1 P + q_0 + q + \frac{1}{P}\sum_{i=2}^{m} \frac{\mu_i^2}{2x_i} + \frac{\mu_1^2}{2x_1 P + q}\right)^{-1} \qquad (3)$$

(2) and (3) are just the two energy denominators of (1). (2) is of the order P. (3) will also be of the order P if the following condition is satisfied:

$$2x_1 P + q_0 + q = 0. \qquad (4)$$

This may then be written in the following form

$$Q^2 + 2x_1 P_\mu q_\mu = (q - q_0)(2x_1 P + q_0 + q) = 0. \qquad (5)$$

which is just the elastic scattering condition of the electron by the parton.

The above derivation is valid when $\mu_i^2 \ll P$. We shall consider first the case of deep inelastic scattering of the pion. (3) and the vertex function V_2 represent the final state interaction. The vertex function $V_1(x_1, x_2)$ corresponds to the distribution function in the parton picture. In the usual treatment the distribution function is left undetermined by the theory. We shall assume that the motion of quarks inside the hadrons is the simple harmonic

oscillation. This certainly is consistent with the mass spectra of the hadrons given by the formula [1] $M^2 = -M_0^2 + \lambda(\frac{3}{2} + \ell + 2n)$ where $\lambda \cong 1$ GeV^2, n and ℓ are respectively the principle and orbital quantum numbers. We may consider the particle x_1 as the quark (or anti-quark) which will absorb the virtual photon later on, and the particle x_2 as the remaining part of the pion which contains the anti-quark (or quark) together with gluons and sea quarks. The vertex function V_1 of the pion may then be given by

$$V_1 = \gamma_5 f_1(x_1, x_2) = \gamma_5 \exp\{-4\lambda p_\perp^2 - \lambda(x_1 - x_2)^2 M_\pi^2 c^2\} \tag{6}$$

where $f_1(x_1, x_2)$ is the boosted ground state wave function of the simple harmonic oscillator. After the virtual photon is absorbed, the momentum p_1 of particle 1 will become $p_1' = p_1 + q = -(1 - x_1)P$, which is equal and opposite to p_2 of the particle 2. The final state may then be considered as a highly excited one-dimensional oscillator in its rest system, since the oscillation in the transverse direction perpendicular to P becomes now unimportant. At the moment when this excited oscillator is formed, the kinetic energy takes the maximum value and the potential energy is zero. As time increases, the quark and the anti-quark will move away from each other, at the same time the kinetic energy will transform into the potential energy. When the potential energy is large enough to create a quark pair, the system will break into two oscillators. This process of breaking into two parts will repeat again and again until the system becomes a large number of oscillators all in the ground states, each of them is then a stable hadron. Since the excitation must be very high when P is very large, the one-dimensional excited oscillator may be treated classically. The vertex function V_2 may then be approximated by the following expression:

$$V_2 \approx \gamma_5 [(1 - x_1)\delta]^{-1/4} \tag{7}$$

This result is obtained by taking the square root of the probability of finding this classical oscillator at the maximum kinetic energy just when the oscillator is formed. However, as a classical oscillator this probability is found to be infinity. So we have to consider the average probability over a small interval δ.

It should be pointed out in passing that one important consequence of considering the quarks as performing simple harmonic oscillations is that the average potential energy is equal to one-half of the total energy. Since the potential energy is stored in the gluon field, this explains the well-known fact that one-half of the energy P_0 belongs to the gluon field. Recent experiments showed also that the distribution of transverse momentum $p_\perp$ in jets produced by deep inelastic scattering is of the Gaussian type [2,3], instead of the exponential type usually observed in jets produced by hadron-hadron collisions. This may be considered as another evidence that the quarks inside the hadrons do perform the simple harmonic oscillations. The deviation from the Gaussian distribution for jets produced by hadron-hadron collisions may be explained by the fact that gluons also take part in the interaction. The final expression for the pion structure function is finally given by

$$F_2^\pi(x) \sim \sum_i Q_i^2 x(1 - x)^{1/2} \exp\{-2\lambda(2x - 1)^2 M_\pi^2 c^2\} \tag{8}$$

When the hadron in the initial state is a nucleon, V_1 is then given by (6), with the pion mass M_π replaced by the nucleon mass M_N. p_1 represents the quark which will absorb the virtual photon as before, but $p_2 = x_2 P$ now represents the boson containing the remaining part of the nucleon. We assume that this boson has the same quantum numbers as a pion-like state formed by a nucleon and an anti-quark, so V_1 also contains a matrix γ_5. The structure function obtained for the nucleon by similar calculations is

$$F_2^N(x) \sim \sum_i Q_i^2 x(1-x)^{7/2} \exp\{-2\lambda(2x-1)^2 M_N^2 c^2\} \qquad (9)$$

The structure functions $F_2^N(x)$ and $F_2^\pi(x)$ are plotted in Figs. 2 and 3. The dashed curve represents the well-known function $(1-x)^3$.

A different curve for $F_2^\pi(x)$ determined experimentally [4] from the process $\pi^- P \to \mu\bar{\mu}$ using Drell-Yans' result[5] that the structure function of the above process is given by the product of the pion and nucleon structure functions. However, this result is true only when the final state interaction can be overlooked. The true picture of the above process will be like this: As soon as the quark and the anti-quark annihilate into a virtual photon, the remaining parts of the two hadrons will integrate into an excited one dimensional oscillator as in the cases considered before. The result of this consideration will be given else where. This provides a new test of QCD or the asymptotic freedom.

We shall now turn to consider the violation of scaling due to the emission of a gluon k of large transverse component $k_\perp$. The corresponding Feynman diagram is shown in Fig 4. The transition matrix element is

$$\langle k_1 k_2 \cdots k_n | M | P q \rangle = \sum_m \sum_{p_i} \langle k_1 k_2 \cdots k_n | V_2 | k, p_1 - k + q, p_2 \cdots p_m \rangle$$
$$\frac{1}{P_0 + q_0 - \varepsilon_0 - E_1'' - E_2 \cdots - E_m} \langle p_1 - k + q | J_\perp | p_1 - k \rangle \frac{1}{P_0 - \varepsilon_0 - E_1' - E_2 \cdots - E_m}$$
$$\langle p_1 - k | J_k | p_1 \rangle \frac{1}{P_0 - E_1 - E_2 \cdots - E_m} \langle p_1 p_2 \cdots p_m | V_1 | P \rangle \qquad (10)$$

where ε_0, E_i, E_1' and E_1'' are energies corresponding to the momenta k, p_i, $p_1 - k$, and $p_1 - k + q$ respectively. Introducing

$$p_i = x_i P, \quad k = (1-z) p_1 = x_1 (1-z) P, \quad 0 \le x_i \le 1, \quad 0 \le z \le 1 \qquad (11)$$

we obtain

$$\varepsilon_0 \approx x_1(1-z)P + k_\perp^2 / 2x_1(1-z)P, \quad E_1 \approx x_1 P + k_\perp^2 / 2x_1 P$$
$$E_1' \approx x_1 z P + k_\perp^2 / 2x_1 z P, \quad E_1'' = -q - x_1 z P - k_\perp^2 / 2(q + x_1 z P) \qquad (12)$$

μ_i^2 being neglected in comparison with $k_\perp^2$. Inserting (12) in the energy denominator of (10), we obtain further

$$(P_0 - E_1 - E_2 \cdots - E_m)^{-1} \approx P / \sum_i \mu_i^2 x_i \qquad (13)$$

$$(P_0 - \varepsilon_0 - E_1' - E_2 - \cdots - E_m)^{-1} \approx P/[\frac{1}{x_1(1-z)} + \frac{1}{x_1 z}]\, k_\perp^2 \qquad (14)$$

$$(P_0 + q_0 - \varepsilon_0 - E_1'' - E_2 - \cdots - E_m)^{-1} \approx [q_0 + q + 2x_1 z P - (\frac{1}{x_1(1-z)} + \frac{1}{(1-x_1 z)})\frac{k_\perp^2}{P}] \qquad (15)$$

(13) and (14) are of the order P. (15) will also be of the order P if the following condition is satisfied

$$q_0 + q + 2x_1 z P - (\frac{1}{x_1(1-z)} + \frac{1}{1-x_1 z})\frac{k_\perp^2}{P} = 0$$

Multiplying by $q - q_c$ as before , we obtain

$$Q^2 + 2x_1 z P_\mu q_\mu - (\frac{1}{x_1(1-z)} + \frac{1}{1-x_1 z})(1-x_1 z)\, k_\perp^2 \cong 0 \qquad (16)$$

The third term represents the deviation from the condition of the elastic scattering condition(5). From (16) we get

$$d[\ln (Q^2 - Q_1^2)] = d(\ln k_\perp^2), \qquad Q_1^2 = 2x z P_\mu q_\mu \qquad (17)$$

which is different from the following result obtained in the usual treatment based on the leading logarithm approximation:

$$d(\ln Q^2) = d(\ln k_\perp^2) \qquad (18)$$

The final equation describing the violation of scaling for the non-singular distribution function $q^{NS}(x)$ is given by

$$\frac{d}{dt} q^{NS}(x,t) = g^2 \int_0^1 \frac{dx_1}{x_1} q^{NS}(x_1,t) P_1(\frac{x}{x_1}), \quad dt = d[\ln (Q^2 - Q_1^2)]$$
$$P_1(z) = \frac{g^2}{16\pi^2}\frac{1}{2} z(1-z) \sum_{spin} \frac{|\bar{u}\Gamma u|^2 x_1}{k_\perp^2}, \qquad (19)$$

When the final state interaction is important, it would be unjustified to consider the gluon k as a free particle with transverse polarizations only, as was done in the usual treatment. As a virtual particle it must have 4 polarimations, or at leat three polarizations if it materializes into a vector meson. With 4 polarizations the same result of scaling violation will be obtained for Yang-Mills gluon as the scalar, pseudo-scalar and vector gluons apart from the different t dependence of the coupling constants.

REFERENCES

1) N. Hu, Scientia Sinica, 22 295 (1979)
2) C. del Papa et al, Phys. Rev. 13D 2934 (1978)
3) B. A. Gordon et al Phys. Rev. Lett. 41 615 (1978)
4) Lederman, 19th International Conf. on High Energy Phys. Tokyo, P-26 (1978)
5) S. D. Drell and T. M. Yan, Ann. of Phys. N. Y. 66 578 (1971)

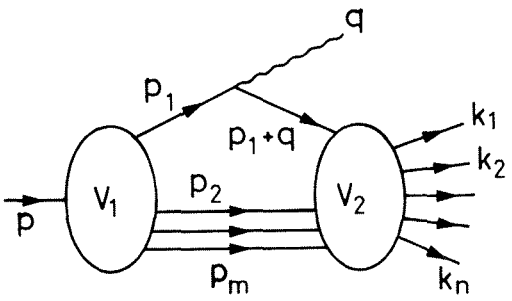

Fig. 1

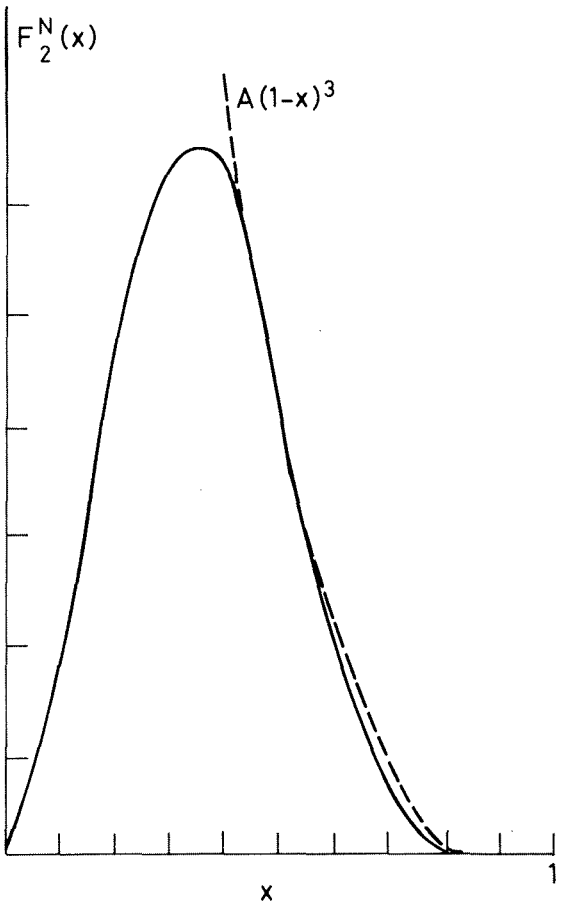

Fig. 2

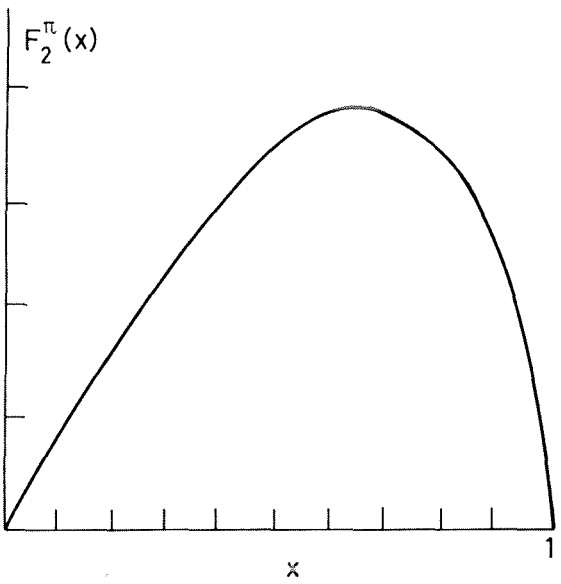

Fig. 3

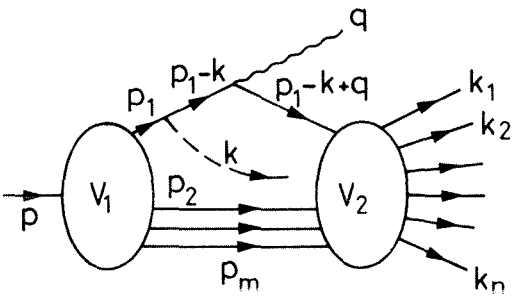

Fig. 4

SESSION V

CHARGED LEPTON PHYSICS

Chairmen: R.A. Salmeron
S.C.C. Ting

Sci. Secretaries: C. Best
M. Bozzo
H. Gennow
P. Gregory

Rapporteur's talk:

E. Gabathuler	Experimental review of deep inelastic electron and muon scattering

Invited papers:

G. Altarelli	Lepton pair production in hadronic collisions
C.W. Fabjan	Direct production of single photons at the CERN Intersecting Storage Rings

Contributed papers:

G. Matthiae	Experimental determination of the pion and nucleon structure functions by measuring high-mass muon pairs produced by pions of 200 and 280 GeV/c on a platinum target
S.C. Loken	Study of rare muon-induced processes
S.H. Pordes	A measurement of the production of massive e^+e^- pairs in proton-proton collisions at $\sqrt{s}$ = 62.4 GeV
F. Janata	Jets in deep inelastic electroproduction
U. Becker	Dimuon spectra from 62 GeV proton collisions

EXPERIMENTAL REVIEW OF DEEP INELASTIC ELECTRON AND MUON SCATTERING

E. Gabathuler
CERN, Geneva, Switzerland

1. INTRODUCTION

In this review of inelastic electron and muon scattering, emphasis will be placed on the new data in this field which have appeared since the Tokyo Conference[1], and on the areas where there are apparent discrepancies between the experimental results and the most successful theoretical prescription of the present day given by quantum chromodynamics (QCD). This theory provides a mechanism of introducing non-scaling effects into the quark-parton model (QPM) to take account of gluon emission off the quarks. The value of the quark-gluon coupling constant is given by

$$\alpha_s = \frac{4\pi}{(11-\frac{2}{3}F)\ \log\ (Q^2/\Lambda^2)} ,$$

where F = No. of flavours and Λ (GeV) is determined from a moments analysis of the structure functions. However, since $\alpha_s \approx 0.1$, then the inclusion of higher-order corrections complicates the simple leading-order theory where Λ is independent of the moment.

For the first time there are good quality multimuon data presented at this Conference, with significant statistics to show that multimuon final states can be used to study production of new flavours in the multi-GeV region. The energy dependence of the cross-section can be used to make further tests of QCD through the fusion mechanism of a photon + gluon → → heavy quark-pair production. The extension of these experiments to detect $\geq$ 3 charged leptons incorporating missing energy and p_T imbalance will provide a sensitive method of enhancing new flavours.

The study of final-state hadrons by electron-muon interactions is still to be pursued in high-energy regions where the current and target fragmentation regions can be separated, and only very general global properties will be discussed. The complete final hadronic state in inelastic lepton scattering is an evolvement of quarks and gluons into hadrons, and therefore specific tests will be forthcoming when sufficiently large data samples of complete events have been collected. Here the monochromatic muon beam provides many more high-energy events compared to a broad-band neutrino beam in H_2 or D_2. For many aspects of quark fragmentation studies, the ability to distinguish the different particles and to define large statistical subsets of events in x, Q^2, x_F, p_T, and W far outweighs the advantage of knowing the target quark uniquely.

2. THE DETERMINATION OF R

The determination of R, the ratio of the cross-sections for the absorption of longitudinal and transverse photons, has been experimentally very difficult. It is only possible to change the amount of polarization over a very limited range at the same value of (x, Q^2) by changing the kinematic variables (E, θ), and therefore systematic errors dominate the measurement.

In terms of the QPM

$$R = \frac{4[m_Q^2 + p_T^2]}{Q^2} ,$$

where m_Q, p_T are the mass and transverse momentum of the quark in the nucleon. For a quark of spin ½, then $\sigma_L = 0$ for $m_Q = p_T = 0$. However, it is well known from Drell-Yan measurements that $p_T \neq 0$ and is therefore x-dependent. If the contribution to QCD is included, then

$$R = \frac{4\langle p_T^2(x)\rangle}{Q^2} + \frac{F(x)}{\log\,(Q^2/\Lambda^2)} .$$

In the first term, $p_T^2(x)$ will behave like $(1 - x)$ at large x and be constant at small x. The second term will behave like $(1 - x)^3$, enhancing the small x region.

The most precise data on R come from the lower-energy SLAC-MIT measurements[2], which are illustrated in Fig. 1 in terms of Q^2 and W^2. It is interesting to note that the consistency of the data points is very good, and that there is no obvious decrease with Q^2 over the whole kinematic range. From all these measurements, the value $\langle R\rangle_{wt.av.} = 0.21 \pm 0.1$ is obtained. A determination of R over a limited range of $x < 0.1$ has been made by the Chicago-Harvard-Illinois-Oxford (CHIO) Collaboration from their H_2 measurements at different muon energies[3]. The data are plotted against x in Fig. 2 and indicate that R increases at small x values, which is expected from the QCD contribution. In Fig. 3 both sets of data are used to illustrate the x dependence for fixed Q^2 ranges in the regions of overlap. The QCD prediction of Reya[4] is indicated by the dotted curve. The separate contributions of the dynamical and primordial components are given for $Q^2 = 3$ $(GeV/c)^2$. In spite of the fact that the uncertainty on R is large in these small intervals of Q^2, it is obvious that in the larger x regions the experimental points are well above the theoretical predictions.

The value of R can also be determined from the y distributions in neutrino interactions through the Callan-Gross relationship[5]. Although there is no *a priori* reason why they should be identical in both reactions, at least similar trends are expected. The values of R given at this Conference[6] are tabulated in Table 1 below and are consistent with zero for $Q^2 \geq 1$ $(GeV/c)^2$. However, it should be noted that by integrating over the x variable, the magnitude of R will in general be reduced.

Table 1

Experimental results on R from neutrino data

Exp	$R = \frac{F_2 - 2xF_1}{F_2}$	Q^2 $(GeV/c)^2$
GGM	0.32 ± 0.15	$Q^2 < 1$
BEBC	0.11 ± 0.14	$Q^2 < 1$
CDHS	-0.03 ± 0.05	$\langle Q^2\rangle \sim 20$
HPWF	0.10 ± 0.06 (± 0.04) a)	$\langle Q^2\rangle \sim 20$
FMII	-0.12 ± 0.16	$\langle Q^2\rangle \sim 5$
CDHS	0.03 ± 0.05 (± 0.1) a)	$\langle Q^2\rangle \sim 20$

a) With radiative correction

A very interesting model of the nucleon has been proposed[7], when two of the valence quarks form a diquark state. This model enhances the larger x region as illustrated in Fig. 4. The diquark system can consist of a (ud) spin-zero combination of charge $\frac{1}{3}$, or a (uu) spin-1 combination of charge $\frac{4}{3}$, which could lead to differences between neutrino and muon scattering in the larger x region.

It is therefore important to make further precision measurements of R in the higher Q^2 and larger x region. Figure 5 shows the uncertainty in measuring R for one of the new CERN experiments, which is indicated by the shaded regions assuming a total integrated luminosity of 10^{38}, six different energies, and a 3% systematic measuring uncertainty. A long-term commitment by the experimental groups over several years will be required to resolve these differences between theory and experiment. However, since the understanding of the p_T behaviour of the quarks in the nucleon is one of the most important inputs in our understanding of hadronic interactions, measurements of R will be of the utmost interest.

3. STRUCTURE FUNCTIONS

3.1 Heavy targets

Deep inelastic electron and muon scattering mainly through the inelastic electron scattering has given the most precise data on structure functions, in particular the x and Q^2 dependence of F_2. From this basic platform has evolved the QCD theory, and from further precise scattering data the parameters (α_s, Λ) should eventually be determined. At present there is over-all reasonable agreement between the theoretical predictions and experiment, except for one experiment which because of its high luminosity extends the ranges of Q^2 and x well beyond that of any existing data. This experiment has been carried out by an FNAL-Michigan group using 275 GeV/c muons on an iron-calorimeter target, and has recorded 10^6 deep inelastic events with $Q^2 \geq 5$ $(GeV/c)^2$. The results of this experiment have been published[8] and are presented at this Conference.

In Fig. 6, the value of $F_2(x, Q^2)$ is plotted against Q^2 for different x regions, where the curves are obtained from a QCD parametrization given by Buras and Gaemers[9] using a value of $\Lambda = 0.4$ (dotted line) and $\Lambda = 0.5$ (solid line). A value of $R = 0.25$ has been used in the extraction of F_2. From the results, there is a clear deviation between theory and experiment which appears as an enhancement in the region $10 < Q^2 < 50$ $(GeV/c)^2$ in the lower x regions. This can be seen more easily in Fig. 7, where the ratio of the experimental determination of F_2 to the theoretical one given by QCD ($\Lambda = 0.5$) is plotted versus Q^2. The dotted line shows the effect of changing Λ from this value of 0.5 to 0.4. However, this enhancement appears to have a fairly strong threshold effect in Q^2 and also is most pronounced in the region $0.1 < x < 0.3$. Since x and Q^2 are related through ν or W, the total centre-of-mass hadronic energy, it is important to establish which variable is producing the effect. Figure 8 gives the ratio of the observed value of F_2 and the predicted value as a function of W^2. The solid lines are separate fits for $W^2 < 80$ GeV^2 and $W^2 > 80$ GeV^2, and other fits are for a linear dependence and step function in W^2. The results indicate that the deviation in the structure function is due to a threshold effect at $W \approx 9$ GeV. The effect cannot be explained by any kinematic uncertainties or known corrections.

Three new experiments have presented preliminary results at this Conference. At this early stage of their analysis, an over-all normalization uncertainty of ±15% is given for

each experiment. As these experiments are presented for the first time, a brief description will be given, since the experimental techniques are very different in the three experiments.

At FNAL, an experiment has been carried out by a Berkeley-FNAL-Princeton (BFP) Collaboration using a large iron multimuon spectrometer consisting of 18 modules of 5 × 10 cm thick iron plates, magnetized in the vertical direction. Scintillation counters together with proportional and drift chambers are interspersed between the iron as illustrated in Fig. 9, to provide triggering and a measurement of the muon trajectory and the hadronic energy. The uncertainty in Q^2 is $\sim$ 10% and the resolution (ΔE) on the hadronic energy measurement is $1.5\sqrt{E}$ (GeV). Data have been taken at 219 GeV using 4×10^{11} μ^+ with some μ^- running at that energy, and also at 100 GeV using 5×10^9 μ^+. The total luminosity achieved was 1.5×10^{39} cm^{-2}. The results presented here correspond to $\sim$ 17% of the 219 GeV data set.

At CERN, two experiments are at present data-taking in the North Area muon beam:

The NA4 experiment: a Bologna-CERN-Dubna-Munich-Saclay (BCDMS) Collaboration have carried out measurements at 280 GeV using a carbon target. The apparatus, illustrated in Fig. 10, consists of 10 identical toroidal iron modules which are magnetized. The carbon target extends throughout the complete 50 m length of the apparatus. Proportional chambers and liquid scintillation counters are inserted throughout the spectrometer to provide triggering and to measure the muon trajectories which spiral in the magnetized iron. The uncertainty in Q^2 is $\lesssim$ 10% for focalized tracks and between 10-20% for defocalized trajectories (opposite sign). The apparatus has a high rate capability since hadronic showers are absorbed in the iron. Data have been collected at 280 GeV using 10^{11} μ^+ giving a total luminosity of 5×10^{38} cm^{-2}. The results presented here correspond to 30% of these data.

The NA2 experiment: a CERN-DESY-Freiburg-Kiel-LAPP-Lancaster-Liverpool-Oxford-Rutherford-Shrivenham-Turin Collaboration (European Muon Collaboration, EMC) have carried out measurements using an iron scintillator calorimeter target with a hadronic energy resolution (ΔE) given by $0.41E^{0.6}$ (GeV). The apparatus consists of a large conventional spectrometer magnet using proportional and drift chambers to measure the scattered muons together with the forward hadrons. Scintillation counters are used for triggering, and the muons are distinguished by their ability to penetrate the calorimeter and magnetized iron absorber as illustrated in Fig. 11. The multiple scattering in the iron target determines $\Delta x/x = 0.15$. Data have been collected at 280 GeV using 8×10^{10} μ^+ and at 250 GeV using 5×10^{11} μ^+ for a total luminosity of 7×10^{38} cm^{-2}. The results presented here represent 15% of the data collected, and are confined to the 280 GeV sample only.

For the EMC data, the value of $F_2(x, Q^2)$ is plotted against Q^2 for different x regions in Fig. 12a. The minimum range of Q^2 is determined by the fact that the data have been taken at 280 GeV with a minimum angle cut $\sim$ 1 degree ($Q^2_{min} \propto EE'\theta^2_{min}$). This cut has been introduced by the present level of confidence in the measurement of the scattered muon at small angles close to the incident beam direction. It is interesting to note that the data do not show any large variations with Q^2 in the range of (x, Q^2) presented. This is, of course, consistent with what is expected in QCD, where the deviations from scaling given by $\log (Q^2/\Lambda^2)$ are largest in the lower Q^2 region owing to the smallness of Λ. This can be seen in Fig. 12b, where data from SLAC[10] on inelastic electron-deuteron scattering are presented together with EMC iron data. Allowing for the uncertainty in the normalization of the EMC data at this stage, it is evident that the largest variations in F_2 with Q_2 occur in

the region $Q^2 < 20$ (GeV/c)^2. Figure 12 clearly shows the importance of having in one experiment a complete set of data spanning the low- and high-Q^2 regions for all x.

Figure 13 presents a comparison between the EMC data and those of the FNAL-Michigan experiment. At present there is no indication of an enhancement in the EMC data similar to that observed in the FNAL experiment. The disagreement between the two experiments in the larger x region should not be taken seriously at present, since in this x region the method of defining the centre of the x bin can introduce large differences in F_2. However, even allowing for an over-all normalization displacement of the two data sets, there is no indication of an enhancement in the EMC data in the range $0.1 < x < 0.3$.

It is of considerable interest to compare F_2 as measured by muons and by neutrinos, since there is a simple relationship which states that $F_2^{\mu N} = {}^5/_{18}\, F_2^{\nu N}$ when the strange, charm, etc., sea contributions are neglected. The comparison between the EMC data and those of CERN-Dortmund-Heidelberg-Saclay (CDHS)[11] can be seen in Figs. 14a and 14b, where $F_2(x, Q^2)$ is plotted against Q^2 in the same x intervals. The agreement between the two experiments is very good and provides further proof of the simple concepts of the QPM.

The preliminary results of the BCDMS Collaboration giving $F_2(x, Q^2)$ as a function of Q^2 for different x regions are illustrated in Fig. 15 and, as a comparison with the CDHS neutrino experiment, in Fig. 16. The minimum Q^2 is again limited by the muon energy and the minimum angle accepted by the spectrometer. However, the over-all Q^2 dependence has a behaviour similar to that given by the EMC data, as illustrated in Fig. 17 where the two data sets are compared.

The BFP Collaboration have determined the structure function $F_2(x, Q^2)$ using a parametrization for R given by $R = 1.2(1-x)/Q^2$, whereas the two CERN experiments assumed a constant value of $\simeq 0.2$, and the results from that experiment are illustrated in Fig. 18. A comparison between the BFP results and the EMC results is given in Fig. 19, showing excellent agreement in normalization and Q^2 dependence in view of the over-all ±15% uncertainty quoted by both experiments at this time.

From these three new experiments, which have been made using iron and carbon targets, the following conclusions can be drawn. Although the data are preliminary at this stage, there is reasonably good agreement between all three experiments. The structure functions do not show any large deviations with Q^2, in particular for $Q^2 \geq 20$ (GeV/c)^2 which is consistent with QCD predictions. There is no evidence of the enhancement seen by the FNAL-Michigan experiment, although further data will be required to rule out smaller effects around the 10% level. There is good agreement between $F_2(x, Q^2)$ as measured by muons and neutrinos when the coupling to the quark charges is taken into account. Data will have to be analysed at lower energies in order to achieve lower Q^2 coverage before a meaningful moments analysis can be made. High-precision data from muon and neutrino experiments off an iron target will become available in the near future, which should allow the possibility to look for small differences in the behaviour of the structure functions. This may even shed some light on R if the sea contributions can be properly taken into account through dilepton-neutrino studies.

3.2 Hydrogen targets

At present, the existing data on H_2 have been obtained by the CHIO Collaboration[12] and from the SLAC experiments[13]. Figure 20 shows the combined data for $F_2(x, Q^2)$ as a

function of x for different Q^2 regions. The best data at large x in the low Q^2 region come from the SLAC measurements, while the data up to a $Q^2 = 50$ $(GeV/c)^2$ come mostly from the CHIO experiment. The EMC Collaboration have collected data at an energy of 280 GeV using 10^{12} μ^+ and at 240 GeV using 5×10^{11} μ^+ for a total luminosity of 4×10^{37} cm^{-2}. A similar amount of data have been taken in deuterium at 280 GeV.

The data presented at this Conference correspond to 10% of the 280 GeV H_2 data. The value of $F_2(x, Q^2)$ is plotted in Fig. 21 against Q^2 for different x regions and extends the existing data up to $Q^2 = 100$ $(GeV/c)^2$. A value of $R = 0.2$ has been used in the extraction of F_2. Although the data are preliminary the trends of the scaling violations are clearly visible, the data extending down to much lower values of Q^2 than for the iron target data. It is interesting to compare the EMC data with the CHIO data, and this is illustrated in Fig. 22. Here the agreement is quite good, in particular at larger x. This can also be seen in the comparison (Fig. 23) between the CHIO and the EMC variations of F_2 versus x in the region $30 < Q^2 < 50$ $(GeV/c)^2$. Clearly more work is required in order to resolve the differences in the small x region, where many of the corrections due to radiative corrections, experimental systematic uncertainties, etc., have to be carefully studied.

In order to see to what extent the deviations from scaling correspond to the predictions of QCD, it is considered advantageous to study the behaviour of the moments of the structure functions rather than the structure functions themselves. In general the predictions are simplest for the flavour non-singlet structure functions such as $F_2^P - F_2^N$ in electron-muon scattering or xF_3 in charged-current neutrino scattering. The determination of the moments from which a value for Λ_N can be determined has become a very active industry, where the simple understanding has become somewhat obscured in the treatment of higher-order corrections. Figures 24a and 24b show the variation of Λ_N with N for $F_2^P - F_2^N$ and for xF_3, together with the theoretical predictions of Sachrajda[14] and Duke and Roberts[15]. In the muon experiment, the same data-set forms the basis of the two independent analyses, one by Quirk et al.[16] and the other by Duke and Roberts[15]. In the neutrino determination of xF_3, both the BEBC[17] and CDHS[18] experiments are essentially determining the same quantity using different lower Q^2 data in conjunction with their own measurements. Theoretically, QCD predicts that Λ_N rises with N, but clearly the extraction of a value of Λ from the existing data is non-trivial. This can be seen from a prediction given by Ross[19] in Fig. 25, where the effect of changing Λ by a factor of 2 in leading order changes the structure function by an amount ($\sim$ 10%) similar to that obtained by including the first higher-order correction in α_s. The need for a complete set of measurements for $F_2(x, Q^2)$ which span the whole x and Q^2 regions is evident. It is not yet clear whether it will be possible to separate $1/\log(Q^2/\Lambda^2)$ from $1/Q^2$ behaviour when the higher-order corrections are also taken into account.

4. MULTIMUONS

The production of multimuons by muons is more complicated than, for example, in neutrino physics owing to the electromagnetic-hadronic nature of the photon, which means that QED and vector dominance Drell-Yan processes dominate over all other processes at low masses. The various processes which contribute to the final state of ≥ 2 prompt muons are illustrated in Fig. 26. It is interesting to note that QED and Compton processes are identical in their final states, and therefore it is possible to check aspects of quark-lepton universality

through the interference amplitudes in the differential cross-sections. Multimuons produced in a high-luminosity heavy target can be used as indicated in the flavour-changing process to signature quark cascades through leptonic decays giving large p_T muons. Bound states produced by $q\bar{q}$ formation can be detected as narrow $\mu^+\mu^-$ resonances. In the vector dominance picture, where the photon behaves like a $q\bar{q}$ vector state, opposite-sign pairs can be produced by the annihilation of a $\bar{q}$ from the $q\bar{q}$ vector state with a quark from the nucleon or vice versa.

The behaviour of the cross-section for different processes is presented in Figs. 27a and 27b for an incident energy of 280 GeV with kinematic cuts of $E_\mu > 5$ GeV and $\theta_\mu > 5$ mrad for the fastest muon of like sign to the beam. Figure 27a illustrates the well-known rapid fall-off in the yield when the four-momentum transfers to the muon vertex and to the quark-target vertex are increased. Figure 27b shows how the cross-section of the $\mu^+\mu^-$ varies with longitudinal energy and invariant pair mass for the various coherent and incoherent processes. It is evident that the electromagnetic and Drell-Yan processes dominate over all other processes unless selective kinematic selections are made. For example, it should be possible to increase charm production over background if the simple Q^2 dependence of the cross-section given by $\left[1 + (Q^2/M_\psi^2)\right]^{-2}$ actually works for masses much bigger than the proton mass. In addition, for calorimeter targets the missing neutrino energy provides a possible signature of prompt D decays. Figure 28 shows that in both the BFP and EMC experiments like-sign and unlike-sign dimuon inelastic events have $\sim$ 20 GeV missing energy when compared to the normal deep inelastic process. The muon mass spectra of the BFP and of the EMC iron target experiments are illustrated in Figs. 29 and 30 where the muon of like sign to the beam with the largest p_L or smallest θ_s for high ν events is the main criterion used to define the scattered muon. The BCDMS experiment has studied multimuon production from carbon and the $\mu^+\mu^-$ mass spectrum for those muons entering the toroids is plotted in Fig. 31. All three experiments have a clear peak in their dimuon spectrum at the J/ψ mass, achieving a mass resolution of $\sim$ 10%, which is consistent with that given by the detection apparatus. The BCDMS experiment has a very small acceptance ($\sim$ 1%) at a mass of 3 GeV, rising to $\sim$ 60% at 10 GeV. However, at that mass the small number of events is consistent with QED predictions. In order to enhance the $\Upsilon \to \mu^+\mu^-$ decays, it will be necessary to select muons of large angle, since the cross-section for QED has a steeper θ dependence than that for vector meson production. Figures 32 and 33 illustrate the Q^2 dependence of the elastic J/ψ cross-section for the BFP and EMC experiments, where the elastic events are defined as those events with a total observed energy $\leq$ 5 GeV consistent with radiated energy loss from the muons. For the first time there is clear evidence that the shallow Q^2 dependence behaves like an $\sim$ 3 GeV mass effect in the propagator dependence. This confirms the previous statement that it is possible to enhance charm production (assumed mediated by J/ψ production) over the background of strange particle production (mediated by ϕ production) by tuning the Q^2 dependence defined by the scattered muon.

The energy dependence of the J/ψ-production cross-section, given by $(d\sigma/dt)$ $(Q^2 = 0, t = 0)$, has been obtained using the Q^2 dependence of J/ψ production and the t-dependence taken from photoproduction[20]. The cross-section rises rapidly from threshold and flattens out at a value $\sim$ 50 nb/(GeV/c^2), as illustrated in Fig. 33. Systematic errors ($\sim$ 20%) are not included.

It is useful to compare the behaviour of J/ψ production with that of ϕ production. Figures 34a and 34b illustrate the Q^2 dependence and the energy dependence of ϕ electroproduction[21] and photoproduction experiments[22]. The results are clearly in agreement with vector dominance model (VDM) predictions using the mass scale of the ϕ meson. The relationship between the photon-gluon (QCD) process and VDM process in predicting the energy dependence of the cross-section should provide further insight into our understanding of hadronic interactions within the QCD framework.

An attempt has been made by the Michigan-FNAL group[23] to establish evidence for charm using a large dimuon sample. The dimuon kinematic distribution is presented in Fig. 35 in terms of the produced dimuon momentum and transverse momentum relative to the virtual photon direction for 275 GeV incident muons. The contributions expected from QED, charm production, and decays are also indicated. However, since it was indicated in Fig. 27b that background QED and vector dominance Drell-Yan processes have a behaviour similar to that shown here, it is therefore necessary to understand the precise shape and normalization of each background contribution. Again it would be advantageous to look at the events which dominate the low p_T and low p_L dimuon mass spectra in order to confirm missing energy.

In conclusion, the multimuon data presented provide the first evidence for virtual photoproduction of J/ψ through their muon decay, and are in agreement with the VDM in their Q^2 dependence. The energy dependence of elastic and inelastic J/ψ production should provide clean tests of QCD since heavy quark masses are involved. Future detailed studies are necessary to look for a unique charm signature, but the average small missing energy of $\sim$ 15 to 20 GeV makes this problem difficult. The possibility of measuring longitudinal components in the photon interaction can in principle be studied through the decay angular distribution of the dimuon events.

5. FINAL-STATE HADRONS

The study of final-state hadrons in deep inelastic scattering provides a very useful test of our ideas on how quarks and gluons fragment into hadrons. However, apart from low-energy experiments carried out at electron accelerators, there has not yet been a detailed study of complete hadronic final states at high energies. Since the quark jets etc. are expected to have an opening angle of $\sim \pm 30°$ at FNAL/SPS energies, it is necessary to carry out experiments with a large-solid-angle detector. At present, all the studies of final-state hadrons at high energies have been made using limited-acceptance forward spectrometers.

The transverse momentum of single hadrons with respect to the direction of the virtual photon is important in that $\langle p_T^2 \rangle$ is expected to reflect the primordial p_T of the quark in the nucleon, the gluon (or pair production) emission off the quark, and the fragmentation of the quark back into a hadron. Figure 36 shows the $\langle p_T^2 \rangle$ versus Q^2 for the CHIO[24] and BEBC neutrino experiment[25] for all hadrons with $Z > 0.2$. The results show good agreement between the muon and neutrino measurements of the $\langle p_T^2 \rangle$. However, the absolute value of the $\langle p_T^2 \rangle$ is somewhat higher than the QCD prediction given by $Q^2/\log(Q^2/\Lambda^2)$ although the over-all Q^2 dependence is in qualitative agreement. The $\langle p_T^2 \rangle$ rises with Z, which is known as the seagull effect, and therefore it is not possible to draw any simple conclusions since

$$\langle p_T^2 \rangle = \left[\langle p_T^2(\text{prim.}) \rangle + \langle p_T^2(\text{QCD}) \rangle\right] Z^2 + \langle p_T^2(\text{frag.}) \rangle \ .$$

Figure 37 presents the W^2 dependence of the $\langle p_T^2 \rangle$ of the hadrons for inelastic electron[26], muon[24], and neutrino[25] scattering, as well as that from electron-positron collisions[27]. The straight lines (log W^2) are obtained by fitting the e^+e^- data and transposing that dependence to the inelastic lepton data. The agreement is reasonably good in the W^2 dependence and it is expected that the $\langle p_T^2(e^+e^-) \rangle$ is less than $\langle p_T^2(\ell h) \rangle$ since the jet axis is defined in the e^+e^- hadronic events by minimizing the p_T distributions (sphericity axis). The QCD prediction that $\langle p_T^2 \rangle$ depends on Q^2 rather than log W^2 cannot yet be proven because of the small range in W over which the measurements have been carried out.

A comparison of the sphericity axis and the virtual photon axis has been made by the DESY-Cornell (DECO)[28] Collaboration using data obtained from a streamer chamber in the kinematic range $1 < Q^2 < 6$ $(GeV/c)^2$ and $9 < W^2 < 16$ GeV^2. In order to avoid contamination from diffractive processes, only events with three charged tracks in the final state were accepted. Figure 38 shows the distribution of events versus $|\cos \theta|$, where θ is the angle between the sphericity axis and the vertical photon axis in the centre-of-mass system. The two axes are closely correlated but are not identical. Figure 39 presents the $\langle p_T \rangle$ and $\langle p_L \rangle$ distributions of all the hadrons as a function of $W' = W - M_N + m_\pi$ for $n_{ch} > 3$. It is interesting to note that there is a smooth continuation in the W' dependence when the sphericity axis is used for ep and e^+e^- events, whereas this is not so when the virtual photon axis is used in ep. These results suggest that the p_T of the initial quark has a most likely value given by $0.5 < p_T < 0.9$ GeV/c. However, it is again obvious that carrying out the same exercise at higher energies will provide a better test, since the present W range has a very limited multiplicity in which to carry out sphericity analyses.

The whole range of single-arm measurements in terms of the usual lepton and hadron final-state variables does not indicate any features which are different from those where hadrons are used as the incident particles. In order to look for specific quark or gluon effects, it is necessary to bin the data in discrete intervals of the different variables. The quality and quantity of the present data are not yet sufficient for carrying out such detailed studies.

6. CONCLUSIONS

In a rather short period of time, the study of deep inelastic scattering has given us initially through scaling a very good dynamical theory of quarks within the nucleon (QPM) and the addition of the gluon concept through non-scaling (QCD). Clearly, future work in this field requires a detailed study of what is actually meant by QCD tests, i.e. what particular facet of the theory is actually being tested.

With future high-statistics experiments on the same targets, it will be possible to make detailed comparisons between muon and neutrino structure functions for F_1 and F_2. The study of multimuons and hadronic final states is still very much in its infancy, but muon beams provide the highest energy, highest luminosity interactions on hydrogen targets with which to study the interplay between quarks, gluons, and leptons at high energies. In conclusion, the results of a little-known experiment which has been carried out at FNAL by a Cornell-Krakow-Michigan-Washington (CKMW) group[29], using 5.6 litres of emulsion exposed to a 150 GeV muon beam, illustrate the need for a comprehensive understanding of hadronic final states. This group has measured the angular distributions of the hadrons and compared the

pseudo-rapidity distributions with those of pion- and proton-induced reactions at the same centre-of-mass energy. The results illustrated in Fig. 40 show that while there is good agreement between all experimental data in the forward and backward directions, there is a clear discrepancy in the central region. If this effect is not caused by a large statistical fluctuation or measuring uncertainty, then it is interesting at least to ask the question whether this can be explained by the different absorption of quarks and gluons in nuclear matter. QCD as a theory of the strong interactions should eventually be able to answer this question.

Acknowledgements

I wish to express my thanks to all my colleagues in the EMC experiment for their help in the preparation of this report. I also express my thanks to W. Chen, R. Clifft, J. Davies, Y. Declais, S.C. Loken, P. Payre, I. Savin and G. Smadja for their individual contributions to this Conference.

* * *

REFERENCES

1) E. Gabathuler, Proc. 19th Int. Conf. on High-Energy Physics, Tokyo, 1978 (Physical Society of Japan, Tokyo, 1978), p. 841.

2) M.D. Mestayer, A measurement of the proton structure functions using inelastic electron scattering, SLAC-214, Thesis (1978).

3) H.L. Anderson et al., Fermilab-Pub-79/30-EXP, submitted to Phys. Rev. D.

4) M. Gluck and E. Reya, Nucl. Phys. B142, 24 (1978).

5) C.G. Callan and D.J. Gross, Phys. Rev. Lett. 21, 311 (1968).

6) R. Turlay, Charged weak currents, Rapporteur's talk at this Conference (see p. 50).

7) L.F. Abbott, E.L. Berger, R. Blankenbecler and G.L. Kane, SLAC-PUB-2327 (1979).

8) R.C. Ball et al., Phys. Rev. Lett. 42, 866 (1979).

9) A.J. Buras and B.G.F. Gaemers, Nucl. Phys. B132, 249 (1978).

10) E.M. Riordan et al., SLAC-PUB-1634 (1975).

11) J.H.G. De Groot et al., Phys. Lett. 82B, 292 (1979).

12) B.A. Gordon et al., Phys. Rev. Lett. 41, 615 (1978).

13) R.E. Taylor, Proc. Int. Symp. on Lepton and Photon Interactions at High Energies, Stanford, 1975 (Stanford Univ., Calif., 1975), p. 679.

14) A. Para and C.T. Sachrajda, preprint TH.2702-CERN (1979).

15) D.W. Duke and R.G. Roberts, Rutherford Laboratory preprint RL-79-025 (1979).

16) T.W. Quirk, J.B. Mac Allister, W.S.C. Williams and C. Tao, Non-singlet moments in charged lepton scattering, Oxford Univ., Nuclear Physics Dept. preprint (1979).

17) P.C. Bosetti et al., Nucl. Phys. B142, 1 (1978).

18) CDHS Collaboration, Structure function, A parameter and the Callan-Gross relation, presented by J. Wotschack at the parallel session No. 2 on Deep inelastic phenomena.

19) D.A. Ross, Preprint CALT-68-699 (1979).

20) W. Lee, Proc. Int. Symp. on Lepton and Photon Interactions at High Energies, Hamburg, 1977 (DESY, Hamburg, 1977), p. 555.

21) R. Dixon et al., Phys. Rev. Lett. 39, 516 (1977).

22) R.M. Egloff et al., Phys. Rev. Lett. 43, 657 (1979).

23) D. Bauer et al., Phys. Rev. Lett. 43, 1551 (1979).

24) W.A. Loomis et al., Fermilab-Pub-78/94, submitted to Phys. Rev.

25) B. Tallini, Hadronic final states, Rapporteur's talk at this Conference (see p. 81).

26) J.F. Martin and L.S. Osborne, Phys. Rev. Lett. 38, 1193 (1977).

27) G. Wolf, Results from PETRA, Rapporteur's talk at this Conference (see p. 220).

28) F. Janata, Jets in deep inelastic electroproduction, this Conference (see p. 775).

29) L. Hand et al., Acta Phys. Polon. B9, 1087 (1978).

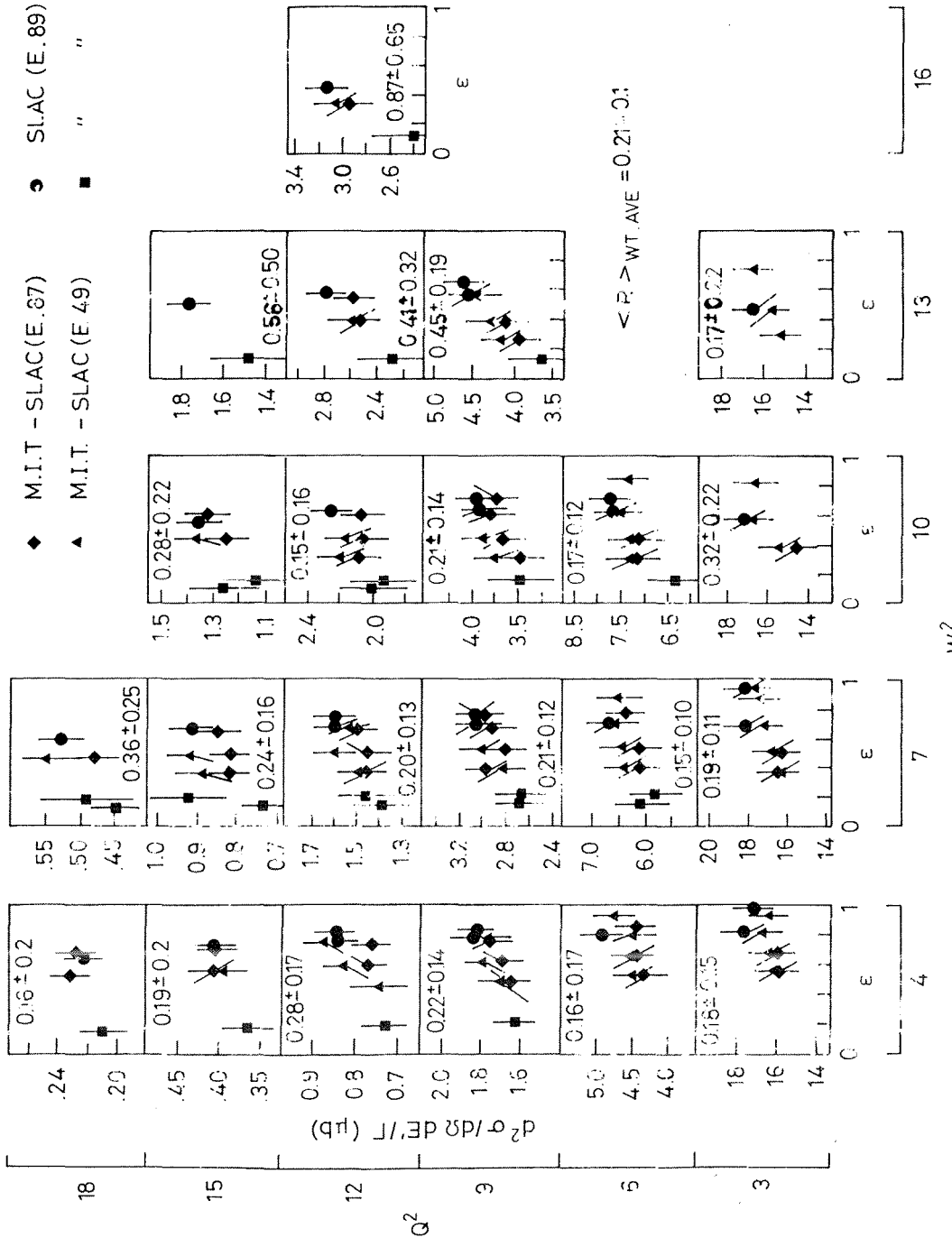

Fig. 1 Value of R determined from MIT-SLAC data in bins of Q^2 and W

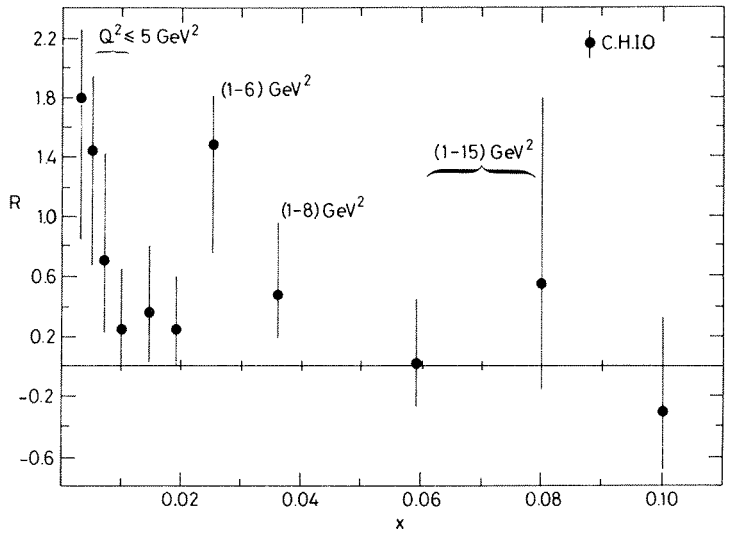

Fig. 2 The value of R determined from CHIO data

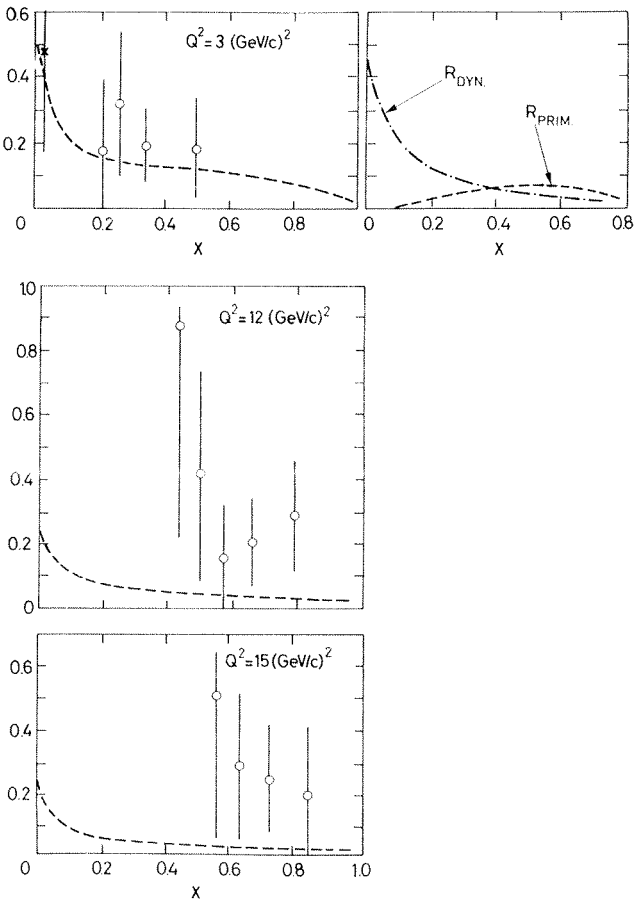

Fig. 3 The value of R determined for different Q^2 values as a function of x for SLAC (O) and CHIO (×). Dotted curve is QCD prediction.

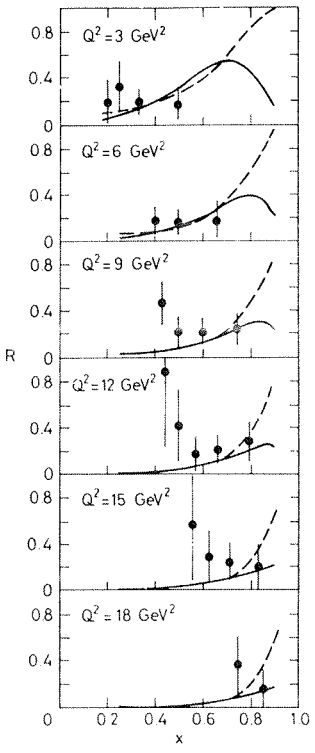

Fig. 4 Theoretical prediction of R versus x for different Q^2. The two models are given in Ref. 7.

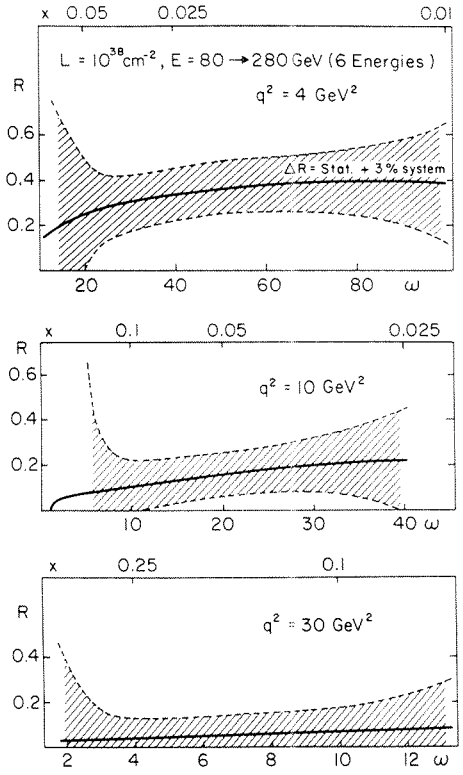

Fig. 5 The theoretical value of R versus x for different Q^2 ranges for the EMC experiment. The shaded area gives the uncertainty in the measurement of R for six energies, luminosity 10^{38} cm^{-2} and 3% systematic error for each measured cross-section.

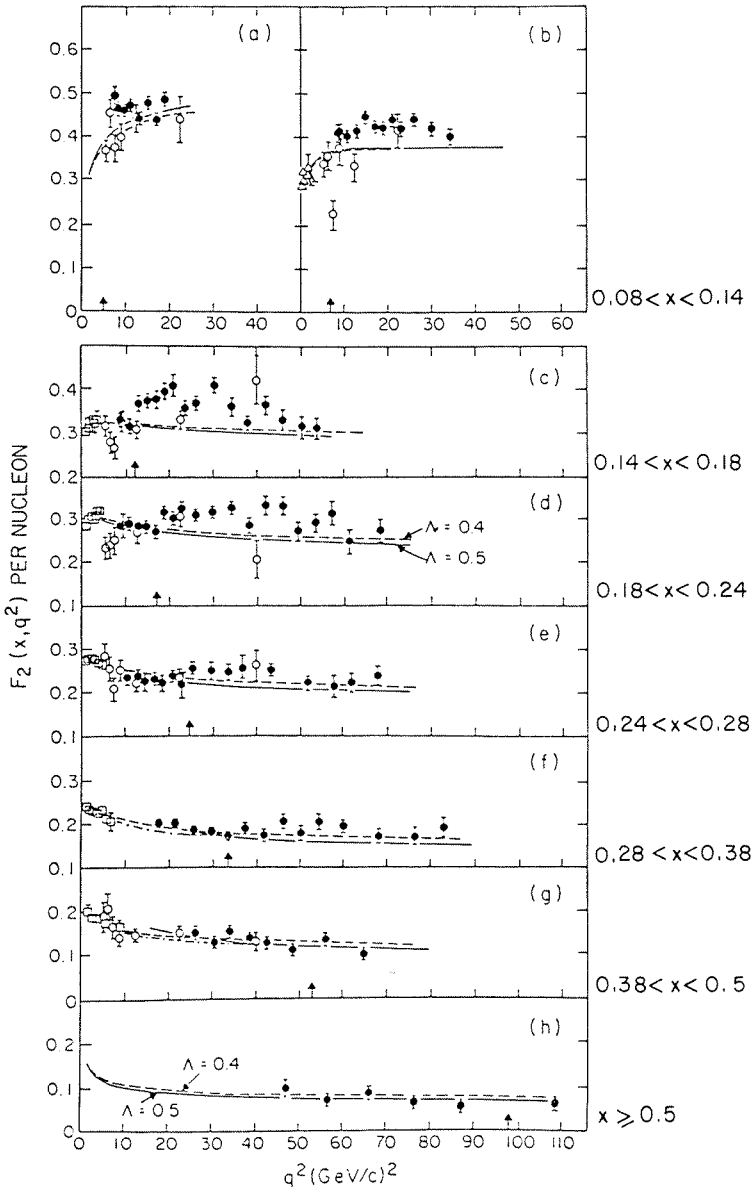

Fig. 6 $F_2(x, Q^2)$ versus Q^2 for different x regions for the Michigan-FNAL experiment (●). Also shown are SLAC e-D data (□) and CHIO data (○) corrected for n-p difference. The solid and dashed lines are QCD predictions.

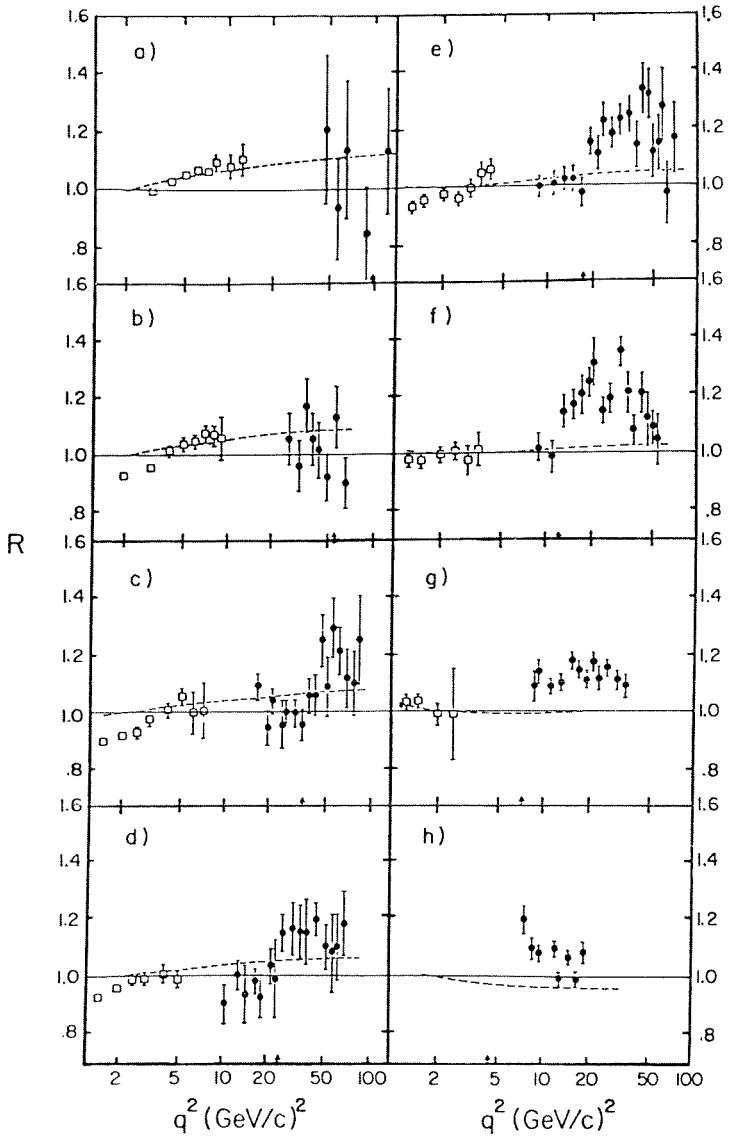

Fig. 7 The ratio of observed/calculated (QCD) $F_2(x, Q^2)$ for the Michigan-FNAL experiment (●). Also shown are SLAC e-D data (□).

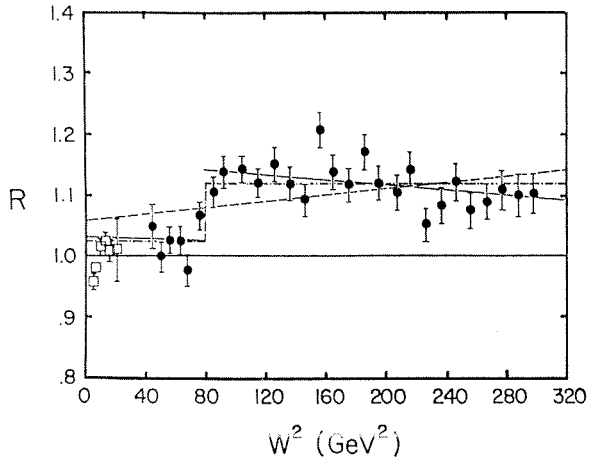

Fig. 8 The ratio of observed to calculated (QCD) structure function versus W^2, for all x and Q^2

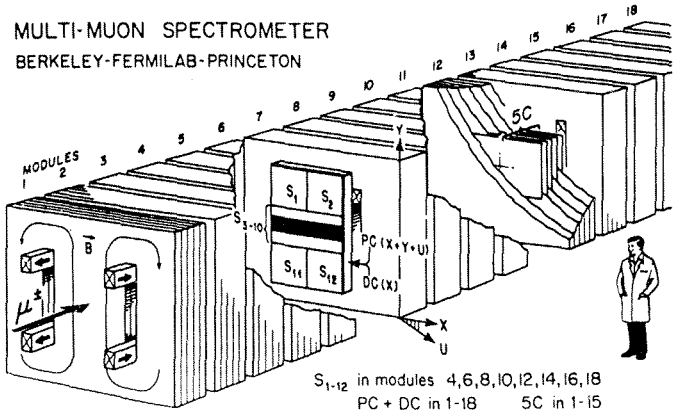

Fig. 9 The layout of the Berkeley-FNAL-Princeton multimuon spectrometer

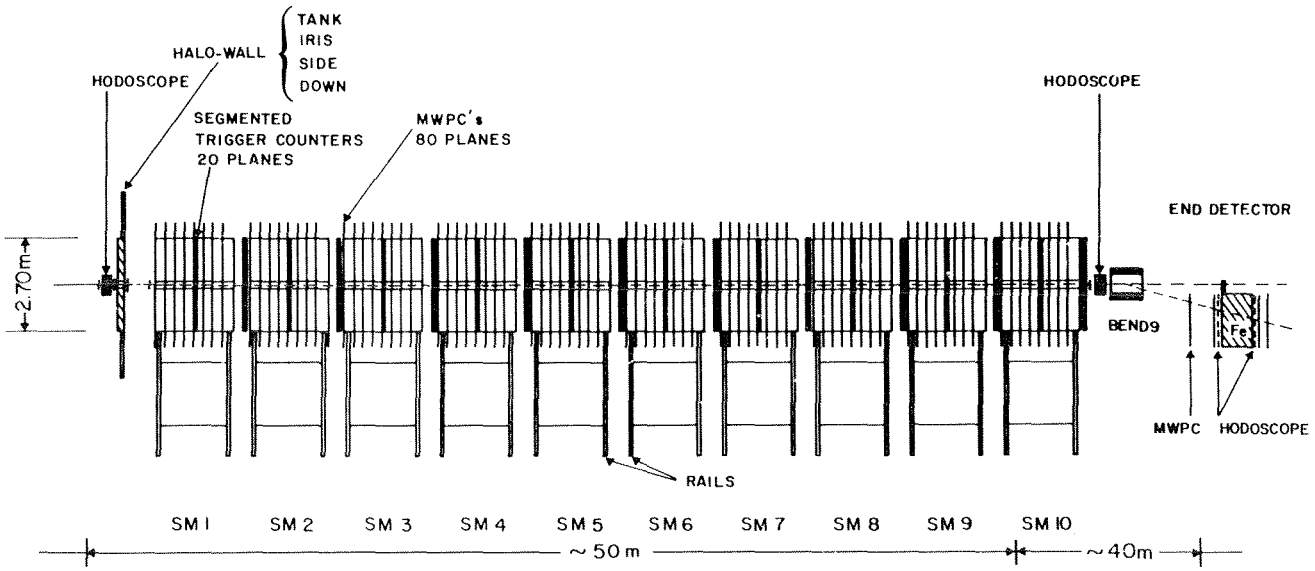

Fig. 10 The layout of the BCDMS (CERN-NA4) experiment

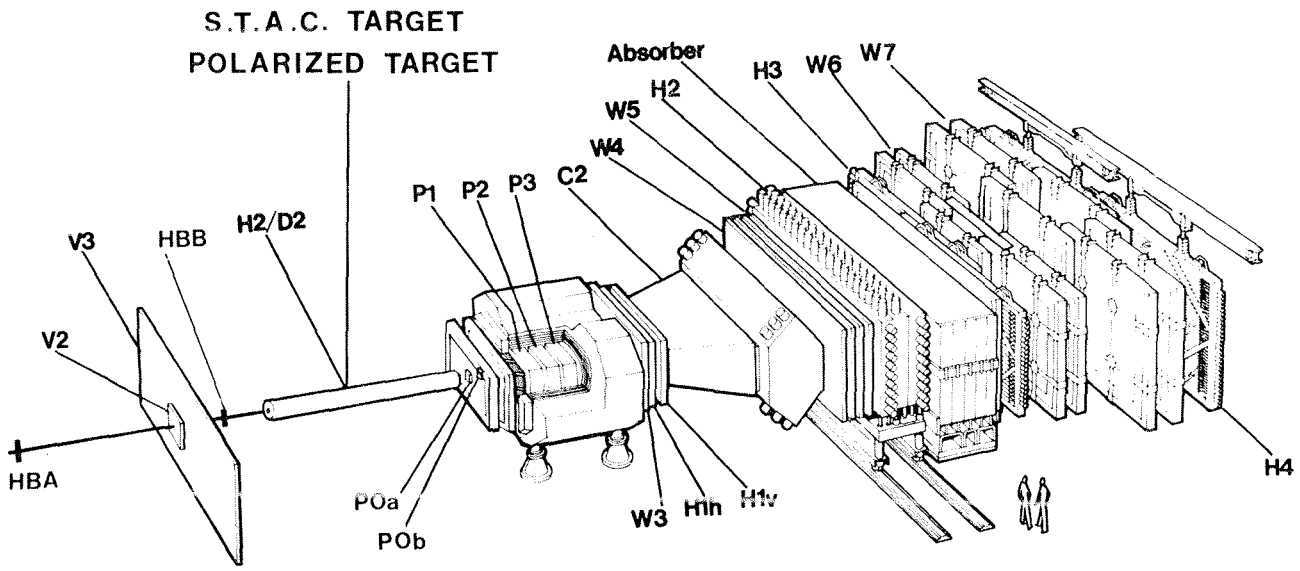

Fig. 11 The layout of the EMC (CERN-NA2) experiment

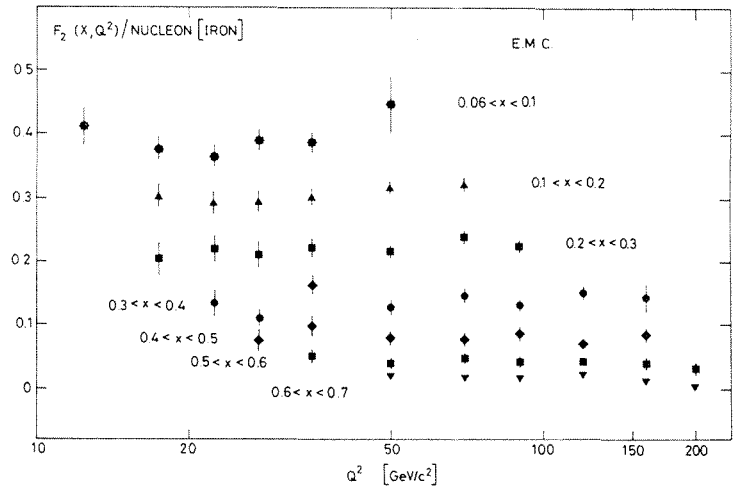

Fig. 12(a) $F_2(x, Q^2)$ versus Q^2 for different values of x for the EMC experiment

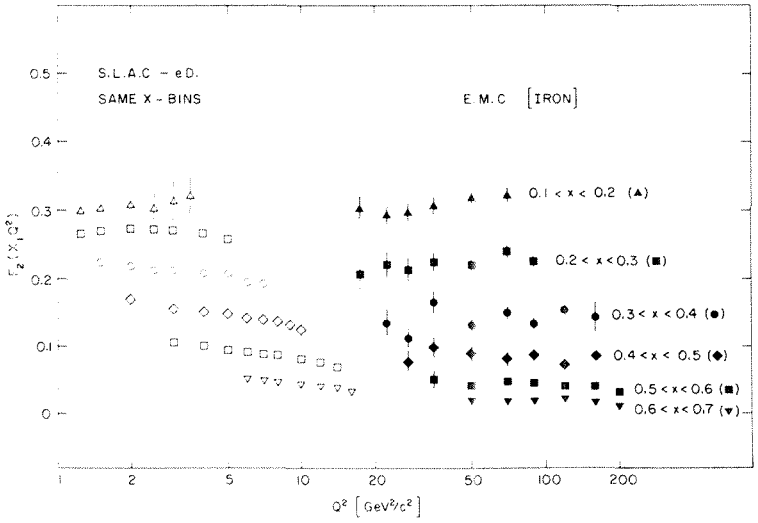

Fig. 12(b) Comparison of $F_2(x, Q^2)$ for the EMC muon-iron data and SLAC e-D data

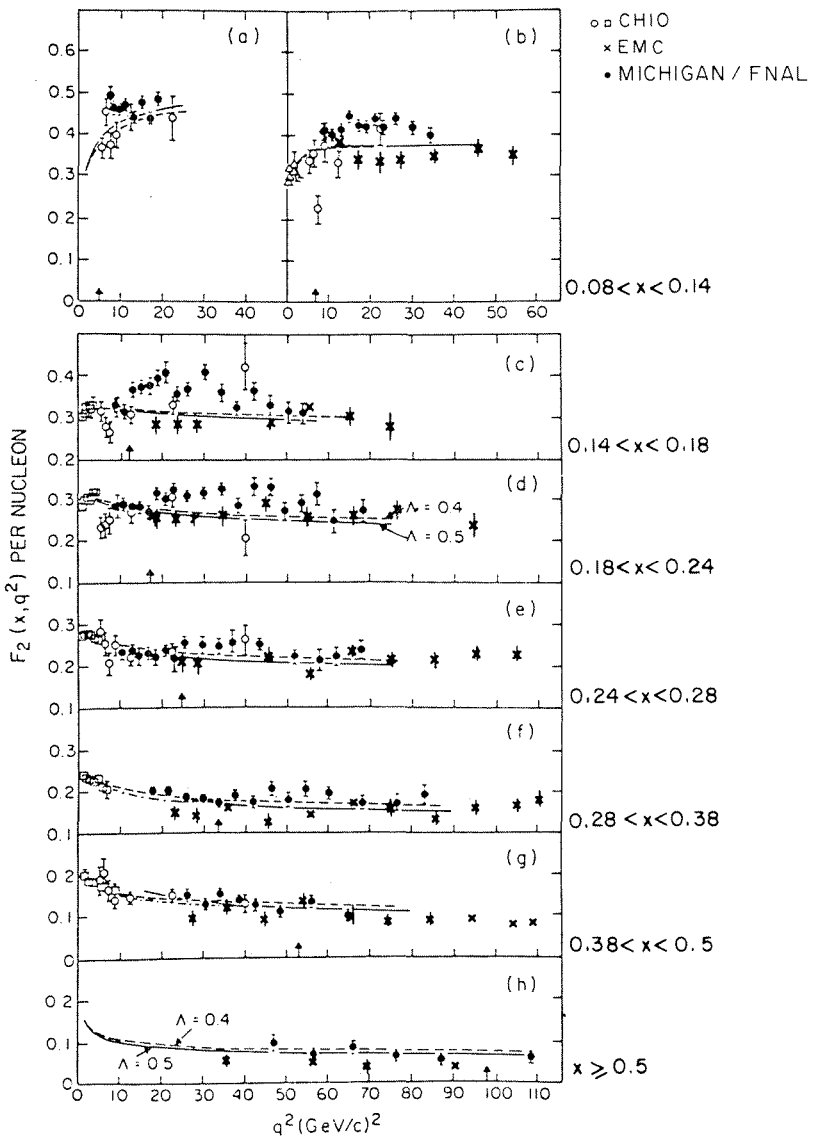

Fig. 13 Comparison of $F_2(x, Q^2)$ for the EMC and Michigan-FNAL muon-nucleon experiments

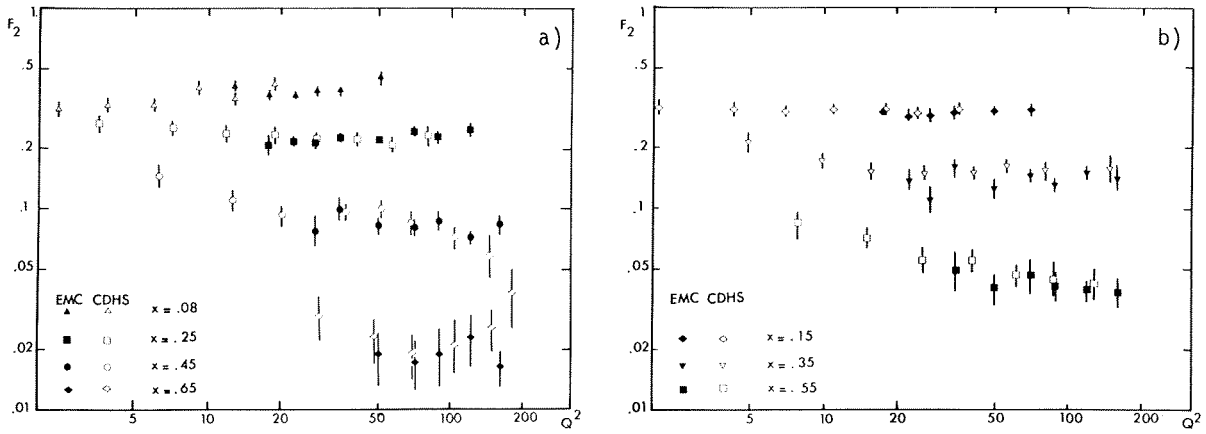

Fig. 14 (a) and (b) Comparison of $F_2(x, Q^2)$ for μ-N (EMC) and ν-N (CDHS) data

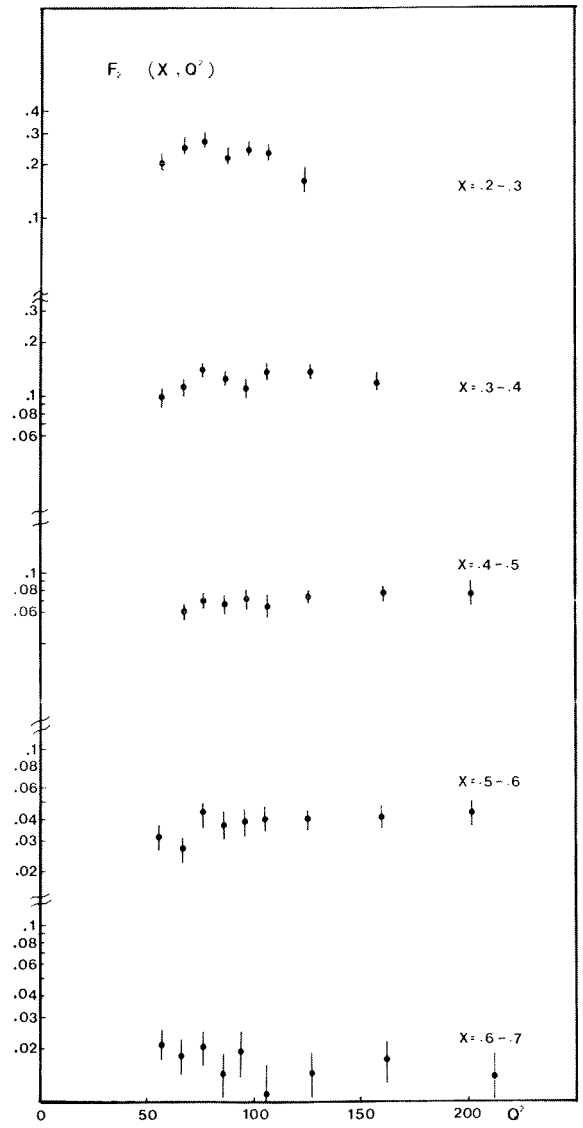

Fig. 15 $F_2(x, Q^2)$ versus Q^2 for different x bins for the BCDMS experiment

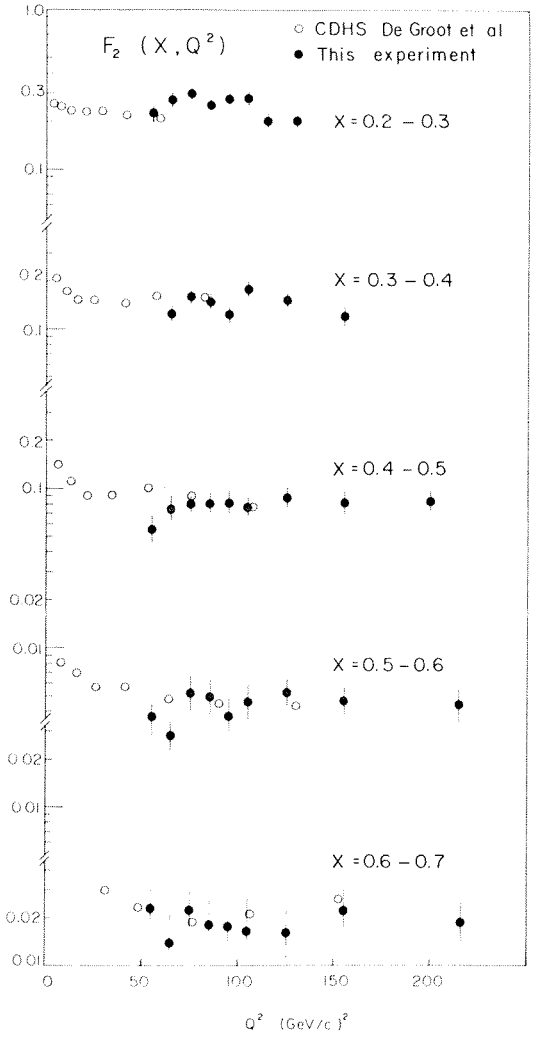

Fig. 16 Comparison of $F_2(x, Q^2)$ versus Q^2 in different x bins for the BCDMS (●) and CDHS experiments (○)

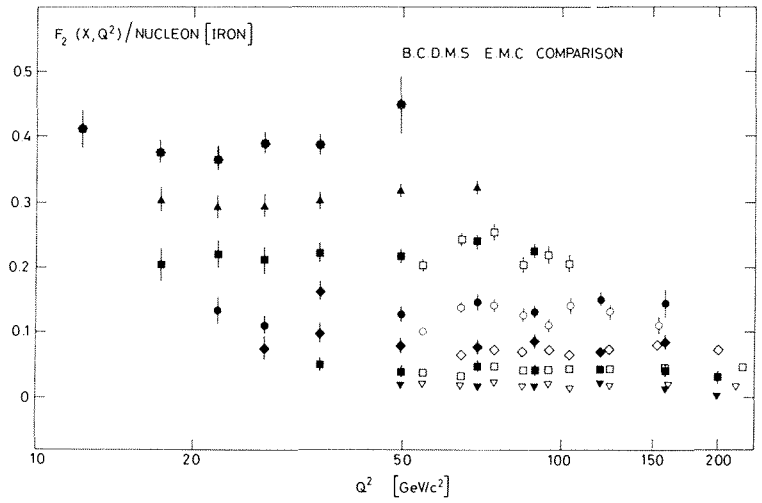

Fig. 17 Comparison of $F_2(x, Q^2)$ versus Q^2 in different x bins for BCDMS (open points) and EMC (full points) experiments

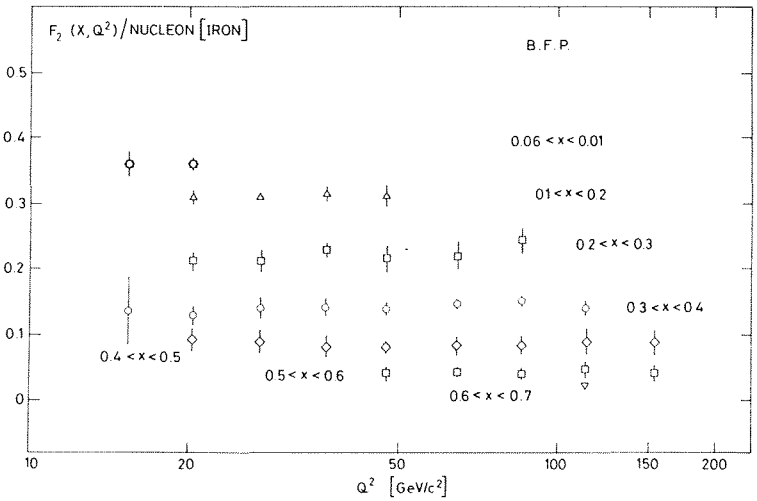

Fig. 18 $F_2(x, Q^2)$ versus Q^2 in different x bins for the BFP experiment

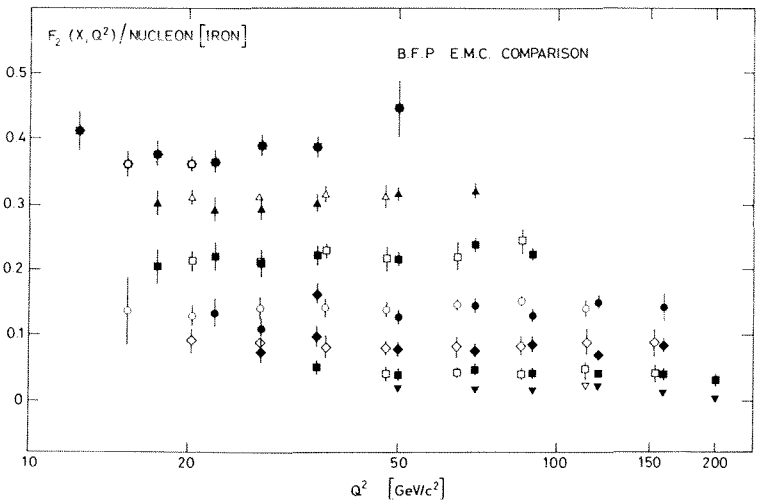

Fig. 19 Comparison of $F_2(x, Q^2)$ for the BFP and EMC experiments

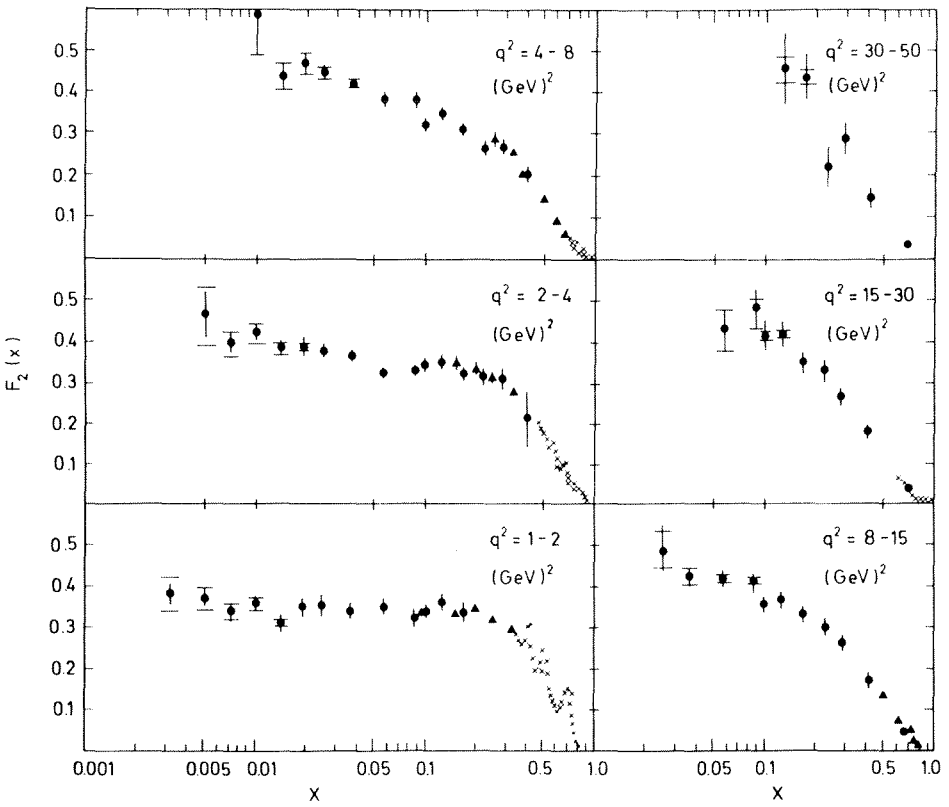

Fig. 20 $F_2(x, Q^2)$ versus x for various q^2 regions for CHIO data (●). Also shown are SLAC data (×). The large horizontal bars indicate a total change of R of 0.5.

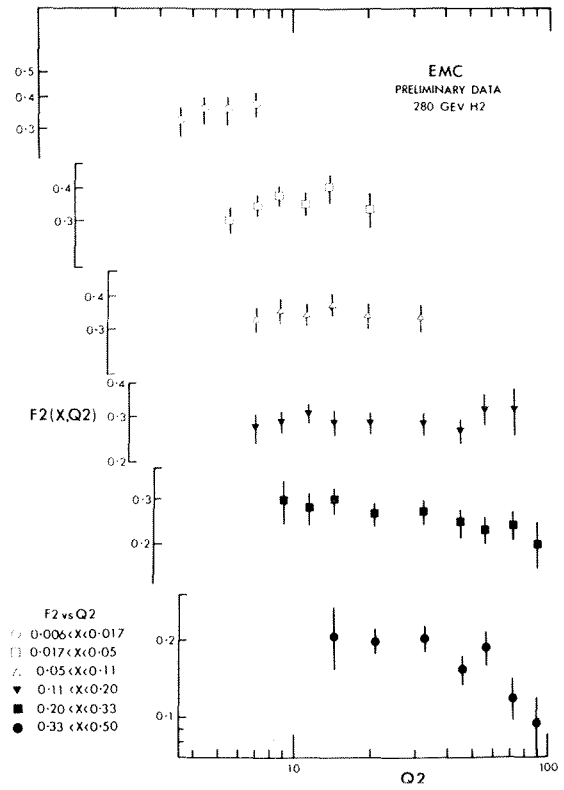

Fig. 21 $F_2(x, Q^2)$ versus Q^2 for various x regions for the EMC experiment

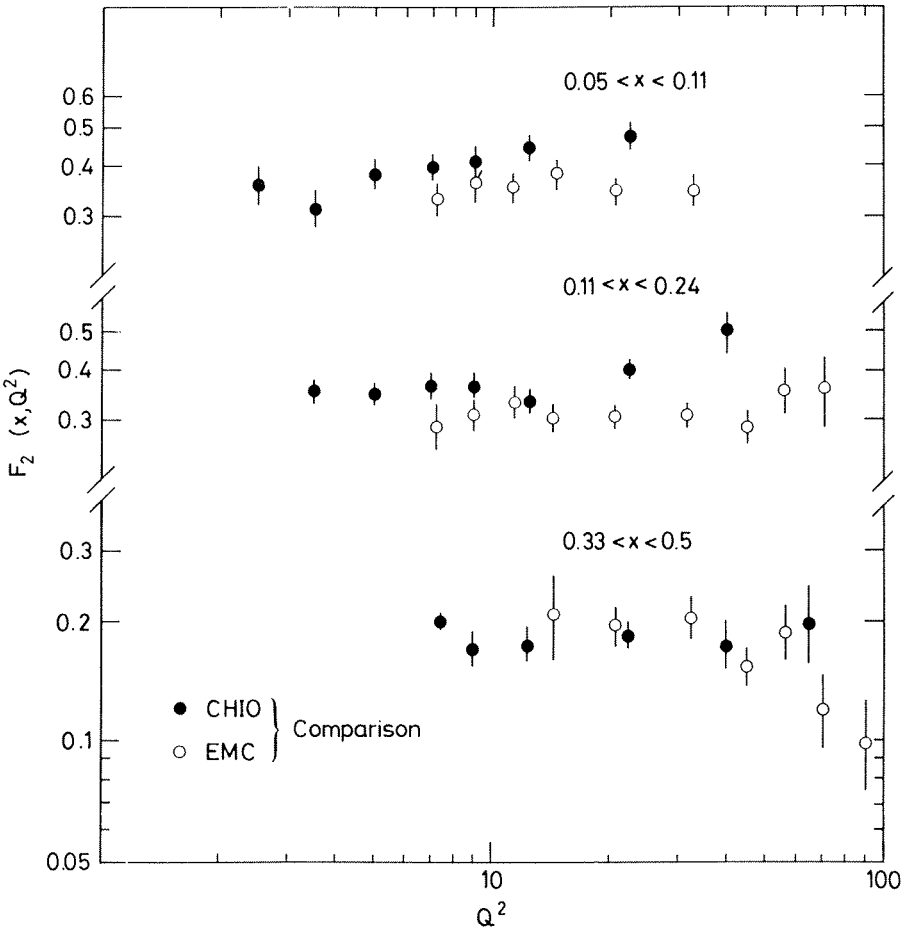

Fig. 22 A comparison of $F_2(x, Q^2)$ versus Q^2 for the CHIO and EMC experiments

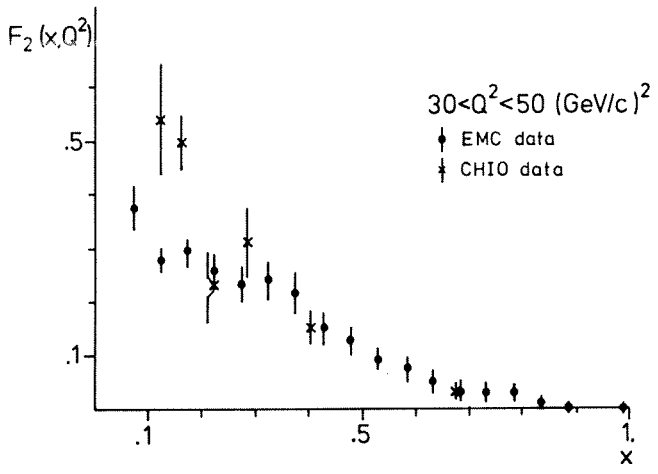

Fig. 23 A comparison of $F_2(x, Q^2)$ versus x in the range $30 < Q^2 < 50$ $(GeV/c)^2$ for the EMC and CHIO experiments

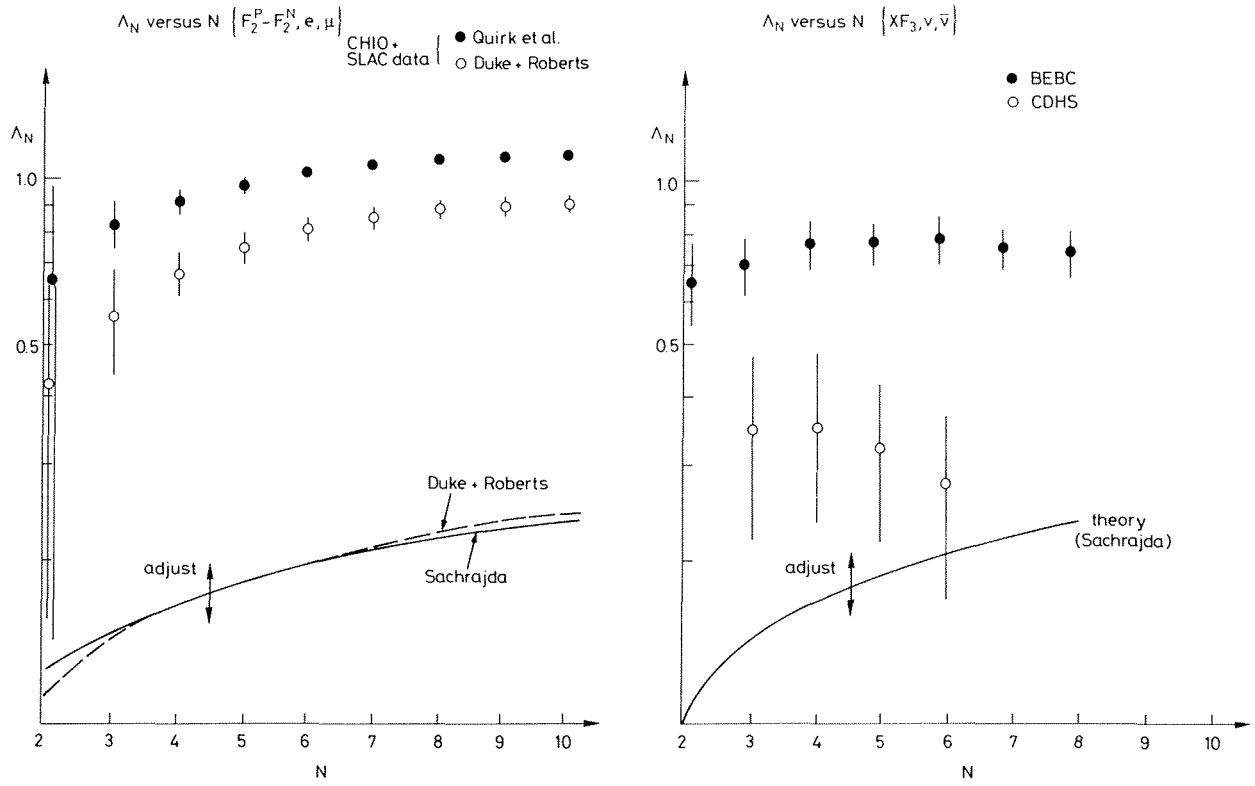

Fig. 24 a) Variation of Λ_N versus N from $F_2^P - F_2^N$ measurements. b) Variation of Λ_N versus N from xF_3 measurements. Also shown are QCD predictions.

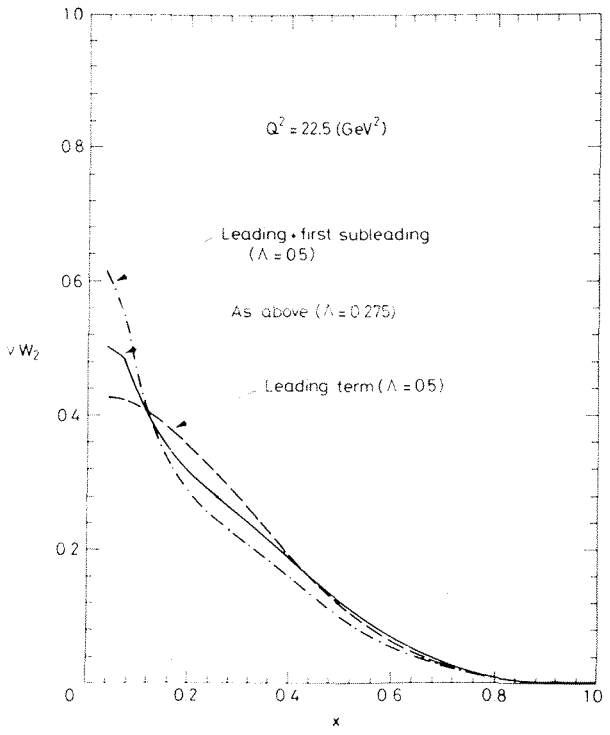

Fig. 25 The variation of νW_2 versus x for $Q^2 = 22.5\ (GeV/c)^2$ illustrating the dependence on higher-order corrections

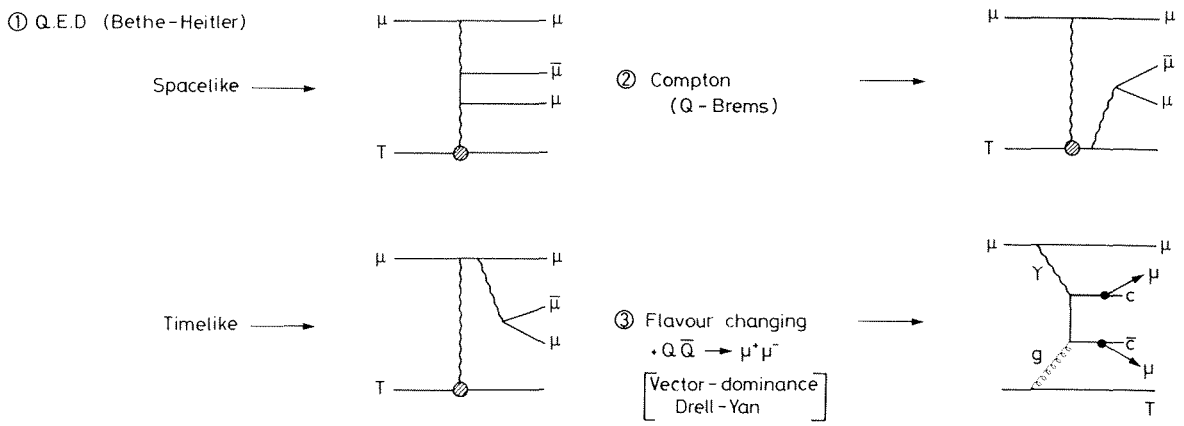

Fig. 26 Different processes which contribute to the production of multimuons by incident muons

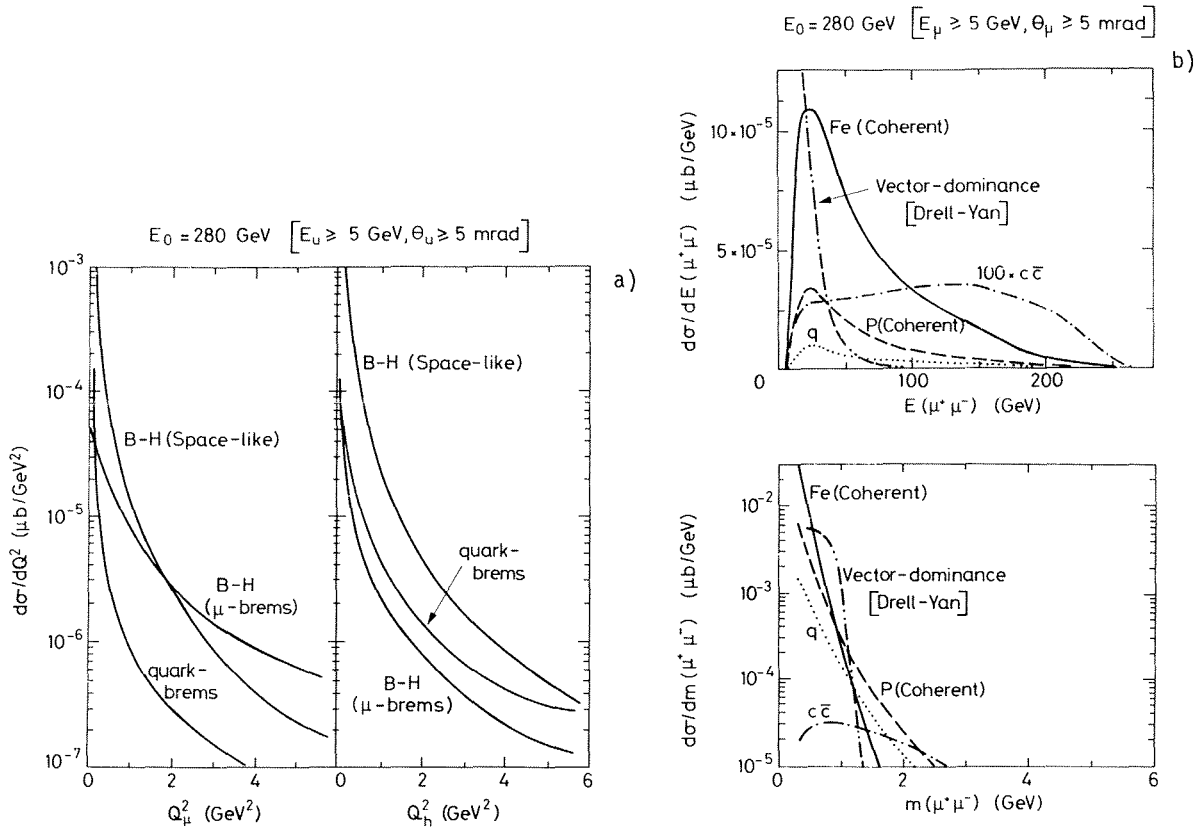

Fig. 27 a) The differential cross-section for the production of muon pairs versus Q^2_μ and Q^2_h for the given processes for 280 GeV and cuts as given. b) The differential cross-section for the production of muon pairs versus $E(\mu^+\mu^-)$ and $m(\mu^+\mu^-)$ for 280 GeV and cuts as given.

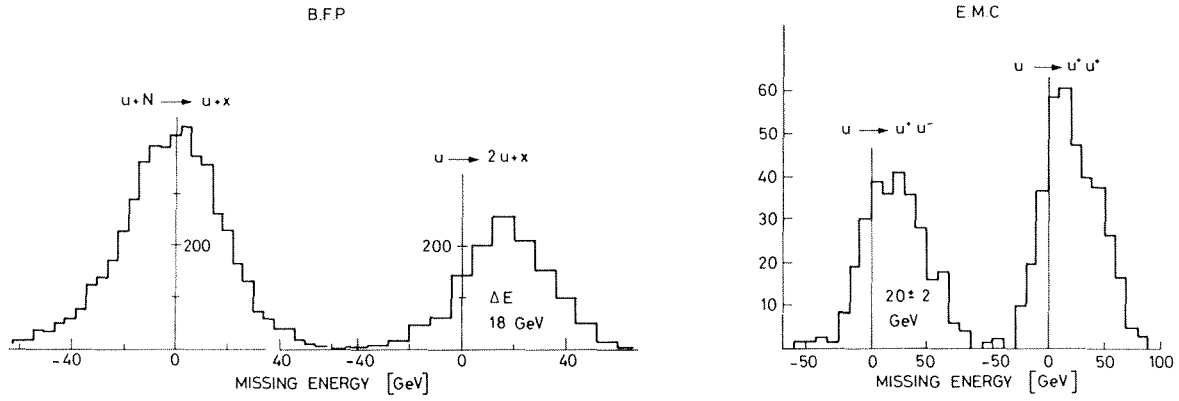

Fig. 28 The missing energy in the final state for dimuons compared to single-muon inelastic scattering

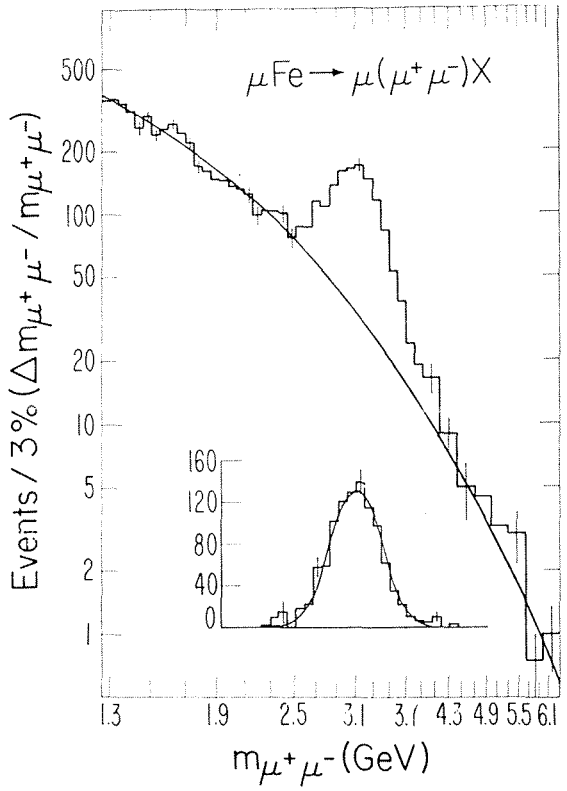

Fig. 29 The elastic dimuon mass spectrum for the BFP experiment

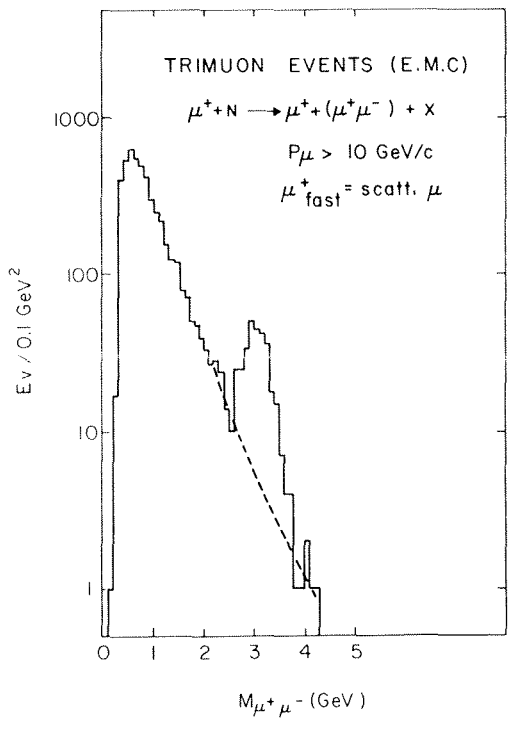

Fig. 30 The elastic dimuon mass spectrum for the EMC experiment

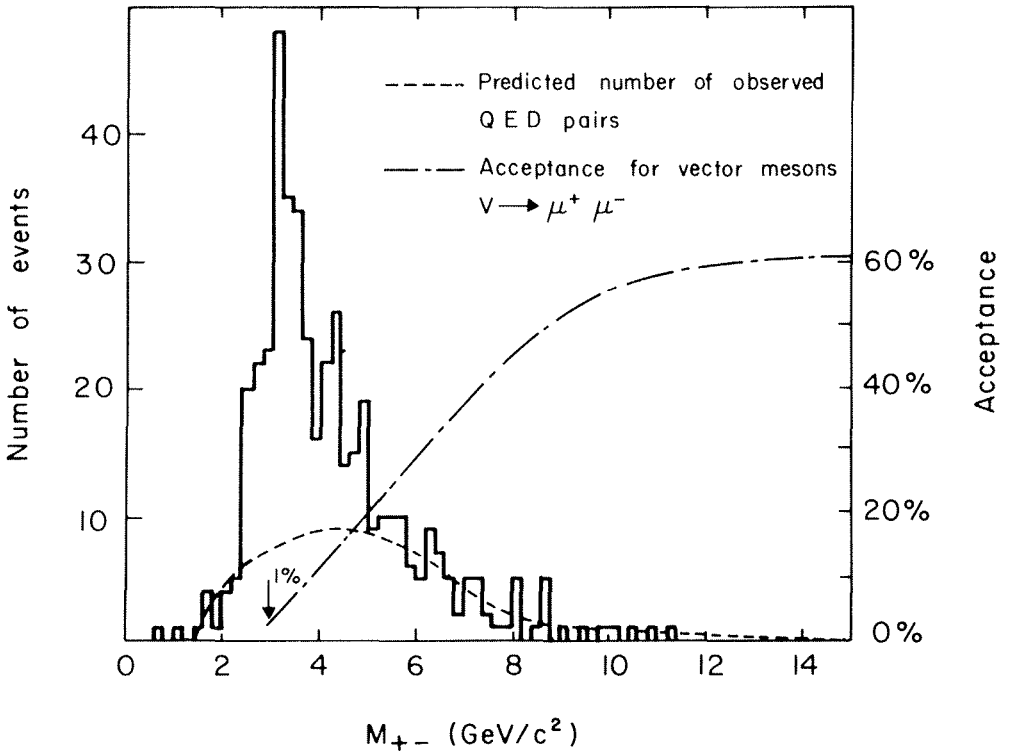

Fig. 31 The total dimuon mass spectrum for the BCDMS experiment

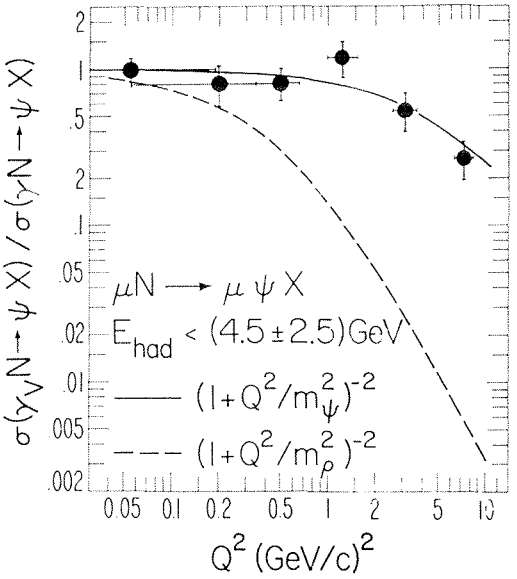

a) The Q^2 dependence of muon production of J/ψ for the BFP experiment

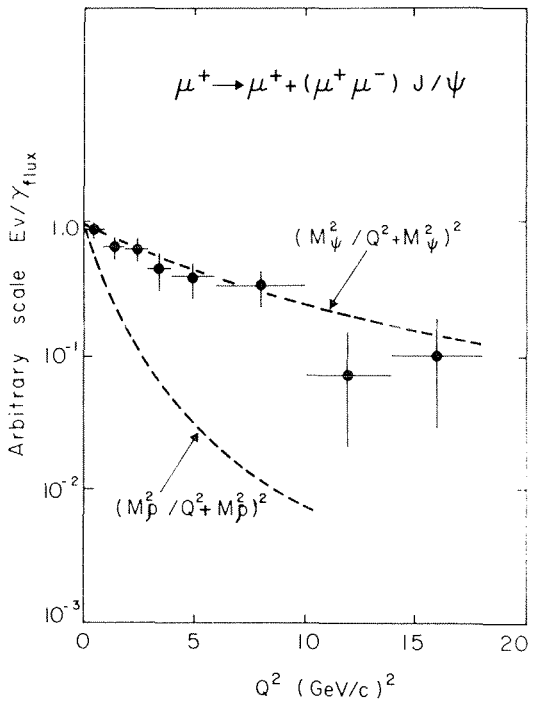

b) The Q^2 dependence of muon production of J/ψ for the EMC experiment

Fig. 32

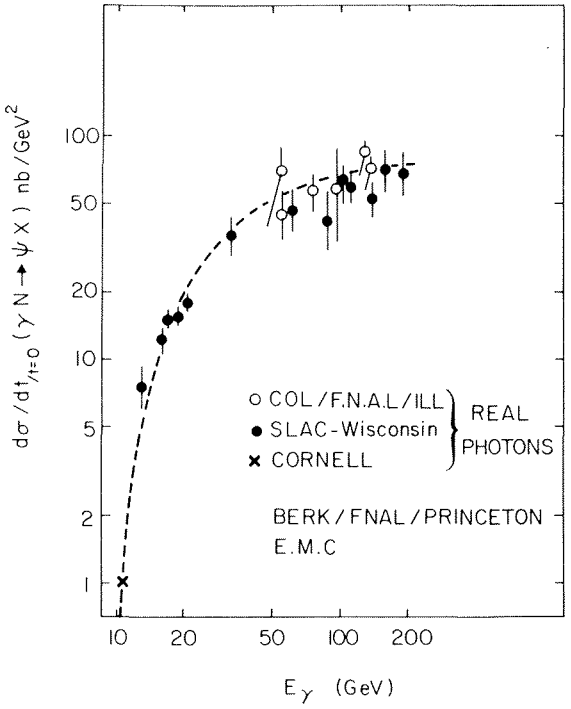

Fig. 33 The energy dependence of the J/ψ cross-section

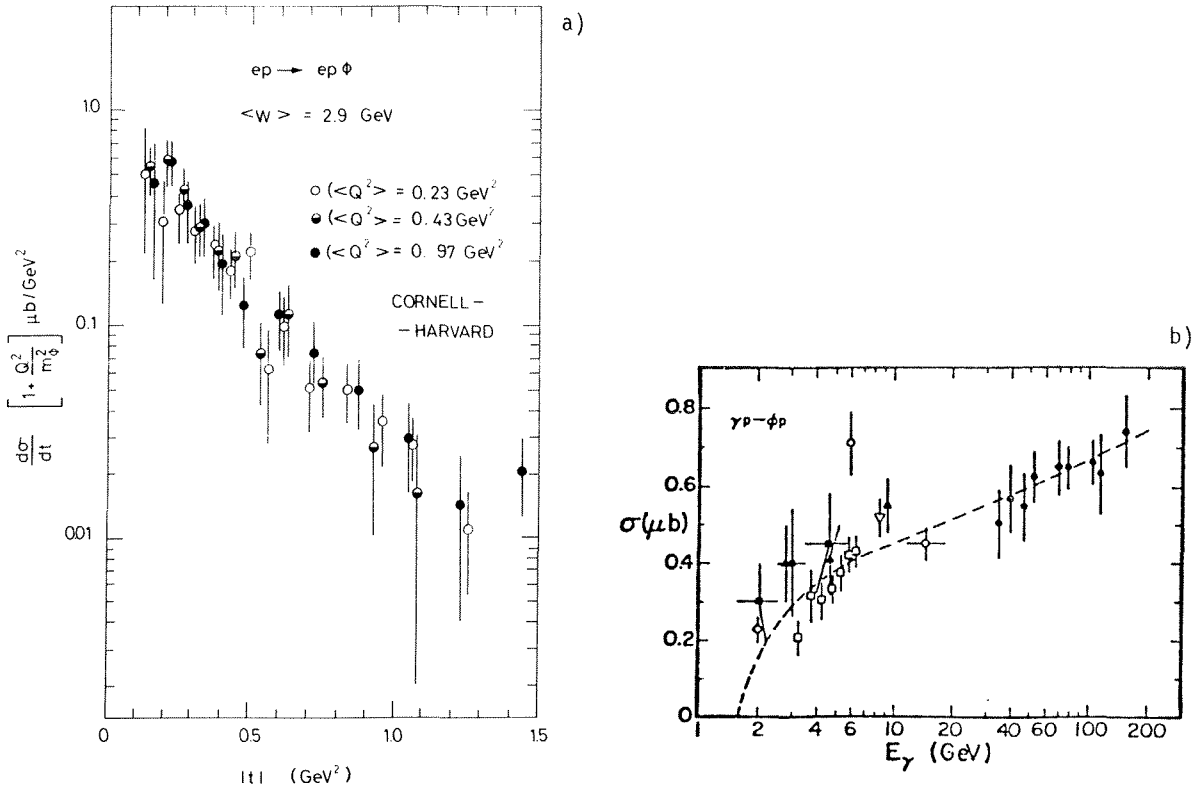

Fig. 34 a) The Q^2 dependence of the φ cross-section. b) The cross-section for φ photoproduction versus E_γ. For the references of experimental data, see Ref. 22.

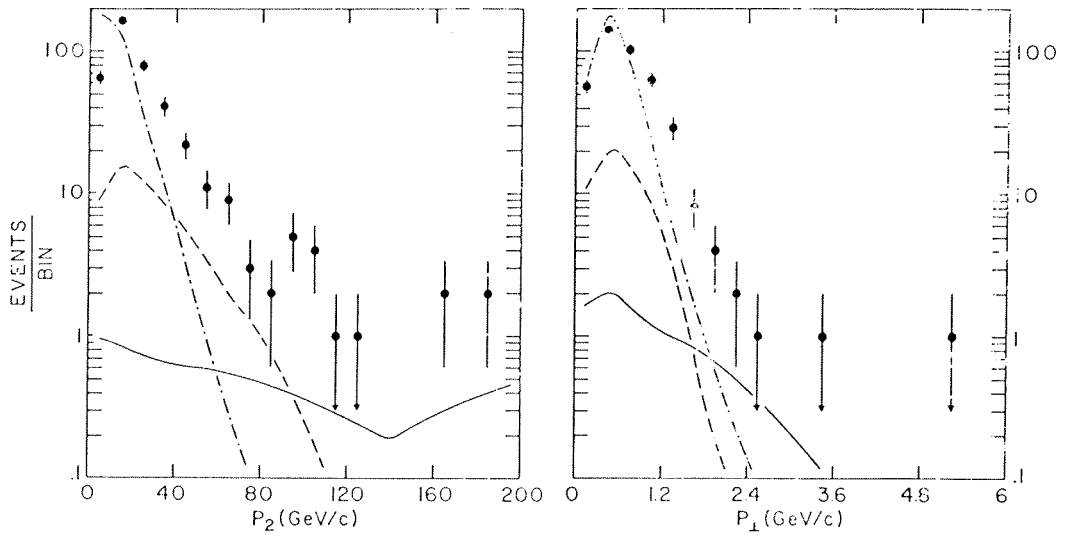

Fig. 35 The dimuon spectrum for the Michigan-FNAL experiment as a function of longitudinal and transverse momenta

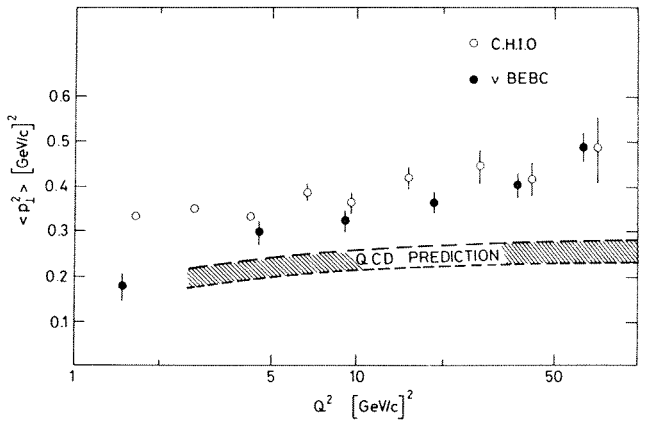

Fig. 36 The $\langle p_T^2 \rangle$ distribution versus Q^2 for hadrons in BEBC and CHIO

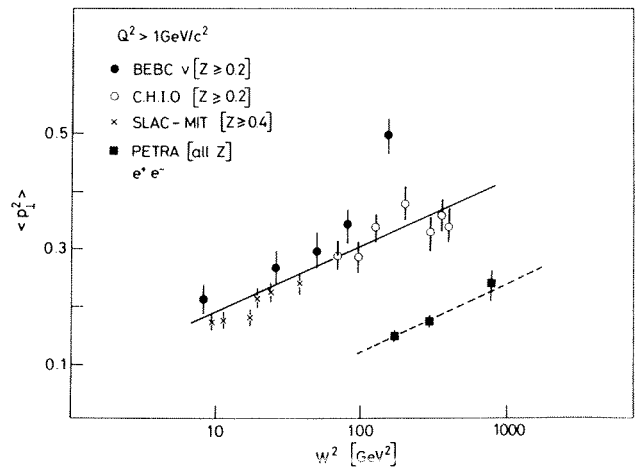

Fig. 37 The $\langle p_T^2 \rangle$ distribution versus W^2 for hadrons in electron and muon production, neutrino production, and e^+e^- collisions

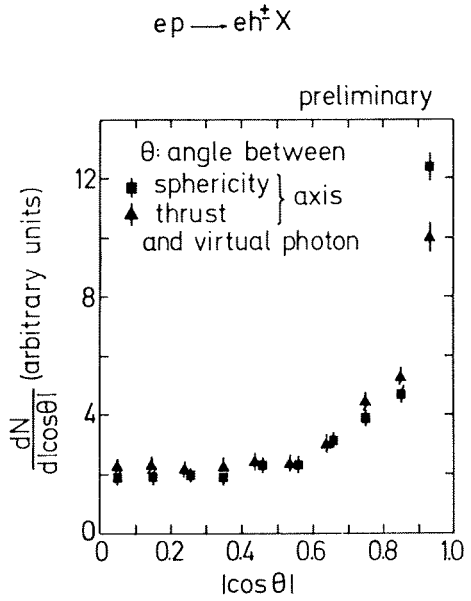

Fig. 38 The angular distribution in electroproduction (DECO) for the angle between the photon direction and the sphericity or thrust axis

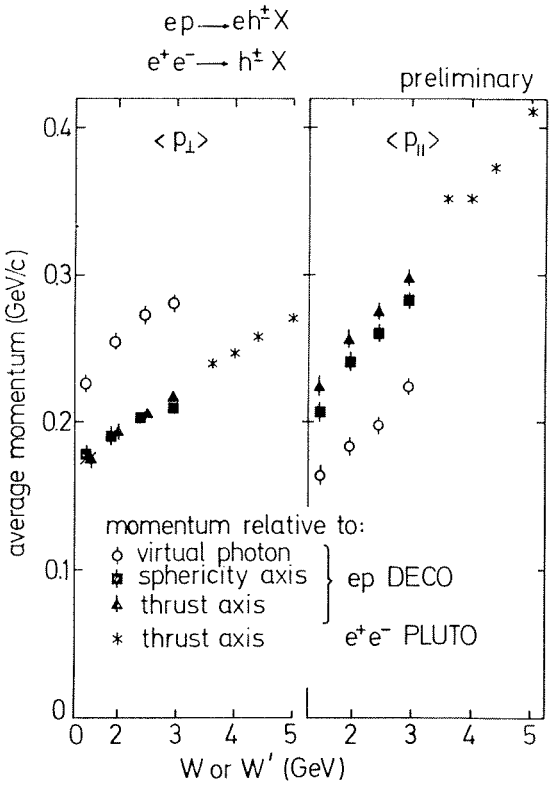

Fig. 39 The $\langle p_T \rangle$ and $\langle p_L \rangle$ dependence for hadrons in electroproduction (DECO) versus W, the c.m. hadronic energy

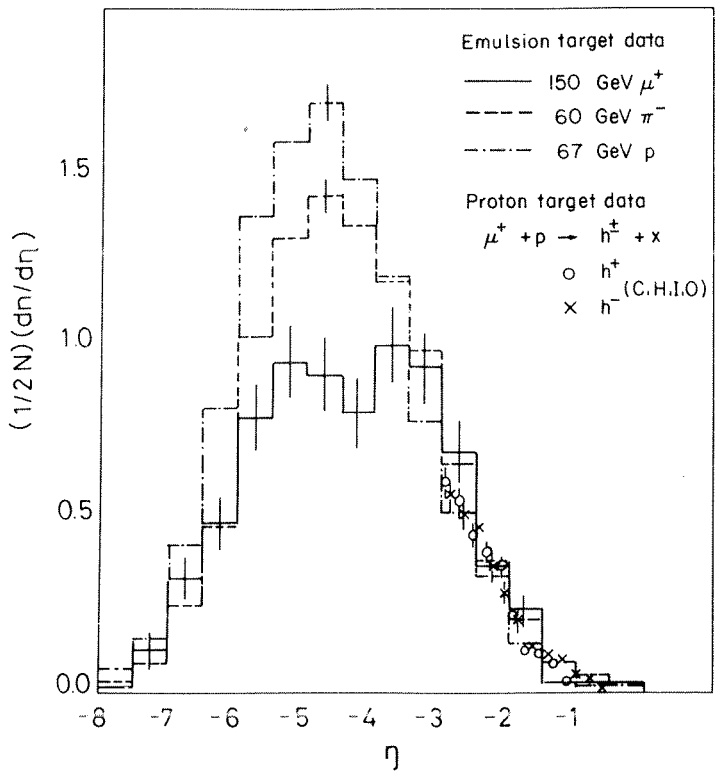

Fig. 40 The rapidity distribution for hadrons produced in emulsion by 140 GeV muons

DISCUSSION

Chairman: S.C.C. Ting

Sci. Secretaries: C. Best and H. Gennow

S.J. Brodsky (comment): As emphasized by a number of authors (e.g. Blankenbecler and Schmidt, Abbot and Barnett, Abbot et al.) effects from high twist terms can seriously affect the QCD analyses. In Okun's words, any fit which has logarithmic terms *only* will always set Λ^2 just where the power law effects are rapidly changing. Thus the "true" Λ^2 could be much smaller than the usually quoted values.

G. Preparata (comment): I would like to have your permission to show again the prediction from a "non-naive" approach to QCD (the Massive Quark Model), which illustrates that the BEBC and CDHS data can be explained without having to resort to two values of Λ.

Also I would like to point out that in our analysis (P. Castorina, G. Nardulli and G. Preparata) we predict larger scaling violations in μp than in μn, which is clearly indicated in the H_2 data you presented from the European Muon Collaboration.

P. Minkowski: I was confused by two different plots of $\langle p_T \rangle$ versus W (hadron energy): one seemed to show a logarithmic behaviour whereas the e^+e^- $\langle p_T \rangle$ analysis clearly indicates a linear dependence

$$\left\{ \langle p_T \rangle \propto \frac{\log W}{W} \right\}$$

Could you clarify this point?

E. Gabathuler: I plotted the data on a log scale to get it all in. Owing to the short lever arm for e^+e^- data you can fit it either linearly or logarithmically. The neutrino data would obviously prefer a linear dependence. Now if I look at the ep μp data then the best fit would be logarithmic but you still cannot rule out a linear fit. We have to extend the lever arm in W and get better precision.

N.S. Craigie: On the question of $R = \sigma_L/\sigma_T$, do I understand correctly that there is no indication of Λ/Q^2 effects or even the $1/\log Q^2$ effects predicted by QCD. Is this likely to be a question of experimental uncertainty or is it likely to be a real dynamical effect?

E. Gabathuler: I feel that if you really look into the data rather than do the experiment yourself it is hard to tell. A large amount of effort has been put into trying to compare all the data, and the points I showed in that table were in fact a summary of data taken at many different values of the polarization and there is a consistency in the data. I myself tend to believe that the data points are correct and we still have a lot of explaining to do as to why we are seeing this behaviour. R is very sensitive to many effects, particularly in the small x to large x transition region.

G. Barbiellini: Neutrino and muon data on deep inelastic scattering show some difference in σ_L/σ_T ratio, that you said could be explained in terms of some quark states in the nucleon. Do you know if this explanation will produce some other differences in neutrino and charged lepton deep inelastic scattering?

E. Gabathuler: I am not an expert on this but when I talked to Callan, who is, he told me that there is no reason why the neutrino value of R and the e/μ value of R should be the same. After all one is dealing with different currents. However, the agreement on F_2 looks remarkably good.

J. Soffer: From what we heard yesterday it seems that elastic form factors are important in the tests of QCD. Can we hope to have a better experimental determination of the proton elastic form factor in the near future?

E. Gabathuler: It is very hard to measure the elastic scattering much above 10 GeV incident energy at large Q^2. The question of whether one has to include the elastics or not in the moments analysis I think in some sense indicates that we still do not properly understand the systematic errors in all these experiments. Therefore, until one has a complete data set from a single experiment over a large Q^2 and x region from, say 3 GeV^2 to 100 GeV^2 with good precision, can one say whether effects of elastics should be included or not. There is a controversy here; some people say that elastics should be included as one is measuring the total cross-section, other people say what has an elastic cross-section got to do with deep-inelastic phenomena.

S.J. Brodsky: Form factors are very important tests of QCD since they directly test the scaling and spin dependence of internal qq interactions. In addition one can predict the power law behaviour of structure functions at fixed W^2, namely

$$\text{for } Q^2 >> W^2 \quad F_{2N} \sim (W^2/Q^2)^3$$

(modulo calculable logarithmic anomalous dimensions from the short distance nucleon wave-function). There are also many tests of QCD scaling behaviour and of the gluon spin which are reflected in the helicity dependence of meson and baryon form factors.

E. Gabathuler: Unfortunately like all of these tests the better the test the more difficult the experiment.

V.A. Khoze: Are the data on high-energy ϕ production in good quantitative agreement with the vector dominance model? And was the cross-section $\sigma_{tot}(\phi p)$ used in the comparison with data extracted from quark-model calculations?

E. Gabathuler: Yes, the agreement with vector dominance is very good. The dashed curve which I showed is a vector dominance fit. There is a slight question of normalization depending on which value of γ_ϕ^2 you use but if you just fit the over-all curve the agreement is very good.

E.L. Berger (comment): There are several physical effects which contribute to a non-zero value of $R = \sigma_L/\sigma_T$. These include:

1) QCD gluonic radiation effects which tend to generate a significant σ_L only at low x, falling as $1/\log Q^2$.
2) Constituent transverse momentum fluctuations (the "primordial" k_T effects), which yield a rather flat x dependence.
3) "Higher twist" effects in QCD associated in part with diquark substructure in the nucleon.

The higher twist effects grow with x at fixed Q^2, and fall with Q^2 as an inverse power. These higher twist diquark effects are discussed by Abbot, Berger, Blankenbecler and Kane in SLAC-PUB-2327, where additional tests are also proposed.

The different physical effects contributing to σ_L may be isolated by a detailed study of both the x and Q^2 dependences of the data.

LEPTON PAIR PRODUCTION IN HADRONIC COLLISIONS

G. Altarelli
Istituto di Fisica dell'Università - Roma
Istituto Nazionale di Fisica Nucleare, Sezione di Roma

1. INTRODUCTION

In this talk I shall briefly summarize our present understanding of lepton pair production in hadronic collisions. I shall limit my discussion to continuum production (i.e. for lack of time I shall not consider ψ and Υ production) and the main emphasis will be on recent progress with respect to the situation as it looked last year and was neatly reviewed by Lederman [1] at the Tokyo Conference.

Consider the inclusive production of a lepton-antilepton pair of total invariant mass Q in the collision of two hadrons H_1 and H_2 with total invariant mass $\sqrt{S}$. As usual one defines:

$$\tau = Q^2/S \tag{1}$$

The Drell-Yan [2] mechanism is the basis of our theoretical understanding of these processes in the deep inelastic region i.e. for $Q^2 \longrightarrow \infty$ with τ fixed. In this picture the lepton pair is produced via the pointlike, one photon, annihilation of a quark (antiquark) from H_1 and an antiquark (quark) from H_2. At the naive parton model level this corresponds to the simple Drell-Yan [2] formula:

$$Q^2\frac{d\sigma}{dQ^2} = \frac{4\pi\alpha^2}{3S}\frac{1}{3}\int\frac{dx_1dx_2}{x_1x_2}\left[\sum_i e_i^2\, q_i^{H_1}(x_1)\,\bar{q}_i(x_2) + 1\leftrightarrow 2\right]\delta\left(1-\frac{\tau}{x_1x_2}\right) \tag{2}$$

where the index i runs over flavors, $q_i^H(x)$ are the densities for a quark q_i with charge e_i in the hadron H, x is the fraction of longitudinal momentum carried by the quark, and a factor of $1/3$ arises from color. The cross section at fixed $X_F = 2P_L/\sqrt{S}$, where P_L is the total longitudinal momentum of the pair in the overall center of mass, is given by a simpler formula that reads:

$$\frac{d\sigma}{dQ\,dx_F} = \frac{8\pi\alpha^2}{3Q^3}\frac{1}{3}\left[\sum_i \frac{e_i^2}{x_1+x_2}\, q_i^{H_1}(x_1)\,\bar{q}_i^{H_2}(x_2) + 1\leftrightarrow 2\right] \tag{3}$$

$$x_{1,2} = \frac{1}{2}\left[\pm x_F + \sqrt{x_F^2+4\tau}\right] \tag{4}$$

Leaving for the moment aside all corrections that perturbative QCD im-

poses on eqs.(2,3) we stress that the validity of the Drell-Yan mechanism implies a number of striking signatures that all seem to be well supported by the available experimental evidence. We recall here the main tests of the Drell-Yan mechanism.

a) Intensity rules. We know from deep inelastic scattering that in the nucleon valence quarks are dominant over sea quarks especially at large x. We have no reasons to doubt that this ought to be true for hadrons other than the nucleon. Thus the Drell-Yan formula predicts much larger cross sections for processes where the lepton pair can be produced by valence-valence annihilation ($\pi^{\pm}$ N, K^{-}N, $\bar{P}$N) than processes where only valence-sea annihilations are possible (PN,K+N). This should be more and more true the larger is τ, because the bulk of the production arises at small X_F and at X_F=0 we have $X_{1,2}=\sqrt{\tau}$ as follows from eq.(4). Thus for large enough τ where the sea can be neglected we also expect for example (on isoscalar targets) $\sigma(\pi^{+}N(I=0))/\sigma(\pi^{-}N(I=0)) \cong 1/4$. New data on $\pi^{\pm}$, $K^{\pm}$ and $\bar{P}$ cross sections have been collected over the last year by the CIP collaboration [3] at FNAL and, at CERN, by the NA3 [4] and the Goliath [5] groups. Also new results obtained at CERN-ISR by the CCOR [6] and the R209 [7] collaborations were reported. Most of these new data have been presented at this conference for the first time and added new evidence to the above mentioned intensity rules. All of them appear to be quite well supported by the data.

b) Angular distribution of the leptons. On general grounds the angular distribution of the lepton in their center of mass for production through one photon exchange must be of the form:

$$\frac{d\sigma}{dQd\cos\theta} = W_T(Q)\left(1+\cos^2\theta\right) + W_L(Q)\sin^2\theta \qquad (5)$$

The Drell-Yan mechanism predicts the longitudinal component W_L to be absent because the quark spin is 1/2. For non vanishing transverse momentum of the pair there is some ambiguity in the choice of the reference axis that defines θ. Apart from detailed QCD effects [8)9)] this ambiguity can only be important at finite energies. In fact within the present error bars it makes no difference whether for example the Gottfried-Jackson (G.J.) or the Collins-Soper [10] (C.S.) definitions for the angle are adopted. The available data are in fair agreement with the expected angular distribution. New data have been presented. The results can be summarized by giving the measured value of λ obtained by fitting the observed angular distribution with a form $1+\lambda\cos^2\theta$. In πN collisions the reported values are (pion ener-

gies $\sim$ 200 GeV, $3.5 < Q < 9$ GeV)

CIP [3]	$\lambda = 1.30 \pm 0.23$	(C.S.)	
NA3 [4]	$\lambda = 0.80 \pm 0.16$	(G.J.)	(6)
	$= 0.85 \pm 0.17$	(C.S.)	

In PP collisions a value for λ was obtained at ISR by the R209 [5] collaboration:

$$\lambda = 1.6 \pm 0.7 \qquad \text{(C.S.)}$$

c) Atomic number dependence. Since the cross section is proportional to the number of quarks or antiquarks in the target one expects a linear A dependence in the Drell-Yan domain of validity. This is well supported by the data on PN collisions and to a lesser extent also for πN collisions. Precisely by introducing a parameter α defined from $\sigma \simeq A^{\alpha}$ one obtains (above the Ψ region):

CFS [11]	$\alpha = 1.02 \pm 0.018 \pm 0.059$	(P N)	
CIP [3]	$\alpha = 1.12 \pm 0.05$	(π N)	(8)
NA3 [4]	$\alpha = 1.02 \pm 0.03$	(π N)	

It is important in the following to keep in mind that taking $A^{1.12}$ as opposed to A^{1} makes a difference of about a factor of 2 when the cross section per nucleon is derived from data on a tungsten target, as is the case for the CIP experiment.

d) Approximate scaling. The adimensional quantity $Q^3 \frac{d\sigma}{dQ}$ can only be a function of τ in the naive parton limit. A rather good evidence in support of this approximate scaling law is obtained by comparing the FNAL data in the range $\sqrt{S} \simeq 20 \div 27$ GeV among themselves and with the ISR data at $\sqrt{S} \simeq 62$GeV. Unfortunately there is only a limited overlap in the τ ranges at FNAL and ISR. Further evidence for the approximate scaling law is obtained from the π-N data of CIP, NA3 and Goliath, provided of course the same A dependence is used.

We can therefore conclude that the Drell-Yan mechanism seems to be a firm starting point for the analysis of lepton pair production. As for other processes we think the naive parton model to be only a rough approximation, to be implemented with scaling violations and other effects that are computable if QCD is right.

2. THE PION STRUCTURE FUNCTION

I make at this point a digression to discuss the recent important results on the pion structure function as measured in lepton pair production from π beams. Three experimental groups have reported results on this. They are CIP [3] (FNAL) with about 2000 events analyzed from 225 GeV/c π^- on tungsten, NA3 [4] (CERN) with 8000 events on platinum from both π^- and π^+ at 200 GeV/c, plus over 3000 π^- at 280 GeV/c, Goliath [5] (CERN) with 500 events from π^- on berillium at 150 and 175 GeV/c. The measured values at different ν and X_F are analyzed in terms of eq.3 and the following quantity is determined for an array of different X_1 and X_2 values:

$$\sigma(x_1,x_2) = V_\pi(x_1)\,Q_N(x_2) + S_\pi(x_1)\,H_N(x_2) \qquad (9)$$

where $V_\pi(x)$ and $S_\pi(x)$ are the valence and the sea densities in the pion and $Q_N(x)$ and $H_N(x)$ are combinations of valence and sea distributions in the nucleon. CIP and Goliath neglect $S_\pi(x)$, while the π sea is also determined in the NA3 analysis that includes both π^- and π^+ results. The fitted forms for $V_\pi(x)$ are given by:

$$\begin{aligned}
&\text{NA3 [3]} && xV_\pi(x) \simeq x^{0.4\pm0.06}\,(1-x)^{0.90\pm0.06} \\
&\text{CIP [4]} && \simeq \sqrt{x}\,(1-x)^{1.27\pm0.06} \qquad (10) \\
&\text{Goliath [5]} && \simeq \sqrt{x}\,(1-x)^{1.56\pm0.18}
\end{aligned}$$

The above shapes obtained by the three groups are in fair agreement (the smaller exponent of (1-x) obtained by NA3 is compensated by the smaller exponent of X). We shall discuss the important issue of normalization later in this talk. The sea distribution obtained by NA3 is given by

$$xS_\pi(x) \simeq (0.09\pm0.06)\,(1-x)^{4.4\pm1.9} \qquad (11)$$

which confirms the expectations that the sea in the pion is of the same order as in the nucleon. The flatter x dependence of the π sea in comparison with the nucleon sea is also reasonable in view of the similar difference in the valence x distributions.

On the theoretical side an interesting prediction for the behavior of the π structure function near x=1 was made by Berger and Brodsky [12]. On the same lines as for the quark counting rules [13], they make a QCD model for the higher twist operators that we know must be important in the region near x=1. In this limit almost all of the π momentum is carried by one of

its constituent quarks (all non valence parton densities can be neglected near x=1). That requires a large momentum transfer between the two constituent legs. It is argued that this interaction is well approximated by a single hard gluon exchange. Neglecting all normal gluon radiative corrections that lead to scaling violations (which however may be large near x=1), the resulting predictions for the lepton pair cross section near x=1 is of the form:

$$\sigma_{\ell^+\ell^-} \simeq (1-x)^2 (1+\cos^2\theta) + \frac{4}{9} \frac{\langle k_T^2 \rangle}{Q^2} \sin^2\theta \qquad (12)$$

It has been checked by the CIP [14] collaboration that eq.(12) provides a good fit to the data on the π structure function for $x > 0.5$ with $\langle k_T^2 \rangle = 1.1 \pm 0.2$ (GeV/c)^2. Also clear evidence is indicated by the data[14] for the predicted shift of the angular distribution toward a $\sin^2\theta$ angular dependence near x=1. This is not in contradiction with the previously mentioned test of the Drell-Yan mechanism which predicts $1+\cos^2\theta$, because only a small fraction of events is at large values of X_F.

3. QCD EFFECTS IN DRELL-YAN PROCESSES

We have seen that the Drell-Yan formula is well supported by the data at the naive parton model level. We now consider the corrections to it implied by our present understanding of QCD [15] and the related tests that can be checked in the data.

The first of these effects is the replacement in the Drell-Yan formula of the scaling quark densities with effective Q^2 dependent densities. These are the same as in leptoproduction and satisfy the same Q^2 evolution equations in spite of q^2 being spacelike in one process and timelike in the other. Thus in the leading approximation in QCD (i.e. when additional terms of order $\alpha_s(Q^2)$ can be neglected as well as terms down by powers of Q^2) the Drell-Yan formula is replaced by:

$$Q^2 \frac{d\sigma}{dQ^2} = \frac{4\pi\alpha^2}{3S} \frac{1}{3} \int \frac{dx_1 dx_2}{x_1 x_2} \left[\sum_i e_i^2 q_i^{H_1}(x_1, Q^2) \bar{q}_i^{H_2}(x_2, Q^2) + 1 \leftrightarrow 2 \right] \delta\left(1 - \frac{\tau}{x_1 x_2}\right) + O\left(\alpha_s^2(Q^2)\right) \qquad (13)$$

This is a consequence of a general factorization theorem [16] that was recently extended by diagrammatic techniques also to processes where the operator expansion method [17] cannot be applied.

The available data are not precise enough to establish the existence

of the predicted scaling violations directly. Some indirect evidence is obtained by analyzing the PN data in the FNAL energy range [1]. If the nuclear structure function as measured at a fixed value of Q^2 ($Q^2 \simeq 10 GeV^2$) is taken as an input then the resulting sea distribution that one obtains by fitting the data with the Drell-Yan formula is definitely steeper in X than the sea distribution as measured in leptoproduction. Typically one obtains [1] $(1-x)^n$ with $n \simeq 10$. On the other hand, by using as an input $F_2(x,Q^2)$ as measured in leptoproduction Q^2 by Q^2, then the sea x dependence turns out to be $S(x) \simeq (1-x)^{8.5 \pm 0.1}$ (in the SU(3) symmetric case) in fair agreement with the CDHS extimate of $(1-x)^{8.4 \pm 0.7}$ from ν scattering [18].

A more practical way of detecting a sign of QCD effects is provided by a study of the transverse momentum distribution of the lepton pairs. Most of the lepton pairs are produced with small transverse momentum together with two hadronic jets opposite in momentum arising from the fragments of the two incoming hadrons. However a small fraction of events of order $\alpha_s(Q^2)/\pi$ should contain a pair with large $P_\perp \sim \sqrt{Q^2}$ with three accompanying hadronic jets, i.e. the two hadron fragmentation jets plus a third parton jet. These events arise from the possibility that the incoming quark or antiquark radiates a hard gluon with large $p_\perp$ before annihilating. Alternatively a quark or antiquark may interact with a gluon from the other hadron to produce a massive photon and a final, high $p_\perp$, quark or antiquark. Notice that the lepton pair directly measures the sum of the transverse momenta of the interacting partons. So the actual $P_\perp$ distribution is a superposition of the intrinsic $P_\perp$ distribution of the partons inside the hadrons and of gluon effects including a long tail (up to $P_\perp \sim Q$) arising from hard parton interactions. The tail of $\frac{d\sigma}{dP_\perp^2}$ can be computed [19] in perturbation theory and it behaves at large $P_\perp$ as $1/P_\perp^2$. It is precisely this same effect that leads to the scaling violations in the cross section. We understand that its importance is enhanced if we look at the average $P_\perp$ ($\langle P_\perp \rangle$) or better at higher $P_\perp$ moments. A general and unambiguous prediction of QCD in the increase [19] of $\langle P_\perp \rangle$ with energy at fixed τ :

$$\langle P_\perp \rangle = \alpha_s(Q^2)\sqrt{S} \int (\tau, \alpha_s(Q^2)) + \text{CONST.} \qquad (14)$$

The linearly rising term is computable in perturbation theory while the constant term is affected by wave function effects from the intrinsic $P_\perp$ and is mainly non perturbative.

The available data on PN collisions for $\langle P_\perp \rangle$ are shown in Fig.1. Notice that at fixed S the dependence of $\langle P_\perp \rangle$ with Q is flat at not

too small Q. That is no evidence against eq.(14) because a meaningful comparison independent of the shape of $f(\tau,\alpha_s)$ (apart from the log dependence on Q^2 though $\alpha_s(Q^2)$) must be done at fixed τ. It is clear for example that at $\tau = 0$ and $\tau = 1$ $\langle p_\perp \rangle$ must go to zero because of phase space, and therefore $f(\tau,\alpha_s)$ cannot be monotonic. The τ value of the ISR point at the highest Q is the same as the points at FNAL energies for $Q \simeq 4 \div 5$ GeV. If we take advantage of the empirical flatness of $\langle p_\perp \rangle$ in τ at fixed S for making some averaging in τ, we obtain a plot as in Fig.2 for the observed rise of $\langle p_\perp \rangle$ with energy. The observed slope is well consistent with theoretical estimates [20] within the uncertainties in the calculation due to the lack of knowledge of the gluon density, the ambiguity on the value of α_s ($\alpha_s(Q^2)$, $\alpha_s(S)$ etc.), the non leading terms. All this taken into account the increase of $\langle p_\perp \rangle$ with $\sqrt{S}$ appears to be the clearest evidence so far for QCD effects in Drell-Yan processes.

A more difficult theoretical problem is the prediction of $\frac{d\sigma}{dp_\perp^2}$ at smaller $p_\perp$. An important step in this direction was achieved by extending the calculable domain from the case of a single large scale (i.e. $p_\perp^2 \sim Q^2$) to the case of two large scales ($M^2 \ll p_\perp^2 \ll Q^2$). This involves keeping track to all orders of terms in $\log p_\perp^2/Q^2$ that could be neglected in the previous case. The result is the famous DDT formula [21]:

$$\frac{Q^2 d\sigma}{dQ^2 dp_\perp^2 dy} = \frac{4\pi\alpha^2}{9S} \frac{1}{p_\perp^2} \frac{\partial}{\partial \ln p_\perp^2} \sum_i \left[e_i^2 q_i^{H_1}(x_1, p_\perp^2) \bar{q}_i^{H_2}(x_2, p_\perp^2) + 1 \leftrightarrow 2 \right] T^2\left(\frac{Q^2}{p_\perp^2}\right) \qquad (15)$$

with

$$T(\lambda) = \int_1^z dz \exp - \frac{1}{z^2} \frac{2}{3\pi} \alpha_s \ln \lambda \qquad (16)$$

In the available data the applicability of this formula is only marginal due to the limited Q and $p_\perp$ range explored so far. Actually perhaps the most important quantitative difference in practice is the realization that the use of $\alpha_s(p_\perp^2)$ rather than $\alpha_s(Q^2)$ is more appropriate in the calculation of the $p_\perp$ moments. The result is a reduction of the amount of intrinsic $p_\perp$ needed to reproduce the actual distribution [22]. Last year it was thought to be around $p_\perp \sim 600$ MeV (intrinsic per parton). Now it is considerably lower [22]: $p_\perp \sim 400$ MeV.

We now turn to a third effect of QCD that has to do with the calculation of non leading corrections. In eq.(13) all terms down by a power of $\alpha_s(Q^2)$ were neglected. To evaluate the first order corrections it is pre-

liminarly necessary to precisely specify what we mean by quark densities. This can be done [23] by specifying that the quark densities are to be measured from the structure function F_2 in leptoproduction. That is F_2 is related to the quark densities by the familiar parton formula valid by definition with no corrections of order $\alpha_s(Q^2)$. The advantage of choosing F_2 as a standard is that it turns out that quark densities so defined satisfy [13] the valence sum rules:

$$\int_0^1 dx \left[u(x,Q^2) - \bar{u}(x,Q^2) \right] = 2 \tag{17}$$

etc., with no corrections of order $\alpha_s(Q^2)$. Once the quark densities are so defined one can compute in a non ambiguous way the corrections of order $\alpha_s(Q^2)$ to the parton formulae for all other processes. In the Drell-Yan case the improved formula is as follows: [23)24)25)]

$$Q^2 \frac{d\sigma}{dQ^2} = \frac{4\pi\alpha^2}{9S} \int \frac{dx_1 dx_2}{x_1 x_2} \left\{ \left[\sum_i e_i^2 q_i^{H_1}(x_1,Q^2)\, \bar{q}_i^{H_2}(x_2,Q^2) + 1 \leftrightarrow 2 \right] \left[\delta(1-z) + \right.\right.$$

$$\left.\left. + \alpha_s(Q^2)\, \theta(1-z)\, f_q(z) \right] + \left[\frac{1}{x_1} F_2^{H_1}(x_1,Q^2)\, G^{H_2}(x_2,Q^2) + 1 \leftrightarrow 2 \right] \alpha_s(Q^2)\, \theta(1-z)\, f_G(z) \right\} \tag{18}$$

where $z = \frac{\tau}{x_1 x_2}$, $F_2^H(x,Q^2) = x \sum_i e_i^2 \left[q_i^H(x,Q^2) + \bar{q}_i^H(x,Q^2) \right]$ and

$$\alpha_s f_q(z) = \frac{4}{3} \frac{\alpha_s}{2\pi} \left[\left(1 + \frac{4\pi^2}{3} \right) \delta(1-z) + 2(1+z^2) \left(\frac{\ln 1-z}{1-z} \right)_+ + \frac{3}{1-z_+} - 6 - 4z \right]$$

$$\alpha_s f_G(z) = \frac{1}{2} \frac{\alpha_s}{2\pi} \left[\left(z^2 + (1-z)^2 \right) \ln(1-z) + \frac{8}{2} z^2 - 5z + \frac{3}{2} \right] \tag{19}$$

It turns out that the gluon correction is normal, i.e. it can be neglected at not too larger values of τ in all processes where the quark term is of valence-valence type, while it makes a non negligible correction for valence-sea processes [23)26)]. On the other hand the quark correction is quite large at present energies with currently accepted values for $\alpha_s(Q^2)$. The most dangerous term is the δ function term that renormalizes the point like cross section. It arises mainly from the continuation from spacelike q^2 in leptoproduction to timelike q^2 in Drell-Yan processes. The other terms in f_q are rapidly increasing with τ and arise from the difference in

phase space between leptoproduction (the heavy photon in the initial state) and Drell-Yan processes (the heavy photon in the final state). The situation is summarized in Fig.3 for πN collisions at $\sqrt{S} \simeq 21$ GeV. The gluon correction is in this case negligible and it is not displayed. It is important to notice that in the τ range of the data the result amounts essentially to a large change in the over all normalization in the cross section in excess with respect to the naive prediction. Of course being the first order correction so large we cannot trust the present approximation beyond a semi quantitative level.

Note that all tests of the Drell-Yan mechanism discussed in the first part of this talk are essentially unaffected by the above results. In fact the predictions of a linear A dependence, approximate scaling, linear rise of $\langle P_\perp \rangle$ at fixed τ are not changed. The intensity rules are not qualitatively altered. Also the $1+\cos^2\theta$ angular distribution is not changed, because it turns out that the large corrective terms are not in the longitudinal part but only in the transverse part.

In view of this large non leading terms it is interesting to inquire whether the experiments allow to draw some conclusion on the measured scale of the cross section in comparison with the prediction of the naive Drell-Yan formula. It is remarkable that actually there are consistent indications in the data for a cross section larger than expected. We consider first the new data on πN collisions. Let us introduce a scale factor defined as

$$\left(\frac{d\sigma}{dQ^2}\right)_{EXP} = K \left(\frac{d\sigma}{dQ^2}\right)_{NAIVE\ D.Y.} \tag{20}$$

The parton densities can be normalized by requiring the validity of the valence sum rules:

$$\int_0^1 V_\pi(x)\, dx = 1 \tag{21}$$

for the pion and similarly for the nucleon (see eq.(17)). Then the situation appear to be as follows. The Goliath group takes the nucleon structure functions from Buras-Gaemers [27] and obtains $K \simeq 3$. The NA3 [4] collaboration finds $K \simeq 2.2 \div 2.5$ if the CDHS [18] nucleon densities are taken and $K \simeq 1.4$ if they take the nucleon densities from their own fit (which however contains a large sea component, so that only 20÷30 % of the momentum is left for gluons in the nucleon). The CIP [3] collaboration finds $K \simeq 1$ if the cross section per nucleon is extracted from the data on tungsten by using the measured $A^{1.12}$ dependence. That means they would end up with

$K \simeq 2$ for a linear A dependence.

Finally in PN collisions we learn from refs.(1,11) that the CFS group finds the amount of sea required to fit the Drell-Yan data to correspond to a fraction of momentum as high as 6% (per species). In ν scattering CDHS[18] only finds about 2.5 %. This is also illustrated by a study of Berger[28] who compares at correspondent values of Q^2 and x the CDHS sea with the Drell-Yan sea. In the overlap region a discrepancy of about a factor of two is observed (see Fig.4).

Note that the predicted departures from the naive Drell-Yan formula should dramatically increase when τ approaches 1, where prominent factorization breaking effects should also be present. Finally we recall that instanton effects are also possibly dangerous for the Drell-Yan picture[29].

4. CONCLUSIONS

The data accumulated so far are enough to conclude that the Drell-Yan mechanism for leptoproduction appears to be physically correct. The problem is now to go beyond the naive parton model and establish or disproof the presence of the departures from this first approximation as predicted by QCD. The only reasonably verified signature so far is the rise of $\langle P_\perp \rangle$ with $\sqrt{s}$ at fixed τ. The normalization issue seems to be a crucial point to be checked. πN collisions are promising in this respect, but the problem of the A dependence must be settled before one can derive firm conclusions.

I think it is clear by now that a solid confirmation of QCD can only arise from a patient work exploring at the same time different processes where the same basic quark gluon interactions are at work. In this respect Drell-Yan processes will play an important role.

* * *

REFERENCES

1) L.M.Lederman, Proc. XIX International Conference on High Energy Physics, Tokyo, 1978.

2) S.D.Drell, T.M.Yan, Phys.Rev.Letters 25, 316 (1970), Annals of Physics 66, 578 (1971).

3) CIP collaboration: K.J.Anderson et al., Phys.Rev.Letters 42, 944 (1979); G.E.Hogan et al., ibidem 948; C.B.Newman et al., ibidem 951.

4) NA3 collaboration: presented by G.Matthiae and Ph.Miné, These Proceedings; J.Badier et al., papers presented at this Conference.

5) Goliath collaboration, presented by R.Heinz, these Proceedings, M.A.Abolins et al., papers presented at this Conference.

6) CCOR collaboration, presented by S.H.Pordes, these Proceedings.

7) R209 collaboration, presented by U.Becker, these Proceedings.

8) K.Kajantie, J.Linfors, R.Raitio, Phys.Letters 74B, 384 (1978).

9) J.Cleymans, M.Kuroda, Phys.Letters 80B, 385 (1979); J.C.Collins, Phys. Rev.Letters 42, 291 (1979).

10) J.C.Collins, D.E.Soper, Phys.Rev. D16, 2219 (1977).

11) CFS collaboration, J.K.Yoh et al., Phys.Rev.Letters 41, 684 (1978).

12) E.L.Berger, S.J.Brodsky, Phys.Letters 42, 940 (1979).

13) S.J.Brodsky, G.R.Farrar, Phys.Rev.Letters 31, 1153 (1973) and Phys.Rev. 11D, 1309 (1975); V.A.Matveev, R.M.Muradyan, A.N.Tavkhelidze, Lett.Nuovo Cimento 7, 719 (1973);Z.F.Ezawa, Nuovo Cimento 23A, 271 (1974); G.R.Farrar, D.R.Jackson, Phys.Rev.Letters 35, 1416 (1975), see also A.I. Veinshtain, V.I. Zacharov, Phys.Letters 72B, 368 (1978).

14) K.J.Anderson et al., presented at this Conference by J.E.Pilcher.

15) For reviews see: H.D.Politzer, Phys.Reports 14C, 129 (1974); W.Marciano, H.Pagels, Phys.Reports 36C, 137 (1978); G.Altarelli, Proceedings of the 1978 Advanced Summer Institute on New Phenomena in Lepton Hadron Physics, Karlsruhe, Germany, 1978. Rome preprint n.132 (1979).

16) C.H.Llewellyn Smith, Talk at the "XVII Internationale Universität-swochen für Kernphysik", Schladming, Austria, 1978; Oxford Preprint (47/78).
Yu.L.Dokshitser, D.I.D'yakanov and S.I.Troyan, "Hard Semi-Inclusive Processes in QCD", Leningrad Preprint and Proceedings of the 13th Leningrad Winter School (1978), available in English as SLAC Trans.-183.
D.Amati, R.Petronzio and G.Veneziano, Nucl.Phys. and CERN Preprint TH-2527 (1978).
R.K.Ellis, H.Georgi, M.Machacek, H.D.Politzer and G.C.Ross,Phys.Lett.78B, 281 (1978) and Nucl.Phys. B152, 285 (1979).
G.Sterman and S.Libby, Stony Brook Preprint ITP SB78-41, 42 (1978).
G.Sterman, Phys.Rev. D17, 2773, 2789 (1978).
A.H.Mueller, Columbia Univ. Preprint CU-TP-125 (1978).
W.R.Frazer, J.F.Gunion, Univ. of Calif. at Davis, Preprint 78/3 (1978).

17) H.Georgi, H.D.Politzer, Phys.Rev. D9, 129 (1974); D.J.Gross, F.Wilczek, ibidem 980.

18) CDHS collaboration, J.G.H. de Groot et al., Zeitschrift fur Physik C1, 143 (1979).

19) I.Hinchliffe, C.H.Llewellyn Smith, Physics Letters 66B, 281 (1977); A.V.Radyushkin, Phys.Letters 69B, 245 (1977); G.Altarelli, G.Parisi, R. Petronzio, Physics Letters 76B, 351,356 (1978).

20) K.Kajantie, R.Raitio, Nucl.Physics B139, 72 (1978); K.Kajantie, J.Lindfors, R.Raitio, Phys.Letters 74B, 384 (1978); H.Fritzsch, P.Minkowski, Physics Letters 73B, 80 (1978); F.Halzen, D.Scott, Phys.Rev. Letters 40, 1117 (1978); E.L.Berger, Argonne Preprint ANL-HEP-PR-78-12.

21) Y.L.Dokshitzer, D.I. D'yakonov, S.I.Troyan, Phys.Letters 78B, 290 (1978).

22) K.Kajantie, J.Lindfors, Helsinki University, Preprint HU-TFT 78-33. G.Parisi, R.Petronzio, CERN Preprint TH 2627 (1979).

23) J.Kubar-André, F.E.Paige, Phys.Rev. D19, 221 (1979); G.Altarelli, R.K. Ellis, G.Martinelli, Nucl.Physics B143, 521 (1978), E B146,544 (1978), MIT Preprint CTP-776-March 1979 (Nuclear Physics in press).

24) K.Haroda, T.Taneko, N.Sakai; CERN Preprint TH 2619 (1979) and Erratum.

25) B.Humpert, W.L. van Neerven CERN Preprint 2654 (1979). The claim is made in this paper that ambiguities may arise for off shell quarks.

26) A.P.Contogouris, J.Kripfganz, McGill Preprint (1978).

27) A.J.Buras, K.J.F. Gaemers, Nucl.Phys. B132, 249 (1978).

28) E.L.Berger, SLAC-PUB-2314 (1979).

29) J.Ellis, M.K.Gaillard, W.J.Zakrzewski, Phys.Letters 81B, 224 (1979).

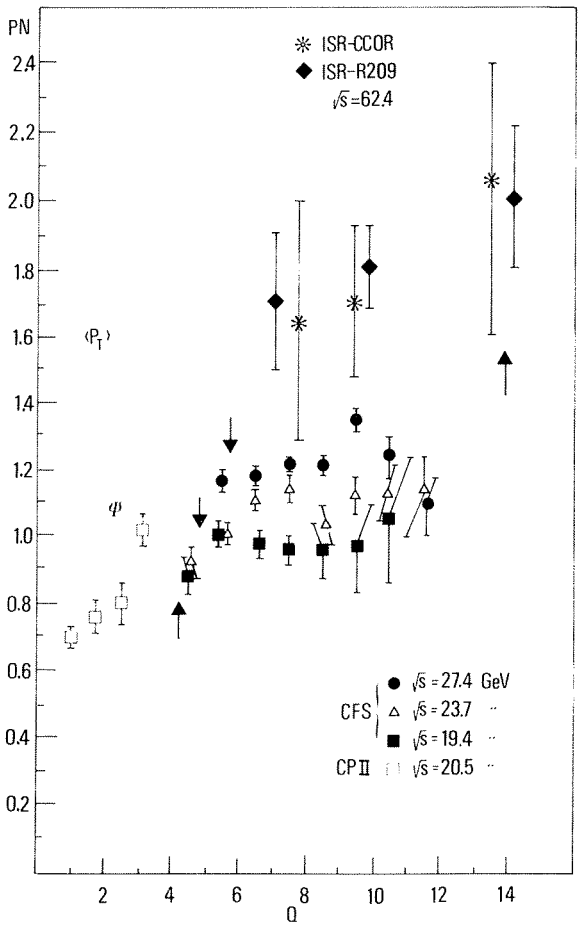

Fig. 1 Average $\langle P_\perp \rangle$ for PN lepton pair production. The arrows indicate points with same τ.

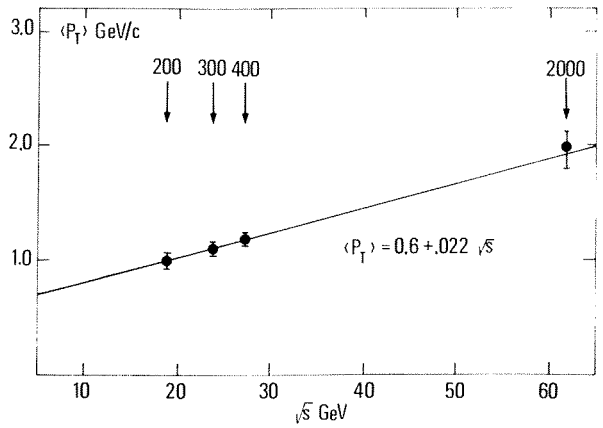

Fig. 2 Average $\langle P_\perp \rangle$ VS $\sqrt{S}$. The point at $\sqrt{S}$ = 62 is from ISR CCOR and R209 collaborations.

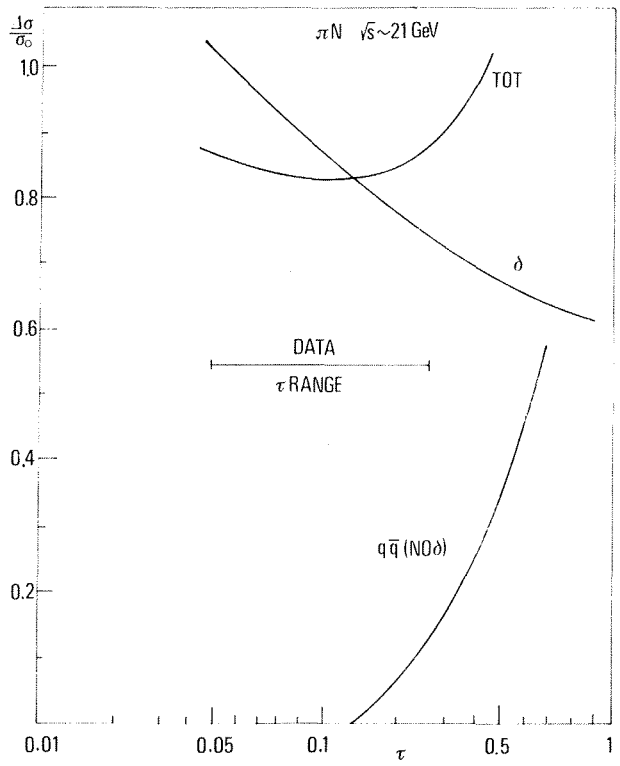

Fig. 3 Effect of non leading corrections to the π^-N cross section. A similar result also holds for PN collisions.

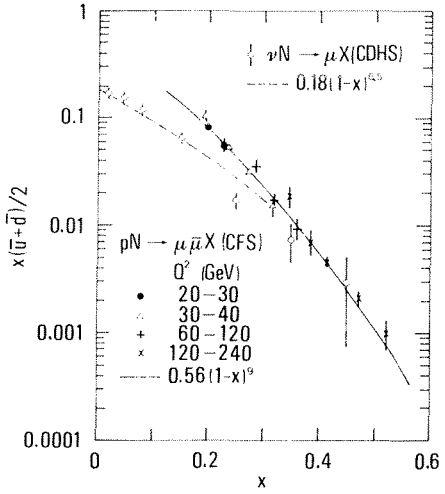

Fig. 4 The sea from ν scattering VS the sea extracted from PN Drell-Yan processes. At same values of x and Q^2 we note a factor two discrepancy. (Figure taken from ref. 28.)

DISCUSSION

Chairman: S.C.C. Ting

Sci. Secretaries: C. Best and H. Gennow

E.L. Berger: For the next to leading $1/\log Q^2$ corrections to the Drell-Yan formula, do the corrections due to the initial $g + q$ diagrams dominate, or are the $q\bar{q}$ diagrams more significant? I am thinking of the possibility of subtracting π^+N from π^-N cross-sections to remove the higher order, non-leading $1/\log Q^2$ terms. If the qq set wins, this subtraction could be motivated.

G. Altarelli: In general the gluon term is completely negligible for valence dominated processes unless you go to very large τ.

R.C. Hwa: A year ago CP data showed no significant dependence of $\langle p_T \rangle_{\mu^+\mu^-}$ on x_F. That ruled out QCD contributions as an important effect because the large p_T of $\mu^+\mu^-$ accompanied by a gluon recoil in $q+q \to (\mu^+\mu^-) + g$ should be seen mainly at low x_F, not large x_F. Have the data changed since then at higher energies?

G. Altarelli: No, the data did not change at that energy.

A. Bodek: Do you see any mechanism for making the Drell-Yan cross-section bigger than $A^{1.0}$? Normally an A-dependence bigger than 1.0 can be obtained by multiple scattering of the final state. However, here the final state is two muons. Interaction of the initial state hadron in the nucleus, losing energy and re-interacting again tends to make the A-dependence smaller than 1.0.

G. Altarelli: Well, the final state is not only leptons, there are also hadron fragments which could contribute. I do not know however of any detailed theory for an A-dependence.

S.J. Brodsky: Regarding the A-dependence of the massive lepton-pair cross-section: an effect that seems reasonable physically is that one expects the incoming hadron to lose energy in the nucleus by standard particle production (Glauber) processes. The energy loss and rearrangement of the Fock space of the incident hadron before the $q\bar{q}$ annihilation evidently destroys simple factorization arguments. Should not such effects be taken into account at some level?

G. Altarelli: I would not be so impressed by finding $A^{1.12}$. I only pointed out this fact because it is very important for knowing our cross-sections per nucleon. I would not expect more than, say, a 10% departure from a linear A-dependence because otherwise I would conclude that the parton model cannot be the full story, since the cross-section is not proportional to the number of partons you have around. So if you see a large effect, this is not impossible to imagine, but certainly a blow against the parton approach.

The experimental evidence is contradictory because from proton beams we would say it is perfectly linear. From pion-nucleus collisions there is contradictory evidence from different groups, so the situation is more confused on a measurement point level than for theory to worry about.

DIRECT PRODUCTION OF SINGLE PHOTONS AT THE CERN INTERSECTING STORAGE RINGS

Athens-Athens-Brookhaven-CERN Collaboration

M. Diakonou, C. Kourkoumelis and L.K. Resvanis
University of Athens, Athens, Greece.

T.A. Filippas, E. Fokitis and C. Trakkas
National Technical University, Athens, Greece.

A.M. Cnops, J.H. Cobb[1], E.C. Fowler[2], D.M. Hood[3], S. Iwata[4], R.B. Palmer, D.C. Rahm, P. Rehak and I. Stumer
Brookhaven National Laboratory[5], Upton, NY, USA.

C.W. Fabjan, T. Fields[6], D. Lissauer[7], I. Mannelli[8], W. Molzon, P. Mouzourakis, K. Nakamura[9], A. Nappi[8] and W.J. Willis
CERN, Geneva, Switzerland.

(Presented by C.W. Fabjan)

ABSTRACT

Single-photon production in pp collisions at $30 < \sqrt{s} < 62$ GeV has been measured with liquid-argon/lead calorimeters at the CERN ISR. This process, indicative of direct constituent interaction, remains approximately constant with increasing $\sqrt{s}$. For fixed $\sqrt{s}$, the single-photon to π^0 ratio increases strongly with increase in p_T; γ/π^0 is 0.25 ± 0.08 at $5.0 < p_T < 6.5$ GeV/c for these interactions.

1. INTRODUCTION

Hadron-induced production of single photons has been investigated rather extensively in recent years, both experimentally and theoretically. Early interest in these studies was partly motivated by the conjecture[1] that the level of direct γ production, and in particular its $\sqrt{s}$ dependence, might discriminate in a sensitive way between different models of constituent scattering and therefore help in the understanding of large transverse momentum phenomena. At present, within the framework of QCD analyses, copious production of direct photons is one of the clearest predictions of this theory: provided this reaction is probed at large enough transverse momentum, the point-like coupling of the photon to the quarks should be at the origin of the dominant source for direct photons.

---

1) Now at Lancaster University, England.
2) Permanent address: Purdue University, W. Lafayette, Ind., USA.
3) Now at David Lipscomb College, Nashville, Tenn., USA.
4) Permanent address: Nagoya University, Nagoya, Japan.
5) Research supported under the auspices of the US Department of Energy.
6) Permanent address: Argonne National Laboratory, Argonne, Ill., USA.
7) Permanent address: Tel-Aviv University, Israel.
8) On leave of absence from the University of Pisa, and INFN, Sezione di Pisa, Italy.
9) Permanent address: University of Tokyo, Japan.

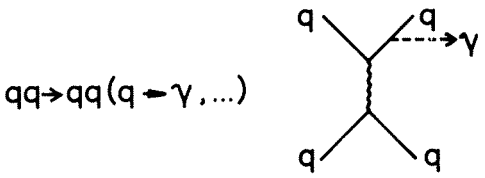

Fig. 1 Lowest-order QCD diagram for "final bremsstrahlung" of high p_T photons. There are also related processes of gq, gg, $q\bar{q}$, and $g\bar{q}$ scattering.

Fig. 2 QCD diagrams contributing to "prompt" production of high-p_T photons

Several theoretical groups have studied γ production within the framework of QCD [2]. Some of the lowest-order diagrams are shown in Figs. 1 and 2. The physics indicates the consideration of two distinct classes of γ sources. As represented in Fig. 1, the photon may fragment in a bremsstrahlung-like process from the scattered quark and be observed together with the other quark fragments in a jet. Dominating however, and very different in the structure of the final state, are subprocesses where the photon participates directly in the scattering. Two diagrams for such "prompt" processes are shown in Fig. 2. For the reaction

$$q\bar{q} \to \gamma g$$

the corresponding invariant cross-section is found to be

$$E\frac{d\sigma}{d^3p}(pp \to \gamma) = C\left[f_q(x), f_{\bar{q}}(x)\right]\frac{(1 - x_T)^{11}}{p_T^4},$$

where $C\left[f_q(x), f_{\bar{q}}(x)\right]$ contains the dependence on the quark and antiquark distribution functions. In pp collisions, the dominant subprocess is, however, the gluon equivalent of Compton scattering:

$$gq \to \gamma q ,$$

for which the pp production cross-section is calculated to be

$$E\frac{d\sigma}{dp^3}(pp \to \gamma) = C'\left[f_q(x), f_g(x)\right]\frac{(1 - x_T)^8}{p_T^4}.$$

Should this description be valid, one would expect to observe events with a most striking signature: a high-p_T photon, unaccompanied by other particles, recoils against a high-multiplicity jet of hadrons. Moreover, in the kinematical region where this reaction dominates, single-photon production provides a probe of the gluon distribution function: these single-photon studies of the gluon distributions are analogous to quark distribution studies in deep-inelastic lepton-nucleon scattering.

2. EXPERIMENTAL APPROACHES

Different experimental approaches are summarized in Table 1.

Table 1

Experimental approaches

Measurement	Technique	Comments
Low-mass, high-p_T virtual γ	e pairs from internal conversion	Very clean signature, reduced sensitivity
High-p_T, real γ	Identification of photons and discrimination against π^0's	Good sensitivity, devastating background
	Measurement of conversion probability in external converter	Statistical method

The method of slightly virtual photons (low mass, large transverse momentum) is characterized by the experimentally very clean signature of electron pairs resulting from internal conversion, albeit with greatly reduced sensitivity. Alternatively, real high-p_T photons may be identified by appropriate experimental techniques. The method offers good sensitivity provided that the devastating background from trivial sources, such as π^0 and η decay, can be treated experimentally. In a variation of this identification method, the conversion probability into e^+e^- pairs of neutral electromagnetic clusters is measured in an appropriately chosen external converter. Hence one determines the average number of photons per cluster and may evaluate the level of the direct one-photon contribution. This is a statistical method and does not allow event-by-event identification of possible direct photons.

All three techniques have provided results, which will be discussed in the following section.

3. RESULTS

3.1 Virtual photon measurements

Results on low-mass, high-p_T electron pairs and their implication on the level of direct γ production were published some time ago[3]. The mass range chosen was

$$200 \text{ MeV} < m_{ee} < 600 \text{ MeV} .$$

A comparison with the simultaneously measured inclusive ρ production, $pp \to \rho(\rho \to e^+e^-) + X$, allowed a sensitive check of systematic experimental effects. The experiment was rate-limited for $p_T \gtrsim 3$ GeV/c.

The measured production of electron pairs from virtual photons implies an expected level of direct photon production[4]:

$$(q^2 + m^2)^{1/2} \frac{d\sigma(\gamma \to ee)}{d^3q dm^2} = \frac{\alpha}{2\pi m^2} R \left(\frac{\gamma}{\pi^0}\right) \left[E \frac{d\sigma(\pi^0)}{d^3p}\right] ,$$

where we have assumed m_T scaling and evaluated the invariant π^0 cross-section for given q and m^2 by the relations $p_L = q_L$ and $p_T^2 = q_T^2 + m^2$. The ratio $R(\gamma/\pi^0)$ of direct photon to π^0 production is expected to have a small p_T dependence, evaluated to be between a constant and p_T^2 in most models, and is not very significant over the small p_T range covered by the experiment. This measurement found as an upper limit for direct γ production

$$R\left(\frac{\gamma}{\pi^0}\right) = (0.55 \pm 0.92)\% \quad \text{for} \quad 2.0 \leq p_T \leq 3.0 \text{ GeV/c} .$$

Later, a similar result was obtained by another group working at the ISR[5].

3.2 Real photon measurements

The characteristics of the A^2BC apparatus that are relevant for the single-photon programme are summarized in Table 2. The apparatus consists essentially of up to four large-solid-angle electromagnetic shower detectors[6]. The modularity permitted several different experimental layouts (Fig. 3) and, as a consequence, control of some important systematic

Table 2

A^2BC γ work: relevant apparatus aspects

Features	Parameters	Consequences
Modular, electromagnetic shower detector	4	Vary layout (and some systematics)
Large area	65×170 cm^2/module	
Highly segmented	Transv. $\sim 2 \times 140$ cm^2 4-fold longitudinal read-out	$\delta x \approx 5$ mm γ/hadron discrimination in trigger and off-line
Liquid-argon ion chamber technique	Photon with $E_\gamma \gtrsim 300$ MeV identified	Stability and reproducibility of operating conditions

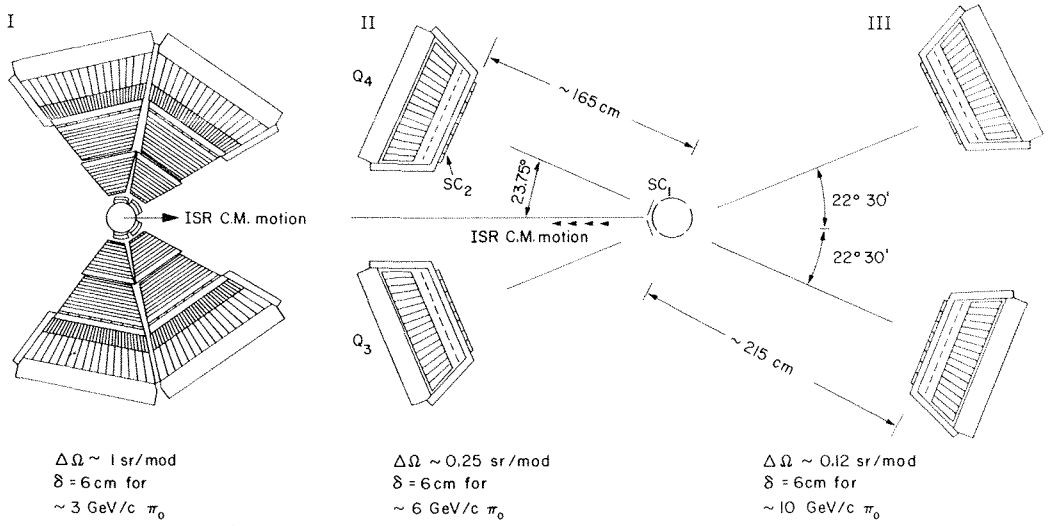

Fig. 3 The apparatus of the A^2BC Collaboration showing schematically the various phases of high-p_T photon studies. The large solid-angle layout (Phase I) has been used for the measurement of very high p_T π^0's, e^+e^- pairs, and single photons up to $p_T \sim 3$ GeV/c. Single-photon data obtained with layout II are discussed here. A recent run (layout III) aimed at the independent verification of the result of II.

effects. The high spatial segmentation achievable with the liquid-argon ion chamber technique resulted in a spatial resolution of typically $\sigma \sim 5$ mm and allowed us to separate the two photons from symmetric π^0 decays, up to ~ 10 GeV/c depending on the experimental layout. The fourfold longitudinal subdivision allowed effective hadron-photon discrimination already at the triggering stage.

As emphasized in the Introduction, the success of this photon identification method has to be based on two requirements:

- identification of the single photons and discrimination against hadrons through detailed study of the longitudinal and transverse shower distribution in the calorimeter;
- discrimination against photons originating from decays of π^0's, η's, η''s, ω's, etc. This imposes two contradictory constraints on the experimental apparatus: identification of near-by showers from π^0 decay requires the highest achievable spatial resolution; on the other hand, the background from very asymmetric decays has to be minimized by using detectors of adequate geometrical acceptance.

Details of the data selection are given in Table 3. The evaluation of the efficiency of these requirements was based on measurements (in test beams and at the ISR) and on computer simulations of the performance of the apparatus[7]. Note that the selection of photons or π^0's unaccompanied by any additional photon or charged particle within the solid angle covered by one calorimeter module introduces a physics bias: the yield of γ's and π^0's measured under these experimental conditions is not truly inclusive.

Table 3

Selection requirements on data

Requirement	Comment
Triggering	Localized energy deposit consistent with electromagnetic shower development; trigger efficiency measured to be 0.95 ± 0.05 for photons with $E_\gamma > 3$ GeV and 0.7 ± 0.05 for π^0's with $E_{\pi^0} > 3$ GeV.
Off-line reconstruction of photons	Calorimeter provides four independent views allowing stereo reconstruction of showers; a minimum of 200 MeV energy deposit is demanded per view; consistency of longitudinal and transverse energy deposit with electromagnetic shower is required.
"Unassigned" energy less than 35 MeV	Unassigned energy corresponds to total energy deposit in the front sections of the calorimeter, which is not reconstructed as a shower. Eliminates e.g. accompanying hadrons.
Fiducial area, 0.3 m × 1.2 m concentric with active calorimeter area of 0.56 m × 1.5 m	For single γ: only one shower in fiducial volume and no shower in veto area. For π^0 (or η): two showers inside fiducial volume, reconstructing to give a consistent mass value, and no shower in veto area.

The measured γ/π^0 ratio has to be corrected for two trivial sources of apparent single photons: asymmetric decay of mesons (π^0, η, η', ω) will result in topologies where one photon satisfies all criteria and the other one misses the detector completely. The correction is based on the meson yields measured in the same apparatus[8] and on Monte Carlo

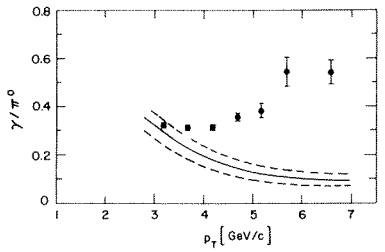

Fig. 4 Observed ratio of γ to π^0 for data from all energies. The error bars give statistical errors only. The smooth line indicates the Monte Carlo prediction for the ratio assuming no direct γ production. The dashed lines indicate the one standard deviation systematic errors on the Monte Carlo simulation.

evaluation of the specific experimental conditions. Also, the two photons from π^0 decay may be close enough to appear "merged" after shower reconstruction. These results of the Monte Carlo calculation are summarized in Fig. 4, showing the apparent γ/π^0 ratio. This has to be compared (Fig. 4) with the observed yield, showing a net excess which rises from approximately 0% to about 25% at the highest transverse momentum.

4. DISCUSSION OF RESULTS

4.1 Background

Several other sources may produce an apparent excess of single showers.

The level of hadron background is estimated from a test beam exposure of the calorimeter to hadrons and electrons. Applying the same data selection criteria as that used in the γ analysis, we obtain

$$\frac{\text{acceptance of a } \pi^-}{\text{acceptance of a } e^-} \approx 0.4\% \ .$$

Assuming pessimistically that other hadrons are equally likely to simulate a photon, we arrive at an upper limit on the hadron background of $\lesssim 2\%$.

Cosmic rays or *beam-gas interactions* may also be confused with single photons. The effect of this background was estimated to be below 2% of the observed γ/π^0 ratio.

A *non-linear energy response* of the calorimeter, rising faster than linear with incident photon energy, would contribute to the γ/π^0 ratio. Information on the energy response of our calorimeter modules is shown in Fig. 5 together with the level of non-linearity, which would be required to reproduce our measurements with this effect alone. The effect of a non-linearity has been included in the systematic errors.

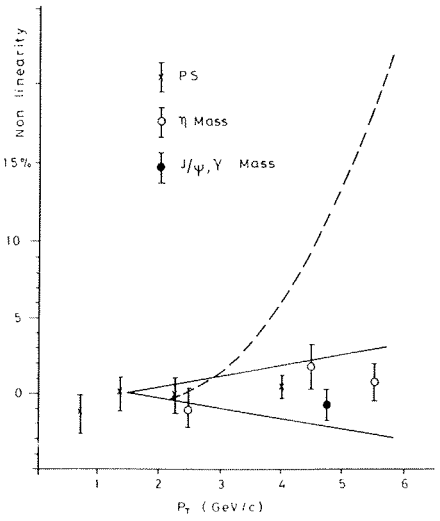

Fig. 5 Differential energy linearity of the liquid-argon calorimeter. Crosses are from an exposure to a momentum-analysed electron beam. Open circles are obtained from the reconstruction of $\eta \to \gamma\gamma$ events over the interval $1.5 < p_T < 8$ GeV/c. The closed circle is based on a comparison of the J/ψ and Υ masses. Also shown is the required non-linearity if this effect alone were to explain the measured γ/π^0 ratio (dashed line). Systematic errors given in the text are based on the non-linearity shown by the solid lines.

4.2 Summary of experimental results

In Fig. 6 we show the results obtained with set-up II at three $\sqrt{s}$ values. Error bars shown include both systematic and statistical errors. The results are consistent with preliminary data of a recent run (set-up III), where some of the critical experimental parameters, such as the effective solid angle, were changed. This indicates, for example, that the physics bias of some of the previously described cuts does not affect the data in a drastic way. For comparison, we also show (Fig. 7) three different theoretical curves, estimated for the *inclusive* ratio γ/π^0. Besides the subprocesses mentioned earlier, the prediction of Rückl et al.[2] assumes also different CIM mechanisms, estimated to contribute particularly at the intermediate p_T values.

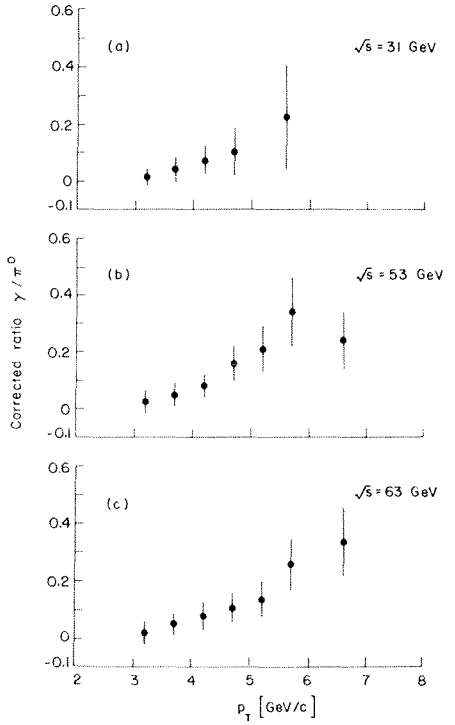

Fig. 6 The measured γ/π^0 ratio at three $\sqrt{s}$ values after subtraction of all sources of apparent γ production.

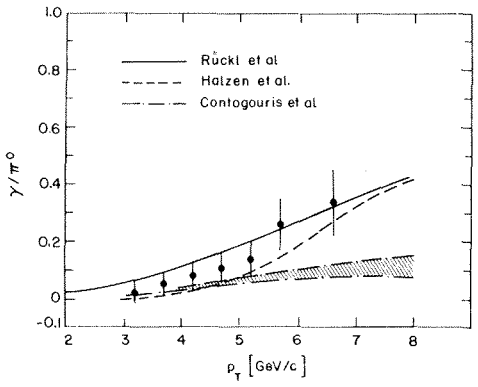

Fig. 7 The measured γ/π^0 ratio ($\sqrt{s}$ = 63 GeV) and comparison with three different theoretical estimates. The calculation of Contogouris et al. was carried out for $\sqrt{s}$ = 52 GeV and for two different sets of structure functions (shaded area).

Also shown is a calculation [Contogouris et al.[9]] where scale-breaking effects were explicitly included in the treatment, resulting in a rather strong suppression at large transverse momenta.

Some information on direct γ production is available from other groups and is summarized in Figs. 8 and 9. The data of the CERN-Rome-BNL Collaboration[10] show, within very large errors, the trend of an increasing γ/π^0 ratio, not inconsistent with our measurements. Data of the FNAL-Johns Hopkins Group[11] also show a similar p_T dependence. Note the rather substantial value for γ/π^0 at 2 GeV/c, which may perhaps be explained by the rather large $x_{\parallel}$ acceptance of this experiment. Another experiment at the ISR, using the "external converter method", reports an upper limit of $\gamma/\pi^0 \leq 30\%$ at p_T = 10 GeV/c [12].

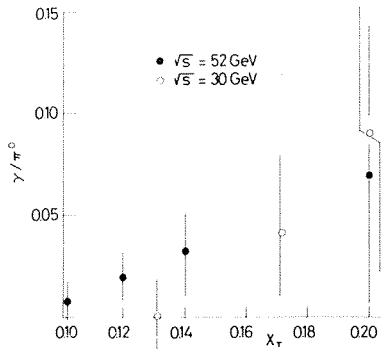

Fig. 8 Results on γ/π^0 obtained by the CERN-Rome-BNL Collaboration at the CERN ISR.

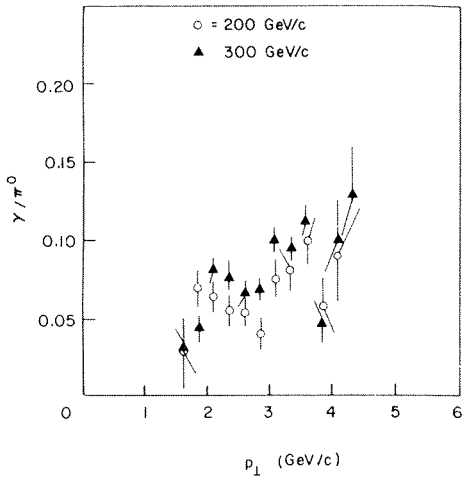

Fig. 9 Preliminary results of the FNAL-Johns-Hopkins Group on γ/π^0 production.

5. CONCLUSIONS

We have presented experimental evidence for direct production of photons in pp collisions. The ratio γ/π^0 rises from below $\sim 1 \pm 1\%$ at $p_T \approx 2.5$ GeV/c to about $25 \pm 8\%$ at $p_T \approx 7$ GeV/c. The p_T dependence of this ratio is consistent with the production level predicted by QCD. The very large p_T regime (up to and beyond 10 GeV/c), where scale-breaking effects are expected to be observable, remains to be explored. The study of direct photon production should be developed into a probe of the gluon distribution: this requires experiments combining the measurement of the complete event structure together with excellent photon identification capabilities.

REFERENCES

1) G.R. Farrar, Phys. Lett. 67B, 337 (1977).

2) We mention, in particular, the results of two groups, which have been used in comparison with our data:
R. Rückl, S.J. Brodsky and J.F. Gunion, Phys. Rev. D 18, 2469 (1979).
F. Halzen and D.M. Scott, COO-881-21 (1978).

3) J.H. Cobb et al., Phys. Lett. 78B, 519 (1978).

4) G.R. Farrar and S.C. Frautschi, Phys. Rev. Lett. 36, 1017 (1976).

5) A. Chilingarov et al., Contribution submitted to the 19th Int. Conf. on High-Energy Physics, Tokyo, 1978.

6) J.H. Cobb et al., Nucl. Instrum. & Methods 158, 93 (1979).

7) The Monte Carlo program of the electromagnetic cascade is described in: R.L. Ford and W.R. Nelson, SLAC-210 (1978).

8) C. Kourkoumelis et al., Phys. Lett. 84B, 270 and 277 (1979).
C. Kourkoumelis et al., Inclusive η' and ω production at the CERN ISR, in preparation.

9) A. Contogouris et al., Phys. Rev. D 19, 2607 (1979).

10) E. Amaldi et al., Phys. Lett. 84B, 360 (1979).

11) B. Fox, private communication.

12) A.L.S. Angelis et al., Phys. Lett. 79B, 505 (1978).

DISCUSSION

Chairman: S.C.C. Ting

Sci. Secretaries: C. Best and H. Gennow

J.F. Gunion: It was not clear to me whether the γ/π^0 ratios you showed increased primarily as a function of p_T or primarily as a function of x_T. Theoretically higher twist (CIM) contributions predict a rise with p_T^2 even at fixed x_T, while QCD contributions predict a constant result at fixed x_T as p_T increases. Does your data discriminate between these alternatives?

C. Fabjan: Absolutely right. Look at the data and you would at first say that x_T scaling does not seem to be very clearly exhibited, but what can we say?

Firstly the lever region squared of s is not very large, at 15 GeV we run out of statistics very early on, so I would think that this detailed comparison would have to wait the second round of experimentations, where the 15 GeV points have to be sharpened up to answer this question -- not quite ready yet.

EXPERIMENTAL DETERMINATION OF THE PION AND NUCLEON STRUCTURE FUNCTIONS BY MEASURING HIGH-MASS MUON PAIRS PRODUCED BY PIONS OF 200 AND 280 GeV/c ON A PLATINUM TARGET

C.E.N., Saclay[1]-CERN[2]-Collège de France, Paris[3]-Ecole Polytechnique, Palaiseau[4]-Laboratoire de l'Accélérateur Linéaire, Orsay[5]

J. Badier[4], J. Boucrot[5], G. Burgun[1], O. Callot[5], Ph. Charpentier[1], M. Crozon[3], D. Decamp[2], P. Delpierre[3], A. Diop[3], R. Dubé[5], B. Gandois[1], R. Hagelberg[2], M. Hansroul[2], W. Kienzle[2], A. Lafontaine[1], P. Le Dû[1], J. Lefrançois[5], Th. Leray[3], G. Matthiae[2], A. Michelini[2], Ph. Miné[4], H. Nguyuen Ngoc[5], O. Runolfsson[2], P. Siegrist[1], J. Timmermans[2], J. Valentin[3], R. Vanderhagen[4], S. Weisz[4]

ABSTRACT

We measured the production of massive muon pairs on a platinum target by pions of 200 and 280 GeV/c. The following number of dimuon events have been collected for $M > 4$ GeV/c^2. (a) π^- of 200 GeV/c: $\sim$ 5900 events; (b) π^+ of 200 GeV/c: $\sim$ 2200 events; (c) π^- of 280 GeV/c: $\sim$ 5700 events. These data were analysed in terms of the Drell-Yan model in order to obtain the pion and nucleon structure functions, which are parametrised with expressions of the form $x^\alpha(1 - x)^\beta$. Our results are compared to the structure functions obtained in other experiments.

1. INTRODUCTION

We have performed a series of experiments to measure the production of massive muon pairs in hadron-hadron collisions at the CERN SPS. One of the aims of the experiment was to obtain the structure functions of unstable hadrons like pions and kaons, difficult to probe by lepton scattering, by making use of the Drell-Yan mechanism of quark annihilation.

In this paper we present detailed results on the pion and nucleon structure functions. Data on dimuon production by kaons, protons and anti-protons are discussed in another contribution[1)] to this conference.

2. THE EXPERIMENTAL APPARATUS

The general layout of the experiment is shown in fig. 1(a). The beam is an unseparated secondary particle beam produced by protons of 400 GeV/c on a 50 cm Be target. Particle identification is done by two differential Čerenkov counters (CEDAR's) for $K^\pm$ and $\bar{p}$, and two threshold Čerenkov counters for π^+. The particle fluxes were in the range (1 - 3) 10^7 part/pulse. At 200 GeV/c the fraction of π^- in the negative beam was about 96%. A 2m long CH_2 absorber was used to enhance the π^+ percentage of the positive beam to about 36%.

Platinum targets, 6 cm long for the 200 GeV run and 11.1 cm for the 280 GeV run, were used. At 200 GeV we have also used a 30 cm long liquid hydrogen target.

After passing through the targets, the beam is absorbed in a beam dump which starts 40 cm downstream of the Pt target. It consists of a 1.5 m long block of stainless steel with a heavy (tungsten and uranium) conical plug of ± 30 m rad aperture inserted in the centre, in order to minimize the total beam dump length.

The large acceptance magnetic spectrometer consists of:

i) a large superconducting dipole magnet with vertical field ($\int B\, dl = 4.0$ Tm) in an airgap of cylindrical shape of 1.6 m diameter;

ii) a set of six multiwire proportional chambers (31 planes with a total of about 26 000 wires) ranging in size from 0.6 x 0.6 m^2 (PC1) up to 4.2 x 4.0 m^2 (PC6);

iii) muon filtering, behind the beam dump, is provided by the electron calorimeter (12 cm of lead), by the hadron calorimeter (1 m of iron) and by an additional iron absorber 80 cm thick;

iv) the trigger system consists of two symmetric telescopes of counters and chambers placed above and below the horizontal plane.

A "pretrigger" is provided by three planes of counter hodoscopes:

- T_1 placed at the end face of the beam dump consisting of 12 counters;
- T_2 which is in fact the second layer of the electron calorimeter, subdivided in 50 horizontal strips;
- T_3 is the last hodoscope made of 44 horizontal sheets.

The last two hodoscopes cover vertical angles from ± 6 mrad up to ± 165 mrad. The pretrigger requires at least 2 particles in the coincidence T_2T_3 and at least one in T_1. The pretrigger provides a fast strobe for the proportional chambers PC1, PC2, M1 and M2.

The trigger acts on the vertical component P_t^V of the transverse momentum of the muons. The p_t^V selection is achieved by two planes of cathode-readout chambers M1 and M2 covering vertical angles from ± 30 mrad up to ± 165 mrad. The cathodes are printed in 18 separated horizontal bands, each subdivided into 64 cells corresponding to equal intervals of the tangent of the azimuthal angle. The correlation between cells of a given band provides a cut-off in the magnetic deflection angle and thus in p_t^V, which in turn, defines a rough lower cut in the muon pair effective mass. The trigger conditions in the course of the experiment were either $p_t^V > 0.7$ GeV/c for both muons,

or $p_t^v > 1$ GeV/c for one muon, without cut on the other muon. Events with both muons in the 30 mrad cone of the W/U core of the beam dump were not accepted. The trigger system is illustrated in fig. 1(b).

The overall acceptance of the apparatus, as determined by the geometry of the detector and by the p_t^v cut is shown in fig. 1(c) as a function of the dimuon mass and of the variable $x = 2p_L^*/\sqrt{s}$, where p_L^* is the longitudinal momentum of the dimuon in the c.m. system.

3. DATA ANALYSIS

We analyse our data in the framework of the Drell-Yan mechanism, assuming that an antiquark $\bar{q}$ and a quark q of the beam and target hadrons annihilate electromagnetically into a virtual photon which then decays into a muon pair, according to the diagram

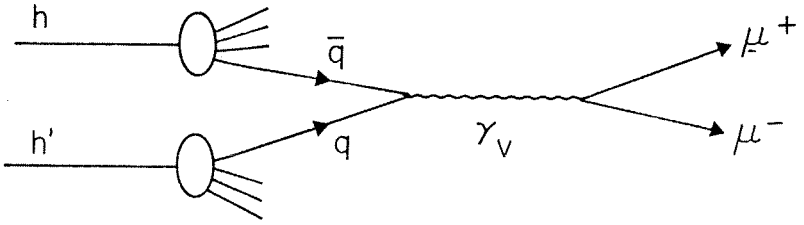

The muon pair momentum and invariant mass M determine the kinematical variables of the colliding $\bar{q}q$ pair, if transverse momentum is neglected, as

$$M^2 = x_1 x_2 s, \quad x = x_1 - x_2$$

where x_1 and x_2 are the fractional momenta of the quarks in the beam and target particle respectively.

The Drell-Yan formula can be written as

$$\frac{d^2\sigma}{dx_1\, dx_2} = \frac{\sigma_0}{3} \Sigma_i \frac{Q^2_i}{x_1^2\, x_2^2} \left[f_i(x_1)\, f_{\bar{i}}(x_2) + f_{\bar{i}}(x_1)\, f_i(x_2) \right], \qquad (1)$$

where $\sigma_0 = 4\,\pi\alpha^2(\hbar c)^2/3s$ and the structure function f_i for quarks of flavour i and charge Q_i have a valence and a sea contributions, $f_i = f_{iv} + f_{is}$. The factor of 3 due to the colour hypothesis is displayed explicitly in eq. (1).

For the pion there is a single valence function, that we call $V(x_1)$, defined by:

$$V(x_1) = \bar{u}_V^{\pi^-}(x_1) = d_V^{\pi^-}(x_1) = u_V^{\pi^+}(x_1) = \bar{d}_V^{\pi^+}(x_1).$$

For the nucleon there are two independent valence functions, that we define for the proton as $u(x_2)$ and $d(x_2)$ for the up and down quarks respectively:

$$u^p(x_2) = d^n(x_2) = u(x_2),\ d^p(x_2) = u^n(x_2) = d(x_2).$$

The valence structure functions are normalized to the corresponding number of valence quarks i.e.

$$\int \frac{V(x_1)}{x_1}\, dx_1 = 1, \int \frac{u(x_2)}{x_2}\, dx_2 = 2, \int \frac{d(x_2)}{x_2}\, dx_2 = 1.$$

The sea distributions are taken to be SU3 symmetric. For each flavour, we define $S_n(x_2)$ for the nucleon and $S_\pi(x_1)$ for the pion.

In the analysis of our results we compare the experimentally determined cross section to the one calculated by the Drell-Yan formula using:

$$\left(\frac{d^2\sigma}{dx_1\, dx_2}\right)_{exp} = K \left(\frac{d^2\sigma}{dx_1\, dx_2}\right)_{D.Y.}, \tag{2}$$

where K is a scale factor, related either to our experimental normalization error or to a multiplicative correction factor due to QCD effects[2].

The general form of the cross section for pion-nucleon interaction is,

$$\frac{d^2\sigma}{dx_1\, dx_2} = \frac{K\sigma_0}{3x_1^2 x_2^2}\left[V(x_1)\ G(x_2) + S_\pi(x_1)\ H(x_2)\right], \tag{3}$$

where, for Pt target (Z/A = 0.40), the nucleon functions $G(x_2)$ and $H(x_2)$ take the following form,

$$\begin{aligned} G &= 1/9\ (1.6u + 2.4d + 5S_n) \quad \text{for } \pi^- \\ G &= 1/9\ (0.6u + 0.4d + 5S_n) \quad \text{for } \pi^+ \\ H &= 1/9\ (2.2u + 2.8d + 12S_n) \quad \text{for } \pi^\pm . \end{aligned} \tag{4}$$

The raw data of the experiment come in the form of $\mu^+\mu^-$ events for which we know the mass and the longitudinal momentum. From these we extract values of x_1 and x_2 for each event and we obtain an array as shown in fig. 2.

We have calculated by Monte Carlo method the acceptance at each value of x_1 and x_2, by integrating on the observed p_t distribution and on the $\cos\theta$ and ϕ distribution[1] which was taken to be $P(\theta,\phi) \propto (1 + \cos^2\theta)$. The experimental errors ($\Delta p/p$, multiple scattering) and the Fermi motion of the nuclear target distort slightly the distribution of events in the x_1, x_2 array. The main effects are that the $\Delta p/p$ error produces a $\Delta x_1/x_1$ of about 3% at high x_1, while Fermi motion and multiple scattering induces $\Delta x_2/x_2$ of about 10% and 6% respectively. The resulting effects on dN/dx_1 are sizeable only at high x_1 or x_2 and in any case do not exceed 10%.

From the x_1, x_2 array, corrected for acceptance, we extract the pion and nucleon structure functions by three different methods illustrated in the following sect. 3.1, 3.2, 3.3.

We exclude the mass regions where resonances are present, by the following cuts, $4 < M < 8.5$ GeV/c^2 at 200 GeV/c and $4.5 < M < 8.5$ GeV/c^2 at 280 GeV/c. In the resulting arrays we have 5607 events for 200 GeV/c π^-, 2073 events for 200 GeV/c π^+ and 3441 events for 280 GeV/c π^-.

3.1 Factorization method

In this method we perform a first analysis of our π^- data by assuming that for the range of x_1 values explored by this experiment, the sea of the pion can be neglected in comparison to the valence. In that case the observed cross section for incident π^- can be written as (see eq. 3)

$$\frac{d^2\sigma}{dx_1\, dx_2} \propto \frac{1}{x_1^2\, x_2^2}\, V(x_1)\, G(x_2).$$

For each bin of given x_1 (N_1 bins in total) we have an unknown value of $V(x_1)$, for each bin of given x_2 (N_2 bins in total) we have an unknown value of $G(x_2)$. We thus have $N_1 + N_2$ unknown and $N_1 \cdot N_2$ independent cells. We exclude from the analysis the cells where the acceptance is less than 3%. By minimizing the global χ^2, we obtain the numerical value of the function $V(x_1)$ for N_1 different values of x_1 and the numerical value of $G(x_2)$ for N_2 values of x_2.

The results of this analysis are shown for the 200 GeV π^- run in fig. 3(a) together with results from a similar analysis by Newman et al.[3] on their 225 GeV π^- data. The χ^2 of our fit is 95 for 67 degrees of freedom. This value of the χ^2 indicates that in our kinematical range of the variable x_1 and x_2, the factorization hypothesis may not be adequate.

We can also perform a simultaneous analysis of our π^- and π^+ data without any assumptions on the pion sea. In fact the subtraction of the π^+ induced

Drell-Yan cross section from the π^- induced cross section, allows to eliminate the terms involving the sea of the pion and those involving the sea of the nucleon, which are the same for incident π^+ and π^-. For the Pt target (Z/A = 0.40), the combination of up and down valence quark that we obtain is u + 2d

$$\left(\frac{d^2\sigma}{dx_1\ dx_2}\right)_{(\pi^- Pt)\ -\ (\pi^+ Pt)} \propto \frac{1}{x_1^2\ x_2^2}\ V(x_1)\ 1/9\ [u(x_2) + 2d(x_2)].$$

The analysis was done by subtracting in each x_1, x_2 cell the π^+ events from the π^- events, both normalized to the same number of incident pions. This normalization was obtained by using the observed number of J/ψ events and the measured equality (within ± 2%) of the production cross section for J/ψ on Pt by incident π^+ and π^-[4]. The results are presented in fig. 3(b). The χ^2 of this $\pi^- - \pi^+$ difference fit is 43 for 59 degrees of freedom. In the present analysis by the factorization method we have made no attempt of normalization of our data.

3.2 Parametrization method

We assume the following simple x-dependence for the various structure functions[5]:

$$V(x) = Ax^{\alpha}(1 - x)^{\beta}$$
$$S_{\pi}(x) = B(1 - x)^{n}$$
$$u(x) = A'_u x^{\alpha'}(1 - x)^{\beta'}$$
$$d(x) = A'_d x^{\alpha'}(1 - x)^{\beta'+1}$$
$$S_n(x) = B'(1 - x)^{n'}.$$

The choice of $\alpha'_u = \alpha'_d$ and $\beta'_d = \beta'_u + 1$ is the result of theoretical prejudices.

As explained in sect. 3, the parameter A, A'_u, A'_d are fixed in terms of α and β by the normalization condition to the number of valence quarks.

If we use simultaneously the information from our π^- and π^+ data, it is possible to determine the parameters of the sea in addition to the valence. In fact the π^+/π^- ratio gives the relative importance of the sea and the valence contribution, the variation of this ratio as a function of x_1 and x_2 fixes the relative importance of the pion sea and the nucleon sea.

The results of this global fit, done by a maximum likelihood method, on the 200 GeV data are given below:

$\alpha = 0.40 \pm 0.06$ $\quad$ $\alpha' = 1.02 \pm 0.15$

$\beta = 0.90 \pm 0.06$ $\quad$ $\beta' = 4.04 \pm 0.4$

$B = 0.09 \pm 0.06$ $\quad$ $B' = 0.35 \pm 0.07$

$n = 4.4 \pm 1.9$ $\quad$ $n' = 6.0 \pm 1.3$

$A = 0.55$ $\quad$ $A'_u = 10.5$ $\quad$ $A'_d = 6.31$.

Only the relative normalization of the π^+ to the π^- data (known within ± 2%) is used in this fitting procedure. The absolute normalization, which is however affected by a large error, will be exploited in the following method to evaluate the factor K as defined by eq. (2).

3.3 Projection method

By projecting the content of the x_1, x_2 array on the two axes we get the distribution dN/dx_1 and dN/dx_2. If L is the integrated luminosity calculated from the integrated beam intensity and from the useful number of target nucleons assuming a linear A dependence[1] of the cross section, we can get from eq. (3) and (4) an expression where only the variable x_1 appears

$$F_\pi(x_1) \equiv \frac{dN/dx_1}{\frac{\sigma_0}{3}\frac{L}{x_1^2} I(x_1)} = K\left[V(x_1) + \frac{J(x_1)}{I(x_1)} S_\pi(x_1)\right]. \qquad (5)$$

In this equation the quantities $I(x_1)$ and $J(x_1)$ are integrals involving the nucleon structure functions $G(x_2)$ and $H(x_2)$ and the calculated acceptance of the apparatus $A(x_1, x_2)$

$$I(x_1) = \int \frac{G(x_2)}{x_2^2} A(x_1, x_2)dx_2, \quad J(x_1) = \int \frac{H(x_2)}{x_2^2} A(x_1, x_2)dx_2.$$

These integrals have been evaluated in two different ways:

i) using the results of the fit to our data discussed in sect. 3.2;

ii) using the results of the CDHS[6] parametrization.

The quantity $J(x_1)/I(x_1)$ is nearly constant (± 7%) in the relevant x_1 range and is ~ 1.4 for the π^- data and ~ 3.7 for the π^+ data. In fig. 4(a) we present the results for the pion structure function.

A procedure similar to the one which leads to eq. (5) can be used to derive the nucleon structure function using as input the pion structure function from our fit. In this case for the π^- the valence part is 1.6u + 2.4d and $J/I \sim 5.3$, for the π^+ the valence part is 0.6u + 0.4d and $J/I \sim 4.5$. The results are given in fig. 4(b).

The numerical value of K is obtained from the integration of eq. (5)

$$K = \frac{\int F_\pi(x_1)\, dx_1}{\int \left[V(x_1) + \frac{J(x_1)}{I(x_1)} S_\pi(x_1) \right] dx_1} ,$$

where $V(x_1)$ and $S_\pi(x_1)$ are the normalized valence and sea structure functions as determined in sect. 3.2. The results on K are given in table 1.

4. DISCUSSION

a) First we should note that the shape of the pion structure function is rather insensitive to the choice of the nucleon structure function used in the projection method of sect. 3.3. Furthermore, the pion and nucleon valence structure function curves obtained from our fit fall nicely on the values obtained from the factorization method (sect. 3.1) using the $\pi^- - \pi^+$ data (fig. 3(b)); this checks the consistency of the two methods. The π^- structure function which we derive from the factorization method agrees in shape with the result of Newman et al.[3]. However, the nucleon structure functions, derived by the same methods, are incompatible (fig. 3(a)).

b) Using the parameters obtained from our fit in sect. 3.2, we find:

$$2 \cdot \int V(x_1)\, dx_1 = 0.34 \qquad 6 \cdot \int S_\pi(x_1)\, dx_1 = 0.10 .$$

These fractions of the π momentum carried respectively by the valence quark and the sea agree with general expectation.

On the other hand, using the parameters from the same fit, we find:

$$\int \Big(u(x_2) + d(x_2) \Big)\, dx_2 = 0.47 \qquad 6 \cdot \int S_N(x_2)\, dx_2 = 0.3 .$$

Our nucleon structure functions (and their integrals) are about twice as high as those obtained in the parametrization of CDHS. It should be noticed however that in our fit we are very sensitive to extrapolation of the structure function to $x_2 = 0$ and hence the values given above, both for the sea and valence, depend on the choice of the analytical representation of $F_N(x_2)$ at small x_2 [7]. It should also be noticed that a large value of the nucleon sea momentum, compatible with ours, is obtained in the analysis of the FNAL proton data[8,9].

c) The values of the scale factor K given in table 1 are affected by different sources or errors; they are listed in table 2.

REFERENCES

1) J. Badier et al., "Muon pair production above 4 GeV (Drell-Yan continuum) by $\pi^{\pm}$, $K^{\pm}$, $\bar{p}$ and p at 200 GeV/c and by π^{-} at 280 GeV/c on platinum and hydrogen targets", International Conference on High Energy Physics, Geneva 1979.

2) G. Altarelli et al., MIT Report CTP No 776, 1979.
J. Kubar-André and F.E. Paige, Phys. Rev. D19 (1979) 221.

3) C.B. Newman et al., Phys. Rev. Lett. 42 (1979) 951.

4) J. Badier et al., "Dimuon resonance production from 200 and 280 GeV/c tagged hadron beam", International Conference on High Energy Physics, Geneva 1979.

5) A.J. Buras and K.J.F. Gaemers, Nucl. Phys. B132 (1978) 249.

6) J.G.H. de Groot et al., Phys. Lett. 82B (1979) 456.

7) The larger acceptance error in the case of the fit with our data alone is due to the strong dependence of the integral $\int F_N(x_2)/x_2 dx_2$ on the acceptance at small x_2.

8) L.M. Lederman, Proc. of the 19th International Conference on High Energy Physics, Tokyo, 1978.

9) E.L. Berger, SLAC-PUB-2314, 1979.

Table 1

Results on the scale factor K

	π^+ 200 GeV/c	π^- 200 GeV/c	π^- 280 GeV/c
$G(x_2)$, $H(x_2)$ from this experiment (sect. 3.2)	1.4	1.4	1.5
$G(x_2)$, $H(x_2)$ from CDHS fit	2.4	2.2	2.5

Table 2

Estimated errors on the scale factor K

	K obtained using for the nucleon $G(x_2)$ and $H(x_2)$ from CDHS	K obtained using for the nucleon $G(x_2)$ and $H(x_2)$ from our fit
Luminosity error of our experiment	± 15%	± 15%
statistical error	± 10%	± 15%
Systematic error from the acceptance uncertainty	± 10%	± 15%
CDHS normalisation error	± 5%	-

FIGURE CAPTIONS

Fig. 1(a) General layout of the NA3 spectrometer for the study of dimuon production in hadronic collision.

(b) Sketch of the trigger system.

(c) The acceptance of the apparatus as a function of x and M as calculated by a Monte-Carlo method.

Fig. 2 Two-dimensional plot in the x_1, x_2 plane of the 200 GeV/c π^- Pt dimuon events. A cut was applied at M = 4 GeV/c^2.

Fig. 3(a) The data points are the result of the factorization method (sect. 3.1) applied on the π^- data at 200 GeV/c. Data points from ref. 3) are also plotted with arbitrary relative normalization. The shape of the structure functions obtained by the parametrization method (sect. 3.2) is also shown.

(b) The data points are the result of the factorization method (sect. 3.1) applied to the $\pi^- - \pi^+$ data at 200 GeV/c. The shape of the structure functions obtained by the parametrization method (sect. 3.2) is also shown.

Fig. 4(a) The data points represent $F_\pi(x_1)$ as defined by eq. (5), using:
- nucleon structure function of our fit (1)
- nucleon structure function from CDHS fit (2)
  i) dashed curves represent the valence structure function of the pion obtained from our fit.
  ii) solid curves represent the (valence + sea) pion structure function as defined by eq. (5).

The curves have been scaled up by a factor K:
(K = 1.4 for (1), K = 2.5 for (2))

(b) The data points represent $F_N(x_2)$, as defined in sect. 3.3, using the pion structure function from our fit.
- dashed curves represent the valence part of the nucleon structure function: $1.6u(x_2) + 2.4d(x_2)$ for π^-
  $0.4d(x_2) + 0.6u(x_2)$ for π^+
- solid curves represent (valence + sea) nucleon structure function as defined in sect. 3.3.

The curves have been scaled up by a factor K:
(K = 1.4 using our fit; K = 2.5 using CDHS fit).

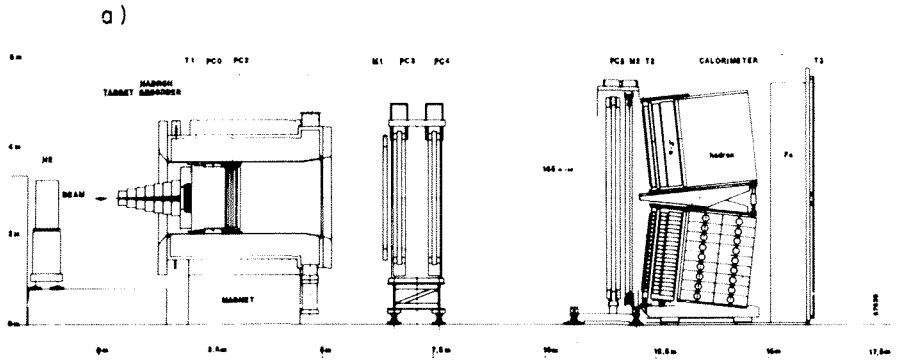

Experimental layout / side view

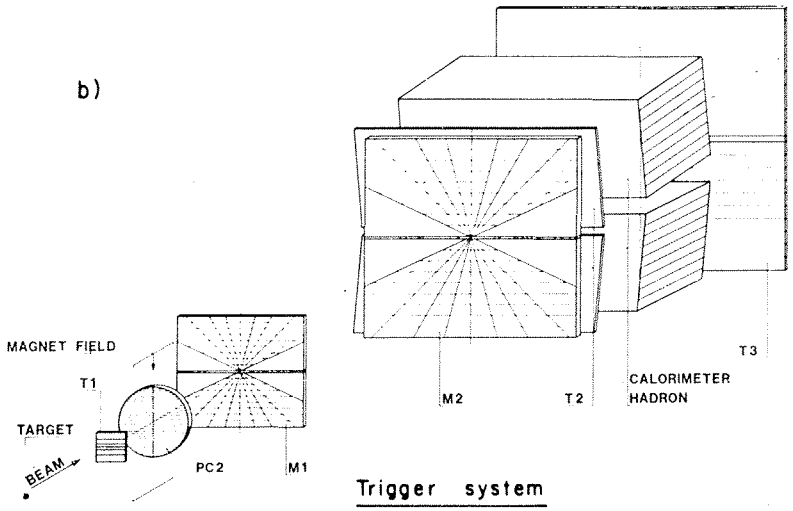

Trigger system

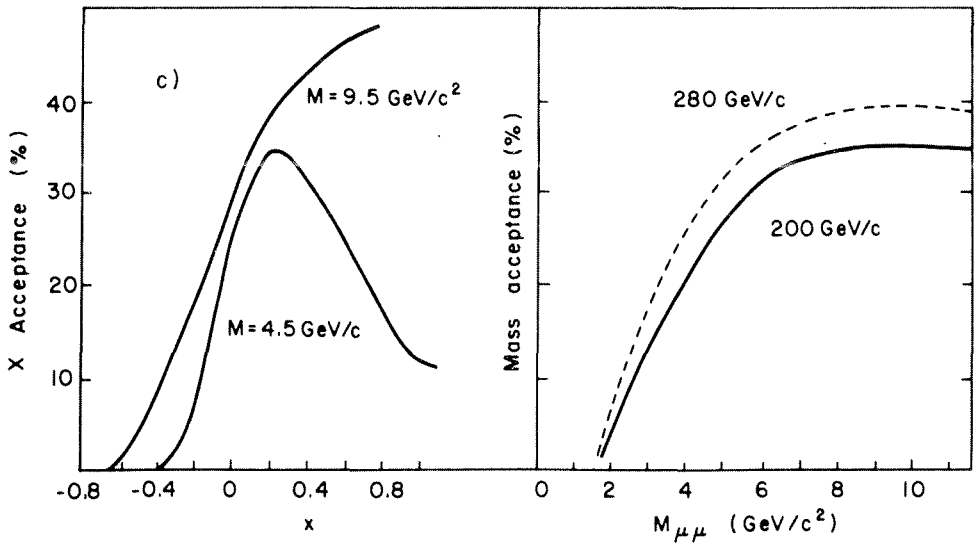

Acceptance

Fig. 1

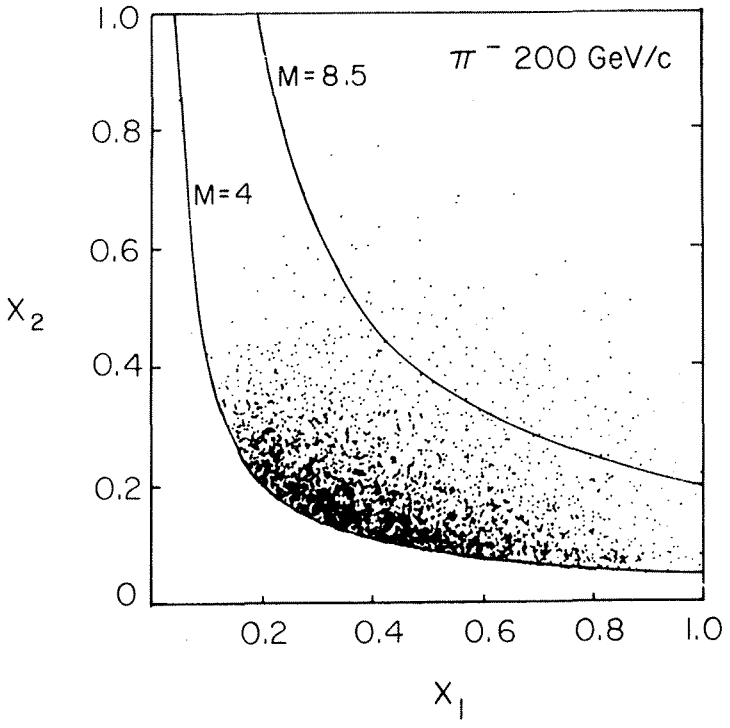
1.0
0.8
0.6
0.4
0.2
0
X_2
M=8.5
M=4
π^- 200 GeV/c
0.2
0.4
0.6
0.8
1.0
X_1

Fig. 2

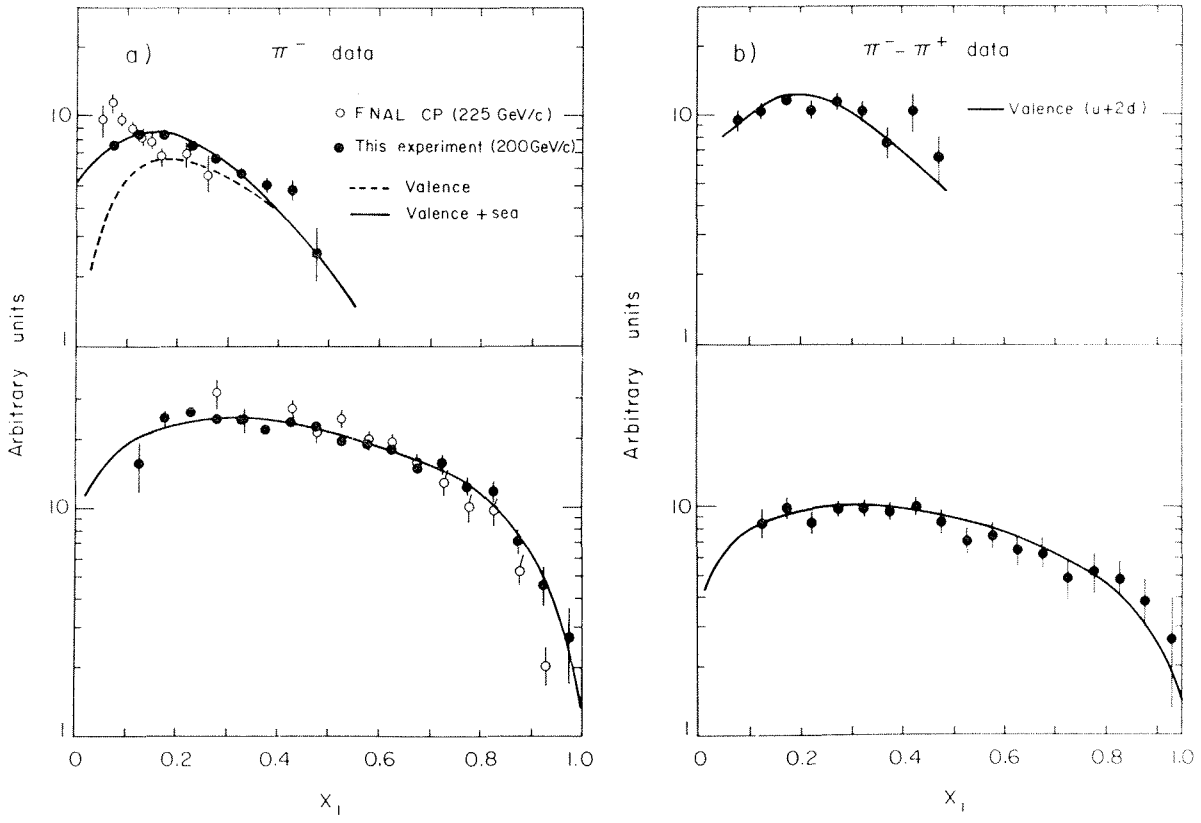
a) π^- data
○ FNAL CP (225 GeV/c)
● This experiment (200GeV/c)
---- Valence
—— Valence + sea
b) $\pi^- - \pi^+$ data
—— Valence (u+2d)
Arbitrary units
10
1
0
0.2
0.4
0.6
0.8
1.0
X_1

Fig. 3

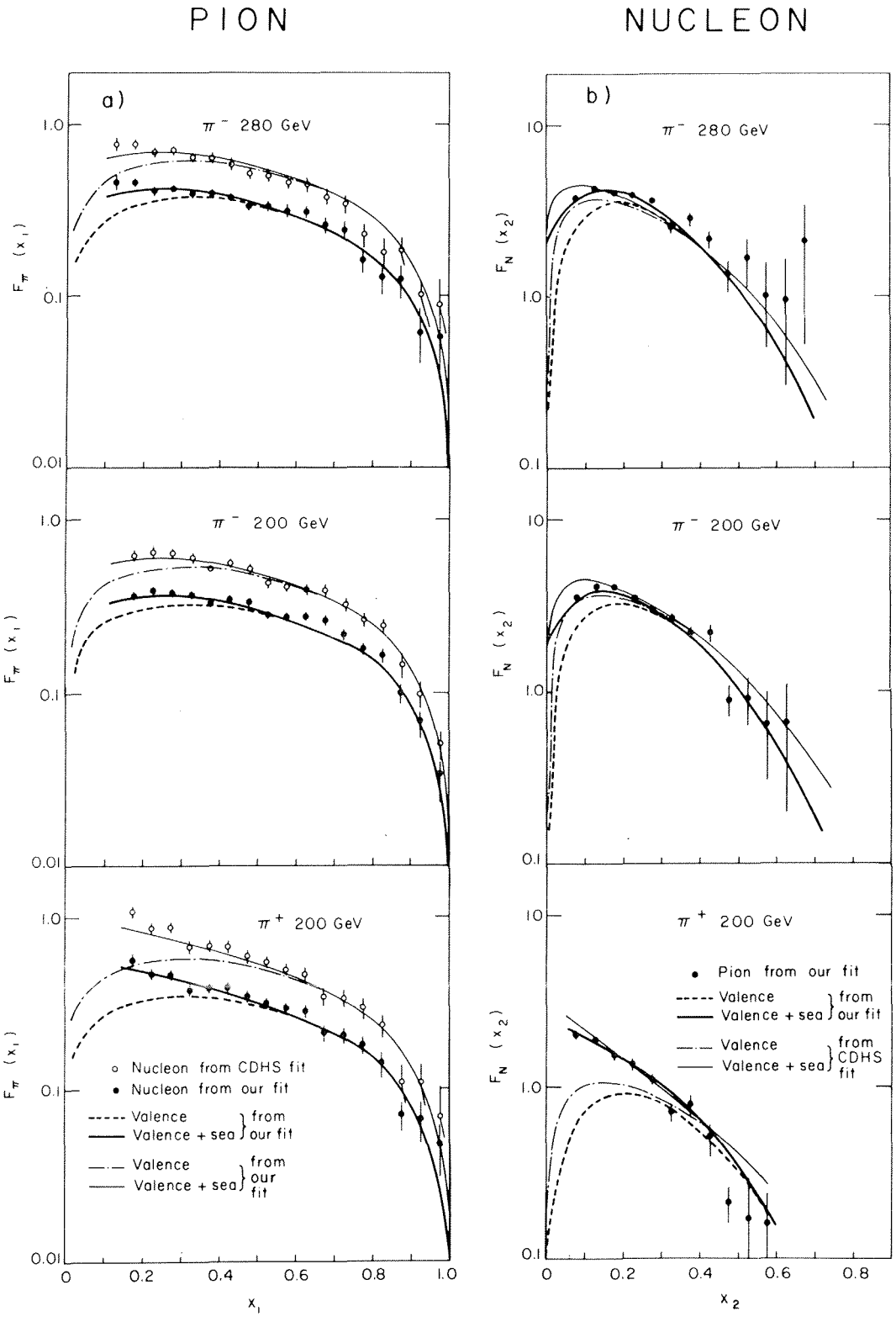
PION
NUCLEON
a)
b)
π⁻ 280 GeV
π⁻ 200 GeV
π⁺ 200 GeV
F_π (x_1)
F_N (x_2)
x_1
x_2
Nucleon from CDHS fit
Nucleon from our fit
Valence
Valence + sea
from our fit
from our fit
Pion from our fit
from CDHS fit

Fig. 4

STUDY OF RARE MUON INDUCED PROCESSES

A.R. Clark, K.J. Johnson, L.T. Kerth, S.C. Loken, T.W. Markiewicz, P.D. Meyers, W.H. Smith, M. Strovink, W.A. Wenzel
Lawrence Berkeley Laboratory, Berkeley, California, USA

R.P. Johnson, C. Moore, M. Mugge, R.E. Shafer
Fermi National Accelerator Laboratory, Batavia, Illinois, USA

G.D. Gollin, F.C. Shoemaker, P. Surko
Princeton University, Princeton, New Jersey, USA

ABSTRACT
Interactions of the type $\mu N \to (n\mu)X$ (n=1,2,3,4,5) are being studied with high sensitivity in the Multimuon Spectrometer in the Fermilab muon beam. Results are reported on inelastic structure functions, production of $\psi(3100)$ and exotic multimuon final states.

INTRODUCTION

Data have been collected using the Multimuon Spectrometer recently constructed in the Fermilab muon beam. To achieve the desired luminosity ($>10^{39}$ cm^{-2}/experiment) the experiment uses a massive target (5 kg/cm^2). An integrated spectrometer magnet provides high acceptance along the length of the target even for tracks along the beam direction.

The apparatus shown in Fig. 1, consists of 18 modules of 5 10-cm thick steel plates each followed by a calorimeter scintillator (5C). A 25 cm gap between modules contains a drift chamber (DC) for precise determination of track position in the bend plane and a proportional chamber which reads out 3 coordinates to resolve multi-hit ambiguities.

Signals from banks of trigger scintillators S_1-S_{12} are used to form parallel triggers for >1, >2, >3 muons in the final state. The single muon trigger incorporated a veto on a hit in the beam area; the two muon trigger required deposition of approximately 20 GeV in the hadron calorimeter. Three muons triggered only on multiplicity.

Beam tracks were momentum-analyzed by 2 separate upstream bends. Accepted outgoing tracks, registering >4 proportional chamber hits in 2 views and >3 hits in the third, were required to intersect a common vertex optimized by iteration. Extra hits due mainly to small showers induced by direct electron pairs, were identified and rejected using a complex momentum-fitting algorithm which solves for the Coulomb-scattering in each module.

The acceptance and resolution of the spectrometer were modelled for each final state by Monte Carlo simulation. Coordinates of randomly sampled beam muons are used as input and all energy loss and scattering processes are included for each iron plate. Trajectories were deflected in each plate using measured field maps. Simulated interactions occurred between muons and nucleons in Fermi motion or coherently between muons and iron nuclei. These simulated events were output in the same format as raw data and were reconstructed and momentum-fit exactly as the data.

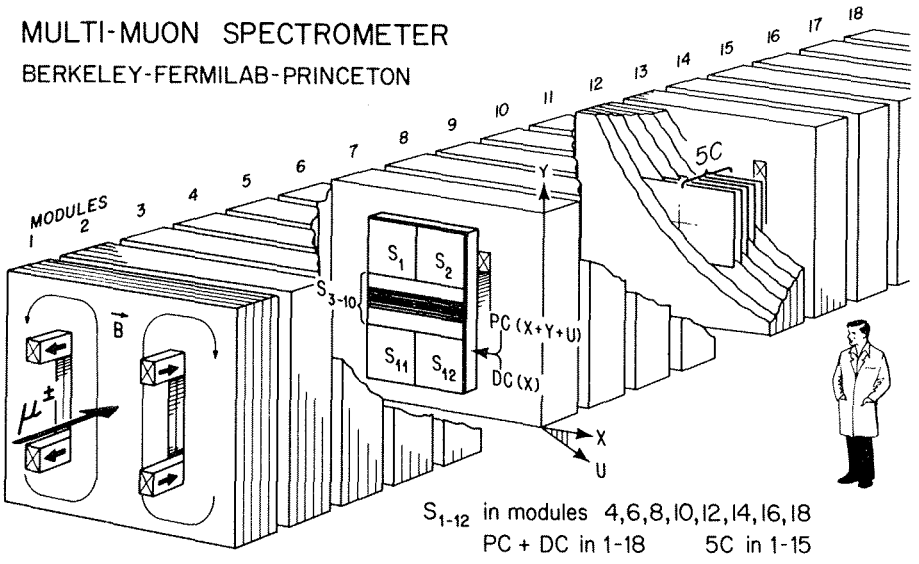

Figure 1. Schematic view of the apparatus. S_1-S_{12} are trigger scintillators. PC and DC are proprotional and drift chambers. The scintillators labelled 5C form a hadron calorimeter.

EXOTIC MULTIMUON FINAL STATES

Identification of exotic events begins in the reconstruction and fitting programs. Events satisfying normal analysis criteria which possess unusual characteristics are saved on microfilm containing tabulated data and computer-generated track pictures. Events are double scanned by physicists and are refit using hand-selected information as a consistency test.

Table 1 presents the properties of four rare events found in an initial scan of 20% of the data. The three muon event with two missing μ^- or ν_μ is similar to events seen in the CDHS neutrino experiment[1]. In this case also, the small pair masses and transverse momenta favor interpretation as π/K decay contamination of dimuon events.

Two events with 5 muon final states have been observed. Event 1208-3386 possesses characteristics similar to those of the more abundant (by $\sim\alpha^{-2}$) muon tridents. Event 851-11418, however, does not seem consistent with any plausible QED process.

The four muon event, 1191-5809, has properties which differ significantly from those of the three reported events in neutrino experiments[2,3,4]. The softest lepton has at least 4 times the energy and the lightest $\mu^+\mu^-$ daughter has at least 4 times the mass of any neutrino-induced counterpart. The most obvious potential background, single muon production due to any process in random association with $\mu^+\mu^-$ pair production due to any process within the same diagram, has been estimated using measured properties of 2 and 3 muon final states in this experiment to be less than 7×10^{-4}.

TABLE 1

Properties of Exotic Events

Event	Scattered Muon	Energies (GeV)	Masses (GeV/c^2)	Unseen $p_\perp$ to $\gamma\gamma$ (GeV/c)
851-5726 $\mu^-\to\mu^-\mu^+\mu^+$ 1 2 3 4	2 Q^2=0.1±0.1 ν =160±6	E_3= 19± 2 E_4= 11± 2 E_{had}=103±15 E_{miss}= 27±17	M_{34}=0.5±0.1	0.3±0.1
1191-5809 $\mu^+\to\mu^+\mu^+\mu^-\mu^-$ 1 2 3 4 5	2 Q^2=0.3±0.2 ν =158±7	E_3= 26± 3 E_4= 18± 2 E_5= 25± 4 E_{had}> 57±11 E_{miss}< 31±14	M_{34}=3.0±0.3 M_{35}=3.2±0.3 M_{345}=4.6±0.3	2.0±0.2
1208-3386 $\mu^+\to\mu^+\mu^-\mu^-\mu^+\mu^+$ 1 2 3 4 5 6	2 Q^2=0.2±0.2 ν =149±9	E_3= 50± 5 E_4= 27± 3 E_5= 61± 6 E_6= 10± 2 E_{had}= 6± 3 E_{miss}= -4±13	M_{35}=1.3±0.2 M_{36}=0.3±0.1 M_{45}=0.4±0.1 M_{46}=0.5±0.1 M_{3456}=2.0±0.2	0.1±0.3
851-11418 $\mu^-\to\mu^-\mu^-\mu^+\mu^+\mu^-$ 1 2 3 4 5 6	2 Q^2=3.5±0.6 ν =61±12	E_3= 13± 2 E_4= 19± 2 E_5= 15± 2 E_6= 10± 2 E_{had}= 5± 3 E_{miss}= -1±13	M_{34}=2.3±0.2 M_{35}=2.0±0.2 M_{46}=0.5±0.1 M_{56}=0.3±0.1 M_{3456}=3.5±0.3	1.8±0.4

INELASTIC STRUCTURE FUNCTIONS

The values of the inelastic structure function $F_2(x,Q^2)$ are extracted using a Monte Carlo simulation to correct for acceptance and resolution. The simulation uses fits to F_2 and $R(x,Q^2)=\sigma_L/\sigma_T$ determined from earlier experiments[5] with the neutron-proton ratio a parameterization of electron data[6].

The values of F_2/nucleon averaged for iron are presented in Figure 2b. This represents 17% of the data on tape. Systematic uncertainties in the energy calibration and resolution, and in trigger efficiency are folded in quadrature with the statistical. There is an overall normalization uncertainty of ±14%.

The data indicate less dependence on Q^2 than measured in earlier experiments[5] although the result is not inconsistent with those. The values of F_2 fall approximately 20% below the extrapolation of fits to those lower Q^2 data at all values of x. Changing the value of R from the form $R=1.2(1-x)/Q^2$ to a large value would increase the measured F_2 particularly at larger values of Q^2. The data presented here are in good agreement with values measured in neutrino scattering from iron[7].

ψ(3100) PRODUCTION BY MUONS

Previous experiments at Fermilab, SLAC, and Cornell have measured ψ photoproduction. We report here 1000±80 $\mu^+\mu^-$ pairs from ψ decay drawn from 16834 muon interactions producing 3 fully-reconstructed muon tracks in the final state. These represent 12% of the data on tape.

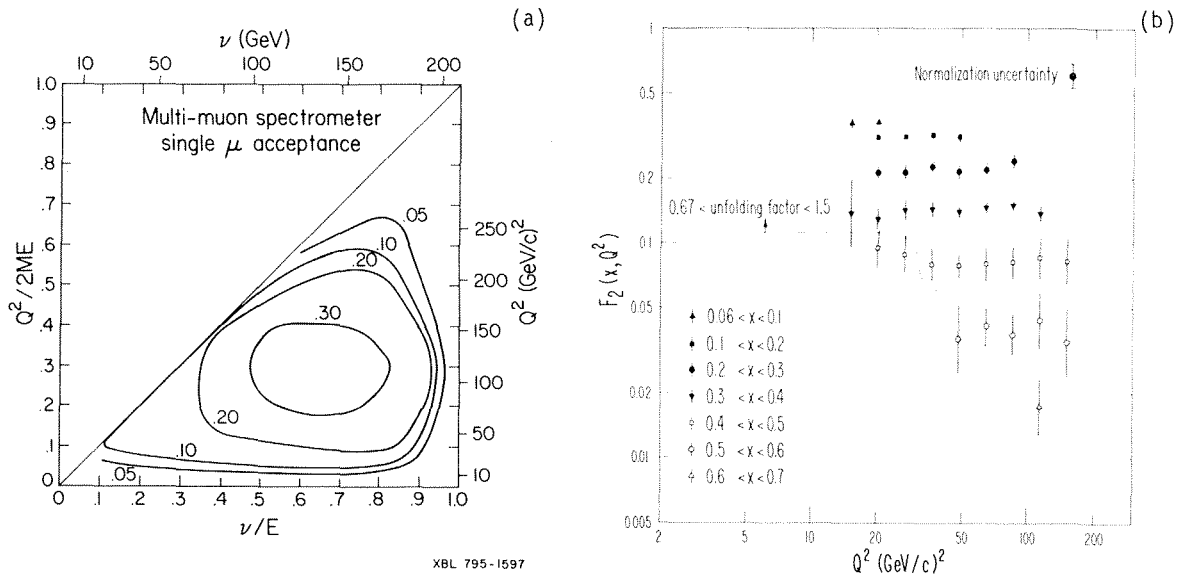

Figure 2. (a) Calculated efficiency for inelastic muon scattering vs. Q^2 and ν, averaged over full target length. (b) Measurements of $F_2(x,Q^2)$ for bins of x. Points above the dashed line have been corrected by a factor less than 1.5 for smearing. Errors shown include statistical and systematic uncertainty.

Only one choice of $\mu^+\mu^-$ pairing is plotted in the mass spectrum of Figure 3(a). The centroid of 3(b) is consistent with 3.1 GeV and the width of 9% agrees with Monte Carlo predictions and with direct calculations. The $\psi'(3685)$ is not resolved.

Data taken at low intensity with interactions restricted to the upstream 8 spectrometer modules were used for determination of the total cross-section

$$\sigma/\text{nucleon}\ (\mu Fe \to \mu\psi X) = 0.76 \pm 0.22\ \text{nb}$$

allowing for the 7% $\psi \to \mu^+\mu^-$ branching fraction. Monte Carlo corrections for nuclear coherence, shadowing and $|t|_{min}$ effects yield

$$\sigma(\mu N \to \mu\psi X) = 0.67 \pm 0.20\ \text{nb}$$

where the error is due to normalization uncertainty. A calculation using a photon-gluon-fusion model is consistent with this result[8].

To make contact with other data at small t, the t-dependence of the cross section was assumed in the Monte Carlo simulation using parameters based on other experiments. The E_γ dependence of Figure 3(c) is insensitive to reasonable variations of the parameters.

Above 30 GeV, the cross sections vary less steeply than is predicted by a photon-gluon-fusion calculation (shaded band). The broken line is the shape of the kinematic factor $(p^{\psi}_{c.m.}/p^{\gamma}_{c.m.})^2$. In the simplest VMD interpretation the ratio of solid to broken lines in Fig. 3(c) gives the energy dependence of the square of the ψ-nucleon total cross section.

The shallow Q^2-dependence in Fig. 3(d) is fit by $(1+Q^2/M^2)^{-2}$ with $M=2.7\pm0.5$ consistent with a ψ propagator; the choice $M \approx m_\rho$ is ruled out.

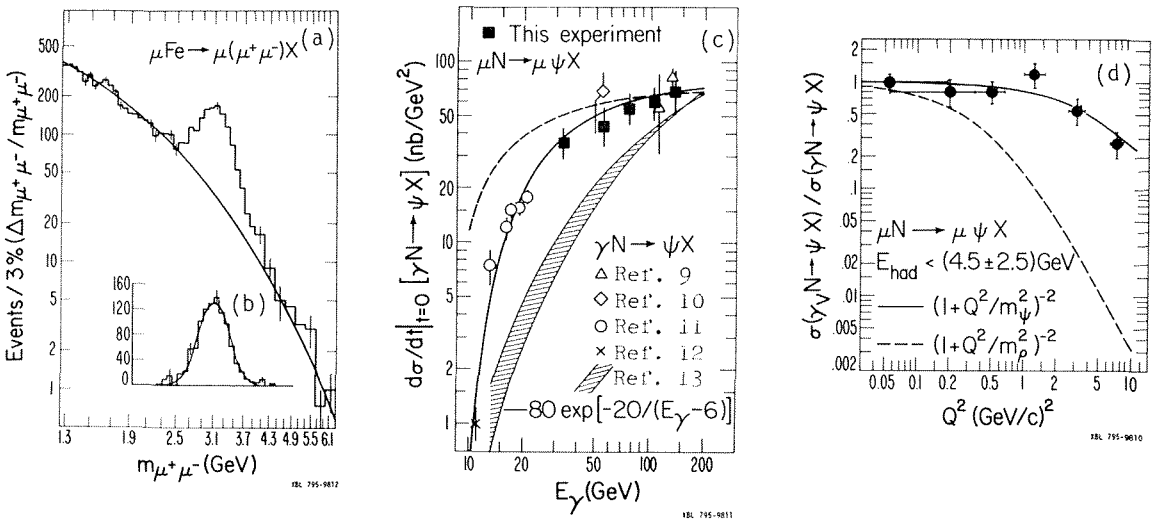

Figure 3. $\mu^+\mu^-$ mass spectrum before (a) and after subtraction (b). Cross sections for ψ production by equivalent virtual photon flux as a function of E_γ (c) and Q^2 (d).

If the charmed quark mass is approximately half of the ψ mass, the kinematics of the photon-gluon-fusion produce a Q^2-dependence similar to that in VMD. Data like that of Fig. 3 may provide a critical test of a more exact QCD calculation.

* * *

REFERENCES

1) T. Hansl et al., Phys. Lett. 77B, 114 (1978).

2) M. Holder et al., Phys. Lett. 73B, 105 (1978).

3) R.J. Loveless et al., Phys. Lett. 78B, 505 (1978).

4) A. Benvenuti et al., Phys. Rev. Lett. 42, 1024 (1979).

5) H.L. Anderson et al., Fermilab Pub. 70/30EXP, submitted to Physical Review.

6) S. Stein et al., SLAC PUB. 1585 (1975).

7) J.G.H. deGroot et al., Z. Physik C. Particles and Fields 1, 143 (1979).

8) V. Barger, W.Y. Keung, and R.J.N. Phillips, Univ. of Wisconsin preprint C00-881-83 (1979).

9) B. Knapp et al., Phys. Rev. Lett. 34, 1040 (1975); W.Y. Lee, in Proc. Int. Symp. on Lepton and Photon Interactions at High Energies (DESY, Hamburg, 1977); M. Binkley, private communication.

10) T. Nash et al., Phys. Rev. Lett. 36, 1233 (1976).

11) U. Camerini et al., Phys. Rev. Lett. 35, 483 (1975).

12) B. Gittelman et al., Phys. Rev. Lett. 36, 1616 (1975).

13) M. Glück and E. Reya, Phys. Lett. 79B, 453 (1978); M. Glück and E. Reya, DESY preprint 79/05 (1979). In Fig. 3(c) we have multiplied their result for σ by 2.4 to obtain dσ/dt(t=0).

This work was supported by the High Energy Physics Division of the US Department of Energy under contract Nos. W-7405-Eng-48, EY-76-C-02-3072, EY-76-C-02-3000.

A MEASUREMENT OF THE PRODUCTION OF MASSIVE e^+e^- PAIRS IN PROTON-PROTON COLLISIONS AT $\sqrt{s}$ = 62.4 GeV

CERN-Columbia-Oxford-Rockefeller (CCOR) Collaboration

A.L.S. Angelis, H.-J. Besch, B.J. Blumenfeld, L. Camilleri, T.J. Chapin, R.L. Cool, C. del Papa, L. Di Lella, Z. Dimcovski, R.J. Hollebeek, L.M. Lederman, D.A. Levinthal, J.T. Linnemann, C. Newman, N. Phinney, B.G. Pope, S.H. Pordes, A.F. Rothenberg, R.W. Rusack, A.M. Segar, J. Singh-Sidhu, A.M. Smith, M.J. Tannenbaum, R.A. Vidal, J.S. Wallace-Hadrill, J.M. Yelton and K.K. Young.

ABSTRACT

An apparatus consisting of a superconducting solenoid magnet, cylindrical drift chambers, and two arrays of lead-glass Cerenkov counters has been used at the CERN ISR to study the production of e^+e^- pairs of invariant mass above 6.5 GeV/c^2.

The production of massive electron-positron pairs in proton-proton collisions has been measured at the CERN ISR at a centre-of-mass energy ($\sqrt{s}$) of 62.4 GeV, as part of a general study of high transverse momentum processes [1,2]. In this report, after a description of the apparatus and event selection procedure, three topics are discussed : the e^+e^- continuum for $m_{e^+e^-} > 6.5$ GeV/c^2 [3], the cross-section for the Υ family of resonances [4], and the mean transverse momentum, $\langle p_T \rangle$ of the lepton pair for both the continuum and the resonances. The data presented here come from an integrated luminosity of $8.5 \times 10^{37} cm^{-2}$.

The experimental apparatus (Fig. 1) can be considered in two parts. The inner detector, designed to track charged particles, consisted of a set of 4 double-gap cylindrical drift-chambers inside a thin-walled superconducting solenoid magnet [5,6] (B = 1.4 Tesla). The outer detector, used to identify electrons and photons and measure their energies, consisted of two large arrays of lead-glass Cerenkov counters [1], one on either side of the intersection region. The pulse-heights recorded in the scintillation counters 'B' on the outer face of the magnet were used to correct, event by event, for the apparent energy loss of electrons passing through the magnet coil and cryostat (1 radiation length of aluminium). This correction was typically 260 MeV. The r.m.s. momentum resolution of the tracking system was $\Delta p/p = 6\% p$ (p in GeV/c). The mass of the electron pair was calculated using the energies as measured in the lead-glass counters, with an r.m.s. resolution of 4% at 10 GeV/c^2. The geometric acceptance covered the range $-0.5 < y < 0.5$ and was 9% for this interval assuming a cross-section flat in y, the rapidity of the lepton pair. The acceptance did not depend significantly on the decay angular distribution.

The trigger required that more than 2 GeV be deposited in a cluster of 3 x 3 counters in each lead-glass array, and was dominated by π^0 pairs. Off-line, tracks in the inner detector and the clusters in the lead-glass

arrays were reconstructed independently, and only events with tracks pointing to clusters in both arrays retained. The genuine electron pairs formed less than 6% of this sample which consisted of backgrounds in roughly equal amounts from three sources : (a) the spatial overlap of a charged hadron with a π^0, (b) electrons and positrons from Dalitz decays of π^0's and external conversions in the beam-pipe and the first layer of the innermost drift-chamber and (c) charged hadrons which deposited most of their energy in the lead-glass arrays after interacting in the magnet coil or the lead-glass itself. To reduce these backgrounds, some further cuts were made, of which the most important were to require that the momentum of each track match the energy of its corresponding cluster and that the energy in the cluster be concentrated appropriately around the track direction The overall analysis efficiency was 50 ± 5%.

Of the remaining 226 events, there were 174 where the two particles were of opposite charge, and 52 where they were of the same charge. It is assumed that the contribution of background processes to the opposite-charge class is given by the number of events in the same-charge class. This assumption is valid for both the electromagnetic backgrounds (b) and the hadronic backgrounds [7]. Since the apparatus acceptance for positive and negative particles was the same, a direct subtraction was performed to obtain the electron-positron signal (Fig. 2).

The cross-section $\left.\frac{d^2\sigma}{dmdy}\right|_{y=0}$ for $m > 6.5$ GeV/c^2 is given in Fig. 3. The peak in the mass region 8.5 → 11 GeV/c^2 corresponds to the T resonances[8,9] and there is a continuum region below 8.5 GeV/c^2 and above 11 GeV/c^2; the line is a fit excluding the T region. In addition to the statistical errors shown, uncertainties in the luminosity measurement, analysis efficiency and acceptance give an overall uncertainty of 12%, and there is an uncertainty of 5% in the mass scale. The scaling hypthesis [10] predicts that the quantity $m^3 \left.\frac{d^2\sigma}{dmdy}\right|_{y=0}$ or equivalently $s^{3/2} \left.\frac{d^2\sigma}{dmdy}\right|_{y=0}$ should be a function of $(m/\sqrt{s})$ only. To test this we compare our data with results from Fermilab [8]. The fit given in ref. 8 implies that the cross-section at $\sqrt{s} = 62.4$ should exceed that at $\sqrt{s} = 27.4$ by a factor of 4 at a mass of 7 GeV/c^2 and a factor of 200 at 14 GeV/c^2. Figure 4 shows that the values for the scaled cross-sections from the two experiments are quite consistent with this prediction.

The excess of 40 events above the continuum fit in the mass range 8.5 - 11 GeV/c^2 is due to the T family of resonances and corresponds to a cross-section $B \left.\frac{d\sigma}{dy}\right|_{y=0} = (9 \pm 2) \times 10^{-36}\text{cm}^2$ for the T, T' and T''; the error includes the uncertainty from the continuum subtraction. This value is much lower than the value of $(59 \pm 34) \times 10^{-36}\text{cm}^2$ from another ISR experiment [11], although the two results are consistent given the quoted errors. Our cross-section is 25 times the cross-section at $\sqrt{s} = 27.4$ and it is interesting to note that the behaviour of the cross-section for T

production is similar to that of the J/ψ as a function of m/√s with a relative magnitude of 10^{-3} (Fig. 5). The ratio of the resonances cross-section $B \frac{d\sigma}{dy}_{y=0}$ to the continuum $\frac{d^2\sigma}{dmdy}_{y=0}$ at 9.5 GeV/c^2 is 3 ± 0.7 in the present experiment, compared to the value 1.66 ± 0.06 measured at √s = 27.4 [9]. No event is observed in the present experiment with mass > 16 GeV/c^2 which implies a 95% confidence level upper limit on $B \frac{d\sigma}{dy}_{y=0}$ for any heavier resonances of 7.5 x 10^{-37} cm^2.

The mean transverse momentum of the lepton pair for the mass 6.5 → 8.5, 8.5 → 11 and above 11 GeV/c^2 is shown in Fig. 6. Except for the first point, which is affected by the energy threshold in the trigger and where the error has been increased accordingly, the mean p_T is essentially independent of the form taken for the p_T distribution, and is also independent of the decay angular distribution of the leptons. The trend for $\langle p_T \rangle$ to increase with √s at a fixed mass as observed at Fermilab [8] is clearly continued to the ISR energy range.

Acknowledgements

We are particularly grateful to our secretary and data aide M.A. Huber, our technician R. Gros, and to Dr. C. Onions who provided invaluable programming assistance. We should like to acknowledge the excellent performance of the ISR machine itself.

REFERENCES

1) A.L.S. Angelis, et al., Phys. Letters 79B (1978) 505.

2) A.L.S. Angelis, et al., Physica Scripta 19 (1979) 116.

3) D.C. Hom, et al., Phys. Rev. Lett. 36 (1976) 1236.

4) S.W. Herb, et al., Phys. Rev. Lett. 39 (1977) 252.

5) L. Camilleri, et al., NIM 156 (1978) 275.

6) M. Morpurgo, Cryogenics 17 (1977) 89.

7) M. Albrow, et al., Nucl. Phys. B145 (1978) 305.

8) J.K. Yoh, et al., Phys. Rev. Lett. 41 (1978).

9) K. Ueno, et al., Phys. Rev. Lett. 42 (1979) 486.

10) S. Drell and T-M Yan, Phys. Rev. Lett. 25 (1970) 316.

11) J. Cobb, et al., Phys. Letters 72B (1977).

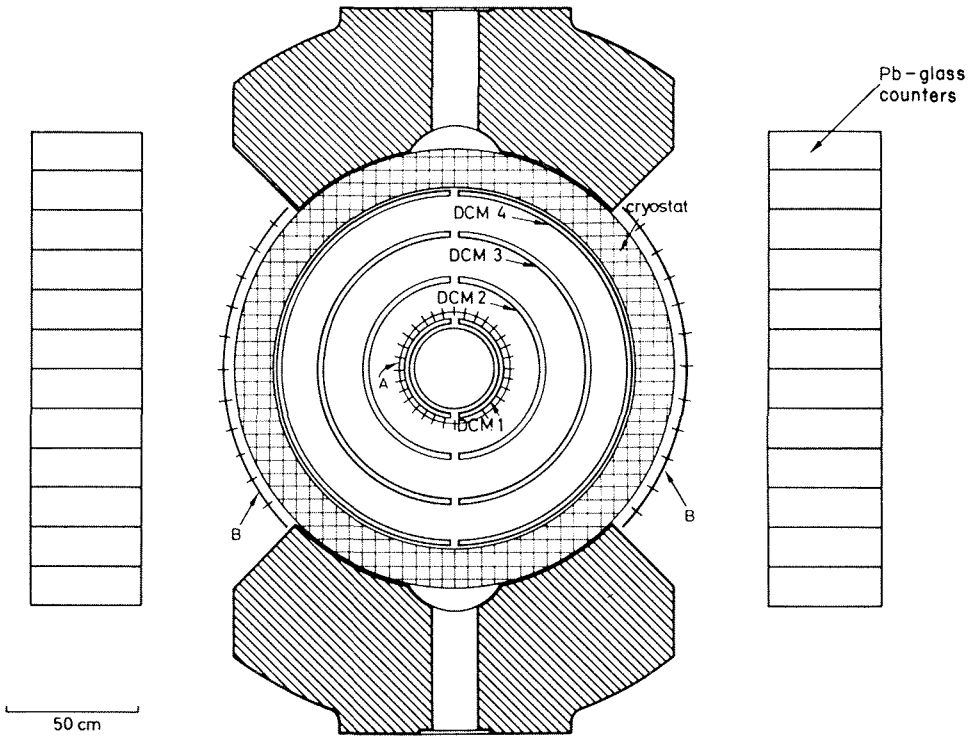

VIEW PERPENDICULAR TO THE BEAMS

Fig. 1

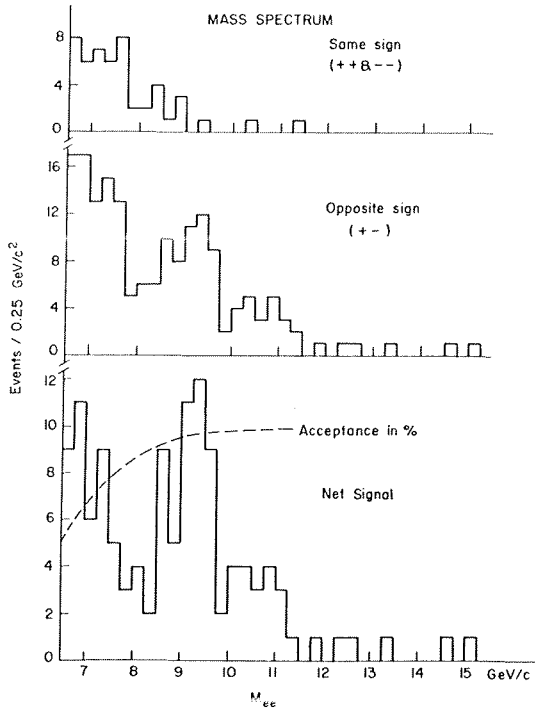

Fig. 2

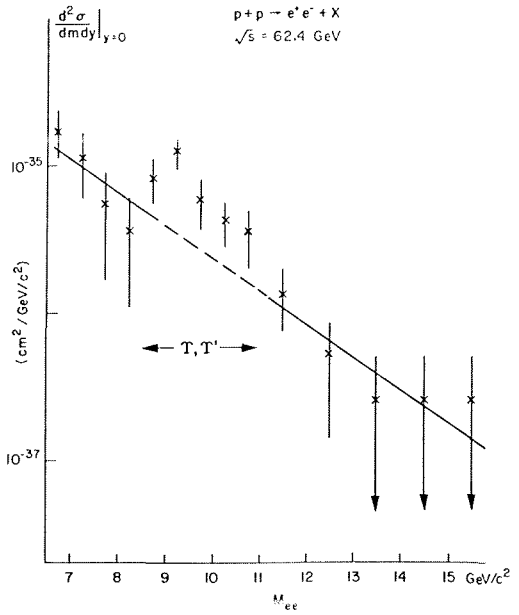

Fig. 3

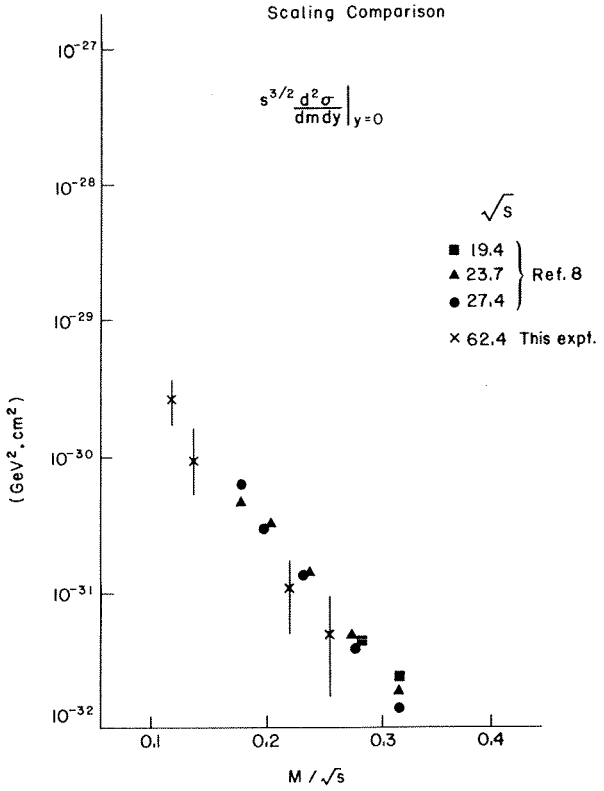

Fig. 4

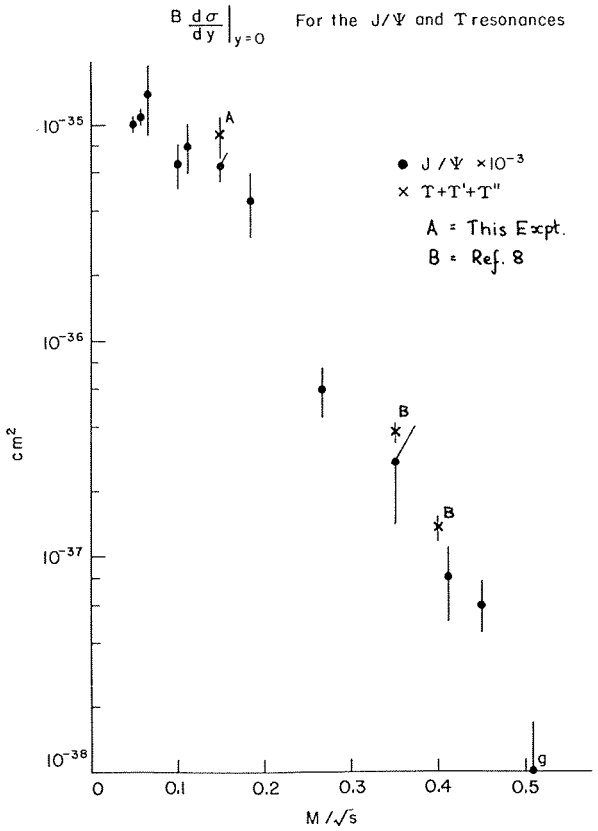

Fig. 5

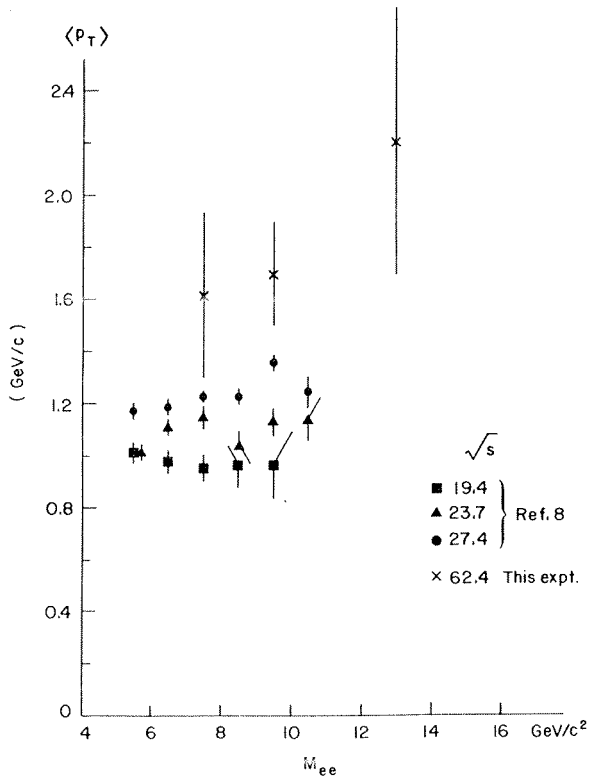

Fig. 6

JETS IN DEEP INELASTIC ELECTROPRODUCTION

DECO Collaboration
G. Drews, W. Gebert, F. Janata, P. Joos, A. Ladage, H. Nagel*), H. Preissner and P. Söding
II. Institut für Experimentalphysik der Universität Hamburg
and Deutsches Elektronen-Synchrotron DESY, Hamburg

I. Cohen, R. Erickson, F. Messing**), E. Nordberg, R. Siemann, J. Smith-Kintner and P. Stein
Cornell University, Ithaca, N.Y. 14853

A. Sadoff
Ithaca College, Ithaca, N.Y. 14850

ABSTRACT

Results on jet structure of the hadronic final state in electron-proton scattering are presented. The kinematic range includes $1 < Q^2 < 6$ GeV^2 and $9 < W^2 < 16$ GeV^2. The correlation between the jet axis determined with sphericity or thrust and the direction of the virtual photon is measured. Comparison with data from e^+e^--annihilation is made. A method to estimate the intrinsic transverse momentum of the quark in the target proton is presented.

In the framework of the quark-parton model the fast final state hadrons from electron-proton scattering are interpreted as quark or diquark fragments. The hadronic final state is expected to exhibit a dominant two jet structure. In its center-of-mass system these jets are collinear. The extent to which the jet axis agree with the direction of the virtual photon will depend on the intrinsic transverse momentum of the quark in the target proton.

We present results on jet structure from an electron-proton scattering experiment performed in an 11.5 GeV electron beam at the Wilson Synchrotron Laboratory. The apparatus, the main part of which was a streamer chamber, is described in Ref. 1. The kinematic region is 1 GeV^2 < Q^2 < 6 GeV^2 and 9 GeV^2 < W^2 < 16 GeV^2 ($-Q^2$,W^2 are the squares of the invariant masses of the virtual photon and the final state hadrons respectively). To suppress contributions from diffractive processes, predominantly $ep \to ep\rho^0(\to\pi^+\pi^-)$, only events with more than three charged hadrons in the final state are accepted. The quantities used are sphericity[2,3,4]

$$S = \frac{3}{2} \min\left(\sum_i p_{i\perp}^2 \Big/ \sum_i p_i^2 \right) \tag{1}$$

and thrust[3,5]

$$T = \max\left(\sum_i |p_{i\parallel}| \Big/ \sum_i |p_i| \right). \tag{2}$$

Since in this experiment neutral hadrons were not detected the summations in formulae (1) and (2) run only over charged hadrons.

In Fig. 1 the distribution of $|\cos\Theta|$ is shown where Θ is the angle between the sphericity or thrust axis and the direction of the virtual photon in the center-of-mass system.

---

*) Now at Beiersdorf AG. Hamburg
**) Now at Carnegie-Mellon University, Pittsburgh, PA.

The data exhibit a strong correlation between the jet axis and the photon direction as expected. For the Lorentz-transformation to the center-of-mass system the hadrons have to be identified as pions, kaons or protons. This is done on a statistical basis using parametrizations of hadron structure functions[6]. Even when all charged hadrons are treated as pions the results remain qualitatively the same.

In Fig. 2 $\langle p_\perp \rangle$ and $\langle p_{||} \rangle$ of all hadrons with respect to the directions of the virtual photon and the sphericity and thrust axis are presented as function of W' where $W' = W - m_N + m_\pi \approx W - 0.8$ GeV. For comparison the results from PLUTO[3] on $\langle p_\perp \rangle$ and $\langle p_{||} \rangle$ relative to the thrust axis are included. The use of W' instead of W for the ep data serves as a rough correction for the kinematic effect of the final baryon. Although the ranges of W and W' covered by the e^+e^- and ep data do not overlap the figure shows clearly that the ep data continue the trend defined by the e^+e^- data when the sphericity or thrust axes are used. This does not hold however when $p_\perp$ and $p_{||}$ are defined with respect to the virtual photon direction.

The deviations of the sphericity and thrust axes from the calculated direction of the virtual photon seen in Fig. 1 and Fig. 2 may be due to several causes: a) radiative effects, b) missing neutrals, c) non-identification of protons and kaons, d) the fact that the sphericity and thrust axes are only approximations to the real jet direction at finite energies, e) transverse momentum of the quark in the target proton. In order to eliminate the first three causes for the following investigation events were selected that satisfy a kinematic 4c fit e.g. for the reaction type $ep \to ep\pi^+\pi^+\pi^-\pi^-$. To disentangle the influences of the last two causes listed above a Monte Carlo model was developed. This model is based on Field and Feynman's parametrization of quark fragmentation[7] which was found to be in

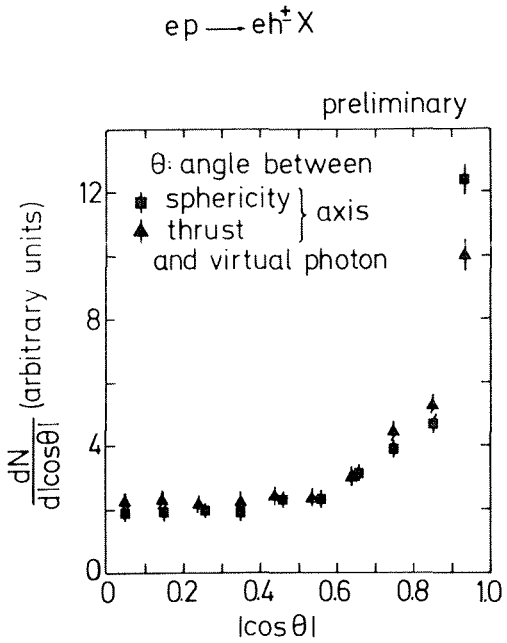

Fig. 1 The distribution of $|\cos\Theta|$ for events with more than three observed final state hadrons at $9 < W^2 < 16$ GeV^2 and $Q^2 > 1$ GeV^2.

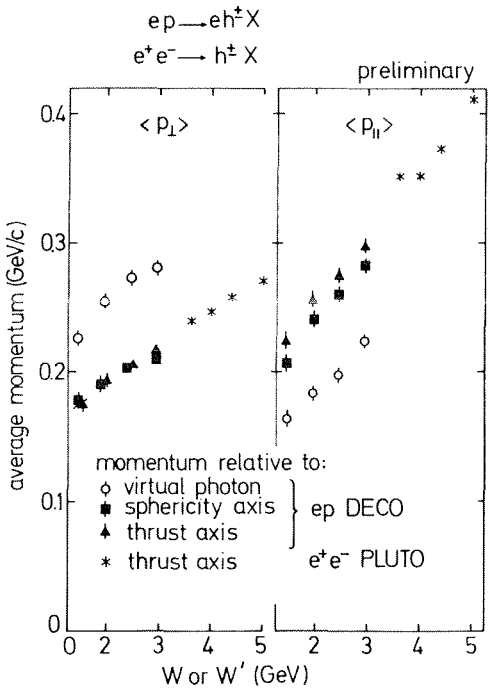

Fig.2 The average transverse and longitudinal momentum of all final state hadrons as a function of $W' = W - m_N + m_\pi$ for events with more than three observed hadrons. The PLUTO[3] data are shown as function of W.

good agreement with the pion fragmentation functions determined in this experiment[6]. It is assumed that the fragmentation of the diquark system is equal to that of the quark except for the fact that the first rank hadron is always a baryon. The quark and diquark jets with energy W/2 each and opposite directions are first calculated independently. Then the two jets are combined whereby in an iterative way the momenta of the hadrons are changed according to momentum and energy conservation[8].

Comparison between the experimental events and the results of the Monte Carlo model shows good agreement in the distributions of momenta, sphericity, $m_{\pi^+\pi^-}$, $m_{p\pi^+}$, $m_{p\pi^-}$, and $p_\perp^2$ with respect to the sphericity axis. This gives confidence that the model serves as a good description of the final hadronic system in our experiment.

On the other hand, the average angle between the direction of the parent quark and the jet axis in the Monte Carlo model comes out significantly smaller than the angle between the virtual photon direction and the jet axis in the real events. This suggests that the fragmenting quark did have a primordial transverse momentum distribution. Assuming this distribution to be of the form $\exp(-k_\perp^2/2\sigma^2)dk_\perp^2$, it is found that the most likely value for $\langle k_\perp \rangle_{quark}$ lies between 0.5 and 0.9 GeV/c (see Fig. 3).

In summary our investigation of jet structure of the hadronic final state in ep scattering provides further support for the quark-parton model. The data show a strong correlation between the direction of the virtual photon and the jet axis. The mean transverse and longitudinal momenta of the hadrons with respect to the jet axis in ep scattering and e^+e^- annihilation follow a common trend. The width of the angular distribution between virtual photon and jet direction is consistent with an intrinsic transverse momentum of the quark in the target proton of 0.7 ± 0.2 GeV/c.

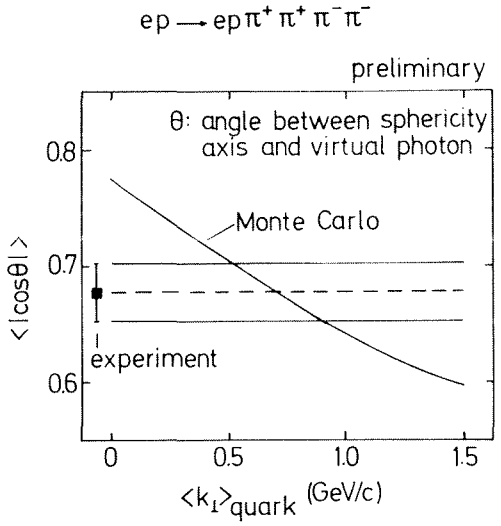

Fig.3 Comparison between the experimental result on $\langle|\cos\theta|\rangle$ and a Monte Carlo model with varying intrinsic transverse momentum $k_\perp$ of the quark in the target proton.

This work was supported in part by the Bundesministerium für Forschung und Technologie and the National Science Foundation. We gratefully acknowledge the support of Professor B.D. McDaniel, Professor H. Schopper, and Professor G. Weber, and the staffs of the Wilson Synchrotron Laboratory and DESY.

* * *

REFERENCES

1) I. Cohen et al., Phys. Rev. Lett. 40, 1614 (1978).

2) G. Hanson et al., Phys. Rev. Lett. 35, 1609 (1975).

3) PLUTO Collaboration, Ch. Berger et al., Phys. Lett. B78, 176 (1978).

4) J.D. Bjorken and S.J. Brodsky, Phys. Rev. D1, 1416 (1970).

5) E. Fahri, Phys. Rev. Lett. 39, 1587 (1977).

6) G. Drews et al., Phys. Rev. Lett. 41, 1433 (1978).

7) R.D. Field and R.P. Feynman, Nucl. Phys. B136, 1 (1978).

8) H.G. Sander (TASSO Collaboration), private communication.

DIMUON SPECTRA FROM 62 GeV PROTON COLLISIONS

CERN-Harvard-Frascati-MIT-Naples-Pisa Collaboration

D. Antreasyan, W. Atwood, V. Balakin, R. Battiston, U. Becker, G. Bellettini, P.L. Braccini, J.G. Branson, J. Burger, F. Carbonara, R. Carrara, R. Castaldi, V. Cavasinni, F. Cervelli, M. Chen, G. Chiefari, T. Del Prete, E. Drago, M. Fujisaki, M. Hodous, T. Lagerlund, P. Laurelli, O. Leistam, R. Little, P.D. Luckey, M.M. Massai, T. Matsuda, L. Merola, M. Morganti, M. Napolitano, H. Newman, D. Novikoff, L. Perasso, K. Reibel, J.P. Revol, R. Rinzivillo, G. Sanguinetti, C. Sciacca, P. Spillantini, K. Strauch, S. Sugimoto, S.C.C. Ting, W. Toki, M. Valdata-Nappi, C. Vannini, F. Vannucci, F. Visco and S.L. Wu

(Presented by U. Becker)

ABSTRACT

Results from an experiment studying $pp \to \mu^+\mu^- X$ at the ISR with the highest possible energy of $\sqrt{s}$ = 62 GeV are presented. With relatively high statistics at these energies, the measurements extend to very high muon-pair masses. Associated hadron multiplicities are observed.

The continuum of the pair spectra exhibits scaling. The data allow the extraction of the explicit dependence on x_{Feyn}, the transverse momentum p_T, and the decay angle θ. The angular distribution is flat at the Υ, and $1 + \cos^2\theta$ otherwise. J and Υ are seen and measured, as well as very high mass events. Limits of resonance production are estimated.

Here we present data from experiment R209 [1] measuring

$$pp \to \mu^+\mu^- X \ , \qquad (1)$$

which was carried out at the CERN Intersecting Storage Rings (ISR) from the beginning of 1978 to March 1979, with $\sqrt{s}$ = 62 GeV and an integrated luminosity of 1.06×10^{38} cm^{-2}. Observing 11,000 muon pairs with invariant mass above 2.8 GeV, these data provide the best statistical measurement in the range of high masses.

The experiment was designed to study heavy photons in $pp \to \gamma_V X$, with $\gamma_V \to \mu^+\mu^-$, by measuring the pair mass spectrum from 3-20 GeV and the angular distribution together with the multiplicities of the residual hadrons X.

The second aim was to search for new resonances Z, decaying into muon pairs $Z \to \mu^+\mu^-$. For this the detector was designed to accept very high pair masses. It also required the highest possible energy -- as available only on the CERN ISR.

1. THE DETECTOR

The detector is shown in Fig. 1a. Seven toroids of magnetized iron surround the interaction region. Muons are identified by penetration, requiring a minimum of 1.8 GeV/c momentum. Hadrons are absorbed in 450 tons of material with 8-11 absorption lengths along the path.

Made from low-carbon steel of the Carnegie-Mellon cyclotron, the rectangular yokes 1a,b,c, 2a,b, and the round ones 3 and 4, are excited by toroidal coils to a rather uniform magnetic field of 1.75 T. This was measured by Hall probes to < 3%, and also independently confirmed by pick-up coils around the yokes.

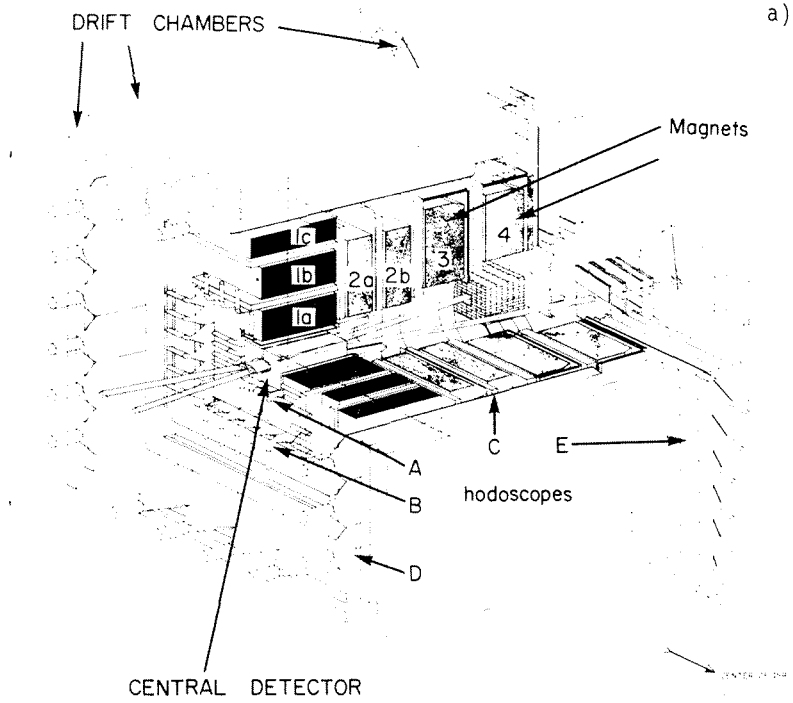

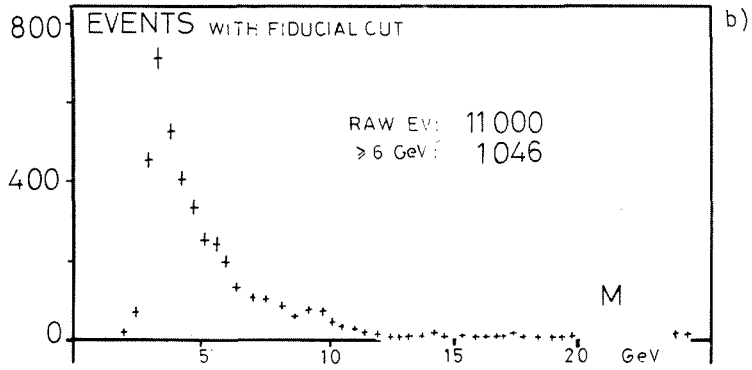

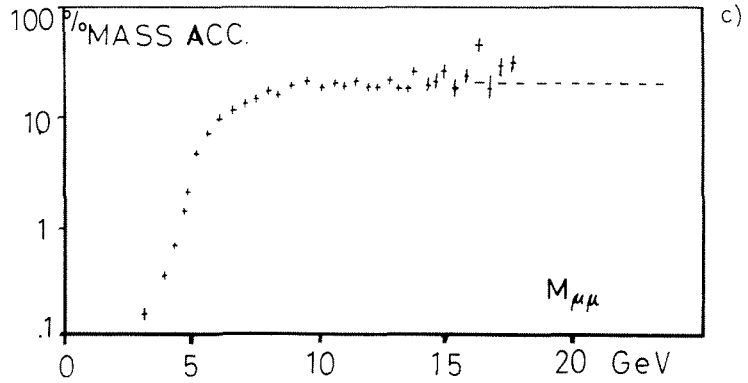

Fig. 1 a) Detector with one quadrant removed for clarity. Shaded areas are the toroidal magnets cut orthogonal to the field lines. b) Event distribution versus reconstructed mass. c) Mass acceptance versus computer-generated mass.

Large-size drift chambers between the magnets and around the detector determine the muon momenta. These chambers have dimensions of up to 6.5 × 2.7 m^2, and a total of 5000 wires spaced by 101.6 mm. With four planes per chamber[2] measuring x,y twice, the left-right ambiguity is resolved and the angle of incidence determined. All the chambers were tested extensively and the resolution was found to be 430 μm. After installation and survey, cosmic rays were used to check their final position with small calibration chambers. Covering ∿ 800 m^2, they contain 60 m^3 of argon + isobutane (75:25% vol. mixture), supplied from a 95% recycling and purifying system.

Immediately around the intersection, an array of 136 precision drift chambers with 544 wires and 272 delay lines indicates all outgoing tracks by 3-5 points, accurate to 0.2 mm along the beam and 2 mm transverse to it. The muon tracks are observed and, together with the hadron tracks, a vertex is determined. The multiplicity and directions of the associated hadrons are measured. An additional system of 34 drift chambers, with 361 wires and 187 delay lines, measure tracks at an angle of 30° down to 1° to the proton beams.

Hodoscopes A, B, C, D, and E form the pair trigger to read out the chambers; their times are precisely recorded on 160 TDCs. Covering 200 m^2, special precautions were necessary to suppress environmental background. Hodoscope D, with elements of 0.83 × 4.0 m^2, has fast 5-inch tubes at both ends. The time difference determines the muon position to 25 cm, which can be checked against the chambers; this eliminates multitrack background and accidentals. In addition, fast "mean timers" give position-independent signals which enable the rejection of cosmic rays, these signals being 15 ns out of time. The toroids have a roughly circular field; bending affects the polar angle θ but not the azimuthal angle φ (around the beam). The B, C, D, (E) hodoscopes form 24 (48) equal φ sectors. Even the worst (3σ) multiple scattering is confined to one sector. Therefore matching combinations (BD, etc.) are formed, allowing also the adjacent elements to define a coarse μ track in the logic. Two tracks at 180° ± 50° yield a trigger.

In summary, the detector has a large acceptance

$$15° < \theta < 130° \quad , \quad p_\mu > 1.8 \text{ GeV} \quad .$$

The π and K decays are small, because the absorber already starts at 40 cm from the vertex.

Figure 1c shows the resulting mass acceptance obtained from a Monte Carlo calculation accounting for multiple scattering energy loss, chamber efficiency, and fiducial cuts as applied to real events. The production mechanism used is consistent with our data.

The momentum resolution is limited by the multiple scattering in iron rather than by the chamber accuracy. One expects Δm/m = 11% almost independent of mass.

2. DATA AND CHECKS

The raw events observed with this apparatus in a year, with $\int L\,dt = 1.06 \times 10^{38}$ cm^{-2}, are more than any other measurement in this energy range and are presented in Fig. 1b. To safeguard against systematic errors, half of the data were taken at each magnet polarity. All time and pulse-height recording equipment was frequently recalibrated and compared to pulser signals. The gas composition was tightly controlled by a chromatograph to avoid efficiency fluctuations.

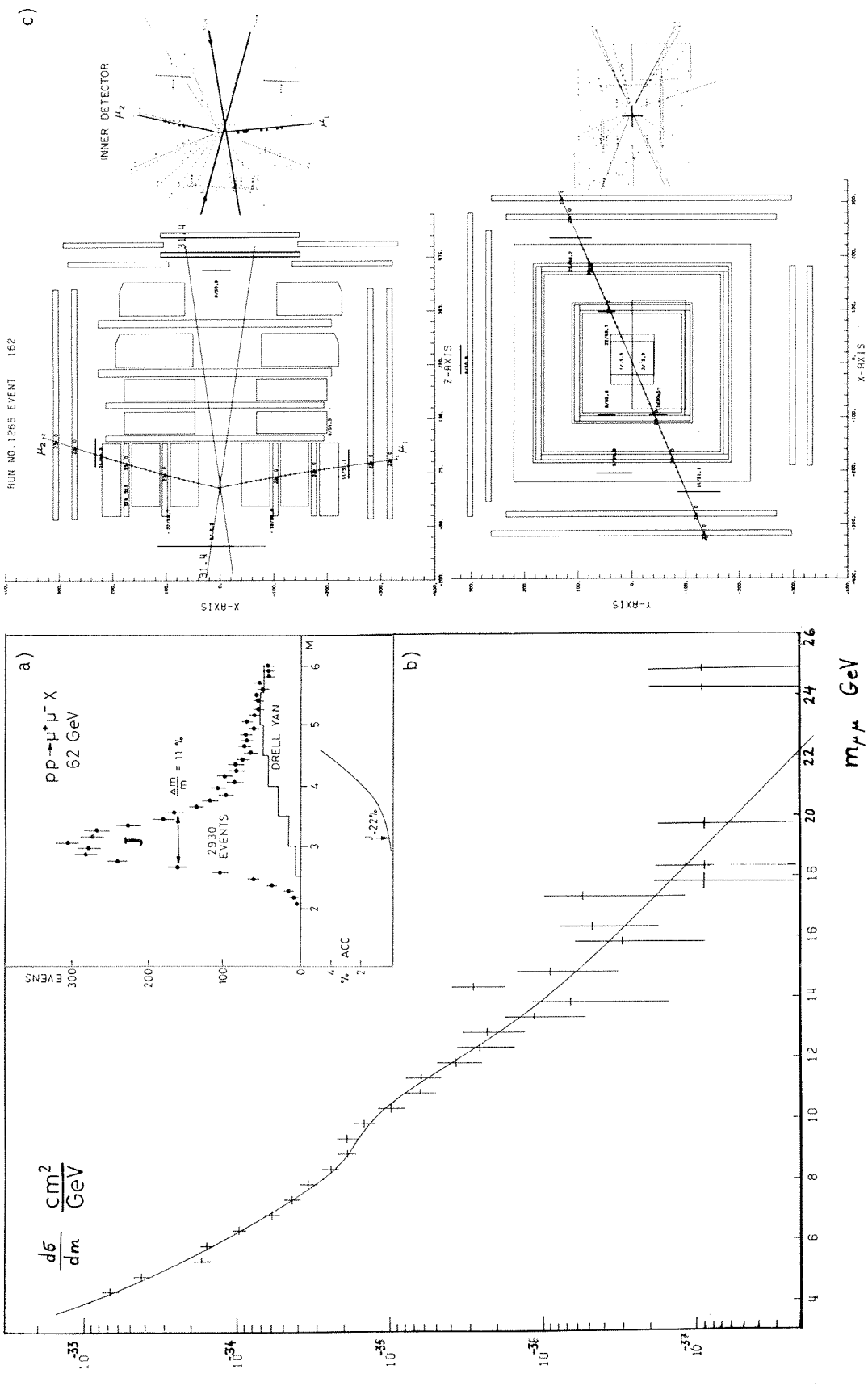

Fig. 2 a) Events in the J region, showing the mass resolution and Drell-Yan contribution. Lower: mass acceptance vs. generated mass. b) Cross-section with simultaneous fit for continuum and $\Upsilon + \Upsilon' + \Upsilon''$ contributions (see text). c) Computer-reconstructed picture of a high mass event. Top view and front view of the detector, accompanied by enlarged view of the tracks in the hadron detector. M = 24.9 GeV, p_T = 1.2 GeV, and x_F = 0.2.

All events were required to originate from the interaction diamond, as "seen" by the inner detector.

Recording cosmic-ray data with magnetic field and comparing the independently fitted momenta of the upper and lower half of the detector yielded $\Delta p/p \approx 16\%$ as expected, confirming the recognition program. From this the mass resolution is estimated to be $\Delta m/m \simeq 16\%/\sqrt{2}$, almost independent of mass. A very direct check is given by observing the J with an apparent width of 780 MeV as in Fig. 2a, in good agreement with the expected 11% mass resolution.

3. J AND T RESONANCES

Kinematically, the muons from J's produced at rest have 1.55 GeV/c momentum and cannot penetrate the iron (1.8-2 GeV). Instead, we measure J's produced forward with $x_F = p_L/p_{L_{max}} \simeq 0.2$. In this case the decay muons have $p > 2.8$ GeV/c. The acceptance is very small and difficult to calculate, and is accounted for by the conservative errors of the cross-section

$$B_{\mu\mu} \left.\frac{d\sigma}{dy}\right|_0 (J) = \left(1^{+1.0}_{-0.5}\right) \times 10^{-32} \text{ cm}^2 .$$

Figure 2b shows the mass spectrum from 4 to 26 GeV, obtained from the events of Fig. 1b and the acceptance incorporating a $(1 - x)^3$ dependence in the Feynman variable x_F, $\exp(-1.0\, p_T)$ for transverse momentum, and $(1 + \cos^2 \theta^{CS}_{\mu^+})$ for angular distribution. All dependences are verified by our data and shown later. The sensitivity to the p_T and x dependence is small, since the detector covers almost the full range. However, taking a flat angular distribution instead of $1 + \cos^2 \theta$ increases the acceptance by 20%. The ansatz

$$\frac{d\sigma}{dm} = A \frac{\left[1 - (m/\sqrt{s})\right]^{10}}{m^4/\sqrt{s}} + B \left\{ \exp\left[- \frac{(1 - 9.4/m)^2}{2\sigma^2} \right] + 0.3 \exp\left[- \frac{(1 - 10/m)^2}{2\sigma^2} \right] \right.$$

$$\left. + 0.15 \exp\left[- \frac{(1 - 10.4/m)^2}{2\sigma^2} \right] \right\}$$

with $\sigma = 10\%$ was fitted to the data of Fig. 2b. With $\chi^2/DF = 17.2/21$, we obtain

$$B_{\mu\mu} \cdot \sigma(\Upsilon) = 10 \pm 3.5 \text{ pb}$$

using a flat angular distribution. The result for the continuum can be recast into the familiar scaling form[3]:

$$m^3 \frac{d\sigma}{dm} = (7.7 \pm 0.4) \times 10^{-33} (1 - \sqrt{\tau})^{10}/\sqrt{\tau} \text{ GeV}^2 \text{ cm}^2$$

with $\tau = m^2/s$. In addition to the quoted errors, the over-all normalization has an uncertainty of 40%.

4. HIGH-MASS EVENTS

As seen in Fig. 2b, both the data and the scaling prediction decrease to less than 2×10^{-37} cm^2 above 20 GeV mass. However, after a gap of several GeV there are two more events at $\sim$ 25 GeV (and one not shown from older data at 28 GeV). The computer-reconstructed picture of one event at 24.9 GeV is shown in Fig. 2c. The front view gives the event in the non-bending plane. Each track has complete sets of coordinates linking to the tracks of the inner detector shown at the right-hand side. The counters initiating the trigger are all within 1.6 ns. The top view displays the excellent momentum fit. The tracks form an angle, seen also in the hadron detector, and with the time information this clearly excludes a cosmic ray. Together with 12 more charged hadrons they emerge from a point well within the interaction diamond. Also indicated is the position using the time difference of both phototubes at the D hodoscope. This matches nicely with the tracks observed with chambers. The event is clean, i.e. does not contain spurious chamber coordinates. This feature is quite common to all events, demonstrating the effectiveness of the iron shielding.

5. ASSOCIATED HADRONS

The hadron detector allows the multiplicity and directions of charged hadrons to be determined. Momenta are not measured. Looking at the track distribution with respect to one of the muons, no correlation was observed. As a function of the dimuon energy $E_{\mu\mu}$ the total multiplicity decreases consistently with the multiplicity expected at the lower energy of $\sqrt{s} - E_{\mu\mu}$.

The multiplicity increases with p_T of the muon pair. Interestingly, this increase happens exclusively in the hemisphere opposing the transverse momentum of the μ pair (see Fig. 3a).

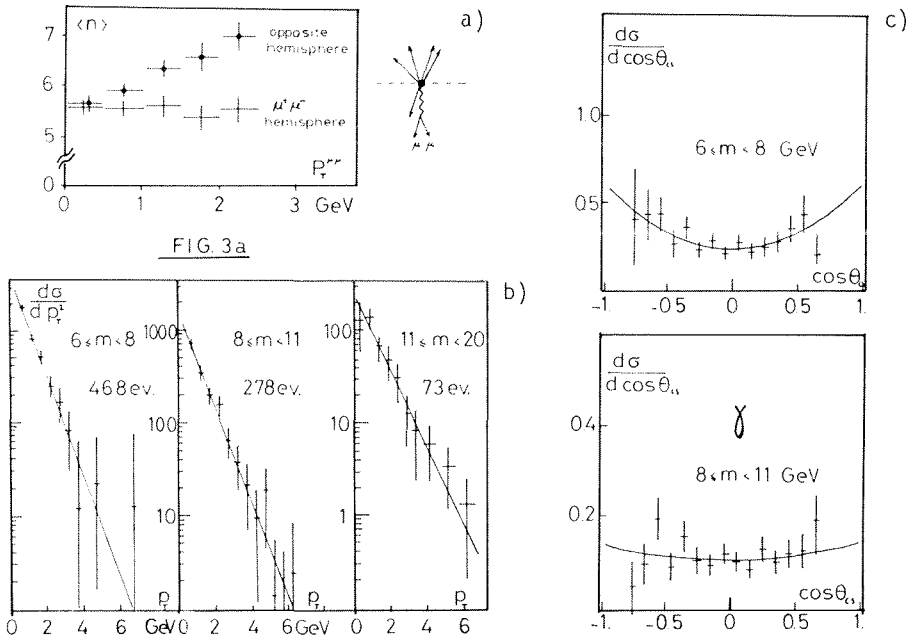

Fig. 3 a) Charged-track multiplicity in the hemisphere of the μ pair. Notice the rise in the opposite one. b) p_T dependence of the dimuons in the 6-8 GeV, the 8 GeV, and the hitherto unexplored 11-20 GeV regions. c) Collins-Soper angular distribution of μ^+.

6. x_F AND p_T DEPENDENCE

Above m = 6 GeV the acceptance is reasonably flat. Comparing the cross-section measured in $-0.1 < x_F < 0.7$ with the form

$$(1 - |x|)^A$$

we find for

468 events in $6 < m < 8$ GeV , $A = 3.0 \pm 0.3$

and

278 events in $8 < m < 11$ GeV , $A = 3.2 \pm 0.3$.

For the same intervals and, additionally, for $11 < m < 20$ GeV the cross-sections $(1/p_T)(d\sigma/dp_T)$ are shown in Fig. 3b in relative units. Neglecting the first (low) bin, a good fit to exp $(-bp_T)$ can be obtained with the result:

$b = 1.20 \pm 0.11 \quad 1.18 \pm 0.10 \quad 0.97 \pm 0.17$ GeV^{-1}

for

m = 6-8 8-11 11-20 GeV .

No difference for the 8-11 region containing the T is seen when this is compared with the other regions. This observation and the measured shape are in good agreement with recent calculations[4].

7. AVERAGE TRANSVERSE MOMENTUM $\langle p_T \rangle$

Three different complementary methods were used to determine $\langle p_T \rangle$:

a) from $d\sigma/dp_T^2 \sim e^{-bp_T}$ there follows: $\langle p_T \rangle = 2/b$;

b) directly (correcting for acceptance): $\langle p_T \rangle = (1/N)\Sigma_{i=1}^{N} p_T^i$;

c) change e^{-bp_T} in the Monte Carlo generation until the best match to the observed event distribution is obtained. This ensures best treatment of the resolution.

The results are summarized in Table 1 for three ranges of dimuon mass.

Table 1

Average transverse momentum in GeV/c

Mass range	6-8	8-11	11-20
a)	1.60 ± 0.15	1.70 ± 0.17	$2.0^{+0.5}_{-0.25}$
b)	1.68 ± 0.19	1.77 ± 0.10	2.0 ± 0.20
c)	1.8 ± 0.2	1.7 ± 0.26	2.1 ± 0.4

These values are definitely higher than those observed at FNAL[3], at the same mass but with $\sqrt{s} = 27.4$ GeV, and suggest a substantial $\sqrt{s}$ dependence.

8. DECAY ANGULAR DISTRIBUTION

Crucial to the Drell-Yan picture of parton antiparton annihilation are the predictions of

i) SCALING: $m^3 \frac{d\sigma}{dm} = F\left(\tau = \frac{m^2}{s}\right)$, and

ii) angular distribution

$$\frac{d\sigma}{d\Omega} \sim 1 + \cos^2 \theta_{\mu^+}$$

following from the spin $\frac{1}{2}$ constituents.

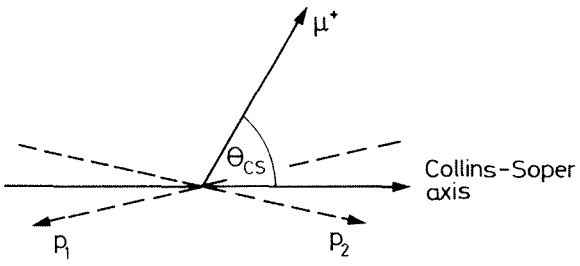

However, the original model ignores p_T. Choosing the reference axis z of Collins and Soper[5] which averages the proton directions p_1, p_2, as seen from the μ-pair c.m.s., one should see to leading order the $1 + \cos^2 \theta_{CS}$ distribution. Figure 3c supports this for

$$6 < m < 8 \text{ GeV} \qquad \text{with} \qquad 1 + (1.6 \pm 0.7) \cos^2 \theta_{CS} \ .$$

However it is remarkably less pronounced and consistent with being flat in the ϒ region:

$$8 < m < 11 \text{ GeV} \qquad \text{with} \qquad 1 + (0.3 \pm 0.6) \cos^2 \theta_{CS} \ ,$$

suggesting another production mechanism. With $\chi^2/DF = 8.2/12$ and $11/12$ these are reasonable fits. The data were integrated over all $x < 0.7$.

9. MULTIMUONS

In order to penetrate the iron of the detector, muons must have $p > 1.8$-2.2 GeV depending on the geometry. The geometrical angular acceptance for each muon is 0.4. Trigger constraints will reduce trimuons by 0.5. Six trimuon events were observed with an integrated luminosity of 1.06×10^{38} cm^{-2}. Two of these events clearly involved a vector-meson mass (J) in one $\mu^+\mu^-$ combination and a third track of bad quality. The remaining four events can be used to pose an upper 2σ limit

$$\sigma(3\mu) < \frac{8 \text{ events} \times 10^{38}}{0.5 \times 0.4^3 \times 1.06} = 2.4 \text{ pb} \ ,$$

for $pp \to 3\mu + X$ with $p_\mu > 2$ GeV, which includes channels such as $B\bar{B}$ production with subsequent cascade decays[6] into muons.

10. CONCLUSION

Measuring $pp \to \mu\mu X$ at $\sqrt{s} = 62$ GeV we find:

$$B \left.\frac{d\sigma}{dy}\right|_0 (J) = \left(1 \begin{smallmatrix} + 1 \\ - 0.5 \end{smallmatrix}\right) \times 10^{-32} \text{ cm}^2 \ ,$$

$$B\sigma(\Upsilon) = 10 \pm 3.5 \text{ pb} \ .$$

Three high-mass events with m > 24 GeV enable a 2σ upper limit to be set on resonance production above 20 GeV:

$$B\sigma < \frac{3 + 2\sqrt{3}}{Acc \cdot L} = 40 \times 10^{-38} \text{ cm}^2 ,$$

where Acc = 0.15 is the acceptance and L = 1.06×10^{38} cm^{-2} is the luminosity. The continuum is measured to small values of τ and is compatible with scaling[3]:

$$m^3 \frac{d\sigma}{dm} = (7.7 \pm 0.4) \times 10^{-33} (1 - \sqrt{\tau})^{10}/\sqrt{\tau} \text{ GeV}^2 \text{ cm}^2 .$$

The associated hadron multiplicity diminishes with $E_{\mu\mu}$ but increases with p_T in the opposite hemisphere.

The $(1 + \cos^2 \theta_{CS})$ distribution is seen, but not at the T, and $\langle p_T \rangle \simeq 1.8 \pm 0.2$ GeV is markedly higher than the values measured at lower $\sqrt{s}$.

Acknowledgement

It is a pleasure to thank CERN and particularly the ISR groups for continuous support.

REFERENCES

1) G. Diambrini-Palazzi, U. Becker, P.J. Biggs, G. Everhard, R. Little, K. Strauch and S.C.C. Ting, Proposal CERN/ISR 73-28 (1973) and Colloquium talk by S.C.C. Ting at CERN, December 1978.

2) U. Becker, J.D. Burger, D. Novikoff and L. Perasso, Nucl. Instrum. Methods 128, 593 (1975).

3) K. Kinoshita, H. Satz and D. Schildknecht, Phys. Rev. D 17, 1834 (1978). The coefficient was determined by fit and agrees with L. Lederman, 19th Int. Conf. on High-Energy Physics, Tokyo, 1978 (Physical Society of Japan, Tokyo, 1979), p. 706.

4) Z. Kunszt, E. Pietarinen and E. Reya, DESY preprint 79/28 (1979), submitted to Phys. Lett.

5) J.C. Collins and D.E. Soper, Phys. Rev. D 16, 2219 (1977).

6) A. Ali, Z. Phys. 1C, 25 (1979).

SESSION VI

A NEW PHYSICS FACILITY

Chairman: S. Fubini

Sci. Secretaries: H. Hoffmann
P. Mouzourakis

Rapporteur's talk:

C. Rubbia Some significant physics objectives of the $p\bar{p}$ collider

SOME SIGNIFICANT PHYSICS OBJECTIVES OF THE $p\bar{p}$ COLLIDER*)

C. Rubbia,
CERN, Geneva, Switzerland.

1. INTRODUCTION. The $p-\bar{p}$ collider will open a new range of centre-of-mass energies with at least five years of advance with respect to ISABELLE and presumably before the corresponding programme at Fermilab. It is clearly impossible within the available time to give a comprehensive review of the major experimental activities. I shall therefore discuss a few topics which, I believe, are particularly significant:

(1) large p_T-effects for jets and single particles
(2) search for intermediate bosons
(3) search for Higgs particles
(4) weak interactions without bosons?
(5) production of very narrow charmonium-like resonances.

At the end I would like to describe briefly the general-purpose detector which is planned for one of the interaction regions around the SPS (LSS5).

2. STRONG INTERACTION EFFECTS: LARGE p_T PHENOMENA. The recent developments in QDC have considerably increased the significance of high momentum transfer phenomena. QDC is believed to be more than a phenomenological model[1]. It is a precise and complete theory purporting to be an ultimate explanation of all hadronic experiments. There one starts with the world of point-like partons, i.e. quarks and vector gluons which interact amongst each others. However higher collisions, which are of great mathematical complexity, are replaced by an effective "non-scaling" parton distribution and fragmentation functions.

This approach has been remarkably successful for the case of deep inelastic electron scattering. The higher order graphs modify the bare, scale invariant cross-section. If the total cross-section is hardly affected, the higher order effects simulate a decrease of hard partons (large-x) and an increase of soft (low-x) partons. The moments

---

*) This report is an extract from CERN SPC/423, 18 September 1978.

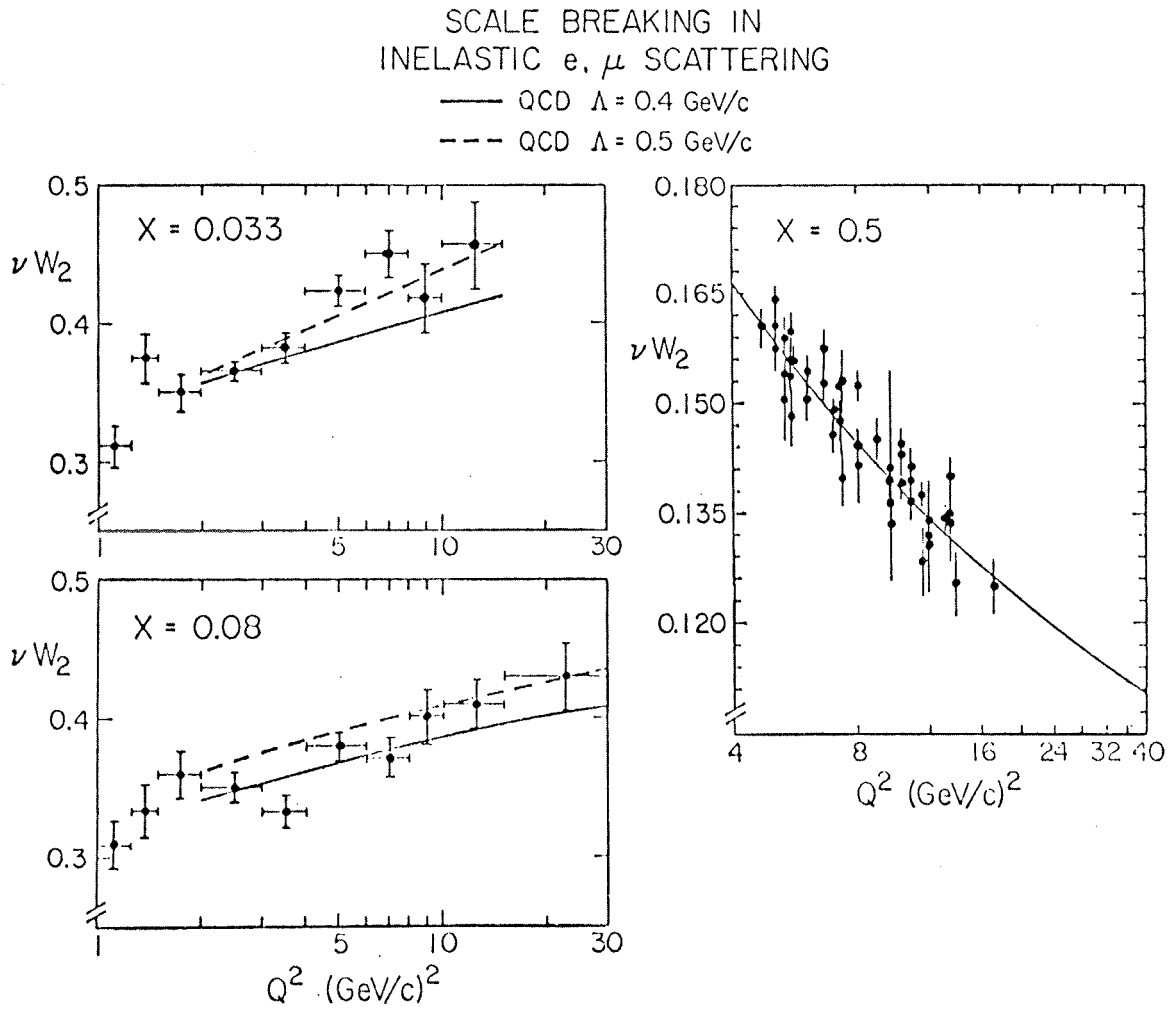

Figure 1. Comparison of the scale breaking effects (Q^2 dependence) expected from an asymptotically free theory with data on ep and μp inelastic scattering at x = 0.033 and 0.08 and at x = 0.5. The theory comes from the analysis of Ref.1 using A = 0.4 GeV/c (solid curve) and A = 0.5 GeV/c (dashed curve).

of the parton distribution then fall as *known* powers of $\ell n\, q^2/\lambda^2$. The experimental results on scale breaking in inelastic muon and electron scattering experiments (Figure 1) are in excellent agreement with this description and suggest $\Lambda \simeq 0.4 - 0.5$ GeV/c.

Hadron-lepton scattering at large momentum transfer is then accounted for very well in terms of a simple perturbation theory on point-like objects, plus an "effective non-scaling of partons" (in order to account for the higher order diagrams, which are too complicated to account for). However, when the theory is extended to *hadron-hadron* collisions, the picture becomes far less clear. Let us consider for instance large p_T experiments, like for instance $pp \to \pi^0 X$ or $p + p \to \text{Jet} + X$ at the ISR. At what was thought to be a high enough p_T, one finds experimentally p_T^{-8} behaviour, instead of the p_T^{-4} expected from point-like scattering (possibly with additional logarithmic modifications). However, as shown by Feynman, Field and Fox[1], QCD tells us clearly why it is so and it predicts correctly experimental findings (Figure 2) provided *one takes into correct account:*

(i) non-scaling distributions ($\Lambda \simeq 0.4$)

(ii) gluon distributions

(iii) transverse momentum of partons, which is measured to be $\langle p_T \rangle \simeq 848$ MeV/c as a fit to the Drell-Yan distributions (Figure 3).

The situation is simply that the energy (p_T) is *still too low* and there are too many non-asymptotic effects still acting. However, at high energies, the distributions must quickly approach the p_T^{-4} fall-off (Figure 4). One can see (Figure 5) that the SPS collider will provide sharp, quantitative tests of the QCD theory as soon as turned on. Note for instance that jet cross-sections are $\sim 10^3$ times larger than single particle production. It is not clear however in which form quark and gluon jets will appear at very large p_T (like $p_T \simeq 30$ GeV/c). If QCD is correct there will be no well collimated object. Instead we shall observe fat, multiply headed jets made of many subjects (Fractiles).

It must be stressed that even if QCD predictions are very complete and essentially parameter-free, the high energy behaviour of

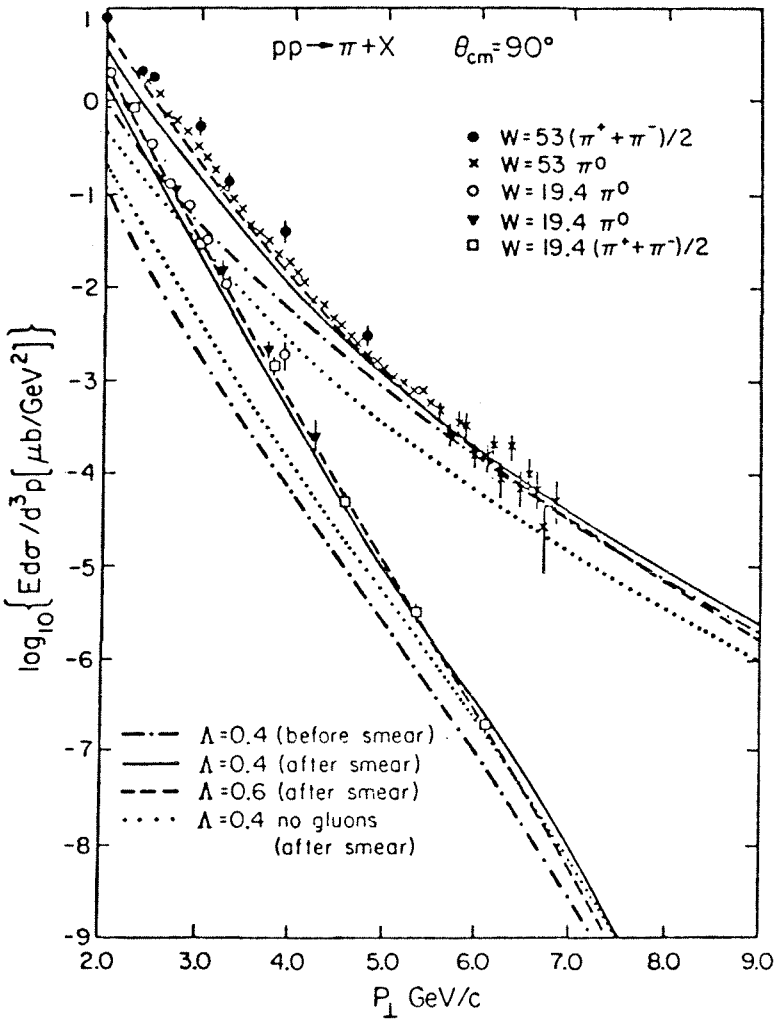

Figure 2. Comparison of a QCD model (normalized absolutely) with data on large p_T pion production in proton-proton collisions at $W = \sqrt{s} = 19.4$ and 53 GeV/c with $\theta_{cm} = 90^0$. The dot-dashed and solid curves are the results before and after smearing, respectively, using $\Lambda = 0.4$ GeV/c and $\langle k_T \rangle_{h \to q} = 848$ MeV and the dashed curves for $\Lambda = 0.6$ GeV/c (after smearing). The contribution arising from quark-quark, quark-antiquark, and antiquark-antiquark scattering (i.e., no gluons) is shown by the dotted curves (after smearing). (From Ref. L7).

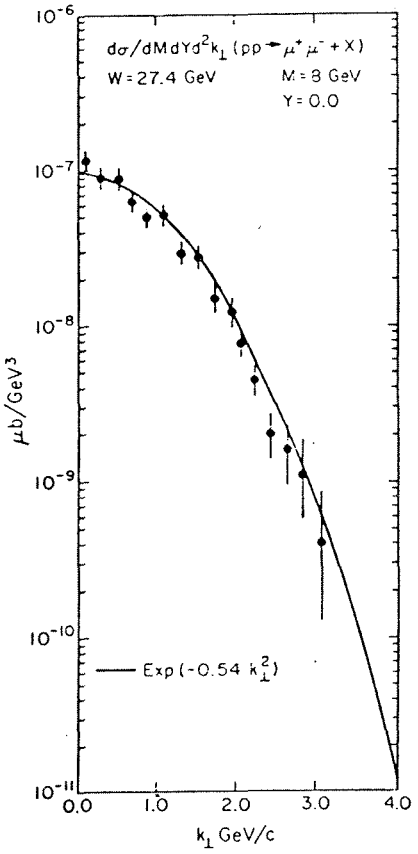

Figure 3. The transverse momentum spectrum, $d\sigma/dMdYd^2k_T$, of muon pairs in pp collisions at W = 27.4 GeV, $M_{\mu\mu}$ = 8 GeV and rapidity Y = 0. Also shown is a Gaussian fit of the form $\exp(-0.54\ k_T^2)$ which yields $\langle k_T \rangle_{\mu\mu} \simeq 1.2$ GeV and is interpreted as implying $\langle k_T \rangle_{h\to q} = 848$ MeV. (From Ref. 1).

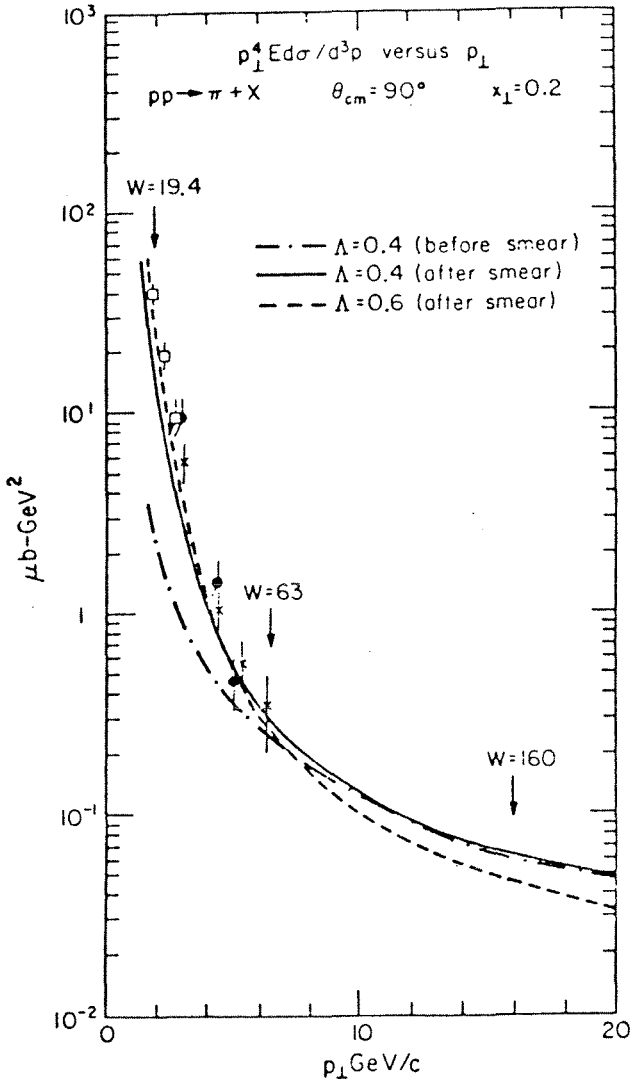

Figure 4. The data on p_T^4 times $Ed\sigma/d^3p$ for large p_T pion production at $\theta_{cm} = 90^0$ and $x_T = 0.2$, compared with the predictions (with absolute normalization) of a model that incorporates all the features expected from QCD. The dot-dashed and solid curves are the results before and after smearing, respectively, using $\Lambda = 0.4$ GeV/c and the dashed curves are the results using $\Lambda = 0.6$ GeV/c (after smearing). (From Ref. 1).

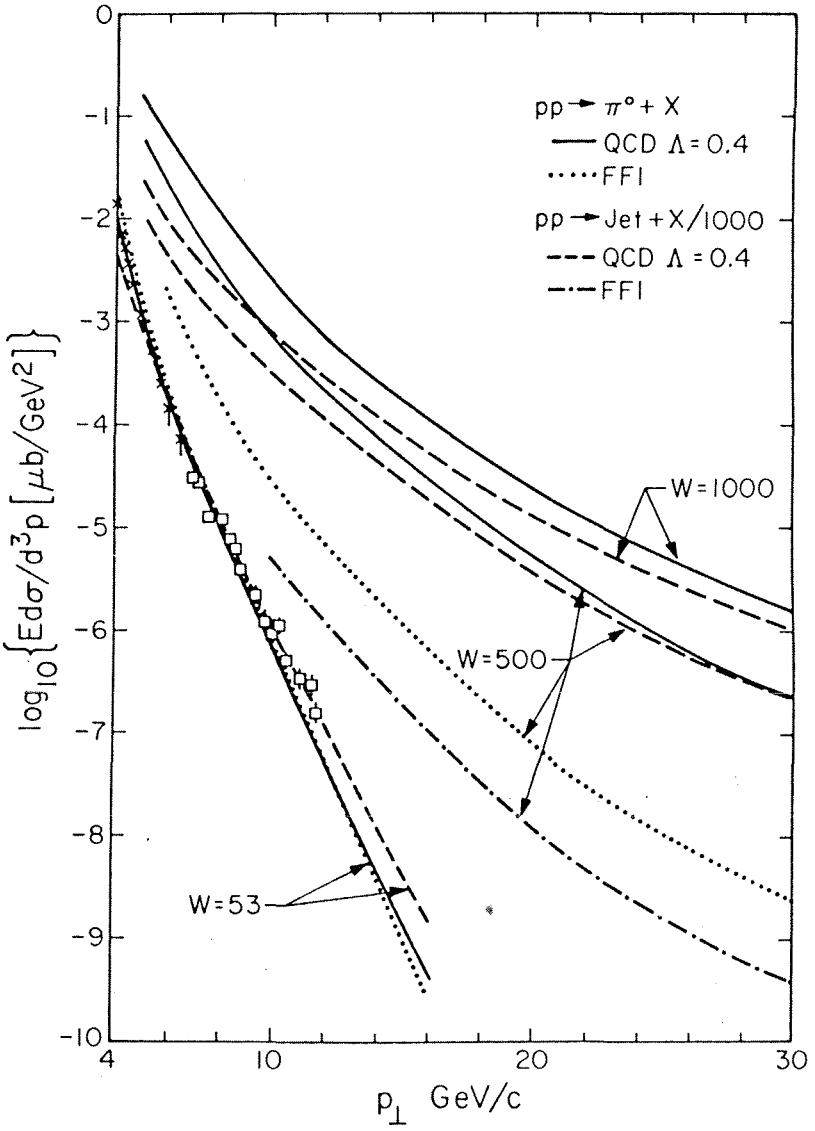

Figure 5. Comparison of the results on the 90° π^0 cross-section, $Ed\sigma/d^3p$, from the QCD approach with Λ = 0.4 GeV/c (solid curve) and the quark-quark "black-box" model FF1 (dotted curves). Both models agree with the data at W = 53 GeV where the open squares are the "preliminary" data from the CCOR collaboration normalized to agree with the lower p_T experiments. The QCD approach results in much larger cross-sections than the FF1 model at W = 500 and 1000 GeV. The FF1 results at 1000 GeV (not shown) are only slightly larger than the results at 500 GeV. Also shown are the cross-sections for producing a jet (quark) at 90° (divided by 1000) as predicted by the QCD approach (dashed curves) and the FF1 model (dot-dashed curve).

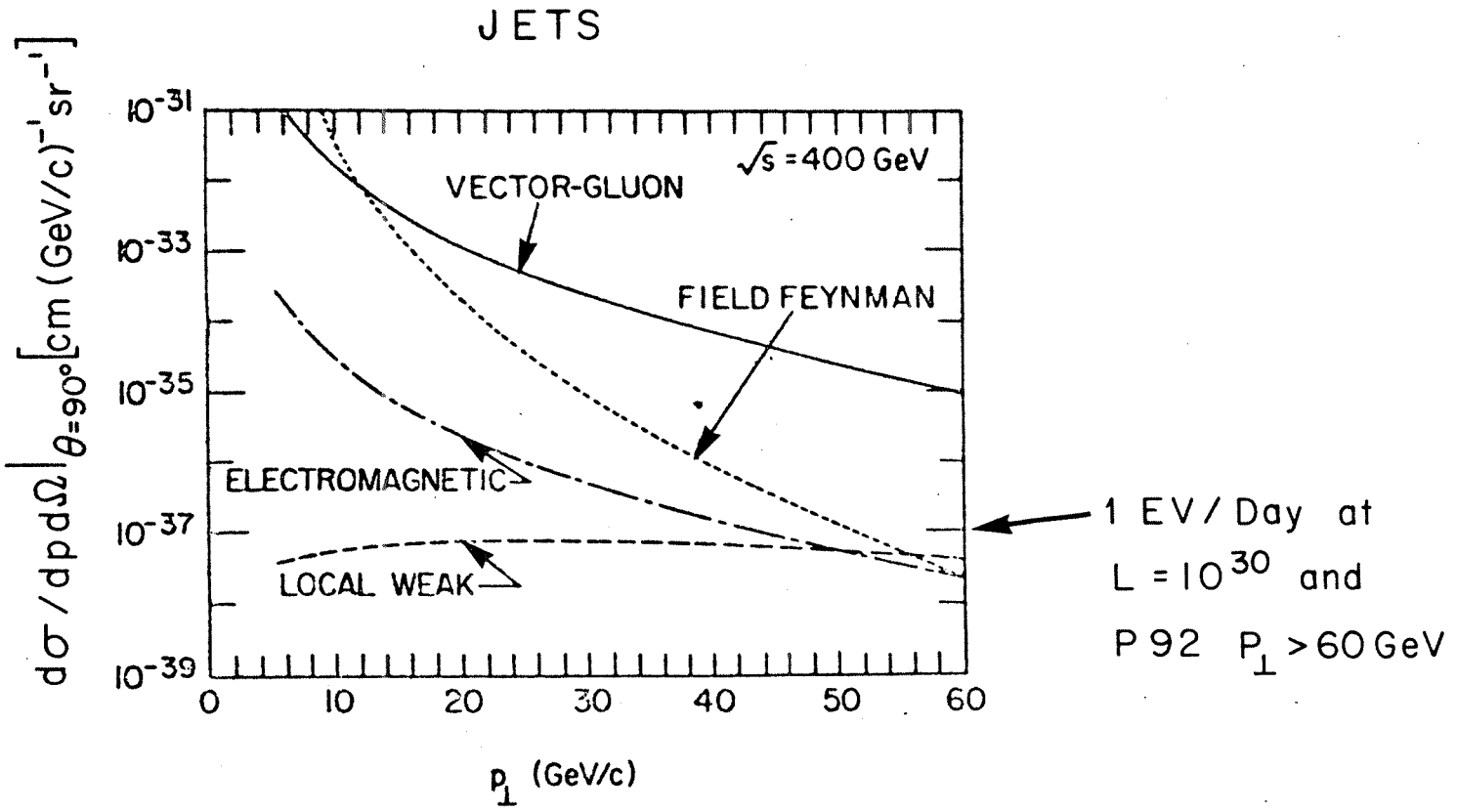

Figure 6. Jet cross-sections at 90^0 for strong, electromagnetic jets and $\sqrt{s}$ = 400 GeV.

large p_T hadrons is one of the most fundamental questions to be elucidated by the SPS-collider.

In general we shall test how weak the parton-parton interaction becomes at small distances. This is shown in Figure 6 where the differential jet cross-section is given as a function of the transverse momentum. Will strong interactions continue to weaken as p_T^{-8}, until the known weak and electromagnetic effects, which go like p_T^{-4} (plus logarithmic corrections) eventually emerge? Note at this point that local weak interactions will contribute with about 1 event/day and $p_T > 60$ GeV/c for the general purpose detector in LSS5 and at luminosity of 10^{30} cm^{-2} sec^{-1}.

3. PRODUCTION OF THE W MESONS. One of the most important justifications to the p-$\bar{p}$ collider is an early exploration of "the first threshold in weak interactions" namely where the four Fermion theory ceases to be valid and vector bosons are essential.

The most significant evidence for this new energy domain would be the direct observation of the W-mesons[2]. From the presence of both charged and neutral currents, we expect at least three of such objects.

Even if we had no idea of which mass to expect, the opening up of the new kinematic range offerd by the p-$\bar{p}$ collider would make the search for W an important objective. Current theoretical ideas establish a close connection between W-mesons and the photon and give to all of them a comparable intrinsic strength. This leads to the mass estimate:

$$m_W \simeq (e/G_F)^{\frac{1}{2}} \simeq 100 \text{ GeV/c}^2$$

where e is the elementary charge and G_F the Fermi constant.

More specific theories allow detailed predictions. The Weinberg-Salam model gives masses and width as a function of $\sin^2\theta_W$ as calculated in Figure 7. The recently favoured value $\sin^2\theta_W \simeq 0.22$ gives about equal masses for W^0 and $W^{\pm}$, around 80 GeV/c^2.

More general models of the same class predict a larger number of W mesons, in the same mass range as the W-S model. It is therefore evident that the presence or absence of W mesons in this mass range is of considerable importance.

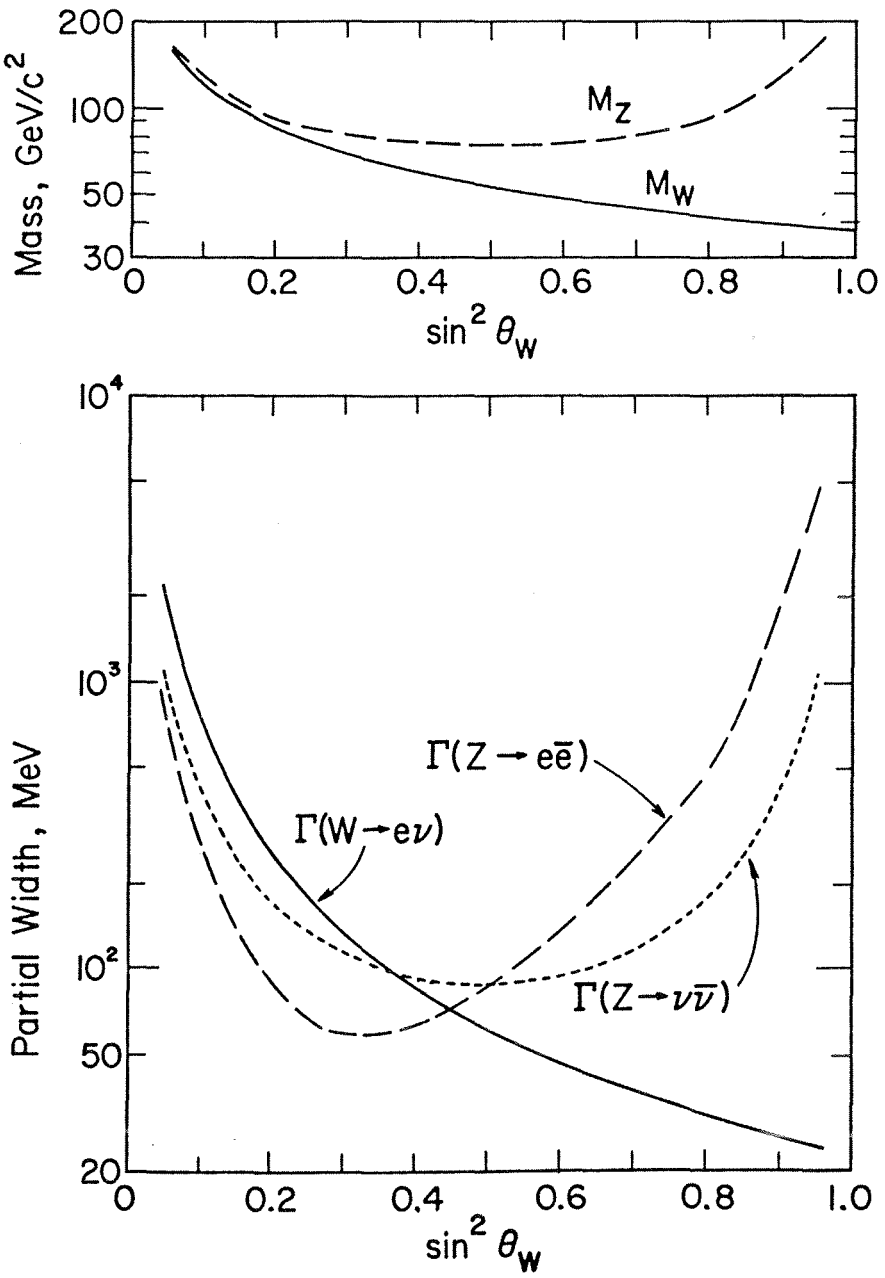

Figure 7. Masses and leptonic partial widths for charged and neutral vector boson in the Weinberg and Salam model.

Is there an upper limit to the mass of the intermediate bosons in the unified gauge theories? Bjorken [3] has discussed this problem in the framework of a unified theory of weak and e.m. interactions with one dimensionless constant and found:

$$m_{W^0} \leq 200 \text{ GeV}/c^2 \qquad m_{W^\pm} \leq 75 \text{ GeV}/c^2$$

which are well within the capabilities of the SPS-collider. However, there are extreme models which explain the neutral currents as exchange of two $W^\pm$ bosons and which predict extremely massive charged bosons. Their limits are $m_{W^\pm} \leq 450 \text{ GeV}/c^2$.

It must be noted that for $m_W \geq 300 \text{ GeV}/c^2$ the decay total width which grows like M_W^3 exceeds its mass. In these cases bosons cannot be experimentally observed as particle states and the phenomenology becomes practically indistinguishable from four fermion theory with unitary cut-off. This "observability bound" appears well matched to the potentialities of the SPS-collider.

How reliable really are W cross-section estimates? There is now very strong support for the notion of point like constituents in the hadron, obtained from lepton-hadron scattering and very high energy neutrino experiments. The experimental detection of weak interaction processes in hadronic collisions almost certainly involves quark-antiquark annihilation very much like e^+e^- collisions.

In order to estimate the cross-sections in $p\bar{p}$ collisions, the structure functions of partons must be known. Neutrino and charged lepton scattering experiments provide the necessary structure functions and have set limits (> 20 GeV) on any non-locality in the parton form factor. The main difference with respect to e^+e^- annihilation is that now the kinematics is largely smeared out by the internal motion of the q's and $\bar{q}$'s. Apart from this "Fermi motion" effect, the production processes initiated by leptons or quarks appear equally fundamental and reliable.

Calculations on the production cross-sections have been reported by several authors [4]. They usually invoke parton-antiparton annihilation, scaling and CVC to relate the Drell-Yan process to the W-production. Some corrections may be required because of scaling deviations due for instance to asymptotic freedom. These effects have been considered and found relatively unimportant at least for $M_W \leq 100$ GeV.

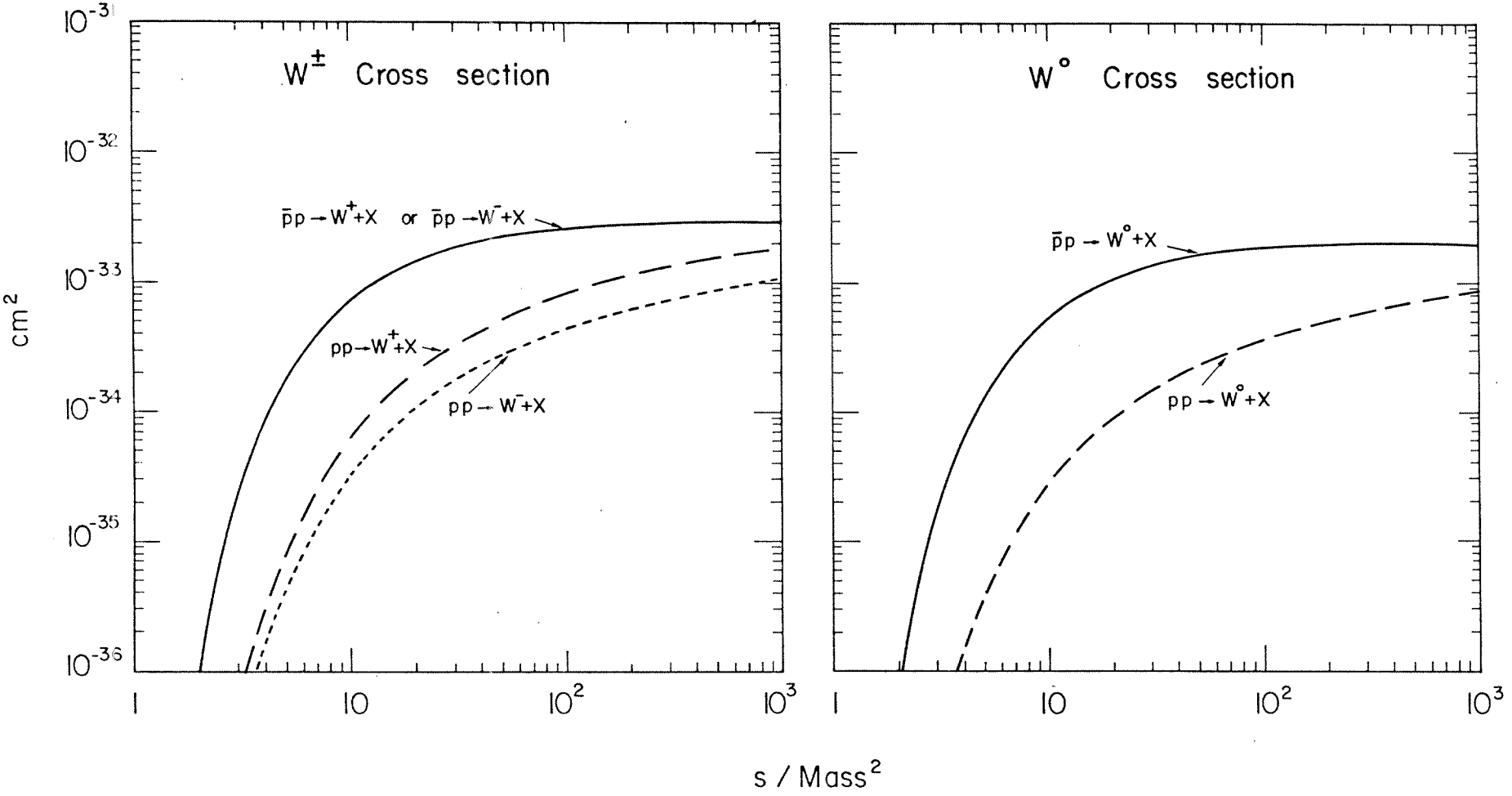

Figure 8a. $W^{\pm}$ production cross-section in $p\bar{p}$ collisions from quark-parton model as a function of the mass M. $\sqrt{s}$ is the centre of mass energy.

Figure 8b. The same as Figure 8a, except for W^{o} production.

Cross-sections are summarized in Figure 8 a and 8 b. Expectations give a total cross-section of about 5×10^{-33} cm^2 for $M_{W^\pm} \lesssim 100$ GeV. We would like to stress that the estimates for $p\bar{p}$ are more reliable than those for pp since the former involve mostly valence quarks which have been accurately investigated in deep inelastic lepton scattering experiments.

One can compare these cross-sections with the ones for LEP and CHEEP colliding beam machines (Table 1.). It appears that $p\bar{p}$ is definitely superior in all cases. Production of W^o by e^+e^- collisions on the resonance is clearly superior to $p\bar{p}$. However the charged W production stands a much better chance with $p\bar{p}$ than e^+e^-. It may be stressed at this point that for $\sin^2\theta_W = 0.21$, $m_{W^+} = 80$ GeV and pair production will be possible only with LEP 100.

A practical search for intermediate bosons requires an unambiguous experimental signature. Leptonic decay branching ratios could be related by CVC to the value of R measured in e^+e^- annihilation at an energy equal to the mass of the W^o. We can either extrapolate R or use the Weinberg-Salam model. It is plausible that the result should be approximately the same in any non-exotic model since it depends mainly on the number of possible quark and leptonic final states. (Quarks are counted three times because of colour and with appropriate allowance being made for the Cabibbo angle). For the branching ratios we take the following values:

$$B(W^\pm \to e^\pm + \nu) = 0.12 \qquad B(W^o \to e^+ + e^-) = 0.05$$

Partial widths in the leptonic channels estimated by standard graphs and the value of the Fermi constant are:

$$\Gamma(W^\pm \to e^\pm + \nu) = 140 \text{ MeV}$$
$$\Gamma(W^0 \to e^+ + e^-) = 60 \text{ MeV} \qquad (\sin^2\theta_W = 0.3)$$

Table 1. Comparison between cross-section for intermediate boson production from e^+e^-, $p\bar{p}$ and $\bar{e}p$ colliding beams. (W-Salam model and $\sin^2\theta_W = 3/8$).

Process	Neutral boson	Single charged boson	Pair production of charged B $\sin^2\theta_W = 3/8$ $m_W = 62$ GeV	Pair production of charged B $\sin^2\theta_W = 0.22$ $m_W = 80$ GeV
e^+e^- $\sqrt{s} = 200$ GeV		$\sigma(e^+e^- \to W^+e\nu) =$ 6.5×10^{-37} cm^2	$\sigma(e^+e^- \to W^+W^-) =$ 0.7×10^{-35} cm^2	$\sigma(e^+e^- \to W^+W^-) =$ 1.4×10^{-35} cm^2
e^+e^- $\sqrt{s} = 150$ GeV		$\sigma(e^+e^- \to W^+e^-\nu) =$ 5×10^{-37} cm^2	$\sigma(e^+e^- \to W^+W^-) =$ 1.1×10^{-35} cm^2	(below threshold)
e^+e^- $\sqrt{s} = m_{W^o}$	$\sigma(e^+e^- \to W^o)_{peak} =$ 4.6×10^{-32} cm^2	$\sigma(e^+e^- \to W^+e\nu) \cong$ 10^{-38} cm^2		
$\bar{p}p$ $\sqrt{s} = 540$ GeV	$\sigma(\bar{p}p \to W^o + X) =$ 2×10^{-33} cm^2	$\sigma(\bar{p}p \to W^+ + X) =$ 5×10^{-33} cm^2		
ep $s = 27{,}000$ GeV^2	$\sigma(ep \to W^o + e + X)$ $\simeq 10^{-37}$ cm^2	$\sigma(ep \to W^+ + \nu + X) =$ 2×10^{-38} cm^2		

Combining partial widths and branching ratios we get total widths, which are relatively large and at least in the case of W^o accessible to experimental observation:

$$\Gamma(W^{\pm} \to \text{all}) = 1.2 \text{ GeV}/c^2 \qquad \Gamma(W^o \to \text{all}) = 1.2 \text{ GeV}/c^2$$

We would like to stress at this point that the decay branching ratios for the W^o depend critically on the *total* number of neutrinos in nature since they are most certainly light enough to be amongst the Z^o decay products.

The leptonic decay channels of both the neutral and charged bosons represent the most obvious way of detection. In the case of the W^o a pair of charged leptons are emitted. A narrow resonant peak (reminiscent of the ψ/J signature) is easy to detect (Figure 9). In the case of the charged boson, a substantial fraction of the emitted leptons are confined close to the maximum of the transverse momentum (Figure 10). Furthermore a large fraction of the transverse momentum will be missing because of the emitted neutrino. Detectors are capable of recording such a missing momentum.

Figure 11 shows the calculated product $\sigma.B$ for the process:

$$p + p \to W^{\pm} + X$$
$$\qquad\qquad \hookrightarrow e^{\pm} + \nu$$

as a function of the $W^{\pm}$ mass. The large C.M. energy available allows us to investigate the existence of such particles up to masses of about 300 GeV/c^2. The rapidity distribution of the emitted leptons is shown in Figure 12. We remark that only 50% of W^o emit *both* leptons in the angular range $30^o < \theta < 150^o$ ($|y| \leq 1.3$) and 96% of the leptons are contained in the angular acceptance of the general purpose detector of LSS5[5], $5^0 < \theta < 175^0$ ($|y| < 3$).

An important signature of the weak decay of the intermediate boson can be found in the lepton angular distribution. The lepton distributions from the charged W show a strong forward-backward asymmetry (Figure 13a). This asymmetry is specific to $p\bar{p}$ collisions. The asymmetry for the W^o is expected to be small (Figure 13b). On the

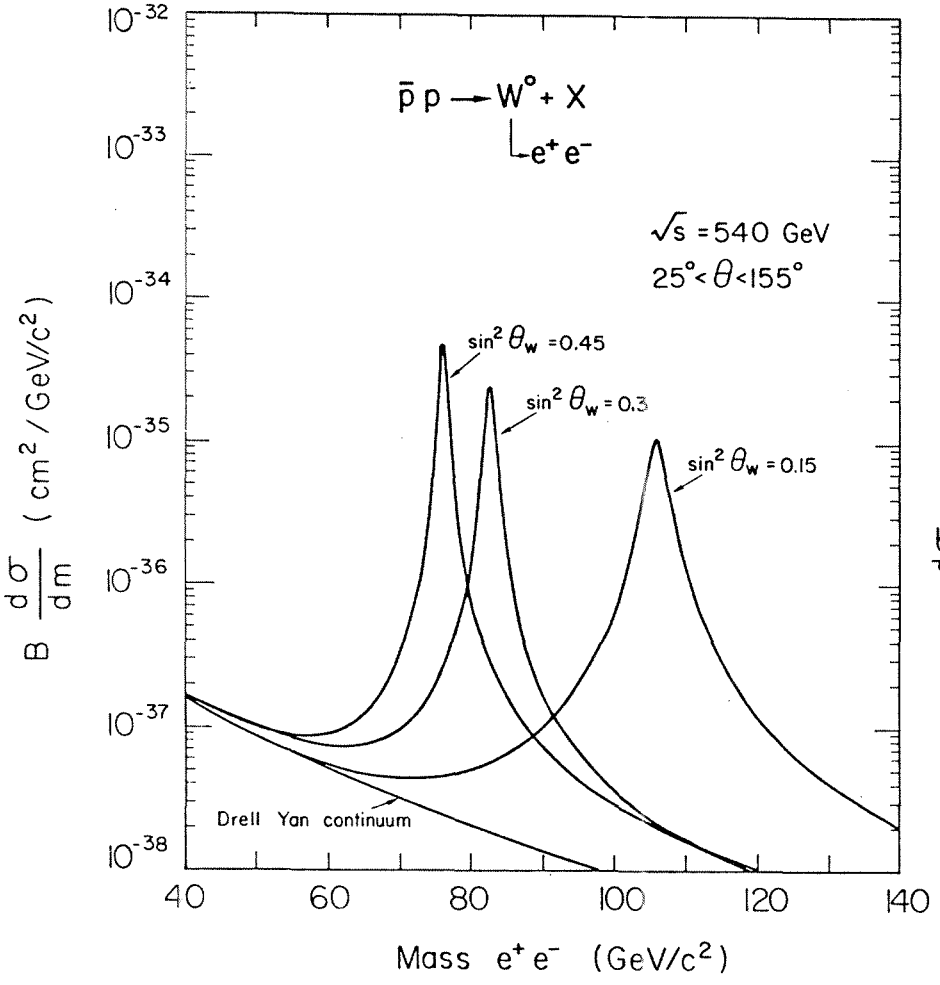

Figure 9. Dilepton invariant mass from $W^0 \rightarrow e^+e^-$ decay integrated over the angular acceptance $25^o < \theta < 155^o$ for $p\bar{p}$ collisions at $\sqrt{s}$ = 540 GeV and for different values of the Weinberg angle θ_W. Drell-Yan continuum is also shown for comparison.

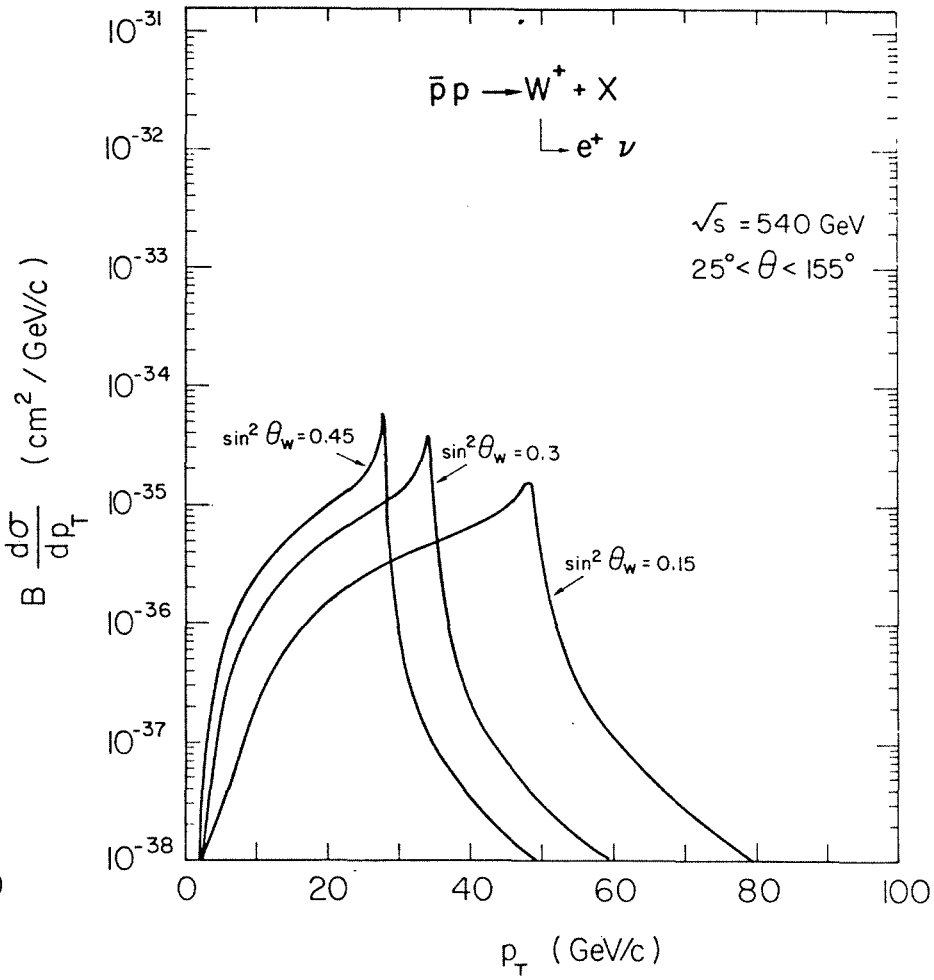

Figure 10. Single charged lepton distribution integrated over the angular range $25^o < \theta < 155^o$ from $W^+ \rightarrow e^+ + \nu$ decay and $p\bar{p}$ collisions at $\sqrt{s}$ = 540 GeV according to the quark parton model for various values of the Weinberg angle θ_W.

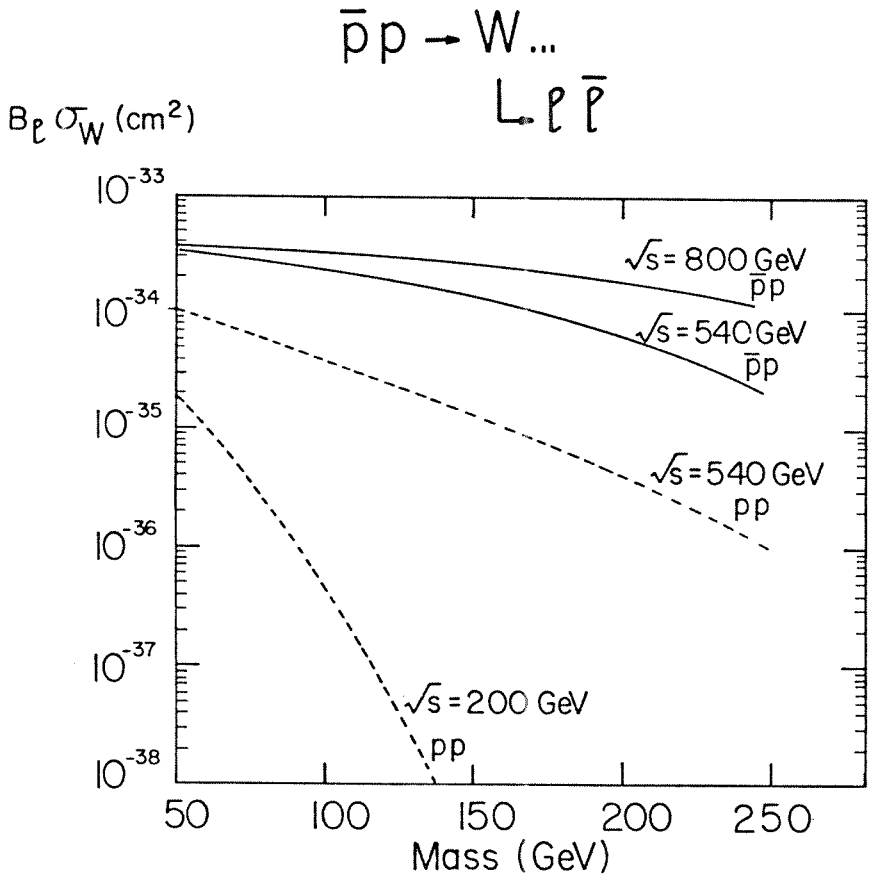

Figure 11. Total cross-section σ_W times leptonic branching ratio B_ℓ for the process of $W^\pm$ production by $p\bar{p}$ collisions and decay, given as a function of the mass and for different centre of mass energies. Proton-proton initiated curves are shown for comparison[16].

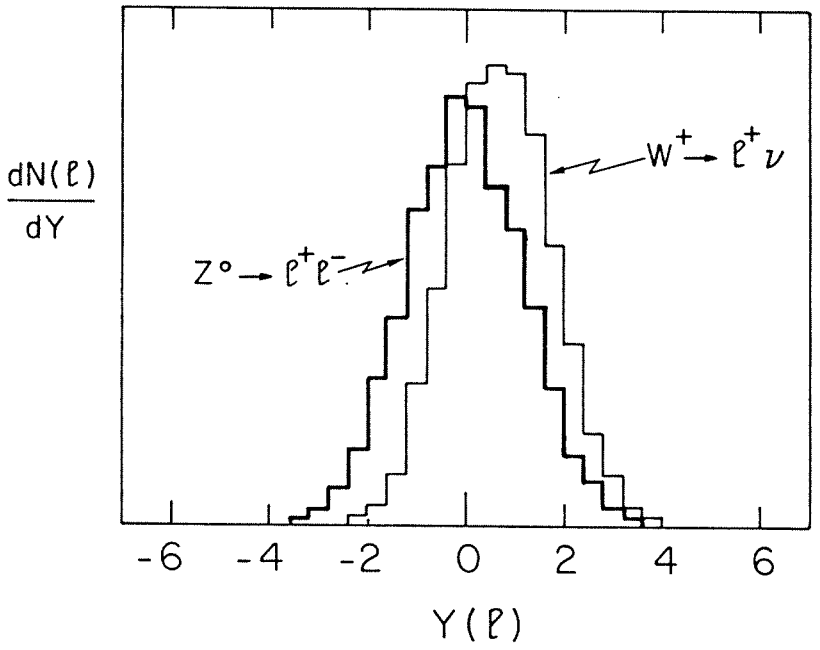

Figure 12. Rapidity distribution of the charged lepton emitted in $p\bar{p}$ collisions by the decays $W^o \rightarrow e^+e^-$ and $W^+ \rightarrow e^+\nu$

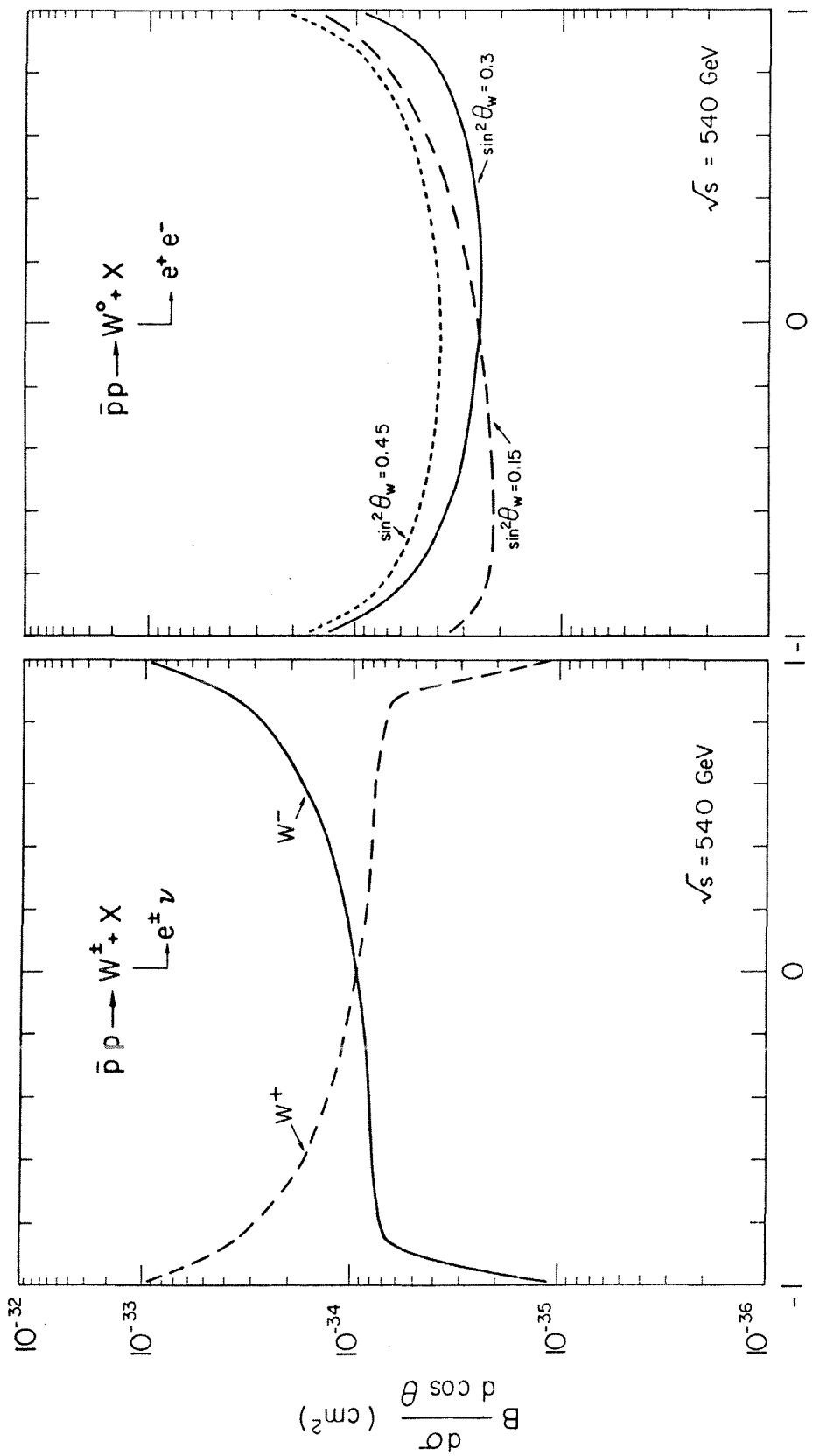

Figure 13a. Charge asymmetry for leptonic $W^{\pm}$ decays from $p\bar{p}$ collisions and $\sqrt{s} = 540$[16].

Figure 13b. Charge asymmetry for $W^0 \rightarrow e^+e^-$ from $p\bar{p}$ and collisions various values of the Weinberg angle θ_W[16]) Note the rapidity variation of the distribution with $\sin^2\theta_W$.

contrary, in pp collisions, the lepton distributions are symmetric in $\cos\theta$.

Recently spectacular hadronic jets have been observed in e^+e^- annihilation experiments at DORIS. According to CVC the W should also decay into two hadronic jets. Observing the transverse momentum of the jet is most likely not a sufficient criterion to separate out the W signal from the (probably) more abundant background of hadronic origin. However if the mass of the W is determined by observing *both* jets, the situation is far more promising and, depending on the actual backgrounds and mass resolution, it might be possible to isolate the signal.

A crucial question is what is the minimal luminosity which is needed for an early realistic observation of the charged and neutral W's. In order to clarify this point we should take the most pessimistic point of view on the cross-sections and leptonic branching ratios. Let us consider charged W's. There are several reasons to believe that the canonical estimates could turn out to be optimistic. Firstly asymptotic freedom and other scaling violations may reduce the production cross-section by perhaps as much as a factor two. Secondly the decay branching ratio B may be lower if additional leptons and quarks exist in the mass range of W^+ decays. Assuming that three new leptons and three new quarks are to be found in this mass range, we get $B_{e\nu} = 0.05$. Therefore for conservative estimates one might then introduce a factor four of safety and use $\sigma.B = 1.0 \times 10^{-34}$ cm^2.

A realistic detector with sensitivity for both $e^\pm$ and $\mu^\pm$ channels might have an overall efficiency of about 1/2, when all effects of kinematical cuts, geometry, off-line and on-line losses are included. The average luminosity <L> needed to collect N useful events during a time t is then given by:

$$\langle L \rangle = \frac{N}{4 \times (\sigma.B) \times 0.5 \times t}$$

($e^\pm, \mu^\pm$; detection eff.)

Taking $\sigma.B = 1.0 \times 10^{-34}$ cm^2 (i.e. the lower limit to the estimate)

N = 20 and 500 hours of actual running time (corresponding to 25% of SPS over a first year at 50% overall efficiency to take into account beam manipulation errors, initial hardware problems and so on) one gets:

$$\langle L \rangle = \frac{20}{4 \times 1.0 \times 10^{-34} \times 0.5 \times 3.6 \times 10^{3} \times 500} = 5.5 \times 10^{28}\ \mathrm{cm}^{-2}\ \mathrm{s}^{-1}$$

This is about a factor twenty below the target luminosity and well within the expectations for the first running-in year of the project(*).

Of course the question is if N = 20 is a reasonable estimate. In the past several crucial discoveries (two neutrinos, CP-violation, Ω^-) and more recently the F^+ at DESY have been conclusively demonstrated on a relatively small number of events. The key issue has been in all cases the avaliability of a large number of redundant pieces of information for each event. As we shall see this is the case for the detectors planned for the first generation of experiments, which are capable of determining the neutrino momentum by missing energy and hence the invariant mass of the $W^{\pm}$ for individual events to about 10% accuracy.

The situation for the W^o where a mass peak is easily obtained is however more complex. Estimates of mass and cross-sections are somewhat more uncertain and much more model-dependent. Standard values give $\sigma.B$ which is substantially smaller than for $W^{\pm}$. As already mentioned the decay branching ratio into charged leptons depends critically on the total number of neutrinos in Nature. Finally there is almost no obvious way of distinguishing the narrow peak due to the Z^o from the one of yet another massive vector particle of the Υ or ψ type, as long as the charge asymmetry is as small as predicted by the Weinberg-Salam model. The minimal luminosity to carry out realistically this phase of the programme is then about an order of magnitude larger than the one for the charged W's, still within the expectations of the SPS collider project.

(*) This roughly corresponds to the luminosity obtained by collisions between one p and one $\bar{p}$ bunch of standard emittances and about 5×10^{10} particles. The AA ring is expected to produce this number of $\bar{p}$'s in about 2 hours.

In conclusion the search for the charged W's with the appropriate detector is truly a first generation experiment for the SPS collider.

4. SEARCH FOR HIGGS PARTICLES. A common feature of gauge theories is that the masses of the gauge bosons and renormalizability are obtained using the Higgs mechanism. Every gauge theory has at least one physical neutral scalar Higgs boson. Therefore looking for such particles should be an integral part of any programme to study weak interactions at high energies. In the simplest W-S model there is only one of such neutral Higgs bosons, H. The Higgs boson could be less massive than the $W^{\pm}$ and W^{o}. Other possibilities exist for instance in which Higgs particles are much heavier than the intermediate vector bosons. Their self interactions could be large and a whole new set of effects could emerge at centre of mass energies $\geq$ 200 - 300 GeV.

The Higgs particle is elusive and plays a negligible role in low-energy phenomenology. This is because it couples to particles according to their mass, and is only very weakly coupled to the quark and lepton constituents of ordinary matter.

It goes without saying that the cleanest laboratory test for associated Higgs production is e^+e^- annihilation. The total cross-section for the process

$$e^+e^- \rightarrow Z \rightarrow Z + H$$

is shown in Figure 14, relative to the QED rate for $e^+e^- \rightarrow \mu^+\mu^-$. At fixed energy this rate is essentially independent of M_H until close to threshold, when it drops rapidly. As the energy is increased, however, the relative rate decreases substantially. (Below threshold, some smaller cross-section for H production proceeds through virtual Z^o state which decays for instance in $\mu^+\mu^-$ pairs). It can be noted from Figure 9 that LEP70 will be sensitive to H production to a mass of about 40 GeV/c^2 and with $\sigma(HZ) \simeq 4 \times 10^{-36}$ cm^2.

A similar process is expected to occur from the initial annihilation of $(q\bar{q})$ pairs in proton-antiproton collisions, namely

$$q + \bar{q} \rightarrow (Z \text{ or } W^{\pm}) + H$$

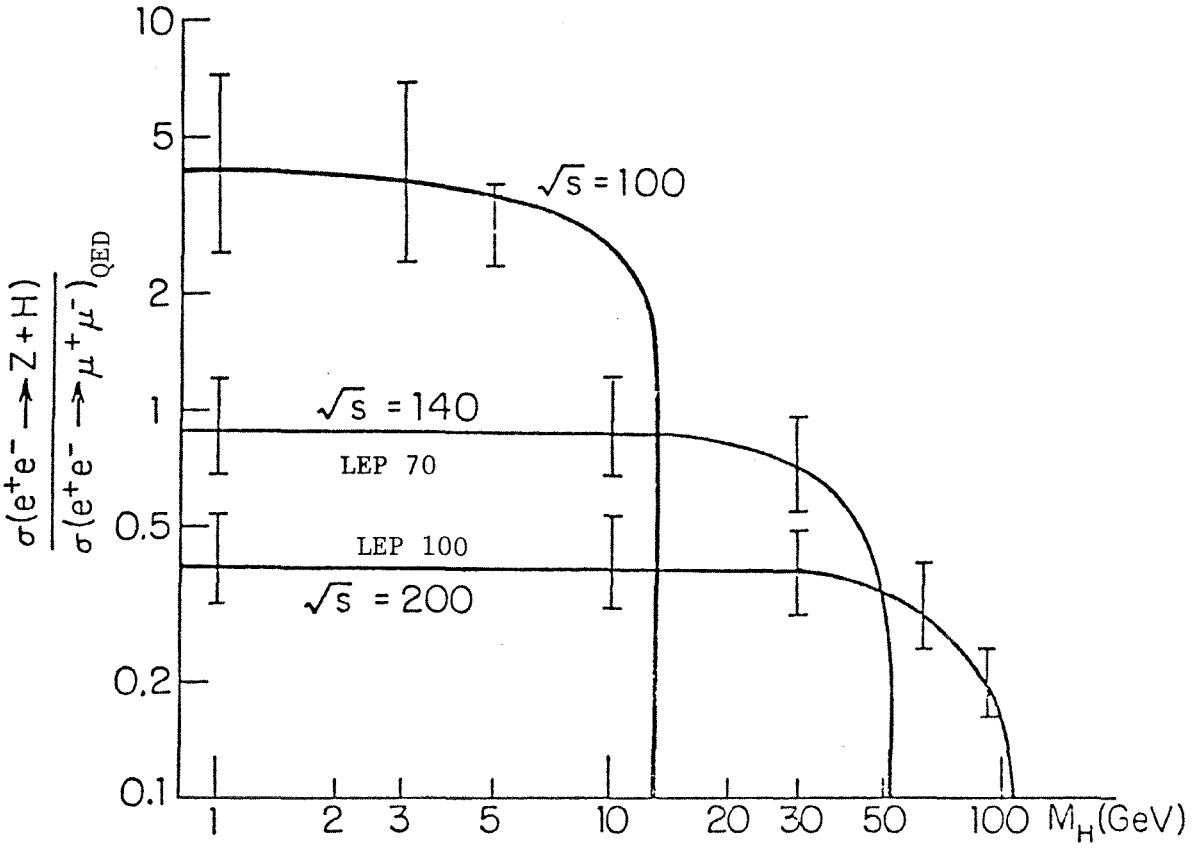

Figure 14. Associated H,Z production cross-section for e^+e^- colliding beams. The cross-section is $\sigma(e^+e^- \to \mu^+\mu^-)_{QED} = 4.1 \times 10^{-36}$ at $\sqrt{s}$ = 140 GeV and about 2×10^{-36} at $\sqrt{s}$ = 200 GeV. At this last energy and for $\ell = 10^{32}$ $cm^{-2}sec^{-1}$ we expect about two events/day for a Higgs mass $\leq$ 50 GeV/c^2 over the full solid angle and 100% detection efficiency.

The cross-sections are easily calculated by convolution of the appropriate quark and antiquark distribution functions, which will smear somewhat the nice plateau of Figure 14. (See Figure 15).

The association of a $W^{\pm}$ or Z with H provide a dramatic experimental signal for H production, provided a non-negligible fraction of produced $W^{\pm}$ or Z's are accompanied by an H, whose decay scheme is by its very nature, as bizarre as is kinematically permitted. For masses between $\sim$ 4 GeV and 10 GeV, the $\tau\bar{\tau}$ and $\bar{c}c$ decay modes are accessible and dominant. The experimental signature is then the presence of at least one additional lepton in the debris of the W-producing event. If the mass is greater than $\sim$ 10 GeV, H decays mostly into hadrons containing the Υ constituents. Until the next hadronic or leptonic threshold is encountered (corresponding to yet another flavour of lepton or quark), these decay modes will predominate. There may be the possibility that the new upsilon-related hadrons are stable. Another alternative is that the Υ belongs to yet another flavoured set of quarks which enjoys weak couplings to other flavours. In this case the new hadrons will decay by weak cascades producing multi-leptons or multi-strange particle final states.

Detectors planned for the SPS-collider have a specific sensitivity to such a process. It is estimated that an integrated luminosity $\ell = 10^{36}$ cm^{-2} could bring evidence for Higgs particles of masses up to 30 GeV/c^2. A second generation run of 10^3 hours and $\ell \cong 10^{31}$ cm^{-2} sec^{-1} could test the existence of H particles up to masses of 80 GeV/c^2, thus matching the sensitivity of LEP to these processes. A realistic way of obtaining such an increased luminosity for the SPS $\bar{p}$-p collider is offered by the relativistic electron cooling techniques [6].

Finally we shall note that the sensitivity of the experiment increases relatively slowly with $\sqrt{s}$ as shown in Figure 11. Hence the SPS-collider is not too bad even when compared with the F-NAL energy doubler-collider. However, significant gains may be achieved by ISABELLE, because of the much greater luminosities.

5. WEAK INTERACTIONS WITHOUT SIMPLE W's?. Although the existence of narrow W-states seems for today the most plausible assumption, it is not excluded that intermediate bosons could turn out to be exceedingly

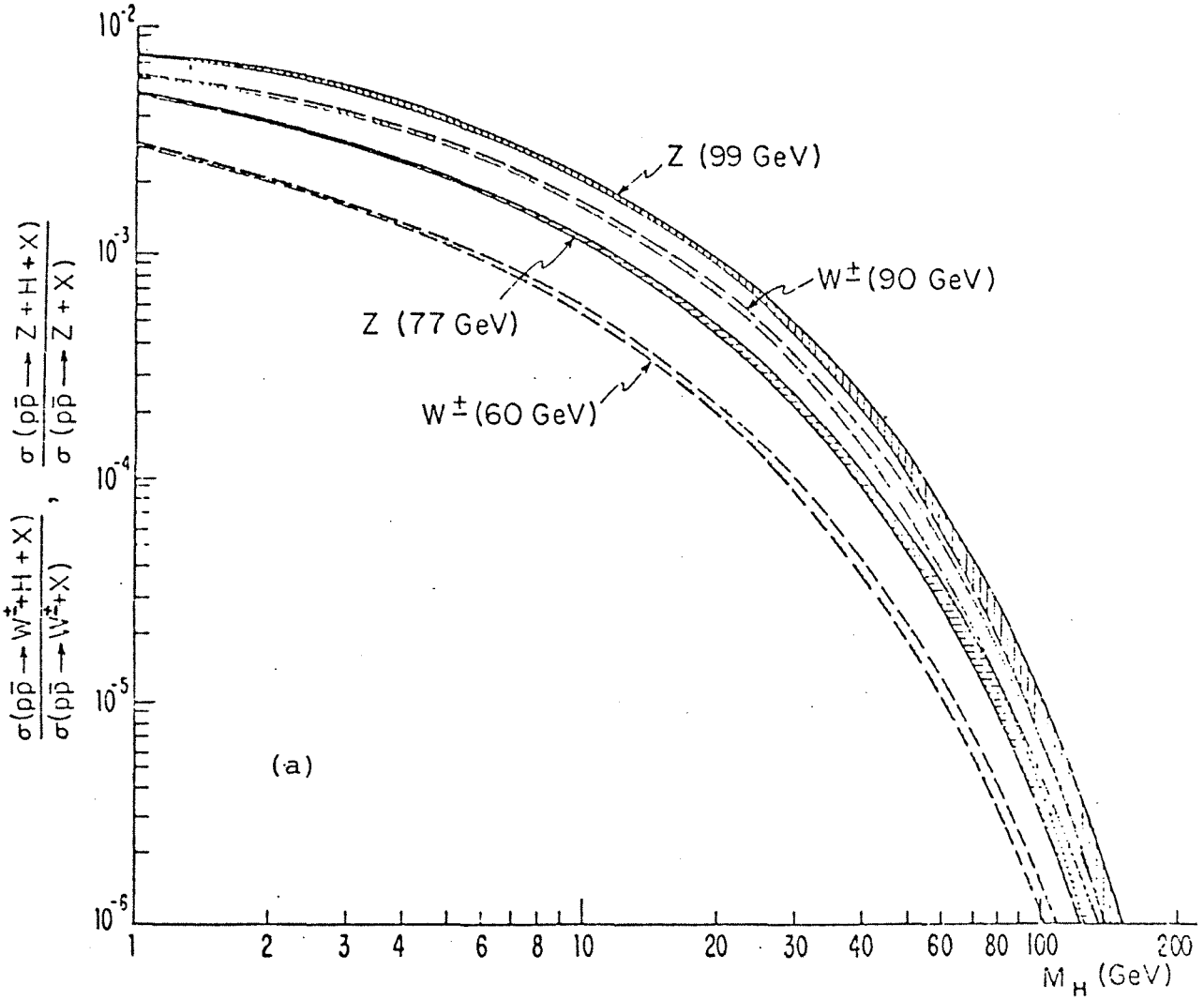

Figure 15. Rate of associated production of the Higgs meson with $W^{\pm}$ or with Z, versus M_H, expressed as a fraction of total $W^{\pm}$ or Z production. In $p\bar{p}$ collisions at $\sqrt{s}$ = 540 GeV. Production with $W^{\pm}$ is indicated by the dotted bands, with Z by slashes. Bands are shown for M_W = 60 GeV (M_Z = 77 GeV) (lower curves) and for M_W = 90 GeV (M_Z = 99 GeV) (upper curves). Bands indicate the range of variation due to different quark distribution function parametrizations.

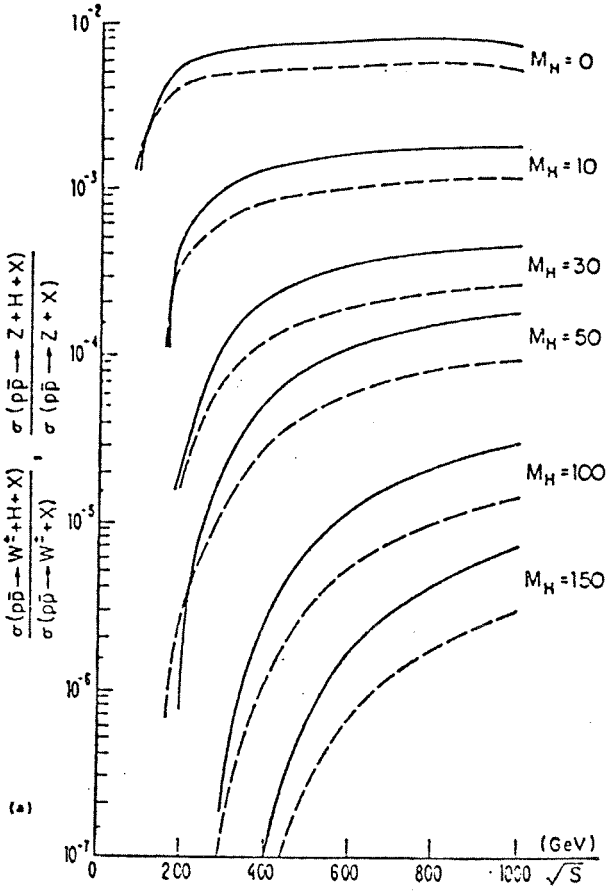

Figure 16. Rate of associated production of the Higgs meson with W^+, W^- or Z, versus energy $\sqrt{s}$, expressed as a fraction of total W^+, W^- or Z production. a) In $p\bar{p}$ collisions. Rates are shown for several M_H values, all using M_W = 75 GeV (M_Z = 86.6 GeV), corresponding to x_W = 0.25.

massive and very wide. Interactions between W's could become strong. There could be many W-W resonances of various spins, W's could lie on a Regge trajectory, there could be a strong interaction W-bootstrap etc. Alternatively strong effects could be concentrated in the Higgs sector.

The relatively high energy available in the $\bar{p}$-p system allows one to reach a broad sensitivity to such phenomena. As already noted, W^+ masses in excess of 300 GeV give detectable event rates. Corrections due to asymptotic freedoms are significant and have to be included. In order to define the sensitivity of $p\bar{p}$ collider to high energy phenomena we have plotted in Figure 17 the fractional probability that in the collision the total energy in the $\bar{q}$-q system will exceed a threshold value. One can see that collisions up to about 350 GeV in the centre of mass of the q-$\bar{q}$ system can be effectively studied. The inverse beta decay process:

$$q + \bar{q} \rightarrow e + \nu$$

can be observed experimentally provided the cut-off Λ is at least 250 GeV or greater. These events are characterized by a spectacular large p_T electron and a large transverse missing energy for the neutrino and no clear peak in the (νe) invariant mass plot.

6. PRODUCTION OF NEW, MASSIVE CHARMONIUM-LIKE VECTOR MESONS. If massive new quarks exist there should also be narrow vector mesons analogous to the J/ψ and Υ. A question of primary interest is the production of heavy vector mesons with hidden quantum numbers beyond charm. We can attempt to infer the production cross-sections for such states from the measured cross-sections for J/ψ production. Gaisser, Halzen and Paschos [7] have proposed the scaling rule for the production of such a meson of mass M:

$$\sigma = \frac{\Gamma}{M^3} F(s/M^2)$$

where Γ is the total width into hadrons and $F(s/M^2)$ is a universal dimensionless function.

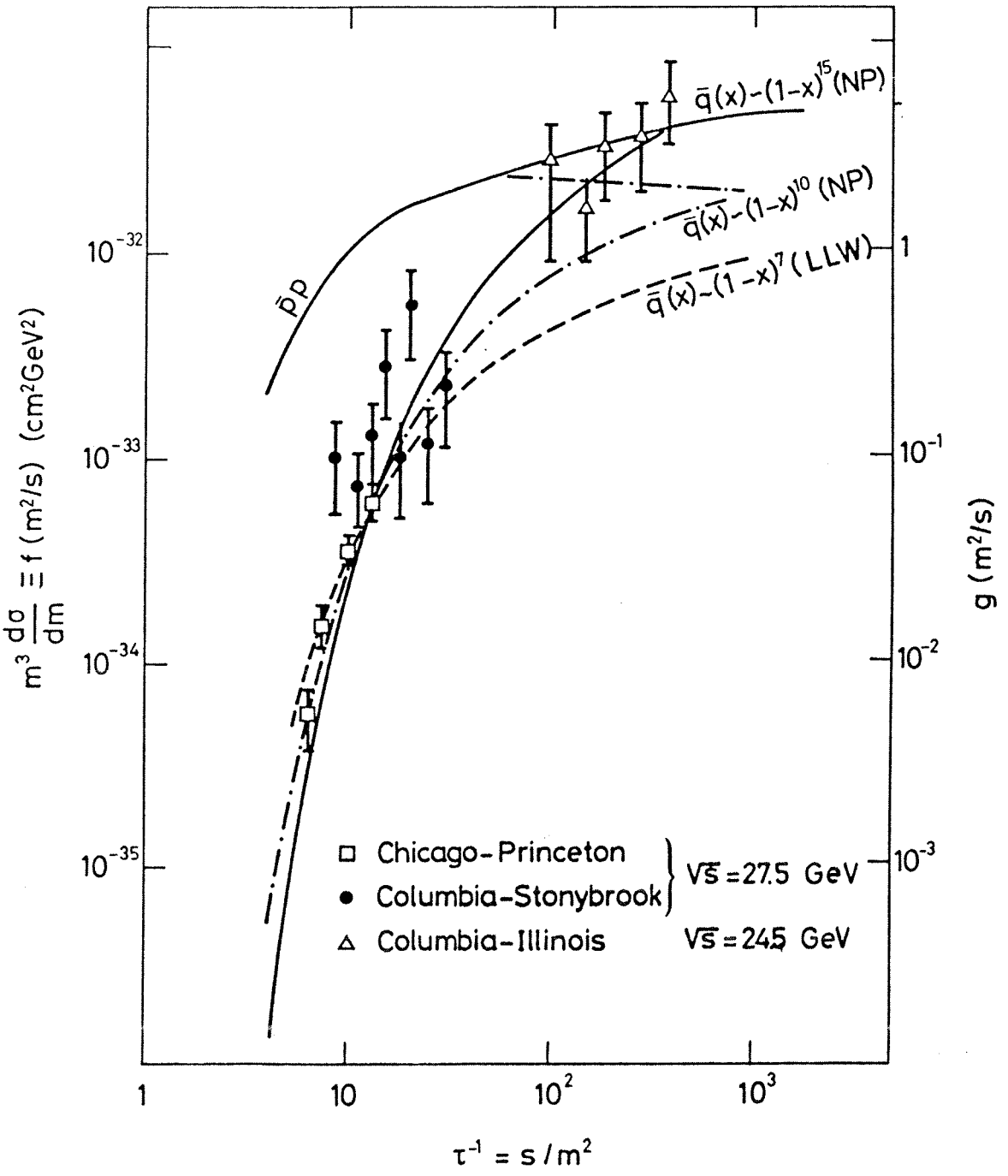

Figure 17. Drell-Yan cross-sections compared with parton model predictions. The scale to the right $g(m^2/s)$ represents the number of effective parton-parton collisions of total energy m at each proton-antiproton collision.

The meson should decay into lepton pairs e^+e^- with a branching ratio $B_{e^+e^-}$. Thus it could be observed as a narrow peak in the lepton pair invariant mass with a cross-section:

$$B_{e^+e^-}\ \sigma = \frac{\Gamma_{e^+e^-}}{M^3} F(s/M^2)$$

which is independent of Γ. Assuming that $\Gamma_{e^+e^-}(J/\psi)$, we can estimate production from J/ψ data. It is interesting to remark that this procedure gives approximately the cross-section for $\Upsilon \to e^+e^-$ observed at the ISR.

Scaling according to M^2 rather than M^3 is also conceivable and it is not ruled out by the experimental data. The event rates, assuming the M^3 scaling law, a detection efficiency of 70% and a cross-section with the same rapidity distribution as for the W^o, are summarized in Table 2. One can see that already an early run can significantly improve the PEP-PETRA range and that an ultimate, high luminosity run can probe massive vector mesons to masses of about 100 GeV/c^2. This justifies the following question: suppose one finds a narrow peak in e^+e^- say at 60 GeV/c^2. How do we know that we have found the W^o, rather than a bound $q\bar{q}$ states? The answer evidently rests on the observation of the asymmetry in the leptonic charge.

Table 2. Massive vector meson rates into lepton pairs

M_V(GeV/c^2)	$B_{e^-e^+}\ \sigma_V$(cm^2)	$N_{\ell\ell}$(for $\ell = 10^{36}$)	$N_{\ell\ell}$(for $\ell = 3\times10^{37}$)
9.5	6×10^{-33}	5400	1.62×10^5
15.0	1.5×10^{-33}	1350	4×10^4
30.0	1.9×10^{-34}	171	5130
70.0	1.5×10^{-35}	13	390
100	5.16×10^{-36}	4.46	134

7. A BRIEF DESCRIPTION OF THE GENERAL PURPOSE DETECTOR IN LSS5.

A collaboration between eleven Institutions [5] has proposed a 4π solid angle detector which is expected to be ready at the turn-on of the collider. The physics motivations discussed and the exploratory nature of the experimental programme have provided the following guide-lines for the design of such a detector.

(i) In order to collect the largest amount of unbiased information at each event the detector must cover the largest possible fraction of the solid angle. In practice we have succeeded in ensuring detection of particles down to about one degree from the beam axis.

(ii) The simultaneous detection of large transverse momentum electrons, muons and neutrinos, the last ones by missing energy, is of importance when searching for a broad class of new physical phenomena.

We need energy measurements both by magnetic curvature and calorimetry. Global energy flow measurement remains of significance even for configurations where the local particle density is too large for the visual detectors to give meaningful curvature measurements. Likewise an electromagnetic shower detector complements the energy resolution of magnetic analysis for high energy electrons, like for instance from decays of the type $W^0 \to e^+e^-$. It is also less sensitive to internal radiative corrections and to bremsstrahlung in the vacuum chamber walls.

(iv) The detector must operate with minimum disruption of the SPS programme and in an environment which is relatively hostile because of high radiation levels, backgrounds and so on. Only unsophisticated and reliable equipment must be chosen. The problem of debugging and maintaining efficiently complex equipment in the SPS tunnel should not be underestimated.

(v) The nature of our proposal is basically evolutionary and several separate elements (building blocks) are designed in such a way as to be operated almost independently and may eventually be installed in successive phases matched to the available luminosity and to the advances of civil engineering.

(vi) Data acquisition and trigger should be arranged in order to

collect the maximum of information at each event and per unit of time.

Although the inner core of our detector could be installed in the SPS tunnel without major modifications for a first exploratory experiment, we have reached the conclusion that the minimum overall disruption to the SPS programme is achieved by breaking-in of the new area before the beginning of the experimental activity. Furthermore a series of successive installation phases will inevitably delay some of the most challenging explorations to the advantage of ISABELLE which is expected to operate few years after the present proposal. However our design is sufficiently flexible to permit substantial modifications in case a different strategy should be chosen.

We shall describe briefly the set-up, refering to Figure 18 . The complete detector is about 10 m long and 5 m wide. The magnet is a dipole of nominal field value of 0.7 Tesla and it has an internal magnetic volume of 80 m^3 (7.0 x 3.4 x 3.4 m^3). The coils |7| (numbers refer to Figure 18) are made of Aluminium in order to minimize the number of collision lengths. They are 13 cm thick and weigh about 25 Tons. We have chosen a rather conservative current density of 5A/mm^2 giving a total dissipated power of 5.8 MW. The total thickness of the instrumented iron yoke is 96 cm and is subdivided into 16 C-shaped elements |2| each one about 90 cm wide and of about 52 Tons. Each element can be in principle removed independently with its own instrumentation (hadron calorimetry).

The chambers of the central detector |1| are of drift type with image read-out. The third coordinate is obtained by current division. The sensitive volume around the vacuum pipe |3| is roughly a cylinder about 6 m long and 1.22 m radius. It can be separated in 6 blocks which can be easily removed and replaced with another standard element in case of failure. All wires travel along the horizontal plane. The wire spacing is 3 mm and the maximum wire length is 2.5 m. Since we plan to use 40 μ wires, this span can be covered without supporting wires. The drift distance is 20 cm and it is matched to the time lag between bunches, i.e. the collection of electrons must be completed before the next crossing takes place. We hope to achieve a spatial resolution of 250 μ on each wire, and a longitudinal localization to

EXPERIMENTAL AREA FOR $P\bar{P}$ IN LONG STRAIGHT SECTION 5 OF THE SPS

-Vertical section in beam direction.

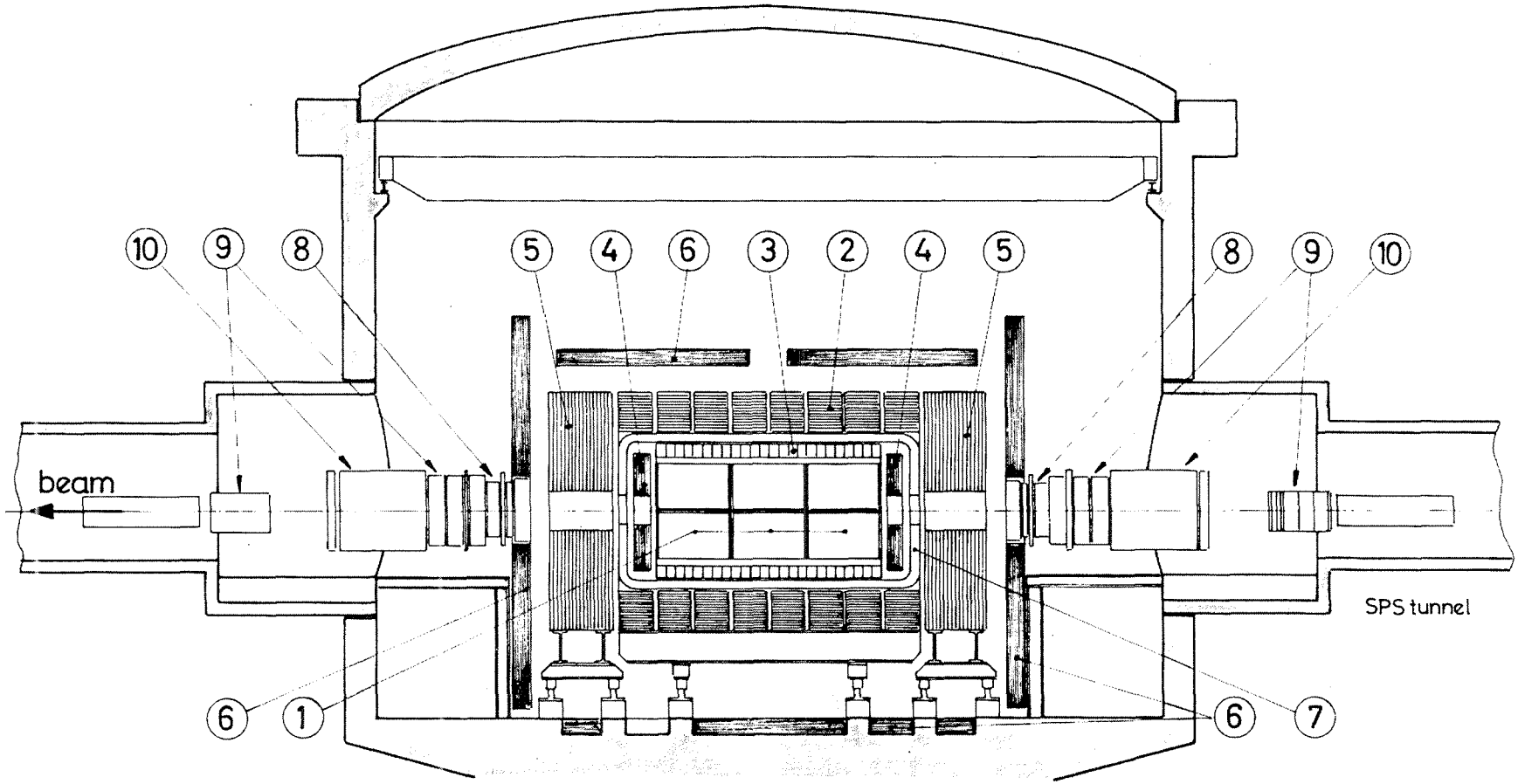

1. Central detector with image readout.
2. Large angle calorimeter and magnet yoke.
3. Large angle shower counter.
4. End cap shower counter.
5. End cap calorimeter.
6. Muon detector.
7. Aluminium coil.
8. Forward chambers
9. Forward shower counters and calorimeters
10. Compensator magnet.

Figure 18.

about ± 1% of its length. The large number of points measured on each track makes it possible to determine the ionization of tracks down to ± 6%.

The chambers are surrounded by an electromagnetic calorimeter |3| of lead-scintillator type, about 30 radiation length deep. The calorimeter is segmented in 52 half-moon gondolas which have an internal radius of 1.3 m, a width of 22.5 cm, corresponding to four gondolas for each magnet unit |2|. They weigh about 1.8 Tons each. A scintillation counter is mounted in front of each gondola for dE/dx and time of flight measurements. The thickness of the lead-scintillator stack is about 36 cm. Each gondola can be separately removed. Similar units |4| cover the end caps. They are segmented in ten angular ranges of a width modulated to achieve iso-rapidity gaps over the radii between 30 cm and 1.2 m.

The hadron calorimeters are actually built inside the magnet C's |2| and end-caps |5|. There are in each of the C's ten subdivisions in ϕ. In total there are 8 subdivisions in θ, one for each one of the C's. The standard scintillator plate size is 88 x 80 x 0.7 cm^3. About 2000 m^2 of scintillator are needed. The total number of phototubes for the C's is 640. The two end-caps (270 Tons) are instrumented with about 360 tubes and 1000 m^2 of scintillator.

The detector can be easily opened by rolling the two halves of the magnet apart. In this way the chambers are made immediately accessible. PM's can be replaced easily with a quick disconnect technique. The rest of the detector is very rugged and should need only very rarely direct maintenance. An artist's view of the detector is shown in Figure 19.

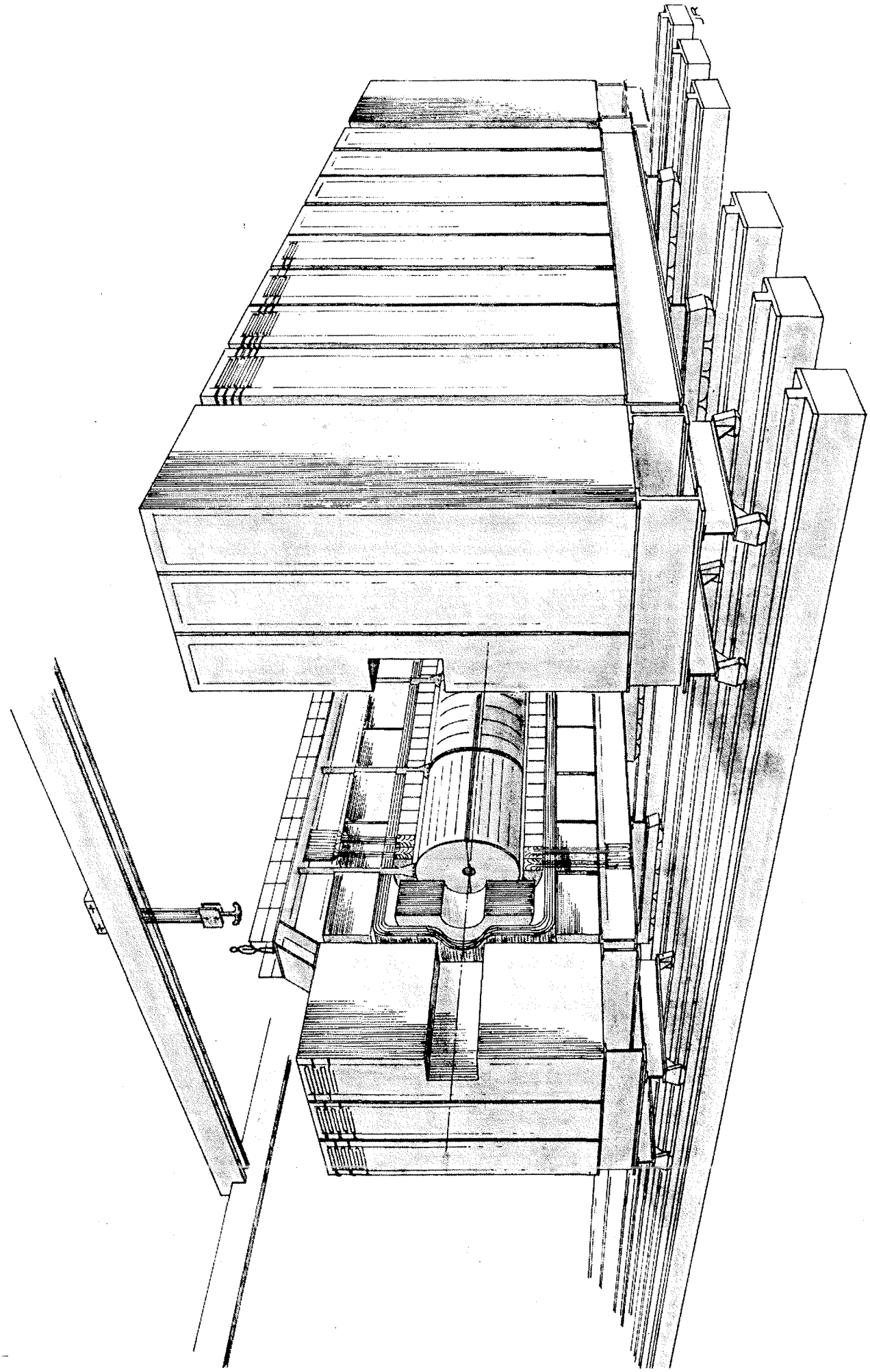

Figure 19. Artist's view of the detector of Ref. 5.

REFERENCES

(1) R.P. Feynman, R.D. Field and G.C. Fox, CALT-68-651, (1978). A substantial part of section 2 has been derived from this work. See also R.P. Feynman, paper presented at the Joint LBL-FNAL Workshop for a High Luminosity $\bar{p}$-p, Berkeley, March 1978.

(2) C. Rubbia, P. McIntyre and D. Cline in Proceedings of Aachen Neutrino Conference, 1976 (pag. 683).

(3) J.D. Bjorken, Phys. Rev. D15, 1330 (1977).

(4) G. Quigg, Rev. Mod. Phys. 49 (1977) 297;
F. Halzen, Wisconsin preprint COO-573 (Oct. 76);
M. Chase and W.J. Stirling, unpublished;
P.V. Landshoff: "Parton physics and hunting the W with hadron beams", in Proceedings Varenna Summer School, July 1977 (North Holland Publisher).
R. Palmer et al., Phys. Rev. D14 (1976) 118;
J. Finjord, Nordita preprint 76/22 (1976);
Yu. A. Golukhov et al., Soviet J. Nucl. Phys. 18 (1979) 203.
Okun-Voloshin, ITEP preprint 111 (1976).

(5) A. Astbury et al., CERN SPSC/70-06, January 1978.

(6) C. Rubbia, "Relativistic electron cooling for high luminosity colliding beams, paper contributed to the Joint LBL-FNAL Workshop for High Luminosity $p\bar{p}$, Berkeley, March 1978.

(7) T.K. Gaisser, F. Halzen and E.A. Paschos
Phys. Rev. D15 2572 (1977).

SESSION VII

FUTURE EUROPEAN ACCELERATOR POSSIBILITIES

Chairman: V.F. Weisskopf

Sci. Secretaries: H. Hoffmann
P. Mouzourakis

Rapporteur's talk:

M. Vivargent Future European accelerator possibilities

FUTURE EUROPEAN ACCELERATORS POSSIBILITIES

M. Vivargent
LAPP, Annecy-le-Vieux, France.

INTRODUCTION

Only two laboratories are now running big accelerators in Europe: CERN and DESY. In these two laboratories, research in subnuclear physics is performed by international collaborations. DESY is a national laboratory; CERN is an international one financed through the contributions of 12 member states.

Before reporting on the projects of future accelerators for Europe, let me briefly review the present situation.

1. PRESENT SITUATION FOR ACCELERATORS IN EUROPE

1.1 DESY-PETRA

Since the middle of 1978, DESY has been running a large e^+e^- collider with the following characteristics. The machine consists of a single ring, 2.3 km in circumference, in which e^+ and e^- bunches are circulating in opposite directions. The bending radius for the particles is 194 m. They can interact in eight intersection regions when four bunches are accelerated in each beam. The centre-of-mass energy ranges from 10 to 38 GeV. The maximum luminosity of 1.2×10^{32} cm^{-2} s^{-1} per intersection should be achieved with four bunches.

1.1.1 Present situation

The machine is now running at 27.72 GeV, with a maximum luminosity of 3×10^{30} cm^{-2} s^{-1}, giving a mean value of 10^{30} with two circulating bunches in each beam; four interaction regions are used for experiments; four huge detectors installed at these intersections are now taking data: JADE, MARK J, TASSO, PLUTO. Another one, CELLO, is in assembly in the same experimental hall as PLUTO, where installations for supplying superconducting magnets are available.

The schematic view (Fig. 1) shows the detector layout. All the detectors with the exception of MARK J have a solenoidal coil providing an axial field parallel to the beam direction.

JADE and TASSO have conventional coils. PLUTO and CELLO are equipped with superconducting coils.

1.1.2 Plan for PETRA

The main task is to understand the beam dynamics, improve the tuning, and obtain higher luminosities.

Thirty-two RF cavities are now installed for an energy of 34 GeV. By adding another 32 cavities the energy can be pushed up to 38 GeV. By doubling the number of cavities (not in the original project) it would be possible to reach 46 GeV.

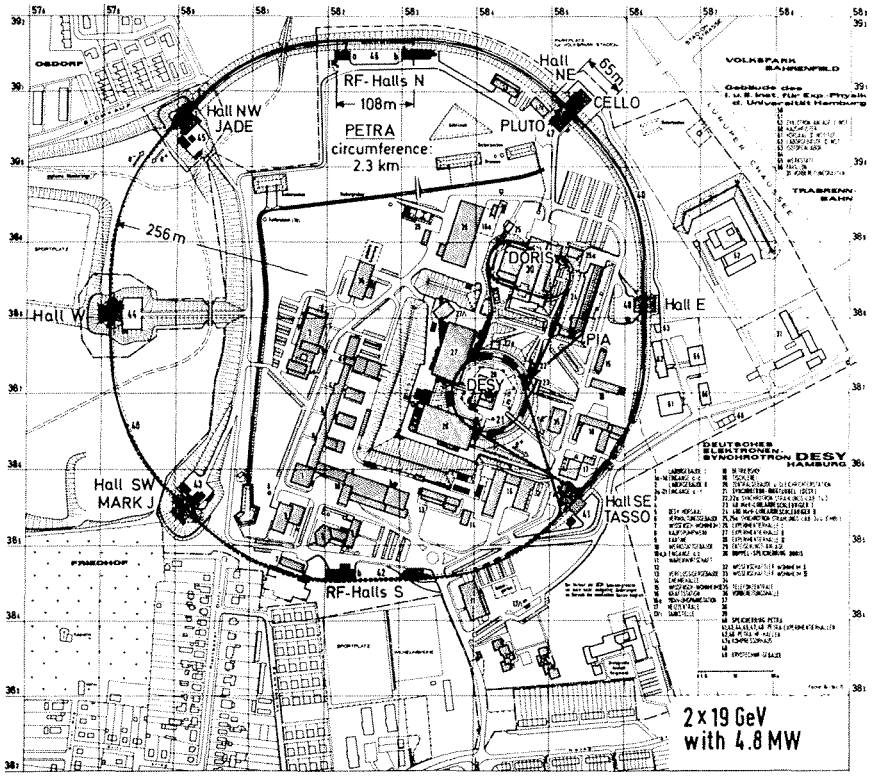

Fig. 1

1.2 CERN

1.2.1 SPS

The SPS is now running at an energy of 400 GeV with an intensity of 2×10^{13} ppp at its maximum value and with a cycle of 10.8 s.

a) Fixed-target experiments

Up to now, the SPS has been used for fixed-target experiments installed in two experimental areas (Fig. 2).

i) West Experimental Area (Fig. 3)

The general layout of this area includes

- the West Hall, with seven hadron beams and one electron beam originating from a 240 GeV proton beam;
- the West Area neutrino facility, with N_1 and N_3 beams, whose parents may have a momentum of up to 400 GeV/c.

ii) The North Area (Fig. 4)

This area is split into three halls:

- EHN 1, with several hadron beams and one high-energy electron beam;
- EHN 2, with an intense muon beam;
- EHN 3, with the full proton beam providing an intense π beam and an intense e,γ beam.

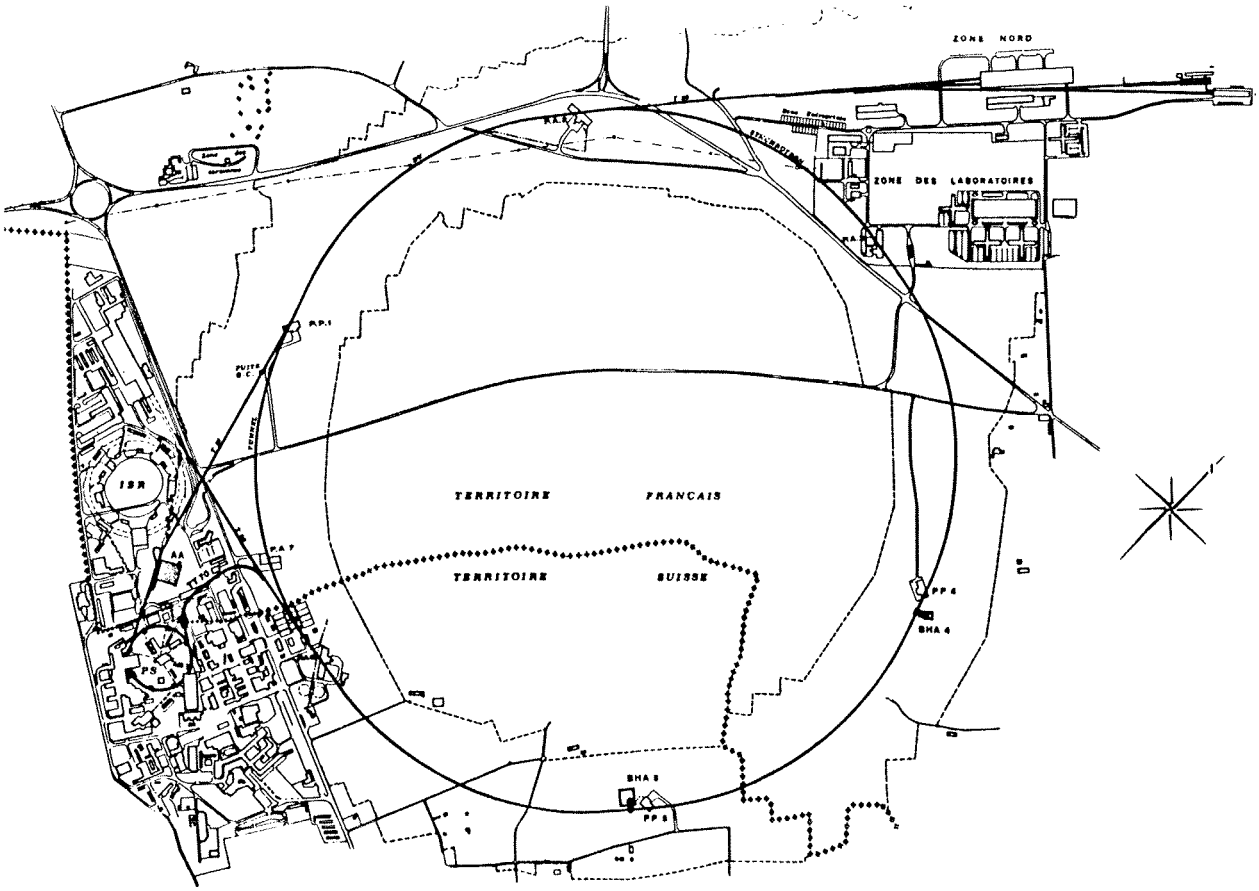
ZONE NORD
ZONE DES LABORATOIRES
TERRITOIRE FRANCAIS
TERRITOIRE SUISSE
ISR
PP 1
PP 4
BHA 4
BHA 5
PP 5

Fig. 2

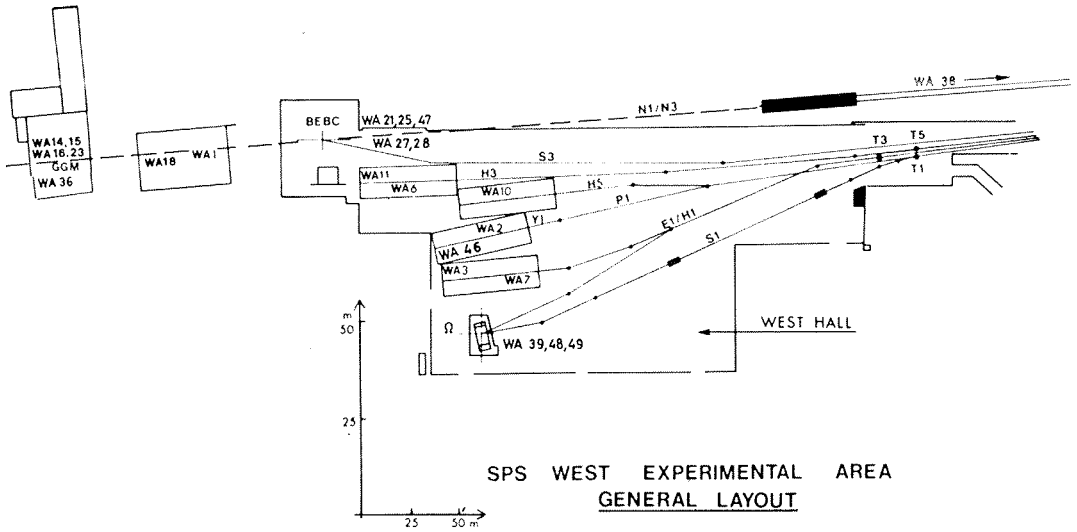
WA14, 15
WA16, 23
GGM
WA 36
WA18
WA1
BEBC
WA 21,25,47
WA 27,28
N1/N3
WA 38
T3
T5
T1
S3
WA11
WA6
H3
WA10
H5
P1
WA2
Y1
E1/H1
WA 46
WA3
WA7
S1
Ω
WA 39,48,49
WEST HALL
m
50
25
25
50 m
SPS WEST EXPERIMENTAL AREA
GENERAL LAYOUT

Fig. 3

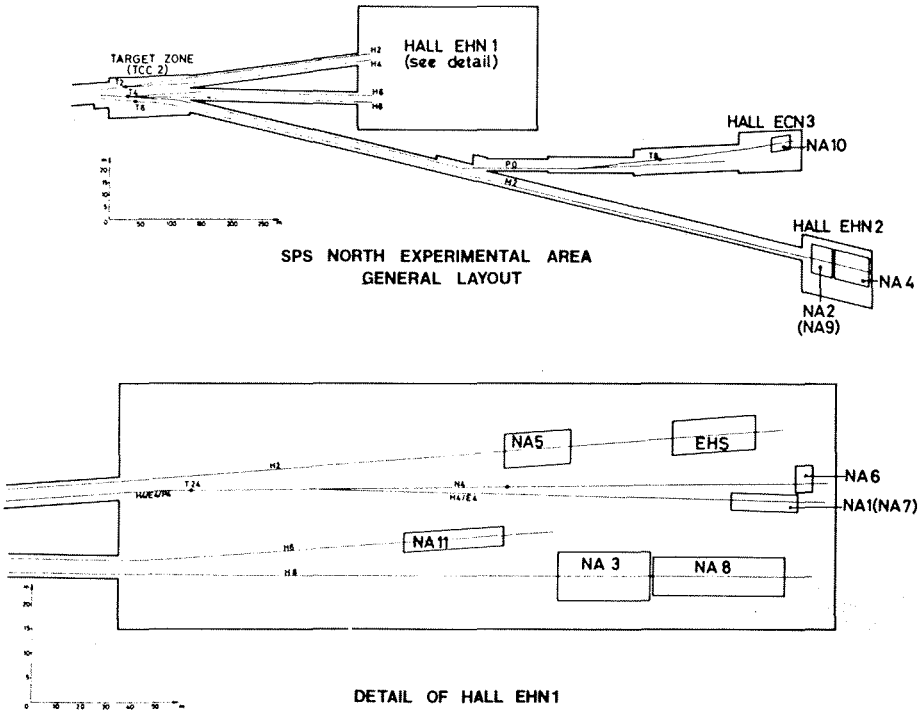

Fig. 4

b) $p\bar{p}$ collider

The stochastic cooling of antiprotons is achieved in the Antiproton Accumulator at 3.5 GeV/c. Antiprotons are then injected into the PS, where they are accelerated to 26 GeV/c in 12 bunches of 5×10^{10} particles. Finally they are injected into the SPS through TT 70. The number of bunches is reduced to six and these are accelerated to 270 GeV. They collide with six bunches of protons circulating in the opposite direction at the same energy (Fig. 5).

Modifications have to be made in almost all the long straight sections (LSS) during the SPS shutdown scheduled from 15 June 1980 to the beginning of March 1981. Two experimental halls will be built at LSS 5 and LSS 4, in preparation for the installation of experiments UA1 and UA2 (Figs. 6 and 7).

The first $\bar{p}$ are expected to be injected into the SPS in autumn 1981. The luminosity at the end of 1981 could be of the order of 10^{29} cm^{-2} s^{-1}.

c) Improvement program for the SPS

The SPS energy will be increased up to 450 GeV before the end of 1979. The intensity will be increased by the following means:

i) The addition of one RF cavity to correct instabilities observed in the beam, at the beginning of 1980. A modest increase in intensity is hoped for.

ii) By doubling the power of each RF cavity. The intensity will reach 3×10^{13} ppp at the end of 1981. The machine cycle will go from 10.8 s to 12 s. The total SPS power consumption will be $\sim$ 100 MW.

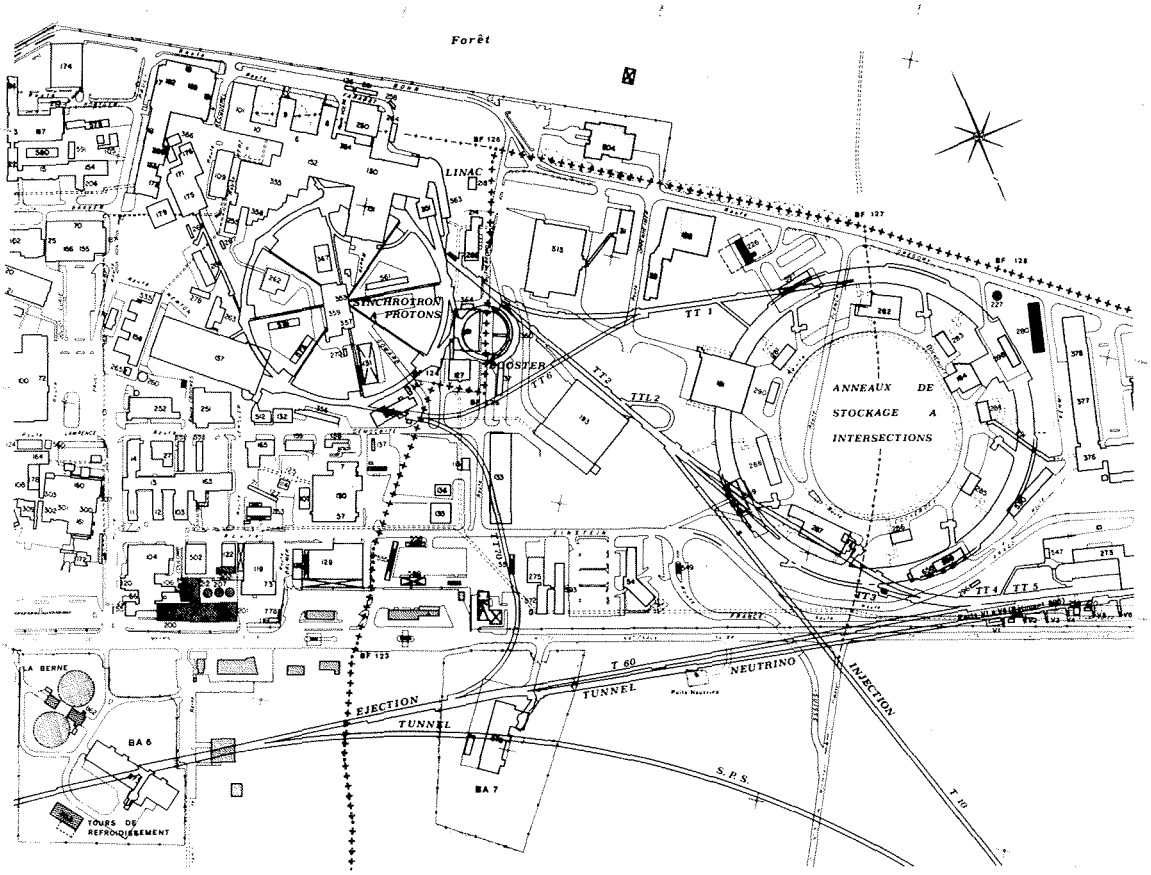
Forêt
LINAC
SYNCHROTRON A PROTONS
BOOSTER
TT1
TT2
TTL2
ANNEAUX DE STOCKAGE A INTERSECTIONS
TT4
TT5
TT9
BF 123
BF 126
BF 127
BF 128
T 60
TUNNEL
NEUTRINO
INJECTION
EJECTION
TUNNEL
S.P.S.
T 10
LA BERNE
BA 6
BA 7
TOURS DE REFROIDISSEMENT

Fig. 5

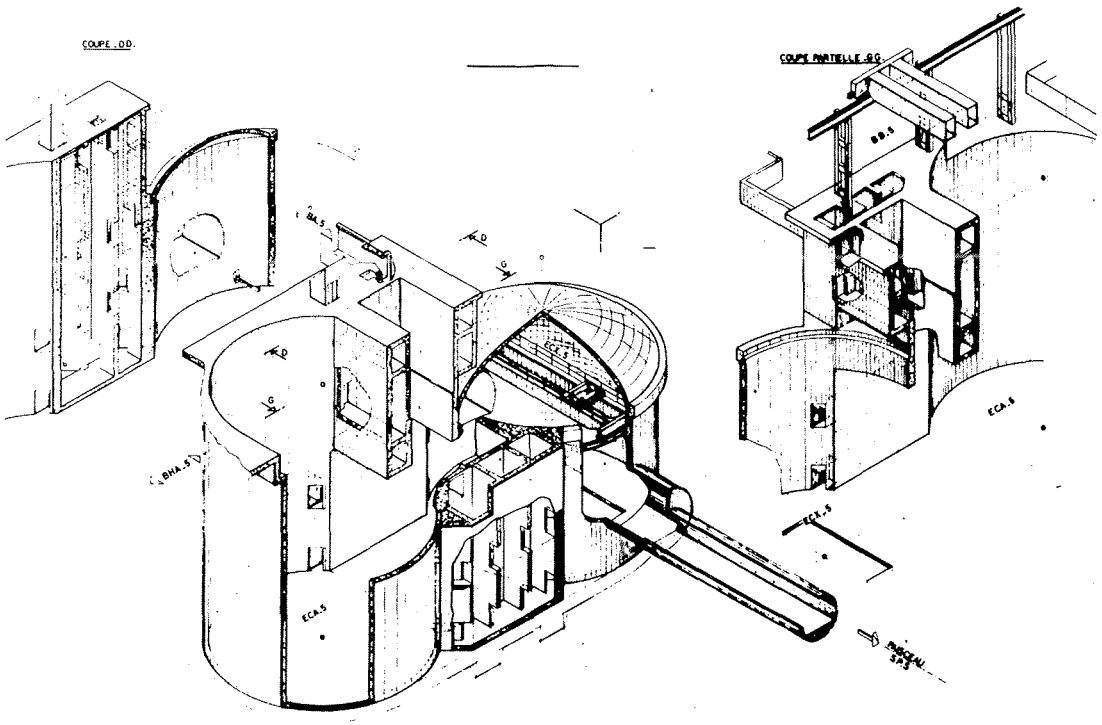
COUPE .OD.
COUPE PARTIELLE .BG
BA.5
ECA.5
ECA.4

Fig. 6

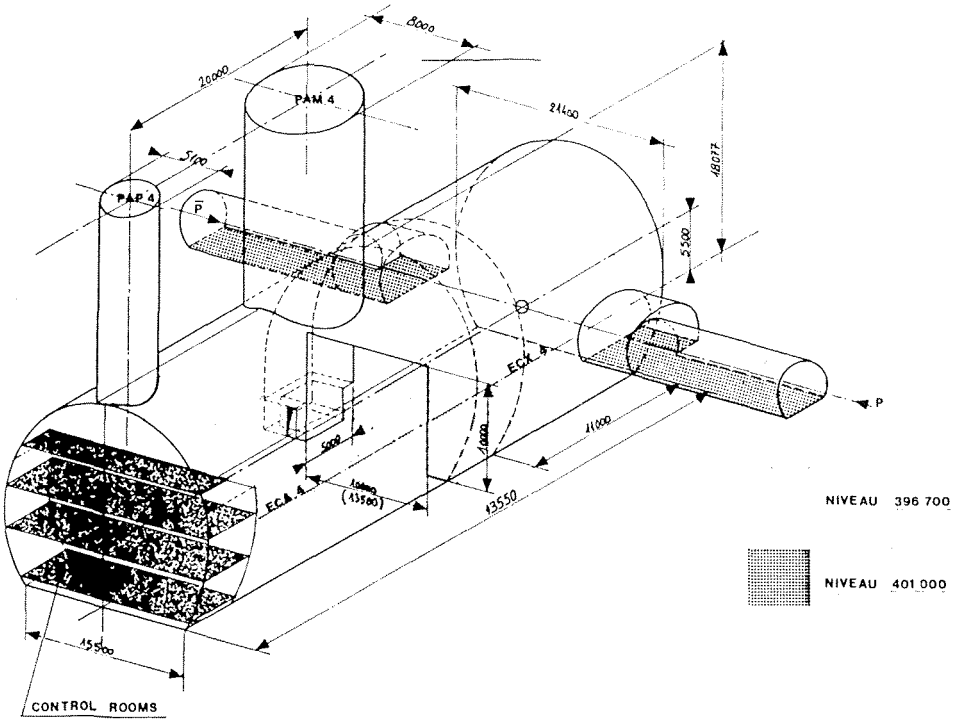

Fig. 7

1.2.2 ISR

This machine gives the highest centre-of-mass energy available in proton-proton collisions. This c.m. energy can go up to 62.4 GeV. The luminosity is constantly increasing (Fig. 8). Its value for normal intersections is 2.2×10^{31} cm^{-2} s^{-1} and it is 4.5×10^{31} cm^{-2} s^{-1} for the steel low-β intersection (I1).

About 120 physicists are involved in the experiments running at the ISR (Fig. 9).

a) Normal improvement program

A low-β superconducting intersection will be installed at I8. It will provide for a luminosity of up to 1.32×10^{32} cm^{-2} s^{-1} for experiment R 807.

b) New program

Antiprotons will be injected into the ISR in autumn 1980. Experiments will start in January 1981. The luminosity is expected to be 10^{30} cm^{-2} s^{-1} in I8 and 2×10^{29} cm^{-2} s^{-1} in the other intersections.

From this brief review, we can conclude that, before the starting up of the Doubler at Fermilab and of ISABELLE at Brookhaven, Europe will continue to hold a very strong position in subnuclear research. But, in the second half of the 1980's, a new generation of accelerators has to be brought into operation.

ISR LUMINOSITY AVAILABLE FOR PHYSICS AT $\sqrt{S}$ = 62.4 GeV

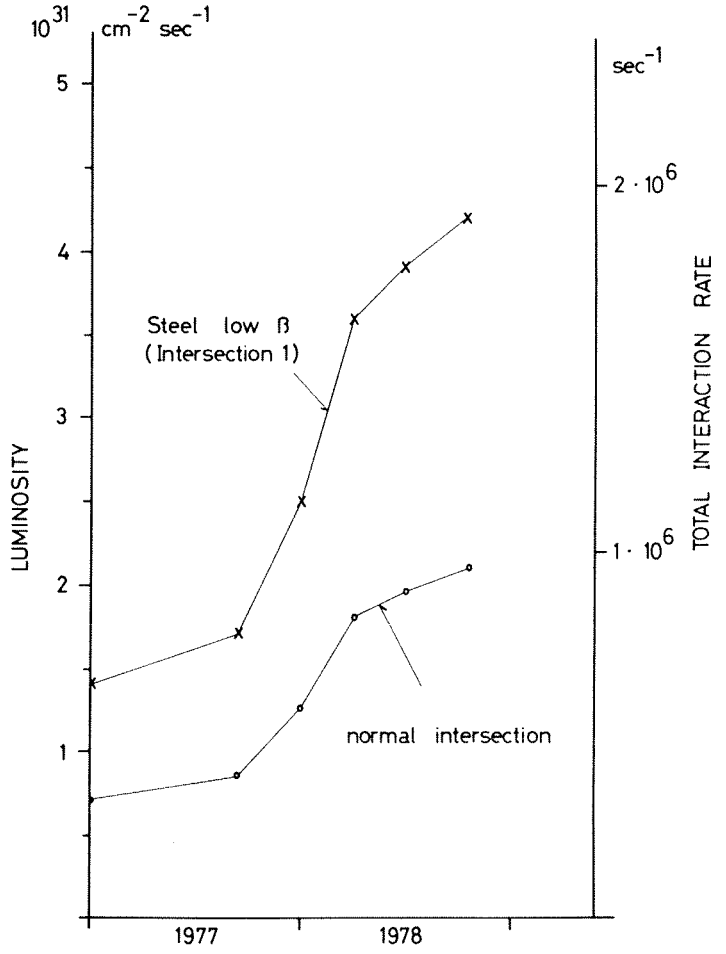

Fig. 8

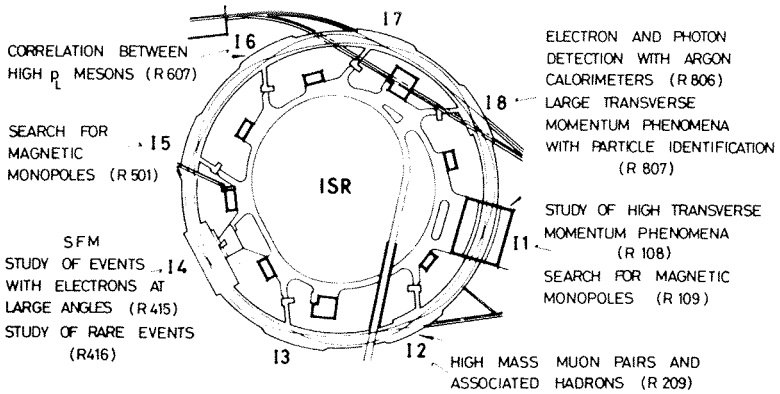

ISR Layout of Approved Experiments

Fig. 9

2. e^+e^- COLLIDER PROJECTS

In May 1977, ECFA recommended that:

1) An e^+e^- storage ring of about 200 GeV c.m. energy, possibly with an initial phase at 140 GeV, be considered by the high-energy physics community as prime candidate for a major European project for the 1980's.

2) As a first step, a location near the Meyrin site should be investigated by CERN.

3) The technical, scientific, and financial aspects of such a European project be further studied to allow the high-energy physics community via CERN and ECFA to submit a proposal for this project to the CERN Scientific Policy Committee.

4) Technical research and development of importance to the project be taken up or pursued at CERN and the laboratories of Member States, in particular on superconducting RF cavities, high-power coupling devices, etc.

5) Studies of the design of the machine and its operation, on which preliminary results were reported at the ECFA Study Week at DESY, be pursued with high priority.

6) The interest of non-CERN Member States in joining such a project be actively explored.

CERN started to actively study a LEP project. CERN-ECFA Working Groups with restricted participation were set up at the end of 1977, to look at the technical and scientific aspects of the project. Later on, in April 1978, ECFA felt it necessary to involve all the members of the community more deeply in the study and the definition of the LEP project.

Professor A. Zichichi agreed to chair the ECFA-LEP Working Group to look at all the problems concerning the machine and the physics to be performed with it. More than 350 physicists and engineers belonging to all the European laboratories replied enthusiastically to Professor Zichichi's appeal. The ECFA-LEP Working Group started its activities in July. The Working Group on high-energy physics activities in the CERN Community has to examine the consequences of the LEP construction on the future of the European laboratories. It is chaired by Professor J. Mulvey.

The design of one project was completed in the middle of 1978. The description of this project was issued in August 1978 in a Blue Book distributed to all the European laboratories. The title was: "Design study of a 15 to 100 GeV e^+e^- colliding beam machine (LEP)".

3. LEP-70 PROJECT

Let me recall the main parameters (Table 1) and the interaction region parameters (Table 2) of that machine, which is sometimes called LEP-70. I will not enter into the technical details; these I will present with the new version of the machine.

3.1 Machine

The machine has a single ring located in an underground tunnel of 3.5 km radius at an average of 60 m below the surface. This tunnel is externally tangent to the SPS tunnel in order to provide for ep collisions (Fig. 10). The tunnel bored in the "molasse" has a

Table 1

Over-all machine parameters at nominal energy

Energy per beam	70 GeV
Number of intersections	8
Number of bunches	4
Machine circumference	22.208 km
Average machine radius	3.535 km
Horizontal betatron wave number	66.208
Vertical betatron wave number	74.273
Momentum compaction factor	3.125×10^{-4}
Circulating current/beam	10.50 mA
Number of particles/beam	4.835×10^{12}
Transverse damping time	11.6 msec
Uncorrected chromaticities	-118.3 -186.5
Energy variation of damping partition number	-446
Natural r.m.s. energy spread	1.23×10^{-3}
Natural r.m.s. bunch length at I = 0	12.5 mm
r.m.s. bunch length for I ≠ 0	45 mm
Coupling	0.25
Beam-beam bremsstrahlung lifetime	6.52 h
Quantum lifetime	24 h

Table 2

Intersection region parameters

Luminosity	10^{32}	0.5×10^{32}	$cm^{-2}\ s^{-1}$
Horizontal amplitude function	1.6	3.2	m
Dispersion	0	0	
Horizontal r.m.s. beam radius	318.01	449.71	μm
Vertical r.m.s. beam radius	19.87	28.11	μm
Maximum beam-beam tune shift	0.0592	0.0592	
Crossing angle	0	0	
Free space around crossing points	±5	±10	m
Vertical amplitude function	0.1	0.2	m

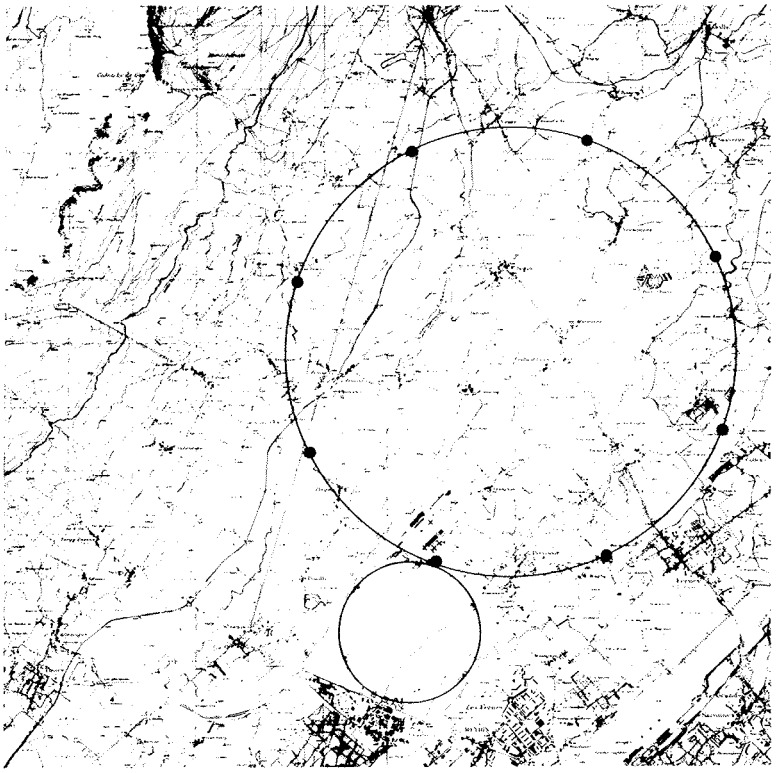

Fig. 10

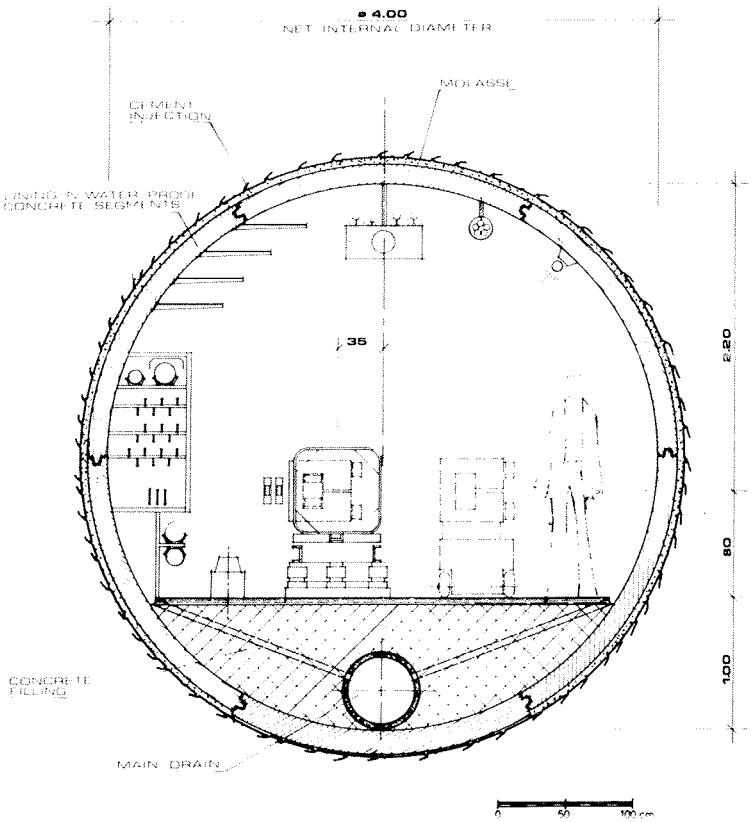
ø 4.00
NET INTERNAL DIAMETER
MOLASSE
CEMENT INJECTION
LININGS WATER PROOF CONCRETE SEGMENTS
35
220
80
100
CONCRETE FILLING
MAIN DRAIN
0
50
100 cm

Fig. 11

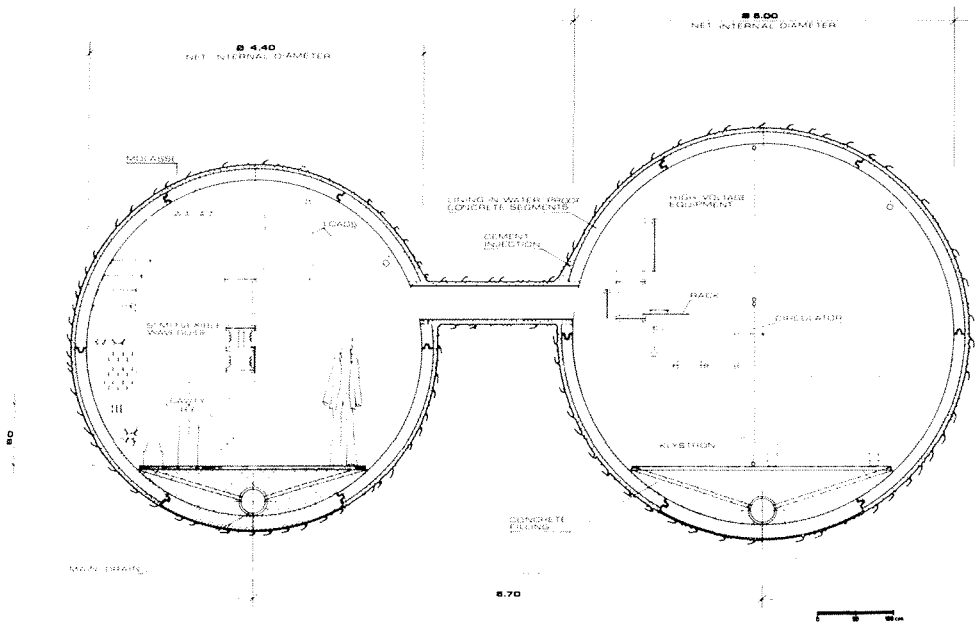

Fig. 12

circular cross-section of 4 m in diameter (Fig. 11). This is doubled, at the straight sections where beams collide in the experimental halls, by another tunnel of the same diameter in which klystrons feeding the cavities have to be installed (Fig. 12).

3.2 Experimental areas

The underground tunnel has eight access shafts corresponding to the eight intersections. These are for the transport of machine and experimental components, personnel, and services. On top of every access shaft, there is an auxiliary equipment building containing power distribution, power supplies, water pumps and exchangers. Experimental areas are designed to house two experimental facilities, one taking data, the other being accessible for maintenance.

3.3 Luminosity

The luminosity to be achieved with conventional RF cavities and superconducting RF cavities is shown in Figs. 13 and 14.

In September 1978, CERN and ECFA organized two study weeks at Les Houches to assess the contents of the Blue Book, and to review the physics to be done with a large e^+e^- collider.

More than 80 engineers and physicists coming from European laboratories and from outside laboratories took part.

The machine design was considered to be good evidence of the feasibility of a large e^+e^- machine and as a good basis for the design of a final project. Nevertheless, studies on several points revealed the need to improve the present technique or to find new solutions to reduce the cost. Many physicists found that the experimental halls were too small.

The physics was unanimously found to be extremely exciting and promising. The majority felt it necessary to push the machine energy as high as possible with conventional cavities in order to retain the possibility of studying W pair production and even going above this threshold.

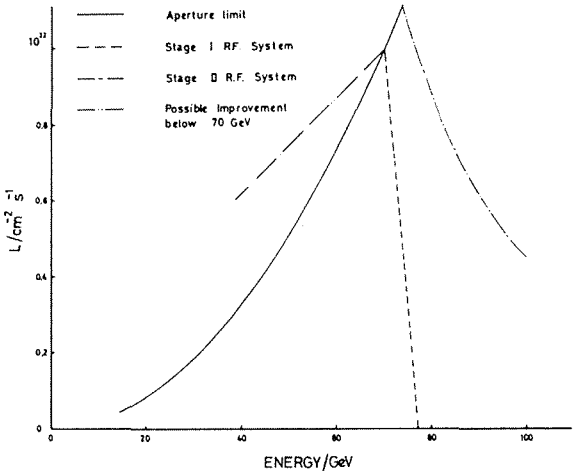

Fig. 13

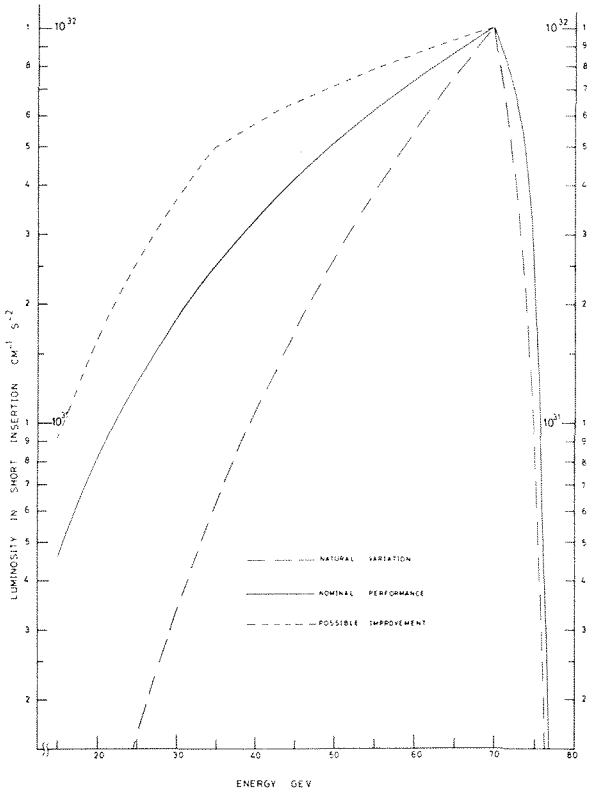

Fig. 14

4. LEP VERSION 8

After the meeting at Les Houches, it was decided to study a new project of a machine providing collisions at higher energies. A new design has been studied by CERN, in collaboration with European national laboratories. It will be issued in a Pink Book at the end of August.

4.1 Machine

The machine is a single ring in an underground tunnel of the same cross-section as LEP-70 and 30.608 km in circumference. Because of the large size of the tunnel, one part of it lies under the Jura, giving a very large depth for three of the eight intersections (3 = 179 m, 4 = 860 m, 5 = 524 m) (Fig. 15).

4.1.1 Lattice cells

Particles are bent in eight magnetic sectors and collide in eight straight sections at eight interaction points corresponding to four bunches in each beam. In the bending sectors composed of elements with separated functions, each cell comprises dipoles, quadrupoles, sextupoles, and one variable multipole (Fig. 16).

Since the LEP-70 design, a big improvement has been achieved in the construction of the dipoles by designing and testing magnets with concrete in them (⅔ concrete, ⅓ iron) (Fig. 17). Cost is thus greatly reduced.

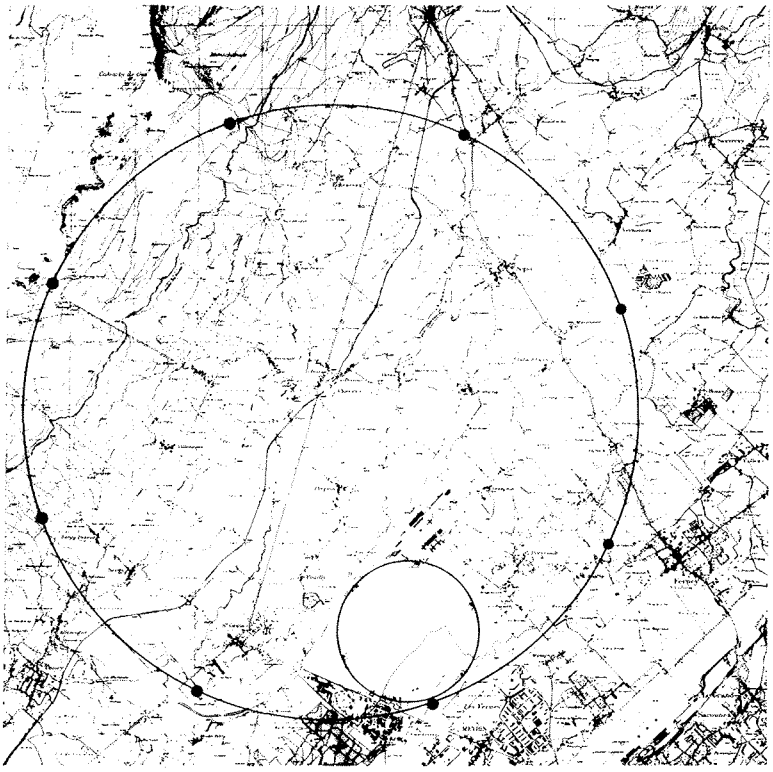

Fig. 15

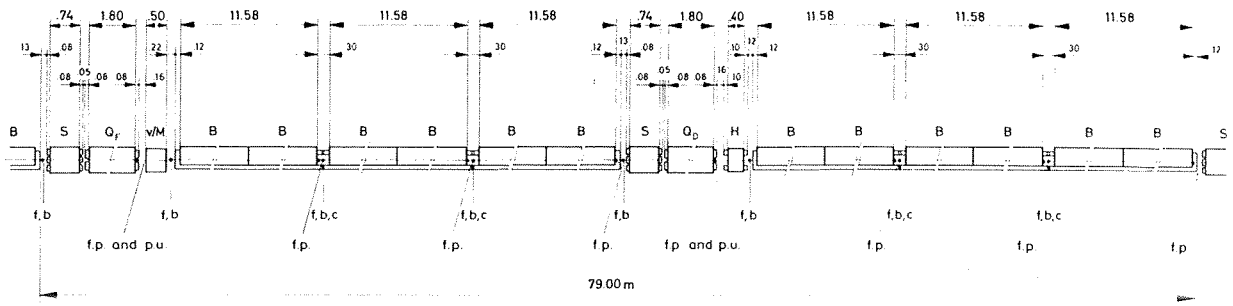

STANDARD CELL

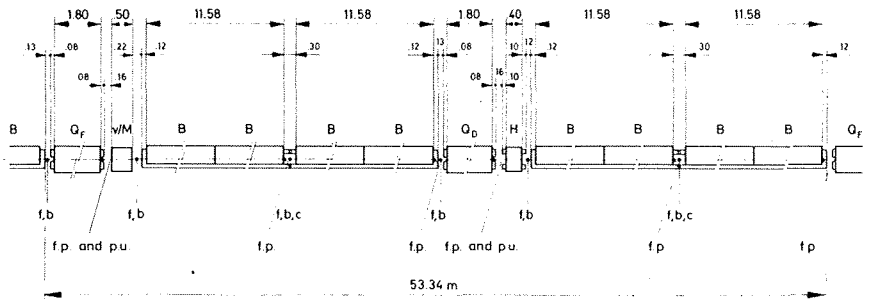

DISPERSION SUPPRESSOR CELL

B - bending magnet
Q_F, Q_D - quadrupoles
S - sextupole
H - horizontal-field dipole
M - multipole

f - flange
b - bellows
c - connections
f.p - fixed point
p.u - pick-up
v - valve

Fig. 16

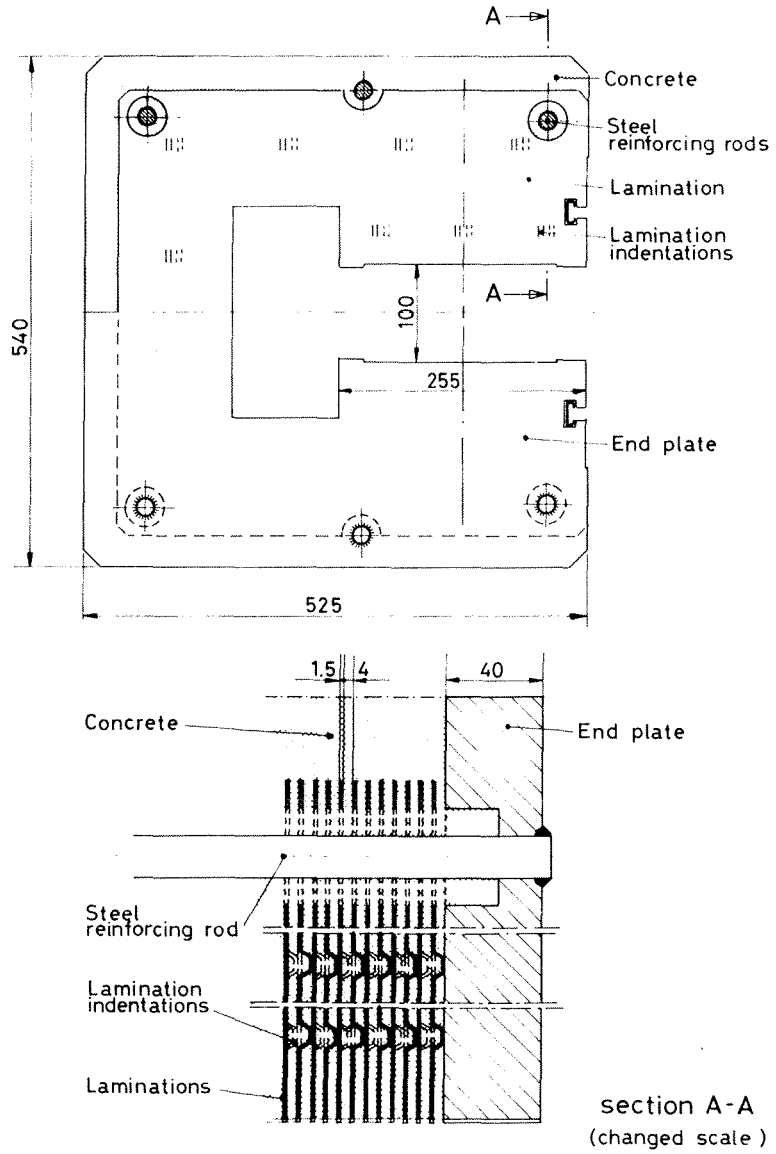

Fig. 17

4.1.2 RF system

Particles are accelerated in straight sections on either side of the intersection point by RF cavities powered by klystrons (Fig. 18). Four stages are foreseen for the running of LEP, corresponding to the number of working cavities.

Another big improvement has been made here by the introduction of storage cavities which reduce the power consumption and allow a small increase in the energy (Fig. 19).

4.1.3 Experimental areas

Experimental areas are larger than those foreseen in the LEP-70 project. Two are accessible from the surface (2 and 6: -30 m) (Fig. 20); three by shafts (1: -58.3 m, 7: -42 m, 8: -57 m) (Fig. 21); three by tunnel (4, 5, 6).

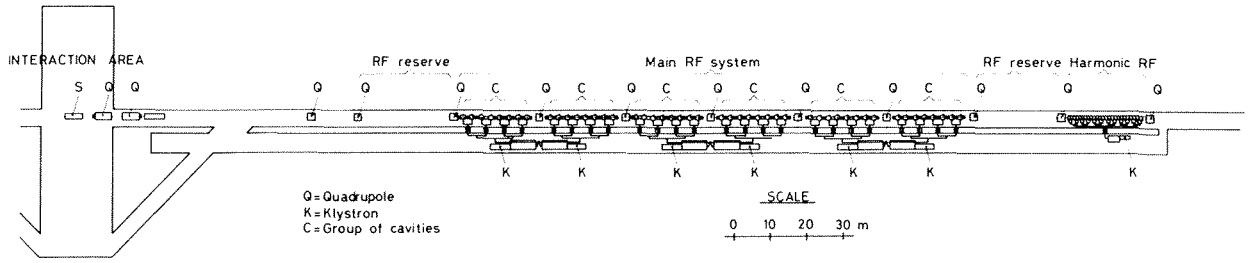

Fig. 18

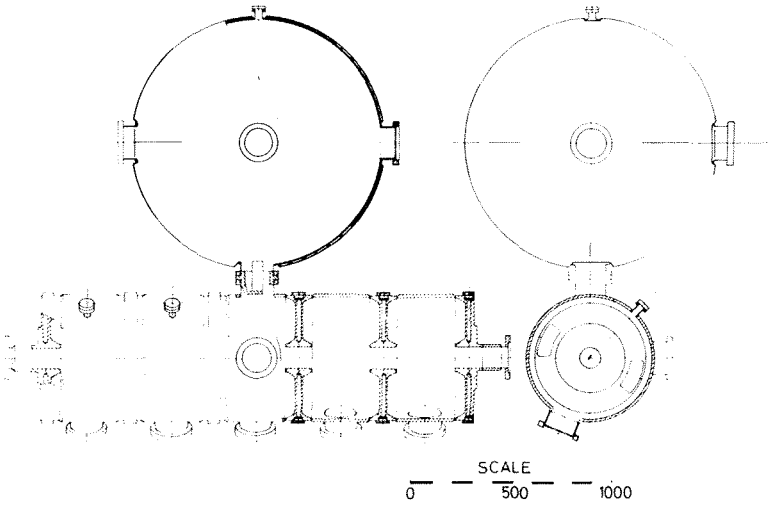

Fig. 19

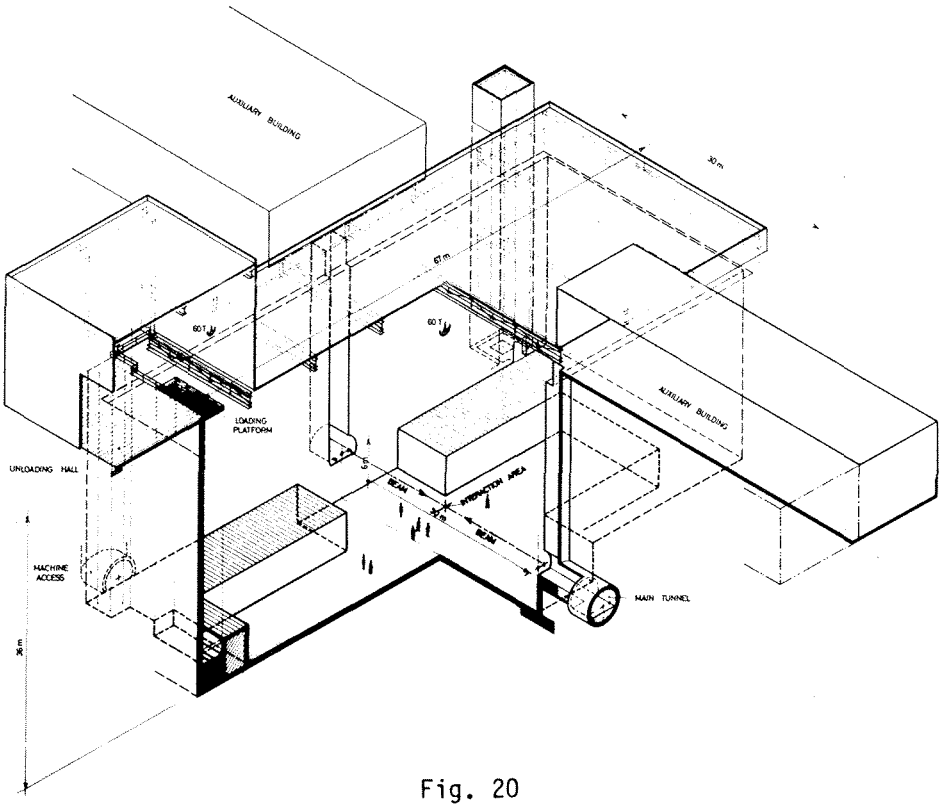

Fig. 20

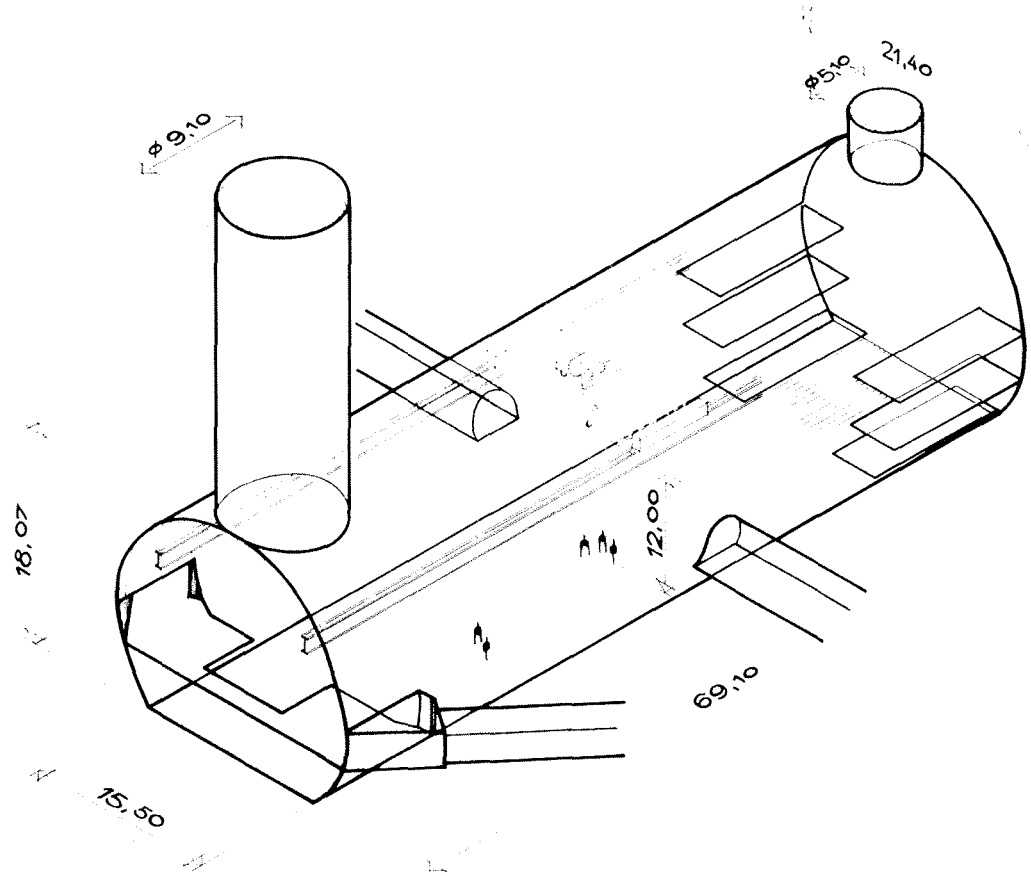

Fig. 21

4.1.4 Energy

Four stages are foreseen with normal cavities (Table 3):

Stage 1/6	49.4 GeV
Stage 1/3	62.3 GeV
Stage 1	86.11 GeV
Stage 4/3	92.86 GeV .

The main RF system parameters, corresponding to stage 1, are given in Table 4. Superconducting cavities with an accelerating gradient of up to 5 MV/m are required to push the energy up to 130 GeV with good luminosity.

4.1.5 Luminosity

The luminosities corresponding to the different stages are shown in Fig. 22.

4.2 Injector

Electrons and positrons will be injected into LEP by a 22 GeV synchrotron, possibly built by using ISR magnets (Fig. 23).

Since I am speaking of new e^+e^- colliders, I have to quote two other national projects.

Table 3

Possible stages of LEP

		Stage 1/6	Stage 1/3	Stage 1	Stage 4/3	Unit
Design energy	E	49.4	62.3	86.11	92.86	GeV
Circulating current per beam	I	5.71	7.20	9.15	9.15	mA
Design luminosity	L	3.85×10^{31}	6.16×10^{31}	1.07×10^{32}	1.15×10^{32}	$cm^{-2}\ s^{-1}$
Frequency	f_{RF}	353.39	353.39	353.39	353.39	MHz
Number of RF stations		8	8	16	16	
Number of klystrons		16	32	96	128	
Active RF cavity length	L_c	271.5	542.9	1628.8	2171.7	m
Number of five-cell cavities (each one coupled to a storage cavity)		128	256	768	1024	
Shunt impedance	Z	40.0	40.0	40.0	40.0	$M\Omega \cdot m^{-1}$
Parasitic impedance, RF cavities		1.63	3.25	9.75	13.0	GΩ
Parasitic impedance, chamber		2.25	2.25	2.25	2.25	GΩ
Parasitic impedance, total		3.88	5.5	12.0	15.25	GΩ
Synchrotron energy loss/turn	U_0	182	420	1370	1853	MeV
Parasitic energy loss/turn	U_{hm}	22	40	110	140	MeV
Peak RF voltage a)	V_{RF}	364	694	1949	2593	MV
Accelerating field	V_{RF}/L_c	1.34	1.28	1.20	1.19	$MV \cdot m^{-1}$
Stable phase angle a) (from zero crossing)	ϕ_s	145.9	138.6	130.6	129.8	degrees
Synchrotron radiation power (two beams)	P_b	2.08	6.05	25.07	33.91	MW
Parasitic mode losses (two beams)	P_{hm}	0.25	0.57	2.01	2.55	MW
Cavity dissipation and reflection	P_d	12.47	22.98	61.72	81.94	MW
Waveguide losses		1.2	2.4	7.2	9.6	MW
Total RF generator power	P_g	16.0	32.0	96.0	128.0	MW
Number of synchrotron oscillations/turn	Q_s	0.1015	0.1187	0.1576	0.1736	

a) Overvoltage factor calculated allowing for turbulent bunch widening.

Table 4

Main RF system parameters, Stage 1

Design energy	E	86.1	GeV
Design luminosity	L	1.07×10^{32}	$cm^{-2}\ s^{-1}$
Synchrotron energy loss/turn	U_0	1370	MeV
Parasitic energy loss/turn	U_{hm}	110	MeV
Peak RF voltage/turn	V_{RF}	1949	MV
Stable phase angle (from zero crossing)	ϕ_s	130.6	degrees
Frequency	f_{RF}	353.4	MHz
Number of synchrotron oscillations/turn	Q_s	0.158	
Length of active RF structure	L_c	1628.8	m
Shunt impedance/unit length	Z	40.0	$M\Omega \cdot m^{-1}$
Fundamental mode cavity dissipation and reflection	P_d	61.7	MW
Synchrotron power (two beams)	P_b	25.1	MW
Waveguide losses		7.2	MW
Parasitic mode losses (two beams)	P_{hm}	2.0	MW
Total RF generator power	P_g	96.0	MW
Number of RF stations		16	
Total number of klystrons		96	
Total number of five-cell cavities (each one coupled to a storage cavity)		768	

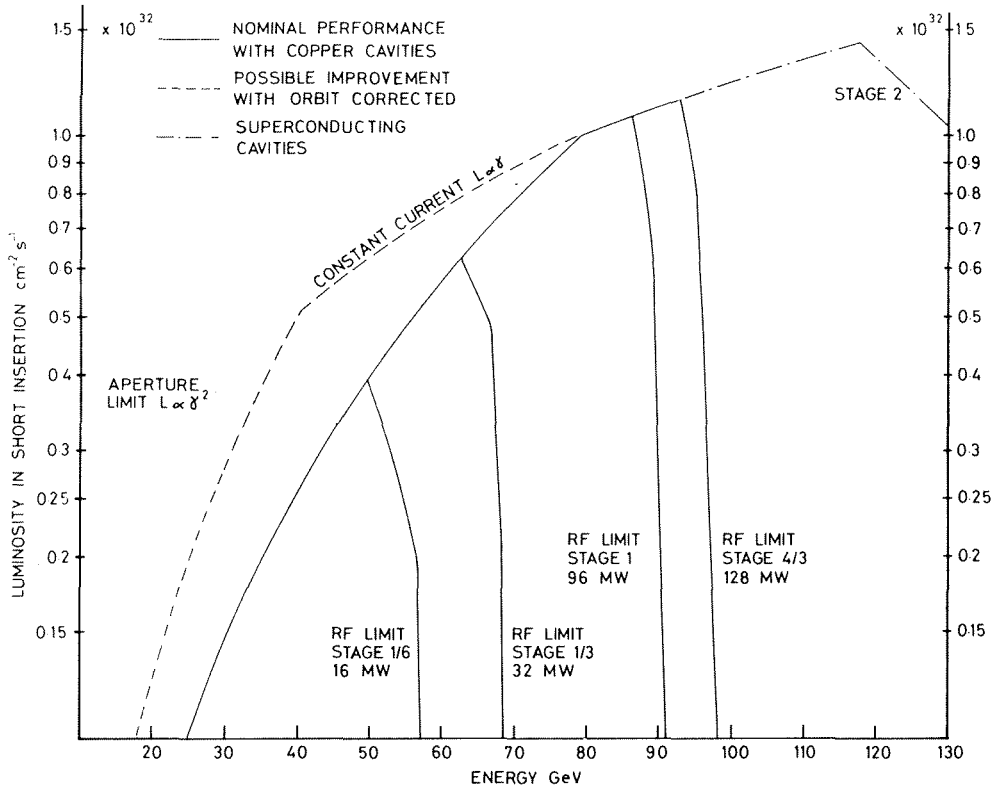
x 10^32
NOMINAL PERFORMANCE WITH COPPER CAVITIES
POSSIBLE IMPROVEMENT WITH ORBIT CORRECTED
SUPERCONDUCTING CAVITIES
STAGE 2
CONSTANT CURRENT L∝γ
APERTURE LIMIT L∝γ²
RF LIMIT STAGE 1/6 16 MW
RF LIMIT STAGE 1/3 32 MW
RF LIMIT STAGE 1 96 MW
RF LIMIT STAGE 4/3 128 MW
LUMINOSITY IN SHORT INSERTION cm⁻² s⁻¹
ENERGY GeV

Fig. 22

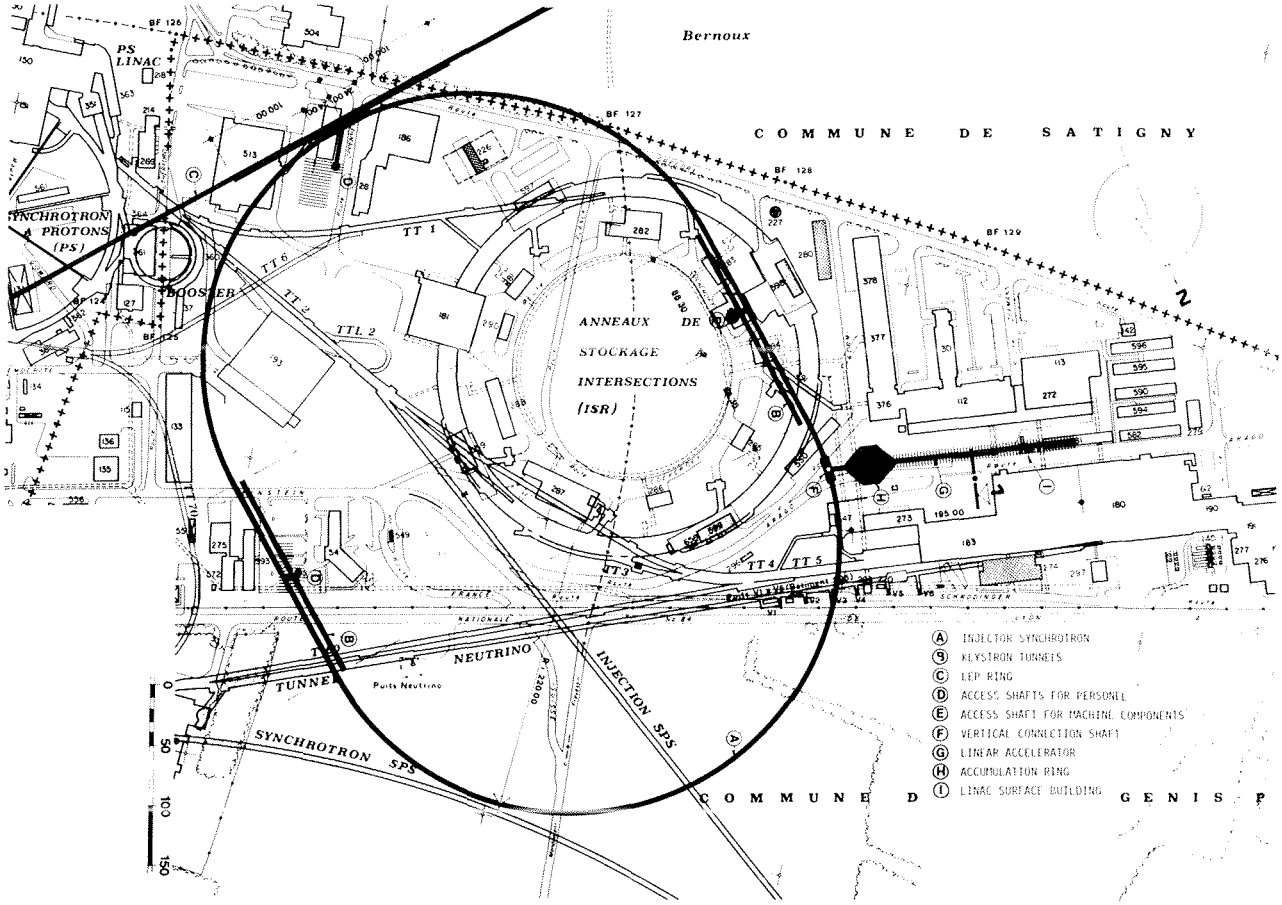
Bernoux
COMMUNE DE SATIGNY
PS LINAC
SYNCHROTRON A PROTONS (PS)
BOOSTER
TT 1
TT 2
TT 6
TTL 2
ANNEAUX DE STOCKAGE INTERSECTIONS (ISR)
TT 3
TT 4
TT 5
NEUTRINO
TUNNEL
Puits Neutrino
INJECTION SPS
SYNCHROTRON SPS
COMMUNE D GENIS P
A INJECTOR SYNCHROTRON
B KLYSTRON TUNNELS
C LEP RING
D ACCESS SHAFTS FOR PERSONEL
E ACCESS SHAFT FOR MACHINE COMPONENTS
F VERTICAL CONNECTION SHAFT
G LINEAR ACCELERATOR
H ACCUMULATION RING
I LINAC SURFACE BUILDING

Fig. 23

5. DESY

New ring in the PETRA tunnel: PETRA 45

i) Principles: Very low β^*: through very small quadrupoles very close to the intersection point;
Very small ε: through very strong focusing lattice;
Very small electron current at same ΔQ, i.e. very small beam power.

ii) Luminosity: Luminosity can be kept constant if ΔQ = cst and ε/β_z^* = cst, as may be deduced from the following formulae:

$$L = \frac{c}{2r_e^2} \frac{n_b (\Delta Q)^2 \varepsilon (1 + k)\gamma^2}{R\beta_z^*}$$

$$\Delta Q = \frac{r_e}{2\pi} \frac{N}{n_b \varepsilon \gamma} .$$

iii) Energy: 45 GeV. Needs superconducting cavities.

6. FRASCATI

ALA

i) ALA is a very attractive project for two reasons:

a) The low energy range of the machine is well adapted to the study of resonances between 1 GeV and 2.4 GeV.

b) This project is proposed by the laboratory from which originated the ideas and the techniques for this type of machine. It would be a great pity for the community if this machine were not built. I am sure that the chairman of the INFN, Professor A. Zichichi, will do his best for the success of the project.

ii) Characteristics

- Circumference: 70 m. Bending radius: 2.5 m.
- Energy from 1 GeV to 2.4 GeV.
- Two low-β intersection regions; 3 m for experiments.
- Luminosity $\sim E^4$ for $0.5 < E_e < 0.75$ GeV:

  1.6×10^{30} at 0.5 GeV (1 GeV total),
  9×10^{30} at 0.75 GeV (1.5 GeV total);
  $\sim E^{2.6}$ for $0.75 < E_e < 1.2$ GeV:
  1.5×10^{31} at 1.2 GeV (2.4 GeV total).

7. ep COLLIDER PROJECTS

An ep collider has been considered by ECFA as the best complementary machine to LEP. This collider could be built either by making use of existing proton or electron machines or by constructing a new machine.

In order to look at all the problems concerning ep machines and physics, ECFA has organized studies with the strong support of European laboratories. The latest study of an ep facility for Europe was organized by ECFA and DESY, and held at DESY on 2 and 3 April 1979.

More than 300 physicists and engineers participated in these studies, showing their strong interest in this field of physics. Proceedings will be issued at the end of August.

ECFA has decided to continue the studies and has set up four small groups coordinated by U. Amaldi. They are working on the following subjects:

i) superconducting magnets;

ii) machine design;

iii) experiments;

iv) theory.

This decision has been taken in view of the fact that ep physics is one of the future programs now envisaged at DESY. The corresponding project has to be defined by the beginning of 1980, in order to be ready for a decision on the future DESY program in 1981. The ECFA Working Group will contribute to the definition of the DESY project. Two possibilities are under consideration, PROPER and SUPERPROPER.

7.1 PROPER

PROPER consists of the addition of a proton ring to PETRA. The electron ring is the PETRA ring modified in the straight sections only. No changes in the tunnel building are required (Fig. 24).

There will be up to six ep interaction points, two in the long straight sections E and W, and four in the short straight sections (NE, SE, SW, NW).

Beams collide head on.

The electron spin is turned longitudinally by a simple antisymmetric vertical bending arrangement that causes minimum depolarization. There would be 100% longitudinal polarization in the long straight sections and 60% in the short straight sections if the PETRA beam were fully polarized.

The free length for ep experiments is typically 15 m in the long straight sections and 10 m in the short ones.

The proton ring is alternately underneath and above the electron ring, crossing it at each ep interaction point. It is a superconducting ring whose magnets would be an adaptation of the Fermilab or Brookhaven magnets.

The energies range as follows: $6.3 < E_e < 17.5$ GeV and $100 < E_p < 280$ GeV.

The luminosity stays above 10^{32} cm^{-2} s^{-1} with a maximum at 11/176 GeV (Fig. 25).

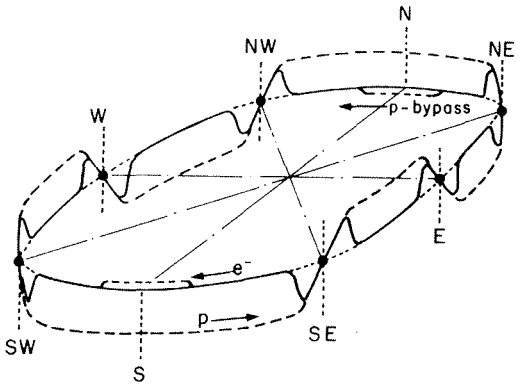

Fig. 24

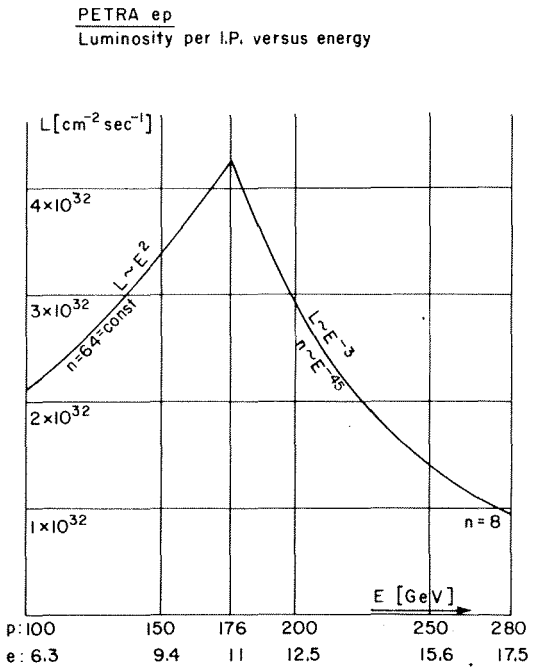

Fig. 25

Three options have been considered:

1) 4 T (NbTi), E_p = 225 GeV,
   Magnets construction: $2\frac{1}{2}$ years.

2) 5 T (NbTi), E_p = 280 GeV,
   Study of the new magnets: not before the end of 1986.

3) 8 T (NbSn), E_p = 450 GeV,
   Full studies of dipoles and multipoles: not before the end of 1988.

Construction time after the definition of the project for option (1): 5 years.
Problems: interaction between the two beams;
interaction regions.

7.2 SUPERPROPER or PROPER II ($\sim$ 6 km circumference)

Preliminary studies of an ep machine installed in a 6 km circumference ring near PETRA have been conducted at DESY.

The new scheme proposed by Steffen for an e^+e^- ring has been adopted for these studies. It includes mini-β, mini-emittance, mini-intensity.

The characteristics of such a machine using this new scheme are as follows:

- Energy of the electrons: up to 40 GeV,
- Energy of the protons with conventional magnets: 380 GeV,

Total c.m. energy: 214 GeV for E_e = 30 GeV,

Luminosity: 1.7×10^{32} cm^{-2} s^{-1}.

- Energy of the protons with superconducting magnets: 1000 GeV,

  Total c.m. energy: 346 GeV,

  Luminosity: 4.6×10^{32} cm^{-2} s^{-1}.

8. CONCLUSION

Important choices have to be made at both national and international levels, it is hoped as soon as possible. These choices will fully commit the future of the subnuclear physics community and will affect all its members. The high quality of the physicists and engineers in the European laboratories is a guarantee of the technical quality of the projects. ECFA has to organize the participation of the maximum number of physicists and engineers in the study and definition of the future accelerators for Europe.

This is why the ECFA-LEP Working Group has been set up. For more than one year, over 350 physicists and engineers have been studying all the problems concerning LEP (machine, experiments, detectors, theory), in 20 specialized study groups.

Two study weeks will be held in September in Rome. At the end of the study weeks, the ECFA-LEP Working Group will draw its conclusions on the machine. It will continue to study other aspects of the project.

In the same spirit, ECFA has set up a working group on an ep facility for Europe, and ECFA will carefully follow the work of this group in order to make the most effective contribution to the project studies.

The twenty-fifth anniversary of CERN has naturally given the opportunity to emphasize the success of the CERN laboratories. Let me nevertheless recall that this success is mainly due to the good collaboration among the European laboratories and universities, which, by virtue of their own vitality, are able to perform high-quality research programs at the CERN accelerators. This vitality has to be preserved.

ECFA has therefore set up a working group to study the consequences of LEP construction on the activities of the subnuclear physics laboratories in the community. The group is studying ways in which these activities can be maintained at the highest level during and after the LEP construction. It will also give its first conclusions in September.

ECFA will have to formulate recommendations concerning ep machines and LEP by taking into account the conclusions of its three working groups. ECFA will thus have fully assumed its responsibilities.

The national and European bodies will have to face up to their own responsibilities in choosing from among the various candidates the projects which will satisfy the national and European communities and which are compatible with the economic constraints imposed.

With the realization of the new projects, and particularly with the building of LEP, Europe will have complemented the machines under construction in the world (Doubler at FNAL, ISABELLE at Brookhaven, UNK at Serpukhov).

We are now entering an era where all the accelerators and other facilities in the world have to be open to all physicists irrespective of their national origin.

ECFA will encourage this step in international collaboration, which will inevitably be followed in the next stage by the study of an international machine in an international centre run by all the nations of the world.

SESSION VIII

CLOSING SESSION

Chairman: A. Zichichi

Sci. Secretaries: A. Benvenuti
S. Reucroft

Rapporteur's talk:

A. Salam A gauge appreciation of developments in particle physics - 1979

Before giving the floor to Professor Abdus Salam I would like to make it clear that his lecture is not going to be a summary of the Conference.

I have asked Professor Salam to concentrate on those aspects of the Conference that are relevant to a gauge theorist. And in particular, starting from today's results, to elaborate on what could happen in the distant future. This implies discussing matters such as the so-called DESERT, supergravity, SO(8), etc. Fascinating topics, just mentioned in my opening lecture, but ones to which not much time has been devoted during the Conference.

A. Zichichi

A GAUGE APPRECIATION OF DEVELOPMENTS IN PARTICLE PHYSICS - 1979

A. Salam,
ICTP, Trieste, Italy, and
Imperial College, London, England.

I. INTRODUCTION

A conference so vast and many-sided is impossible to summarize in forty-five minutes, and I will not even attempt to do so. My major theme is a gauge-theorist's appreciation of the developments in particle physics reported at the conference. In particular I wish to address myself to the question raised by Professor Zichichi in his opening address: Can we now indeed chart the course of the subject nearly up to Planck energies, of the order of 2×10^{-5} grams (1.2×10^{19} GeV)? If so, is there likely to be a long stretching Grand Plateau, unbroken by any high peaks of new physics, which is predictable on the basis of the gauge revolution of this decade?

There is no question as to the fact that the central feature of particle physics of this decade has been the recognition that the fundamental forces of nature appear to be governed by a universal gauge principle - a principle which made its first appearance with Maxwell and Einstein, whose hundredth anniversaries of death and birth, respectively, we celebrate this year. This principle has not only provided us with a quantitative theory of weak nuclear forces; it has also forced upon us a unification of the weak with the electromagnetic, in the electroweak $SU(2) \times U(1)$. Combined with the hope that the strong nuclear force is controlled by the gauge group $SU_C(3)$, one has been led to an elaboration of a standard model. There is then the natural and tantalizing hope that these weak nuclear, strong nuclear and electromagnetic gauges ($SU(2) \times U(1) \times SU_C(3)$) will combine, perhaps in a direct extrapolation, into the ELECTRO-NUCLEAR gauges of a grand unified theory and eventually perhaps into (gauged) super-gravity. As we know, it is this vast extrapolation which, within the context of particular grand unifying schemes, appears to lead to the "plateau" syndrome. And central to these schemes is the circular hypothesis that essentially no new forces (besides those described by $SU(2) \times U(1) \times SU_C(3)$) will manifest themselves, before one reaches the end of the plateau, deduced on this basis to extend nearly up to Planckian energies.

Now in this half century, in the science of biology, the analogue of our universal gauge principle was found in 1953 with the discovery of the double helix. Likewise in another scientific discipline, nearer to ours, a standard model was elaborated with the discoveries of the expanding universe

and the big bang. However neither of these (admittedly intellectually inferior!) disciplines of science have on the basis of present knowledge entertained the death-wish for an unrelieved wasteland for all tomorrow. In fact, the universality of the double helix principle has not obscured from the biologist the fact that far from being the "end of molecular biology", this was only a beginning. "Something quite essential is missing in our basic understanding of life and we have not the slightest idea about the nature of lacunae in our knowledge"[1]. I believe that precisely the same applies to particle physics. As I would like to stress in the course of this talk, the remarkable successes of the gauge principle and the understanding of the fundamental forces it has given us should not obscure from us the fact that before we believe our vast extrapolations, we must fill in some glaring lacunae in our knowledge. There is something fundamentally essential missing in our understanding of the nature of the (flavour and colour) charges with which the gauging starts. In this respect, not till we match, at the very least, the type of understanding reached by Einstein (when he comprehended gravitational charge in terms of space-time curvature), can our quest in particle physics acquire the qualitative depth attained for example by gravity, nor more importantly, its quantitative freedom from some of the presently ad hoc parameters.

I shall divide my remarks about the conference into five parts:

1) Status of the Three Families of what we consider to-day as the elementary entities of matter;
2) Status of the electroweak $SU(2) \times U(1)$;
3) Status of QCD - the gauge theory of colour;
4) From the electroweak to the electro-nuclear (grand unification);
5) Post-Planck physics and Einstein's dreams, i.e. a unification of gravity with matter; and a comprehension of the nature of (flavour and colour) charges within space-time geometry or space-time topology.

II. THE THREE FAMILIES

1. The physics of the two familiar Families consisting of 15 (or if the neutrinos are massive, 16) two-component objects (ν_e, e_L, e_R; u_L, u_R, d_L, d_R; quarks in three colours) plus (ν_μ, μ_L, μ_R, c_L, c_R, s_L, s_R) is in good shape. In particular:

a) Charm is produced by hadrons as demonstrated both by indirect (prompt e, μ, ν, eμ) and direct (bump hunting and emulsion) methods. (The

first paper presented at the conference was the emulsion picture of $\Lambda_c^+ \to p\pi^+K^-$; $m_{\Lambda_c} = 2.29 \pm 0.15$ GeV and (theoretically expected) lifetime $\tau = (7.3 \pm 0.1) \times 10^{-13}$ s.) The production mechanism is not quantitative yet, but presumably soon will be.

b) The detailed knowledge provided by e^+e^- annihilation of $\bar{c}c$ states (J/ψ, ψ', ψ'',..., P states χ) is however matched by the new problems of the charmed pseudoscalars reportedly missing at 2830 MeV and 3455 MeV.

2. Regarding the Third Family, assuming that it also follows the pattern of the first Two Families:

a) There is no evidence for toponium up to the centre-of-mass e^+e^- energies ≈ 27.4 GeV at PETRA.

b) Naked beauty has most likely been seen by the fortunate few in the SISI collaboration in $B \to (J/\psi) + \bar{K} + \pi$ [incident π^-'s (150-170 GeV), BR.σ = 0.8 nb, and estimated B production $\approx$100 nb, if B.R. $\approx$1% for the channel quoted].

The status of the Third Family is thus at a tantalizing stage. It may not follow the pattern of the first Two Families (though after the observed b-decay, the case for a (t-b) doublet has become stronger). If it does, I would consider it evidence - in analogy with the universality of the double helix - that nature has discovered a dynamical stability about the system of the 15 (or 16) objects which constitute the first Two Families and that almost certainly there is a more basic layer of structure underneath.

III. THE ELECTROWEAK SU(2) × U(1)

After the beautiful presentations of Dydak (who emphasised the degree of precision achieved now in measuring the model independent parameters in neutrino neutral-current physics) and of Prescott, there is little that I can add about the agreement of the SU(2) × U(1) theory (containing one theoretically undetermined coupling, $\sin^2\theta = 0.230 \pm 0.015$) with all the currently measured weak and electromagnetic phenomena below 100 GeV or so. [2]

Perhaps the most remarkable measurement in this respect is that of the parameter $\rho = \left(\frac{m_W}{m_Z \cos\theta}\right)^2$ which is currently determined from the ratio

THE NEUTRAL CURRENT COUPLING CONSTANTS (Dydak)

	Experiment	SU(2) × U(1)	$\sin^2\theta = 0.23$
u_L	0.32 ± 0.03	$\frac{1}{2} - \frac{2}{3}\sin^2\theta_W$	0.347
d_L	-0.43 ± 0.03	$-\frac{1}{2} + \frac{1}{3}\sin^2\theta_W$	-0.423
u_R	-0.17 ± 0.02	$-\frac{2}{3}\sin^2\theta_W$	-0.153
d_R	-0.01 ± 0.05	$\frac{1}{3}\sin^2\theta_W$	0.077
g_V	0.06 ± 0.08	$-\frac{1}{2} + 2\sin^2\theta_W$	-0.040
g_A	-0.52 ± 0.06	$-\frac{1}{2}$	-0.500
$\tilde{\alpha}$	-0.72 ± 0.25	$-1 + 2\sin^2\theta_W$	-0.54

$$\sin^2\theta = 0.230 \pm 0.015$$

$$\rho = 1.00 \pm 0.02$$

of neutral to charged current cross-sections. The predicted value $\rho = 1$ for weak iso-doublet Higgs is to be compared with the experimental $\rho = 1.00 \pm 0.02$. Presumably like (g-2) in QED, the radiative corrections to ρ from SU(2) × U(1) will provide important information, not only on the basic theory involved, but also about the masses of charged elementary fermions - and in particular leptons - which contribute to the radiative corrections [3] of ρ. (According to Ellis, the present accuracy of ρ appears to suggest $m_{lep} \lesssim 100$ GeV for a one-loop calculation.)

But why does nature favour the simplest suggestion of SU(2) × U(1) theory of the Higgs being iso-doublet? Is there just one physical Higgs?

Of what mass? Could the Higgs phenomenon be a manifestation of a dynamical breakdown of the symmetry?

Personally I see no theoretical reason for a prejudice against an elementary spin-zero object. The real problem with Higgs - and this is one of those unresolved problems which I mentioned earlier and one which calls for greater depth in our theories - is the large number of parameters - 21 out of 26 in the standard 6-quark, (K-M) SU(2) × U(1) × $SU_C(3)$ model - attributable to the Higgs sector [4]. What is needed is an extension of the gauge (or a similar) principle to embrace the Higgs sector.

IV. THE HIGGS SECTOR

I shall briefly comment on some of the ideas expressed in the theoretical sessions of the conference relating to the Higgs sector, particularly as I shall need some of these ideas later.

1) **Higgs mass:** Bjorken discussed in detail the attractive suggestion (Gildener and Weinberg; Ellis, Gaillard, Nanopoulos, Sachrajda) to use the Coleman-Weinberg mechanism to generate Higgs mass (one-loop) radiatively. With the assumption of one iso-doublet with bare mass zero, a low physical mass m_H is predicted

$$m_H \approx (38.53)\ \left[\frac{3\alpha}{8\pi}\ \left[\frac{2 + \sec^4\theta}{\sin^4\theta}\right]\right]^{1/2}\ \text{GeV}$$

$$\approx 9.35\ \text{GeV}\quad (\sin^2\theta = 0.23)\quad .$$

2) The rival suggestion that if $m_H \geq \sqrt{\frac{8\pi\sqrt{2}}{3G_F}} \approx 1$ TeV, partial wave unitarity is not respected at the tree level, and the Higgs sector is truly a strong interaction sector, has its own attractions for Isabelle and other accelerators in that energy range. This has been made quantitative by Grisaru and Schnitzer in a contribution to the conference: Assuming that SU(2) × U(1) is made part of a larger non-Abelian gauge group, and assuming that $m_H \geq 300$ GeV, one may expect Regge recurrences of $W^{\pm}$, Z^0 and the photon occurring around 2-4 TeV. If $m_H \leq 100$ GeV, these recurrences would still occur but regrettably near Planck energies $\approx m_W \exp\frac{c}{g^2}$.

3) To reduce the arbitrariness of the Higgs couplings and to motivate their iso-doublet character, one suggestion is to use supersymmetry [5]. Recall that supersymmetry is a Fermi-Bose symmetry, so that iso-doublet leptons for example must be accompanied in the same multiplet by iso-doublet Higgs.

Unhappily the concrete realization of supersymmetry has always necessitated adding in of further (heavy) multiplets. For example, in the simplest SU(2) × U(1) supersymmetric model that I know of, the three leptons (ν_L, e_L, e_R) must be accompanied by 9 new leptons before a realistic theory emerges. Likewise for quarks and other leptonic families. Frightful inflation!.

4) And finally in the context of the Higgs mechanism emerging as dynamical symmetry breaking (Dimopoulos, Susskind, Weinberg) (with assumed non-zero expectation values of bilinear products of Fermi fields ($\langle \bar{\psi}\psi \rangle \neq 0$), there is the attractive idea of technicolour.
One introduces a set of technicoloured quarks (and in extended versions of the theory, techni-gauge fields)but no Higgs. The techni-forces are <u>new</u> forces of which we have no cognizance at present low energies; these and the corresponding particles manifest themselves in the 1-100 TeV range. Once again, like supersymmetry, there is a vast inflation of new particles. For example, the three leptons (ν_L, e_L, e_R) must appear as humble members of a set of $5 + 5 + 5 + \overline{10}$ multiplets of $SU(5)|_{tech}$ - an inflation nearly three times worse as that for supersymmetry.

Clearly, there is no fear of any "desert" of new particles or of new forces, in the few TeV region if these or similar ideas (devised to diminish Higgs and their arbitrary couplings) make physical sense.

V. STRONG INTERACTIONS AND GAUGED COLOUR

The bulk of the conference was occupied by the parton model and the theory of gauged colour, with a special session on the status of QCD, addressed by de Rujula and Preparata. So I can be brief.

To one coming as an outsider to the subject of strong interactions the first reaction is one of profound wonderment at the sureness of touch displayed in the initial formulation of the parton model. The second reaction is again of wonderment at how remarkable a theory QCD is - principally on account of its unique property of asymptotic freedom (shared possibly only by Einstein's gravity, as surmised by Fradkin and Vilkovisky[6]). The third reaction is still of wonderment, but this time at how little impress, quantitative QCD of quarks and gluons has yet made on the broad spectrum of strong interaction physics, in spite of a large number of exceedingly brilliant contributions made to the subject, particularly during the last year.

The present role of QCD is essentially one of <u>perturbatively</u> renormalizing the quark (and gluon) parton model, with which QCD is compatible

but which it does not yet predicate. As Preparata and de Rujula both agreed, this situation will not change till QCD solves:

i) The problem of confinement of quarks and gluons in hadrons;

ii) The converse problem of hadronization of quarks and gluons;

iii) And the problem of determination of the spectrum of physical states (though we heard from de Rujula of the exciting prospect of qualitative considerations of E. Witten who has shown in the context of an $\frac{1}{N}$ expansion in an N colour $SU_C(N)$ that baryons for example may be understood as $\frac{1}{N}$ analogues of "monopole solitons").

5.1 Theoretical considerations

The next table summarizes the elucidation achieved of the inter-relation between the ideas built into the parton model and the quantitative impress made on these by perturbative QCD. [7] (This is after the perturbative expansion is summed either through the operator product expansion method,or more generally, through the solution of an appropriate Bethe-Salpeter equation.)

5.2 Tests of QCD

The tests of QCD, discussed at the conference, fall into three categories:

1) The gluon: Since $SU(3)|_{colour}$ is a theory of spin-one gluons and their mutual self-interactions, the most positive evidence for QCD would be: discover the gluon G and test for $G \to 2G$, $G \to 3G$.

2) Negative tests:

(a) As emphasised at the Conference, QCD predicts

$$\langle p_T^2 \rangle \approx (\bar{g}^2/4\pi)\, Q^2 \quad .$$

This is unlike most other tests which depend on $\log Q^2$. If $\langle p_T^2 \rangle$ does not eventually exhibit a rising trend with Q^2, QCD must be discarded.

(b) Likewise, it should die if in hadron-hadron collisions, the cross-sections fail eventually to exhibit a behaviour like p_T^{-4} (rather than the(once)empirical p_T^{-8}). Both these are negative tests.

3) Indirect tests of perturbative QCD: i.e. scale breaking, Q^2-dependence of the structure and fragmentation functions and their moments. These tests include

(a) The (Reya-Gluck) characteristic prediction for coloured QCD: i.e. $\int F_2(x,Q^2)\, dx$ must decrease as Q^2 increase;

Parton model: Built-in features	Perturbative QCD and the manner of its "renormalization" of the built-in features of the parton model
Factorization $\{F(x) \times D(z)\}$ $F(x)$: Hadronic structure function $D(z)$: Parton fragmentation function	QCD replaces $\{F(x) \times D(z)\}$ by $\{F(x,Q^2) \times F(z,Q^2)\}$ or more precisely, in terms of moments [8] by $F^N_{\text{parton}}\left(\bar{g}^2 \ln \frac{Q^2}{\Lambda^2}\right) D^M_{\text{parton}}\left(\bar{g}^2 \ln \frac{Q^2}{\Lambda^2}\right)$ $\times \left\{ f^N\left(\bar{g}^2, \ln \frac{\Lambda^2}{m^2}\right) \times d^M\left(\bar{g}^2, \ln \frac{\Lambda^2}{m'^2}\right) + O(\bar{g}^2) \right\}$
Scaling	QCD gives a perturbative calculation of the F^N's and the D^M's. In the leading log order these scale-breaking factors behave like $\left(\ln \frac{Q^2}{\Lambda^2}\right)^{-d_N}$, though the theory does not predict the magnitude of Λ^2. The f^N's and d^M's are QCD non-calculable probability amplitudes, universal in the same sense as the parton model's $F(x)$'s and $D(z)$'s are.
Jets are soft	1) Jets are characeristically hard: 2) There is the complementary theoretical development of "safe" jet variables, following the pioneering work of Sterman and Weinberg. Here one attempts to define such measurable quantities for which a reliable perturbation expansion exists in terms of $\bar{g}^2 \approx \left(\ln \frac{Q^2}{\Lambda^2}\right)^{-1}$ rather than for the mass-singularity-containing parameter $\bar{g}^2 \ln \frac{Q^2}{m^2}$.
Hadronization of partons: soft transfer of quantum numbers	Domains of perturbative QCD and of confinement phenomena shown to be distinct [9),10)].

(b) Log moment versus log moment plots for both structure and fragmentation functions;

(c) Corresponding plots of (moment)$^{-1/d}$ versus log Q^2;

(d) And predicted QCD corrections to Drell-Yan.

The status of these indirect tests have been discussed in detail at the conference by Gaillard, de Rujula, Preparata and (for Drell-Yan) by Altarelli. Battles have raged over the significance of singlet versus non-singlet structure functions, over higher than leading log corrections, over higher twist and resonance regime effects - over whether the present tests really do test QCD fairly. I make no comment, except to express, as always, a theorist's profound admiration to our experimental colleagues in making the theory commit itself by extracting significant numbers from difficult data.

5.3 The direct test; Discovery of the gluon (G)

Fig.1 shown by Brandt exhibits the status of $T \to 3G$ versus phase-space Monte-Carlo (plots of thrust, triplicity and other jet parameters). As Professor Schopper told us, in the next few months, the statistics on these jets are likely to improve vastly, but if we accept tentatively that $T \to 3G$ is the likeliest decay mode, one could in principle determine gluon spin, using ideas of Koller, Walsh and Kraseman who define a function $(\alpha(T))$ (T = thrust of the fastest jet)and plot the thrust axis angular distribution relative to the beam direction in terms of this.

Fig.2 shows the sharp distinction between spin-one and spin-zero gluons. The paucity of statistics makes an experimental comparison with theory difficult at present. As stressed by Gaillard, however, one may compute thrust averaged $\langle \alpha(T) \rangle$, and plot the corresponding angular distribution (Fig.3). The results favour spin-one.

One does not wish to rush into a conclusion, which the cautious men(and women) from PETRA themselves have not drawn. However, one might predict, that with the Cornell accelerator soon coming on stream, and more statistics from DORIS, the gluon is likely to be discovered sooner than the $W^{\pm}$'s and the Z^0.

To test for the $G \to 2G$ and $G \to 3G$ vertices, characteristic of QCD, one of the clearest tests will be the comparison of the evolution of gluon jets and in particular the moments of the gluon fragmentation for $T \to 3G$ versus the $t\bar{t} \to 3G$, once $t\bar{t}$ is discovered (Fig.4) (Koller, Walsh and Zerwas).

5.4 The negative tests

Figs.5 and 6 are plots of $\langle p_T^2 \rangle$ presented to the conference by Gabathuler and Altarelli consolidating the data on e, μ, ν, (e^+e^-) and Drell-Yan. As Gabathuler remarked, there is no agreement whether $\langle p_T^2 \rangle$ varies with W^2 or $\log W^2$; all one may infer at present is that $\langle p_T^2 \rangle$ is not flat, but rises. QCD lives. Fig.7 was presented by Jacob, showing the progressive transition trend from p_T^{-8} to p_T^{-4} in inclusive π^0 yield, when p_T increases from 3 to 15 GeV/c. Again prognosis for QCD's life and health is good. [11]

To conclude:

1) QCD is a remarkable gauge theory, particularly on account of its asymptotic freedom;

2) It is not yet a theory of strong interaction and will not be till the problems of confinement and hadronization are solved;

3) Its present successes (or otherwise) lie in the field of perturbative QCD. However, there are serious problems at present in estimating corrections to the various predictions.

4) The gluon may have been discovered, together with its spin determination.

VI. GRAND UNIFICATION, THE ELECTRONUCLEAR FORCE AND THE ISSUE OF THE GRAND PLATEAU

6.1 The electronuclear force

Besides QCD, the second area of intense revival this year has been the attractive extension of the ELECTROWEAK unification to embrace strong forces as well - i.e.the emergence of the ELECTRONUCLEAR unification (of the weak nuclear, the strong nuclear and the electromagnetic forces). Related to this - as Professor Zichichi told us - is the issue of the possible existence of a GRAND PLATEAU with no high peaks of new physics to be scaled, except near Planck energies.

The main stages of the ELECTRONUCLEAR unification which go back to the years 1972-1974 are the following:

1) Embed $SU(2) \times U(1) \times SU_C(3)$ into a simple (or a semi-simple) non-Abelian gauge group G; all quantum numbers (flavour, colour, lepton and quark numbers) are then automatically quantized. [12]

2) A gauging of this group G will assure asymptotic freedom [13] for the full ELECTRONUCLEAR theory, provided the numbers of fermion fields (and Higgs) is restricted.

3) The gauge theory based on a technically "simple" (or with appropriate discrete symmetries, a "semi-simple") group contains one basic gauge constant, which manifests itself physically above the unification mass M exceeding all particle masses in the theory.

4) These particle masses must be introduced through the familiar Higgs mechanism, which breaks the symmetry through one or more mass stages down to $SU(2) \times U(1) \times SU_C(3)$ for low energies $\mu \approx 100$ GeV. Given the pattern of symmetry breaking and these mass stages [14], the magnitudes of the observed couplings [15] $\alpha_s(\mu)$, $\alpha(\mu)$ (i.e. why, SU(3) forces are strong and SU(2) forces weak at low energies) as well as the ratio of the two electroweak couplings ($\sin^2\theta(\mu)$) can in principle be determined by the renormalization group equations [37].

5) Clearly grand unified theories must treat leptons on par with quarks. This psychological break was first implemented in 1972 by grouping quarks and leptons in the same multiplet of the unifying group G. From this follows (through the processes of gauging) the prediction of the existence of lepto-quark gauge bosons - necessarily heavy, since they will induce exotic phenomena, particularly proton decays into leptons. The following two tables summarize the development of these ideas

Quark-lepton unification

Semi-simple groups *) (with left-right symmetry)	$G_L \to \begin{pmatrix} q \\ \ell \end{pmatrix}$, $G_R \to \begin{pmatrix} q \\ \ell \end{pmatrix}_R$ $G_L \times G_R$ $\quad L \longleftrightarrow R$	Exotic gauge particles Lepto-quarks $\to (\bar{q}\ell)$	Proton decay Lepto-quarks $\to W +$ (Higgs) or Proton $= qqq \to \ell\ell\ell$
Simple groups	$G \to \begin{pmatrix} q \\ \ell \\ \bar{q} \\ \bar{\ell} \end{pmatrix}_L$	diquarks $\to (qq)$ dileptons $\to (\ell\ell)$ leptoquarks $\to (\bar{q}\ell), (q\ell)$	$qq \to \bar{q}\bar{\ell}$ or Proton $P = qqq \to \bar{\ell}$

*) Grouping (q and ℓ) (Pati et al. 1972) together, implies treating lepton number as the fourth colour, i.e. $SU_C(3)$ extends to $SU_C(4)$.

The emergence of the grand unifying groups

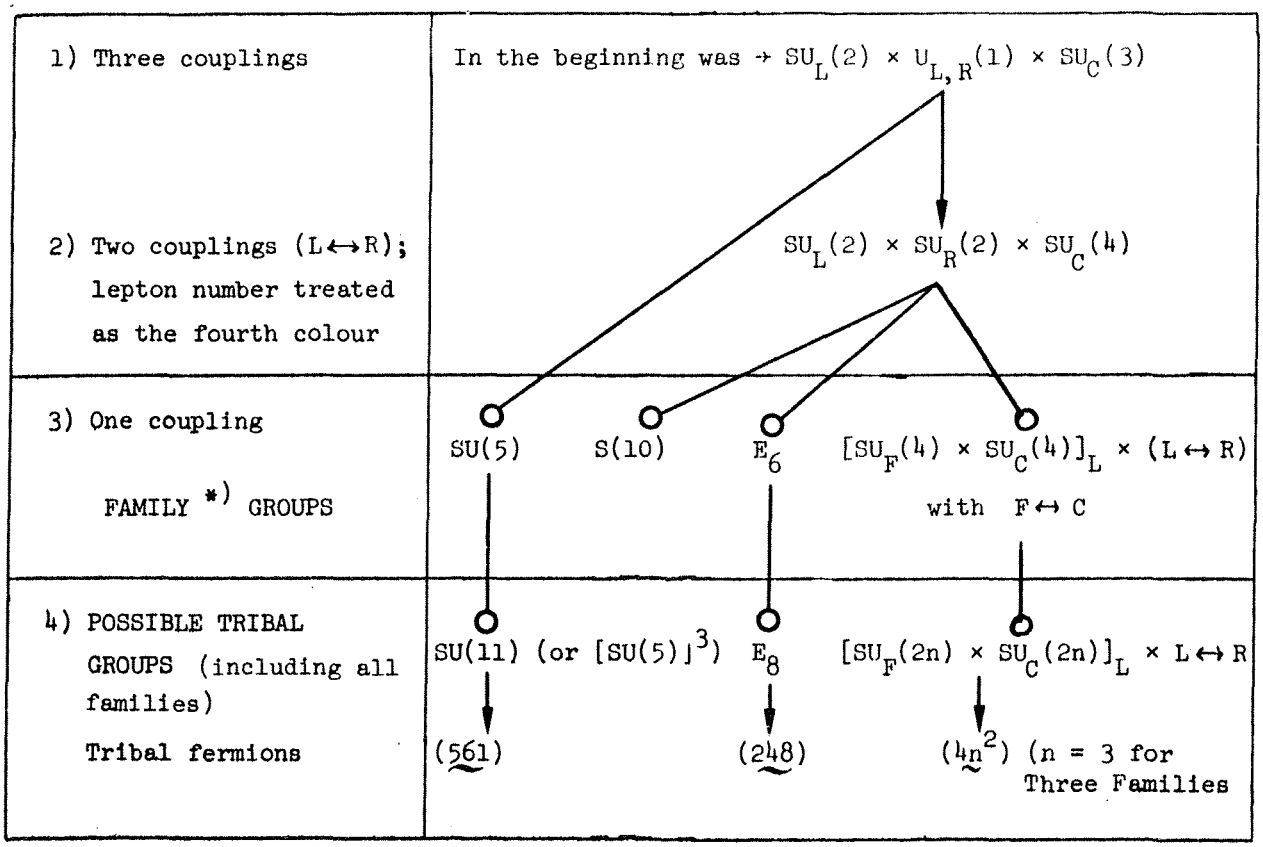

) The representations ($\underset{\sim}{5}$ + $\underset{\sim}{10}$) and ($\underset{\sim}{16}$), respectively, of the family groups SU(5) and SO(10) each describe One Family, while the basic representations [16] of E_6 and $[SU(4)]^4$ describe Two Families ((e,...) and (μ,...)).

6) An unresolved mystery is the replication of families, if this indeed is what is happening. Is there a larger "TRIBAL" group (as distinct from the smaller FAMILY groups) whose basic representation contains all the families? (Note the fermion-inflation for Tribal groups.)

6.2 Tests of grand unification

The most characteristic prediction from the existence of the ELECTRONUCLEAR force is proton decay, first discussed in the context of grand unification at the Aix-en-Province Conference of 1973 - and if memory serves right - in the same session in which the first experimental discovery of the electroweak neutral currents was announced. It is indeed deeply gratifying that both in Europe and in the United States there now is intense interest in improving the half-life limits for the proton. For unifying groups with multiplets containing quarks and leptons only the lepto-quark masses are, as a rule, rather moderate $\sim 10^4 \sim 10^5$ GeV. For such models the characteristic

proton decays (proceeding through exchanges of three lepto-quarks) conserve quark number + lepton number, i.e. $P = qqq \to \ell\ell\ell$, ($P \to 3\nu + \pi^+ \sim 80\%$; $\to 3\nu + \pi^+ + \pi^- + \pi^+ \sim 5\text{-}8\%$; $N \to 2\nu + e^- + \pi^+ \sim 80\%$; $\tau_P \sim 10^{29}\text{-}10^{34}$ years). On the contrary, for the "simple" unifying groups like SU(5), SO(10) and E_6 (with multiplets containing anti-quarks and anti-leptons as well $(q,\ell,\bar{q},\bar{\ell})$) and decays proceeding through an exchange of one lepto-quark, the decay of the proton is to an anti-lepton, with $P \to \ell$ or 3ℓ forbidden [17]. ($P \to e^+ + \pi^0$, ρ^0, ω^0, $\eta^0 \sim 75\%$; $\mu^+ + K^0 \sim 10\%$; $\bar{\nu} + \pi^+$, $\rho^+ \sim 15\%$; $N \to e^+ + \pi^-$, $\rho^- \sim 75\%$.)

An intriguing possibility in this context is that investigated recently by Pati et al. for the maximal unifying group SU(16) - i.e. the largest group to contain a 16-fold fermionic multiplet $(q,\ell,\bar{q},\bar{\ell})$. This can permit (irrespective of quark charges) the decay modes: $P \to 3\ell$ as well as $P \to \bar{\ell}$, $P \to \ell$ (e.g. $P \to e^- + \pi^+ + \pi^+$) and $P \to 3\bar{\ell}$ (e.g. $P \to 3\bar{\nu} + \pi^0$, $N \to 2\bar{\nu} + e^+ + \pi^-$), the relative magnitudes being model-dependent on how precisely SU(16) breaks down to SU(3) × SU(2) × U(1). Quite clearly, it is the central fact of the existence of the proton's decay (rather than precise details of its decay modes) for which the present experiments must be designed. [18]

Finally, grand unifying theories predict mass relations like:

$$\frac{m_d}{m_e} = \frac{m_s}{m_\mu} = \frac{m_b}{m_\tau} = \left[\frac{\alpha_s(\mu)}{\alpha_s(M)}\right]^{\frac{4}{11 - \frac{2}{3}f}} \approx 2.8$$

for 6 (or at most 8) flavours (f) below the unification mass. The important remark for proton decay, for mass relations of the above type (or for baryon excess) [19], is that these are essentially characteristic of the fact of grand unification - rather than of specific models.

It is also worth remarking that even for the simplest of grand unifying theories (Georgi & Glashow's SU(5) with just two Higgs (a $\underset{\sim}{5}$ and a $\underset{\sim}{24}$)) the number of ad hoc parameters needed (most of them attributable to the Higgs sector) is still unwholesomely large - 22, to compare with 26 of the six-quark Kobayashi-Maskava model based on the humble SU(2) × U(1) × $SU_C(3)$. We cannot feel proud.

6.3 The unifying mass, $\sin^2\theta$ and the grand plateau [20]

As discussed by Iliopoulos, the decoupling theorem of Applequist and Carazonne, as applied by Georgi, Quinn and Weinberg to grand unification, relates the observed low-energy couplings $\alpha(\mu)$ and $\alpha_s(\mu)$ ($\mu \approx 100$ GeV) to the grand unifying mass M and the observed value of $\sin^2\theta$. The demonstration that this leads inevitably to a grand plateau, stretching up to nearly Planckian energies, depends, very sensitively (qualitatively and

quantitatively) on a number of assumptions which are strong extrapolations from present trends. In view of the importance of the subject, I wish to examine these assumptions critically, even though this makes this part of the talk heavy.

My conclusions (stated more fully later) are first: that even extrapolating from present theoretical ideas, the unifying mass M (and thus the stretch in energy scale for which new physics may not manifest itself) depends critically on the assumptions made by particular unifying models and may vary between 10^4-10^5 to 10^{13}-10^{15} GeV. Second, that even for those models which call for $M \sim 10^{13}$-10^{15} GeV there is an inevitable breaking up of the plateau by newer "heights" of physics at intermediate energy scales. This last result follows from the (rather high) value of $\sin^2\theta \approx 0.23$ suggested by the present data at this Conference.

6.4 The measure of the plateau problem (Occam's razor):

1) Given a grand unifying group G, there can, in general, exist a succession of stages of its descent, down to the low-energy gauge symmetry $SU(2) \times U(1) \times SU_C(3)$, with a hierarchy of mass stages $M_1 > M_2 > \ldots > \mu$ and corresponding stages of symmetry breaking. [21]

Clearly, at each stage, new physics enters, with the corresponding new gauge particles, new sets of interactions, new Higgs, new selection rules, new Regges, new monopoles [22] and new dyons.

To speak of a plateau, we must prove from internal consistency (or as is the more common practice, simply assume) that such hierarchies, either do not exist or - if they are forced upon us by experimental data - that they are few and far between.

2) However - for this descent, from G down to $SU(2) \times U(1) \times SU_C(3)$ - even if other complicated [21] intermediate stages are eschewed, two types of stages may not be rejected out of hand. i) The Family stage: The low-energy $SU_L(2)$ may have descended (as the diagonal sum) of $SU^I(2) \times SU^{II}(2) \times SU^{III}(2) \times \ldots$, where I, II, III,... refer to the various families [23] $(e,\ldots)$, $(\mu,\ldots)$ and $(\tau,\ldots)$. ii) The Chiral stage: The low-energy $SU_C(3)$ may, likewise, have descended (as the diagonal sum) from the chiral colour symmetry $SU_{CL}(3) \times SU_{CR}(3)$ as well as from the diverse families [24]. The physics of this situation is profoundly different from the physics of a straightforward descent to $SU(2) \times U(1) \times SU_C(3)$ but only for energies well above the (possibly high) masses of the fields orthogonal to $W^{\pm}$, Z^0 and

G's. Once again, the neglecting of such possibilities implies assuming from the start that the corresponding peaks of new physics simply do not exist: (OCCAM'S RAZOR).

3) Finally an absolutely crucial role in determining M and $\sin^2\theta$ is played by the parameter $\sin^2\theta_0 = \sin^2\theta(M^2) = \sum T_3^2 \to SU(2) \Big/ \sum Q^2$, and the conventional assumption that for fermions (including any superheavy ones with masses near M) [25] $\sin^2\theta_0 = \frac{3}{8}$.

The details of the demonstration of the statements below are given in the Appendix. Here I summarize the results.

6.5 Summary

A) The gauge plateau is the consequence of two assumptions:

1) That there is a gauge plateau! - more soberly, of the assumption that no new gauge forces except those represented by $SU(2) \times U(1) \times SU_C(3)$ exist, until we reach the grand unifying mass.

2) For certain grand unifying family groups (like SU(5) and SO(10)) the unifying mass M does edge towards the Planck mass [39] ($M \approx 10^{13}$ GeV, for $\sin^2\theta = 0.23$). This happens because together with assumption (1), we have also assumed that all fundamental fermions - past, present and future - (including any superheavy ones, to be discovered with masses $\approx 10^{13}$ GeV) belong to that representation of the eventual tribal group for which $\sin^2\theta_0 = \sin^2\theta(M^2)$ equals $\frac{3}{8}$.

This assumption may be correct [26] (and one of the goals of particle physics is to find this out [27]), but one should appreciate its full import in determining M.

B) There are other tribal grand unifying groups for which $\sin^2\theta_0 = \sin^2\theta(M^2)$ is different from $\frac{3}{8}$ (e.g. for the 6-flavoured $[SU(6)]^4$ with $\sin^2\theta_0 = \frac{9}{28}$). For these the unifying mass M can be much smaller. For $[SU(6)]^4$ it is $\approx 10^6$ GeV. If there are eight flavours i.e. $[SU(8)]^4$, M is even smaller $\approx 10^4$ GeV. The plateau has shrunk vastly.

c) A family group like SU(5) may be currently disfavoured on the basis that it cannot easily accommodate the experimental $\sin^2\theta \approx 0.23$ unless α_s is unseasonably small ≈ 0.07, see Appendix). Even if SU(5) could accommodate $\sin^2\theta \approx 0.23$, it gives a proton lifetime estimate [39] ($\tau_p \approx 10^{23}$ years) which may be too small, unless there are 15 Higgs doublets. The "simple" SO(10) may overcome these disabilities; however, at the price of introducing intermediate symmetry-breaking stages. But then, by definition, new physics does appear for energies considerably lower than the grand unifying mass. The plateau is not a plateau after all.

To conclude, I do not think any experimental physicist, who is still with me, need seriously worry about an unbroken plateau where there are no new physics heights to be scaled. I have tried to show that this holds even within the theoretical framework represented by a direct extrapolation of the present ideas to the highest energies. In some of the remaining parts of the talk I shall be questioning two of the notions which have gone into this direct extrapolation - first, do quarks and leptons represent the correct elementary[27] fields, which should appear in the matter Lagrangian, and which are structureless for renormalizability; second, could some of the gauge fields themselves be composite?

6.6 The quest for elementarity, prequarks (preons and pre-preons)

While the rather large number (15) of elementary fields (for example, for the family group SU(5)) already makes one feel somewhat queasy, the number 561, for the three-family tribal group SU(11) (of which presumably $3 \times 15 = 45$ objects are of low and the rest of Planckian mass) is distinctly baroque. Is there any basic reason for one's instinctive revulsion when faced with these vast numbers?

The numbers by themselves would perhaps not matter so much. After all, Einstein in his description of gravity, chose to work with 10 fields ($g_{\mu\nu}(x)$) rather than with just one (scalar field) as Reissner and Nordström had done before him. Einstein was not perturbed by the multiplicity he chose to introduce, since he relied on the sheet-anchor of a fundamental principle - (the equivalence principle) - which permitted him to relate the 10 fields for gravity $g_{\mu\nu}$ with the 10 components of the physically relevant quantity, the tensor $T_{\mu\nu}$ of energy and momentum. Einstein knew that nature was not economical of structures; only of principles of fundamental applicability. The question we must ask ourselves is this: Have we yet discovered such principles in our quest for elementarity, to justify having fields with such large numbers of components as elementary.

Recall that quarks carry at least three charges (colour, flavour and a family number). Should one not, by now, entertain the notions of quarks (and possibly of leptons) as being composites of some more basic entities (PRE-QUARKS or PREONS), which each carry but one basic charge. These ideas have been expressed before but they have become more compulsive now, with the growing multiplicity of quarks and leptons. Recall that it was similar ideas which led from the eight-fold of baryons to a triplet of (Sakatons and) quarks in the first place.

The preon notion is not new. In 1975, among others, Pati et al. introduced 4 chromons (the fourth colour corresponding to the lepton number) and 4 flavons, the basic

group being SU(8) - of which the family group $SU_F(4) \times SU_C(4)$ was but a subgroup. (With the preon stage, the gauge group does not change; the fermionic multiplet changes.) As an extension of these ideas, we now believe these preons carry magnetic charges and are bound together by very strong short-range forces, with quarks and leptons as their magnetically neutral composites.

In another form the preon idea has been revived this year by Curtright and Freund, who motivated by ideas of extended supergravity(to be discussed in the next section), reintroduce an SU(8) of 3 chromons (R,Y,B), 2 flavons and 3 familons (horrible name). The family group SU(5) could be a subgroup of this SU(8). (Recall that of the two representations used by SU(5) to describe quarks and leptons, the 10^* could in any case be considered as a three-fold anti-symmetric composite of the fundamental $\underset{\sim}{5}$ - though unfortunately the quark-lepton numbers do not quite match. In a sense then, the preon idea is implicit in SU(5).) In the Curtright-Freund scheme, the $\underset{\sim}{3} \times \underset{\sim}{15} = \underset{\sim}{45}$ fermions of SU(5) can be found among the $\underset{\sim}{8} + \underset{\sim}{28} + \underset{\sim}{56}$ of SU(8) (or alternatively the $3 \times \underset{\sim}{16} = \underset{\sim}{48}$ of SO(10) among the vectorial $\underset{\sim}{56}$ fermions of SU(8)).

A second contribution on preons is due to Harari and(independently) Schupe. In his quest for elementary entities, Harari has followed the approach of starting with two objects, Tohu's (charge $\frac{1}{3}$) and Vohu's (charge zero), making up the set of what he calls Rishons ("basic entities" in Hebrew)(the "chiefs" in Arabic). The eight 4-component fermions in a typical SO(10) (or SU(2) × SU(2) × SU(4)) multiplet (e.g. u, d, ν, e) are composed as follows: [28]

$T\,T\,T \to \bar{e}$	$V\,V\,V \to \nu$
$T\,T\,V \to u_R$	$V\,V\,T \to \bar{d}_R$
$T\,V\,T \to u_Y$	$V\,T\,V \to \bar{d}_Y$
$V\,T\,T \to u_B$	$T\,V\,V \to \bar{d}_B$.

The other Two Families are assumed to be orbital excitations of these (with radii of composites $\lesssim 10^{-24}$ cms., deduced from upper limits on $\mu \to e + \gamma$, $s \to d + \gamma$).

I would personally like to interpret Harari's ideas as referring not to the three families but to pre-preons. In the above table, read flavons in place of e and ν; chromons (R,Y,B) instead of u_R, u_Y, u_B and familons for d_R, d_Y, d_B. The objection that one is trading space-time ideas for internal quantum numbers (with colour a "composite" quantum number - a new

notion; and gluons as "composite" gauge fields - suggested also by Dürr and Saller) can possibly be met in the manner of the converse generation of spin from isospin for dyonic composites discussed several years ago by Goldhaber, Hasenfratz, 't Hooft, Jackiw and Rebbi. Splendid craziness.[29]

Before I conclude this section, I would like to make a prediction regarding the course of physics in the next decade, extrapolating from our past experience of the decades gone by:

DECADE	1950-1960	1960-1970	1970-1980	1980 →
Discovery in early part of the decade	The strange particles	The 8-fold way, Ω^-	Confirmation of neutral currents	W, Z, G, Proton decay
Expectation for the rest of the decade		SU(3) resonances		Grand Unification, Tribal Groups
Actual discovery		Hit the next level of elementarity with quarks		May hit the preon level, composite structure of quarks, and composite gauge fields

VII. POST-PLANCK PHYSICS,[30] SUPERGRAVITY AND EINSTEIN'S DREAMS

I now turn to the problem of a deeper comprehension of the charge concept (the basis of gauging) - <u>which, in my humble view, is the real quest of particle physics</u>. Einstein, in the last thirty-five years of his life lived with two dreams: one was to unite gravity with matter (the photon) - he wished to see the "base wood" (as he put it) which makes up the stress tensor $T_{\mu\nu}$ on the right-hand side of his equation $R_{\mu\nu} - \frac{1}{2} g_{\mu\nu} R = -T_{\mu\nu}$ transmuted through this union, into the "marble" of gravity on the left-hand side. The second (and the complementary) dream was to use this unification to comprehend the nature of electric charge in terms of space-time geometry in the same manner as he had successfully comprehended the nature of gravitational charge in terms of space-time curvature.

In case some one imagines [31] that such deeper comprehension is irrelevant to quantitative physics, let me adduce the tests of Einstein's theory versus the proposed modifications to it (Brans-Dicke for example). Recently (1974), the strong equivalence principle (i.e. the proposition that gravitational forces contribute equally to the inertial and the gravitational masses) was tested to one part in 10^{12} (i.e. to the same accuracy as achieved in particle physics for $(g-2)_e$) through lunar-laser ranging measurements. These measurements determined departures from Kepler equilibrium distances, of the moon, the earth and the sun to better than ± 30 cms. and triumphantly vindicated Einstein.

There have been four major developments in realizing Einstein's dreams:

1) The Kaluza-Klein miracle: An Einstein Lagrangian (scalar curvature) in five-dimensional space-time (where the fifth dimension is compactified in the sense of all fields being explicitly independent of the fifth co-ordinate) precisely reproduces the Einstein-Maxwell theory in four dimensions, the $g_{\mu 5}$ ($\mu = 0,1,2,3$) components of the metric in five dimensions being identified with the Maxwell field A_μ. From this point of view, Maxwell's field is associated with the extra components of curvature implied by the (conceptual) existence of the fifth dimension [32].

2) The second development is the recent realization by Cremmer, Scherk, Englert, Brout, Minkowski and others that the compactification of the extra dimensions - (their curling up to sizes perhaps smaller than Planck length $\lesssim 10^{-33}$ cms. and the very high curvature associated with them) - might arise through a spontaneous symmetry breaking (in the first 10^{-43} seconds) which reduced the higher dimensional space-time effectively to the four-dimensional that we apprehend directly.

3) So far we have considered Einstein's second dream, i.e. the unification of electromagnetism (and presumably of other gauge forces) with gravity, giving a space-time significance to gauge charges as corresponding to extended curvature in extra bosonic dimensions. A full realization of the first dream (unification of spinor matter with gravity and with other gauge fields) had to await the development of supergravity - and an extension to extra fermionic dimensions of superspace (with extended torsion being brought into play in addition to curvature). I discuss this development later.

4) And finally [33] there was the alternative suggestion by Wheeler that electric charge may be associated with space-time topology - with worm-holes, with space-time Gruyère-cheesiness. This idea has recently been developed by Hawking [34] and his collaborators.

Extended supergravity, SU(8) preons and composite gauge fields

Thus far the developments in respect of Einstein's dreams as reported at the Tokyo Conference of 1978. A remarkable new development was reported at this conference by Julia (Julia and Cremmer) which started with an attempt to use the ideas of Kaluza and Klein to formulate extended supergravity theory in a higher (compactified) space-time - more precisely in eleven dimensions. This development links up, as we shall see, with preons and composite Fermi fields - and even more important - possibly with the notion of composite gauge fields.

Recall that simple supergravity is the gauge theory of supersymmetry - the gauge particles being the (helicity ±2) gravitons and (helicity $\pm \frac{3}{2}$) gravitinos. Extended supergravity gauges supersymmetry combined with SO(N) internal symmetry. For N = 8, the (tribal) supergravity multiplet consists of the following SO(8) families.

Helicity	
± 2	$\underset{\sim}{1}$
$\pm \frac{3}{2}$	$\underset{\sim}{8}$
± 1	$\underset{\sim}{28}$
$\pm \frac{1}{2}$	$\underset{\sim}{56}$
0	$\underset{\sim}{70}$.

As is well known, SO(8) is too small to contain SU(2) × U(1) × $SU_C(3)$. Thus this tribe has no place for $W^{\pm}$ (though Z^0 and γ are contained) and no place for μ or τ or the t quark.

This was the situation at Tokyo. This year, Cremmer and Julia attempted to write down the N = 8 supergravity Lagrangian explicitly, using an extension of the Kaluza-Klein ansatz which states that extended supergravity (with SO(8) internal symmetry) has the same Lagrangian in 4 space-time dimensions as simple supergravity in (compactified) 11 dimensions. This formal - and rather formidable ansatz - when carried through yielded a most agreeable bonus. The supergravity Lagrangian possesses an unsuspected SU(8) "local" internal symmetry [35] although one started with an internal SO(8) only.

The tantalizing questions which now arise are the following.

1) Could this internal SU(8) be the symmetry group of the 8 preons (3 chromons, 2 flavons, 3 familons) introduced earlier?

2) When SU(8) is gauged, there should be 63 spin-one fields. The supergravity tribe contains only 28 spin-one fundamental objects which are not minimally coupled. Are the 63 fields of SU(8) to be identified with composite gauge fields made up of the 70 spin-zero objects of the form $V^{-1}\partial_\mu V$; Do these composites propagate, in analogy with the well-known recent result in CP^{n-1} theories, where a composite gauge field of this form propagates as a consequence of quantum effects (quantum completion)?

The entire development I have described - the unsuspected extension of SO(8) to SU(8) when extra compactified space-time dimensions are used - and the possible existence and quantum propagation of composite gauge fields - is of such crucial importance for the future prospects of gauge theories that one begins to wonder how much of the linear extrapolation which went into extrapolating $SU(2) \times U(1) \times SU_C(3)$ to the grand unifying gauges is likely to remain unaffected by these new ideas now unfolding.

But where in all this is the possibility to appeal directly to experiment? For grand unified theories, it was the proton decay. What is the analogue for supergravity? Perhaps the spin $\frac{3}{2}$ massive gravitino, picking its mass from a super-Higgs effect provides the answer. Fayet has shown that for a spontaneously broken globally supersymmetric weak theory the introduction of a local gravitational interaction leads to a super-Higgs effect. The gravitino acquires a mass and an effective interaction, but of conventional weak rather than just the gravitational strength - an enhancement by a factor of 10^{34}. One may thus search for the gravitino among the neutral decay modes [36] of J/ψ. Notwithstanding the enhancement, this will surely tax all the ingenuity of Sam Ting, Burt Richter and their colleagues.

I would like to conclude, as at Tokyo, with a quotation from J.R. Oppenheimer which more than anything else expresses in my view the faith for the future with which this greatest of decades in particle physics ends: "Physics will change even more ..... If it is radical and unfamiliar ..... We think that the future will be only more radical and not less, only more strange and not more familiar, and that it will have its own new insights for the inquiring human spirit."

J.R. Oppenheimer
Reith Lectures BBC 1953.

APPENDIX ON GRAND UNIFICATION

Here are stated the results used in the text which relate grand unifying mass, $\sin^2\theta$, and the intermediate symmetry-breaking stages.

In the sequel, I shall assume that $G \overset{M_1}{\to} [SU(2)]^q \times U(1) \times [SU_c(3)]^p \overset{M_2}{\to} SU(2) \times U(1) \times SU_c(3) \overset{\mu}{\to} U(1) \times SU_c(3)$, where p and q are the possible stages referred to in 2) of Subsec. 6.4 correlated for example with family or chiral symmetries. For simplicity, and without much loss of generality, I shall assume that $M_1 \approx M_2 \approx M >> \mu$, so that all fields not contained in $SU(2) \times U(1) \times SU_c(3)$ are very heavy and the parameters p and q make their explicit appearance only through how the physical α_s and α normalize in terms of the grand unifying coupling $\frac{g^2(M)}{4\pi}$.

Theorem

Assume that $G \overset{M_1}{\to} [SU(2)]^q \times U(1) \times [SU_c(3)]^p \overset{M_2}{\to} SU(2) \times U(1) \times SU_c(3) \overset{\mu}{\to} U(1) \times SU_c(3)$ (and assume for simplicity that $M_1 \sim M_2 \sim M$). One finds from Eqs.(B) and (C) of footnote 37

$$\frac{11\alpha}{3\pi} \ell n \frac{M}{\mu} = \frac{(\sin^2\theta_0 - \sin^2\theta)}{\cos^2\theta_0} \quad . \tag{1}$$

Using (A) of footnote 37 and (1) above one gets:

$$\sin^2\theta(\mu) = \frac{(3q - 2p)\sin^2\theta_0 + \frac{\alpha}{\alpha_s}(2q)\cos^2\theta_0}{(3q - 2p\sin^2\theta_0)} \quad . \tag{2}$$

From this one deduces that

$$\frac{\sin^2\theta_0 - \sin^2\theta}{\cos^2\theta_0} = \frac{2}{3q-2p}\left(p\sin^2\theta - q\frac{\alpha}{\alpha_s}\right) .$$

(If $M_1 \neq M_2$, the left-hand side of (1) reads $11\alpha/3\pi \, \ell n \left[\left(\frac{M_1}{M_2}\right)^q \frac{M_2}{\mu}\right]$, with similar smooth limit ($M_1 \to M_2$) changes to (2).)

1) Note the crucial result: If $\sin^2\theta$ is given, $\ell n \frac{M}{\mu}$ depends only on $\sin^2\theta_0$ (and not explicitly on $\frac{p}{q}$). On the contrary, the expression for $\sin^2\theta$ does depend explicitly on the ratios $\frac{p}{q}$, $\frac{\alpha}{\alpha_s}$ as well as on $\sin^2\theta_0$.

2) For SU(5) and SO(10), $p = 1 = q$ [38], $\sin^2\theta_0 = \frac{3}{8}$ and we obtain [39]

$$\sin^2\theta = \frac{1}{6} + \frac{5}{9}\frac{\alpha}{\alpha_s} \quad \text{and} \quad M = 1.3 \times 10^{13} \text{ GeV}.$$

This value of M is obtained from Eq.(1) if $\sin^2\theta = 0.23$ and $\sin^2\theta_0 = \frac{3}{8}$. It differs from the conventionally stated value of $\approx 10^{15}$ GeV, which is usually derived by substituting $\sin^2\theta = \frac{1}{6} + \frac{5}{9}\frac{\alpha}{\alpha_s}$ into the expression for $\ell n \frac{M}{\mu}$. The following remarks are in order:

i) Note the extreme sensitivity of M on the presumed value of $\sin^2\theta$ (the conclusions below depend on $\sin^2\theta \approx 0.23$).

ii) The empirically indicated value of $\sin^2\theta$ is compatible with the SU(5) formula $(\frac{1}{6} + \frac{5}{9}\frac{\alpha}{\alpha_s})$ for an α_s which appears to be small ($\alpha_s \approx 0.07$).

iii) With M as small as 1.3×10^{13} GeV (small compared with 10^{19} GeV of Planck energies), one finds that the proton half-life τ_p as estimated by Marciano [39] is $\approx 6 \times 10^{23}$ years - perhaps already excluded experimentally. (Fifteen isodoublet Higgs [39] are needed to remedy this.)

3) For the semi-simple tribal group $[SU_F(6) \times SU_C(6)]_L \times [SU_F(6) \times SU_C(6)]_R$ (with p = 2, q = 3) describing six quark flavours [25] and colours, $\sin^2\theta_0 = \frac{9}{28}$. Thus $M \approx 10^6$ GeV and $\sin^2\theta = \frac{5}{24} + \frac{19}{36}\frac{\alpha}{\alpha_s}$ (≈ 0.23 for $\alpha_s \approx 0.18$).

Note the enormous difference between the predicted values for the grand unifying masses (10^6 GeV versus 10^{13} GeV) for the two cases of the "simple" versus the "semi-simple" groups considered. The size of the plateau has considerably shrunk for the latter case. It could shrink still more, with more flavours [40] and colours. (For $[SU(8)]^4$, $M \sim 10^4$ GeV.)

4) For the family groups SU(5) and SO(10), we have noted that a straight descent to $SU(2) \times U(1) \times SU_c(3)$ (p = q = 1) gives a small M (for comfort with the proton's life) and too small α_s (≈ 0.07) if $\sin^2\theta \approx 0.23$. Now SU(5) cannot admit any intermediate stages but SO(10) is larger and can, as noted by Georgi and Nanopoulos and Shafi and Wetterich (CERN Th.2667 (1979)). [41]

Could such stages help in resolving the problem of the "large" $\sin^2\theta$ and the "small" M? (Clearly the existence of such stages would mean that the plateau is broken up with peaks of new physics.) To concretize - and simply as an illustration - consider just one stage, i.e. take the simple case [42] of $G \xrightarrow{M} SU(2) \times U(1) \times SU(n) \xrightarrow{M_1} SU(2) \times U(1) \times SU_C(3)$. Formulae (1) and (2) for $\ell n \frac{M}{\mu}$ and $\sin^2\theta$ still hold; however p must be replaced by

$$\frac{(3p)}{np(1-z) + 3z} \quad \text{where} \quad z = \ell n \left(\frac{M_1}{\mu}\right) \Big/ \ell n \left(\frac{M}{\mu}\right) .$$

For SO(10), with n = 4 (four colours) and $SU_C(4) \to U_C(1) \times SU_C(3)$, one may indeed secure $\sin^2\theta = 0.23$, for $\alpha_s \approx \frac{1}{7}$, provided [43] $M_1 \sim 10^7$ GeV.

In the preparation of this report I had assistance from: U. Amaldi, G. Altarelli, D. Amati, J. Augustin, E.L. Berger, J.D. Bjorken, S.J. Brodsky, J. Chadwick, M. Conversi, N.S. Craigie, V. Elias, J. Ellis, P. Fayet, S. Ferrara, G. Flügge, H. Fritzsch, S. Fubini, E. Gabathuler, M.K. Gaillard, R. Gatto, I.G. Halliday, J. Iliopoulos, M. Jacob, H.F. Jones, K. Koller, C.H. Llewellyn Smith, L. Maiani, B. Nagel, D.V. Nanopoulos, J. Nilsson, J.C. Pati, D. Perkins, J. Prentki, G. Preparata, S. Rajpoot, C. Rubbia, A. de Rujula, L.M. Sehgal, W.G. Scott, P. Söding, B. Stech, J. Steinberger, P.M. Stevenson, J. Schwarz, D. Storey, B. Tallini, J.G. Taylor, D. Treille, R. Turlay, S. Weinberg, B. Wiik, K. Winter, G. Wolf and A. Zichichi.

FOOTNOTES

1) "The End of Molecular Biology", by A. Sibatani, Trends in Biochemical Sciences, International Union of Biochemistry (Elsevier, North-Holland, 1979), Vol.4, No.7.

2) The situation for atomic physics was summarized by L.M. Barkov who gave $\frac{\langle R_{exp.} \rangle}{R_{theor.}} = 1.07 \pm 0.14$ as the ratio of the Novosibirsk bismuth measurements of atomic parity violation compared with the predictions of SU(2) × U(1). Into this comparison is folded the atomic theory calculations of Khriplovich et al. for the complicated bismuth atom. Since the Oxford group contest (among other things) this atomic theory, which has gone into Barkov's comparison, the issue of atomic parity violation is a problem for atomic physicists, rather than a problem for particle physics.

3) While on the subject of radiative corrections, it is worth mentioning that Marciano (and independently Goldmann and Ross) have examined the renormalization group corrections to the fine structure constant and find

$$\alpha^{-1}(m_W) = \alpha^{-1}(0) - \frac{80}{3\pi} \approx 128.5 \quad .$$

Here $\alpha(0)$ is the Josephson value, while $\alpha(m_W)$ is the quantity relevant for present low energy neutrino experiments. This 6% correction in α^{-1} reflects itself in the revised mass formulae for m_W and m_Z which, according to Marciano (COO-2232-B-1979) register a surprising 3% increase; surely of some concern tc the running of LEP at the m_Z peak.

$$\left[\begin{array}{l} m_W \approx \dfrac{38.53}{\sin\theta} \\ \left.\begin{array}{l} m_W \approx 77 - 84 \text{ GeV} \\ m_Z \approx 89 - 95 \text{ GeV} \end{array}\right\} \quad 0.25 \gtrsim \sin^2\theta \gtrsim 0.21 \end{array}\right] .$$

4) The 26 dimensionless parameters of the standard model are: 3 gauge couplings, 6 quark + 6 leptonic masses (assuming $m_\nu \neq 0$), 4 + 4 mixing angles, m_H, m_W and two "instanton" angles corresponding to non-Abelian SU(2) and $SU_c(3)$.

5) A different, somewhat more economical suggestion to motivate iso-doublet Higgs is the use of dimensional reduction. (I shall have occasion to mention this idea later in the context of extended supergravity.) Start with a gauge theory in 6 dimensions (x_μ, x_5, x_6; $\mu = 0,1,2,3$). Reduce 6 dimensions to 4 in the sense of assuming that all fields are independent of the extra co-ordinates x_5 and x_6. On reducing to 4 dimensions, the 6-component vectorial field (A_μ, A_5, A_6) in 6 dimensions comprises a conventional spin-one gauge field A_μ plus a doublet of spin-zero Higgs fields A_5 and A_6.

For one concretization of these ideas (due to Y. Ne'eman, D. Fairlie, J.G. Taylor and others) embed SU(2) × U(1) into a graded internal symmetry SU(2|1) AND work in 6 dimensions. The combination of higher dimensions and the higher internal symmetry (1) makes an iso-doublet Higgs compulsive, (2) specifies the Higgs-Higgs coupling uniquely as part of the basic gauge coupling, (3) predicts $\sin^2\theta = \frac{1}{4}$ and (4) predicts $m_H = 2m_W$. This is fine; unfortunately, the theory as developed so far is not satisfactory, since to avoid ghosts characteristic of an internal graded SU(2|1), this symmetry must be broken explicitly. The hope however is that a more agreeable version may emerge where the desirable features like a compulsive "gauge" iso-doublet Higgs and $\sin^2\theta = \frac{1}{4}$ may remain, without the undesirability of the explicit symmetry breaking.

6) This statement refers to the sign of the one-loop computation of the analogue of QCD's β function in gravity theory. Since gravity, (on present ideas) is non-renormalizable, higher loops are (as yet) intractable, though they may not long remain so. If gravity is indeed asymptotically free, there may be no initial big bang singularity due to the progressive weakening of the effective Newtonian constant with diminishing radius of the universe.

7) While on the subject of perturbative QCD, I would like to quote a remark made by Res Jost at the Sienna Conference of 1963: "To my mind, the most striking feature of theoretical physics in the last thirty-six years is the fact that not a single new theoretical idea of a fundamental nature has been successful. The notions of relativistic quantum theory, so clearly in need of improvement, have been in every instance stronger than the revolutionary ideas of - as the saying goes - a great "number of highly talented theoretical physicists". We live in a dilapidated house and we seem to be unable to move out. The difference between this house and a prison is hardly noticeable". To Jost's words "relativistic quantum theory" in this quotation I would like to add "perturbative", for surely it is ironic, that in fifty-two years since Dirac's invention of QED, we have no quantum solution for QED (or for QCD) except the perturbative.

8) Note the independence of the F^N's and D^M's from mass ($m \to 0$) singularities ($\ell n \frac{\Lambda^2}{m^2}$). These are junked into the primordial (empirical)parton factors f^N, d^M. The parton model factorization survives up to the leading order ($\{F \times D\} \to \{f^N \times d^M\}$) but breaks down in the next to the leading order (i.e. for terms of order $O(\bar{g}^2)$ in the { } brackets). As a rule this non-leading order is large for Drell-Yan processes and may necessitate a different type of resummation of perturbative QCD. Evidence relating to the "non-factorization" in non-leading logs was presented at the conference, This will surely be a major area of progress in the coming year.

9) A dramatic example of the independence of the domains of perturbative QCD and phenomena attributable to confinement has recently been provided by Davis and Elias and Rajpoot. Davis has defined a safe jet variable (to all orders of perturbation theory) which has the remarkable property of measuring charge (including fractional charge) in final states within a phase space "horn". The experimental failure to detect fractional charges must then imply at the very least that "perturbation theory apparently gives no signal of its own failure".

10) If confinement is indeed a non-perturbative dynamical phase (and has no status as an absolute selection rule), the question arises: is it under all circumstances absolutely exact? Using appropriate Higgs, could $SU_C(3)$ be broken spontaneously, with massive gluons, and with confinement only partial, in the sense of an Archimedes effect,i.e. QCD with Higgs may solve in such a way that quarks and gluons may exhibit an effective mass variation; light and

partially confined within an interaction zone; heavy, unconfined and liberated outside it. Practically nothing would need changing in the conventional parton model ideas and in their QCD perturbative renormalization, except for an additional type of "fragmentation" function, describing mass barrier penetration and the probability of finding massive physical quarks and gluons in the final states.

(Even without the heavy non-perturbative theory needed for confinement, one may understand the growth of the running gluon and quark masses as momenta diminish, as a consequence of the renormalization group. The Archimedes effect suggests that this growth is non-perturbatively sharper than logarithmic though not infinite as for full confinement.)

An illustrative mass formula for quarks and gluons exhibiting the Archimedes effect has been suggested by de Rujula, Giles and Jaffe on the basis of a string model of gluonic interactions (mass outside - mass inside) $\propto$ (gluon mass inside)$^{-1}$ times an essentially group-theoretic factor. For zero inside gluon mass (exact $SU_C(3)$) the quark and gluon masses outside are infinite and exact confinement ensues. For inside gluon masses of the order of 20-30 MeV, the outside quark masses could be in excess of several Gev. Bjorken described to the conference a quark model of this variety within a spontaneously broken QCD, to explain the high density hadronic droplets accreting around a liberated fractionally charged quark. (Such droplets are needed in his explanation of the peculiar Centauro events discovered in cosmic rays.)

Such ideas of eventual quark and gluon liberation and the Archimedes effect are unconventional but in view of the lack of any basic understanding of the confinement mechanism, I would like to rephrase for the remembrance of our experimental colleagues what Iliopoulos remarked in another context: "A test of quark-gluon liberation is too important to be left to vagaries of theoretical dogmas".

Earlier than this, Pati et al. had used the Archimedes effect and partial confinement to propose another unconventional version of spontaneously broken QCD. This is the gauge theory of (Han-Nambu) integer-charge quarks and gluons ($Q = Q_{flavour} + Q_{colour}$). Here the excitation of Q_{colour} in lepton-hadron collisions is automatically suppressed by a factor of the type

$$\frac{m^2(q^2)}{|q^2|\,(|q^2| + m^2(q^2))} \quad J_{lepton}\, J_{colour}$$

(compared with the usual factor $\frac{1}{|q^2|} J_{lepton} J_{flavour}$ for flavour-charge interaction with a mass relation of the type $m^2_{out} \approx c\mu^2 \exp \int_{g(m_{in})}^{g(\mu)} \frac{dx}{\beta(x)}$. (Using dispersion relations for $e^+e^- \to \mu^+\mu^-$, Okun, Voloshin and Zakharov, have attempted to show that in a spontaneously-broken $SU_C(3)$ with integer charges, the gluon mass must be $\lesssim 1$ GeV. Unfortunately this demonstration takes no account of the ideas of partial confinement and the Archimedes effect associated with the contribution of the intermediate gluonic state in this model, and thus has no bearing on what the (non-perturbative) physical mass of the gluon is.

11) In the context of the parton model, one of the important results presented at the conference concerns the efficacy of anti-quarks relative to quarks - (pions versus protons) producing T; $(\sigma_\pi \to T)/(\sigma_p \to T) \gtrsim 30$ (Cern NA3; 200 GeV π^+; $(\sigma \cdot B)_T = 2.10^{-36}$ cm^2). This augurs very well for the prospects for Z^0 and $W^\pm$ production at the $P\bar{P}$ collider as emphasised by Rubbia.

12) The proton charge thus equals the positron's, without further hypotheses.

13) The necessity of requiring asymptotic freedom for the ELECTRONUCLEAR force on its own, for energies beyond Planckian ($m_P \approx 1.2 \times 10^{19}$ GeV) has been questioned by Cabibbo, Maiani, Parisi and Petronzio. They argue that by then gravity would profoundly affect the entire discussion. On this basis, they suggest (working essentially to a one-loop approximation) that the numbers of families below Planck mass must not exceed eight. They also give bounds on the expected Higgs and fermion masses. On the contrary, Oehme and Zimmerman (EFI/79/28) have deduced (from the positivity of the transverse gluon propagator) a <u>lower</u> bound on the number of quark flavours.

14) Ideally one would wish all these mass stages to emerge as radiatively generated multiples of the Planck mass - possibly with magnitudes $\sim \alpha m_P$, $\alpha^2 m_P$, $\alpha^3 m_P$, ... or alternatively of magnitudes like $m_P \exp - \frac{c_n}{\alpha}$ (c_n's are constants). The problem of a "natural" generation of such mass hierarchies is another aspect of the unsolved problem of Higgs.

15) Likewise (from the renormalization group equations for the fermion mass ratios) one may hope to deduce the ratios of the physical quark to the lepton masses, the ratios at the grand-unifying M being specified by the Higgs couplings assumed.

16) The topless version of E_6 predicts b-quark decays to charmless quarks (B. Stech, private communication). The observed b-decays involving

charm may thus imperil E_6. (The suggestion of SU(11) as the tribal extension of Georgi and Glashow's simple SU(5) is due to Georgi; the suggestion of E_8 extending Gürsey et al.'s E_6 is due to Achiman and Stech.)

17) These decay modes have been brought into prominence during the last year through an improvement in the renormalization group estimates (for example, of $\alpha^{-1}(m_W)$ - 6% diminution [3] from $\alpha^{-1}(0)$ and a corresponding diminution in the estimates for τ_P which are now typically $\sim 10^{29}$-10^{33} years if unification masses range between 5×10^{14} and 3×10^{15} GeV and $\sin^2\theta$ ranges [3] between 0.210 and 0.20),

18) "Proton decay is too important to be left to theoreticians alone." - Iliopoulos.

19) The one really new feature of this year's work has been the estimation, within the context of grand unification, of baryon excess in the universe - more precisely an estimate of the ratio of the photon number N_γ to the baryon numbers N_B, which is empirically known to be $\approx 10^8$-10^9. The suggestion that baryon excess may be a consequence of baryon-non-conservation plus CP violation was first made by Yoshimura at the Tokyo Conference. The present quantitative estimates (which by and large - more "by" and less "large" - agree with data) were reviewed by Mohapatra for models with supermassive multi-Higgs and lepto-quarks (10^{15} GeV) and "hard" CP violation; as well as for models with low-mass lepto-quarks ($\sim 10^4$-10^5 GeV) and CP violation which is "soft".

20) Yet each man kills the thing he loves
By each let this be heard
Some do it with a bitter look
Some with a flattering word
The coward does it with a kiss
The brave man with a sword.

Oscar Wilde - The Ballad of the Reading Goal.

21) For example, for the Family group SO(10) of Fritzsch, Minkowski and Georgi, there is the possible chain (see Appendix)

$$SO(10) \xrightarrow{M} SU_L(2) \times SU_R(2) \times SU(4) \xrightarrow{M_1} SU_L(2) \times SU_R(2) \times U_C(1) \times SU_C(3) \xrightarrow{M_2} SU_L(2) \times U(1) \times SU_C(3) \xrightarrow{\mu} U(1) \times SU_C(3).$$

22) According to 't Hooft's theorem, a monopole corresponding to the $SU_L(2)$ gauge symmetry is expected to possess a mass of the order of $\frac{m_W}{\alpha}$. Even if such monopoles are (conveniently) confined, their indirect effects must manifest themselves, if they exist.

23) This is assuming that the concept of "families" which make up a "tribe", makes sense for ultimate grand unification.

24) Similar remarks apply to the U(1) in $SU(2) \times U(1) \times SU_C(3)$.

25) Even if it is assumed that all fermions are singlets or doublets of SU(2) and singlets or triplets of $SU_C(3)$, there is no reason for $\sin^2\theta_0$ to equal $\frac{3}{8}$. To see this note that with this assumption - which incidentally excludes supersymmetric gauge fermions in the adjoint representations - $\sin^2\theta_0 = (9N_q + 3N_\ell)/(20N_q + 12N_\ell)$, where N_q and N_ℓ are the numbers of quark and lepton doublets, respectively. Only if we make the further assumption that $N_q = N_\ell$, from anomaly cancellation between quarks and leptons, do we recover $\sin^2\theta_0 = \frac{3}{8}$. This assumption however is not compulsive; for example, anomalies cancel if (superheavy) mirror fermions exist, without the need for assuming $N_q = N_\ell$. This is the case for $[SU(2n)]^4$. (The anomalies also automatically cancel for the adjoint representations of the supersymmetric gauge fermions.) Note however that if $[SU(3)]^p \times [SU(2)]^q \times U(1)$ is embedded within a non-Abelian symmetry and the manner of descent specified, one can express $\sin^2\theta_0$ as a function of p and q.

26) The universal urge to **extrapolate** from what we know to-day and to believe that nothing new can possibly be discovered, is well expressed in the following:

"I come first, My name is Jowett
I am the Master of this College,
Everything that is, I know it
If I don't, it isn't knowledge" -

The Balliol Masque.

27) So long as we work with the concepts of elementary fields and fundamental Lagrangians, it is clear that some day we must hit the level of elementary fermions. Thus it does not dismay me that the succession of flavours and colours (or families) may end. But we cannot really argue about these matters on the basis of one-loop approximations.

I would here like to quote Feynman in a recent interview to the "Omni" magazine: "As long as it looks like the way things are built with wheels within wheels, then you are looking for the innermost wheel - but it might not be that way, in which case you are looking for whatever the hell it is you find!" In the same interview he remarks, "a few years ago I was very sceptical about the gauge theories..... I was expecting mist, and now it looks like ridges and valleys after all".

28) Zero mass neutrinos are the hardest objects to conceive of as composites.

29) Harari was kind enough to send me a pre-copy of his paper. He wondered if I considered his ideas were crazy enough in the sense of Niel Bohr's famous remark. I am afraid I had to express some reservations; from a follower of the world's first great monotheistic religious tradition, I would have appreciated one pre-preon rather than two.

30) I have called this "Post-Planck" physics, assuming that the thrust of the ideas discussed will be felt at and beyond Planck energies (10^{19} GeV). But let us make no mistake - the ideas are quite general and their import might be felt much earlier.

31) The following quotation from Einstein is relevant here. "Experiment alone can decide on truth ..... But how wrong are those theorists who believe theory comes inductively from experiment - and this includes the great Newton with his "Hypotheses Non Fingo"." I believe this is the only place where Einstein departed somewhat from his total veneration for Newton.

32) What is electric charge in this theory? To answer this, one must introduce charged matter - and in the last analysis, fermions. Kaluza and Klein foreshadowed the answer - charge corresponds to the variable conjugate to the fifth dimension - quantized if the fifth dimension curls onto itself. Perhaps the most detailed and elegant working out of this idea is due to Olive and Witten (reported by Olive at the conferance). Consider a supersymmetric Georgi-Glashow model in six-dimensional compactified space-time. One can show that all objects in this theory (elementary fields, monopoles, dyons) satisfy a light-like mass relation (exact, including quantum corrections):

$$P_\mu^2 - P_5^2 - P_6^2 = 0 \quad .$$

Here P_5 and P_6 are the momenta conjugate to x_5 and x_6 and one shows by an explicit calculation that P_5 = m x electric charge, topologically defined $\rightarrow \int \partial_i F_{i0}\, d^3x$ and P_6 = m x magnetic charge on the particle, defined similarly. Thus by an explicit construction one demonstrates that momenta conjugate to the extra dimensions correspond to (topologically defined) electric and magnetic charges.

33) An attractive suggestion pursued recently by Budini and Raczka ascribes the existence of higher internal symmetries to the Cartan reflections in conformal space (projectively realized in 6 dimensions).

34) The Einstein Lagrangian allows large fluctuations of metric and topology on Planck-length scale. Hawking has surmised that the dominant contributions to the path integral of quantum gravity come from metrics which carry one unit of topology per Planck volume. On account of the intimate connection (de Rham, Atiyah-Singer) of curvature with the measures of space-time topology (Euler number, Pontryagin number) the extended Kaluza-Klein and Wheeler-Hawking points of view may not be so different after all.

An example of the possible relevance of topological ideas is a result of Kiskis, who shows that under certain conditions a space-time with handles would permit global violations of charge. One wonders if this result extends to other (violated) charges (like I-spin, hypercharge,...) and what its significance for the topology of our space-time may then be.

In a very different context, I might mention a recent topological result of Witten. In a Yang-Mills theory, he shows that for a theory with a non-zero "vacuum" angle θ, dyons must carry (possibly fractional or even irrational) electric charges = $\left(n + \frac{\theta}{2\pi}\right) e$. Physics, as we have known it, may be made to stand on its head by an infusion of topology.

35) The full result is this: The Lagrangian in [11]-dimensions possesses an invariance as large as $E_7|_{\text{global}} \times SU(8)|_{\text{local}}$. The analogy is with Weyl's version of Einstein's gravity theory which has the invariance $GL(4,R)|_{\text{global}} \times SO(3,1)|_{\text{local}}$. Now the graviton in Weyl-Einstein theory with its 16 - 6 = 10 components lives in the coset space $\frac{GL(4,R)}{SO(3,1)}$ with its 10 generators. Likewise the coset space $\frac{E_7}{SU(8)}$ with its 133 - 63 = 70 generators can carry 70 spin-zero objects which are the "gravitons" of the internal space. These are just the 70 spin-zero fields in the N = 8 supergravity tribe.

36) Fayet estimates, for a light gravitino, a rate 10^{-5}-10^{-7} to compare with $\Gamma(\psi \to \text{unobserved neutrals}) \approx 7 \times 10^{-3}$ and $\Gamma(\psi \to e^+e^-) = (7 \pm 1) \times 10^{-2}$. He has made the assumption that the (spontaneous) breakdown of supersymmetry occurs at masses $\approx m_W \approx m_P \exp(-c/g^2)$. (There is the alternative proposal of a linear progression from grand unification to extended supergravity which suggests that the characteristic mass for the breakdown of supersymmetries - and for all the unwanted supersymmetric partners of $W^{\pm}$, Z^0, , etc - as well as for the gravitinos - is of the order of Planck mass m_P.)

37) This follows from the standard one-loop renormalization group equations:

$$\alpha_s^{-1}(\mu) = p(4\pi g^{-2}(M)) - 3.\ \frac{11}{6\pi}\ \ell n\ \frac{M}{\mu} \qquad (A)$$

$$\alpha^{-1}(\mu)\ \sin^2\theta(\mu) = q(4\pi g^{-2}(M)) - 2.\ \frac{11}{6\pi}\ \ell n\ \frac{M}{\mu} \qquad (B)$$

$$\alpha^{-1}(\mu)\ \cos^2\theta(\mu) = q(4\pi g^{-2}(M))\ \cot^2\theta_0\ . \qquad (C)$$

For simplicity we have ignored the effects of the fermionic (and the Higgs) loops on the right-hand side. These are discussed by Marciano [39].

38) These family groups are too small to permit $p, q > 1$. The tribal group SU(11) however may accommodate larger p's and q's.

39) W.J. Marciano (COO-2232-B-173) who gives the same result for $\frac{11\alpha}{3\pi}\ \ell n\ \frac{M}{\mu}$, as above, except that the factor 11 is replaced by $\frac{109}{9}$ if one takes fermion and one Higgs loops into account. For N_H Higgs isodoublets, replace 11 by $\frac{110 - N_H}{9}$. Thus for $N_H \sim 15$, $\sin^2\theta \simeq 0.23$ is compatible with $M \approx 10^{15}$-10^{16} GeV. The extreme sensitivity of M on assumptions relating to renormalizations should be stressed once again.

40) For the semi-simple group $[SU(2n)]^4$ describing $2n$ flavours of quarks (and $4n^2 - 6n$ leptons; the majority possibly superheavy), Elias and Rajpoot give:

$$\sin^2\theta_0 = \frac{3n}{4(3n - 2)}$$

$$\sin^2\theta = \frac{3n-4}{12(n - 1)} + \frac{\alpha}{\alpha_s}\ \frac{9n-8}{18(n - 1)}$$

$$\frac{11\alpha}{\pi}\ (n - 1)\ \ell n\ \frac{M}{\mu} = 1 - (2n - \tfrac{4}{3})\ \frac{\alpha}{\alpha_s}\ .$$

41) Consider one more example of the introduction of intermediate energy scales - and the plateau-breaking peaks - which may have their location almost anywhere, so far as the internal logic of the symmetry-breaking is concerned. The example is that of the tribal group $SU^I(5) \times SU^{II}(5) \times SU^{III}(5)$ corresponding to the Three Families. Assume each $SU^i(5)$ breaks to $[SU(2) \times U(1) \times SU_C(3)]^i$, i = I, II, III, with mass scales M^i. The final breaking stage corresponds to the emergence of the diagonal sum $[SU(2) \times U(1) \times SU_C(3)]^{I+II+III}$ ($\supset U(1) \times SU_C(3)$) with the associated scale M. The results of the computations of $\sin^2\theta$ and the unifying masses are:

$$\sin^2\theta = \frac{1}{6} + \frac{5}{9}\frac{\alpha}{\alpha_s}$$ (i.e. the same result as for the Family group SU(5)); and

$$\frac{\alpha_s}{\alpha} = \frac{8}{3}\left[1 - \frac{11\alpha}{\pi}\,\ell n\,\frac{M^I M^{II} M^{III}}{\mu M^2}\right] .$$

For $M^I = M^{II} = M^{III} = M$, we recover the well-known Family SU(5) result. Now M^I may be restricted on account of proton decay, but the restrictions on the locations of M^{II} and M^{III} need not be too stringent. (Elias has conjectured that the ratios of fermionic masses among the three Fermi Families may differ on account of the three differing mass scales M^I, M^{II}, M^{III}. The point is that not till we understand the deeper relationship of the Family and the Tribal groups can we reject such possibilities.)

42) This analysis is relevant also if there exist new forces of which we may, at present, have no apprehension – for example the techni-colour forces of Dimopoulos and Susskind, with $G = SU(10) \to SU(2) \times U(1) \times SU(8) \to SU(2) \times U(1) \times SU_C(3) \times SU_{tech}(5)$. (The Higgs needed to break the symmetry this particular way have to be specially chosen.)

43) In Shafi and Wetterich's analysis the intermediate stage is through the breaking of $SU_R(2)$ at around 10^6 GeV, i.e. (V+A) forces make their appearance then. I believe both types of stages may be necessary to shore up $\sin^2\theta$, as well as M and τ_P.

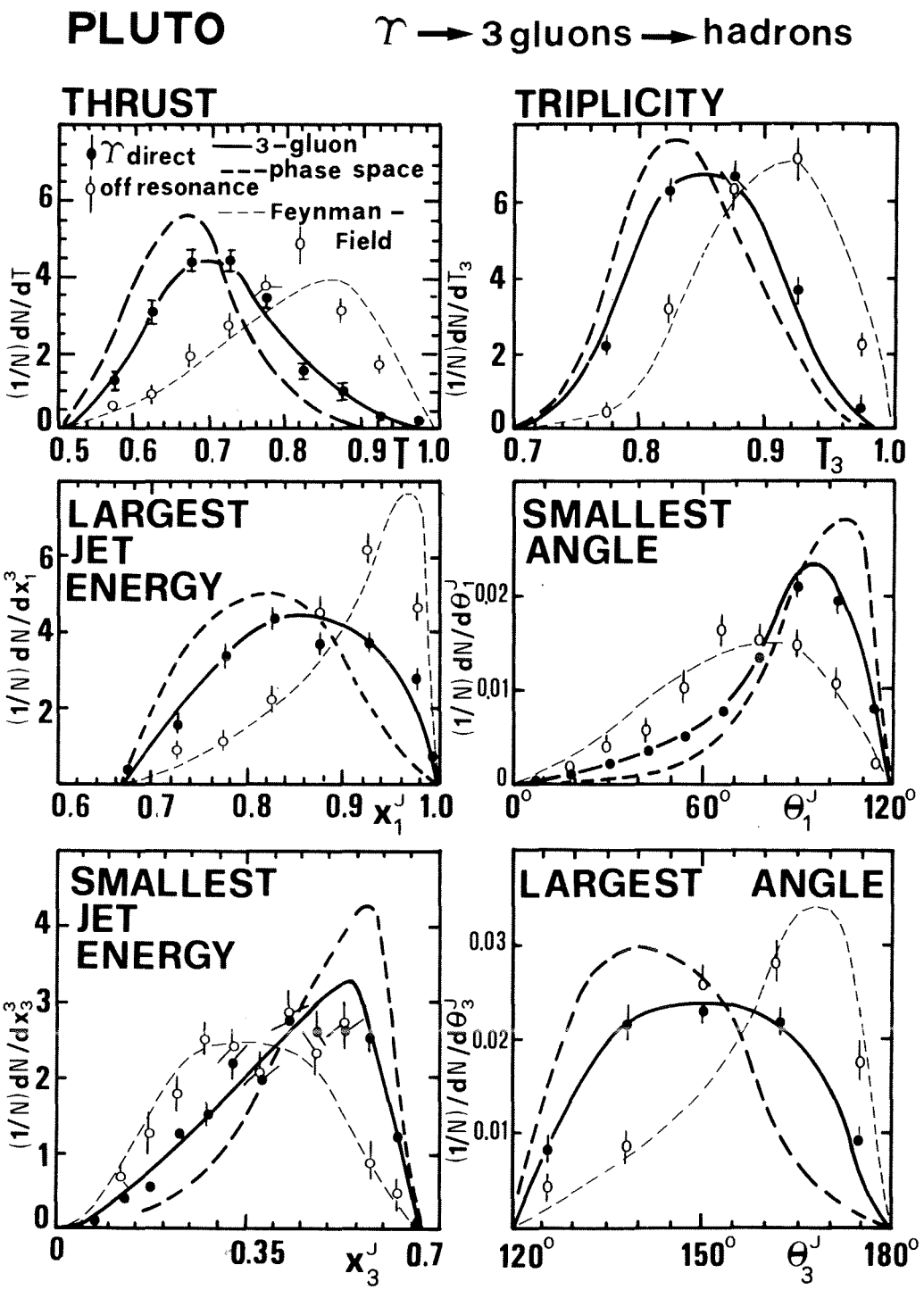

Experimental distributions of thrust T, triplicity T_3 reconstucted gluon energies x_1^J, x_3^J and reconstructed angles θ_1^J, θ_3^J between gluons, compared to Monte-Carlo calculations based on various models

Fig. 1

GLUON SPIN TEST

$\Upsilon \rightarrow$ 3 GLUONS

THRUST AXIS ANGULAR DISTRIBUTION

$$\frac{1}{\sigma_{3g}}\frac{d\sigma_{3g}}{dT} \cong 1+\alpha(T)\cos^2\Theta_T$$

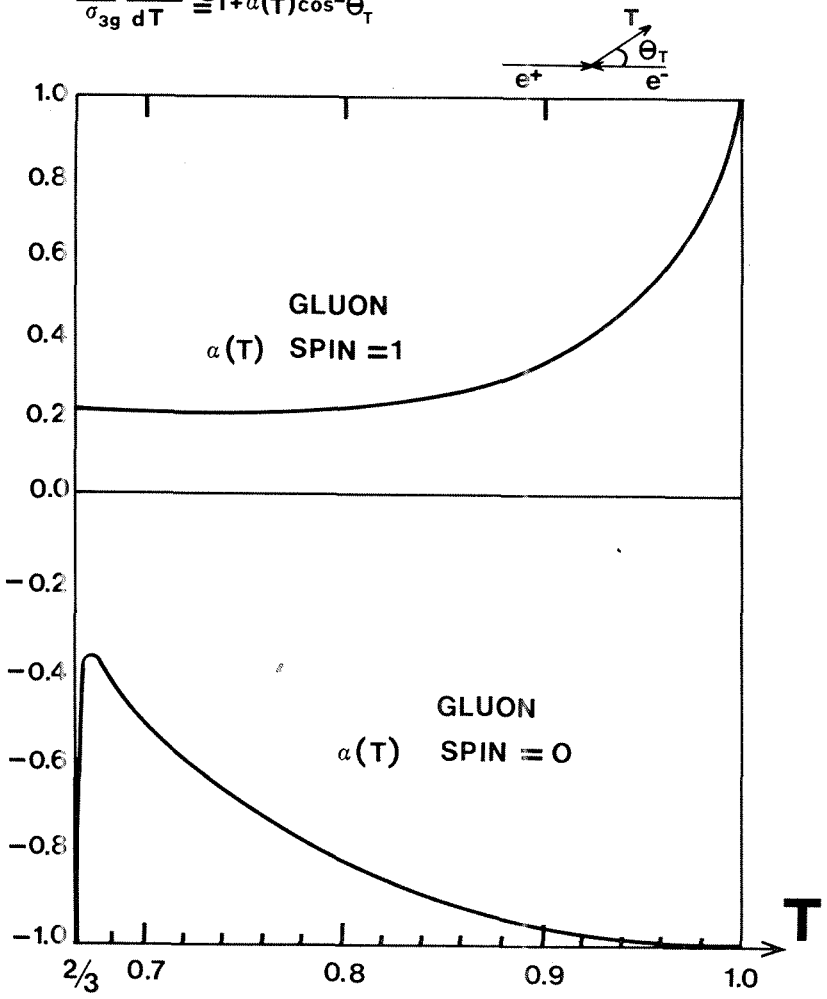

Fig. 2

THRUST AVERAGE
ANGULAR DISTRIBUTION

$\langle\alpha(T)\rangle = 0.39$ GLUON SPIN=1

$\langle\alpha(T)\rangle = -0.99$ GLUON SPIN=0

$\langle\alpha(T)\rangle = 0$ NAIVE PHASE SPACE

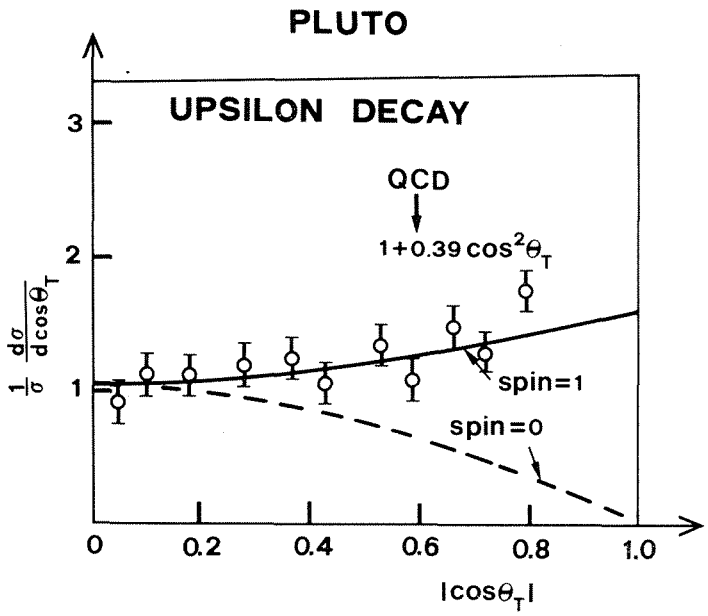

Fig. 3

Measuring presence of 3 gluon vertex

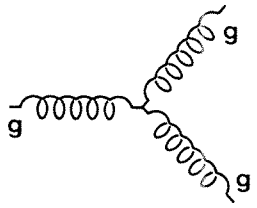

M^2 Evolution of Gluon Jets

Fragmentation function Moments

$D_g(n,M^2)$ $n=2,3,4...$

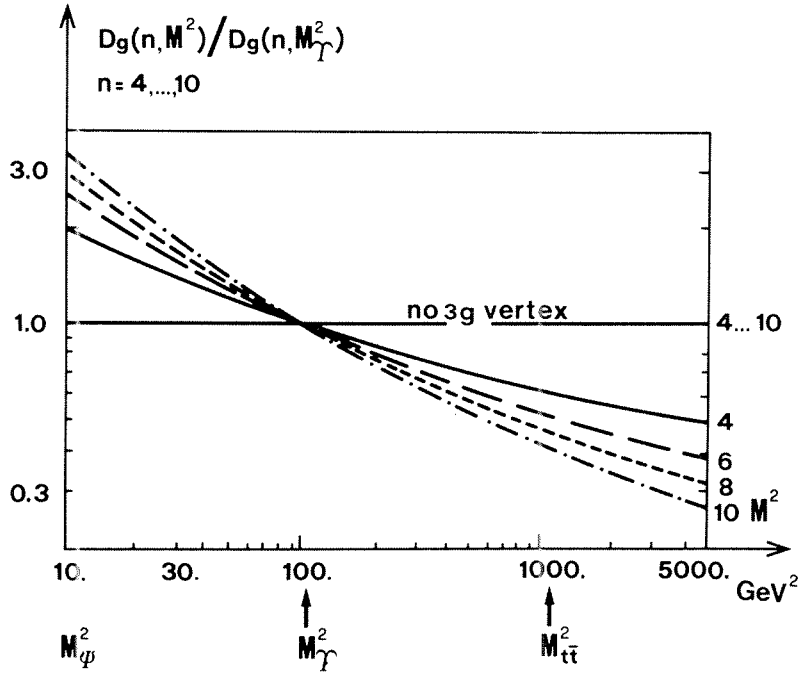

Fig. 4

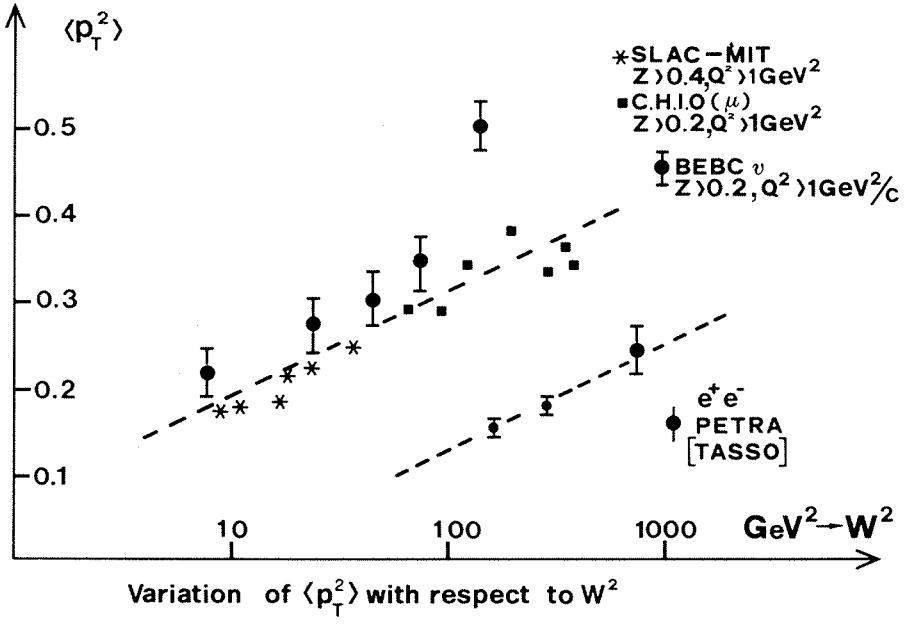

Fig. 5

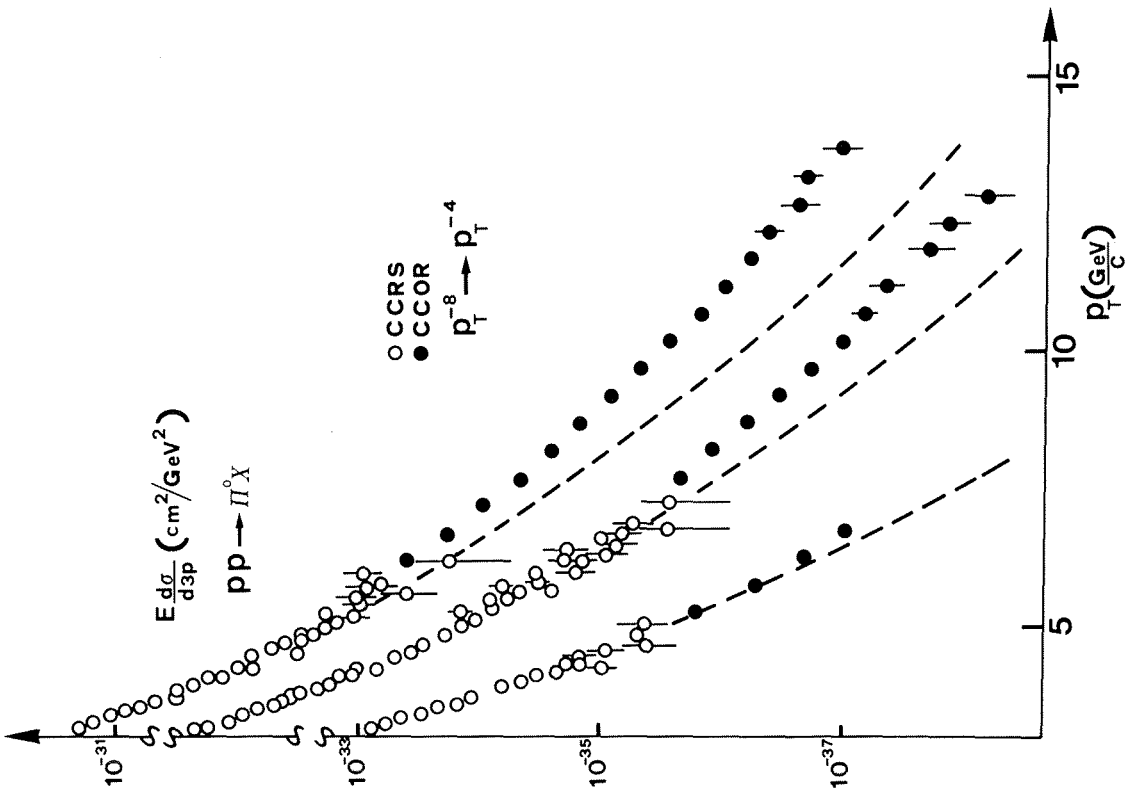
$E\frac{d\sigma}{d3p}$ (cm²/GeV²)
pp → π°X
○ CCRS
● CCOR
$p_T^{-8} \rightarrow p_T^{-4}$
10^{-31}
10^{-33}
10^{-35}
10^{-37}
5
10
15
p_T(GeV/c)

Fig. 7

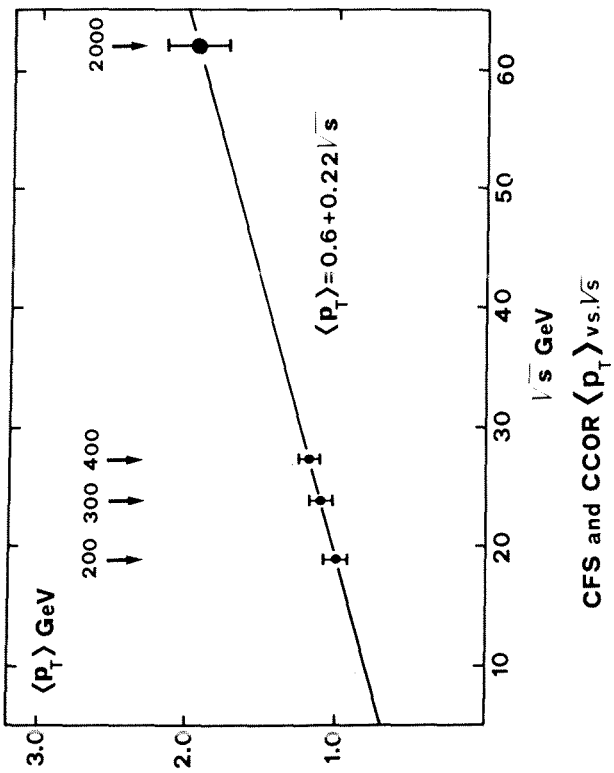
⟨p_T⟩ GeV
3.0
2.0
1.0
200 300 400
2000
⟨p_T⟩=0.6+0.22$\sqrt{s}$
10
20
30
40
50
60
$\sqrt{s}$ GeV
CFS and CCOR ⟨p_T⟩ vs.$\sqrt{s}$

Fig. 6

PARALLEL DISCUSSION SESSION 1

HIGH-ENERGY HADRON-INDUCED REACTIONS

Chairman: J.C. Sens

Sci. Secretaries: B.S. Nielsen
S. Weisz

Summary report of the Chairman

SUMMARY OF THE MOST SIGNIFICANT RESULTS REPORTED IN THIS SESSION

J.C. Sens
NIKHEF-H, Amsterdam, Netherlands
and
CERN, Geneva, Switzerland

The most interesting although speculative result is the observation of a *4 standard deviation effect at 5.3 GeV* in the $\psi K^0\pi^-$ and $\psi K^-\pi^+$ mass plots (SPS Exp. WA11) with a cross-section of 180 nb (assuming 1% branching ratio). This is a candidate bare b-state.

The next most significant experimental result is the observation of Λ_c^+ at the CERN Intersecting Storage Rings (ISR). This state was discovered at BNL by Samios et al. and has since been seen in several neutrino experiments. It was seen at the ISR by Lockman et al. about a year ago (reported at Budapest) but not in a convincing way. The analysis has now been improved, and the result shows a peak which is most clearly present in the summed $\Lambda(3\pi)^+$ and $K^-p\pi^+$ mass spectra. The signal has furthermore been seen in Exp. R606 (reported by F. Muller in this parallel session) in both $\Lambda 3\pi$ and $pK^-\pi^+$. The most convincing signal comes from the Split-Field Magnet (SFM) in $K^-p\pi^+$. The three observations together, all at the ISR, make this an outstanding result of the conference, although it is *not* a *new* discovery.

Very interesting contributions have been made by Brodsky and Berger on *higher-twist effects*. This, in my opinion, is going to strongly influence the phenomenological analysis in the future. One prediction, the dependence of α in $1 + \alpha \cos^2\theta$ in $\pi p \to \mu\mu$ on $X(\mu\mu)$, has been verified by experiment (reported in Aubert's session by Pilcher).

Also figuring high on the list of new developments are data as well as models for understanding parton dynamics in all-hadronic reactions. The work of Gunion, Hwa, and others, and a number of experiments (Kp at 110 GeV, ϕ production, correlations at the ISR, etc.) are of interest, but not fully conclusive at this stage. One might say that the *Brodsky-Gunion counting rule is dead* but it is not clear with what to replace it.

List of papers prepared for this session

1. RECENT PHOTOPRODUCTION RESULTS FROM FERMILAB
   S.D. Holmes
   (Columbia Univ., NY).

2. DIFFRACTIVE PRODUCTION OF THE CHARMED BARYON Λ_c^+ AT THE CERN ISR
   K.L. Giboni et al.,
   Aachen-CERN-Harvard-Munich-Northwestern-Riverside Collaboration
   (Presented by F. Muller, CERN)

3. CHARMED BARYON PRODUCTION AT THE CERN ISR
   D. Drijard et al.,
   ACCDHW Collaboration
   (Presented by H. Frehse, Heidelberg)

4. ON THE PRODUCTION OF CHARMED MESONS IN HIGH-ENERGY PROTON-PROTON COLLISIONS (CERN/ISR)

   A. Chilingarov et al.,
   CERN-CEN Saclay-ETH Zurich Collaboration

   (Presented by A. Clark, CERN)

5. EVIDENCE FOR Λ_c^+ IN INCLUSIVE $pp \to (\Lambda^0\pi^+\pi^+\pi^-) + X$ AND $pp \to (K^-\pi^+p) + X$ AT $\sqrt{s}$ = 53 AND 62 GeV

   W. Lockman et al.,
   UCLA-Saclay Collaboration

   (Presented by P. Schlein, UCLA)

6. FIRST OBSERVATION OF A COMPLETE DECAY OF A $\bar{D}^0$ PRODUCED IN A HIGH-ENERGY PHOTON INTERACTION IN EMULSIONS

   (Presented by A. Conti, Florence)

7. UPS AND DOWNS IN THE SEARCH FOR BARYONIUM STATES

   M.N. Kienzle-Focacci,
   University of Geneva

8. RESULTS OF A BEAM-DUMP EXPERIMENT USING THE BEBC BUBBLE CHAMBER

   (Presented by P. Schmid, CERN)

9. BEAM-DUMP EXPERIMENT WA1

   CDHS Collaboration

   (Presented by S. Loucatos, CEN Saclay)

10. RESULTS FROM A BEAM-DUMP NEUTRINO RUN AT THE SPS

    J.V. Allaby et al.,
    CHARM Collaboration

    (Presented by P. Monacelli, Rome)

11. DIMUON RESONANCE PRODUCTION FROM A 200 GeV TAGGED MESON BEAM

    J. Bordier et al.,
    CEN Saclay-CERN-Collège de France-Ecole Polytechnique-Orsay Collaboration

    (Presented by P. Delpierre, Collège de France, Paris)

12. DIMUON CONTINUUM PRODUCED IN pp AT FNAL (E 288)

    (Presented by W. Innes, SLAC)

13. EXCLUSIVE PROCESSES AT LARGE MOMENTUM TRANSFER IN QCD AND THE INCLUSIVE-EXCLUSIVE CONNECTION

    S.J. Brodsky and G.P. Lepage

    (Presented by S.J. Brodsky, SLAC)

14. UNIFIED QCD AND CIM APPROACH TO LARGE p_T AND LOW p_T INCLUSIVE REACTIONS

    J.F. Gunion,
    Univ. Calif., Davis

15. HADRONIZATION OF PARTONS IN THE RECOMBINATION MODEL

R.C. Hwa,
Univ. Oregon

16. INCLUSIVE ϕ-MESON PRODUCTION -- RELATION TO J/ψ AND Υ PRODUCTION

D.R.O. Morrison,
CERN

17. SUMMARY OF SOME RECENT CORRELATION EXPERIMENTS

R.C. Hwa,
Univ. Oregon

18. INCLUSIVE γ-PRODUCTION IN $p\bar{p}$ AT 0.76 GeV/c AND SEARCH FOR DIRECT γ-PRODUCTION

S. Banerjee et al.,
Tata Institute, Bombay
(Presented by S.N. Ganguli, Tata Inst., Bombay)

19. A MEASUREMENT OF PARTICLES PRODUCED AT LARGE p_T BY PIONS

(Presented by B. Pope, Univ. Princeton)

20. A SEMICLASSICAL MODEL FOR THE POLARIZATION OF INCLUSIVELY PRODUCED Λ^0's

B. Andersson et al.
(Presented by G. Gustafson, Univ. Lund)

21. SOFT MULTIHADRON PRODUCTION FROM PARTONIC STRUCTURE AND FRAGMENTATION FUNCTIONS

A. Capella et al.
(Presented by A. Capella, Orsay)

PARALLEL DISCUSSION SESSION 2

DEEP INELASTIC PHENOMENA

Chairman: J.J. Aubert

Sci. Secretaries: E. Longo
H. Wahlen

Summary report of the Chairman

SUMMARY OF THE MOST SIGNIFICANT RESULTS REPORTED IN THIS SESSION

J.J. Aubert
LAPP, Annecy-le-Vieux, France

This session has mostly been orientated towards experimental results, with only three theoretical presentations dedicated to a better comprehension of the significance of these results.

There has been a presentation of four new measurements of the μp structure function, by the Berkeley-FNAL-Princeton and EMC Collaborations on an iron nucleus, by the Bologna-CERN-Dubna-Munich-Saclay Collaboration on a carbon nucleus, and by the EMC Collaboration on a hydrogen target. Although all the data are preliminary, they agree reasonably well; they do not seem to reproduce the step observed in the W distribution (W is the mass of the hadronic final state) by the Michigan State University-FNAL Collaboration, and they show a flat behaviour at large Q^2 ($15 < Q^2 < 200$ GeV/c^2). E. Reya has explained what tests of QCD are provided by the nucleon structure function, and P. Castorina has presented an alternative description of deep inelastic structure functions which agree very well with the data.

J. Wotschack from CDHS has made a useful clarification of the Λ parameter determination. Part of the difference between the data of CDHS and BEBC is explained by the difference in data handling; namely, the number of flavours, radiative corrections, and effects of Fermi motion; and part of the difference comes from the fact that they do not rely on the same Q^2 range for their data.

New results on the elastic muoproduction of the J has been presented by the EMC Collaboration; their data support the Q^2 behaviour of the vector dominance model production and show an energy dependence that is rather flat above 100 GeV.

Recent measurements of the Drell-Yan pair production ($\pi^{\pm}$, $K^{\pm}$, $p^{\pm}$ induced data) from the CERN-Collège de France-Ecole Polytechnique-Orsay-Saclay Collaboration have been reported. Results on scaling, A dependence, absolute comparison of $\pi^{\pm}$, $K^{\pm}$, $p^{\pm}$ induced mass spectra, p_T dependence, and decay angular distributions have been presented. The Chicago-Illinois-Princeton Collaboration, using π-induced dimuons, have measured the helicity angular distribution; their data show evidence for a $\sin^2\theta$ term for x close to one. This is a new and interesting result which is consistent with a calculation based on QCD. E. Berger gave a comprehensive review of the significance of the experimental data and compared the information from deep inelastic scattering and the Drell-Yan pairs.

List of the papers presented

1. STRUCTURE FUNCTION IN μp SCATTERING
   Berkeley-FNAL-Princeton Collaboration
   (Presented by S.C. Loken, Berkeley)

2. DEEP INELASTIC SCATTERING OF 280 GeV/c μ^+ ON CARBON
Bologna-CERN-Dubna-Munich-Saclay Collaboration
(Presented by G. Smadja, Saclay)

3. DETERMINATION OF NUCLEON STRUCTURE FUNCTIONS FOR MUON SCATTERING ON A HEAVY TARGET
European Muon Collaboration
(Presented by P. Payre, CERN)

4. DEEP INELASTIC MUON SCATTERING ON HYDROGEN
European Muon Collaboration
(Presented by Y. Declais, LAPP, Annecy)

5. STRUCTURE FUNCTION IN μp SCATTERING AND MULTIMUON FINAL STATES
Michigan State University-FNAL Collaboration
(Presented by K.W. Chen, Michigan State University)

6. MULTIMUON PRODUCTION BY 280 GeV/c μ^+ ON CARBON
Bologna-CERN-Dubna-Munich-Saclay Collaboration
(Presented by I.A. Savin, Dubna)

7. J/ψ PRODUCTION IN MUON NUCLEON SCATTERING
European Muon Collaboration
(Presented by J. Davies, Oxford)

8. HOW TO TEST QCD WITH NUCLEON STRUCTURE FUNCTIONS
(Presented by E. Reya, DESY)

9. A REALISTIC DESCRIPTION OF DEEP INELASTIC STRUCTURE FUNCTION
P. Castorina, G. Nardulli and G. Preparata
(Presented by P. Castorina, Bari)

10. MUON PAIR PRODUCTION AT MASSES ABOVE 4 GeV/c^2 (DRELL-YAN CONTINUUM) BY $\pi^{\pm}$, $K^{\pm}$, $\bar{p}$, AND p of 200 GeV/c AND BY π^- OF 280 GeV/c ON PLATINUM AND HYDROGEN TARGETS
CEN Saclay-CERN-Collège de France-Ecole Polytechnique Palaiseau-LAL Orsay Collaboration
(Presented by Ph. Miné, Ecole Polytechnique)

11. EVIDENCE FOR LONGITUDINAL PHOTON POLARIZATION IN MUON-PAIR PRODUCTION BY PIONS
Chicago-Illinois-Princeton Collaboration
(Presented by J.E. Pilcher, Chicago)

12. QUARK STRUCTURE FUNCTIONS OF MESONS, DEEP INELASTIC SCATTERING AND THE DRELL-YAN PROCESS
(Presented by E.L. Berger, SLAC)

13. CHARM PRODUCTION ON νp WITH BEBC
Aachen-Bonn-CERN-Munich-Oxford Collaboration
(Presented by D. Lanske, Aachen)

14. STRUCTURE FUNCTION, Λ PARAMETER AND THE CALLAN-GROSS RELATION
CERN-Dortmund-Heidelberg-Saclay Collaboration
(Presented by J. Wotschack, Heidelberg)

15. STRANGE SEA DETERMINATION WITH DIMUONS PRODUCED ON ν-NUCLEON SCATTERING
CERN-Dortmund-Heidelberg-Saclay Collaboration
(Presented by J. Rander, Saclay)

PARALLEL DISCUSSION SESSION 3

HADRON SPECTROSCOPY

Chairman: R.T. Van de Walle

Sci. Secretaries: A. Burns
P. Gavillet

Report of the Chairman

SUMMARY OF THE MOST SIGNIFICANT RESULTS REPORTED IN THIS SESSION

R.T. Van de Walle
University of Nijmegen, Netherlands

In the following a summary is presented of five parallel sessions on *light quark* hadron spectroscopy. In general all topics which were discussed in the plenary sessions, and for which the proceedings contain separate (invited) papers, will be left out; only occasionally (and for reasons of completeness) will we make a reference to these presentations.

Several other restrictions can be made. Nearly all papers submitted to the (parallel) hadron spectroscopy sessions were experimental[1], the only exceptions being a series of four theoretical papers on the baryonium problem. Furthermore, there was virtually no new information concerning the 'classical' baryons. In particular, no new facts were submitted on the problem of the possible existence of baryon states outside the so-called minimal spectrum, i.e. outside $\{56,L^{+}_{even}\}$ and $\{70,L^{-}_{odd}\}$, the existence of the $\{20\}$'s, and the existence of (baryon) exotic states. There was one contribution on a 'possible' new Ξ^{*} [2], and a report on the final measurement of the Σ^{+} magnetic moment with the HYBUC bubble chamber[3]. Recent work on πN phase-shift analysis was presented in the plenary sessions[4]. The remaining baryon contributions were on searches for narrow states.

As a result of the situation described above, this summary will to a large extent deal with *meson* spectroscopy only, both with the conventional mesons ($q\bar{q}$ - see Section 1) and with the narrow and broad mesons coupled mainly to $B\bar{B}$ (see Section 2). In (a short) Section 3 we will mention the results of the narrow *baryon* searches. For the $q\bar{q}$ mesons the data obtained will be discussed in the framework of simple SU(6). For the other topics a more 'enumerative' approach will be necessary.

1. THE $q\bar{q}$ MESONS

Figure 1 gives a summary of the different nonets expected. The x-coordinate is a variable proportional to the $(\text{mass})^2$ of the multiplets; the y-coordinate gives the (internal) orbital angular momentum. In general there are four nonets for each L-value (except for L = 0 where there are only two). Each nonet is classified by the usual quantum numbers:

$$J = L + S$$
$$P = (-1)^{L+1}$$
$$C = (-1)^{L+S} ,$$

where S (0 or 1) is the spin of the $q\bar{q}$ system.

The mass-ordering in Fig. 1 is of course potential-dependent. The one shown corresponds to the harmonic oscillator potential, but this assumption will not enter into our discussions; Fig. 1 will only be used as a guide line. In general one would also expect all multiplets to repeat themselves at higher masses as a result of radial excitations. Actually such states have indeed been observed for the low-lying 0^{-+} and 1^{--} multiplets. Again, no new facts concerning the existence of such states were reported to this conference and we leave them out of Fig. 1 for reasons of clarity. This will allow us to discuss the various nonets in terms of their L-grouping only.

1.1 The L = 0 states (0^{-+}, 1^{--})

The L = 0 multiplets present a stationary picture; the only new facts concern singlet-octet mixing angles for the 0^{-+} nonet[5] and new data on rare decays (such as $\omega \to \pi^0\mu^+\mu^-$) [6].

1.2 The L = 1 states (0^{++}, 1^{++}, 1^{+-}, 2^{++})

1.2.1 0^{++} mesons

The scalar meson situation is essentially unchanged. The $\delta(980)$ and $S^*(980)$ are well established[7] and the $\varepsilon(800)$ and $\kappa(1500)$ are healthy but still in need of further confirmation. The I = 1 $\delta'(1300)$ S-wave $K\bar{K}$ resonance reported in $\pi^-p \to K^0K^-p$ [8] and the presumably I = 0 $\varepsilon'(1300)$ S-wave structure observed in neutral $(\pi\pi)$ and neutral $(K\bar{K})$ [9] are also still alive, but for the latter Martin et al. have shown that the I = 0 assignment is highly model-dependent, and therefore still in doubt[10]. Whatever the outcome of this isospin assignment problem, however, the fact that additional 0^{++} I = 0/I = 1 states seem to exist around 1300 MeV keeps feeding the speculation of a second 0^{++} nonet due to multiquark $(qq\,\bar{q}\bar{q})$ states[11]. However, as before, a successful allocation of the known 0^{++} states over these two types of nonets is still missing.

1.2.2 1^+ mesons

i) There were several new developments for the 1^+ mesons. The A_1 lived up to its reputation of an on-off problematic state through the results reported by the ACCMOR Collaboration in $\pi^-p \to \pi^-\pi^-\pi^+p$ at 63 and 94 GeV/c [12]. The A_1 is observed, but at a mass of (1280 ± 40) MeV, i.e. approximately 200 MeV higher than has been seen by most of the experiments up to now[12].

More welcome information was that of the J^{PC} determination of the E(1420) meson observed in $\pi^-p \to K^0_S K^\pm\pi^\mp n$ at 4 GeV/c by the CERN-Collège de France-Madrid-Stockholm Collaboration[13]. A Zemach spin parity analysis, sensitive to the sign of the interference between the two possible K*'s in the decay modes *)

$$E \to K^{*+}K^-(K^{*+} \to K^0_S\pi^+)$$

and

$$E \to K^{*0}K^0_S(K^{*0} \to K^\pm\pi^\mp) \ ,$$

favours the C = +1 assumption and a 1^+ J^P value (see Figs. 2a and 2b).

ii) Partial wave analyses of the $(K\pi\pi)^-$ systems in the Q_1-Q_2 *region* of the reactions $K^-p \to (K\pi\pi)^-p$ at 4.2 GeV/c yield results[14] which are essentially in agreement with the ones reported by the SLAC group[15]. In the reaction $\pi^-p \to (K\pi\pi)^0\Lambda$ at 4.0 GeV/c, not only the 1^+S $Q_1(\to K\rho)$ was observed but also a $K^*\pi$ contribution in the mass region of the Q_2 (1.33-1.43 GeV) [16]. The partial wave analysis of this second peak is not yet completed. If it turns out to contain a sizeable 1^+ contribution, this finding would contradict the generally observed absence of the Q_2 in non-diffractive reactions.

iii) For the 1^{+-} *mesons* there is still no trace of the I = 0 members; were it not for these states, the L = 1 multiplets would be complete.

---

*) And thus also sensitive to C-parity, C = +1 corresponding to a constructive interference and C = -1 to a destructive one.

iv) Irving pointed out that 1^+ *meson* spectroscopy can be substantially modified by production mechanisms, and that these modifications can (sometimes) be parametrized in a consistent way[17]. An example in case are the production and decay relations for the Q/C mesons; taking into account such relations it is possible to retrieve uniquely defined SU(3) states from the different types of Q-bumps seen in forward and backward production, diffractive and non-diffractive production, etc.

1.3 The L = 2 states

A substantial amount of confirmatory evidence was presented for the (L = 2) 2^{-+} and 3^{--} nonets.

1.3.1 The 2^{-+} mesons

The ACCMOR Collaboration raised the status of the I = 1 $f^0\pi^-$ enhancement at 1640 MeV (called the A_3 meson and up to now labelled as 'a not well established resonance') to respectability by establishing the resonant nature of the 2^- S$(f^0\pi^-)$ wave, and by showing a coupling of the A_3 mass bump to the $(\rho^0\pi^-)$ and $(\varepsilon^0\pi^-)$ channels[18] [see Figs. 3a, b, c*)].

Recent information concerning the L meson, i.e. the I = 1/2 member of the 2^{-+} nonet, comes from a partial wave analysis of the $(K\pi\pi)^-$ system in the L-region using $K^-p \to (K^-\pi^+\pi^-)p$ data at 10, 14, and 16 GeV/c [19] (not presented to the conference but mentioned during the discussions). No *new* evidence for the resonant nature of the L was found, but the general dominance of an S-wave $[K^*(1420)\ \pi]$ 2^{-+} wave was confirmed. However, the authors stress that this contribution does not fully explain the L-enhancement.

1.3.2 The 3^{--} mesons

An amplitude analysis by the Bari-Bonn-CERN-Daresbury-Glasgow-Liverpool-Milano Collaboration[9] of the K^+K^- system produced in the reaction $\pi^-p \to K^+K^-n$ at 10 GeV/c yields clear confirmation of the g(1680)/ω(1670) resonances in the (zero helicity) F-wave. The $d\sigma/dt$ distribution furthermore suggests that this $|F_0|^2$ structure is mainly g^0 production.

In the backward production of ω(1670) in the reactions $K^-p \to \pi^+\pi^-\omega\Lambda$ at 8.25 GeV/c [20], evidence was found for the decay of ω(1670) into $B^\pm\pi^\mp$. A branching ratio for $B^\pm\pi^\mp/\omega\pi^+\pi^- =$ $= (1.00 \pm 0.25)$ was obtained, or alternatively $B\pi/\text{total} = (0.56 \pm 0.16)$.

Finally, confirmatory evidence for the production of K*(1780) in $K^-p \to \bar{K}^0\pi^-p$ and $\bar{K}^0\pi\pi N$ at 8.25 GeV/c was presented[21]. The angular distributions of the decay K*(1780) $\to \bar{K}^0\pi^-$ are consistent with $J^P = 3^-$. An enhancement near 1.8 GeV observed in the K(3π) mass spectra of the same experiment (and mainly associated with $K^{*-}\rho^0$) could not be positively identified as being due either to the K*(1780) or to the L(1770) [22].

1.4 The L ≥ 3 states

Further analysis of the K^+K^- system in the reaction $K^-p \to K^+K^-n$ now also suggests a new 2^{++} state at approx. 1.8 GeV with $\Gamma \sim 200$ MeV [9]. It could either enter into the L = 3 nonet or else be a radial recurrence of the A_2 meson. Further confirmation is needed however. Previously, this same analysis had shown evidence for the h meson at 2 GeV and a new ($J \geq 4$) structure at 2.2 GeV [23] (in addition to the g/ω* confirmation mentioned above).

*) Figure 3d shows evidence for a further possibly resonant 2^{-+} structure in the 2^- D$(f^0\pi)^-$ wave at 1850 MeV. In principle this could be a radial excitation of the A_3, but the fact that such a state would lie only about 200 MeV higher than the A_3 would be rather surprising. Actually the authors themselves caution against accepting this structure as a new 2^{-+} resonance before other explanations (e.g. in terms of interferences between resonance production and Deck amplitudes) are more fully explored.

The ACCMOR Collaboration provided the first real evidence for the existence of a spin-5 boson in $\pi^- p \to K^+K^- n$ at 62 GeV/c [24]. The mass and width found are (2300 ± 10) MeV and (272 ± 32) MeV, respectively. These values are not incompatible (within errors) with the state claimed at 2.2 GeV/c by C. Evangelista et al.[23]. It would have to belong to the L = 4 level.

2. THE $B\bar{B}$ MESONS

2.1 The narrow $B\bar{B}$ states (baryonium)

We refer to the plenary reviews of Povh[25] and Chan[26] for a status report on baryonium search and theoretical background.

2.1.1 Theory - Baryonium

In the parallel sessions Fukugita examined various theoretical aspects of baryonia spectroscopy in a mini-report, including four theoretical contributions presented to the Conference[27-30]. A review of the different spectrum models now used for $qq\bar{q}\bar{q}$ (= diquonium) states and of the decay properties of these states, led him to conclude that much more experimental information is needed [especially for key states such as the narrow 2.02 GeV and 2.20 GeV states[31]] in addition to a more unified understanding of meson and baryon spectroscopy, before the baryonium problem can make decisive progress.

2.1.2 The S(1936) meson

Coming back to the experimental baryonium contributions, the highlight was the report from an LBL (Berkeley)-BNL Collaboration[32] on a (low-energy) $p\bar{p}$ formation experiment nearly identical to the one performed by Carroll et al.[33]. The latter experiment is generally regarded as providing the best evidence for the $p\bar{p}$ resonance S(1936). In this new experiment (which in principle should have smaller systematic effects, e.g. as a result of a much reduced target length) no evidence for such a narrow resonance is observed, at least not for one of the magnitude seen by Carroll et al. (An upper limit of 2-4 mb is quoted.) Figure 4 illustrates the discrepancy in the *total* $p\bar{p}$ cross-section; the dashed line shows the peak expected from the Carroll et al. experiment*). The disagreement is also present in the annihilation channel $p\bar{p} \to n\bar{n}$, the total *absorption* cross-section, and the backward elastic pp scattering.

A re-analysis of old Brookhaven 30" bubble chamber data on total and partial $\bar{p}d$ cross-sections for incident momenta between 260 and 460 MeV/c was presented[34]. A discrepancy with the recent LBL-BNL experiment[32] is present, but no definite conclusion as to the existence or non-existence of the S(1936) could be drawn from this.

Kluyver[35] pointed out that in a model in which the S meson is assumed to be a baryonium state composed of I = 1 diquarks and anti-diquarks only, the S-*formation* cross-section ratios -- as they were known before the results of Ref. 32 -- can be understood as a result of I-spin conservation in the s-channel (combined with quark additivity).

*) 1936 MeV corresponds to a laboratory momentum of 500 MeV/c. Incidentally, a mass of 2020 MeV corresponds to 805 MeV/c; here, too, no structure is observed.

2.1.3 Search for other narrow $B\bar{B}$ states

A search for narrow $p\bar{p}$ and $p\bar{p}\pi$ states produced diffractively (i.e. *forward*) in the reaction $\pi^+ p \to pp\bar{p}\pi^+$ at 150 GeV/c led to a negative result[36]. In the mass ranges 2.2 GeV < $< M(p\bar{p}) < 4.0$ GeV and $1.9 < M(p\bar{p}\pi) < 2.7$ GeV and at a level of 25 nb, no states were found. The above mass bands cover the 2.02 GeV and 2.20 GeV narrow states observed by the CERN-Collège de France-Ecole Polytechnique-Orsay Collaboration[31]; it should be remembered, however, that the latter states were observed in a baryon exchange process*).

2.2 The broad $B\bar{B}$ states

2.2.1 The T, U, V mesons

An analysis of the differential cross-section data on $p\bar{p} \to \pi^+\pi^-$ in the 1-2 GeV/c laboratory momentum range[37] by Carter et al.[38] had previously led to the conclusion that the three broad resonances at 2.17, 2.33, and 2.48 GeV [known as the T, U, and V mesons since their first detection as bumps in $\sigma(\bar{p}N)$ many years ago] were mesons with $J = 3^{--}$, 4^{++}, and 5^{--}, respectively. However, to reach these conclusions some simplifying assumptions had to be made. A new analysis by Martin et al.[39] using simultaneously the $p\bar{p} \to \pi^+\pi^-$ data and recently published $p\bar{p} \to \pi^0\pi^0$ data[40] confirmed an earlier analysis by Dulude et al.[41] which had shown that the Carter solutions are ruled out by the $\pi^0\pi^0$ data. The new situation is that a $J = 5$ assignment for the V meson is still tenable, but that the resonant character of the U bump is unclear and that the T bump -- if at all a resonance -- should have a spin parity 1^- or 2^+.

2.2.2 Search for strange $B\bar{B}$ states

In a study of the reactions $K^+p \to (\bar{\Lambda}p)p$ and $K^-p \to (\Lambda\bar{p})p$ at an incident momentum of 50 GeV/c, evidence has been sought for strange counterparts of the broad $p\bar{p}$ mesons[42]. In a mass region extending up to 3 GeV, a moment analysis of the $\bar{\Lambda}p$ and $\Lambda\bar{p}$ c.m. angular distributions provides evidence for a 2^- state at 2.26 GeV and a 4^- state at 2.50 GeV, both with a width of approximately 250 MeV.

3. SEARCH FOR NARROW BARYON RESONANCES

The interest of these searches stems from the fact that they may give information on five-quark ($qqqq\bar{q}$) systems forming (narrow) colour isomers which decay dominantly into multiparticle (≥ 3) final states.

i) A search for narrow high-mass Y* hyperons by the Birmingham-CERN-Glasgow-Michigan State-Paris LPNHE Collaboration[43] in K^-p at 8.25 GeV led to the observation of a significant enhancement ($\gtrsim 5\sigma$) at a value of (3170 ± 5) MeV in the combined mass spectra of various $\Sigma|S| \geq 3$ final states (such as $R^+ = \Lambda K\bar{K}$ + pions, $\Sigma K\bar{K}$ + pions or ΞK + pions recoiling against a π^-) (see Fig. 5). The observed width is ≤ 20 MeV. Recently the ACNO Collaboration[44] has claimed the existence of a 5σ enhancement (with $\Gamma \leq 40$ MeV) at 2.58 GeV in the $\Sigma^-K^+K^0_S$ mass spectrum of the reaction $K^-p \to \Sigma^-K^+K^0_S$.

*) In this respect it might be relevant to point out that the narrow resonance reported at 2.95 GeV in the *forward* direction by another Omega spectrometer collaboration [C. Evangelista et al., Phys. Lett. 72B, 139 (1977)] was recently retracted on the basis of an experiment by essentially the same collaboration but with twelve times the original statistics [T. Armstrong et al., Phys. Lett. 85B, 304 (1979)].

ii) A (preliminary) negative result was reported[45] of a search for narrow baryon resonances coupled to the $\pi^- p$ channel. With a sensitivity for resonance detection in terms of width of $\sim$ 200 keV and in terms of elastic branching ratio of $\sim$ 5%, no evidence was found in a mass region extending from 3.5 to 5 GeV.

4. CONCLUSIONS

- There is no progress in experimental baryon spectroscopy.
- In $q\bar{q}$ meson spectroscopy there is healthy progress, especially for the L = 1 nonets, albeit that the 0^{++} situation is still unclear.
- The 'ancestor' of the narrow $B\bar{B}$ meson resonances -- the S(1936) -- is 'experimentally' in trouble. New experiments (also covering the 2.02 and 2.20 GeV narrow states) are necessary.
- The J^P assignments of the broad U, T, V states are again an open question. In the meanwhile, new (broad, but) strange states are ready to join the group of meson states coupling predominantly to $B\bar{B}$.
- Another high-mass Y* decaying into $\geq$ 3-body final states (with $\Sigma|S| \geq 3$) has been observed.

* * *

REFERENCES

1) For a review of new theoretical insights, see A.J. Hey, Particle systematics, Session IV: Hadron Physics.

2) A 3.3σ enhancement observed in K^+p interactions at 32 GeV/c decaying into $\bar{\Lambda}K^+$. Mass = (2137 ± 4) MeV. Width ≤ 20 MeV. No J^P information was obtained. E. De Wolf et al., CERN (Brussels, Mons) - Soviet Union (Serpukhov) Collab., Paper 63.

3) The final result obtained is $\mu_{\Sigma^+} = (2.30 \pm 0.14)\mu_N$, to be compared with a world average (prior to the HYBUC measurement) of $\mu_{\Sigma^+} = (2.62 \pm 0.41)\mu_N$. The new result has consequences for mass-splitting hypotheses inside quark models. S. Reucroft et al., MPI-Vanderbilt Collab., Paper 166.

4) G. Hohler, High-energy phase-shift analyses, Session IV: Hadron Physics.

5) W. Apel et al., USSR (Serpukhov) - CERN Collaboration, Paper 265.

6) R.I. Dzhelyadin et al., Observation of $\omega \to \pi^0\mu^+\mu^-$ decay, post-deadline paper submitted to this conference.

7) And the latter one, e.g. confirmed in $\pi^- p \to K^0_S K^0_S n$ at 4.0 GeV/c, R. Armenteros et al., CERN-Collège de France-Madrid-Stockholm Collab., Paper 185 *(presented by P. Loverre)*.

8) A.D. Martin et al., Nucl. Phys. B121, 154 (1977).

9) See, for example, G. Costa et al., Bari-Bonn-Daresbury-Glasgow-Liverpool-Milano-Vienna Collab., Paper 232.

10) A.D. Martin and E.N. Ozmutlu, Paper 249 *(presented by A.D. Martin)*.

11) R.L. Jaffe, Phys. Rev. D 15, 267 (1977).

12) See paper presented by G. Thompson (ACCMOR Collab.) for more details: The A_1 meson produced at 63 and 94 GeV/c in the reaction $\pi^- p \to \pi^-\pi^-\pi^+ p$, Session IV: Hadron Physics.

13) R. Armenteros et al., CERN-Collège de France-Madrid-Stockholm Collab., Paper 191 *(presented by C. Dionisi)*.

14) J. Vergeest et al., ACNO Collab., Paper 131.

15) G. Brandenburg et al., Phys. Rev. Lett. 36, 703 (1976).

16) S. Holmgren et al., CERN-Collège de France-Madrid-Stockholm Collab., Paper 184.

17) A. Irving, Liverpool preprint LTH 51 and post-deadline paper.

18) G. Thompson et al., ACCMOR Collab., Paper 57.

19) G. Otter et al., Nucl. Phys. B147, 1 (1979).

20) J.M. Scarr et al., Birmingham-CERN-Glasgow-Michigan State-Paris LPNHE Collab. Paper 77.

21) R. Zitoun et al., Birmingham-CERN-Glasgow-Michigan State-Paris LPNHE Collab., Paper 68.

22) R. Zitoun et al., Birmingham-CERN-Glasgow-Michigan State-Paris LPNHE Collab., Paper 70.

23) C. Evangelista et al., Nucl. Phys. B154, 381 (1979).

24) B. Alper et al., ACCMOR Collab., Paper 53 *(presented by E. Lorenz)*.

25) B. Povh, Very narrow states, Session IV: Hadron Physics.

26) C. Chan, Theoretical implications of very narrow states, Session IV: Hadron Physics.

27) C.S. Kalman et al., Paper 18.

28) M. Fukugita, Paper 84.

29) I.M. Barbour and D.K. Ponting, Paper 220.

30) G.R. Goldstein and J. Maharana, Paper 239.

31) P. Benkheiri et al., Phys. Lett. 68B, 483 (1977).

32) M. Alston-Garnjost et al. *(presented by R. Tripp)*, In search of baryonium (post deadline paper).

33) A.S. Carroll et al., Phys. Rev. Lett. 32, 247 (1974).

34) T. Kalogeropoulos et al., Paper 177.

35) J.C. Kluyver, Paper 156 *(presented by G. Wolters)*.

36) W.E. Cleland et al., Geneva-Lausanne-Pittsburgh Collab., Paper 204 *(presented by C. Nef)*.

37) E. Eisenhandler et al., Nucl. Phys. B96, 109 (1975).
A.A. Carter et al., Nucl. Phys. B127, 202 (1977).

38) A.A. Carter et al., Phys. Lett. 67B, 117 and 122 (1977).

39) A.D. Martin and M.R. Pennington, Paper 248.

40) R.S. Dulude et al., Phys. Lett. 79B, 329 (1978).

41) R.S. Dulude et al., Phys. Lett. 79B, 335 (1978).

42) W.E. Cleland et al., Geneva-Lausanne-Pittsburgh-Durham-CERN Collab., Paper 203 *(presented by C. Nef)*.

43) A. Burns et al., Birmingham-CERN-Glasgow-Michigan State-Paris LPNHE Collab., Paper 78.

44) C. Dionisi et al., ACNO Collab., CERN/EP Phys. 78-24 (1978).

45) P. Baillon et al., CERN-Collège de France-Ecole Polytechnique-Caen Collab., Paper 31.

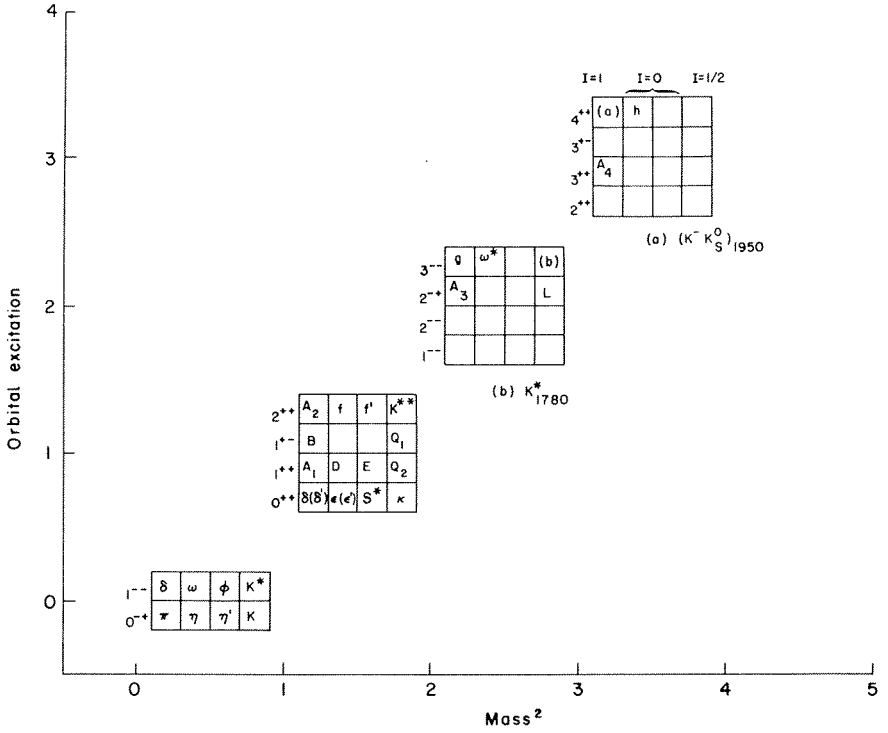
Orbital excitation
Mass²
I=1 I=0 I=1/2
(a) h
A4
(a) (K⁻ K⁰S)1950
ω*
(b)
A3
L
(b) K*1780
A2 f f' K**
B Q1
A1 D E Q2
S* κ
δ ω φ K*
π η η' K

Fig. 1

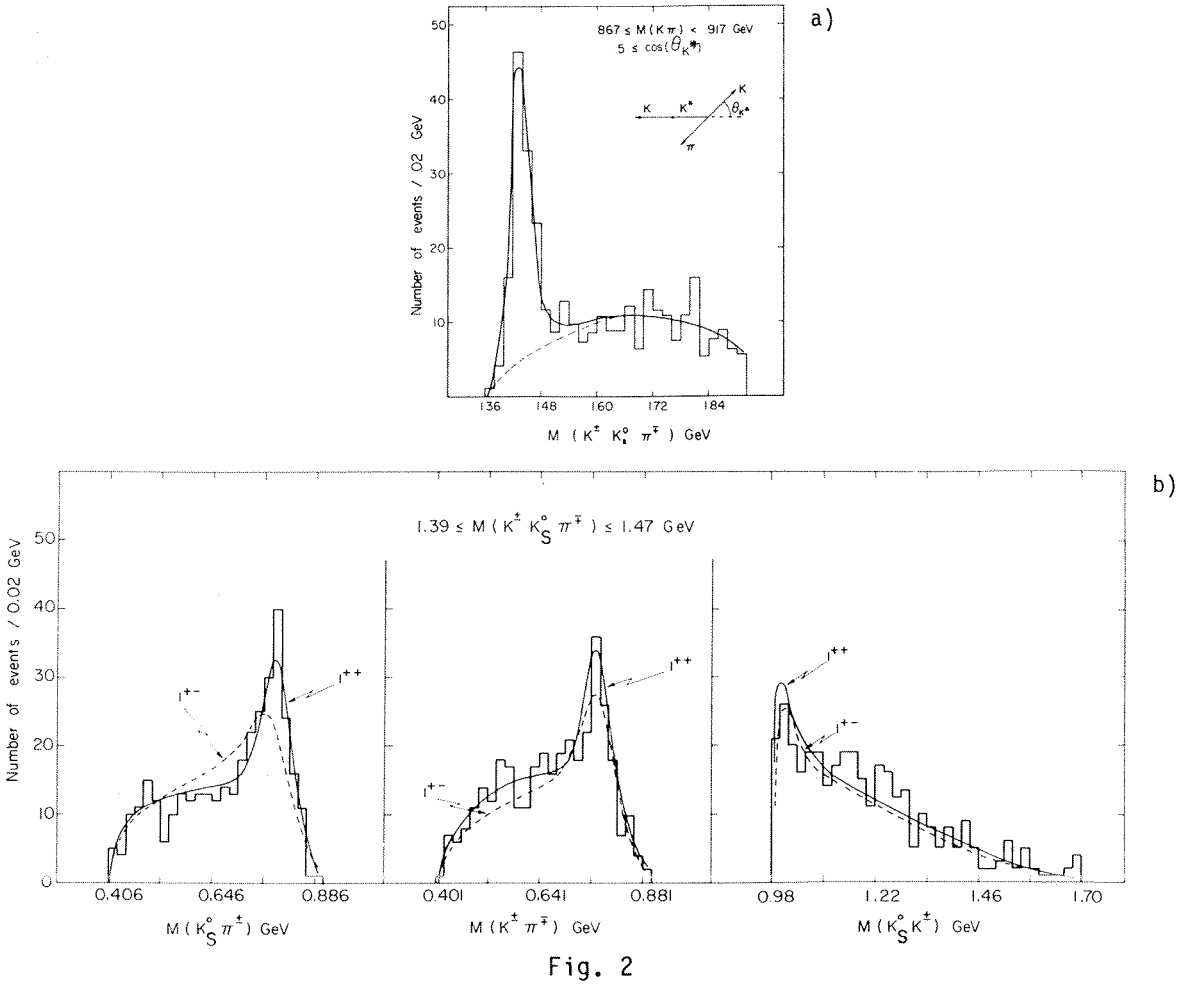
a)
867 ≤ M(Kπ) < 917 GeV
5 ≤ cos(θK*)
Number of events / .02 GeV
M (K± K°S π∓) GeV
b)
1.39 ≤ M (K± K°S π∓) ≤ 1.47 GeV
Number of events / 0.02 GeV
M (K°S π±) GeV
M (K± π∓) GeV
M (K°S K±) GeV

Fig. 2

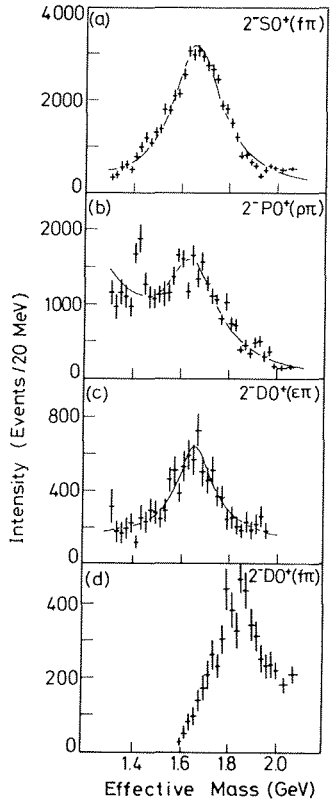

Fig. 3

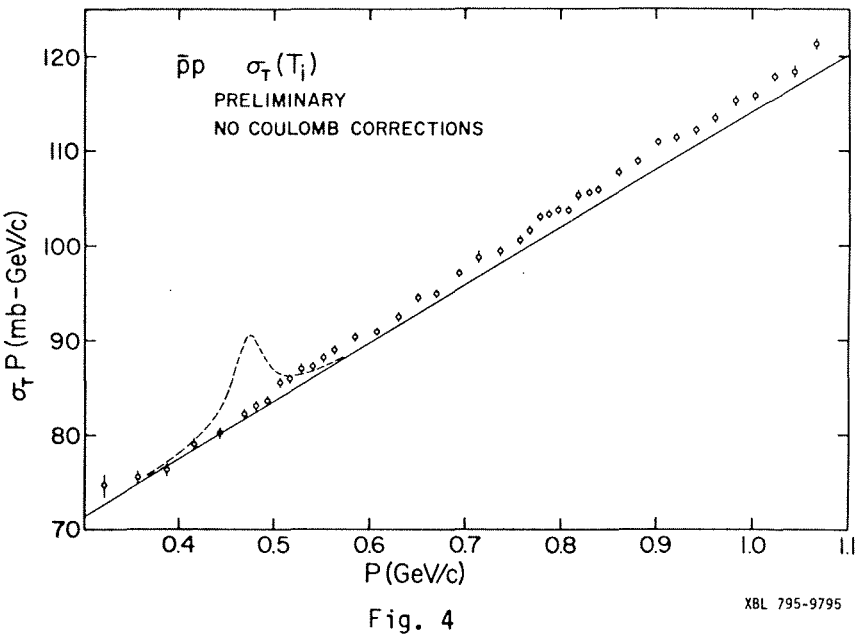

Fig. 4

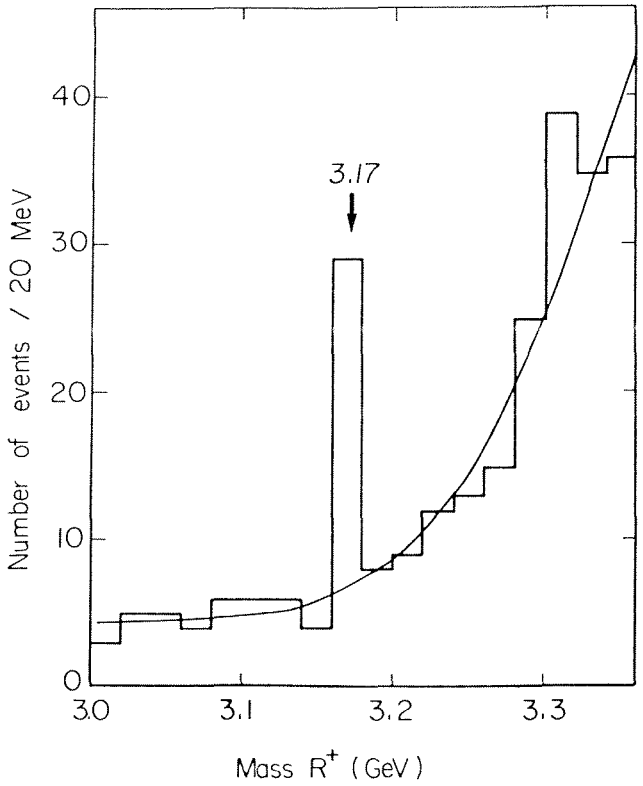

Fig. 5

PARALLEL DISCUSSION SESSION 4

WEAK INTERACTIONS AND GAUGE THEORIES

Chairman: R. Gatto

Sci. Secretaries: J. Finjord
B. Humpert

T. Appelquist	Low energy features of a 1 TeV Higgs sector
G. Segré and H.A. Weldon	Natural flavor conservation and weak mixing angles
S. Dimopoulos	Mass without scalars (abstract)
R.N. Mohapatra and G. Senjanović	Broken symmetries at high temperatures and the problem of baryon excess of the Universe
J. Ellis	SU(5)
D. Olive	Magnetic monopoles
B. Julia	Technological applications of N = 8 supergravity
S. Ferrara	Formulation of supergravity without superspace
J.G. Taylor	The ultra-violet divergences of superfield supergravity

LOW ENERGY FEATURES OF A 1 TEV HIGGS SECTOR

Thomas Appelquist

J. W. Gibbs Physics Laboratory, Yale University, New Haven, Conn., 06520, U. S. A.

ABSTRACT

It seems very likely that the Higgs sector of a spontaneously broken gauge theory could be heavy ($M \simeq 1$ TeV) and strongly interacting. By exploiting the intimate connection of such theories to nonlinear σ models, it is possible to show under quite general conditions what sort of impact the heavy Higgs sector can have on low energy experiments ($E \ll 1$ TeV). In this talk, the techniques and results will be summarized for an SU(2) gauge theory. The analysis of the Weinberg-Salam and other realistic theories will appear in a forthcoming paper.

1. INTRODUCTION

A unified theory of weak and electromagnetic interactions, based on a spontaneously broken SU(2) x U(1) gauge theory, continues to be an attractive possibility. Unfortunately, although our understanding of gauge theories has developed considerably over the last decade, we have made almost no progress in understanding the origin of spontaneous symmetry breakdown. Even if the basic gauge theory framework is correct, the dynamical origin of the Higgs symmetry breakdown remains mysterious and we continue to describe it by the ad hoc introduction of elementary, weakly self-coupled scalar fields into the Lagrangian. In the minimal model, a complex SU(2) doublet is used, providing three Goldstone bosons (longitudinal W bosons) and one physical massive scalar.

Even though dynamical symmetry breakdown is at best poorly understood, some qualitative features are to be expected. The necessary existence of zero mass Goldstone bosons to drive the Higgs mechanism suggests the presence of strong forces and that, in turn, leads to a natural guess for the mass scale of the physical spectrum in the Higgs sector. A rough estimate of this scale can be gotten in a vari y of equivalent ways. The relation $M_W = \frac{g}{2}\langle\phi\rangle$ between the W boson mass and the vacuum expectation value of an effective (or elementary) scalar field tells us that $\langle\phi\rangle \simeq 300$ GeV and so this must be a natural scale of the Higgs sector. If the forces are of unit

strength on this scale, then a mass scale on the order of or somewhat more than 300 GeV is expected.

Another way to see that this kind of mass scale is to be expected for a strongly interacting Higgs sector is to consider the conventional complex doublet theory. The ϕ^4 expansion parameter $\lambda/4\pi$ can be written in the form

$$\frac{\lambda}{4\pi} = \frac{g^2}{32\pi M_W^2} \quad M_H^2 = \frac{1}{4\sqrt{2}\pi} G_F M_H^2 \tag{1}$$

where G_F is the Fermi constant and M_H is the mass of the Higgs boson. Then as $\frac{\lambda}{4\pi} \to 1$ and perturbation theory begins to break down, $M_H \to 1$ TeV.

If the Higgs sector is heavy and strongly interacting, it is important to study its impact on the low energy ($E \ll 1$ TeV) structure of the gauge theory. Currently available center of mass energies are considerably below 1 TeV and it will be some time before 1 TeV energies are available in elementary channels such as e^+e^- or $q\bar{q}$. In this talk I will report some recent work on this problem. Part of the work is a collaboration with R. Shankar[1] which is already published and part is an ongoing collaboration with C. Bernard[2] which will be reported on in more detail in a forthcoming paper. The question being asked is to some extent independent of the detailed mechanism of spontaneous symmetry breakdown. It is really the question of whether we can learn anything about this 1 TeV world of strong interactions, whatever its origin and structure, by doing experiments at $E \ll 1$ TeV. The answer, unfortunately but perhaps not surprisingly, is that it will be very difficult.

The results I will report in this talk will be restricted to an SU(2) gauge theory. The techniques are easily extendable to the realistic SU(2) x U(1) case or any other gauge theory of interest. Some discussion of the SU(2) x U(1) model will be included in Ref. 2.

2. THE HIGGS THEORY AS AN EFFECTIVE LOW ENERGY THEORY

We use a conventional Higgs theory with elementary scalar fields, but regard the Higgs sector as a phenomenological low energy Lagrangian. The mass M_H of the physical Higgs particle(s) is regarded as a regulator for the theory when it is used beyond tree approximation. It provides a measure of low energy experimental sensitivity to a strong 1 TeV Higgs sector.

The results are expected to be quite general, depending only on the assumed symmetry properties of the Higgs sector. The situation should not be unlike pion chiral dynamics where the phenomenological Lagrangian used in tree approximation reproduces the results of current algebra and PCAC.

The first observation is that some sensitivity to M_H is indeed expected. Since the theory without the physical Higgs particles is non-renormalizable, the limit $M_H \to \infty$ does not exist: that is, the heavy sector does not decouple from the low energy physics.[2] Perhaps the best known example of this phenomenon involves the ratio $\frac{M_Z^2}{M_W^2}\cos^2\theta_W$ in the Weinberg-Salam model where $\sin\theta_W \equiv e/g$. It is constrained to be one at the tree level and has been measured experimentally to be $0.98 \pm .05$ [3]. At one loop,

$$\frac{M_W^2}{M_Z^2} = \cos^2\theta_W - \frac{11\alpha}{24\pi}\ell n\,\frac{M_H}{M_W} \qquad (2)$$

for $M_H >> M_W$ showing that the limit $M_H \to \infty$ does not exist. However even for $M_H \simeq 1$ TeV, the correction term is only of order .002 so that the measurement of this ratio isn't likely to tell us much about the heavy Higgs sector.

Every spontaneously broken gauge theory has examples of the above phenomenon : tree graph or "natural" relations which are corrected at one loop and beyond . They provide the best sensitivity to the heavy Higgs sector, and I will describe a new way of viewing these corrections and M_H sensitivity in general. It will be shown that the greatest one loop sensity to M_H is $\ell n\ M_H$ and that this arises only in the deviations from natural relations.

The Higgs sector of the model will be taken to be the minimal one which can be written in terms of a complex doublet field or, more conveniently for our purposes, in terms of the matrix field

$$M(x) = \sigma(x) + i\vec{\tau}\cdot\vec{\pi}(x) \qquad (3)$$

of the linear σ model. This exhibits the $SU(2)_L \times SU(2)_R$ symmetry of the scalar sector which plays a central role in the analysis. The left handed SU(2) is gauged leading to the Lagrangian terms $\mathrm{Tr}(F_{\mu\nu})^2$ and $\mathrm{Tr}\, D_\mu M(D^\mu M)^+$ along with the scalar potential. The choice of Landau gauge keeps M_π (the Higgs ghost mass) equal to zero so that the $SU(2)_L \times SU(2)_R$ Goldstone realized symmetry is manifest. Fermions can be introduced with couplings to

the gauge fields and scalar fields.

A convenient way to search for M_H sensitivity, which continues to keep the Goldstone realized $SU(2)_L \times SU(2)_R$ symmetry manifest, is to formally take the $M_H \to \infty$ limit at the beginning. This leads to a gauge theory coupled to the nonlinear σ model with constraint $M^+M = MM^+ = \frac{(2M_W)^2}{g^2} \equiv f^2$. This nonrenormalizable theory is equivalent to a Yang-Mills theory in which a mass term is introduced by hand rather than by Higgs. Note in particular that, from this point of view, the massive theory does not involve a broken gauge symmetry but rather a nonlinearly realized symmetry.

If higher order computations are done with this theory, the nonrenormalizability leads to divergences which force the introduction of new counterterms. These terms must be $SU(2)_L \times SU(2)_R$ symmetric and it is fairly straightforward to list the structures that can be generated at one loop. Some dimensional analysis then shows that these terms are at most logarithmically sensitive to the cutoff, which can be taken to be M_H of the original linear theory. These new terms will contain some of the vertices of the original Lagrangian and so the natural relation corrections referred to above simply reflect the presence of the new terms.

3. ONE LOOP ANALYSIS

A complete list of the new structures generated at one loop will be given in Ref. 2. I will here only describe two of them which are representative and which I will use to illustrate several important points including the natural relation corrections.

The first is $L_1 = \frac{\alpha}{f^4} [\mathrm{Tr}\, D_\mu M (D^\mu M)^+]^2$ where $D_\mu = \partial_\mu - \frac{ig}{2} \vec{\tau}\cdot\vec{W}_\mu$ and α is a dimensionless constant. This contributes a term to a π-sector Green's function proportional to four powers of the external momenta. It also gives rise to a 4W vertex with no momentum factors, but whose tensor structure differs from that arising from $\mathrm{Tr}(F_{\mu\nu})^2$ [4]. That α behaves like $\ell n\, M_H$ can be seen most easily by looking at the 4π amplitude. A power dependence on M_H would require more inverse powers of f but there are simply no more to be had at one loop. The $\ell n\, M_H$ behavior can be seen by noting that the relevant diagrams contain two particle unitarity cuts and therefore terms like $\ell n \sqrt{-(p_1+p_2)^2}$. By scale invariance, the argument of the logarithm must be $\sqrt{-(p_1^2+p_2^2)}/M_H$. This estimate of α is made completely within the nonlinear

σ model sector of the theory but the symmetry-enforced counterterm structure then links it to the gauge particle sector.

Another one-loop term is $L_2 = \frac{\beta}{f^2} g^2 \, \mathrm{Tr}\, D_\mu M (D_\nu M)^+ F^{\mu\nu}$. It has a 3W and 4W vertex as well as mixed vertices like ππW and WWπ. The estimate that $\beta \sim \log M_H$, following from unitarity and dimensional considerations, is most easily made using the ππW vertex. There is only one graph, which arises essentially from the nonlinear σ model sector, and the W is really only an external probe. The induced 3W vertex has the same structure as the one coming from $\mathrm{Tr}\, F^2$ and its presence leads to the breaking of a natural relation. To see this, let me introduce a left-handed fermion into the theory. Then, with only the Lagrangian terms of dimension four, the fermion coupling g_{ffW} must equal the 3W coupling g_{3W}. At one loop, this relation is known to be corrected according to

$$\frac{g_{ffW}}{g_{3W}} = 1 + \frac{1}{12} \frac{g^2}{16\pi^2} \log \frac{M_H}{M_W} \qquad (4)$$

Clearly the correction is due to the presence of terms like L_2 and the connection with the nonlinear σ model makes it clear that the sensitivity to M_H can be only logarithmic. The coupling g_{ffW} can be measured through $W \to f\bar{f}$ decay or fermion scattering while g_{3W} enters into processes like $f\bar{f} \to W^+W^-$. Thus the M_H dependence, while only logarithmic, is in principle a measurable effect.

In higher orders, terms of order $(\frac{M_H^2}{f^2})^P = (\, g^2 \frac{M_H^2}{4M_W^2} \,)^P$ can arise, where P is some positive integer. These terms are of order one in the limit of interest so that they cannot be reliably estimated using perturbation theory. Nevertheless, they will all be multiplied by at least one overall power of g^2 so that the corrections such as Eq. 2 and Eq. 4 might be expected to remain weak.

4. CONCLUSIONS

1. For the SU(2) model examined in detail, one loop computations can lead at most to a logarithmic sensitivity to a heavy Higgs sector. Although the perturbation expansion breaks down within the Higgs sector in this limit, the strong amplitudes within it will be shielded from the probing of gauge particles by at least one factor of g^2 (except for the logarithms I have been discussing).

2. These results depend critically on the use of the $SU(2)_L \times SU(2)_R$ symmetry of the scalar sector. It is expected that any Higgs theory which has the symmetry will lead to the same result.

3. With this symmetry, which seems rather natural from the point of view of dynamical symmetry breakdown, the heavy Higgs sector will be very difficult to see with energies below 1 TeV. Explicit one loop computations of $e^+e^- \to W^+W^-$ in the Weinberg-Salam model show small effects even at E_{CM}=200 GeV.[5]

* * *

REFERENCES

1) T. Appelquist and R. Shankar, On Gauge Theories with Heavy Higgs Bosons, to be published in Nuclear Physics.

2) T. Appelquist and C. Bernard, manuscript in preparation.

3) M. Sehgal, Invited talk at Neutrino -78, Purdue University, April-May 1978.

4) K. Shizuya, Renormalization of Two-dimensional Massive Yang-Mills Theory and Non-renormalizability of Its Four-dimensional Version, Nuclear Physics B121(1977) 125-140.

5) M. Veltman and M. Lemoine, Radiative Corrections to $e^+e^- \to W^+W^-$ in the Weinberg Model, Utrecht preprint, 1979.

NATURAL FLAVOR CONSERVATION AND WEAK MIXING ANGLES

G. Segrè and H. A. Weldon

University of Philadelphia, Pennsylvania

ABSTRACT

We show that if neutral Higgs couplings conserve flavor, mixing angles are trivial (0 or $\pi/2$). Examples and implications are discussed.

I. INTRODUCTION

During the past five years the extensive set of neutrino and polarized electron-nucleon scattering experiments have convincingly established the validity of $SU(2)_L \times U(1)$ as a phenomenological model for the weak and electromagnetic interactions[1]. Most of us believe it is more than that, and expect the discovery of the Z and $W^{\pm}$ gauge bosons to confirm the basic structure of the theory.

Even if this were to occur, there are however, still several unanswered questions. A few of these are: 1) unification problem, 2) CP problem, 3) determination of mixing angles and masses. The three may be related to one another, but in this talk the emphasis will be on problem three in isolation. Limiting ourselves to the quark sector and to $SU(2)_L \times U(1)$ models we see that for N quark doublets we have as fields

$$\psi_{iL} = \begin{pmatrix} p_i \\ n_i \end{pmatrix}_L \qquad p_{iR} \qquad n_{iR} \qquad i = 1 \ldots N \qquad (1)$$

where the p_i have charge 2/3 and the n_i charge -1/3. We have 2N quark masses, N(N-1)/2 mixing angles and $N^2 - (2N-1) - N(N-1)/2$ phases. All of these are a prior undetermined parameters, by no means a satisfactory state of affairs.

1. FOUR QUARK MODEL

For pedagogic purposes, let us concentrate on a simple four quark model with one Higgs doublet. The Yukawa couplings are then

$$\mathcal{L}_{yuk} = \sum_{i,j=1,2} \left\{ \bar{\psi}_{iL} \Gamma_{ij} \varphi n_{jR} + \bar{\psi}_{iL} \Gamma'_{ij} \tilde{\varphi} p_{jR} \right\} \qquad (2)$$

with $\tilde{\varphi} = i\sigma_2 \varphi$; Γ, Γ' are two by two matrices. The quark mass matrices M and M' for respectively n and p type quarks are:

$$M_{ij} = \lambda \Gamma_{ij} \qquad M'_{ij} = \lambda \Gamma'_{ij} \qquad (3)$$

where λ is the vacuum expectation value (v.e.v.) of the neutral component of φ. In the four quark model, we have five parameters, namely the four masses $m_{u,c,d,s}$ and the mixing angle θ_c. As usual[2] λ is related to G_F by $\lambda^{-2} = 2\sqrt{2}\, G_F$, but the arbitrariness in Γ and Γ' is such that there is no relation between the four quark masses and the mixing angle θ_c. For this to occur we must place some restriction on Γ and Γ' so that there are no more than four free parameters in $\mathcal{L}_{yuk}$.

Our line of attack is the following: we shall demand $\mathcal{L}$ be invariant under $SU(2)_L \times U(1) \times R$, where R is some discrete symmetry (in practice it may also be continuous and gauged[3]). R is such that the gauge couplings are automatically R invariant, but the Yukawa couplings are constrained by the invariance. The first important result, due to Barbieri, Gatto and Strocchi[4], is that a relation between quark masses and mixing angles can only follow if the Higgs mesons transform non-trivially under R. This automatically excludes the one Higgs field model since φ can only be transformed by a phase factor. The model in

which a single φ couples to n quarks and another Higgs field χ, instead of $\tilde{\varphi}$, couples only to p quarks is similarly excluded. We must allow therefore for at least two Higgs fields, φ_1, and φ_2, transforming non-trivially under R.

Let us illustrate these ideas with a very simple model, originally proposed by Pakavasa and Sugawara [5]. The discrete symmetry is the permutation group of three objects, S_3.[6,7] Consider three fields $\psi_{a,b,c}$; under S_3 we can form a singlet ψ_0 and a doublet $\psi_{1,2}$

$$\begin{aligned} \psi_0 &= \frac{1}{\sqrt{3}}\left(\psi_a + \psi_b + \psi_c\right) \\ \psi_1 &= \frac{1}{\sqrt{2}}\left(\psi_a - \psi_b\right) \\ \psi_2 &= \frac{1}{\sqrt{6}}\left(\psi_a + \psi_b - 2\psi_c\right) \end{aligned} \tag{4}$$

It isn't necessary for us to go into any details of S_3, except to note that under S_3 the coupling of two doublets is given by

$$2 \times 2 = 2 + 1 + 1^A$$

where 1 is a singlet and 1^A is an antisymmetric singlet. The model assumes the two $_L$ isospin doublets belong to an S_3 doublet; similarly the isospin singlets n_{1R} and n_{2R}, but the isospin singlet p_R fields both belong to S_3 singlets. There are two Higgs isospin doublets transforming like an S_3 doublet, hence non-trivially under S_3. The S_3 invariant Yukawa coupling is

$$\begin{aligned} \mathcal{L}_{Yuk} &= \bar{\psi}_i \left(\Gamma_\alpha\right)_{ij} \varphi_\alpha n_{jR} + \bar{\psi}_i \left(\Gamma'_\alpha\right)_{ij} \tilde{\varphi}_\alpha p_{jR} \\ &= f\left[\left(\bar{\psi}_1 n_{2R} + \bar{\psi}_2 n_{1R}\right)\varphi_1 + \left(\bar{\psi}_1 n_{1R} - \bar{\psi}_2 n_{2R}\right)\varphi_2\right] \\ &\quad + g\left[\bar{\psi}_1 \tilde{\varphi}_1 + \bar{\psi}_2 \tilde{\varphi}_2\right] p_{1R} + g'\left[\bar{\psi}_1 \tilde{\varphi}_1 + \bar{\psi}_2 \tilde{\varphi}_2\right] p_{2R} \end{aligned} \tag{5}$$

corresponding respectively to the S_3 doublet and S_3 singlet in the decomposition of two times two in S_3. Remember that despite the labels $p_{1,2R}$, both p_{1R} and p_{2R} are S_3 singlets (perhaps we should have called them p_{oR} and p'_{oR}).

Let us now count parameters; phases may be absorbed into the definition of quark fields in the four quark model, so we are left with four parameters, the magnitudes of[8]

$$f, g, g', \lambda_1/\lambda_2$$

in terms of which we wish to express the four quark masses and the mixing angle θ_c. Clearly there will be a non-trivial restriction .

We now look for the unitary transformations which diagonalize the mass matrices

$$\begin{aligned} U_L^\dagger \Gamma_\alpha \lambda_\alpha U_R &= \hat{M} = \begin{pmatrix} m_d & 0 \\ 0 & m_s \end{pmatrix} \\ U_L'^\dagger \Gamma'_\alpha \tilde{\lambda}_\alpha U'_R &= \hat{M}' = \begin{pmatrix} m_u & 0 \\ 0 & m_c \end{pmatrix} \end{aligned} \tag{6}$$

where we neglect the phases of the coupling constants which can be reabsorbed. The results are

$$U_L = \frac{1}{\sqrt{2}}\begin{pmatrix} 1 & 1 \\ -i & i \end{pmatrix} \qquad U_R = \frac{1}{\sqrt{2}}\begin{pmatrix} -i & i \\ 1 & 1 \end{pmatrix} \qquad m_{d,s} = f\left|\frac{\lambda_1 \pm i\lambda_2}{\sqrt{2}}\right| = f\lambda_\pm$$

$$U_L' = \frac{1}{\lambda}\begin{pmatrix} \lambda_2 & \bar{\lambda}_1 \\ -\lambda_1 & \bar{\lambda}_2 \end{pmatrix} \qquad U_R' = \frac{1}{\sqrt{g^2+g'^2}}\begin{pmatrix} -g' & g \\ g & g' \end{pmatrix} \qquad m_c = \lambda\sqrt{g^2+g'^2} \qquad (7)$$

$$m_u = 0$$

where of course, $\lambda = \sqrt{|\lambda_1|^2+|\lambda_2|^2}$. The relation between masses and mixing angles follows by transforming the gauge coupling to the physical basis

$$W^\mu \bar{p}_{iL}\gamma_\mu n_{iL} = W^\mu(\bar{u}_L\ \bar{c}_L)\, U_L'^{\dagger}\gamma_\mu U_L \begin{pmatrix} d_L \\ s_L \end{pmatrix}$$

$$= W^\mu(\bar{u}_L\ \bar{c}_L)\,\gamma_\mu A \begin{pmatrix} d_L \\ s_L \end{pmatrix} \qquad (8)$$

$$A = U_L'^{\dagger}U_L = \frac{1}{\lambda}\begin{pmatrix} \lambda_+ & -\lambda_- \\ \lambda_- & \lambda_+ \end{pmatrix}$$

which implies

$$\tan\theta_c = \lambda_-/\lambda_+ = m_d/m_s \qquad (9)$$

so we have the desired relation between masses and mixing angles. A further interesting feature of the model can be seen from the unitary transformations in equation (7), namely $U_{L,R}$ are independent of λ and f. This means that they diagonalize not only $\Gamma_\alpha \lambda_\alpha$, but $\Gamma_\alpha \varphi_\alpha$ as well.

$$U_L^{\dagger}\Gamma_\alpha \varphi_\alpha U_R = \varphi_1\begin{pmatrix} f & 0 \\ 0 & f \end{pmatrix} + \varphi_2\begin{pmatrix} -if & 0 \\ 0 & -if \end{pmatrix} \qquad (10)$$

This says that the Higgs couplings are diagonal in the physical quark basis, i.e. no $\bar{d}_L s_R$ or $\bar{s}_L d_R$ terms are present. For the u and c quarks $\bar{u}_L c_R$ and $\bar{c}_L u_R$ terms are present however as one readily sees by evaluating

$$U_L'^{\dagger}\Gamma_\alpha'\tilde{\varphi}_\alpha U_R'$$

The model has several problems (only four quarks, $m_u = 0$, pseudo Goldstone bosons[6] etc), but the two features we wish to focus on are

1) calculability of θ_c
2) flavor changing neutral Higgs couplings

The question is can we preserve 1) while avoiding 2). A priori it seems possible; the S_3 assignment we tried was

$$\psi \in 2 \qquad \varphi \in 2 \qquad n_R \in 2 \qquad p_R \in 1 \oplus 1$$

We could assign instead p_R to the two representation, but this doesn't work since θ_c is then equal to zero, as there is obviously no difference between U_L and U_L'. A more subtle change is to have $p_R \in 2$, but to have p_R couple to two new Higgs fields χ_o, χ_o' belonging to the 1 and 1^A representation of S_3 rather than to $\tilde{\varphi}$ and n_R couple only to φ. Miraculously[9] enough, the diagonalization of the p mass matrix through the transformations

$$U'_L = U'_R = \frac{1}{\sqrt{2}} \begin{pmatrix} 1 & 1 \\ i & -i \end{pmatrix}$$

also diagonalizes the p quark Yakawa couplings. However we discover that

$$U'^{\dagger}_L U_L = \begin{pmatrix} 0 & 1 \\ 1 & 0 \end{pmatrix}$$

so $\theta_c = \pi/2$. As we shall see shortly this problem is not specific to the model: natural flavor conservation of Higgs couplings inevitably leads to trivial (0 or $\pi/2$) mixing angles.

II. $\Delta S = 2$ LIMITS

Before we go on to the proof, let us digress briefly on the problems that arise when neutral Higgs couplings are not flavor preserving. Though it may happen, as we have seen, that strangeness is conserved, despite flavor violation, in general we will have neutral Higgs coupling to $\bar{d}_L s_R$ and $\bar{s}_L d_R$ when flavor is not conserved, or an effective $\Delta S = 2$ low energy phenomenological Lagrangian of the form

$$\mathcal{L}^{\Delta S=2} \sim \left\{ f_1^2 (\bar{d}_L s_R)^2 + f_2^2 (\bar{s}_L d_R)^2 \right\} / M_H^2 \qquad (11)$$

The Higgs couplings $f_{1,2} \sim G_F^{\frac{1}{2}}$ m and, from experience with models, we find characteristically $m \gtrsim \sqrt{m_d m_s}$. The most stringent limits on $\mathcal{L}^{\Delta S=2}$ come from the $K_L - K_S$ mass difference

$$\left(\frac{M_L - M_S}{M_K} \right) = 0.7 \times 10^{-14}$$

Using (11), sandwiched between K^0 and $\bar{K}^0$ states we find that compatibility with experiment requires $M_H \gtrsim$ 1 Tev. If the coupling constants $f_{1,2}$ are complex, the limits imposed by CP violation on the imaginary part of the $K^0 - K^0$ mass matrix lead to $M_H \gtrsim$ 10 Tev. In either case such heavy Higgs masses appear to conflict with our naive ideas of Higgs couplings[11].

III. SCENARIOS

At this point let us display the two avenues open to us

1) One Higgs coupling

a) $\mathcal{L}_{YUK.} = \bar{\psi} \Gamma \varphi n_R + \bar{\psi} \Gamma' \tilde{\varphi} p_R$

b) $\mathcal{L}_{YUK} = \bar{\psi} \Gamma \varphi n_R + \bar{\psi} \Gamma' \tilde{\chi} p_R$

$\longrightarrow$ flavor preserving Higgs couplings, but undetermined mixing angles

2) Several Higgs couplings

In general neutral Higgs mesons will mediate flavor changing neutral current interactions (neutral gauge bosons will not; for conditions see ref. 12). We have two choices now

a) If we impose natural flavor conservation of neutral Higgs coupling (natural means independent of values of v. e. v.'s), mixing angles are either zero or $\pi/2$. This remarkable result is proved in Refs. 9 and 13,14. Are there ways around it? Two thoughts leap to mind: the first is to try a larger gauge group such as $SU(2)_L \times SU(2)_R \times U(1)$, but this doesn't work, as shown in Ref. 13. In general larger gauge groups are more restrictive than $SU(2)_2 \times U(1)$ so there is less freedom in the mixing angles. The second thought is to accept vanishing mixing angles at the tree level, but generate them by radiative corrections. In a recent preprint[15] we have shown that this fails: we do this by displaying a discrete symmetry which persists even after the spontaneous symmetry breaking, as long as the mixing angles are zero in tree approximation. Essentially under this discrete symmetry neutral

bosons are unchanged, charged bosons change sign and, in the four quark example

$$d,s,u,c \rightarrow -d,s,u,-c$$

This discrete symmetry remains unbroken and thus forbids Cabibbo mixing to any order in perturbation theory.

b) If we do not impose natural flavor conservation, we may determine the mixing angles in terms of quark masses. The price to be paid is the existence of strangeness changing neutral Higgs couplings; the mesons which mediate this should then probably be made very heavy by adding terms to the Higgs potential along the lines suggested by Georgi and Nanopoulos[16]. Alternatively one could look for models in which there is only partial flavor violation, in particular there are no strangeness changing neutral currents. Examples of this are given in reference nine, one being of course the Pakvasa - Sugawara model itself.

IV. PROOF OF CONFLICT BETWEEN NATURAL FLAVOR CONSERVATION AND NON TRIVIAL MIXING ANGLES

We shall sketch here the first step of the proof of the result mentioned in the beginning of 1a) of section III. Given

$$\mathcal{L}_{Yuk} = \bar{\psi}\,\Gamma_\alpha\,\varphi_\alpha\,n_R + \bar{\psi}\,\Gamma'_\alpha\,\tilde{\chi}_\alpha\,p_R \qquad (12)$$

invariant under a set of discrete symmetries whereby

$$\begin{aligned} p_L &\rightarrow K'_L\,p_L & p_R &\rightarrow K'^{\,\prime}_R\,p_R \\ n_L &\rightarrow K'_L\,n_L & n_R &\rightarrow K'_R\,n_R \\ \varphi_\alpha &\rightarrow D^{i\,*}_{\alpha\beta}\,\varphi_\beta & \tilde{\chi}_\alpha &\rightarrow D^{i\,\prime}_{\alpha\beta}\,\tilde{\chi}_\beta \end{aligned} \qquad (13)$$

the invariance of $\mathcal{L}_{yuk}$ requires

$$\begin{aligned} K'_L\,\Gamma_\alpha\,K'_R &= D^{i\,*}_{\alpha\beta}\,\Gamma_\beta \\ K'_L\,\Gamma'_\alpha\,K'^{\,\prime}_R &= D^{i}_{\alpha\beta}\,\Gamma'_\beta \end{aligned} \qquad (14)$$

where the D^i are unitary matrices. Though p_L, n_L must transform the same way under the discrete symmetry since they form an isospin doublet, the mass eigenstates

$$d_L = U_L^{+}\,n_L \qquad U_L = U_L'\,p_L$$

transform under the discrete symmetry as

$$\begin{aligned} d_L &\rightarrow S^i_L\,d_L & S^i_L &= U_L^{+}\,K^i_L\,U_L \\ u_L &\rightarrow T^i_L\,u_L & T^i_L &= U_L^{+\prime}\,K^i_L\,U'_L \end{aligned}$$

and S^i_L and T^i_L are related by the identity

$$A^{+}T^i_L\,A = S^i_L$$

where A is the mixing matrix

$$A = U_L'^{+}\,U_L$$

The proof consists of two parts: the first is to show that S^i_L, T^i_L are unitary monomial matrices (one non zero entry of unit magnitude in each row and each column). For the Yukawa

couplings to be flavor conserving we must have

$$U_L^\dagger \Gamma_\alpha U_R = \hat{\Gamma}_\alpha \qquad \text{a diagonal matrix} \quad \forall \alpha$$

and (14) then implies that under the discrete symmetries

$$S_L^{i\dagger} \hat{\Gamma}_\alpha S_R^i = D^i_{\alpha\beta}{}^* \hat{\Gamma}_\beta \qquad (16)$$

The diagonal mass matrix M is of course

$$\hat{M} = \hat{\Gamma}_\alpha \lambda_\alpha$$

Multiplying $S_L^{i\dagger} \hat{M} S_R^i$ by its adjoint we see that

$$S_L^{i\dagger} \hat{M} \hat{M}^\dagger S_L^i = \lambda_\alpha \bar{\lambda}_\mu D^i_{\alpha\beta}{}^* D^i_{\mu\nu} \hat{\Gamma}_\alpha \hat{\Gamma}_\nu^\dagger$$

$$= \text{diagonal matrix}$$

As long as the quark masses are non degenerate the matrices S_L^i which take diagonal matrices into diagonal matrices are unitary monomial matrices; ditto for T_L^i.

The second step is to show that A which accomplishes the equivalence between S_L^i and T_L^i is also a unitary monomial matrix (if this is true all mixing angles have cosines equal to zero or one). This involves the assumption that the quark isospin doublets form an irreducible representation of the horizontal symmetry group (when they don't there are some basically uninteresting exceptions to our result, which are sketched in Ref. 9). For thorough discussions see refs. 9,13,14.

REFERENCES

1) S. Weinberg, Phys. Rev. Lett. 19, 1264(1967), A. Salam, Proc. 8th Nobel Symposium, p. 367, (Alimquist and Wiskell, Stockholm 1968).

2) e.g., E. S. Abers and B. W. Lee, Physics Reports, 1973.

3) F. Wilczek and A. Zee, Phys. Rev. Letts. 42(1979), 421.

4) R. Barbieri, R. Gatto and F. Strocchi, Phys. Lett. 74B, (1978), 344.

5) S. Pakvasa and H. Sugawara, Phys. Lett. 73B, (1978), 224.

For recent applications of S_3 with discussions of couplings see:

6) V. Goffin, G. Segrè and H. A. Weldon, "Explicit one Loop Corrections to the Strong CP Violating Phase", Univ. of Penn., preprint UPR-0113T, 6/79.

7) E. Derman, Phys. Lett. 78B, (1978), 497.

8) It is now $\lambda^2 = |\lambda_1|^2 + |\lambda_2|^2$ that equals $\left(2\sqrt{2}\, G_F\right)^{-1}$ so λ_1/λ_2 is a free parameter.

9) These examples are discussed in:
G. Segrè and H. A. Weldon, "The Conflict between Natural Flavor Conservation of Higgs Couplings and Cabibbo Mixing in $SU(2)_L \times U(1)$", Univ. of Penn. preprint UPR 0125T, to be published in Annals of Physics.

10) For a discussion of $\Delta S = 2$ see e.g. J. Ellis, M. K. Gaillard and D. V. Nanopoulos Nucl. Phys. B109, 213, 1976.

11) M. Veltman, Acta Physics Polonica B8, 475 (1977), B. W. Lee, C. Quigg and H. Thacker Phys. Rev. Lett. 38,883 (1977).

12) S. L. Glashow and S. Weinberg, Phys. Rev. D15, 1958, 1977, E. Paschos, Phys. Rev. D15, 1980,1977.

13) R. Gatto, G. Morchio and F. Strocchi, Phys. Lett. 80B, 265, 1979.

14) R. Gatto, G. Morchio and F. Strocchi, Phys. Lett. 83B, 348, 1979.
see also:

R. Gatto, Univ. of Geneva preprint UGVA-DPT, 199, 4/79, G. Sartori, UGVA, 187, 12/78.

15) G. Segrè and H. A. Weldon, Univ. of Penn, preprint UPR 0129T (1979).

16) H. Georgi and D. V. Nanopoulos, Phys. Lett. 82B, 95 (1979).

MASS WITHOUT SCALARS

S. Dimopoulos

Physics Department, Columbia Univ., NY, USA.

ABSTRACT

It is argued that realistic fermion and vector boson masses can arise in theories without fundamental scalars. The scalars are replaced by new strong gauge groups and "heavy" fermions with masses of the order of 1 TeV and 100 TeV. In such models the strong CP problem is solved and a naturally small CP violation can be introduced.

These models are very natural in the sense that physics at large distances ($> 10^{-17}$ cm) does not sensitively depend on minute details of the bare physics at small distances ($< 10^{-28}$ cm). The chief disadvantage is the epicyclic proliferation of new gauge groups.

BROKEN SYMMETRIES AT HIGH TEMPERATURES AND THE PROBLEM OF BARYON EXCESS OF THE UNIVERSE

Rabindra N. Mohapatra* and Goran Senjanović**
Department of Physics, Brookhaven National Laboratory, Upton, New York 11973

ABSTRACT
We discuss a class of gauge theories, where spontaneously broken symmetries, instead of being restored, persist as the temperature is increased. Applying these ideas to the specific case of the soft CP-violation in grand unified theories, we discuss a mechanism to generate the baryon to entropy ratio of the universe.

1. INTRODUCTION

Several years ago it was suggested by Kirzhnitz and Linde[1,2] that the spontaneously broken gauge and global symmetries of nature may be restored if the system is heated to a sufficiently high temperature exactly the same way as heating a superconductor breaks Cooper pairs above the critical temperature and destroys the state of order. Since spontaneously broken gauge theories are excellent candidates for description of weak interactions, above the critical temperature $T_c \sim m_W/g$, the charged and neutral gauge mesons mediating weakinteractions would become massless leading to a basically different form of weak interactions at higher temperatures. This may enable us to test (at least in principle) whether the broken gauge symmetry of weak interactions is real or just a mathematical artifact to arrive at an effective Lagrangian. If this wisdom is accepted the same kind of symmetry restoration would take place for discrete symmetries such as P[3] and CP[4] as well if they were broken softly at low temperature. On the other hand, the recently suggested mechanism[5] to understand the matter-antimatter asymmetry of the universe requires that there must be B as well as CP-violating interactions at extremely high temperature ($T \sim 10^{15}$ GeV) in the very early moments ($t \sim 10^{-36}$ sec.) of the universe[6]. Since, according to the prevaling folklore, the characteristic temperature at which soft CP-violation disappears is $\sim 10^3$ GeV, the Lagrangian describing weak interaction must be CP-violating[7] prior to symmetry breakdown (i.e. hard CP-violation), if we want to tackle the problem of baryon to entropy ratio in these terms. Such a hard CP-violation model, however, would preclude any understanding[8] of the strong CP-problem[9] posed by Quantum Chromodynamics. In order to develop theories, which would simultaneously cure the strong CP-problem as well as provide a mechanism for the cosmological production of baryons via the scenario outlined above, we recently began a careful study[10] of the behaviour of broken gauge symmetries at high temperature in the context of various Quantum Flavor Dynamics models. A plausible basis for our discussion can be given in terms of the following intuitive argument. In flavor

*) Permanent Address: City College of City Univ. of New York, New York 10031.
Work supported by National Science Foundation Grant No. PHY-78-2488 and PSC-BHE research award no. 13096.
**)Present address: Univ. of Maryland, College Park, Md. 20742; work supported by National Science Foundation.

dynamics models with a single order parameter (i.e. one Higgs doublet) the restoration of symmetry at high temperature would appear automatic by the laws of thermodynamics (i.e. entropy must increase!). However, in models with more than one order parameter (more Higgs doublets), the thermodynamic principles simply require that, the entropy of the whole system increase; but it is conceivable that the state of order in one sub-system could be reinforced whereas in the complementary system, the state of order is destroyed as temperature rises. In the context of a large class of gauge models[10] we showed that there exist perfectly acceptable domains of coupling parameters, where one or more Higgs fields $\langle\phi_i\rangle$ remains nonzero while another one $\langle\chi\rangle$ goes to zero above critical temperature as the system is heated. They provide counter examples to the common lore in that in these models, the gauge (or global) symmetry is not restored at high temperature and also in such models, soft CP-violation persists even at ultrahigh temperature. This has important cosmological applications. This review is organized as follows: in sec. II, we summarize the main points of our work in the context of the O(N) gauge model with two vector Higgs multiplets. In sec. III, we discuss the question of cosmological baryon production using these ideas in the context of a grand unified model. There we also summarize our result and conclude our discussion giving other applications.

2. O(N) MODEL WITH BROKEN GAUGE SYMMETRY

Here we discuss a simple O(N) model with spontaneous symmetry breaking occurring at zero temperature. The model consists of two vector representations $\vec{\phi}$ and $\vec{\psi}$. At T=0 the Higgs potential allowed by gauge symmetry is given by

$$V(\vec{\phi},\vec{\psi}) = -\frac{\mu_1^2}{2}\vec{\phi}^2 - \frac{\mu_2^2}{2}\vec{\psi}^2 + \frac{\lambda_1}{4}(\vec{\phi}^2)^2 + \frac{\lambda_2}{4}(\vec{\psi}^2)^2 + \frac{\lambda_3}{2}\vec{\phi}^2\vec{\psi}^2 + \frac{\lambda_4}{2}(\vec{\phi}\cdot\vec{\psi})^2 \quad . \tag{2.1}$$

We look for the minimum of the potential in the form of:

$$\langle\vec{\phi}\rangle^2 = v_1^2, \quad \langle\vec{\psi}\rangle^2 = v_2^2 \quad (v_1,\ v_2 \neq 0). \tag{2.2}$$

We also chose:

$$\lambda_4 > 0$$

In the case, $\langle\vec{\phi}\rangle\cdot\langle\vec{\psi}\rangle = 0$ at the minimum; so we can choose:

$$\langle\vec{\phi}\rangle = \begin{pmatrix} 0 \\ \cdot \\ \cdot \\ \cdot \\ v_1 \end{pmatrix}, \quad \langle\vec{\psi}\rangle = \begin{pmatrix} 0 \\ \cdot \\ \cdot \\ \cdot \\ v_2 \\ 0 \end{pmatrix} . \tag{2.3}$$

The equations for v_1 and v_2 are

$$\begin{aligned} \mu_1^2 &= \lambda_1 v_1^2 + \lambda_3 v_2^2 \\ \mu_2^2 &= \lambda_2 v_2^2 + \lambda_3 v_1^2 \quad . \end{aligned} \tag{2.4}$$

The positivity of Higgs scalar masses leads to further constraints

$$\lambda_1\lambda_2 > \lambda_3^2 \tag{2.5}$$

We now compute the one loop induced temperature dependent terms in the potential $V_1(T)$ using the general form given by Weinberg[2)]

$$V_1(T) = \frac{1}{48} T^2 \left[6g^2(T_\alpha T_\alpha)_{ij} + f_{ijkk}\right] \psi_i\psi_j \tag{2.6}$$

where T_α are the generators of the gauge group; ψ_i counts all the scalar fields and $f_{ijk\ell} \equiv \frac{\partial^4 V}{\partial\psi_i \partial\psi_j \partial\psi_k \partial\psi_\ell}$. In our case, we get

$$V_1(T) = \frac{1}{24} T^2 \left[b_1\vec{\phi}^2 + b_2\vec{\psi}^2\right] \tag{2.7}$$

with

$$b_i = (N+2)\lambda_i + N\lambda_3 + \lambda_4 + \frac{3}{4}(N-1)g^2 \tag{2.8}$$

$i = 1.2$. It is now clear that if we chose $\lambda_3 < 0$ and

$$(N+2)\lambda_1 + \lambda_4 + \frac{3}{4}(N-1)g^2 < N|\lambda_3| \tag{2.9}$$

then $b_1 < 0$. Notice that $b_2 > 0$, since λ_2 has to be taken sufficiently large (still of order g^2) to satisfy (2.5). Therefore, above critical temperature T_C given by

$$12\mu_2^2 = \left[(N+2)\lambda_2 + N\lambda_3 + \lambda_4 + \frac{3}{4}(N-1)g^2\right]T_C^2 \tag{2.10}$$

$\langle\vec{\psi}\rangle$ vanishes, but $\langle\vec{\phi}\rangle$ remains broken at all temperatures. In conclusion, the symmetry remains broken at high temperatures.

An important point to note is that for this to happen, several Higgs couplings (such as λ_2, λ_3) must be bigger than g^2, the square of the gauge coupling constant. Furthermore, at zero temperature, we must have $v_1 >> v_2$. Thus, it is the smaller of the two vacuum expectation values, that vanishes at high temperatures. It is also obvious from eqs. (2.5) and (2.8) that, it is never possible to have both $\langle\vec{\phi}\rangle$, $\langle\vec{\psi}\rangle \neq 0$.

A few remarks are needed regarding the fermions. Up to now we have ignored them completely. Their contribution to $V_1(T)$ can be easily shown to be of order of h^2, where h is a typical Yukowa coupling. In most gauge theories, for all the known fermions $h^2 << g^2$, which means that their inclusion will not affect our analysis.

One further noteworthy feature of this model is the behaviour of the particle masses with temperature. Namely, at high temperatures ($T > T_c$)

$$\langle\vec{\psi}\rangle = 0$$

and

$$|\langle\vec{\phi}\rangle_T| = \sqrt{\langle\vec{\phi}\rangle_{T=0}^2 + c^2T^2} \tag{2.11}$$

where c is a constant $c \gtrsim 1$. Approximately then (at $T >> T_c$)

$$|\langle\vec{\phi}\rangle_T| = cT \ . \tag{2.12}$$

Therefore gauge mesons, and those fermions and Higgs particles that get the

masses from the $<\phi>$ expectation value, will have their masses increase with temperatures

$$m(T) \propto T \tag{2.13}$$

at sufficiently high temperatures. This will become relevant when we discuss a realistic grand unified theories in the subsequent section.

3. GRAND UNIFIED THEORIES AND THE PROBLEM OF BARYON EXCESS

In the preceding sections we have learned how a symmetry may remain broken at high temperatures. Of course, one of the basic motivations for studying such effects as we emphasized in the introduction, is the fact that if CP and baryon nonconserving interactions survive at high temperature then they may be responsible for creating matter-antimatter symmetry out of an originally symmetric universe. In this section we therefore apply these ideas to the grandunified theories[12] which provide a natural basis for such phenomena since they are in general characterized by baryon number violating interactions.

Our analysis is done for the simplest of grandunified theories, the SU(5) model of Georgi and Glashow.[12] In order to discuss CP-violation, we have to recall the Higgs sector of the theory. It consists of two types of multiplets: a $\underline{24}$ dimensional adjoint representation which provides the strong symmetry breaking down to SU(3) x SU(2) x U(1) and gives the masses to superheavy gauge mesons which mediate proton decay and a $\underline{5}$ dimensional fundamental representation which is responsible for the breaking of SU(2) x U(1) down to U(1) (it gives the masses to $W^{\pm}$, Z and fermions).

Now, in the minimal scheme with one five dimensional multiplet, the CP has to be built in the Lagrangian prior to the symmetry breaking through the complex Yukawa couplings, since the vacuum expectation value of $\underline{5}$ can always be chosen to be real by means of a gauge rotation. It is therefore necessary for our purpose of constructing a soft VP violating theory to increase the number of fundamental representations of SU(5). Since the Higgs self-couplings that mix $\underline{24}$ and $\underline{5}$ are small in order not to affect the light mass scale by the heavy one, we cannot rely on such couplings to dominate over positive contributions of gauge mesons of order g^2 in the coefficients of the temperature dependent terms in the potential (for the sake of our discussion, we will safely ignore such couplings). Now, similarly as in the case of the single O(N) model discussed in section II, it turns out that in the model with two $\underline{5}$'s the vacuum expectation values of both the multiplets cannot be nonvanishing at high temperatures. This implies that a necessary condition for soft CP-violation in SU(5) models to persist at high temperatures is that, there must be more than two $\underline{5}$ dimensional Higgs multiplets in the theory, the situation completely analogous to the one in $SU(2)_L$ x U(1) gauge model of weak and electromagnetic interactions where one needs at least three Higgs doublets for the same reason. The $SU(2)_L$ x U(1) model was discussed previously by us in detail.[10]

In conclusion, the soft CP-violation at high temperatures requires three $\underline{5}$'s denoted by ϕ_1, ϕ_2 and χ, with the zerotemperature pattern of symmetry breaking

$$\langle\phi_i\rangle_{T=0} = \frac{1}{\sqrt{2}} \begin{pmatrix} o \\ o \\ o \\ o \\ \rho_i\ e^{i\theta_i} \end{pmatrix}, \quad \langle\chi\rangle_{T=0} = \frac{1}{\sqrt{2}} \begin{pmatrix} o \\ o \\ o \\ o \\ v \end{pmatrix} \tag{3.1}$$

where $\theta_1=0$, $\theta_2=\theta$. If we write the one loop induced temperature dependent term in the potential as

$$V_1(T) = T^2\ [b_i\ \phi_i^+\phi_i\ + b_\chi\ \chi^+\chi] \tag{3.2}$$

then, as we have shown,[10] one can choose

$$b_i < 0,\ b_\chi > 0\ . \tag{3.3}$$

Therefore, above a critical temperature $\langle\chi\rangle = 0$, but $\langle\phi_i\rangle \neq 0$ and increase with temperature, i.e. $\langle\phi_i\rangle \simeq c_i T$ for $T >> T_c$. The CP phase θ also remains nonzero at the minimum at all temperatures.

To dicsuss the baryon production in this model, we have to know how the fermion masses grow tith etmperature and in particular, whether at temperatures of the order of 10^{15} GeV, the fermions are light enough to be produced in the decay of the superheavy bosons, X, Y. It actually turns out that, fermion masses $m_f \simeq 10^{-4}$ T (in GeV). Therefore, at 10^{15} GeV, fermion masses are negligible compared to the masses of X and Y bosons. To see this, note that at high T

$$\langle\phi_i\rangle \simeq T \tag{3.4}$$

so the fermion mass, $m_f(T)$ is for large T given by

$$m_f(T) \simeq h(T)T \tag{3.5}$$

where h(T) refers to Yukawa couplings at temperature T. Now $h(0) \simeq g(0)\ \frac{m_f(0)}{m_W(0)} \simeq 10^{-4}$ where (0) denotes the zero temperature value of relevant couplings. Since Yukawa couplings in gauge theories are asymptotically free, that is they decrease with temperature, we conclude from (3.5) that $m_f(T) \lesssim 10^{-4}T$. This implies that, if $T \sim m_X$, then $m_f/m_X \lesssim 10^{-4}$. The second fact to be considered is that since fermions are still massive at these high temperatures, the interaction of both the superheavy gauge bosons as well as the Higgs mesons, with fermions containing CP-violating pieces, as does the normal W-boson weak interactions of fermions. Now we are ready to discuss the problem of cosmological baryon production.[5] It has already been emphasized in several papers that, if either the X, and Y bosons or the Higgs boson H_i decay into two channels with final state baryon numbers B_1 and B_2, with branching ratios γ and $1-\gamma$ then the baryon to entropy ratio n_B/n_γ is given by:[5]

$$\frac{n_B}{n_\gamma} \simeq \frac{N_X}{N} \Delta B \tag{3.6}$$

where N_X is the concentration of the bosons that mediate B violating interactions and N is the concentration of photons at 10^{15} GeV,

$$\Delta B = (\gamma - \bar{\gamma})\ (B_1 - B_2)\ , \tag{3.7}$$

$\bar{\gamma}$ is the corresponding branching ratio for antiparticles $\bar{X}$, $\bar{Y}$ and $\bar{H}$. N_X/N is of the order of 10^{-2}. To compute $(\gamma-\bar{\gamma})$, we note that, we have to take into account the interference between the Born diagram and the one loop correction to it. Writing the various decay widths

$$\gamma\Gamma_{tot} = |g + h\ A(s + i\varepsilon)|^2 \tag{3.8}$$

$$\bar{\gamma}\Gamma_{tot} = |g^* + h^*\ A(s + i\varepsilon)|^2 \tag{3.9}$$

one gets,

$$(\gamma - \bar{\gamma})\Gamma_{tot} \simeq 2(\mathrm{Im}\ gh^*)\ \mathrm{Im}A \tag{3.10}$$

where ImA stands for the s-channel discontinuity. In our case, the various graphs contributing to eq. (3.10) are shown in fig. 1. It can be shown[13] that for SU(5) grand unified theories, with an arbitrary number of {5̄}-dim Higgs multiplets, the flavor interaction of the gauge (W,X,Y) and Higgs bosons (H_i^a) can be written in the form that involves Cabibbo rotation U and some Yukawa couplings H_i. It is clear from eq. (3.10) that the contribution of the interference between Fig. 1a and fig. 1b to $(\gamma-\bar{\gamma})$ is of the form:

$$\mathrm{Im\ Tr}\ (UU^+UU^+) = 0\ . \tag{3.11}$$

However, the interference between Fig. 1a and 1c is of the form Im Tr $(UU^+H_iH_j^+)$ which is not zero in general and therefore, the contribution to ΔB from such graphs is

$$\Delta B \sim \frac{g^2\,\mathrm{Im\,Tr}(UU^+H_iH_j^+)}{g^2}\ . \tag{3.12}$$

If $H \sim 10^{-2}$ to 10^{-3} $\Delta B \simeq 10^{-4}$ to 10^{-6} leading to $n_B/n_\gamma \sim 10^{-6}$ to 10^{-8}. Our purpose here is not to highlight the prediction for the magnitude of ΔB for that depends on many more details of the model but rather to point out that a mechanism for baryon production capable of yielding reasonable values for n_B/n_γ exists and the potentially dangerous gauge loop graphs (Fig. 1b) do not contribute. A similar kind of contribution also arises from Fig. 2, where again the gauge loop corrections vanish.

We would like now to summarize the main results of this paper and conclude with some additional remarks on the implications of our work. The main point we wish to make is that, contrary to conventional wisdom, broken symmetry may persist at high temperatures if boundary conditions at zero temperature are suitably chosen. Such a model necessarily contains heavy Higgs mesons and leads to fermion and boson masses growing with temperature.

We have also shown how realistic theory of soft CP-violation, constructed within the grand unified theory based on SU(5), retains its CP-violating character at high temperatures.

The phenomenon we have uncovered is similar to the one discovered by Linde[14] earlier. However, Linde's work relies on there being a large neutrino density in the universe which may not necessarily be the case. Furthermore, it is not clear whether a generalization of Linde's work to the case of soft CP-violation is possible.

Acknowledgements

We have benefitted from discussion with P. K. Kabir, F. Paige, B, Sakita and P. Senjanović. We would also like to thank the theory group of the Brookhaven National Laboratory for the warm hospitality extended to us while this work was being performed.

* * *

FOOTNOTES AND REFERENCES

1) D. A. Kirzhnitz: Zh. Exp. Theor. Fiz Pisma Red. 15, 745 (1972) (Soviet Phys. JETP Lett. 15, 529 (1972)); D. A. Kirzhnitz and A. Linde, Phys. Lett. 42B, 471 (1972).

2) S. Weinberg, Phys. Rev. D9, 3357 (1974); L. Dolan and R. Jackiw, Phys. Rev. D9, 2904 (1974); C. Bernard, Phys. Rev. D9, 3312 (1974); D. A. Kirzhnitz and A. D. Linde, Ann. of Physics, (N.Y.) 101, 195 (1976); for a review, see A. D. Linde, Rep. on Prog. in Physics 42, 389 (1979).

3) J. C. Pati and A. Salam, Phys. Rev. D10, 275 (1974); R. N. Mohapatra and J. C. Pati; ibid. D11, 566, 2588 (1975); G. Senjanović and R. N. Mohapatra, ibid. D12, 1502 (1975).

4) T. D. Lee, Phys. Rev. D8, 1226 (1973); R. N. Mohapatra and J. C. Pati, ref. 3.

5) S. Weinberg, in Lectures on Particles and Field Theory, ed. by S. Deser and K. Ford (Prentice-Hall, Inc., Englewood Cliffs, N.J., 1964), p. 482; A. D. Sakharov, Zh. Exp. Theor. Fiz, Pisma Red. 5, 32 (1967); A. Y. Ignatiev, N. Y. Krosnikov, V. A. Kuzmin and A. N. Tavkhelidze, Phys. Lett. 76B, 436 (1978); M. Yoshimura, Phys. Rev. Lett. 41, 381 (1978); S. Dimopoulos and L. Susskind, Phys. Rev. D18, 4500 (1978); D. Touissant, S. Treiman, F. Wilczek and A. Zee, Phys. Rev. D19, 1036 (1979); S. Weinberg, Phys. Rev. Lett. 42, 850 (1979); J. Ellis, M. Gaillard and D. Nanopoulos, Phys. Lett. 80B, 360 (1978); J. C. Pati, Univ. of Maryland preprint (1979); S. Barr, G. Segrè and H. A. Weldon, Pennsylvania preprint UPR-0127T (1979); A. Yildiz and P. Fox, Harvard preprint HUTP-79/A019.

6) See, e.g., S. Weinberg, "The First Three Minutes," Baisc Books, N.Y. (1978).

7) For a review and references see, R. N. Mohapatra, Proceedings of the XIX International Conference on High Energy Physics, Tokyo, Japan (1978), edited by S. Homma, M, Kawaguchi and H. Miyazawa (Physical Society of Japan, Tokyo, 1979), p. 604.

8) M. A. B. Bég and H. S. Tsao, Phys. Rev. Lett. 41, 278 (1978); R. N. Mohapatra and G. Senjanović, Phys. Lett. 79B, 283 (1978); H. Georgi, Hadronic Journal, 1, 155 (1978); G. Segrè and A. Weldon, Phys. Rev. Lett.

42, 1191 (1979), S. Barr and P. Langacker, Phys. Rev. Lett. 42, 1654(1979).

9) R. Peccei and H. Quinn, Phys. Rev. Lett. 38, 1449 (1977); S. Weinberg, ibid. 40, 223 (1978); F. Wilczek, ibid. 40, 279 (1978).

10) R. N. Mohapatra and G. Senjanović, Phys. Rev. Lett. 42, 1651 (1979) and CCNY-HEP-79/3 (1979).

11) T. P. Cheng, E. Eichten and L. F. Li, Phys. Rev. D9, 2259 (1974).

12) J. C. Pati and A. Salam, Phys. Rev. D10, 275 (1973); H. Georgi and S. L. Glashow, Phys. REv. Lett. 32, 638 (1974).

13. R. N. Mohapatra, City College preprint CCNY-HEP-79/5 (1979).

14. A. Linde, Phys. Rev. D14, 3345 (1976).

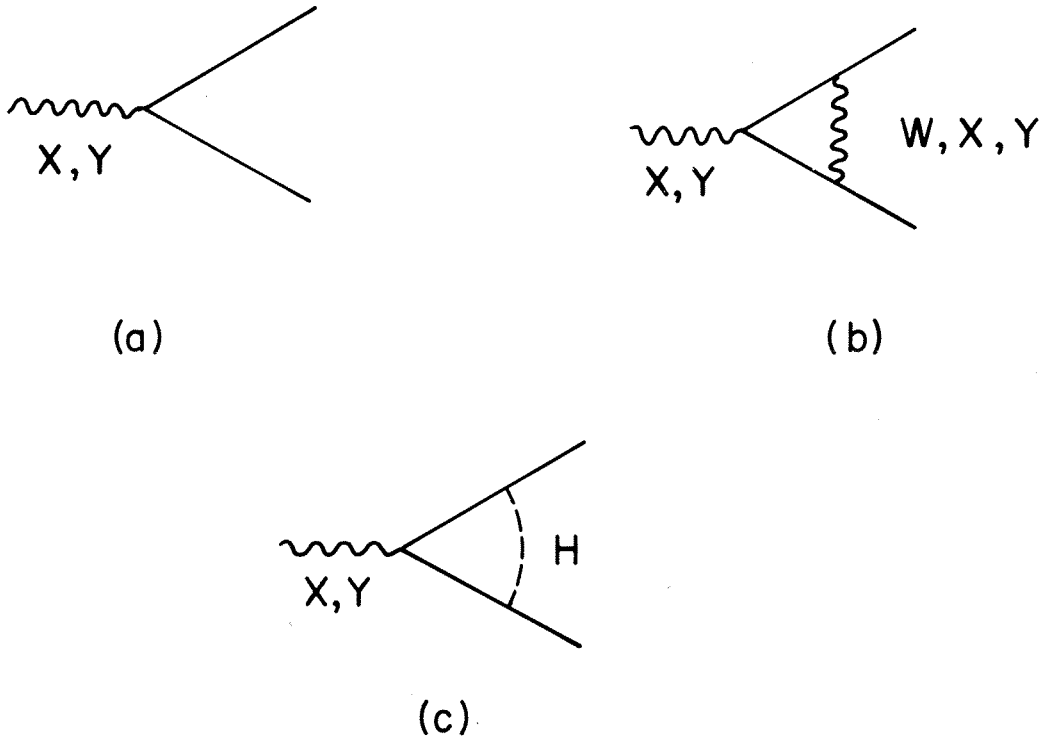

Fig. 1 The Feynman graphs expected to play a role in the generation of baryon excess in the universe, through the decay of heavy gauge mesons. X,Y stand for superheavy gauge mesons and H for superheavy Higgs scalars of SU(5).

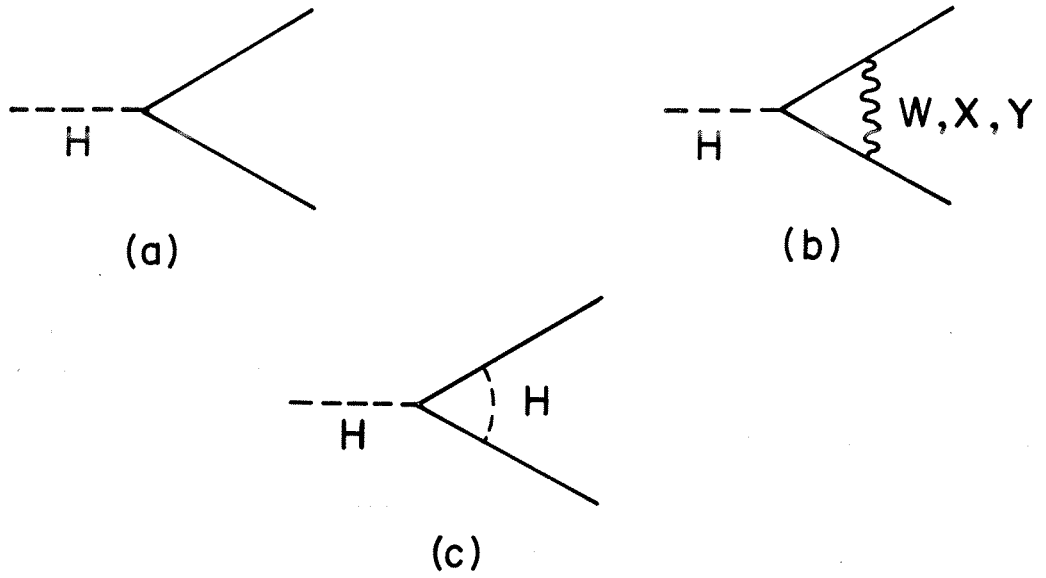

Fig. 2 Baryon number violating decays of superheavy Higgs scalars

SU(5)

J. Ellis
CERN, Geneva, Switzerland

ABSTRACT

We review the past successes, present problems, and future prospects for SU(5) as a prototype grand unified theory of the strong, weak, and electromagnetic interactions.

1. INTRODUCTION

At the moment there is an exponentially growing interest in grand unified theories[1,2] of the strong, weak, and electromagnetic interactions. This stems from the widespread belief that the strong, weak, and electromagnetic interactions are individually solved, and the general insistence that our theories of these interactions [QCD, SU(2) × U(1) Weinberg-Salam[3]] can only be incomplete stepping stones on the path to a greater synthesis. One of the first grand unified theories to be proposed[2] was the simplest one based on the group SU(5). This Georgi-Glashow model[2] is sufficiently elegant in its structure and rich in its content that it may serve as a realistic prototype grand unified theory, in the same way as the SU(2) × U(1) Weinberg-Salam model[3] served for some time as a prototype theory of the partial unification of weak and electromagnetic interactions. It now seems likely that the Weinberg-Salam model is "correct"[4] (whatever that means). It remains to be seen whether the Georgi-Glashow model will be seen to be "correct". Later in this talk we will see reasons why the minimal SU(5) model should be elaborated, a fate which has not yet befallen the Weinberg-Salam model.

This talk is divided into three main parts. First there is a review of the structure of the SU(5) model and a reminder of its "classical" predictions for $\sin^2\theta_W$ and quark masses[5-7]. Then there is a description of recent progress in analysing the model -- refinements in calculations of the proton lifetime[7-9] and decay branching ratios[8,10], the possibility of estimating the baryon number of the universe[11], and studies of the hierarchies of symmetry breaking[12,13]. Finally there is a summary of the prospects and problems facing SU(5). Attempts will be made throughout to discuss the extent to which other grand unified theories resemble or differ from the SU(5) model.

2. REVIEW

2.1 Structure of the model

At low energies the world has a SU(3) [colour] × U(1) [electromagnetism] symmetry. Above 100 GeV this symmetry seems to become SU(3) × SU(2) × U(1) [Weinberg-Salam[3]]. Georgi and Glashow[2] showed that the only rank-4 group capable of grand-unifying these interactions was SU(5). This theory contains 24 gauge vector bosons: the familiar γ, $W^{\pm}$, Z^0, $g_{i=1,\ldots,8}$, and a colour triplet and weak isodoublet $\begin{pmatrix} X \\ Y \end{pmatrix}_{R,Y,B}$ with charges $\frac{4}{3}$ and $-\frac{1}{3}$, together with their antiparticles. These latter bosons acquire their masses at the initial stage of symmetry breaking SU(5) → SU(3) × SU(2) × U(1) which, as we will see later[5-7,9], occurs on a scale of (10^{14} to 10^{15}) GeV. The fermions are considered as forming "generations", each of which comprises 15 left-handed helicity states and is assigned to a

reducible $\bar{5} + 10$ representation of SU(5). The lightest generation is essentially that of (u, d, e^-, ν_e) and is assigned as

$$\bar{5} = \begin{pmatrix} \bar{d}_R \\ \bar{d}_Y \\ \bar{d}_B \\ e^- \\ \nu_e \end{pmatrix}_L , \quad 10 = \frac{1}{\sqrt{2}} \begin{pmatrix} 0 & \bar{u}_B & -\bar{u}_Y & -u_R & -d_R \\ -\bar{u}_B & 0 & \bar{u}_R & -u_Y & -d_Y \\ \bar{u}_Y & -\bar{u}_R & 0 & -u_B & -d_B \\ u_R & u_Y & u_B & 0 & -e^+ \\ d_R & d_Y & d_B & e^+ & 0 \end{pmatrix}_L \tag{2.1}$$

The heavier generations (c, s, μ^-, ν_μ), (t, b, τ^-, ν_τ) (and perhaps others) are assigned to similar representations which will in general mix, giving rise to the generalized Cabibbo angles. The SU(3) × SU(2) × U(1) decompositions of the representations (2.1) are

$$\bar{5} = (\bar{3},1) + (1,2) \qquad 10 = (3,2) + (\bar{3},1) + (1,1) \tag{2.2}$$

which reproduce the conventional SU(3) and SU(2) × U(1) assignments and interactions. Symmetry breaking and mass generation in the SU(5) model is achieved in two stages, using two representations of Higgs fields, a 24 and a 5 respectively:

$$SU(5) \xrightarrow[24 \text{ adjoint}]{} SU(3) \times SU(2) \times U(1) \xrightarrow[5 \text{ vector}]{} SU(3) \times U(1) \tag{2.3}$$

The 24 ϕ has a vacuum expectation value

$$\langle 0|\phi|0\rangle = O(10^{15}\,\text{GeV}) \begin{pmatrix} 1 & & & & \\ & 1 & & & \\ & & -3/2 & & \\ & & & -3/2 & \\ & & & & 0 \end{pmatrix} \tag{2.4a}$$

and generates m_X, m_Y while the 5 H has a vacuum expectation value

$$\langle 0|H|0\rangle = O(10^2\,\text{GeV}) \begin{pmatrix} 0 \\ 0 \\ 0 \\ 0 \\ 1 \end{pmatrix} \tag{2.4b}$$

[note its SU(4) symmetry] and generates m_f, m_W, and m_Z.

2.2 Estimation of grand unification scale

The way this is usually done[5-7,9] is to start from the known coupling strengths (α, $\alpha_3 \equiv \alpha_{strong}$) at a scale $Q^2 = O(10\ \text{GeV}^2)$ and use the renormalization group to compute the scale at which they become essentially equal. The qualitative behaviour of the couplings is shown in Fig. 1: SU(3) is more "asymptotically free" than SU(2), while U(1) is "asymptotically unfree". The rate of approach of α_3 and α_2 is to first order:

$$\frac{1}{\alpha_3(Q^2)} - \frac{1}{\alpha_2(Q^2)} \approx \frac{11}{12\pi} \ln\left(M^2/Q^2\right) \tag{2.5}$$

where M is the grand unification mass at which $\alpha_3 \approx \alpha_2$. Notice that to first order the rate of approach is not only independent of the grand unification group -- it only depends on the sizes of the different components of the intermediate energy symmetry group -- but also

independent of the number of fermion flavours, which appear in the evolution equations for both α_3 and α_2 but cancel in the difference (2.5). Using (2.5) and a strong interaction $\alpha_3(Q^2)$ characterized by the conventional $\Lambda \sim \frac{1}{2}$ GeV, we would naively[7] calculate $M_X \sim$ few $\times 10^{16}$ GeV.

But we must be careful[9,14] about several details of the calculation such as threshold effects[14] at the grand unification mass (see Fig. 2a), which means that the subgroup coupling constants are only effectively equal at scales $Q \sim$ (2 to 3) $\times m_X$. Also important are threshold effects[14] at the switch-on of SU(2) symmetry which cause $\alpha_2(Q^2)$ to evolve in a peculiar way (see Fig. 2b) and reduce m_X by another factor of 2 or 3. A most important refinement[9] is the variation of α between $Q^2 \approx 0$ ($\alpha = \frac{1}{137}$ from the Josephson effect) to $Q^2 \sim 10^4$ GeV^2 ($\Delta\alpha \sim 6\%$) caused by virtual fermion loops (Fig. 3), which was unaccountably neglected by earlier authors[6,7] and reduces the estimate of m_X by an order of magnitude. Higher-order contributions to the renormalization group functions β_3 and β_2 also have some smaller effects[9] on m_X. The net result is to reduce the best estimate of m_X to

$$m_X \sim (1 \text{ to } 2) \times \Lambda \times 10^{15} \text{ GeV} \tag{2.6}$$

where Λ is defined by the second-order QCD formula and may be O(300) MeV to within a factor of 2. The estimate (2.6) is substantially the same in other grand unified theories such as SO(10) [15,16].

2.3 Renormalization of $\sin^2\theta_W$

SU(5) symmetry is badly broken, and symmetry predictions only apply at scales $Q >> m_X$: their renormalization at lower Q^2 can be calculated using the renormalization group. The classic example is $\sin^2\theta_W$, which is $\frac{3}{8}$ in the symmetry limit. In terms of α_2 and an α_1 normalized to equal α_2 at $Q^2 >> m_X^2$,

$$\sin^2\theta_W(Q^2) = \frac{3\alpha_1(Q^2)}{5\alpha_2(Q^2) + 3\alpha_1(Q^2)} \tag{2.7}$$

The couplings $\alpha_1(Q^2)$ and $\alpha_2(Q^2)$ evolve differently at $Q < 10^{16}$ GeV, causing $\sin^2\theta_W$ to be renormalized[5,7] from $\frac{3}{8}$ to

$$\sin^2\theta_W(Q^2 \sim 10^4 \text{ GeV}^2) \approx 0.20 \pm 0.01 \tag{2.8}$$

Present neutral-current experiments measure quantities which are all equal to $\sin^2\theta_W$ ($Q^2 = 10^4$ GeV^2) in the absence of radiative corrections, but which all differ from (2.8) and each other when radiative corrections are taken into account. This has not all[17] been done consistently, but it seems likely that simple SU(5) predicts that present neutral-current measurements should lie in the range (2.8). The present world average is[4]

$$\sin^2\theta_W = 0.230 \pm 0.015 \tag{2.9}$$

There seems to be a 1 or 2 standard deviation discrepancy between SU(5) theory (2.8) and experiment (2.9). It is too early to say if this is really serious, but if $\sin^2\theta_W$ does turn out to be higher than (2.8) we will have to consider modifying or discarding naive SU(5), either by putting more particles (Higgs? superheavy $m \sim 10^{15}$ GeV fermions?) into

theory, or by going to a bigger group such as SO(10) [16] and introducing more stages of symmetry breaking[18].

2.4 Quark and lepton masses

Simple grand unified models such as SU(5) give symmetries between quark and lepton masses which apply when they are measured on scales $Q \gg m_X$, e.g. by defining the effective fermion mass[19] $m_f(Q^2)$ via the inverse propagator

$$S_F^{-1}(Q) = \not{Q} - m_f(Q^2) \tag{2.10}$$

An example is the SU(4) symmetry which occurs in SU(5) for the fermion masses generated by the H-$\bar{5}$-10 couplings, due to the SU(4) symmetry of $\langle 0|H|0\rangle$ (2.4b). This symmetry prediction is[2]

$$m_d = m_e\,, \quad m_s = m_\mu\,, \quad m_b = m_\tau \quad \text{at } Q \gg m_X \tag{2.11}$$

assuming the conventional assignments of quarks and leptons to $\bar{5} + 10$ generations. The dominant[6,7] renormalization at low Q^2 of symmetry predictions such as (2.11) comes from gluon loops (see Fig. 4), which in SU(5) renormalize (2.11) to yield

$$\left[\frac{m_b(Q)}{m_\tau(Q)}\right] = \left[\frac{\alpha_3(Q^2)}{\alpha(m_X^2)}\right]^{\frac{4}{11-\frac{2}{3}f}} \left[1 + \dots\right] \tag{2.12}$$

The dots in (2.12) reflect SU(2), U(1), higher-order SU(3) [20] and finite mass effects which have been estimated to be O(10 to 20)% correction factors. Note the sensitivity in (2.12) to f, the number of quark flavours. If we calculate (2.12) using six quark flavours and evaluating[19] m_q at a scale Q such that $Q = 2m_q(Q)$ (the approximate position of the $q\bar{q}$ threshold), then we hope to get a reasonable value for a heavy quark whose current (short distance) and constituent masses do not differ greatly because we are still in a perturbative régime of Q^2. For the b and s quarks we find[7,20]

$$\left.\begin{aligned} m_b &\sim 5 \text{ to } 5\tfrac{1}{2} \text{ GeV} \\ m_s &\sim \tfrac{1}{2} \text{ GeV} \end{aligned}\right\} \quad \text{for } f = 6 \tag{2.13}$$

with values O(20)% higher for f = 8, and considerably higher for $f \geq 10$ [21]. The estimate (2.13) of m_b is clearly very satisfactory, and is the only phenomenological high-energy physics evidence that there may be only six quarks, but ...

What about m_d? Even though the absolute value of m_d at low Q^2 cannot be calculated, and the qualitative smallness of m_d is correct, we do have the renormalization group invariant prediction[2,7]

$$\frac{m_d}{m_s} = \frac{m_e}{m_\mu} \tag{2.14}$$

which conflicts[7] with current algebra/chiral symmetry estimates that yield

$$\frac{m_d}{m_s} = O\left(\tfrac{1}{20}\right) \text{ not } O\left(\tfrac{1}{200}\right) \tag{2.15}$$

This failure may either reflect some small "slop" in the quark mass matrix which is of the order of a few MeV and does not respect SU(5) symmetry, or it may reflect the existence of a more complicated Higgs structure in SU(5) [22], or it may indicate that SU(5) should be abandoned[18]. It is a well-known problem[7].

What about m_s? It is frequently asserted[23] that $m_s \sim 150$ MeV, on the not very solid theoretical basis that $m_\Lambda - m_N \sim 150$ MeV and that this difference is due to the difference in constituent masses of the s and (u, d) quarks, which is in turn identified with the difference in their current masses. This is clearly not a rigorous short-distance argument. People are generally agreed that the constituent s quark mass is O(500) MeV, but how should this be related to the current quark mass? The previous argument apparently assumes

$$m_q|_{\text{constit.}} \sim m_q|_{\text{current}} + m_q|_{\text{dynamical}} \tag{2.16}$$

where $m|_{\text{dynamical}} \sim 300$ MeV. But perhaps

$$m_q^2|_{\text{constit.}} \sim m_q^2|_{\text{current}} + m_q^2|_{\text{dynamical}} \tag{2.17}$$

in which case $m_s|_{\text{current}} \sim 400$ MeV to be compared with the SU(5) prediction (2.13). In any case, because of the strong coupling problem the m_s prediction (2.13) is probably only correct to ±50%. We conclude that there is no solid evidence that the naive SU(5) prediction of m_s is wrong.

The problems with m_d and perhaps m_s have caused some authors to toy with more complicated Higgs structures for SU(5), involving, for example[22,24], a 45 which would by itself yield the symmetry prediction

$$m_q = \tfrac{1}{3} m_l \tag{2.18}$$

[and could reproduce the correct m_b if there were 10 or 12 flavours[24]] but could be combined with a 5 to give more complicated mass formulae[22].

By the way, the approximate successes (?) of the b, s, d quark mass estimates constitute the only evidence in favour of the conventional "generation" assignments like (2.1).

3. RECENT PROGRESS

3.1 Proton decay

Since grand unified theories put quarks and leptons into the same multiplet, and since gauge theories contain vector bosons linking all particles in a multiplet, there will in general be some interactions, changing quarks into leptons, which violate baryon number conservation[1,2]. In the simple SU(5) model, the X and Y bosons acquire essentially identical masses which yield an effective four-fermion interaction of strength

$$\frac{G_{GU}}{\sqrt{2}} = \frac{g^2}{8 m_X^2} \tag{3.1}$$

which takes the form[7]

$$\tfrac{1}{4}\mathcal{L}_{GU} = \tfrac{1}{\sqrt{2}} G_{GU} \Big[(\epsilon_{ijk} \bar{u}^c_{k_L} \gamma_\mu \gamma_{j_L})(2\bar{e}^+_L \gamma^\mu d_{i_L} - \bar{e}^+_R \gamma^\mu d_{i_R}) + (\epsilon_{ijk} \bar{u}^c_{k_L} \gamma_\mu d_{j_L})(\bar{\nu}^c_{e_R} \gamma^\mu d_{i_R}) + \text{H.c.} \Big] \tag{3.2}$$

The proton decay rate is then clearly $\propto G_{GU}^2$ so that the lifetime is proportional to m_X^4. The classic[7] method of estimating the proton decay rate is to argue that the $q + q \to \bar{\ell} + \bar{q}$ annihilation diagrams of Fig. 5 dominate, and evaluate these using non-relativistic SU(6) for the initial-state wave function, a calculable non-leptonic short-distance enhancement factor, and make the "parton model" assumption that the sum over final-state mesons approximates an inclusive annihilation cross-section. We then find that

$$\tau_{\text{proton, bound neutron}} \sim O(10^3)\,\frac{m_X^4}{m_N^5} \tag{3.3}$$

Combining this with the estimate (2.6) of m_X and making some allowance for uncertainties, we may guess[9]

$$\tau_{\text{proton, bound neutron}} = 10^{31\pm 2}\ \text{years} \tag{3.4}$$

considerably lower than previous estimates[7,14] because of the reduction in m_X. There are still considerable uncertainties -- in Λ, the ratio m_X/Λ, and the rate calculation (one would like to see a calculation of exclusive modes using more traditional current algebra and non-leptonic decay technology) -- but the lifetime (3.4) is temptingly short[25].

Recent attempts have been made to estimate branching ratios into different final states[8,10]. For different quantum numbers in inclusive final states it has been estimated[10] that in SU(5) [SO(10) gives similar results]:

$B(p \to e^+ + \text{nonstrange})$	$\sim 83\%$	$B(n \to e^+ + \text{nonstrange})$	$\sim 76\%$
$B(p \to \bar{\nu} + \text{anything})$	$\sim 15\%$	$B(n \to \bar{\nu} + \text{anything})$	$\sim 22\%$
$B(p \to \mu^+ + \text{nonstrange})$	$\sim 1\%$	$B(n \to \mu^+ + \text{nonstrange})$	$\sim 1\%$
$B(p \to \mu^+ + \text{strange})$	$\sim 1\%$	$B(n \to \mu^+ + \text{strange})$	$< 1\%$
$B(p \to e^+ + \text{strange})$	$< 1\%$	$B(n \to e^+ + \text{strange})$	$< 1\%$

(3.5)

Notice the strong suppression of decay modes involving a μ^+. The different branching ratios arise from different Cabibbo angle and phase-space suppression factors. One may go further and use non-relativistic SU(6) to estimate the ratios of different exclusive final states to the total inclusive rates:

$$\left.\begin{array}{lll} p \to \pi^0 e^+ & \sim 40\% & \to \eta e^+ \sim 14\% \\ \to \rho^0 e^+ & \sim 20\% & \to \omega e^+ \sim 26\% \end{array}\right\} \text{of } p \to e^+ + \text{nonstrange}$$
$$n \to \pi^- e^+ \sim 66\% \quad \to \rho^- e^+ \sim 34\% \quad \text{of } n \to e^+ + \text{nonstrange} \tag{3.6}$$

This gives sizeable branching ratios for both the proton and neutron to decay into readily identifiable two-body final states:

$$B(p \to e^+\pi^0) \sim \tfrac{1}{3}\ , \quad B(n \to e^+\pi^-) \sim \tfrac{1}{2} \tag{3.7}$$

Clearly more theoretical work is needed, particularly on estimating exclusive hadronic decay modes, but there is certainly no need for experimentalists[25] to drag their feet.

3.2 The baryon number of the universe

Grand unified theories provide a framework[11] for discussing the very early evolution of the universe ($T \sim 10^{19}$ to 10^{11} GeV), which suggests a natural mechanism for generating the observed baryon-to-photon ratio

$$\frac{n_B}{n_\gamma} \sim 10^{-8} \text{ to } 10^{-10} \tag{3.8}$$

The general scenario they suggest is that for 10^{19} GeV > T >> 10^{15} GeV, all the known interactions would have to proceed at rates less than the expansion rate of the universe, and so would not have been in thermal equilibrium. At $T \sim 10^{16}$ GeV the strong, weak, and baryon-number-violating interactions would all have come into equilibrium, the interaction rates now being ≥ the expansion rate. Shortly afterwards, between $T \sim 10^{15}$ and 10^{11} GeV, the baryon-number-violating forces would have dropped out of equilibrium because their rates would be slowed by the non-negligible masses $O(10^{14}$ to $10^{15})$ GeV of the baryon-number-violating bosons, while the strong, weak, and electromagnetic interactions would have stayed in equilibrium. During the B-violating drop-out, a C- and CP-violating component of the B-violating forces could[11] have generated the observed baryon-antibaryon asymmetry, and hence (3.8) if there was no entropy-generating dissipation at some later epoch to dilute it.

The simplest SU(5) model[2] contains B-, C-, and CP-violating forces arising from the $Hf\bar{f}$ interactions. With a single $\underline{5}$ of Higgs, the lowest-order diagrams contributing are 8^{th} order[26] (see, for example, Fig. 6): the most important CP-violating phase is not[26] directly related to that connected with CP violation in the K^0 system in the Kobayashi-Maskawa model. The dominant source of baryon number would probably be baryon-number-violating Higgs decays (and possibly interactions). However, these give too small a baryon number $O(10^{-16}$ to $10^{-20})$ in the simplest SU(5) model[26,27]. What to do? It is easily seen that a more complicated Higgs system with more Higgs multiplets[27,28] contributing to the fermion mass matrix could easily give a baryon-to-entropy ratio as large as (3.8), and this would be implemented either in SU(5) or in a larger grand unified theory. However, to get a precise number for n_B/n_γ will probably require "quarkosynthesis" computer calculations for the thermodynamics and interaction rates fully as complicated as the old nuclear physics stellar evolution calculations of a previous physics generation[29].

3.3 Hierarchies of symmetry breaking

Grand unified theories contain many mass scales (m_f, m_H, $m_{W,Z}$, $m_{X,Y}$) which are grotesquely different from each other and from the Planck mass $m_P \sim 10^{19}$ GeV. If we accept without proof that $m_f = O(m_{W,Z})$, then we are left with trying to understand why

$$1 \gg \frac{m_X}{m_P} \gg \frac{m_W}{m_X} \tag{3.9}$$

and what is (are) the mass(es) of the Higgs boson(s)? It can be argued[13] that the hierarchy of gauge hierarchies (3.9) is possible and even plausible in the context of symmetry breaking through radiative corrections[12,30]. In this case there is no explicit mass term $-\mu^2\phi^2$ in the effective potential, and symmetry breaking occurs[12] near a scale Q where the effective

four-Higgs coupling $\lambda(Q) \approx 0$, so that radiative corrections to the effective potential of order $\alpha^2\phi^4 \ln(\alpha\phi^2)$ coming from diagrams of the type of Fig. 7 become important. The logarithmic variations of the different λ with Q then give rise to the exponentially varying ratios (3.9).

A possible general scenario[13] in which physics has only one intrinsic mass scale, the Planck mass, is as follows:

i) The theory has a gauge coupling g and Higgs couplings λ which are $O(g^2)$, but no mass terms $-\mu^2\phi^2$, when the theory is renormalized at the Planck mass at which some new physics must come in.

ii) As the scale Q is decreased, computations[13] reveal that adjoint Higgs couplings [e.g. for the 24 of SU(5)] evolve relatively rapidly because of their large non-Abelian charge, and may become zero already at $Q \sim 10^{-4}\ m_P \sim 10^{15}$ GeV. At this stage, the first stage [e.g. $SU(5) \to SU(3) \times SU(2) \times U(1)$] of symmetry breaking is generated by radiative corrections.

iii) Meanwhile the vector [5 in SU(5)] Higgs couplings evolve relatively slowly, and are still non-zero at $Q \sim 10^{15}$ GeV. At lower Q they evolve even more slowly because many heavy particles drop out of their renormalization group equations. These couplings may[12] therefore become zero at a scale $O(10^2)$ GeV $\ll\ll\ll\ll m_X = O(10^{15})$ GeV, and generate $m_{W,Z}$ at that scale.

This scenario is illustrated in Fig. 8. It explains naturally the ratio $m_X/m_P \sim 10^{-4}$ to 10^{-5} and makes plausible the hierarchy of hierarchies (3.9). To realize the second hierarchy does, however, require[7,12,13] one unnatural condition on the Higgs potential to ensure the absence or negligibility of any $-\mu_H^2H^2$ term in the low-energy ($Q < 10^{15}$ GeV) Higgs potential. If this parameter μ_H is indeed zero (or $\ll$ 10 GeV), then the Weinberg-Salam SU(2) Higgs boson mass is determined by radiative corrections[30,31] and is

$$m_H^2 \approx \frac{3\alpha^2}{8\sqrt{2}\,G_F}\left\{\frac{2+\sec^4\theta_W}{\sin^4\theta_W} - O\left(\frac{m_f}{m_W}\right)^4\right\} \qquad (3.10)$$

which yields

$$m_H \sim 10{\cdot}4\ \text{GeV} \quad \text{if} \quad \sin^2\theta_W = 0{\cdot}20 \qquad (3.11)$$

Such a Higgs boson could be readily detected[31] in the decays of toponium (if/when it is found), or at LEP in processes involving the Z^0 boson[32]. Its discovery would give us a great breakthrough in our understanding of symmetry breaking.

4. PROSPECTS AND PROBLEMS

SU(5)

- has provided us with some successful (?) calculations of previously undetermined quantities: $\sin^2\theta_W$, m_b and m_s.
- Makes some exciting testable predictions: proton lifetime $\sim 10^{31\pm2}$ years with observable decay modes, only three (or at the most four) generations of fermions.

- Suggests intriguing speculations: a mechanism for generating the baryon number of the universe, a motivation for symmetry breaking by radiative corrections which suggests $m_H \sim 10$ GeV.
- Is unsatisfactory because it has ≥ 25 arbitrary parameters (one gauge coupling g, one θ vacuum parameter, three lepton masses, twelve quark masses and mixing angles, eight parameters for the Higgs potential).
- Is incomplete because it does not include gravity. Since the grand unification mass $m_X \ll m_P$, it is reasonable to neglect gravitation in an attempt to unify strong, weak, and electromagnetic interactions, but the resulting grand unified theory must ultimately be combined with gravity at some larger mass scale. It is natural to try to do this via supergravity[33], because of its beauty and a suggestion that it may make matter-coupled gravity less infinite. An embedding of SU(3) × SU(2) × U(1) in a supergravity theory seemed impossible for a long time, since the maximal supergravity theory had a global SO(8) symmetry, too small to accommodate all the known particles. However, Cremmer and Julia[33] have recently pointed out that SO(8) supergravity possesses a concealed non-linear, local SU(8) symmetry, and have conjectured that this may become dynamical, just like the local U(1) in two-dimensional CP^{N-1} models[34]. It is natural to conjecture[35] that all the supermultiplet containing the SU(8) composite vector fields becomes dynamical, including spin $\frac{1}{2}$ particles to be identified with quarks and leptons, and spin 0 particles to be identified as Higgs. All presently observed "elementary" particles would therefore be composites of "preons", which were the naive SO(8) supergravity fields. Indeed, the supermultiplet seems to contain three generations of SU(5) $\bar{5} + 10$ fermions. But it contains a lot of other garbage as well, and we[35] have so far found no way of giving masses to all the unobserved fermions. This and the fact that the SU(8) currents have anomalies, stymies us[35] in our attempt to embed SU(5) in supergravity.
- May be embarrassed by having too many magnetic monopoles[36]. If they were produced in large numbers in the early universe, they would not all have annihilated yet, and would dominate the present matter density of the universe to an unacceptable degree. But estimates of the primordial rate of production of grand unified monopoles are very uncertain, and more work is needed on this problem.
- Has other serious problems: the simplest SU(5) model gets m_d too small, and perhaps has problems with $\sin^2 \theta_W$ and m_s. The simplest model also gives too small a baryon number of the universe. The hierarchy $m_W/m_X \ll 1$, while possible, still seems to us very unnatural. Is there a way in which SU(5) may be cooked so as to solve these problems, or must we go to some other grand unified theory?

There is still a lot to do!

REFERENCES

1) J.C. Pati and A. Salam, Phys. Rev. Lett. 31, 661 (1973).

2) H. Georgi and S.L. Glashow, Phys. Rev. Lett. 32, 438 (1974).

3) S. Weinberg, Phys. Rev. Lett. 19, 1264 (1967).
A. Salam, Proc. 8th Nobel Symposium, Aspenäsgården, 1968 (ed. N. Svartholm) (Almqvist and Wiksell, Stockholm, 1968), p. 367.

4) F. Dydak, Neutral currents, Talk at this Conference.

5) H. Georgi, H.R. Quinn and S. Weinberg, Phys. Rev. Lett. 33, 451 (1974).

6) M.S. Chanowitz, J. Ellis and M.K. Gaillard, Nucl. Phys. B128, 506 (1977).

7) A.J. Buras, J. Ellis, M.K. Gaillard and D.V. Nanopoulos, Nucl. Phys. B135, 66 (1978).

8) C. Jarlskog and F.J. Ynduráin, Nucl. Phys. B149, 29 (1979).

9) T.J. Goldman and D.A. Ross, Phys. Lett. 84B, 208 (1979).
W.J. Marciano, Rockefeller University preprint COO-2232B-173 (1979).

10) M. Machacek, Harvard University preprint HUTP-79/A021 (1979).

11) A.Yu. Ignatiev, N.V. Krosnikov, V.A. Kurmin and A.N. Tavkhelidze, Phys. Lett. 76B, 436 (1978).
M. Yoshimura, Phys. Rev. Lett. 41, 381 (1978).
S. Dimopoulos and L. Susskind, Phys. Rev. D 18, 4500 (1978).
A.D. Sakharov, Zh. Eksp. Teor. Fiz. 76, 1172 (1979).
B. Toussaint, S.B. Treiman, F. Wilczek and A. Zee, Phys. Rev. D 19, 1036 (1979).
J. Ellis, M.K. Gaillard and D.V. Nanopoulos, Phys. Lett. 80B, 360 (1979).
S. Weinberg, Phys. Rev. Lett. 42, 850 (1979).
S. Dimopoulos and L. Susskind, Phys. Lett. 81B, 416 (1979).

12) S. Weinberg, Phys. Lett. 82B, 387 (1979).

13) J. Ellis, M.K. Gaillard, A. Peterman and C. Sachrajda, CERN preprint TH 2696 (1979).

14) D.A. Ross, Nucl. Phys. B140, 1 (1978).

15) H. Georgi and D.V. Nanopoulos, Phys. Lett. 82B, 392 (1979); and Harvard University preprint HUTP-79/A001 (1979). For previous work on SO(10) see
H. Georgi, Particles and fields, 1974 (APS/DPF Williamsburg) (ed. C.E. Carlson) (AIP, New York, 1975), p. 575.
H. Fritzsch and P. Minkowski, Ann. Phys. 93, 193 (1975); Nucl. Phys. B103, 61 (1976).
M.S. Chanowitz, J. Ellis and M.K. Gaillard, Ref. 6.

16) T. Goldman and D.A. Ross, CalTech preprint CALT 68-731 (1979).

17) Some discussions have been given by W.J. Marciano (Ref. 9), and S. Sakakibara and L.M. Sehgal, Aachen preprint PITHA 79/05 (1979).

18) H. Georgi and D.V. Nanopoulos, Harvard University preprint HUTP-79/A039 (1979).

19) H. Georgi and H.D. Politzer, Phys. Rev. D 14, 1829 (1976).

20) D.V. Nanopoulos and D.A. Ross, CERN preprint TH 2536 (1978).

21) W. Grimus, University of Vienna preprint UWThPh. 79-15 (1979) investigates directly the renormalization of the Higgs-fermion-antifermion couplings.

22) H. Georgi and C. Jarlskog, Harvard University preprint HUTP-79/A026 (1979).

23) S. Weinberg, I.I. Rabi Festschrift, Trans. NY Acad. Sci. II, 38 (1977).

24) P.H. Frampton, S. Nandi and J.J.G. Scanio, Ohio State University preprint COO-1545-253 (1979).

25) Proceedings of Seminar on Proton Stability (ed. D. Cline), University of Wisconsin report (1979).
J. Blandino et al., Harvard-Minnesota-Purdue-Wisconsin proposal to the NSF: "A multi-kiloton detector to conduct a sensitive search for nucleon decay" (1979).
For the latest experimental limits on the proton lifetime, see J. Learned, F. Reines and A. Soni, U.C. Irvine preprint 79-54 (1979).

26) See, for example, J. Ellis, M.K. Gaillard and D.V. Nanopoulos, Ref. 11.

27) A. Yildiz and P.H. Cox, Harvard University preprint HUTP-79/A019 (1979).
S. Barr, G. Segrè and H.A. Weldon, University of Pennsylvania preprint UPR-0127 T (1979).
T. Yanagida and M. Yoshimura, Tohoku University preprint TU/79/199 (1979).

28) D.V. Nanopoulos and S. Weinberg, Harvard University preprint HUTP-79/A023 (1979).

29) Projects for such programmes are now under way at CalTech and the University of Chicago, private communication from G. Steigman.

30) S. Coleman and E. Weinberg, Phys. Rev. D 7, 1888 (1973).

31) J. Ellis, M.K. Gaillard, D.V. Nanopoulos and C. Sachrajda, Phys. Lett. 83B, 339 (1979).

32) G. Barbiellini et al., ECFA/LEP Exotic Particles Study Group, DESY preprint 79/27 (1979).

33) See E. Cremmer and B. Julia, Ecole Normale Supérieure preprint LPTENS 79/6 (1979), and references therein.

34) A. D'Adda, P. Di Vecchia and M. Lüscher, Nucl. Phys. B146, 63 (1978).
E. Witten, Nucl. Phys. B149, 285 (1979).

35) J. Ellis, M.K. Gaillard, L. Maiani and B. Zumino, work in slow progress.

36) J.P. Preskill, Harvard University preprint HUTP-79/A028 (1979).
See also Y.B. Zeldovich and M.Y. Khlopov, Phys. Lett. 79B, 239 (1979).

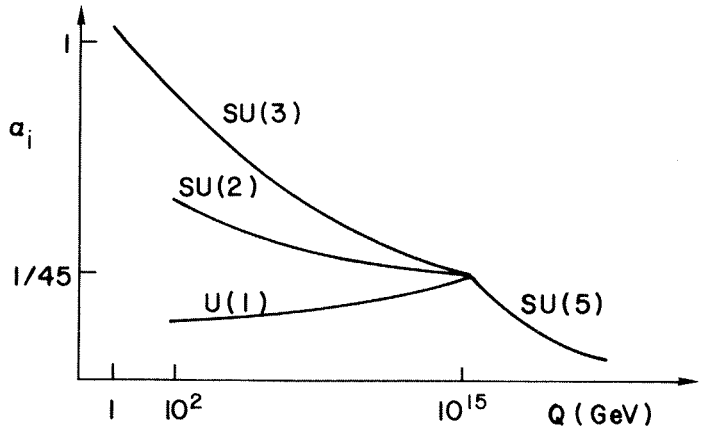

Fig. 1 Qualitative picture of the evolution of the SU(3), SU(2), and U(1) couplings in a grand unified theory such as SU(5)

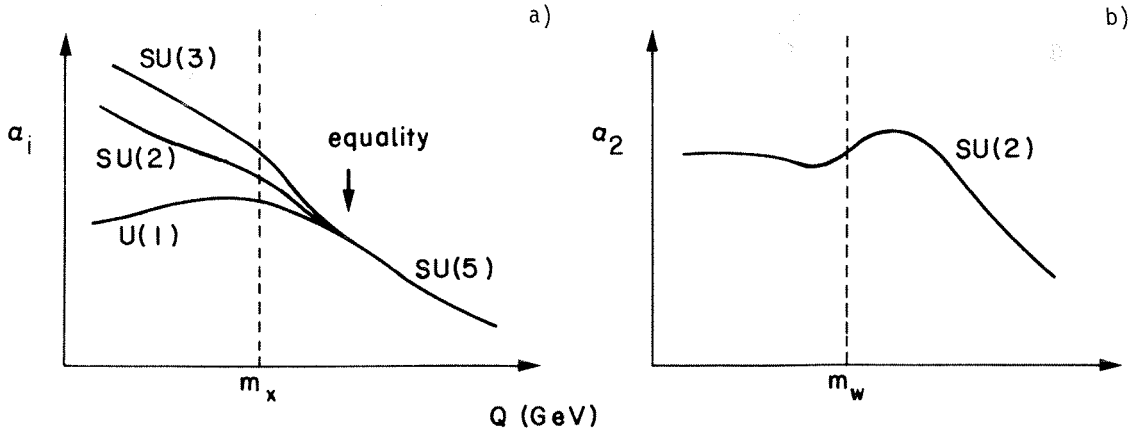

Fig. 2 Important threshold effects (Ref. 14) arise: a) at the grand unification mass, and b) at the weak-electromagnetic stage of unification.

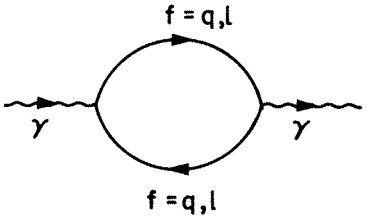

Fig. 3 Graphs renormalizing (Ref. 9) α between $Q^2 = 0$ and 10^4 GeV^2

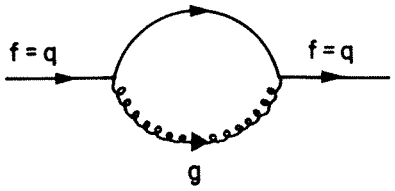

Fig. 4 Gluon loops which make (Refs. 6 and 7) the most important renormalization of the m_q/m_ℓ ratio

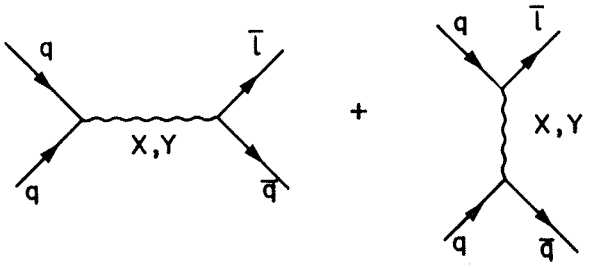

Fig. 5 The graphs dominating (Ref. 7) proton decay in simple grand unified models

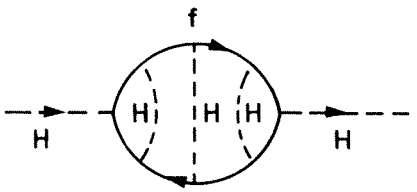

Fig. 6 Typical eighth-order CP- and B-violating diagram in SU(5) (Ref. 26)

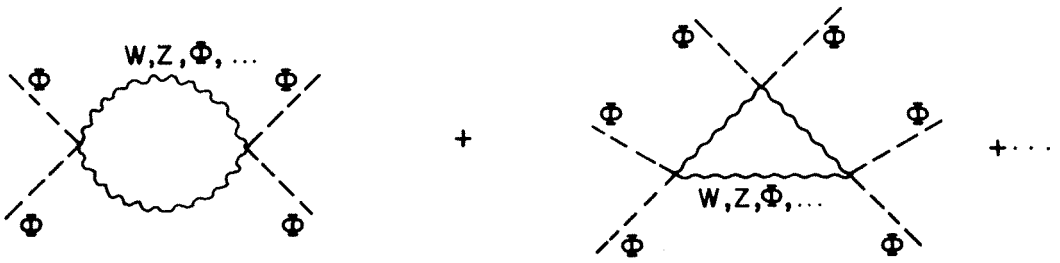

Fig. 7 Typical radiative corrections (Ref. 30) to the effective Higgs potential

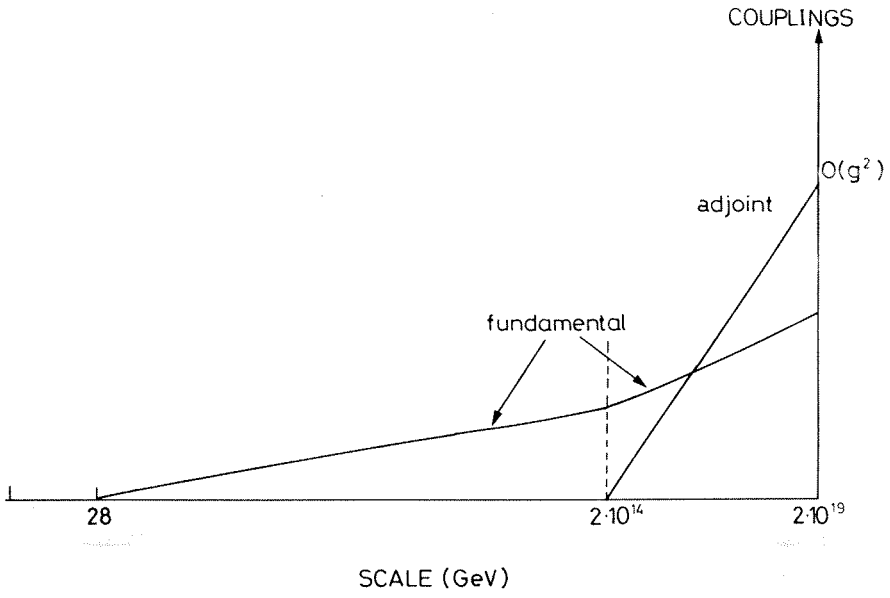

Fig. 8 Qualitative picture of the Q^2 evolution of the effective couplings of fundamental $\underline{5}$ and adjoint $\underline{24}$ Higgs in a simple SU(5) model, illustrating how the hierarchy of hierarchies $\overline{(3.9)}$ may be achieved (Ref. 13)

MAGNETIC MONOPOLES

D. Olive
Imperial College, London, England

The theoretical study of magnetic monopoles was initiated by Dirac nearly 50 years ago[1], but only recently has this study been significantly advanced. The advance has been the realization that magnetic monopoles have a natural tendency to occur as classical solutions in spontaneously broken non-Abelian gauge theories[2]. Such theories are precisely of the types which are now thought to govern the particle interactions, strong and electroweak. Our understanding of monopoles is still extremely incomplete, but it is thought possible that they may have a bearing on two important theoretical problems in particle physics, i) the understanding of quark confinement, and ii) the unification of all the interactions.

Whether or not these possibilities are borne out by future developments, it is clear that we have a lot to learn about the type of theory we must understand. We can already see interesting connections with other theoretical ideas which hitherto appeared to be quite unrelated.

Maxwell's equations *in vacuo* manifest a symmetry with respect to the transformation[3]

$$\underline{E} + i\underline{B} \to e^{i\theta} (\underline{E} + i\underline{B}) ,$$

mixing the electric and magnetic fields $\underline{E}$ and $\underline{B}$. If matter is to respect the symmetry, there should be magnetic charges $g_1, g_2, \ldots$, as well as electric charges $q_1, q_2, \ldots$, in nature. Dirac[1] found that for consistency with quantum mechanics,

$$q_i g_j = 2\pi \hbar\, n_{ij}, \qquad n_{ij} = 0, \pm 1, \pm 2, \ldots .$$

If at least one magnetic charge exists in the universe then the electric charges in nature must be quantized in terms of some unit q_0:

$$q_i = n_i q_0, \qquad n_i = 0, \pm 1 \ldots .$$

This is indeed the pattern of nature with q_0 provided by the electron charge [if we forget about quarks -- which do fit in with the theory if we consider the effect of the SU(3) colour gauge group[4]].

Dirac's monopole was a point-like particle carrying infinite self-energy due to the divergence of the Coulomb magnetic field at the origin. The new development due to 't Hooft and Polyakov[2] is to find a natural way for smoothing out this singularity are thereby gaining a picture of the internal structure and finite mass of the monopole. This picture is related to a feature we have learnt to accept in recent years, that the Lagrangian is governed by a larger non-Abelian gauge symmetry G which is spontaneously broken down to the gauge group H responsible for the long-range fields.

Actually, 't Hooft and Polyakov considered the simplest possibility, the Georgi-Glashow model which has G = SO(3), H = U(1). In this talk, I shall describe a slight generalization of this, paying particular attention to the mass formulae that emerge, their relation to the aforementioned duality, and their further interpretation. This sort of theory does definitely predict monopoles of the type already sought experimentally, but of a mass well beyond present reach.

Let G be the gauge symmetry of the Lagrangian describing a scalar field $\phi(x)$ lying in the adjoint representation of G and coupling minimally to the gauge fields. Suppose that the symmetry G is spontaneously broken owing to the fact that ϕ fails to vanish *in vacuo*. It must, however, be covariantly constant:

$$D^{\mu}\phi_{\alpha} \equiv \partial^{\mu}\phi_{\alpha} + e\, f_{\alpha\beta\gamma}\, W^{\mu}_{\beta}\, \phi_{\gamma} = 0 \ , \tag{1}$$

and so have constant length a:

$$\phi^2 = a^2 \ . \tag{2}$$

The physically observed exact gauge symmetry group H, whose fields are long range, is composed of those elements of G which leave ϕ invariant. Generators X of H therefore satisfy

$$[X, Q] = 0 \ , \tag{3}$$

where

$$Q = e\, \hbar\, \phi_{\alpha}\, T^{\alpha}/a \ . \tag{4}$$

Thus Q itself is a generator of H, while all the others commute with Q. Thus Q generates an invariant subgroup of H which we could identify as the Maxwell gauge group. If we think of the remaining generators as generating a colour group, then Q is a colour singlet, by formula (3) [if the colour group is SU(3), G = SU(4)].

This sort of symmetry breaking, with ϕ in the adjoint representation, occurs frequently in grand unified theories. For example, if G = SU(5), we can get $H = SU(3)_{\text{colour}} \times \times [SU(2) \times U(1)]_{\text{electroweak}}$, with Q the weak hypercharge this time. In a second stage of symmetry breaking a Higgs (5), breaks H down to $SU(3)_{\text{colour}} \times U(1)_{\text{Maxwell}}$. In SO(10) and E_6 grand unified theories, the large symmetry breaking is due to a Higgs field in the adjoint representation.

In what follows we shall think of the earlier example in which Q generates the Maxwell gauge group and hence, when evaluated in the representation appropriate to a given field, is precisely the matrix whose eigenvalues give the electric charges of the particle excitations of that field. Also

$$f^{\mu\nu} = \phi_{\alpha} F^{\mu\nu}_{\alpha}/a \tag{5}$$

satisfies Maxwell's field equations, when Eqs. (1) and (2) hold, and can be identified as the Maxwell field.

The G gauge particles acquire masses due to the ϕ symmetry breaking, according to the formula of Higgs, Englert, Brout, and Kibble[5]:

$$(M^2)_{\alpha\beta} = e^2\hbar^2\, \phi T_\alpha T_\beta \phi \ , \tag{6}$$

which, by Eq. (4), remembering that the T's are antisymmetric structure constants, reduces to the matrix equation

$$M^2 = a^2 Q^2 \ .$$

Diagonalizing and equating eigenvalues, we see

$$M = a|q| \ .$$

In this theory the magnetic monopoles will occur as solitons; that is, smooth classical solutions to the equations of motion, with a finite energy localized in a finite region. Such solitons are familiar from other non-linear equations in physics and can be thought of as solutions which are "waves at rest", this possibility being due to the non-linearity. In general, non-linear equations are difficult to solve, but as Bogomolny[6] and Coleman et al.[6] showed, it is easy to estimate a lower bound on their mass, in terms of their topological quantum number, which is actually the magnetic charge. For

$$E = \frac{1}{2}\int d^3x \left[\mathcal{E}^{i2} + \mathcal{B}^{i2} + \mathcal{D}^0\phi^2 + (\mathcal{D}^i\phi)^2 + V(\phi)\right]$$

$$\geq \frac{1}{2}\int d^3x \left[\mathcal{B}^i \mp \mathcal{D}^i\phi\right]^2 \pm \int d^3x\ \mathcal{B}^i \mathcal{D}^i\phi$$

dropping positive terms. By the Bianchi identity the last term is

$$\int d^3x\, \nabla^i(\mathcal{B}^i\phi) = \int dS^i\ \phi\mathcal{B}^i = a|g| \ ,$$

by Eq. (5), where g is the Maxwell magnetic charge. Hence putting the monopole at rest we deduce that its mass M satisfies

$$M \geq a|g| \ . \tag{7}$$

For a dyon[7], with both electric charge q and magnetic charge g, the argument yields

$$M \geq a\sqrt{q^2 + g^2} \ .$$

Equality is possible if the terms dropped vanish identically, i.e. if the Higgs self-interaction $V(\phi)$ vanishes[8] and if certain first-order differential equations hold.

Finally, let us note that the Higgs particles are massless if $V(\phi) \equiv 0$, and carry zero q and g.

Hence we reach the remarkable conclusion[9] that if $V(\phi) = 0$ (and solitons satisfy certain first-order equations), then all the particle states, monopoles, gauge particles, and Higgs particles, satisfy the single universal formula,

$$M = a\sqrt{q^2 + g^2} \ . \tag{8}$$

This is regardless of their origin as quantum excitations or solitons and respects the dual symmetry $q + ig \to e^{i\theta}(q + ig)$.

This was first noted by Montonen and Olive[9] and one can ask what is the deeper significance of Eq. (8) and whether it is affected by quantum corrections.

Suppose we write down a six-component momentum whose first four components are ordinary four-momentum and whose last two (space-like components) are aq and ag, respectively:

$$\mathbb{P}^\mu = (p^0 p^1 p^2 p^3, aq, ag) \ . \tag{9}$$

Then Eq. (8) is the condition that $\mathbb{P}^\mu$ is light-like in six dimensions:

$$\mathbb{P}^2 = 0 \ . \tag{10}$$

It turns out that this is not accidental; there is a deeper six-dimensional formulation lying behind the theory, explaining the remarkable structure given by Eqs. (8), (9), and (10).

The first clue was the observation that the results depended crucially on the assumption that the Higgs field ϕ lies in the adjoint representation of G, just as do the gauge potentials. This suggests that the Higgs field can be thought of as a fifth component of the gauge potential pointing in an extra, unphysical fifth dimension[10]:

$$\phi = W^5 \ .$$

To fit the kinetic energies together correctly, this dimension must be space-like. Now one can expect an extra gauge invariance with respect to x_5-dependent gauge transformations, even though the original fields would not depend on x_5. This forces $V(\phi) = 0$, and implies[11] that the fifth component of momentum is indeed proportional to the electric charge [Eq. (9)]. Further, if no masses are put in by hand, all particles associated with elementary fields have $g = 0$ and satisfy formula (8). Only the solitons carry non-zero magnetic charge g. The fact that this can be thought of as a sixth component of momentum is in consequence of a new assumption, supersymmetry[11,12]. This assumption seems to be natural in view of the fact that if we can quantize the theory in a supersymmetric way (which is not really known for sure), then the mass formula (8) should be exact in the full quantum theory. We know of no other way of ensuring this remarkable feature.

The appearance of extra dimensions has a long history originating with Kaluza and Klein[13]. Its frequent present-day use in supergravity theory is related to the use above.

REFERENCES

1) P.A.M. Dirac, Proc. Roy. Soc. A133, 60 (1931).

2) G. 't Hooft, Nucl. Phys. B79, 276 (1974).
A.M. Polyakov, JETP Lett. 20, 194 (1974).

3) E. Schrödinger, Proc. Roy. Soc. A150, 465 (1935).

4) E. Corrigan and D. Olive, Nucl. Phys. B110, 237 (1976).

5) P.W. Higgs, Phys. Lett. 12, 132 (1964) and 13, 508 (1964); Phys. Rev. 145, 1156 (1966).
F. Englert and R. Brout, Phys. Rev. Lett. 13, 321 (1964).
T.W.B. Kibble, Phys. Rev. 155, 1557 (1967).

6) E.B. Bogomolny, Sov. J. Nucl. Phys. 24, 449 (1976).
S. Coleman, S. Parke, A. Neveu and C.M. Sommerfield, Phys. Rev. D 15, 554 (1977).

7) B. Julia and A. Zee, Phys. Rev. D 11, 2227 (1975).

8) M.K. Prasad and C.M. Sommerfield, Phys. Rev. Lett. 35, 760 (1975).

9) C. Montonen and D. Olive, Phys. Lett. 72B, 117 (1977).

10) M. Löhe, Phys. Lett. 70B, 325 (1977).

11) D. Olive, Nucl. Phys. B153, 1 (1979).

12) E. Witten and D. Olive, Phys. Lett. 78B, 97 (1978).

13) T. Kaluza, Sitzungsber. Preuss. Akad. Wiss. Berlin, Math. Phys. Kl. Abt. 966 (1921).
O. Klein, Z. Phys. 37, 895 (1926).

TECHNOLOGICAL APPLICATIONS OF N = 8 SUPERGRAVITY

B. Julia
Ecole normale supérieure, Paris, France.

My goal is to report on recent work done in collaboration with Eugène Cremmer and Joël Scherk at the Ecole Normale in Paris. A discussion of historical or technical details can be found in the original papers[1,2], it seems more appropriate to present here the classical Lagrangian in the most compact and symmetric form known today as well as some general observations and concepts of wider applicability.

1. HIGHER SPACE-TIME DIMENSIONS

Space-time is perceived by educated people as being 4-dimensional, and our objective is to construct in closed form the N=8 extended supergravity theory in four dimensions. More precisely one is interested eventually in computing its higher order quantum corrections (d=4) and one would like to generalize the abelian theory[2], where the 28 physical vector fields are gauge fields for $U(1)^{28}$, to a non-abelian theory with non-abelian Yang-Mills fields. In the non-abelian generalization, one would have two independent coupling constants K for gravitation and e the Yang-Mills charge, only for $e \neq 0$ do the scalar fields have non linear (non-derivative) interactions of a potential energy type ; clearly the phenomenological analysis of this theory will require the knowledge of the potential to all orders, even at the classical level. Unfortunately it is a general rule for any number of space-time dimensions that the rescaled bosonic fields $[K\varphi]$ (or KA_μ) are dimensionless ; any iterative construction in successive powers of K is thus potentially infinite as soon as there is one spin zero field in the theory (gauge fields appear with derivatives and consequently to a finite order only). But the most efficient way to construct supergravities is this K-expansion.

Let us recall however that in the pioneering theory of Kaluza and Klein (as extended by Jordan and Thiry) a moving frame in five dimensions decomposes into the usual vierbein, a vector field plus one scalar field in four dimensions ; more precisely in four-dimensional language one has a full Fourier series of particles of each type with increasing masses according to the dependence of the fields on the fifth coordinate.

Our first rule will be to look for gauge fields in higher dimensions ; higher dimensions appear quite naturally here, and the relevant dimension can be inferred from the supersymmetry algebra as we shall see.

2. GENERALIZED GAUGE FIELDS

The most interesting part of the supersymmetry (global) algebra is the set of anticommutators :

$$[Q^a_\varepsilon , \bar{Q}^b_\zeta]_+ = \delta^{ab}(\gamma^\alpha)_{\varepsilon\zeta} P_\alpha \qquad (d=4)$$

ε, ζ are Majorana 4-spinor indices and a, b ... vector indices for an internal symmetry group O(N) ; N labels the so-called extended supersymmetry algebras. Following Salam, Strathdee, Gell-Mann and Ne'eman, one can find the spectrum of states of various models by applying for fixed P_μ ($P^2=0$) the generators of the little group to the state of highest helicity. This analysis explains the very special role played by the N=4 Yang-Mills supersymmetric theory and by the N=8 supergravity theory. Both are realized with irreducible representations of the little group (no CPT doubling is necessary), CPT is built in and one can attempt a field theoretic construction. They are the largest theories having highest spin 1 (resp. 2). Concretely the little group analysis in 4 dimensions suggests, if one wants to avoid spins larger than 2 : 1 spin 2 field e^α_μ , 8 Rarita-Schwinger fields ψ^a_μ , 28 vectors $A^{[ab]}_\mu$, 56 spin $\frac{1}{2}$ fields $\chi^{[abc]}$ and 70 scalars $\Phi^{[abcd]}$, for N=8 supergravity. The irreducibility requirement prevents one from adding any "matter multiplet" ; furthermore such a multiplet would introduce at least one more spin 2 field, if the latter cannot acquire a mass one must stick to the original and thus rather unique field contents. In particular the presence of the 70 scalar fields requires the introduction of extra-dimensions.

Exactly how many, can be seen from the following remark : for $N = 2^k$ the combined index (a,ε) takes 2^{k+2} values and thus corresponds to a single (N'=1) spinor in higher dimensions, typically $d' = 4+2k$. Yet there are some constraints imposed by the existence of a Majorana representation on the signature of space-time ; for N=4 one must go all the way to 10 dimensions (if one requires the extra dimensions to be space-like) the crucial fact is that in 1+9 dimensions Weyl and Majorana properties are compatible. For N=8 the supersymmetry algebra can be reformulated as N'=1, d'=10 supersymmetry (relaxing the Weyl condition). Indeed $\delta^{ab} \times \gamma^\alpha_{\varepsilon\zeta} = \Gamma^\alpha_{(a\varepsilon)(b\zeta)}$ are the first four of 10 Γ matrices for SO(1,9) and the others will not appear in that subsector of the theory (in d' dimensions) corresponding to zero extra-momenta P_5 , P_6 ... = 0 . The field contents in 10 dimensions can be derived from a remarkable hypothesis : the conjecture by Gliozzi, Olive and Scherk of the (local) supersymmetry (as a 10 dimensional field theory) of the spinor dual model of Ramond, Neveu, Schwarz in the zero slope limit. The field contents has also been investigated systematically by Nahm for supersymmetric theories in dimensions $d' \leq 11$. In 10 dimensions one finds in the Bose sector : a metric field g_{MN} or e^A_M , an antisymmetric generalized gauge field A_{MN} (Kalb-Ramond, Nambu) appearing via its field strength $F_{MNP} = 3\,\partial_{[M} A_{NP]}$, and a scalar φ plus a vector A_M and another "gauge field" A_{MNP} . The single scalar φ forces us to go to 11 dimensions à la Kaluza-Klein, itis quite natural in the Fermi sector as well and the final field contents is : a moving frame $e^{A'}_{M'}$ one generalized gauge field $A_{M'N'P'}$ and one 32-component Rarita-Schwinger-Majorana field $\Psi_{M'}$. Altogether 128 bosonic and 128 fermionic physical degrees of freedom,

and corresponding spins are the common features of N=8, d=4 and N'=1, d'=11 supergravities. The full action has been constructed in Ref.[1], it is polynomial in the matter fields in eleven dimensions.

3. ABELIAN DUALITIES

The active reader will have noticed that after dimensional reduction, the 7 $A_{\mu\nu a}$ fields (a = 1 - 7 internal dimension) must be equivalent to 7 scalar fields φ^a . Let us reformulate this in more general terms : in d dimensions a generalized gauge field antisymmetric in p indices appearing in a Lagrangian only via its field-strength can be replaced classically by a dual d-2-p component gauge field leading to the same equations of motion for all fields. The dual potentials appear only through their field strengths which are the algebraic duals of the original field strengths. The dual action can be derived from the original action by simply exchanging the order of two integrations. For example one can consider the field strength as an independent variable (first order formalism) and integrate first on the potential to eliminate it, the dual potential appears when solving this equation of motion, one is then left with a dual action in terms of the dual potential. Provided there is no minimal coupling, there is no difficulty at all, a minimal coupling of the potentials forces the duality transformations to be non-local.

4. COMPLEX INVARIANCES OF REAL FIELDS

Dualities of this type can be found to extend the global symmetry group from O(N) to U(N) or SU(N), here SU(8). It might seem surprising that a real theory possesses complex invariances, but following Ferrara, Scherk and Zumino, one notices that $i\gamma_5$ is real and has square equal to -1 and that in 4-Minkowski space $\frac{1}{2}\,\varepsilon_{\mu\nu\rho\sigma}$ acting on real field strengths $F_{\mu\nu}$ is also real and has square -1 . As was explained in the previous section all dualities act on the equations of motion and change the usual second order Lagrangians, so some of them can be at best invariances of the equations of motion. Actually it is shown in Ref.[2] that there exists a first order action (with constraints) which is fully symmetric under dualities of a special type.

Let us now list the symmetries of the four dimensional N=8 supergravity equations of motion. The expected global SU(8) is a subgroup of a larger non-compact group $E_7(+7)$, to be precise it is its maximal compact subgroup. The global group E_7 is realized non linearly on the scalar fields : they parametrize the homogeneous space $E_7/SU(8)$. This observation leads us to our next rule.

5. NON-LINEAR REALIZATIONS OF (NON)-COMPACT GROUPS

The traditional discussion of non-linear realizations (see the 1969 articles in Physical Review) makes use of a special parametrization of the

homogeneous space G/H . Guided by the analogy with general relativity in the Weyl formalism, we preferred to simplify the transformation rules by relaxing the gauge fixing involved in this parametrization. It is much simpler to describe the coset element of G/H by all the elements gH of G, and this requires a local H (auxiliary) gauge invariance. In our case $G=E_7$, $H = SU(8)$ (compare to the gravitational case[3] $G = GL(4\,\mathbb{R})$, $H = SO(1,3)$) ; besides the global E_7 symmetry we have a local SU(8) gauge invariance which can be visualized by using auxiliary SU(8) gauge potentials. These 63 potentials do not have any kinetic term at the classical level, they are quite distinct from the 28 abelian vector fields $A^{[ab]}$ which are propagating. In view of the phenomenological difficulties of the N=8 theory at the perturbative level, it is very important to check whether or not some of these auxiliary fields (falling into a supersymmetric multiplet) can become dynamical by quantum effects.

The Lagrangian for the scalar fields is simply :

$$L_s = \frac{1}{48} \mathrm{Tr} \left[(\partial_\mu V - h_\mu . V)\, V^{-1} \right]^2$$

where h_μ is the SU(8) auxiliary vector field and V (no gauge fixing) is a general group element of E_7 . For non compact groups the Killing form appearing in the trace is not negative definite, the theory is consequently not positive definite prior to gauge fixing ; but before discussing this point let us state our conjecture that the full N=8 Lagrangian can be put in a simple form (similar to L_s) exhibiting its geometrical nature as a generalized non-linear σ-model in superspace with supergroups. Proving this might explain in turn why E_7 makes its appearance in supersymmetry theory.

6. NON COMPACT GROUPS FOR PHENOMENOLOGY

It is standard lore that internal symmetry groups ought to be compact the reason is very simple ; let us consider a σ model for a non-compact group G, the Lagrangian reads typically :

$$L_s \simeq \mathrm{Tr}(g^{-1}\, \partial_\mu\, g)^2 \quad .$$

The above expression does not have a definite sign, for the maximal compact subgroup H it is negative definite, for the orthogonal Lie algebra elements $(g^{-1}\, \partial_\mu\, g)$, it is positive definite. But one way to avoid this "ghost problem" is to cancel out one of the two types of terms, and this is precisely what is achieved by replacing in L_s the ordinary derivative by a covariant derivative. The arbirary h_μ (after extremization of the classical action) eliminates the negative terms (at the classical level) and one is left with a positive definite energy (and norm).

The case of gravitation is different, one must consider the little group and not the full $GL(4, \mathbb{R})$ [3]. Yet there is a striking similarity

between σ-models and gravitation in any dimension. This can be contrasted with the σ-model form of axisymmetric gravitation theory in four dimensions.

7. CONCLUSIONS

The detour via 11 dimensions allowed the construction of the N=8 supergravity action to all orders in the coupling constant K . The non-linearity seems to indicate a simple group theoretic structure. The topological aspects of this theory remain to be studied, they will be important in the discussion of spontaneous symmetry breaking and for the generalization of the theory to non-abelian physical vector fields. The supersymmetry transformation rules have been[2] partly derived by dimensional reduction, partly guessed by assuming their covariance under E_7 global and SU(8) local. Further simplifications of the action and especially of its fermionic terms are required for efficient computation of quantum corrections.

Finally the appearance of an exceptional group E_7 and the existence of a mathematical "triality" for the group SO(8) must be investigated in view of a possible relation with colour.

REFERENCES

[1] - E. Cremmer, B. Julia and J. Scherk, Phys. Lett. 76B (1978) 409.

[2] - E. Cremmer and B. Julia, Phys. Lett. 80B (1978) 48 ;
E. Cremmer and B. Julia, Nucl. Phys. B (1979), to appear.

[3] - B. Julia, Invited talk at the 2nd M. Grossmann Meeting, Trieste (July 1979), to appear.

FORMULATION OF SUPERGRAVITY WITHOUT SUPERSPACE

S. Ferrara
Laboratori Nazionali di Frascati, INFN, Frascati, Italy.
and
International Centre for Theoretical Physics, Trieste, Italy.

ABSTRACT

Supergravity, the particle theory which unifies under a unique gauge principle the quantum-mechanical concept of spin and space-time geometry, is formulated in terms of quantities defined over Minkowski space-time. The relation between this formulation and the formulation which uses superspace, the space-time supplemented by spinning degrees of freedom, is also briefly discussed.

1. INTRODUCTION

Supergravity [1),2)], the theory of local supersymmetry, is the most sophisticated gauge theory which is known nowadays. It unifies under a unique gauge principle the concept of general co-ordinate transformations of curved space-time and fermionic gauge transformations. The first is the underlying geometrical principle of Einstein theory of gravitation, the last is the basic invariance of the 1941 dated Rarita-Schwinger Lagrangian [3)] and it is also the local extension of supersymmetry transformations among bosons and fermions [4)]. At the global level this latter symmetry permits to overcome previous no-go theorems which previously constituted a barrier against possible extension of space-time symmetries to incorporate internal symmetries in a non-trivial way. At the local level it provides a subtle and perhaps unique interplay between spin-statistics and space-time geometry. The Weyl-Cartan concept of torsion becomes an intrinsic property of space-time in local supersymmetry and fermionic gauge fields appear as space-time connections for the first time. In local extended supersymmetry a unification of the Einstein-Hilbert Lagrangian with Maxwell and Yang-Mills Lagrangians is also possible. At the quantum level supergravity is a better theory of Einstein theory. It furnished, for the first time, finite quantum corrections at the first two loops and in the extended supergravity models, in which higher symmetries are present, it gives hopes (but by no means yet proved) for a renormalizable superunified theory of all particle interactions.

It is the purpose of the present report to focus the attention on the basic aspects which led to the formulation of supergravity and to the most recent formulation which allows us to consider supergravity just as another gauge theory.

2. FORMULATION OF SUPERGRAVITY IN MINKOWSKI SPACE-TIME

Let us make first an excursion to the original formulation of supergravity theory. This theory was approached in two different but equivalent ways: as the gauge theory of the 14-dimensional (10 + 4N dimensional in the extended case if desired) graded Poincaré group [2),5)] (geometric derivation) or as the extension of the Rarita-Schwinger gauge invariance of the free massless spin-$\frac{3}{2}$ field to an interacting theory [1)] (footsteps derivation). The gauge algebra is the local analogue of global supersymmetry. This algebra is the 14-dimensional graded Poincaré algebra whose basic (anti) commutation relations are

$$\{Q_\alpha, Q_\beta\} = -\tfrac{1}{2}(\gamma^\mu C)_{\alpha\beta} P_\mu$$
$$[Q_\alpha, P_\mu] = 0$$
$$[Q_\alpha, M_{\mu\nu}] = (\sigma_{\mu\nu})_\alpha{}^\beta Q_\beta \qquad (1)$$

C is the charge conjugation matrix: $C\gamma_\mu C^{-1} = -\gamma_\mu^T$.

One can define structure constants for a graded Lie algebra

$$[X_A, X_B\} = f_{AB}{}^C X_C \qquad (2)$$

and Lie algebra-valued connection fields (potentials)

$$h_\mu^A X_A = e_\mu^a P_a - \omega_\mu{}^{ab} M_{ab} + \bar{\psi}_\mu{}^\alpha Q_\alpha \qquad (3)$$

and curvatures (field strengths)

$$R_{\mu\nu}^A = \partial_\nu h_\mu^A - \partial_\mu h_\nu^A + f_{BC}^A h_\nu^B h_\mu^C . \qquad (4)$$

Their explicit expression is

$$R_{\mu\nu}^a(P) = \partial_\nu e_\mu^a - \partial_\mu e_\nu^a + \omega_\mu^{ba} e_{b\nu} - \omega_\nu^{ba} e_{b\mu} + \tfrac{1}{2}\bar{\psi}_\mu \gamma^a \psi_\nu , \qquad (5)$$

$$R_{\mu\nu}^\alpha(Q) = \partial_\nu \psi_\mu^\alpha - \partial_\mu \psi_\nu^\alpha + \tfrac{1}{2}\omega_\nu^{ab}(\sigma_{ab})^{\alpha\beta}\psi_{\beta\mu} - \tfrac{1}{2}\omega_\mu^{ab}(\sigma_{ab})^{\alpha\beta}\psi_{\beta\nu} , \qquad (6)$$

$$R_{\mu\nu}^{ab}(M) = \partial_\mu \omega_\nu^{ab} - \partial_\nu \omega_\mu^{ab} + \omega_\mu^{ac}\omega_{\nu cb} - \omega_\nu^{ac}\omega_{\mu cb} . \qquad (7)$$

One gets the following gauge-field variations:

$$\delta(h_\mu^A X_A) = \partial_\mu \eta + [\eta, h_\mu^A X_A] , \qquad \eta = \epsilon^A X_A \qquad (8)$$

i.e.

$$\delta h_\mu^A = (D_\mu \epsilon)^A = \partial_\mu \epsilon^A + f_{BC}^A h_\mu^B \epsilon^C .$$

This gives the rules

$$\delta e_\mu^a = \tfrac{1}{2}\bar{\epsilon}\gamma^a \psi_\mu , \qquad \delta \psi_\mu^\alpha = D_\mu \epsilon^\alpha \qquad (9)$$

for local supersymmetry transformations. Note that general co-ordinate transformations are not the same thing as P gauges since

$$\delta_{gc} h_\mu^A = \partial_\mu \xi^\alpha h_\alpha^A + \xi^\alpha \partial_\alpha h_\mu^A = D_\mu (\xi^\alpha h_\alpha^A) + \xi^\alpha R_{\mu\alpha}^A \ . \qquad (10)$$

Since by construction an action must be general co-ordinate invariant, due to the definition of curvatures, one cannot also require invariance under P gauges, since they would imply counting the translation twice. One can impose a kinematical constraint on the geometry which is equivalent to the second-order formalism of general relativity

$$R_{\mu\nu}^a(P) = 0 \qquad \text{(torsion free space)} \ . \qquad (11)$$

The constraint in (11) solves the spin connection in terms of the vierbein connection $\omega_\mu^{ab}(e)$ and of the spin-$\frac{3}{2}$ contorsion tensor

$$\omega_{\mu ab}(e,\psi) = \omega_{\mu ab}(e) + \frac{1}{4}(\bar\psi_\mu \gamma_a \psi_b - \bar\psi_\mu \gamma_b \psi_a + \bar\psi_a \gamma_\mu \psi_b) \ . \qquad (12)$$

Incidentally, the kinematical constraint (11) can also be interpreted, for Lagrangians linear in the M curvature, as an ω field equation in the first order (Palatini) formalism. However this is no longer the case for more general Lagrangians which are quadratic in the M curvature.

The pure supergravity Lagrangian is

$$\mathcal{L}_{SG} = -\frac{1}{2} e\, e_a^\mu e_b^\nu R_{\mu\nu}^{ab}(M) - \frac{1}{4}\varepsilon^{\mu\nu\rho\sigma}\bar\psi_\mu \gamma_5 \gamma_\nu R_{\rho\sigma}(Q) \qquad (13)$$

and is invariant (up to a four-divergence) under the gauge supersymmetry variations as given by (9) with $\omega_{\mu ab}$ as given by (12).

This ends the discussion of supergravity as the gauge theory of the graded Poincaré group. Supergravity however was originally derived from a fermionic gauge principle and this we would like to discuss now. We have seen already that the spin-$\frac{3}{2}$ field ψ_μ^α is the gauge field of local supersymmetry. If one considers the linearized (quadratic) part of the supergravity Lagrangian given in (13) this is invariant under two separate (abelian) gauge transformations

$$\delta\psi_\mu = \partial_\mu \epsilon \qquad (14)$$

$$\delta h_{\mu\nu} = \delta(g_{\mu\nu} - \eta_{\mu\nu}) = \partial_\mu \xi_\nu + \partial_\nu \xi_\mu \qquad (15)$$

as well as under a global supersymmetry rotation

$$\delta h_{\mu\nu} = \frac{1}{2}\bar\epsilon \gamma_\mu \psi_\nu + \frac{1}{2}\bar\epsilon \gamma_\nu \psi_\mu \ , \quad \delta\psi_\mu = \frac{1}{2}\omega_{\mu ab}^{LIN.}\, \sigma^{ab}\epsilon \ . \qquad (16)$$

At the coupled level the transformations (14) and (16) combine into an irreducible non-abelian symmetry $\delta\psi_\mu = D_\mu \epsilon$. This is entirely analogous to the local Yang-Mills transformation

$$\delta V_\mu^a = D_\mu \Lambda^a = \partial_\mu \Lambda^a + f_{bc}^a V_\mu^b \Lambda^c ,$$

which also in the free case splits into an abelian group transformation and a global Yang-Mills rotation. Eq.(14) is the gauge invariance of the free massless Rarita-Schwinger Lagrangian. Supergravity can be regarded as an extension of this gauge principle to a fully interacting theory. Because of this gauge invariance consistency requirements imply that ψ_μ^α must be coupled to a conserved spinor current $J_\mu^\alpha (\partial^\mu J_\mu^\alpha = 0)$. This implies supersymmetry - on the other hand it is known that under a supersymmetry variation the spinor symmetry current transforms into the stress tensor $T_{\mu\nu}$. Hence the $\bar{\psi}_\mu^\alpha J_{\mu\alpha}$ coupling requires at the same time the $g^{\mu\nu} T_{\mu\nu}$ coupling and therefore gravitation! The final theory derived by this footsteps procedure reproduces again the supergravity Lagrangian as given by Eq.(13).

3. ALGEBRAIC STRUCTURE AND ITS RELATION TO SUPERSPACE

In the last year a significant progress has been made in the understanding of the gauge structure of supergravity. The previous formulations were in fact missing an important point, which we shall describe now. As is well known, supersymmetry requires the same number of bosonic and fermionic degrees of freedom on-mass shell as well as off-mass shell. This was not the case in the description of supergravity in terms of the vierbein and Rarita-Schwinger fields. These fields describe the same number of states on-mass shell (two helicity states both for graviton and gravitino) but off-mass shell $e_{a\mu}$ has 16-10 (gauge invariances) = 6 degrees of freedom, while ψ_μ^α has 16-4 (gauge invariances) = 12 degrees of freedom. Six bosonic degrees of freedom are missing. These are the minimal sets of auxiliary fields of supergravity [6]

$$A_\mu \text{ (axial vector)}, \quad S \text{ (scalar)} \quad \text{and} \quad P \text{ (pseudoscalar)} .$$

The complete gauge multiplet is now

$$(e_{a\mu}, \psi_{\mu\alpha}, A_a, S, P) \tag{17}$$

and the supergravity Lagrangian now reads

$$\mathcal{L}_{SG}^{NEW} = \mathcal{L}_{SG} + \frac{e}{3}(A_a^2 - S^2 - P^2) . \tag{18}$$

The vierbein variation is unchanged, while the new spin-$\frac{3}{2}$ variation is obtained by the replacement

$$D_\mu \to D_\mu + \frac{1}{6}\gamma_\mu (S - i\gamma_5 P) + \frac{i}{2}(A_\mu - \frac{1}{3}\gamma_\mu \not{A})\gamma_5 .$$

Moreover the variations of the new fields A_μ, S, P are proportional to the ψ_μ^α field equations. La "seule raison d'être" of the auxiliary fields is to make the algebra of local supersymmetry a closed algebra. This achievement has the enormous advantage that allows the introduction of a tensor calculus [7] and supergravity can be treated just as

another gauge theory. After the introduction of the auxiliary fields we can study in a model-independent way the composition rule of the gauge algebra and make contact with the superspace formulation of supergravity [8)-9)].

If we denote by $\xi^{\mu}(x)$, $\epsilon^{\alpha}(x)$, $\lambda^{ab}(x)$ the parameters of general co-ordinates, local supersymmetry and local Lorentz transformations, respectively, then the composition law goes as follows:

$$(\xi_1^{\mu}, \epsilon_1^{\alpha}, \lambda_1^{ab}) * (\xi_2^{\mu}, \epsilon_2^{\alpha}, \lambda_2^{ab}) = (\xi_{12}^{\mu}, \epsilon_{12}^{\alpha}, \lambda_{12}^{ab})$$

$$\xi_{12}^{\mu} = \xi_2^{\rho}\partial_{\rho}\xi_1^{\mu} + \frac{1}{4}\bar{\epsilon}_2\gamma^{\mu}\epsilon_1 - (1 \leftrightarrow 2)$$

$$\epsilon_{12}^{\alpha} = \frac{1}{2}\lambda_2^{ab}(\sigma_{ab}\epsilon_1)^{\alpha} + \xi_2^{\rho}\partial_{\rho}\epsilon_1^{\alpha} - \frac{1}{4}\bar{\epsilon}_2\gamma^{\mu}\epsilon_1\psi_{\mu}^{\alpha} - (1 \leftrightarrow 2)$$

$$\lambda_{12}^{ab} = \lambda_2^{ac}\lambda_1^{cb} + \xi_2^{\rho}\partial_{\rho}\lambda_1^{ab} + \frac{1}{4}\left[\bar{\epsilon}_2\gamma^{\mu}\epsilon_1\hat{\omega}_{\mu}^{ab} + \frac{2}{3}\bar{\epsilon}_2\sigma^{ab}(S - \gamma_5 P)\epsilon_1\right] - (1 \leftrightarrow 2) \quad (19)$$

Here $\hat{\omega}_{\mu ab}(e,\psi,A) = \omega_{\mu ab}(e,\psi) - \frac{i}{3}\epsilon_{\mu abc}A^{c}$ is a modified spin connection.

According to Ref.9 we can now deduce the composition rule in superspace [10)] x^{μ}, θ^{α} by comparing table (19) with the composition rule of general co-ordinates $(\xi^{\Lambda}(x,\theta))$ and local Lorentz $(\varepsilon^{ab}(x,\theta))$ variations in superspace. This composition rule is

$$\xi_{12}^{\Lambda}(x,\theta) = \xi_2^{\pi}\partial_{\pi}\xi_1^{\Lambda} + \delta_1\xi_2^{\Lambda} - (1 \leftrightarrow 2)$$

$$\varepsilon^{ab}(x,\theta) = \xi_2^{\pi}\partial_{\pi}\varepsilon_1^{ab} + \varepsilon_2^{ac}\varepsilon_1^{cb} + \delta_1\varepsilon_2^{ab} - (1 \leftrightarrow 2). \quad (20)$$

Here greek indices refer to curved superspace indices and latin indices to flat superspace indices. The extra term in (20) is due to the fact that the superparameters can be field-dependent and δ means variations of the fields inside the parameter.

After identification of the lowest θ component

$$\xi^{\mu}(x,\theta=0) = \xi^{\mu}(x), \quad \xi^{\alpha}(x,\theta=0) = \epsilon^{\alpha}(x), \quad \varepsilon^{ab}(x,\theta=0) = \lambda^{ab}(x) \quad (21)$$

with the parameters over Minkowski space-time, compatibility of tables (19) and (20) enable us to reconstruct all higher θ components in terms of the $\theta = 0$ components and of the fields appearing in the gauge supermultiplet (Eq.(17)). This construction applies for any superfield quantity. For example, the supervierbein $V_{\Lambda}^{A}(x,\theta)$ can be reconstructed after identification of the lowest θ components along "horizontal" vector directions with the vierbein and Rarita-Schwinger fields

$$V_\mu^{\underline{n}}(x,\theta=0)=e_\mu^{\underline{n}}(x) \quad , \quad V_\mu^{\underline{a}}(x,\theta=0)=\psi_\mu^{\underline{a}}(x) . \tag{22}$$

It is important to remark that compatibility of the transformation laws of the supervierbein with those of the gauge multiplet not only determines the higher θ components but also gives the lowest components along "horizontal" spinorial directions

$$V_\alpha^{\underline{n}}(x,\theta=0)=0 \quad , \quad V_\alpha^{\underline{a}}(x,\theta=0)=\delta_\alpha^{\underline{a}} . \tag{23}$$

These directions do not have an analogue over Minkowski space. They correspond to the fact that spinors in superspace live, unlike ordinary space, both in the basic manifold as well as in the tangent space. The determination of the superspace quantities in terms of gauge fields over Minkowski space corresponds to a choice of a specific set of constraints in the superspace geometry. These constraints state that some components of the supertorsion vanish or are constant. This allows us to express the supervierbein in terms of a "prepotential", an axial-vector superfield [11),12)], which therefore is a solution of these constraints. Finally a further gauge choice in superspace, the so-called Wess-Zumino gauge, allows us to express this prepotential in terms of the five fields of the gauge supermultiplet.

* * * * *

REFERENCES

1) D.Z. Freedman, P. van Nieuwenhuizen and S. Ferrara, Phys. Rev. D13, 3214 (1976).

2) S. Deser and B. Zumino, Phys. Letters 62B, 335 (1976).

3) W. Rarita and J. Schwinger, Phys. Rev. 60, 61 (1941).

4) Y.A. Golfand and E.P. Likhtman, JETP Letters 13, 452 (1971); D.V. Volkov and V.P. Akulov, JETP Letters 16, 438 (1972); J. Wess and B. Zumino, Nucl. Phys. B70, 39 (1974).

5) A. Chamseddine and P. West, Nucl. Phys. B129,34 (1977); S.W. MacDowell and F. Mansouri, Phys. Rev. Letters 38, 139 (1977).

6) S. Ferrara and P. van Nieuwenhuizen, Phys. Letters 74B, 333 (1978); K. Stelle and P. West, Phys. Letters 74B, 330 (1978); E. Fradkin and M. Vasiliev, Lettere al Nuovo Cimento 22, 651 (1978).

7) S. Ferrara and P. van Nieuwenhuizen, Phys. Letters 76B, 404 (1978); K. Stelle and P. West, Phys. Letters 77B, 376 (1978).

8) J. Wess and B. Zumino, Phys. Letters 66B, 361 (1977); 74B, 51 (1978); 79B, 394 (1978); R. Grimm, J. Wess and B. Zumino, Phys. Letters 73B, 415 (1978); Nucl. Phys. B152, 255 (1979).

9) L. Brink, M. Gell-Mann, P. Ramond and J.H. Schwarz, Phys. Letters 74B, 336 (1978); Phys. Letters 76B, 417 (1978).

10) A. Salam and J. Strathdee, Nucl. Phys. B80, 499 (1974).

11) V. Ogievetsky and E. Sokatchev, Phys. Letters 79B, 222 (1978).

12) W. Siegel, Nucl. Phys. B142, 301 (1978); W. Siegel and S.J. Gates, Nucl. Phys. B147, 77 (1978).

THE ULTRA-VIOLET DIVERGENCES OF SUPERFIELD SUPERGRAVITY

J. G. TAYLOR
Department of Mathematics, King's College London, England

ABSTRACT

After a brief review of the attempts at obtaining finite answers for superunified theories in which gravity is included with the other forces of nature, we turn to a careful discussion of the use of supersymmetry to achieve ultra-violet divergence cancellations. We present a superfield description of supergravity following as close as possible the analogy of Yang-Mills globally supersymmetric quantum field theories. The constraints required to avoid having spin 3 or 5/2 particles are presented and their use and solution to avoid these higher spins particles is described. A suitable lagrangian and the steps in the field quantisation are then discussed with ultra-violet divergence counting being done for an arbitrary supergraph. We find that superfields do not achieve the hoped-for ultra-violet divergence cancellations for non-extended supergravity, the level of divergence being as for ordinary gravity. A brief argument is presented that extended supergravity should have better ultra-violet divergence cancellation properties and a conjectured power counting law is given for that.

We have heard a lot at this Conference about the possibility of obtaining a unified theory of all of the forces of nature, that is both electroweak and strong and including gravity. Indeed the grand unified models of electroweak and strong interactions require a unification mass which is not many orders of magnitude below the Planck mass of 10^{19}Gev. Thus grand unification already brings us perilously close to having gravity thrust upon us and its subsequent quantisation.

There have been many attempts in the past to quantise gravity, but so far all of these attempts have failed. The basic problem that is presented in quantum gravity, besides various detailed questions of operator ordering, of the various possible quantisation schemes, etc. is that since matter (and gravity itself) is coupled through the energy momentum tensor to the gravitational field that there is always a derivative coupling between gravity and other fields and a self-interaction of gravity with itself. This derivative interaction goes like two powers of a momentum at the vertex being considered and produces an ultra-violet divergence which, for a general graph with L internal loop momenta, has divergence degree 2 (L + 1). In other words quantum gravity is non-renormalisable in the perturbation theoretic sense that there are too many infinities to absorb them all in changes of masses and coupling constants (in this case purely the Newtonian constant G of the particles involved.

t'Hooft and Veltman [1] showed that at least for one loop, pure gravity has a finite

S-matrix. This was proved by the crucial use of field equations. In subsequent years attempts were made to discover forms of matter that would still keep finiteness of the one-loop S-matrix element but were unsuccessful [2].

It was not till the development of supersymmetry [3] and the discovery that through supersymmetry ultra-violet divergences were reduced in virulence [4] that hope rose of finding suitable matter interactions for which the 1-loop gravitational S-matrix elements would then be finite. This was achieved through the remarkable idea of supergravity [5] which is the locally supersymmetric theory of gravity. This theory was shown to have finite 1-loop S-matrix elements [6] by remarkable cancellations occurring, and even to have finite 2-loop S-matrix elements [7]. However this magnificent progress ceased when 3-loop counter terms were written down which did not vanish on mass shell and which showed that there could well be infinite S-matrix elements at the third and higher loop order [8].

In the meantime the ultra-violet divergence cancellation mechanism was being better understood in global supersymmetry by the use of superfield techniques [9] which, when applied to the globally supersymmetric ϕ^4 theory allowed a proof of ultra-violet divergence amelioration to all orders [10]. With this in mind it seems appropriate to attempt to understand whether a superfield theory of supergravity will allow a more complete analysis of the higher loop divergences in the S-matrix elements and possibly show that the coefficients of these higher loop terms that were suggested [8] are in fact zero. That is the purpose of this talk.

It might be appropriate to say at this point that a super-Riemannian theory developed by Arnowitt and Nath [11] as the simplest supersymmetric extension of Einsteinian gravity was proved [12] to be finite in all orders of perturbation theory. However this theory seems to contain unphysical aspects such as ghosts and singular limiting processes and hence it would not appear to be appropriate as a candidate for a superunified theory.

A superfield theory of supergravity at the classical level has been constructed in terms of the differential geometry of a supermanifold [13] that is, of a set of points (x,θ) where x are the usual four spacetime coordinates and θ are anti-commuting coordinates representing a four-component Majorana spinor. In terms of this differential geometry it is possible to construct a superfield theory of supergravity in a geometric form and this was started originally by Wess and Zumino [13]. Members of various groups have since attacked this problem in much more detail [14] [15]. They all use the basic ideas of an achtbein $E_A^{\ M}$ and a superconnection $\Phi_{AB}^{\ \ C}$. However these superfields contain component fields of spins 3 and 5/2 as well as possible spin 2 graviton spin 3/2 gravitino and other

lower spin fields. It is necessary therefore to impose constraints of a geometric form to remove these higher spin fields.

Two approaches have been followed to discover the constraints which are appropriate. The first one of these may be called the torsion constraints approach [14] which imposes suitable conditions on components of the torsion from which the components of the complete curvature tensor may be contained by the use of Bianchi identities. An alternative approach has been to mirror supergravity by analogy with Yang-Mills theories for which a superfield description has been given [16]. The Yang-Mills constraints can then be solved explicitly and a quantisation programme proceeded with. The two approaches may also then by shown to be equivalent [17].

It is then important to discuss the dynamics of the theory in terms of the lagrangian. This is taken to be the simplest possibility which is the volume of the supermanifold, $\det E_A{}^M$ as suggested by Wess and Zumino [14].

The solution to the constraints equations in the Yang-Mills form can be shown to depend completely on an 8 vector prepotential W^M, whose bose component W^m contains the graviton. It is necessary to analyse the quadratic dependence of the lagrangian on W^M to be sure that the field content is correctly that of supergravity; this has been done by various groups [14) 15) 17) 18)]. In particular the Yang-Mills constraint approach has been shown [18] to reduce to the set of fields comprising the graviton spin 2, the gravitino of spin $3/2$ and the auxiliary fields first introduced by Breitenlohner [19].

We now turn to the quantisation problem. Having expressed the achtbein $E_A{}^M$ and superconnection $\Phi_{AB}{}^C$ in terms of the prepotential W^M it is necessary to perform the following steps as usual ones in the quantisation of a gauge field:

a) fix the gauge for the supercoordinate transformation (under which the theory is invariant) as well as that for local Lorentz transformations (if working with torsion constraints);

b) calculate the propagators and ghost propagators by inverting the differential operators which are the coefficients of the quadratic terms in W^M in $\det E_A{}^M$;

c) calculate the vertices including the ghost vertices by expanding the determinant in a power series W^M;

d) discuss the ultra-violet divergences of the resulting expressions using the cancellation mechanism [10] which limits the powers of θ variables that can arise in a given graph.

Steps a) and b) have been taken in both the torsion constraints and Yang-Mills constraints approaches [20) 21)] whilst only in the latter approach have the remaining steps been taken [20].

The results of the power counting [20] is that the degree of divergence for a subset of graphs has been shown to be increasing exactly as in the pure gravity case with no superfield cancellation mechanism; that is that the degree of divergence behaves as 2L, where L is the loop number. This indicates that ordinary superfield supergravity is not renormalisable.

This is very disappointing but we may well ask about the possibility of extended supergravity (which involves more θ variables than one Majorana spinor). Indeed we might expect that this will have a better ultra-violet divergence behaviour, due to the fact that the cancellation mechanism will be even more efficient than before. Such does indeed seem to be the case and if we suppose that there are N Majorana spinors the analogue of the divergence counting for the unextended superfield supergravity case gives the degree of divergence d

$$d = E + (4 - 2N) \times L$$

We see that for N greater than or equal to 2 the divergence degree of an arbitrary diagram no longer increases with the loop number L. This indicates that the theory of extended supergravity may well be renormalisable for such values of N. We must make clear that only the case $N = 1$ has been analysed in some detail and only that case has been proven to be non-renormalisable. It is necessary to perform a similar analysis for N greater than 1 to show that the above conjecture that N greater than 2 is renormalisable is indeed correct. That work is presently proceeding, involving extending the Yang-Mills constraints to higher N and work on this will be reported elsewhere.

We conclude that pure superfield supergravity is not a renormalisable theory, at least according to the most developed methods of achieving ultra-violet divergence cancellations. There is hope that extended supergravity will be renormalisable and that shortly a sensible theory including matter will be accessible to us. It is not however clear that such a theory will be satisfactory as far as superunification is concerned, due to the supposed maximal value of N equal to 8 without the inclusion of higher spin fields. This is a problem which is presently under active discussion; in any way forward it will be necessary to use the criterion for renormalisability as singling out those theories which are sensible from those which nature would have found it not possible to have used.

* * *

RERERENCES

1) G. t'Hooft and M. Veltman, Annals Inst. Henri Poincare 20, 69 (1974).

2) S. Deser and P. van Nieuwenhuizen, Phys. Rev. d 10, 461 (1974).

2) J. G. Taylor and M. Nouri-Moghadam, Proc. Roy. Soc. Lond. A344, 87 (1975).

3) J. Wess and B. Zumino, Nucl. Phys. B 70, 39 (1974).

4) J. Iliopolous and B. Zumino, Nucl. Phys. B 76, 310 (1974).

5) D. Z. Freedman, P. van Nieuwenhuizen and S. Ferrara, Phys. Rev. d 13, 3214 (1976).

6) P. van Nieuwenhuizen and J. A. M. Vermaseren, Phys. Letts. 65B 263 (1976).

7) M. T. Grisaru, Phys. Lett. 66B 75 (1977).

8) S. Deser, J. H. Kay and K. Stelle, Phys. Rev. Lett. 38, 527 (1977).
S. Deser and J. H. Kay, Phys. Lett. 76B, 400 (1978).

9) A. Salam and J. Strathdee, Phys. Rev. D 11, 1521 (1975).

10) D. Capper and G. Leibbrandt, Nucl. Phys. B 85, 492 (1975).
R. Delbourgo, Nuov. Cim. 25A, 646 (1975).
F. Fujikawa and W. Lang, Nucl. Phys. B 88 61 (1975).

11) R. Arnowitt and P. Nath, Phys. Lett. 56B, 177 (1975).

12) J. G. Taylor, Proc. Roy. Soc. Lond. A 362, 493 (1978).

13) J. Wess and B. Zumino, Phys. Lett. 56B, 361 (1977).
S. Downes-Martin and J. G. Taylor, Nucl. Phys. B126, 97 (1977).

14) V. I. Ogievetsky and E. Sokatchev, "Supergravity as a Theory of an Axial Superfield", Dubna preprint 3653, Dec. 1978 (unpublished).
J. Wess and B. Zumino, Phys. Letts. 74B, 51 (1978).

15) J. G. Taylor, Phys. Lett. 78B, 577 (1978);
J. G. Taylor, S. Bedding and S. Downes-Martin, Annals of Physics (to appear).
L. Brink, M. Gell-Mann, P. Ramond and J. H. Schwarz, Phys. Lett. 74B, 336 (1978).

16) J. Wess "Supersymmetry-Supergravity", Lectures at the VIII G.I.F.T. Int. Seminar on Theoretical Physics, Salamanca, June 1977 (unpublished).

17) S. Bedding, S. Downes-Martin, C. Pickup and J. G. Taylor, Phys. Lett. 83B, 59 (1979).
W. Siegel, Nucl. Phys. B 142, 301 (1978).

18) S. Bedding and J. G. Taylor "A Detailed Analysis of the Determinant in Superspace Supergravity", King's College preprint, Feb. 1978.

19) P. Breitenlohner, Nucl. Phys. B 124, 500 (1977).

20) J. G. Taylor "Quantisation of Superfield Supergravity", King's College preprint, May 1979.

21) M. A. Namazie and D. Storey, "Supersymmetric Quantisation of linearised supergravity", I.C.T.P. (Trieste) preprint IC/79/34.
W. Siegel "Supergravity Supergraphs", Harvard preprint HUTP-79/A005, Feb. 1979.

PARALLEL DISCUSSION SESSION 5

QUARK CONFINEMENT

Chairman: H. Joos

Sci. Secretaries: T. Jones
P. Sorba

Summary report of the Chairman

SUMMARY OF THE MOST SIGNIFICANT RESULTS REPORTED IN THIS SESSION

H. Joos
DESY, Hamburg, Fed. Rep. Germany

I. PROGRAM

1. Introduction to the problem of quark confinement (H. Joos).
2. Lattice approximation with contributions by:
   J.M. Drouffe (G. Parisi, N. Sourlas): Lattice gauge theories at large dimensions.
   A. Patkos (P. Rujan): Mean disorder field approximations in lattice systems.
3. Classical solutions; vacuum structure
   A. Chodos: Search for conserved quantities in non-Abelian gauge theories.
   H.B. Nielsen: Upper bounds on the MIT-bag constant; vacuum structure of QCD.
4. Phenomenological implications on quark confinement
   L. Okun': Report on the application of sum rules to $q\bar{q}$, $c\bar{c}$, $b\bar{b}$ and glueball systems.
   J.L. Rosner: Flavour independence of the quarkonium potential.
   J. Rafelski (R.D. Viollier): Tests of QCD with heavy quark bound states.
   J. Stern (J. Gasser, H. Leutwyler, J. Jersák): Spin dependence of the confining potential.
   D. Flamm: Schrödinger approach to strongly bound quarks.
   C.B. Chiu: Perturbative QCD and the finite range confinement criteria.
   B. Schroer: Screening and confinement in two-dimensional models.

II. EVALUATION

The main points of the discussion were

(a) The magnitude of the string constant, a, or the bag constant B, respectively. The value of the MIT-bag $B = (145\ \mathrm{MeV})^4$ differs from the ITEP estimate $B = (\mathrm{GeV}/4)^4$ by nearly a factor of 10. The ITEP value seems more consistent with a string constant of the conventional magnitude $a \sim 0.8$ GeV/c.

(b) The question if the confinement schemes imply the existence of glueballs. Glueballs with a mass between 0.5 GeV and 1 GeV would fit in best in nearly all schemes.

The report by Okun' on the work of the ITEP Group (Moscow) was generally considered as a very important contribution to the discussion of these, and other questions. Also Nielsen work is important for the judgement on the value of the bag constant, which is an important parameter characterizing the confining vacuum structure.

The method of considering the strong coupling approximation to lattice gauge theories by systematic expansions with respect to space-time dimensions (J.M. Drouffe et al.) opens a very interesting approach for the solution of the confinement problem along K. Wilson's line. Besides the investigations on the exact (dense) instanton gas (V.A. Fateev, I.V. Frolov, A.S. Schwarz - ITEP preprint; and B. Berg, M. Lüscher) -- which was not represented at this conference -- I consider this 1/d expansion of lattice gauge theories the most important recent development in the field.

LIST OF PARTICIPANTS

ADAMS, J.B. *CERN, Geneva, Switzerland.*
AKCAY, H. *Middle East Technical University, Ankara, Turkey.*
ALBERI, G. *Istituto di Fisica Teorica dell'Università, Trieste, Italy.*
ALCOCK, J.W. *Dept. of Physics, The University, Bristol, UK.*
ALLES, W. *Istituto di Fisica dell'Università, Bologna, Italy.*
ALLISON, W. *Nuclear Physics Laboratory, University of Oxford, UK.*
ALONSO, J.-L. *Dept. of Theoretical Physics, Universidad de Zaragoza, Spain.*
ALTARELLI, G. *Istituto di Fisica dell'Università, Rome, Italy.*
AMALDI, U. *CERN, Geneva, Switzerland.*
ANDERSSON, B.A. *Inst. for Theoretical Physics, Lund University, Sweden.*
ANDRIC, I. *Dept. of Theor. Physics, Inst. Ruder Bošković, Zagreb, Yugoslavia.*
ANTONIOU, N. *Dept. of Theoretical Physics, University of Athens, Greece.*
APEL, W.-D. *Inst. f. exp. Kernphysik, Kernforschungszentrum Karlsruhe, Fed. Rep. Germany.*
APOSTOLAKIS, A. *Dept. of Nuclear Physics, University of Athens, Greece.*
APPELQVIST, T.W. *Physics Dept., Yale University, New Haven, Conn., USA.*
ARMENISE, W. *Istituto di Fisica dell'Università, Bari, Italy.*
ARMENTEROS, R. *CERN, Geneva, Switzerland.*
AUBERT, B.L. *LAPP, Annecy-le-Vieux, France.*
AUBERT, J.-J. *LAPP, Annecy-le-Vieux, France.*
AUGUSTIN, J.E. *LAL, Université de Paris-Sud, Orsay, France.*
AURENCHE, P. *CERN, Geneva, Switzerland.*
AVILEZ, C. *Inst. de Fisica, Univ. Nacional Autonoma de Mexico, Mexico.*

BAACKE, J. *Theor. Physik III, Universität Dortmund, Fed. Rep. Germany.*
BAAKLINI, N.S. *Int. Centre for Theoretical Physics, Trieste, Italy.*
BABELON, O. *Université de Paris-VI, France.*
BACE, M. *LPTHE, Université de Paris-VI, France.*
BADAWY, O.E. *CERN, Geneva, Switzerland.*
BAGGETT, N. *Dept. of Energy, Washington, DC, USA.*
BAIER, R. *Fakultät für Physik, Universität Bielefeld, Fed. Rep. Germany.*
BAILIN, D. *Dept. of Theoretical Physics, University of Sussex, Brighton, UK.*
BAILLON, P.H. *CERN, Geneva, Switzerland.*
BALDINI, R. *Lab. Nazionali dell'INFN, Frascati, Italy.*
BALDO-CEOLIN, M. *Istituto di Fisica dell'Università, Padua, Italy.*
BALLAM, J.N. *SLAC, Stanford, Calif., USA.*
BANDELLONI, G. *Istituto di Fisica dell'Università, Genoa, Italy.*
BANDER, M. *Dept. of Physics, Univ. of California, Irvine, Calif., USA.*
BANERJEE, H. *Saha Inst. of Nuclear Physics, Calcutta, India.*
BARBIELLINI, G. *CERN, Geneva, Switzerland.*
BARKOV, L.M. *Inst. Nuclear Physics, Siberian Div. Acad. Sci. USSR, Novosibirsk, USSR.*
BARNHAM, K. *Physics Dept., Imperial College, London, UK.*
BARTH, M. *Service de Physique des Particules élémentaires, Univ. Libre de Bruxelles, Belgium.*
BECH NIELSEN, H. *Niels Bohr Institute, Copenhagen, Denmark.*
BECHER, P. *Physikalisches Inst. der Universität Würzburg, Fed. Rep. Germany.*
BECKER, U. *CERN, Geneva, Switzerland.*
BELLINI, G. *Istituto di Fisica dell'Università, Milan, Italy.*
BENVENUTI, A. *CERN, Geneva, Switzerland.*
BERGER, E.L. *Theory Group, SLAC, Stanford, Calif., USA.*
BERGSTROM, L. *Dept. of Theoretical Physics, Royal Inst. of Technology, Stockholm, Sweden.*
BERNABEU, J. *Dept. of Theoretical Physics, Universidad de Valencia, Spain.*
BERTANZA, L. *INFN Pisa, S. Piero a Grado, Italy.*
BERTLMANN, R. *CERN, Geneva, Switzerland.*
BEST, C. *CERN, Geneva, Switzerland.*

BEUSCH, W. *CERN, Geneva, Switzerland.*
BIGI, I. *CERN, Geneva, Switzerland.*
BILLOIRE, A. *Dépt. de Physique théorique, CEN-Saclay, Gif-sur-Yvette, France.*
BINNIE, D.M. *Dept. of Physics, Imperial College, London, UK.*
BISHARI, M. *Dept. of Nuclear Physics, Weizmann Institute, Rehovot, Israel.*
BISI, V. *Istituto di Fisica dell'Università, Turin, Italy.*
BIZOT, J.-C. *LAL, Université de Paris-Sud, Orsay, France.*
BJORKEN, J.D. *SLAC, Stanford, Calif., USA.*
BLASI, A. *Istituto di Scienze, Genoa, Italy.*
BLOBEL, V. *II. Institut f. exp. Physik, Hamburg, Fed. Rep. Germany.*
BLOCH, M. *DPHPE, CEN-Saclay, Gif-sur-Yvette, France.*
BLOODWORTH, I.J. *Dept. of Physics, University of Birmingham, UK.*
BOBBINK, G.J. *NIKHEF-H, Amsterdam, NL.*
BOBISUT, F. *Istituto di Fisica dell'Università, Padua, Italy.*
BODEK, A. *Dept. of Physics and Astronomy, University of Rochester, NY, USA.*
BØGGILD, H. *Niels Bohr Institute, Copenhagen, Denmark.*
BOHM, M. *Physikalisches Inst. der Universität Würzburg, Fed. Rep. Germany.*
BONNEAUD, G. *CERN, Geneva, Switzerland.*
BONNIER, B.J. *Lab. de Physique théorique, Univ. de Bordeaux I, Gradignan, France.*
BORATAV, M. *CERN, Geneva, Switzerland.*
BORG, A. *DPHPE, CEN-Saclay, Gif-sur-Yvette, France.*
BOSETTI, P. *CERN, Geneva, Switzerland.*
BOTNER, O. *Niels Bohr Institute, Copenhagen, Denmark.*
BÖTTCHER, H. *Inst. f. Hochenergiephysik, Akad. Wissensch. DDR, Zeuthen, German Dem. Rep.*
BOTTINO, A. *Istituto di Fisica dell'Università, Turin, Italy.*
BOUQUET, A. *LPTHE, Univ. de Paris VI et VII, France.*
BOURRELY, C. *Centre de Physique théorique I, CNRS, Marseilles, France.*
BOUZOUITA, H. *Int. Centre for Theoretical Physics, Trieste, Italy.*
BOVET, C. *CERN, Geneva, Switzerland.*
BOWCOCK, J.E. *Dept. of Physics, University of Birmingham, UK.*
BOWMAN, J.D. *Los Alamos Scientific Laboratory, NM, USA.*
BOZZO, M. *CERN, Geneva, Switzerland.*
BRABSON, B.B. *High-Energy Physics Dept., Indiana University, Bloomington, Ind., USA.*
BRANDT, S. *Physics Dept., Universität Siegen, Fed. Rep. Germany.*
BRANSON, J.G. *DESY, Hamburg, Fed. Rep. Germany.*
BROADHURST, D.J. *Science Faculty, The Open University, Milton Keynes, UK.*
BROCKMANN, R. *Physikalisches Inst. der Universität Bonn, Fed. Rep. Germany.*
BRODSKY, S.J. *SLAC, Stanford, Calif., USA.*
BROWER, R.C. *Dept. of Physics, University of California, Santa Cruz, Calif., USA.*
BROWN, R.C. *Rutherford Lab., Didcot, UK.*
BUCHMUELLER, W. *Physikalisches Inst. der Universität Bonn, Fed. Rep. Germany.*
BUON, J. *LAL, Université de Paris-Sud, Orsay, France.*
BURKERT, V. *Physikalisches Inst. der Universität Bonn, Fed. Rep. Germany.*
BURNEL, A. *Inst. de Physique de l'Université de Liège, Belgium.*
BURNS, A. *CERN, Geneva, Switzerland.*
BUSCHBECK, B. *Inst. f. Hochenergiephysik, Österreich. Akad. Wissensch., Vienna, Austria.*
BUTTERWORTH, I. *Physics Dept., Imperial College, London, UK.*
BUTTIMORE, N. *School of Mathematics, Trinity College, Dublin, Ireland.*
BUZZO, A. *Istituto di Fisica dell'Università, Genoa, Italy.*

CALUCCI, G. *Istituto di Fisica Teorica dell'Università, Trieste, Italy.*
CALVETTI, M. *CERN, Geneva, Switzerland.*
CANDLIN, D.J. *CERN, Geneva, Switzerland.*
CAPELLA, A. *LPNHE, Université de Paris XI, Orsay, France.*
CARNEGIE, R.K. *Dept. of Physics, Carleton University, Ottawa, Ontario, Canada.*
CARTER, A.A. *CERN, Geneva, Switzerland.*
CARTER, J.R. *CERN, Geneva, Switzerland.*
CASALI, R. *INFN Pisa, S. Piero a Grado, Italy.*
CASHMORE, R. *Nuclear Physics Dept., University of Oxford, UK.*
CASTORINA, P. *Istituto di Fisica dell'Università, Bari, Italy.*
CAVALLI-SFORZA, M. *Dept. of Physics, Princeton University, NJ, USA.*
CENCE, R.J. *Dept. of Physics and Astronomy, Univ. of Hawaii, Manoa, Honolulu, USA.*
CHAN, H.M. *CERN, Geneva, Switzerland.*
CHARAP, J.M. *Dept. of Physics, Queen Mary College, London, UK.*
CHARPENTIER, P. *DPHPE, CEN-Saclay, Gif-sur-Yvette, France.*
CHAURAND, B. *LPNHE, Ecole polytechnique, Palaiseau, France.*
CHAUVEAU, J. *CERN, Geneva, Switzerland.*

CHEN, K.W. *Dept. of Physics, Michigan State University, East Lansing, Mich., USA.*
CHENG, L.S. *Inst. of High-Energy Physics, Academia Sinica, Peking, China.*
CHISHOLM, J.S.R. *Dept. of Applied Mathematics, University of Kent, Canterbury, UK.*
CHIU, C.B. *Max-Planck-Institut, Munich, Fed. Rep. Germany, and University of Texas, Austin, USA.*
CHODOS, A.A. *Dept. of Physics, Yale University, New Haven, Conn., USA.*
CHU, C.Y. *Inst. of High-Energy Physics, Academia Sinica, Peking, China.*
CIFARELLI, L. *CERN, Geneva, Switzerland.*
CLARK, A. *CERN, Geneva, Switzerland.*
COHEN-TANNOUDJI, G. *Dépt. de Physique théorique, CEN-Saclay, Gif-sur-Yvette, France.*
COLLINA, R. *Istituto di Fisica dell'Università, Genoa, Italy.*
COMBLEY, F.H. *Dept. of Physics, University of Sheffield, UK.*
COMTET, A. *Div. de Physique théorique, IPN, Orsay, France.*
CONTI, A. *Istituto di Fisica Sperimentale dell'Università, Florence, Italy.*
CONTIN, A. *CERN, Geneva, Switzerland.*
CONVERSI, M. *Istituto di Fisica dell'Università, Rome, Italy.*
COPLEY, L.A. *Dept. of Physics, Carleton University, Ottawa, Ontario, Canada.*
CORDS, D. *DESY, Hamburg, Fed. Rep. Germany.*
COSTA, G. *INFN, Milan, Italy.*
COSTANTINI, F. *Nevis Laboratories, Columbia University, Irvington, NY, USA.*
COUPLAND, N. *CERN, Geneva, Switzerland.*
CRAIGIE, N.S. *Int. Centre for Theoretical Physics, Trieste, Italy.*
CRAWFORD, R.L. *Dept. of Natural Philosophy, The University, Glasgow, UK.*
CROISSIAUX, M.G. *Centre de Recherches nucléaires, Strasbourg, France.*
CROZON, M. *Lab. de Physique corpusculaire, Collège de France, Paris, France.*

DALPIAZ, P. *Istituto di Fisica dell'Università, Turin, Italy.*
DAVIER, M. *LAL, Université de Paris-Sud, Orsay, France.*
DAVIES, J. *Dept. of Physics, Univ. of Oxford, UK.*
DE ALFARO, V. *Istituto di Fisica dell'Università, Turin, Italy.*
DE BOCK, H.J.M. *Natuurkundig Laboratorium, Univ. of Nijmegen, NL.*
DECLAIS, Y. *LAPP, Annecy-le-Vieux, France.*
DE GROOT, J. *CERN, Geneva, Switzerland.*
DE KERF, E.A. *Inst. of Theor. Physics, Univ. of Amsterdam, NL.*
DE ROO, M. *Inst. Lorentz, Univ. of Leiden, NL.*
DE RÚJULA, A. *CERN, Geneva, Switzerland.*
DE WOLF, E.A. *Dept. Natuurkunde, Univ. Instelling Antwerpen, Wilrijk, Belgium.*
DEL FABBRO, R. *INFN Pisa, S. Piero a Grado, Italy.*
DEL PAPA, C. *CERN, Geneva, Switzerland.*
DELPIERRE, P.A. *Collège de France, Paris, France.*
DEREVSHIKOV, A.A. *IHEP. Serpukhov, USSR.*
DERRICK, M. *Argonne National Lab., Ill., USA.*
DETOEUF, J.-F. *DPHPE, CEN-Saclay, Gif-sur-Yvette, France.*
DEUTSCHMANN, M.N. *III. Physikal. Inst. B, Rhein.-Westf. Tech. Hochschule, Aachen, Fed. Rep. Germany.*
DI CAPORIACCO, G. *Istituto di Fisica Sperimentale dell'Università, Florence, Italy.*
DIAMANT-BERGER, A. *DPHPE, CEN-Saclay, Gif-sur-Yvette, France.*
DIAS DE DEUS, J. *CERN, Geneva, Switzerland.*
DIBON, H. *Inst. f. Hochenergiephysik, Österreich. Akad. Wissensch., Vienna, Austria.*
DICK, L. *CERN, Geneva, Switzerland.*
DICKINSON, B. *Dept. of Physics, University of Manchester, UK.*
DIMOPOULOS, S. *Physics Dept., Columbia University, Irvington, NY, USA.*
DIN, A. *CERN, Geneva, Switzerland.*
DIONISI, C. *CERN, Geneva, Switzerland.*
DOBLE, N. *CERN, Geneva, Switzerland.*
DOLFINI, R. *Istituto di Fisica Nucleare, Università di Pavia, Italy.*
DORFAN, D. *Univ. of California, Santa Cruz, Calif., USA.*
DOTHAN, Y. *Dept. of Physics and Astronomy, Tel Aviv University, Israel.*
DROUFFE, J.-M. *Dépt. de Physique théorique, CEN-Saclay, Gif-sur-Yvette, France.*
DRUMMOND, I.T. *Dept. of Applied Math. and Theoretical Physics, Cambridge Univ., UK.*
DUAN, Y.S. *Dept. of Physics, Lanchow University, China.*
DUERDOTH, I. *Dept. of Physics (High-Energy Group), University of Manchester, UK.*
DUIMIO, F. *Istituto di Fisica Teorica, Università degli Studi, Parma, Italy.*
DUMBRAIS, O. *Institute of Physics, Aarhus University, Denmark.*
DÜRR, H.P. *Max-Planck-Institut f. Physik u. Astrophysik, Munich, Fed. Rep. Germany.*
DYDAK, F. *Inst. f. Hochenergiephysik, Universität Heidelberg, Fed. Rep. Germany.*
DZIEMBOWSKI, Z. *Fysisch Laboratorium, Univ. van Nijmegen, NL, and Warsaw, Poland.*

EBEL, M.E. *Dept. of Physics, Univ. of Wisconsin, Madison, Wis., USA.*
EDWARDS, K.W. *Dept. of Physics, Carleton Univ., Ottawa, Ontario, Canada.*
EKSPONG, G. *Inst. of Physics, Stockholm University, Sweden.*
ELLIS, J. *CERN, Geneva, Switzerland.*
ERNST, W. *Fakultät f. Physik, Universität Bielefeld, Fed. Rep. Germany.*
ESPOSITO, B. *CERN, Geneva, Switzerland.*
ESTEN, M.J. *Dept. of Physics, Univ. College London, UK.*

FABJAN, C. *CERN, Geneva, Switzerland.*
FADEEV, N.G. *JINR, Dubna, USSR.*
FAIRLIE, D.B. *Dept. of Physics, The University, Durham, UK.*
FALK-VAIRANT, P. *CERN, Geneva, Switzerland.*
FERBEL, T. *Dept. of Phys. and Astronomy, University of Rochester, NY, USA.*
FERRARA, S. *Lab. Nazionali dell'INFN, Frascati, Italy.*
FERRARI, E. *Istituto di Fisica, Università degli Studi, Rome, Italy.*
FERREIRA, P.L. *Instituto de Fisica Teorica, Sao Paulo, Brazil.*
FERRO-LUZZI, M. *CERN, Geneva, Switzerland.*
FIALKOWSKI, K. *Inst. of Physics, Jagellonian University, Cracow, Poland.*
FILIPPAS, T.A. *Dept. of Physics B, National Technical Univ., Athens, Greece.*
FILTHUTH, H. *Berthold Laboratory, Wildbald, Fed. Rep. Germany.*
FINE, R. *Nevis Laboratories, Columbia University, Irvington, NY. USA.*
FINJORD, J. *CERN, Geneva, Switzerland.*
FIORENTINI, G. *INFN Pisa, S. Piero a Grado, Italy.*
FIORINI, E. *Istituto di Fisica dell'Università, Milan, Italy.*
FISCHER, H.-G. *CERN, Geneva, Switzerland.*
FLAMINIO, V. *CERN, Geneva, Switzerland.*
FLAMM, D. *Inst. f. theor. Physik der Universität, Vienna, Austria.*
FLÜGGE, G. *DESY, Hamburg, Fed. Rep. Germany.*
FONTANELLI, F. *Istituto di Fisica dell'Università, Genoa, Italy.*
FOSTER, B. *Rutherford Lab., Didcot, UK.*
FRAME, D. *Dept. of Natural Philosophy, The University, Glasgow, UK.*
FRANCIS, W.R. *Dept. of Physics, Michigan State University, East Lansing, Mich., USA.*
FRANÇOIS, T. *LPNHE, Ecole polytechnique, Palaiseau, France.*
FRASER, G. *CERN, Geneva, Switzerland.*
FREDRIKSSON, S. *CERN, Geneva, Switzerland.*
FREHSE, H. *Inst. f. Hochenergiephysik, Universität Heidelberg, Fed. Rep. Germany.*
FRENCH, B. *CERN, Geneva, Switzerland.*
FRISHMAN, Y. *CERN, Geneva, Switzerland.*
FRISKEN, W.R. *Dept. of Physics, York University, Downsview, Ontario, Canada.*
FRITZSCH, H. *Physikalisches Inst., Universität Bern, Switzerland.*
FRODESEN, A.G. *Dept. of Physics, University of Bergen, Norway.*
FROIDEVAUX, D. *LAL, Université de Paris-Sud, Orsay, France.*
FROISSART, M. *Lab. de Phys. corpusculaire, Collège de France, Paris, France.*
FROYLAND, J. *Inst. of Physics, University of Oslo, Norway.*
FRY, M.P. *Inst. of Theor. Physics, Univ. of Groningen, NL.*
FUBINI, S. *CERN, Geneva, Switzerland.*
FUKUGITA, M. *Rutherford Lab., Didcot, UK.*
FURLAN, P. *Ist. di Fisica Teorica dell'Università, Trieste, Italy.*

GABATHULER, E. *CERN, Geneva, Switzerland.*
GAIDOT, A. *DPHPE, CEN-Saclay, Gif-sur-Yvette, France.*
GAILLARD, M.K. *CERN, Geneva, Switzerland.*
GALAKTIONOV, Yu.V. *CERN, Geneva, Switzerland.*
GALBRAITH, W. *Dept. of Physics, University of Sheffield, UK.*
GAMET, R. *CERN, Geneva, Switzerland.*
GANGULI, S.N. *Tata Inst. of Fundamental Research, Bombay, India.*
GARCIA, A. *CIEA, Inst. Politechnico Nacional, Mexico.*
GARCIA CANAL, C.A. *LPTHE, Centre de Recherches nucléaires, Strasbourg, France.*
GATTO, R. *Dépt. de Physique théorique, Université de Genève, Switzerland.*
GAVILLET, P. *CERN, Geneva, Switzerland.*
GEIST, W. *CERN, Geneva, Switzerland.*
GENNOW, H. *CERN, Geneva, Switzerland.*
GENTIT, X. *DPHPE, CEN-Saclay, Gif-sur-Yvette, France.*
GENZEL, H. *I. Physikal, Inst., Rhein.-Westf. Tech. Hochschule, Aachen, Fed. Rep. Germany.*
GERBER, J.P. *Centre de Recherches nucléaires, Strasbourg, France.*
GEWENIGER, C. *Inst. f. Hochenergiephysik, Universität Heidelberg, Fed. Rep. Germany.*
GIACOMO, A. *Istituto di Fisica dell'Università, Pisa, Italy.*

GIDAL, G. *Lawrence Berkeley Lab., Berkeley, Calif., USA.*
GIOVANNINI, A. *Istituto di Fisica dell'Università, Turin, Italy.*
GIUSTI, P. *CERN, Geneva, Switzerland.*
GOGGI, G.V. *CERN, Geneva, Switzerland.*
GOKIELI, R.J. *Inst. of Nuclear Research, Warsaw, Poland.*
GONZALES MESTRES, L. *CERN, Geneva, Switzerland.*
GORDON, H.A. *Brookhaven National Lab., Upton, NY, USA.*
GRACCO, F. *Istituto di Fisica dell'Università, Genoa, Italy.*
GRAFSTROM, P. *CERN, Geneva, Switzerland.*
GREEN, M.B. *Physics Dept., Queen Mary College, London, UK.*
GREEN, M.G. *CERN, Geneva, Switzerland.*
GREGORY, P. *CERN, Geneva, Switzerland.*
GREIN, W. *Inst. f. theor. Kernphysik, Universität Karlsruhe, Fed. Rep. Germany.*
GRIFOLS, J.A. *Dept. of Theor. Physics, Universidad Autonoma de Barcelona, Spain.*
GROSSETETE, B. *LPNHE, Univ. de Paris VI, France.*
GUENIN, M. *Dépt. de Physique théorique, Université de Genève, Switzerland.*
GUNION, J.F. *Dept. of Physics, University of California, Davis, Calif., USA.*
GUSTAFSSON, G. *Inst. for Theor. Physics, Lund University, Sweden.*

HACINLIYAN, A.S. *Dept. of Physics, Bogazici University, Istanbul, Turkey.*
HAGBERG, E. *Gustaf Werner Inst., Uppsala, Sweden.*
HAGELBERG, R. *CERN, Geneva, Switzerland.*
HAISSINSKI, J. *LAL, Université de Paris-Sud, Orsay, France.*
HAMER, C.J. *School of Physics, Univ. of Melbourne, Australia.*
HANSSON, H. *Dept. of Theor. Physics, Chalmers Univ. of Technology, Gothenburg, Sweden.*
HARGROVE, C.K. *Div. of Physics, NRCC, Carleton Univ., Ottawa, Ontario, Canada.*
HARI DASS, N.D. *Raman Research Inst., Bangalore, India.*
HEIMANN, R.L. *Dept. of Physics, Univ. of Oxford, UK.*
HEINZ, R.M. *High-Energy Physics Dept., Indiana University, Bloomington, Ind., USA.*
HELGAKER, P. *CERN, Geneva, Switzerland.*
HEMINGWAY, R.J. *Dept. of Physics, Carleton Univ., Ottawa, Ontario, Canada.*
HENRI, V.P. *Faculté des Sciences, Université de l'Etat, Mons, Belgium.*
HENZI, R. *High-Energy Physics Group, McGill University, Montreal, Quebec, Canada.*
HERCZEG, P. *Los Alamos Scientific Laboratory, N.M., USA.*
HESS, R. *Université de Genève, Switzerland.*
HEUER, R.D. *Physikalisches Inst., Universität Heidelberg, Fed. Rep. Germany.*
HEUSCH, C.A. *High-Energy Physics Div., Univ. of California, Santa Cruz, Calif., USA.*
HEY, A.J.G. *Physics Dept., University of Southampton, UK.*
HIGGS, P.W. *Dept. of Physics, Univ. of Edinburgh, UK.*
HITE, G. *Kaiserslautern, Fed. Rep. Germany.*
HOEHLER, G. *Inst. f. theor. Kernphysik, Universität Karlsruhe, Fed. Rep. Germany.*
HOFFMANN, H. *CERN, Geneva, Switzerland.*
HOFFMANN, L. *CERN, Geneva, Switzerland.*
HØGAASEN, H. *Dept. of Physics, University of Oslo, Norway.*
HOLMES, S. *Nevis Laboratories, Columbia University, Irvington, NY, USA.*
HOLMGREN, S.O. *Physics Inst., Stockholm University, Sweden.*
HOLTHUIZEN, D.J. *NIKHEF, Amsterdam, NL.*
HOPKINS, H. *Physics Dept., College of Technology, Dublin, Ireland.*
HSIEN, T.C. *Inst. of High-Energy Physics, Academia Sinica, Peking, China.*
HU, N. *Dept. of Physics, Peking University, China.*
HUGENTOBLER, M. *Universität Bern, Switzerland.*
HUGHES, R.J. *Nuclear Physics Lab., University of Oxford, UK.*
HUMPERT, B. *CERN, Geneva, Switzerland.*
HUQ, M. *Dept. of Physics, University of Nigeria, Nsukka, Nigeria.*
HWA, R.C. *Dept. of Physics, University of Oregon, Eugene, Oreg., USA.*

ILIOPOULOS, J. *Physics Dept., Rockefeller Univ., New York, NY, USA.*
ILLE, B. *Inst. de Physique nucléaire, Villeurbanne, France.*
INNES, W.R. *SLAC, Stanford, Calif., USA.*
INNOCENTI, P.-G. *CERN, Geneva, Switzerland.*
IORI, M. *DPHPE, CEN-Saclay, Gif-sur-Yvette, France.*
IRVING, A.C. *Dept. of Appl. Maths. and Theor. Physics, University of Liverpool, UK.*
ISO, C. *Tokyo Inst. of Technology, Japan.*

JACOB, M. *CERN, Geneva, Switzerland.*
JANATA, F. *II. Inst. f. exp. Physik, Universität Hamburg, Fed. Rep. Germany.*
JANCSO, G. *Central Research Institute for Physics, Budapest, Hungary.*

JARLSKOG, C. *Dept. of Physics, Univ. of Bergen, Norway.*
JAROSZEWICZ, T. *Inst. of Nuclear Physics, Cracow, Poland.*
JAUNEAU, L. *IN2P3, Paris, France.*
JEANNET, E. *Inst. de Physique, Univ. de Neuchâtel, Switzerland.*
JENTSCHKE, W. *II. Inst. f. exp. Physik, Universität Hamburg, Fed. Rep. Germany.*
JERSAK, J. *Inst. f. theor. Physik, Rhein.-Westf. Tech. Hochschule, Aachen, Fed. Rep. Germany.*
JOHANSSON, E. *CERN, Geneva, Switzerland.*
JONES, C.N.S. *CERN, Geneva, Switzerland.*
JONES, D.R.T. *CERN, Geneva, Switzerland.*
JONES, H.F. *Dept. of Physics, Imperial College, London, UK.*
JONES, K. *NORDITA, Copenhagen, Denmark.*
JOOS, H. *DESY, Hamburg, Fed. Rep. Germany.*
JOSEPH, C. *Université de Lausanne, Switzerland.*
JULIA, B.L.S. *Lab. de Physique théorique, Ecole normale supérieure, Paris, France.*

KAFTANOV, V.S. *CERN, Geneva, Switzerland.*
KALMAN, C.S. *Dept. of Physics, Concordia Univ., Montreal, Quebec, Canada.*
KALOGEROPOULOS, T. *Dept. of Physics, Syracuse University, NY, USA.*
KALTWASSER, J. *JINR, Dubna, USSR.*
KANAREK, T. *JINR, Dubna, USSR.*
KAROWSKI, M. *Freie Univ. Berlin (West).*
KAWARABAYASHI, K. *Dept. of Physics, University of Tokyo, Japan.*
KHOZE, V.E. *Leningrad Inst. of Nuclear Physics, Gatchina, USSR.*
KIENZLE, M.N. *Université de Genève, Switzerland.*
KIESLING, C.M. *SLAC, Stanford, Calif., USA.*
KINNUNEN, R. *University of Helsinki, Finland.*
KINOSHITA, T. *Dept. of Physics, Cornell University, Ithaca, NY, USA.*
KLEINERT, H. *Fachbereich Physik, Freie Univ. Berlin (West).*
KLUBERG, L. *LPNHE, Ecole polytechnique, Palaiseau, France.*
KOBAYASHI, T. *DESY, Hamburg, Fed. Rep. Germany.*
KOCH, W. *DESY, Hamburg, Fed. Rep. Germany.*
KOEGERLER, R. *Inst. f. theor. Physik, Vienna, Austria.*
KOLLER, K. *Theor. Physik der Universität, Munich, Fed. Rep. Germany.*
KONETSCHNY, W. *Inst. f. theor. Physik, Tech. Univ., Vienna, Austria.*
KÖNIGSMANN, K. *Physikalisches Inst., Universität Bonn, Fed. Rep. Germany.*
KONUMA, M. *Research Inst. for Fundamental Physics, Kyoto University, Japan.*
KOTANSKI, A. *Lab. de Physique théorique, Fac. des Sciences, Nice, France.*
KOUNNAS, C. *Centre de Physique théorique, Ecole polytechnique, Palaiseau, France.*
KOURKOUMELIS, C. *Dept. of Physics B, University of Athens, Greece.*
KOZANECKI, W. *CERN, Geneva, Switzerland.*
KRAMMER, M. *DESY, Hamburg, Fed. Rep. Germany.*
KRETZSCHMAR, M. *Institut f. Physik, Universität Mainz, Fed. Rep. Germany.*
KROLL, P. *Fachbereich Naturwissenschaften I, Gesamthochschule Wuppertal, Fed. Rep. Germany.*
KRZYWICKI, A. *LPTHE, Univ. de Paris XI, Orsay, France.*
KUEHNELT, H. *Inst. f. theor. Physik der Universität, Vienna, Austria.*
KUGLER, M. *Dept. of Nuclear Physics, Weizmann Institute, Rehovot, Israel.*
KÜHN, D. *Inst. f. Experimentalphysik, Innsbruck, Austria.*
KÜHN, J.H. *Max-Planck-Inst. f. Physik u. Astrophysik, Munich, Fed. Rep. Germany.*
KUMMER, W. *Inst. f. theor. Physik, Tech. Univ., Vienna, Austria.*
KUNDT, U. *Inst. f. Hochenergiephysik, Akad. Wissensch. DDR, Zeuthen, German Dem. Rep.*
KURODA, M. *Fakultät f. Physik der Universität, Bielefeld, Fed. Rep. Germany.*

LABERRIGUE, J. *LPNHE, Université de Paris VI, France.*
LANCERI, L. *CERN, Geneva, Switzerland.*
LANSKE, D. *III. Physikal. Inst. B, Rhein.-Westf. Tech. Hochschule, Aachen, Fed. Rep. Germany.*
LAPIDUS, L.I. *JINR, Dubna, USSR.*
LAPLANCHE, F. *LAL, Université de Paris-Sud, Orsay, France.*
LEDER, G. *Inst. f. Hochenergiephysik, Österreich. Akad. Wissensch., Vienna, Austria.*
LEFRANÇOIS, J. *CERN, Geneva, Switzerland.*
LEINAAS, J.M. *NORDITA, Copenhagen, Denmark.*
LEITH, D.W.G. *SLAC, Stanford, Calif., USA.*
LEMOINE, M.E. *Instituut v. Theor. Fysica, Rijksuniversiteit, Utrecht, NL.*
LEPELTIER, V.C. *LAL, Université de Paris-Sud, Orsay, France.*
LI LING-FONG *Dept. of Physics, Carnegie-Mellon Univ., Pittsburgh, Penn., USA.*
LIERL, H. *CERN, Geneva, Switzerland.*
LILLESTØL, E. *Dept. of Physics, Bergen University, Norway.*
LIMENTANI, S. *Istituto di Fisica dell'Università, Padua, Italy.*

LINDENBAUM, S.J. *Dept. of Physics, City College of New York, NY, USA.*
LINDFORS, K.J. *CERN, Geneva, Switzerland.*
LLOSA, R. *Exper. High-Energy Group, Junta de Energia Nuclear, Madrid, Spain.*
LOCHER, M.P. *SIN, Villigen, Switzerland.*
LOEHR, B. *Universität Bonn, Fed. Rep. Germany.*
LOKEN, S.C. *Lawrence Berkeley Lab., Berkeley, Calif., USA.*
LONGO, E. *CERN, Geneva, Switzerland.*
LOPEZ, C. *Dept. of Theor. Physics, Universidad Autonoma de Madrid, Spain.*
LORSTAD, B. *Inst. of Physics, Lund University, Sweden.*
LOUCATOS, S. *Comm. Energie atomique, CEN-Saclay, Gif-sur-Yvette, France.*
LOVERRE, P. *CERN, Geneva, Switzerland.*
LUDWIG, J. *Caltech, Pasadena, Calif., USA.*
LUNDBORG, P. *CERN, Geneva, Switzerland.*
LYNCH, J.G. *CERN, Geneva, Switzerland.*
LYONS, L. *Nuclear Physics Lab., University of Oxford, UK.*
LYTH, D.H. *Dept. of Physics, University of Lancaster, UK.*

MACRI, M. *Istituto di Fisica dell'Università, Genoa, Italy.*
MAHARANA, J. *Theory Division, Rutherford Laboratory, Didcot, UK.*
MANDL, F. *Inst. f. Hochenergiephysik, Österreich. Akad. Wissensch., Vienna, Austria.*
MANNELLI, I. *CERN, Geneva, Switzerland.*
MANTON, N. *Lab. de Physique théorique, Ecole normale supérieure, Paris, France.*
MARINELLI, M. *Istituto di Fisica dell'Università, Genoa, Italy.*
MARNELIUS, R.C. *Inst. for Theor. Physics, Gothenburg, Sweden.*
MARTIN, A. *CERN, Geneva, Switzerland.*
MARTIN, A. *Faculté des Sciences, Université de l'Etat, Mons, Belgium.*
MARTIN, A.D. *Dept. of Physics, The University, Durham, UK.*
MARTIN, F. *CERN, Geneva, Switzerland.*
MARTIN, J.P. *CERN, Geneva, Switzerland.*
MARTINIS, M. *Dept. of Theor. Physics, Inst. Ruder Bošković, Zagreb, Yugoslavia.*
MARTYN, H.U. *DESY, Hamburg, Fed. Rep. Germany.*
MARX, G. *Roland Eötvös Physical Society, Budapest, Hungary.*
MASON, P. *Dept. of Physics, Univ. of Liverpool, UK.*
MASSAM, T. *CERN, Geneva, Switzerland.*
MATEEV, M. *JINR, Dubna, USSR.*
MATSUMOTO, S. *CERN, Geneva, Switzerland.*
MATTEUZZI, C. *CERN, Geneva, Switzerland.*
MATTHEWS, P. *University of Bath, UK.*
MATTHIAE, G. *CERN, Geneva, Switzerland.*
MAURY, S. *CERN, Geneva, Switzerland.*
MAY, J. *CERN, Geneva, Switzerland.*
MCKANE, A.J. *Dept. of Applied and Theor. Physics, Univ. of Cambridge, UK.*
MELIN, A.K.S. *Inst. of Physics, Lund University, Sweden.*
MELISSINOS, A. *Dept. of Physics, University of Rochester, NY, USA.*
MENDES, R.V. *Inst. de Fisica e Matematica, Lisbon, Portugal.*
MENESSIER, G. *Lab. de Physique math., Univ. scient. techn. de Languedoc, Montpellier, France.*
MENOTTI, P. *Istituto di Fisica dell'Università, Naples, Italy.*
MERIC DE BELLEFON, A. *CERN, Geneva, Switzerland.*
MERLO, J.-P. *DPHPE, CEN-Saclay, Gif-sur-Yvette, France.*
MERMIKIDES, M.E. *Nuclear Research Centre Demokritos, Athens, Greece.*
MEYER, J. *CERN, Geneva, Switzerland.*
MEYER, P. *Lab. de Phys. théor., Ecole normale supérieure, Paris, France.*
MICHEL, L. *CERN, Geneva, Switzerland.*
MIGNERON, R. *Dept. of Applied Mathematics, Univ. of Western Ontario, London, Ontario, Canada.*
MILLER, D.A. *Dept. of Physics, Purdue University, West Lafayette, Ind., USA.*
MINE, P. *LPNHE, Ecole polytechnique, Palaiseau, France.*
MINKOWSKI, P. *Universität Bern, Switzerland.*
MINTEN, A. *CERN, Geneva, Switzerland.*
MODIS, Th. *Université de Genève, Switzerland.*
MOHAPATRA, R.N. *Dept. of Physics, City Univ. of New York, NY, USA.*
MOLLERUD, R. *Niels Bohr Institute, Copenhagen, Denmark.*
MONACELLI, P. *Istituto di Fisica dell'Università, Rome, Italy.*
MONARI, L. *Istituto di Fisica dell'Università, Bologna, Italy.*
MONTANET, L. *CERN, Geneva, Switzerland.*
MONTONEN, C. *Res. Inst. of Theor. Physics, Univ. of Helsinki, Finland.*
MONTWILL, A. *Exper. Physics Dept., University College, Dublin, Ireland.*
MOREL, A. *DPHPE, CEN-Saclay, Gif-sur-Yvette, France.*

MORGAN, D. *Rutherford Lab., Didcot, UK.*
MORRISON, D.R.O. *CERN, Geneva, Switzerland.*
MOSCA, L. *DPHPE, CEN-Saclay, Gif-sur-Yvette, France.*
MOSER, K. *Fakultät f. Physik, Albert-Ludwigs-Universität, Freiburg, Fed. Rep. Germany.*
MOUZOURAKIS, P. *CERN, Geneva, Switzerland.*
MÜHLEMANN, P. *CERN, Geneva, Switzerland.*
MULLER, F.G.E. *CERN, Geneva, Switzerland.*
MÜLLER-KIRSTEN, H.J.W. *Fachbereich Physik, Universität Kaiserslautern, Fed. Rep. Germany.*
MURTAGH, M.A. *Physics Dept., Brookhaven Nat. Lab., Upton, NY, USA.*
MUSETTE, M. *Theoretische Natuurkunde, Vrije Universiteit, Brussels, Belgium.*
MUZINICH, I.J. *Physics Dept., Brookhaven Nat. Lab., Upton, NY, USA.*

NAGEL, B.C.H. *Royal Inst. of Technology, Stockholm, Sweden.*
NAHM, W. *CERN, Geneva, Switzerland.*
NAKKASYAN, A. *Université de Lausanne, Switzerland.*
NARJOUX, J.-L. *Lab. de Phys. corpusculaire, Collège de France, Paris, France.*
NAROSKA, B. *DESY, Hamburg, Fed. Rep. Germany.*
NASSALSKI, J.P. *Inst. of Nuclear Research, University of Warsaw, Poland.*
NEUHOFER, G. *CERN, Geneva, Switzerland.*
NEWTON, D. *Dept. of Physics, University of Lancaster, UK.*
NIELSEN, B.S. *CERN, Geneva, Switzerland.*
NIELSEN, H. *Inst. of Physics, Aarhus University, Denmark.*
NIELSEN, N.K. *NORDITA, Copenhagen, Denmark.*
NIKITIN, V.A. *JINR, Dubna, USSR.*
NIKITIN, Yu.P. *State Comm. for Atomic Energy of the USSR, Moscow, USSR.*
NINOMIYA, M. *Niels Bohr Institute, Copenhagen, Denmark.*
NÖLDEKE, G.K. *Physikalisches Inst., Universität Bonn, Fed. Rep. Germany.*

O'DONNELL, P.J. *Dept. of Physics, University of Toronto, Ontario, Canada.*
O'NEALE, S.W. *Dept. of Physics, University of Birmingham, UK.*
OADES, G.C. *Institute of Physics, University of Aarhus, Denmark.*
OCHS, W. *Max-Planck-Inst. f. Physik u. Astrophysik, Munich, Fed. Rep. Germany.*
OKUN', L. *ITEP, Moscow, USSR.*
OLIVE, D.I. *Dept. of Physics, Imperial College, London, UK.*
OPAT, G.I. *School of Physics, Univ. of Melbourne, Parkville, Australia.*
ORR, R. *CERN, Geneva, Switzerland.*
OTOKOZAWA, J. *Physics Dept., Nihon University, Tokyo, Japan.*
OTTER, G. *III. Physikal. Inst. B, Rhein.-Westf. Tech. Hochschule, Aachen, Fed. Rep. Germany.*
OTTERLUND, I. *Inst. of Physics, Lund University, Sweden.*
OVERBO, I. *Inst. of Physics, University of Trondheim, Norway.*

PACIELLO, M.L. *INFN Rome, Italy.*
PALMER, W.F. *Dept. of Physics, Ohio State University, Columbus, Ohio, USA.*
PALMONARI, F. *INFN Bologna, Italy.*
PALOMBO, F. *Istituto di Fisica dell'Università, Milan, Italy.*
PAPE, L. *CERN, Geneva, Switzerland.*
PASCUAL, P. *Dept. de Fisica Téorica, Univ. de Barcelona, Spain.*
PATEL, P.M. *Dept. of Physics, McGill Univ., Montreal, Quebec, Canada.*
PATI, J. *Dept. of Physics, University of Maryland, College Park, Md., USA.*
PATKOS, A. *Dept. of Atomic Physics, Eötvös University, Budapest, Hungary.*
PAYRE, P. *CERN, Geneva, Switzerland.*
PEACH, K.J. *CERN, Geneva, Switzerland.*
PEAK, L.S. *School of Physics, University of Sydney, Australia.*
PEIGNEUX, J.-P. *LAPP, Annecy-le-Vieux, France.*
PELLICORO, M. *Istituto di Fisica dell'Università, Bari, Italy.*
PENE, O. *LPTHE, Univ. de Paris XI, Orsay, France.*
PENNINGTON, M.R. *Dept. of Physics, The University, Durham, UK.*
PERKINS, D.H. *Nuclear Physics Laboratory, University of Oxford, UK.*
PERONI, C. *CERN, Geneva, Switzerland.*
PERRIN, D. *Université de Neuchâtel, Switzerland.*
PERROTET, M.C. *Centre de Physique théorique II, CNRS, Marseilles, France.*
PESSARD, H. *LAPP, Annecy-le-Vieux, France.*
PETERSEN, J.L. *Niels Bohr Institute, Copenhagen, Denmark.*
PETERSON, V.Z. *Dept. of Physics and Astronomy, Univ. of Hawaii, Manoa, Honolulu, USA.*
PETERSSON, B.O. *Fakultät für Physik, Universität Bielefeld, Fed. Rep. Germany.*
PETRONZIO, R. *CERN, Geneva, Switzerland.*
PETTORINO, R. *Istituto di Fisica dell'Università, Naples, Italy.*

PEYROU, C. *CERN, Geneva, Switzerland.*
PFEIL, W. *Universität Bonn, Fed. Rep. Germany.*
PHUA, K.K. *School of Physics, University of Melbourne, Australia.*
PICASSO, L.E. *INFN Pisa, S. Piero a Grado, Italy.*
PICCIOTTO, C. *Dept. of Physics, University of Victoria, BC, Canada.*
PILCHER, J. *Enrico Fermi Inst., University of Chicago, Ill., USA.*
PIMIA, M. *CERN, Geneva, Switzerland.*
PINTER, G.F. *Central Research Inst. for Physics, Budapest, Hungary.*
PIRON, C. *Dépt. de Physique théorique, Université de Genève, Switzerland.*
PIROUÉ, P. *Dept. of Physics, Princeton University, NJ, USA.*
PLESS, I.A. *MIT, Cambridge, Mass., USA.*
PLOTHOW, H. *CERN, Geneva, Switzerland.*
POCSIK, G. *Inst. for Theor. Physics, Eötvös University, Budapest, Hungary.*
PONDROM, L.G. *Dept. of Physics, University of Wisconsin, Madison, USA.*
PONS, Y.M.P. *LPNHE, Université de Paris VI, France.*
PONTING, D. *Dept. of Natural Philosophy, The University, Glasgow, UK.*
POPE, B.G. *Dept. of Physics, Princeton University, NJ, USA.*
POPOVIC, D. *Inst. of Physics, Belgrade, Yugoslavia.*
POPPLETON, A.F. *CERN, Geneva, Switzerland.*
PORDES, S.H. *CERN, Geneva, Switzerland.*
POTTER, K. *CERN, Geneva, Switzerland.*
POVH, B. *Max-Planck-Inst. f. Kernphysik, Heidelberg, Fed. Rep. Germany.*
POYER, C. *CERN, Geneva, Switzerland.*
PREDAZZI, E. *Istituto di Fisica dell'Università, Turin, Italy.*
PRENTKI, J. *CERN, Geneva, Switzerland.*
PREPARATA, G. *CERN, Geneva, Switzerland.*
PRESCOTT, C.Y. *SLAC, Stanford, Calif., USA.*
PRETZL, K.P. *CERN, Geneva, Switzerland.*
PROKES, A. *Inst. of Physics, Czechoslovak Acad. of Sciences, Prague, CSSR.*
PROKOSHKIN, Yu.D. *IHEP, Serpukhov, USSR.*
PRORIOL, J. *Lab. de Physique corpusculaire, Université de Clermont, Aubière, France.*
PROSPERI, G.M. *Istituto di Fisica dell'Università, Milan, Italy.*

QUERCIGH, E. *CERN, Geneva, Switzerland.*
QUERROU, M. *Lab. de Physique corpusculaire, Université de Clermont, Aubière, France.*

RAFELSKI, J. *CERN, Geneva, Switzerland.*
RAMM, C.A. *Science Faculty Office, Univ. of Melbourne, Australia.*
RANDER, J. *DPHPE, CEN-Saclay, Gif-sur-Yvette, France.*
RATTI, S. *Istituto di Fisica Nucleare dell'Università, Pavia, Italy.*
REES, M. *Inst. of Astronomy, University of Cambridge, UK.*
REIGNIER, J.G.M. *Th. Natuurkunde, Vrije Universiteit, Brussels, Belgium.*
REINDERS, L.J. *Dept. of Physics, University College London, UK.*
REMIDDI, E. *Istituto di Fisica dell'Università, Bologna, Italy.*
RESVANIS, L.K. *Dept. of Physics B, University of Athens, Greece.*
REUCROFT, S. *CERN, Geneva, Switzerland.*
REYA E. *DESY, Hamburg, Fed. Rep. Germany.*
RICHARD, J.-M. *LPTHE, Univ. de Paris-Sud, Orsay, France.*
RIESTER, J.L. *Centre de Recherches nucléaires, Strasbourg, France.*
RIJKEN, Th. *Instituut voor Theor. Fysica, Univ. van Nijmegen, NL.*
RIJSSENBEEK, M.M.H. *Inst. voor Theor. Fysica, Univ. van Amsterdam, NL.*
RINAUDO, G. *Istituto di Fisica dell'Università, Turin, Italy.*
RIVERS, R.J. *Dept. of Physics, Imperial College, London, UK.*
ROBSON, D. *Dept. of Physics, University of Manchester, UK.*
RODENBERG, R.H.A. *III. Physikal. Inst., Rhein.-Westf. Tech. Hochschule, Aachen, Fed. Rep. Germany.*
ROLLIER, M. *Istituto di Fisica dell'Università, Milan, Italy.*
ROSANOV, A. *ITEP, Moscow, USSR.*
ROSNER, J.L. *School of Physics and Astronomy, Univ. of Minnesota, Minneapolis, Minn., USA.*
ROSS, R.T. *CERN, Geneva, Switzerland.*
ROTHENBERG, A.F. *CERN, Geneva, Switzerland.*
ROUSSET, A. *Délégation générale à la recherche scientifique et technique, Paris, France.*
RUBBIA, C. *CERN, Geneva, Switzerland.*
RUBIO, J.A. *Experimental High-Energy Group, Junta de Energia Nuclear, Madrid, Spain.*
RUMPF, Ch. *II. Inst. f. theor. Physik, Universität Hamburg, Fed. Rep. Germany.*
RYBICKI, K. *High-Energy Physics Dept., Inst. of Nuclear Physics, Cracow, Poland.*

SAARIKKO, H.M.T. *CERN, Geneva, Switzerland.*
SABRY, A.A. *Women's University College, Ain Shams University, Cairo, Egypt.*
SADOULET, B. *CERN, Geneva, Switzerland.*
SAKAI, N. *NORDITA, Copenhagen, Denmark.*
SALAM, A. *Int. Centre for Theoretical Physics, Trieste, Italy.*
SALMERON, R.A. *Centre de Phys. théorique, Ecole polytechnique, Palaiseau, France.*
SALOMONSON, P.A. *Inst. for Theor. Physics, Gothenburg, Sweden.*
SATZ, H. *Fakultät f. Physik, Universität Bielefeld, Fed. Rep. Germany.*
SAVIN, I.A. *JINR, Dubna, USSR.*
SAVOY, C. *Université de Genève, Switzerland.*
SAVRIN, V.I. *CERN, Geneva, Switzerland.*
SCARR, J.M. *Dept. of Natural Philosophy, The University, Glasgow, UK.*
SCHACHT, P. *Max-Planck-Inst. f. Physik u. Astrophysik, Munich, Fed. Rep. Germany.*
SCHECK, F. *Inst. f. Physik, Universität Mainz, Fed. Rep. Germany.*
SCHEGELSKI, V. *Leningrad Inst. of Nuclear Physics, Gatchina, USSR.*
SCHISTAD, B.L. *Dept. of Physics, University of Oslo, Norway.*
SCHLATTER, W.-D. *CERN, Geneva, Switzerland.*
SCHLEIN, P. *Physics Dept., Univ. of California, Los Angeles, Calif., USA.*
SCHMID, C. *ETH, Zurich, Switzerland.*
SCHMID, P. *CERN, Geneva, Switzerland.*
SCHMIDT, M. *Inst. f. theor. Physik der Universität, Heidelberg, Fed. Rep. Germany.*
SCHMITZ, N. *Max-Planck-Institut f. Physik u. Astrophysik, Munich, Fed. Rep. Germany.*
SCHNEIDER, H. *Inst. f. exp. Kernphysik, Kernforschungszentrum Karlsruhe, Fed. Rep. Germany.*
SCHNITZER, H.J. *Dept. of Physics, Brandeis University, Waltham, Mass., USA.*
SCHOPPER, H. *DESY, Hamburg, Fed. Rep. Germany.*
SCHOTANUS, D.J. *Natuurkundig Laboratorium, Univ. van Nijmegen, NL.*
SCHROER, B. *Freie Univ. Berlin (West).*
SCHRÖDER, V. *DESY, Hamburg, Fed. Rep. Germany.*
SCHULKE, L. *Dept. of Physics, Univ. of Siegen, Fed. Rep. Germany.*
SCIARRINO, A. *Istituto di Fisica dell'Università, Naples, Italy.*
SCOTT, W. *CERN, Geneva, Switzerland.*
SEDLÁK, J. *Inst. of Physics, Czechoslovak Acad. of Sciences, Prague, CSSR.*
SEGRÈ, G. *Dept. of Physics, Univ. of Pennsylvania, Philadelphia, Penn., USA.*
SEHGAL, L.M. *III. Physik. Institut A, Rhein.-Westf. Tech. Hochschule, Aachen, Fed. Rep. Germany.*
SEN, S. *School of Mathematics, Trinity College, Dublin, Ireland.*
SENS, J.C. *CERN, Geneva, Switzerland.*
SERDAROGLU, M. *Dept. of Physics, Bogazici University, Istanbul, Turkey.*
SERRA, P. *Istituto di Fisica dell'Università, Bologna, Italy.*
SHAFI, Q. *CERN, Geneva, Switzerland.*
SHAPIRO, A.M. *Dept. of Physics, Brown University, Providence, RI, USA.*
SHIMA, K. *Lab. of Physics, Saitama Inst. of Technology, Japan.*
SIEMANN, R. *Dept. of Physics, Cornell University, Ithaca, NY, USA.*
SIMAK, V. *Inst. of Physics, Czechoslovak Acad. of Sciences, Prague, CSSR.*
SIXEL, P. *III. Physikal. Institut, Rhein.-Westf. Tech. Hochschule, Aachen, Fed. Rep. Germany.*
SKJEVLING, G. *Dept. of Physics, University of Oslo, Norway.*
SLEEMAN, J.C. *LAL, Université de Paris-Sud, Orsay, France.*
SMADJA, G. *DPHPE, CEN-Saclay, Gif-sur-Yvette, France.*
SNELLMANN, H.K. *Dept. of Theor. Physics, Royal Inst. of Technology, Stockholm, Sweden.*
SÖDING, P. *DESY, Hamburg, Fed. Rep. Germany.*
SOERGEL, V. *CERN, Geneva, Switzerland.*
SOFFER, J. *CERN, Geneva, Switzerland.*
SORBA, P. *CERN, Geneva, Switzerland.*
SOURLAS, N. *Ecole normale supérieure, Paris, France.*
SPINKA, H. *Argonne National Lab., Argonne, Ill., USA.*
SPIRO, M. *DPHPE, CEN-Saclay, Gif-sur-Yvette, France.*
STÄHELIN, P. *II. Inst. f. Experimentalphysik, Universität Hamburg, Fed. Rep. Germany.*
STAUDE, A. *Inst. f. theor. Physik der Universität, Munich, Fed. Rep. Germany.*
STERN, J. *Lab. Physique théorique, Particules élém., Univ. de Paris-Sud, Orsay, France.*
STEUER, M. *CERN, Geneva, Switzerland.*
STEVENS, R.A. *DPHPE, CEN-Saclay, Gif-sur-Yvette, France.*
STIPCEVIC, Z. *Inst. of Physics, Sarajevo, Yugoslavia.*
STONE, M. *Dept. of Applied and Theor. Physics, Univ. of Cambridge, UK.*
STRAUMANN, N. *Universität Zurich, Switzerland.*
STRUB, R. *Centre de Recherches nucléaires, Strasbourg, France.*
SUGAR, R.L. *Dept. of Physics, University of California, Santa Barbara, Calif., USA.*
SULAK, L. *Harvard Univ., Cambridge, Mass., USA.*
SUMOROK, K. *CERN, Geneva, Switzerland.*
SUNG, S.C. *Dept. of Physics, Peking University, China.*
SUSINNO, G. *Lab. Nazionali dell'INFN, Frascati, Italy.*

TAKEDA, H. *LICEPP, University of Tokyo, Japan.*
TALLINI, B. *DPHPE, CEN-Saclay, Gif-sur-Yvette, France.*
TARRACH, R.H. *Dept. of Theor. Physics, Universidad de Barcelona, Spain.*
TASSIE, L.J. *Dept. of Theor. Physics, Australian National Univ., Canberra, Australia.*
TAYLOR, J.G. *Dept. of Mathematics, King's College, London, UK.*
TCHRAKIAN, T.H. *Mathematical Physics Dept., St. Patrick's College, Maynooth, Ireland.*
TELEGDI, V.L. *ETH, Zurich, Switzerland.*
TENGSTRAND, G. *Dept. of Theor. Physics, Inst. of Technology, Stockholm, Sweden.*
TEODORO, D. *Université P. et M. Curie, Paris, France.*
TERENTJEV, M.V. *ITEP, Moscow, USSR.*
TERWILLIGER, K.M. *Dept. of Physics, University of Michigan, Ann Arbor, Mich., USA.*
THENARD, J.-M. *LAPP, Annecy-le-Vieux, France.*
THOMPSON, G. *Nuclear Physics Lab., University of Oxford, UK.*
THOMPSON, J.C. *Rutherford Lab., Didcot, UK.*
THUN, R. *Freie Univ. Berlin (West).*
TIEMBLO RAMOS, A. *Inst. de Estructura de la Materia, Madrid, Spain.*
TIMMERMANS, J. *CERN, Geneva, Switzerland.*
TING, S.C.C. *Dept. of Physics, MIT, Cambridge, Mass., USA.*
TOLUN, P. *Dept. of Physics, Techn. University, Ankara, Turkey.*
TORNQVIST, A. *Research Inst. f. Theor. Physics, Univ. of Helsinki, Finland.*
TOVEY, S.N. *CERN, Geneva, Switzerland.*
TREILLE, D. *CERN, Geneva, Switzerland.*
TRIPP, R.D. *Dept. of Physics, University of California, Berkeley, Calif., USA.*
TRUFFIN, C. *Service de Physique générale, Univ. Libre de Bruxelles, Belgium.*
TURLAY, R.P.J. *DPHPE, CEN-Saclay, Gif-sur-Yvette, France.*
TYNDEL, M. *Rutherford Lab., Didcot, UK.*
TZAREV, V. *Physical Institute of the Academy of Sciences, Moscow, USSR.*

UDO, F. *CERN, Geneva, Switzerland.*

VALENTI, G. *CERN, Geneva, Switzerland.*
VALIN, P. *Dept. of Physics, McGill Univ., Montreal, Quebec, Canada.*
VAN DE WALLE, R.T. *Fysisch Laboratorium, Univ. van Nijmegen, NL.*
VAN DER VELDE, C.N. *Service Phys. des Particules élém., Univ. Libre de Bruxelles, Belgium.*
VAN DEURZEN, P.A.J. *Inst. voor Theor. Fysica, Univ. van Amsterdam, NL.*
VAN DONINCK, W.K. *Dienst Elementaire Deeltjes, Vrije Universiteit, Brussels, Belgium.*
VAN HOVE, L. *CERN, Geneva, Switzerland.*
VAN PROYEN, A. *Inst. voor Theor. Fysica, Heverlee, Belgium.*
VAN ROYEN, R.P. *Inst. voor Theor. Fysica, Univ. van Nijmegen, NL.*
VANCURA, A. *Fachbereich Physik, Universität Kaiserslautern, Fed. Rep. Germany.*
VARTAPETYAN, G.A. *Erevan Physical Inst. of the Armenian Academy of Science, Erevan, USSR.*
VAYAKI, A. *Nuclear Research Centre, Athens, Greece.*
VEGNI, G. *INFN and Istituto di Fisica dell'Università, Milan, Italy.*
VENDRAMIN, I. *Istituto di Fisica dell'Università, Padua, Italy.*
VERNOV, Y. *Physical Institute of the Academy of Sciences, Moscow, USSR.*
VIALLE, J.-P. *CERN, Geneva, Switzerland.*
VIRDEE, T.S. *Dept. of Physics, Imperial College, London, UK.*
VIVARGENT, M. *LAPP, Annecy-le-Vieux, France.*
VOLKOV, M.K. *JINR, Dubna, USSR.*
VON SCHLIPPE, W. *Dept. of Physics, Westfield College, London, UK.*

WAGNER, R.W. *DESY, Hamburg, Fed. Rep. Germany.*
WAHL, Heinrich *CERN, Geneva, Switzerland.*
WAHL, Horst *CERN, Geneva, Switzerland.*
WAHLEN, H. *CERN, Geneva, Switzerland.*
WALDEN, P.L. *Dept. of Physics, Univ. of British Columbia, Vancouver, BC, Canada.*
WALTER, M. *Inst. f. Hochenergiephysik, Akad. Wissensch. DDR, Zeuthen, German Dem. Rep.*
WANDERS, G. *Inst. de Physique théorique, Université de Lausanne, Switzerland.*
WARD, D.R. *Dept. of Physics, Cavendish Lab., University of Cambridge, UK.*
WEBBER, D.M. *Dept. of Physics, The University, Liverpool, UK.*
WEGENER, D. *Experimentelle Physik V, Universität Dortmund, Fed. Rep. Germany.*
WEILHAMMER, P. *CERN, Geneva, Switzerland.*
WEISS, J.M. *SLAC, Stanford, Calif., USA.*
WEISSKOPF, V.F. *Dept. of Physics, MIT, Cambridge, Mass., USA.*
WEISZ, S. *CERN, Geneva, Switzerland.*
WENNINGER, H. *CERN, Geneva, Switzerland.*
WESS, J. *Inst. f. theor. Kernphysik, Universität Karlsruhe, Fed. Rep. Germany.*

WETHERELL, A.M. *CERN, Geneva, Switzerland.*
WETZEL, W.S. *Inst. f. theor. Physik der Universität Heidelberg, Fed. Rep. Germany.*
WIGMANS, M.E.J. *NIKHEF, Amsterdam, NL.*
WILLOT, B. *LPNHE, Université P. et M. Curie, Paris, France.*
WINTER, G. *DESY, Hamburg, Fed. Rep. Germany.*
WINTER, K. *CERN, Geneva, Switzerland.*
WOJCIK, W. *LAL, Université de Paris-Sud, Orsay, France.*
WOLF, G. *LAL, Université de Paris-Sud, Orsay, France.*
WOTSCHACK J. *Inst. f. Hochenergiephysik, Universität Heidelberg, Fed. Rep. Germany.*

YAMADA, S. *DESY, Hamburg, Fed. Rep. Germany.*
YAMAGUCHI, Y. *Dept. of Physics, University of Tokyo, Japan.*
YAMDAGNI, N. *Physics Inst., University of Stockholm, Sweden.*
YOSHIKI, H. *KEK National Lab. for High-Energy Physics, Ibaraki, Japan.*

ZACHARIASEN, F. *CERN, Geneva, Switzerland.*
ZAKRZEWSKI, J.A. *Inst. of Exp. Physics, University of Warsaw, Poland.*
ZAKRZEWSKI, W. *CERN, Geneva, Switzerland.*
ZALEWSKI, K. *Inst. of Nuclear Physics, Cracow, Poland.*
ZICHICHI, A. *CERN, Geneva, Switzerland.*
ZIEMINSKI, A. *Inst. of Exp. Physics, University of Warsaw, Poland.*
ZITOUN, R. *LPNHE, Univ. de Paris VI, France.*
ZUMERLE, G. *Istituto di Fisica dell'Università, Padua, Italy.*
ZUMINO, B. *CERN, Geneva, Switzerland.*
ZUPANČIČ, Č. *Inst. f. theor. Physik der Universität, Munich, Fed. Rep. Germany.*